

**A Thesis Submitted for the Degree of PhD at the University of Warwick**

**Permanent WRAP URL:**

<http://wrap.warwick.ac.uk/137751>

**Copyright and reuse:**

This thesis is made available online and is protected by original copyright.

Please scroll down to view the document itself.

Please refer to the repository record for this item for information to help you to cite it.

Our policy information is available from the repository home page.

For more information, please contact the WRAP Team at: [wrap@warwick.ac.uk](mailto:wrap@warwick.ac.uk)

**Biosynthesis and Bioengineering of Antibiotics**  
**in *Burkholderia* Species**

**by**

**Christian Hobson**



Thesis submitted in partial fulfilment of the requirements for the degree  
of Doctor of Philosophy in Chemistry

**University of Warwick, Department of Chemistry**

**June 2019**

## Contents

<b>Contents</b> .....	<b>i</b>
<b>List of Figures</b> .....	<b>iv</b>
<b>List of Schemes</b> .....	<b>ix</b>
<b>List of Tables</b> .....	<b>xii</b>
<b>Acknowledgements</b> .....	<b>xiii</b>
<b>Declaration</b> .....	<b>xiv</b>
<b>Abbreviations</b> .....	<b>xv</b>
<b>Abstract</b> .....	<b>xix</b>
<b>1. INTRODUCTION</b> .....	<b>1</b>
<b>1.1 Antibiotics</b> .....	<b>2</b>
1.1.1 Discovery of Natural Products as a Source of Antibiotics .....	2
1.1.2 Emergence of Antimicrobial Resistance.....	3
1.1.3 Strategies for Improving Antibiotics .....	4
<b>1.2 <i>Burkholderia</i></b> .....	<b>9</b>
<b>1.3 Polyketide Synthases</b> .....	<b>10</b>
1.3.1 Type I Modular PKSs .....	11
1.3.2 Post-PKS Tailoring Enzymes.....	18
1.3.3 <i>trans</i> -AT PKSs .....	20
<b>1.4 Gladiolin</b> .....	<b>24</b>
<b>1.5 Enacyloxin</b> .....	<b>26</b>
<b>1.6 Aims of the Project</b> .....	<b>31</b>
<b>2. RESULTS AND DISCUSSION I: Diene-Forming DH Domains</b> .....	<b>33</b>
<b>2.1 Introduction</b> .....	<b>34</b>
2.1.1 Dehydratase (DH) Domains .....	34
2.1.2 Split Modules .....	38
2.1.3 Aims.....	39
2.1.4 <i>in vitro</i> Assay used to Probe the DH Domain .....	40
<b>2.2 Results and Discussion</b> .....	<b>41</b>
2.2.1 Catalytic Activity of the GbnD5 DH Domain.....	41
2.2.2 Catalytic Mechanism of the GbnD5 DH Domain.....	50
2.2.3 Substrate Tolerance of the GbnD5 DH Domain.....	54
<b>2.3 Conclusions</b> .....	<b>58</b>
2.3.1 Summary .....	58
2.3.2 Diene Synthase Domains in Other Systems.....	59
<b>3. RESULTS AND DISCUSSION II: Enacyloxin IIa Analogues</b> .....	<b>61</b>

<b>3.1</b>	<b>Introduction .....</b>	<b>62</b>
3.1.1	Approaches used for the Generation of Natural Product Analogues .....	62
3.1.2	Previous Work in the Challis Group.....	67
3.1.3	Aims.....	72
<b>3.2</b>	<b>Results and Discussion.....</b>	<b>73</b>
3.2.1	Generation of Analogues via Deletion of Genes Encoding Tailoring Enzymes.....	73
<b>3.3</b>	<b>Conclusions .....</b>	<b>95</b>
3.3.1	Summary.....	95
3.3.2	Rationalizing Changes in Activity.....	96
3.3.3	Future Work .....	99
<b>4.</b>	<b>RESULTS AND DISCUSSION III: DHCCA Biosynthesis.....</b>	<b>103</b>
<b>5.</b>	<b>CONCLUSIONS.....</b>	<b>141</b>
<b>5.1</b>	<b>Elucidation of Biosynthetic Pathways .....</b>	<b>142</b>
5.1.1	Diene-Forming DH Domains .....	143
5.1.2	DHCCA Biosynthesis.....	146
<b>5.2</b>	<b>Engineering Antibiotic Analogues.....</b>	<b>149</b>
<b>6.</b>	<b>EXPERIMENTAL .....</b>	<b>154</b>
<b>6.1</b>	<b>Instruments and Equipment.....</b>	<b>155</b>
<b>6.2</b>	<b>Materials .....</b>	<b>157</b>
6.2.1	General.....	157
6.2.2	Growth and Production Media .....	157
6.2.3	Buffers .....	158
6.2.4	Kits .....	159
6.2.5	Antibiotics.....	160
6.2.6	Bacterial Strains .....	160
6.2.7	Vectors.....	160
<b>6.3</b>	<b>General DNA Manipulation.....</b>	<b>161</b>
6.3.1	Genomic DNA Isolation .....	161
6.3.2	Isolation of Plasmid DNA.....	161
6.3.3	Polymerase Chain Reaction (PCR).....	161
6.3.4	Agarose Gel Electrophoresis.....	162
6.3.5	Fragment DNA Purification.....	162
6.3.6	Restriction Digests and Ligations.....	163
6.3.7	Transformation and Electroporation.....	165
<b>6.4</b>	<b>Genetic Manipulation of <i>Burkholderia</i>.....</b>	<b>166</b>
6.4.1	Gene Deletions in <i>Burkholderia</i> .....	166



6.4.2	Agarose Gels Confirming Gene Deletions.....	168
<b>6.5</b>	<b><i>Burkholderia</i> Metabolite Production and Analysis .....</b>	<b>169</b>
6.5.1	Small-scale Metabolite Production.....	169
6.5.2	Production and Purification of Enacyloxin Derivatives.....	169
6.5.3	Characterization of Enacyloxin Analogues.....	169
6.5.4	Minimum Inhibitory Concentration (MIC) Assays .....	191
<b>6.6</b>	<b>Recombinant Protein Overproduction and Purification .....</b>	<b>191</b>
6.6.1	Recombinant Protein Expression Constructs .....	191
6.6.2	Site-Directed Mutagenesis .....	192
6.6.3	Recombinant Protein Overproduction .....	193
6.6.4	Recombinant Protein Purification .....	193
6.6.5	SDS-PAGE Gel Electrophoresis .....	194
<b>6.7</b>	<b><i>In vitro</i> Biochemical Assays .....</b>	<b>194</b>
6.7.1	Pantetheine Substrate Loading and Dehydration Assay .....	194
6.7.2	Condensation Assay with AHCCA .....	195
6.7.3	CoA Transferase Assay with VbxP .....	195
6.7.4	Intact Analysis of VbxP .....	195
6.7.5	ACP Loading using VbxP.....	196
6.7.6	Enoyl Reductase Assays with VbxN .....	196
6.7.7	Dehydrogenation Assays with VbxM.....	196
6.7.8	Dehydration Assays with VbxL .....	197
6.7.9	Enoyl Reduction Assays with VbxK .....	197
<b>6.8</b>	<b>Homology Modelling and Bioinformatic Analysis .....</b>	<b>198</b>
6.8.1	Homology Modelling of GbnD5 DH Domain.....	198
6.8.2	Phylogenetic Analysis of DH Domains .....	198
<b>6.9</b>	<b>Chemical Synthesis of Substrates .....</b>	<b>199</b>
6.9.1	Diene Synthase Substrates .....	199
6.9.2	Synthesis of DHCCA analogues .....	232
6.9.3	Synthesis of Substrates used to Probe DHCCA Biosynthesis.....	252
<b>7.</b>	<b>REFERENCES.....</b>	<b>262</b>
<b>8.</b>	<b>APPENDICES .....</b>	<b>276</b>

## List of Figures

**Figure 1** The structures of gladiolin and enacyloxin IIa.

**Figure 1.1** The structures of tetracycline (3), streptomycin (2), erythromycin (4), penicillin G (1) and vancomycin (5).

**Figure 1.2** The structures of  $\beta$ -lactams cephalosporin C 6, methicillin 7, clavulanic acid 8 and amoxicillin 9 discovered or developed to combat AMR.

**Figure 1.3** Structures of the semi-synthetic antibiotics plazomicin 10, minocycline 11 and clarithromycin 12 with the synthetic modifications highlighted in red.

**Figure 1.4** The structures of synthetic antibiotics eravacycline 13, carumonam 14 and FSM-100573 15.

**Figure 1.5** The structures of kanamycin A 16, amikacin 17, 1-*N*-AHBA-kanamycin 18, chelocardin 19, CDCHD 20 and the teicoplanin scaffold 21 used to generate glycopeptide analogues (with differing R groups).

**Figure 1.6** The structures of stambomycin A 23, pekiskomycin 22 and teixobactin 24.

**Figure 1.7** The structures of *Burkholderia* produced natural products bongkrekiic acid 25, burkholdine 1215 28, rhizoxin 27, caryoynencin 26, gladiolin 29 and enacyloxin IIa 30.

**Figure 1.8** The structures of natural products erythromycin 4, FR901464 33 and gilvocarcin 34. Post-PKS modifications in their biosynthesis are highlighted in red.

**Figure 1.9** The structures of natural products erythromycin 4, rifamycin B 35 and geldanamycin 36, which have undergone post- or pre-PKS modification (red/blue).

**Figure 1.10** The structures of halogenated polyketide natural products chlortetracycline 37, radicicol 38 and jamaicamide A 39. Halogens introduced by tailoring enzymes are highlighted in red.

**Figure 1.11** The comparison of a typical *cis*-AT PKS module harboring embedded AT and ER domains, with a *trans*-AT PKS module which has a separately encoded AT and ER domains.

**Figure 1.12** Organisation of type A and type B split modules also known as ‘dehydrating bimodules’ in *trans*-AT PKSs.

**Figure 1.13** The enacyloxin congeners isolated by Watanabe and co-workers. The stereocenter marked (*S*) is now believed to be (*R*)-configured.

**Figure 1.14** The crystal structure of enacyloxin IIa 30 bound to the EF-Tu-GDP complex.

**Figure 1.15** The key polar contacts between enacyloxin and the binding site in EF-Tu.

**Figure 2.1** The crystal structure of FabA (PDB: 4B0C) from *Pseudomonas aeruginosa*. **(A)**: The two monomers are shown in blue and green respectively, with the  $\alpha$ -helix of each monomer shown in grey illustrating the “hotdog fold”. **(B)**: The two active sites encompassed

by the dimer with aspartate and histidine residues being provided by each monomer (D,H and D', H' respectively).

**Figure 2.2** The crystal structure of EryDH4 (PDB: 3EL6). (A): The “double hotdog fold” with the antiparallel  $\beta$ -sheets shown in green and the two  $\alpha$ -helices shown in grey. (B): The active site aspartate and histidine residues (D and H).

**Figure 2.3** The domain architecture of type A and type B split modules. The KS<sup>0</sup> domain in type A facilitates chain transfer whereas the KS domain in type B is proposed to result in an additional chain elongation.

**Figure 2.4** Deconvoluted spectra from intact protein MS analyses of the GbnD5 DH-ACP didomain onto which thioesters **53** and **54** were loaded.

**Figure 2.5** Deconvoluted spectra from intact protein MS analyses of the GbnD5 DH-ACP didomain onto which thioesters **64** and **65** were loaded.

**Figure 2.6** Regions of <sup>1</sup>H NMR spectra for **76** and **77**. According to a study by Hodge *et. al.*, the  $\alpha$ -protons (red) of *syn*- and *anti*-Evans' aldol products have diagnostic coupling constants, allowing assignment of relative stereochemistry. The upfield  $\alpha$ -proton of the *syn*-product is predicted to have coupling constants of around 17.6 and 2.7 Hz, and the downfield  $\alpha$ -proton 17.6 and 9.5 Hz. The upfield  $\alpha$ -proton of the *anti*-product is predicted to have coupling constants of around 17.5 and 9.5Hz, and the downfield  $\alpha$ -proton 17.5 and 3.1Hz. The coupling constants for the  $\alpha$ -protons of both **76** and **77** appear to be in agreement with this study.

**Figure 2.7** Deconvoluted spectra from intact protein MS analyses of the GbnD5 DH-ACP didomain onto which thioesters **71** and **72** were loaded. Note the presence of a peak in both spectra corresponding to the *holo*-DH-ACP didomain, This presumably arises from spontaneous  $\delta$ -lactonization of the diols.

**Figure 2.8** Sequence alignment of DH domains predicted to catalyze double dehydrations with canonical DH domains from *cis*-AT PKSs.

**Figure 2.9** The homology model of the GbnD5 DH domain indicating that it contains an additional active site histidine residue (His<sub>158</sub>) compared with the EryAII DH domain active site.

**Figure 2.10** The deconvoluted intact protein MS of the GbnD5 DH-ACP didomain (left) and the H158Y mutant (right) after the loading of pantetheine thioester **86**.

**Figure 2.11** The deconvoluted intact protein MS of the GbnD5 DH-ACP didomain loaded with substrates **78**, **91** and **92**.

**Figure 2.12** The deconvoluted intact protein MS of the GbnD5 DH-ACP didomain loaded with substrates **98** and **99**.

**Figure 2.13** Putative diene-forming DH domains present in leinamycin **105** and macrolactin A **106** biosynthesis.

**Figure 3.1** Feeding of non-proteinogenic amino acids into the cyclosporine (**128**) producing strain results in the production of analogues **129-132**.

**Figure 3.2** The enacyloxin gene cluster. The groups installed by the tailoring enzymes (blue) as well as the DHCCA unit (green) serve as handles for genetic engineering.

**Figure 3.3** The enacyloxin analogues isolated from *B.ambifaria* BCC0203  $\Delta$ 5927,  $\Delta$ 5931 and  $\Delta$ 5930 mutant strains along with their respective activities (Dr. Joleen Masschelein).

**Figure 3.4** The enacyloxin analogues isolated from *B.ambifaria* BCC0203  $\Delta$ 5927 + 5931 and  $\Delta$ 5927 + 5930 double knock-out mutant strains along with their respective activities (Dr. Joleen Masschelein).

**Figure 3.5** The enacyloxin analogues isolated from feeding the *B.ambifaria* BCC0203  $\Delta$ 5912-14 mutant strain with DHCCA analogues **138**, **140** and **143**, along with their activity (Dr. Joleen Masschelein).

**Figure 3.6** The structure of vibroxin **151** compared to enacyloxin IIa **30**.

**Figure 3.7** The construction of in-frame gene deletions in *B. ambifaria* BCC0203.

**Figure 3.8** PCR screening to identify in-frame deletion mutants. The agarose gel corresponds to the deletion of the gene encoding PQQ-dependent dehydrogenase Bamb\_5932. The lanes correspond to the PCR of wild-type *B.ambifaria* BCC0203 genomic DNA, wild-type *B.ambifaria* BCC0203 (colony PCR), pGPI plasmid, single crossover mutant (colony PCR) and double crossover mutant (colony PCR) respectively.

**Figure 3.9** Genes encoding the PQQ-dependent dehydrogenase (Bamb\_5932), responsible for the installation of the ketone, and flavin-dependent halogenase (Bamb\_5928), responsible for the chlorination of the polyene.

**Figure 3.10** **A** UV chromatogram (360 nm) from LC-MS analyses of *B. ambifaria* ( $\Delta$ 5930) extracts. **B** The HRMS for the species eluting at 14.1 min. **C** The structure assigned by NMR spectroscopy and the activity of the analogue against *A. baumannii*.

**Figure 3.11** **A** UV chromatogram (360 nm) from LC-MS analyses of *B. ambifaria* ( $\Delta$ 5928) extracts. **B** The HRMS for the species eluting at 14.1 min. **C** The structure assigned by NMR spectroscopy and the activity of the analogue against *A. baumannii*.

**Figure 3.12** **A** UV chromatogram (360 nm) from LC-MS analyses of *B. ambifaria* ( $\Delta$ 5932 + 30) extracts. **B** The HRMS for the species eluting at 14.0 min. **C** The structure assigned by NMR spectroscopy and the activity of the analogue against *A. baumannii*.

**Figure 3.13** **A** UV chromatogram (360 nm) from LC-MS analyses of *B. ambifaria* ( $\Delta$ 5930 + 31) extracts. **B** The HRMS for the species eluting at 14.0 min. **C** The structure assigned by NMR spectroscopy and the activity of the analogue against *A. baumannii*.

**Figure 3.14** **A** UV chromatogram (360 nm) from LC-MS analyses of *B. ambifaria* ( $\Delta$ 5930-32) extracts. **B** The HRMS for the species eluting at 13.0 min. **C** The structure assigned by NMR spectroscopy and the activity of the analogue against *A. baumannii*

**Figure 3.15** **A** UV chromatogram (360 nm) from LC-MS analyses of *B. ambifaria* ( $\Delta$ 5927-32) extracts. **B** The HRMS for the species eluting at 14.0 min. **C** The structure assigned by NMR spectroscopy and the activity of the analogue against *A. baumannii*

**Figure 3.16** The assignment of the relative stereochemistry of linearmycin A **156** using Kishi's NMR database. The  $^{13}\text{C}$  chemical shifts of enacyloxin analogue **155** appear to be consistent with those of linearmycin A **156** as well as those in the NMR database.

**Figure 3.17** The  $^{13}\text{C}$  NMR shifts of **162** compared with a mixture of diastereomers **165**.

**Figure 3.18** **A** UV chromatogram (360 nm) from LC-MS analyses of extracts of *B. ambifaria* ( $\Delta$ 5912-14) supplemented with DHCCA analogue **157**. **B** The HRMS for the species eluting at 14.4 min. **C** The structure assigned by NMR spectroscopy and the activity of the analogue against *A. baumannii*.

**Figure 3.19** **A** UV chromatogram (360 nm) from LC-MS analyses of extracts of *B. ambifaria* ( $\Delta$ 5912-14) supplemented with DHCCA analogue **167**. **B** The HRMS for the species eluting at 13.4 min. **C** The structure assigned by NMR spectroscopy and the activity of the analogue against *A. baumannii*

**Figure 3.20** **A** UV chromatogram (360 nm) from LC-MS analyses of extracts of *B. ambifaria* ( $\Delta$ 5912-14) supplemented with DHCCA analogue **173**. **B** The HRMS for the species eluting at 14.9 and 15.0 min. **C** The structures assigned by NMR spectroscopy and the activity of the analogues against *A. baumannii*. Note it was not possible to distinguish between **177** and **178**.

**Figure 3.21** **A** UV chromatogram (360 nm) from LC-MS analyses of extracts of *B. ambifaria* ( $\Delta$ 5912-14) supplemented with DHCCA analogue **51**. **B** The HRMS for the species eluting at 15.0 min. **C** The structure assigned by NMR spectroscopy and the activity of the analogue against *A. baumannii*

**Figure 3.22** The results of the *in vitro* assay confirming that AHCCA **192** is a substrate for the condensation domain.

**Figure 3.23** The halogenase enzymes in the enacyloxin cluster (Bamb\_5928 and 5931).

**Figure 3.24** The enacyloxin analogues with increased potency relative to enacyloxin IIa, the features identified as influencing the activity are highlighted in red.

**Figure 3.25** **A** UV chromatogram (360 nm) from LC-MS analyses of extracts of *B. ambifaria* ( $\Delta$ 5912-14+30+32) supplemented with DHCCA analogue **51**. **B** The HRMS for the species eluting at 14.3 min. **C** The structure assigned by NMR spectroscopy and the activity of the analogue against *A. baumannii*

**Figure 3.26** The five enacyloxin analogue with increased potency relative to enacyloxin IIa **30**.

**Figure 3.27** The crystal structure of enacyloxin IIa bound to *E. coli* EF-Tu. The polar contacts between the protein and the antibiotic are highlighted.

**Figure 3.28** The activity of three enacyloxin analogues relative to enacyloxin IIa **30**, which can be explained on the basis of polar contacts observed in the crystal structure.

**Figure 3.29** The activity of two enacyloxin analogues relative to enacyloxin IIa **30**, which cannot be explained solely on the basis of polar contacts observed in the crystal structure

**Figure 3.30** The light-induced isomerization promoted by the C-6 methyl group.

**Figure 3.31** The enacyloxin analogue lacking the methyl group thought to promote isomerization.

**Figure 3.32** Potential enacyloxin analogues that may have increased stability whilst retaining potency.

**Figure 3.33** The simplified amide analogue (**149**) generated in section 3.1.2.3, along with potential additional amide enacyloxin analogues (**209-211**), which are likely to have enhanced potency.

**Figure 5.1** Examples of diene-forming DH domains identified in other PKS systems.

**Figure 5.2** The structures of gladiolin **29** and etnangien **261**.

**Figure 5.3** Engineered enacyloxin analogues with increased potency.

**Figure 5.4** The des-methyl enacyloxin IIa analogue **205** and potential des-methyl enacyloxin analogues (**206-208**) that may retain potency.

**Figure 5.5** The simplified amide analogue (**149**) and potential amide enacyloxin analogues (**209-211**), which are more likely to retain potency.

**Figure 5.6** The structure of vibroxin **151** and the structures of potential improved vibroxin analogues (**262** and **263**)

**Figure 6.1** Agarose gels confirming the gene deletions in *B.ambifaria* BCC0203

**Figure 8.1** The phylogenetic analysis of DH domains from *trans*-AT PKSs. The colored clades correspond to the function of the DH domain as follows: alkene-forming DH (DH<sup>a</sup>), blue; diene-forming DH (DH<sup>d</sup>), red; Enoyl Isomerase (DH<sup>i</sup>), green; Pyran Synthase (DH<sup>p</sup>), orange.

**Figure 8.2** The HRMS corresponding to brominated enacyloxin IIa derivatives **194-203**.

**Figure 8.3** The deconvoluted spectra corresponding to the intact MS of the proteins involved in DHCCA biosynthesis.

## List of Schemes

**Scheme 1.1** The DEBS-catalyzed assembly of 6-deoxyerythronolide **31** followed by post-PKS tailoring steps to afford macrolide antibiotic erythromycin **4**.

**Scheme 1.2** The post-translational conversion of *apo*-ACP domains to their *holo* form.

**Scheme 1.3** The transacylation catalyzed by AT domains, which results in the loading of CoA thioesters onto *holo*-ACP domains.

**Scheme 1.4** The KS domain-catalyzed translocation and elongation reactions resulting in chain elongation by two carbon units.

**Scheme 1.5 A** The (B1-type) KR domain-catalyzed reduction to form a (2*R*,3*R*)-2-methyl-3-hydroxy thioester. **B** The (B2-type) KR domain-catalyzed racemization and reduction to form a (2*S*,3*R*)-2-methyl-3-hydroxy thioester.

**Scheme 1.6 A** The DH-catalyzed dehydration of a (3*R*)-hydroxy thioester intermediate to produce a (2*E*)-enoyl thioester. **B** The dehydration of a (3*S*)-hydroxy thioester intermediate to produce a (2*Z*)-enoyl thioester.

**Scheme 1.7** The ER-catalyzed reduction of a 2-enoyl thioester intermediate to afford stereodefined saturated acyl thioesters.

**Scheme 1.8** The TE-catalyzed offloading of the ACP-bound polyketide chain by macrocyclization (blue arrows) or hydrolysis (red arrows).

**Scheme 1.9** The PS-catalyzed cycloether ring formation observed in *trans*-AT PKSs.

**Scheme 1.10** The HMGS cassette responsible for the installation of a  $\beta$ -methyl group. § denotes a separately encoded ACP domain, \* denotes a megasynthase ACP domain.

**Scheme 1.11** Domain and module organization of the gladiolin **29** *trans*-AT PKS, along with putative ACP-bound intermediates resulting from the reactions catalyzed by each module. The  $\beta$ -methyl 2-enoyl thioesters assembled by modules 1 and 6 (\*) are installed by the HMGS cassette.

**Scheme 1.12** The type B split module present in the gladiolin PKS thought to be responsible for the installation of the (*E,Z*)-diene motif (red).

**Scheme 1.13** The enacyloxin gene cluster and proposed biosynthetic pathway. Note that the domain marked '?' in Bamb\_5917 is of unknown function.

**Scheme 1.14** The off-loading mechanism from the enacyloxin PKS.

**Scheme 1.15** The proposed pathway for DHCCA (**48**) biosynthesis.

**Scheme 1.16** The proposed tailoring steps of the enacyloxin biosynthetic pathway leading to the production of enacyloxin IIa **30** from pre-enacyloxin **46**.

**Scheme 2.1** Biochemically characterized examples of DH domain-catalyzed *syn* eliminations: Dehydration to afford a (2*E*)-enoyl thioester in borrelidin biosynthesis and dehydration to afford a (2*Z*)-enoyl thioester in fostriecin biosynthesis.

**Scheme 2.2** The “base-acid” mechanism whereby the histidine deprotonates at the C-2-position and the aspartate reprotonates the C-3 hydroxyl group to form (*E*)- and (*Z*)-configured alkenes.

**Scheme 2.3** The “single-base” mechanism whereby the histidine both deprotonates at the  $\alpha$ -position and reprotonates the leaving hydroxyl group to form (*E*) and (*Z*)-configured alkenes.

**Scheme 2.4** The type B split module present in the gladiolin PKS thought to be responsible for the installation of the (*E,Z*)-diene motif (red).

**Scheme 2.5** The intact protein MS-based assay used to probe the activity of the GbnD5 DH domain.

**Scheme 2.6** The synthetic route used to prepare (*3R*)-3-hydroxyacyl pantetheine thioester **53**. **54** was generated in similar yields, using an analogous procedure.

**Scheme 2.7** Synthesis of (*2E*)- and (*2Z*)-2-enoyl pantetheine thioesters, **64** and **65**.

**Scheme 2.8** The GbnD5 DH domain catalyzes the interconversion of (*3R*)-3-hydroxyacyl and (*2E*)-2-enoyl thioesters, but cannot interconvert (*3S*)-3-hydroxyacyl and (*2Z*)-2-enoyl thioesters.

**Scheme 2.9** The biosynthetic steps involved in generating the (*3R,5S*)-3,5-dihydroxyacyl thioester intermediate proposed to be the substrate for the GbnD5 DH domain. \* Denotes the PKS domain involved in catalyzing each step.

**Scheme 2.10** Synthesis of (*3R,5S*)-3,5-dihydroxyacyl pantetheine thioester, **71**. (*3S,5S*)-3,5-dihydroxyacyl pantetheine thioester, **78**, was made via the same route.

**Scheme 2.11** Synthesis of (*2E,4Z*)-dienoyl pantetheine thioester, **72**.

**Scheme 2.12** Proposed roles of His<sub>23</sub> and His<sub>158</sub> in the double dehydration reaction catalyzed by the GbnD5 DH domain.

**Scheme 2.13** Synthesis of (*2E,5S*)-5-hydroxy-2-enoyl pantetheine thioester, **86**.

**Scheme 2.14** The proposed mechanism of the double dehydration reaction catalyzed by the GbnD5 DH domain.

**Scheme 2.15** Synthesis of 3,5-dihydroxyacyl pantetheine thioesters, **91** and **92**.

**Scheme 2.16** Syntheses of (*2E,5R*)-5-hydroxy-2-enoyl and (*2E,4E*)-dienoyl pantetheine substrates, **98** and **99**, respectively.

**Scheme 3.1** The deletion of tailoring enzymes to generate analogues of macbecin I (**107**) and ansamitocin P-3 (**109**).

**Scheme 3.2** The inactivation of a KR domain from module 16 of amphotericin biosynthesis resulting in an analogue with an additional ketone group (red).

**Scheme 3.3** A mutasynthetic approach to generating rapamycin analogues. Starter unit mimics **114-119** were incorporated using a mutant lacking the genes required for the assembly of the DHCHC starter unit (red).

**Scheme 3.4** A mutasynthesis approach to generate erythromycin analogues **124-127**.



**Scheme 3.5** The generation of 380 antimycin (**133**) analogues via multiple strategies.

**Scheme 3.6** An A-domain from a NRPS-generated CDA (**134**) was engineered to accept methyl glutamine derivative **135**.

**Scheme 3.7** The use of an engineered malonyl-CoA synthetase, MatB, to generate unnatural extender units. The promiscuous KirCII AT domain primes the extender units onto the relevant ACP domain before incorporation into kirromycin (**137**).

**Scheme 3.8** DHCCA (**48**) analogues **138-144** accepted by the Bamb\_5915 condensation domain during *in vitro* assays.

**Scheme 3.9** The route used for the synthesis of DHCCA analogue **157**.

**Scheme 3.10** The synthetic route to DHCCA analogue **167**.

**Scheme 3.11** The synthetic route used to DHCCA analogue **173**.

**Scheme 3.12** The synthetic route to DHCCA analogue **51**.

**Scheme 3.13** The synthetic route to DHCCA analogue **192**.

**Scheme 3.14** The use of a palladium-catalyzed coupling reaction to derivatize brominated enacyloxin analogue **196**.

**Scheme 5.1** The type B split module present in the gladiolin **29** PKS thought to be responsible for the installation of the (*E,Z*)-diene motif (red).

**Scheme 5.2** The proposed mechanism of double dehydration catalyzed by the GbnD5 DH domain.

**Scheme 5.3** The engineering of a diene-forming DH domain into a canonical *cis*-AT PKS module. DH<sup>A</sup> = canonical alkene-forming DH domain, DH<sup>D</sup> = diene-forming DH domain.

**Scheme 5.4** The proposed pathway for the biosynthesis of DHCCA **48**.

**Scheme 5.5** The DHCCA biosynthetic pathway determined using *in vitro* assays.

**Scheme 5.6** The stereospecific enoyl reduction catalyzed by OYEs along with some representative substrates.

**Scheme 5.7** The *in situ* generation of succinamide-CoA **262** via VbxP and loading of an *apo*-ACP domain.

## List of Tables

**Table 3.1:** Brominated enacyloxin derivatives

**Table 6.1:** Antibiotics used within this project

**Table 6.2:** Bacterial strains used within this project

**Table 6.3:** Vectors used within this project

**Table 6.4:** Typical PCR reaction components

**Table 6.5:** Typical thermocycling conditions for routine PCR reactions

**Table 6.6:** The constructs generated for gene deletions in *Burkholderia* along with associated primers

**Table 6.7:**  $^1\text{H}$  and  $^{13}\text{C}$  assignments for enacyloxin analogue **43**

**Table 6.8:**  $^1\text{H}$  and  $^{13}\text{C}$  assignments for enacyloxin analogue **152**

**Table 6.9:**  $^1\text{H}$  and  $^{13}\text{C}$  assignments for enacyloxin analogue **45**

**Table 6.10:**  $^1\text{H}$  and  $^{13}\text{C}$  assignments for enacyloxin analogue **153**

**Table 6.11:**  $^1\text{H}$  and  $^{13}\text{C}$  assignments for enacyloxin analogue **154**

**Table 6.12:**  $^1\text{H}$  and  $^{13}\text{C}$  assignments for enacyloxin analogue **155**

**Table 6.13:**  $^1\text{H}$  and  $^{13}\text{C}$  assignments for enacyloxin analogue **166**

**Table 6.14:**  $^1\text{H}$  and  $^{13}\text{C}$  assignments for enacyloxin analogue **167**

**Table 6.15:**  $^1\text{H}$  and  $^{13}\text{C}$  assignments for enacyloxin analogue **177**

**Table 6.16:**  $^1\text{H}$  and  $^{13}\text{C}$  assignments for enacyloxin analogue **187**

**Table 6.17:**  $^1\text{H}$  and  $^{13}\text{C}$  assignments for enacyloxin analogue **204**

**Table 6.18:**  $^1\text{H}$  and  $^{13}\text{C}$  assignments for enacyloxin analogue **194**

**Table 6.19:**  $^1\text{H}$  and  $^{13}\text{C}$  assignments for enacyloxin analogue **195**

**Table 6.20:**  $^1\text{H}$  and  $^{13}\text{C}$  assignments for enacyloxin analogue **196**

**Table 6.21:**  $^1\text{H}$  and  $^{13}\text{C}$  assignments for enacyloxin analogue **197**

**Table 6.22:**  $^1\text{H}$  and  $^{13}\text{C}$  assignments for enacyloxin analogue **198**

**Table 6.23:**  $^1\text{H}$  and  $^{13}\text{C}$  assignments for enacyloxin analogue **199**

**Table 6.24:**  $^1\text{H}$  and  $^{13}\text{C}$  assignments for enacyloxin analogue **200**

**Table 6.25:**  $^1\text{H}$  and  $^{13}\text{C}$  assignments for enacyloxin analogue **201**

**Table 6.26:**  $^1\text{H}$  and  $^{13}\text{C}$  assignments for enacyloxin analogue **202**

**Table 6.27:**  $^1\text{H}$  and  $^{13}\text{C}$  assignments for enacyloxin analogue **203**

**Table 6.28:** The constructs generated by Dr. Matt Jenner for recombinant protein overproduction in *E.coli* in order to investigate the functionality of the diene synthase and VbxP

**Table 6.29:** The constructs generated for recombinant protein overproduction in *E.coli* in order to investigate DHCCA biosynthesis

**Table 6.30:** The constructs generated for site-directed mutagenesis

**Table 6.31:** The reagents and volumes used for the preparation of acrylamide SDS-PAGE gels

## **Acknowledgements**

First and foremost, I would like to thank my supervisor, Professor Greg Challis, for giving me the opportunity to work in such a diverse group of researchers and on such interesting and varied projects. The experience and skills I have obtained during my time in the group will be invaluable during my future career.

Secondly, I would like to thank Dr. Matt Jenner, Dr. Joleen Masschelein, Dr. Xinyun Jian and Dr. Lona Alkhalaf for the contributions they made to the work discussed in this thesis, as well as the advice and training they provided me with. Thanks are also owed to Chris Perry and Dr. Doug Roberts for advice and support, as well as the rest of the Challis group members, past and present. Special thanks are also owed to Dr. David Fox, for advice on synthetic chemistry matters, as well as Dr. Lijang Song and Dr. Ivan Prokes for running countless mass spectrometry and NMR samples respectively.

## **Declaration**

I confirm this thesis has been prepared in accordance with the university's guidelines on the presentation of a research thesis for the degree of Doctor of Philosophy. The experimental work reported in this thesis is original research carried out by myself, unless otherwise stated. No material has been submitted in any application for any other degree. Results from other authors are referenced in the usual manner throughout the thesis.

\_\_\_\_\_  
Christian Hobson

Date: \_\_\_\_\_

## Abbreviations

ACP	Acyl carrier protein
AH	Acyl hydrolase
AHCCA	Aminohydroxycyclohexanecarboxylic acid
AMR	Antimicrobial resistance
AT	Acyl transferase
ATP	Adenosine triphosphate
Bcc	<i>Burkholderia cepacia</i> complex
BINAP	2,2'-Bis(diphenylphosphino)-1,1'-binaphthyl
BLAST	Basic local alignment search tool
BSM	Basal salts medium
CCCI	Chemically competent cell
CDA	Calcium-dependent antibiotic
CDCHD	2-Carboxamido-2-deacetyl-chelocardin
CDI	1'-Carbonyldiimidazole
CF	Cystic fibrosis
CFU	Cell forming units
CLSI	Clinical and laboratory standards institute
CoA	Coenzyme A
COSY	Correlation spectroscopy
CYP450	Cytochrome P450
Da	Daltons
DBU	1,8-Diazabicyclo[5.4.0]undec-7-ene
DEBS	6-Deoxyerythronolide B synthase
DEPT	Distortionless enhancement by polarization transfer
DH	Dehydratase
DHCCA	Dihydroxycyclohexanecarboxylic acid
DHCHC	4,5-Dihydroxy-1-cyclohexenecarboxylic acid
DHD	Dehydratase docking
DIBAL-H	Diisobutylaluminium hydride
DIPEA	Diisopropylethylamine
DMAP	Dimethylaminopyridine
DMF	Dimethylformamide
DMSO	Dimethylsulfoxide
DNA	Deoxyribonucleic acid
d.e.	Diastereomeric excess

ECH	Enoyl-CoA hydratase
EDC	1-Ethyl-3-(3-dimethylaminopropyl)carbodiimide
EDTA	Ethylenediaminetetraacetic acid
e.e.	Enantiomeric excess
EF-Tu	Elongation factor thermo unstable
EI	Electron ionization
EIC	Extracted ion chromatogram
ER	Enoyl reductase
ESI	Electrospray ionization
ESBL	Extended spectrum $\beta$ -lactamases
FAD	Flavin adenine dinucleotide
FAS	Fatty acid synthase
FDA	Food and Drug Administration
FMN	Flavin mononucleotide
GDP	Guanosine diphosphate
GE	General electric
GNAT	GCN5-related <i>N</i> -acetyltransferase
GTP	Guanosine triphosphate
HMBC	Heteronuclear multiple bond coherence
HMGS	3-Hydroxy-3-methylglutaryl synthase
HRMS	High resolution mass spectrometry
HSQC	Heteronuclear single quantum coherence
Hz	Hertz
IPTG	Isopropyl $\beta$ -D-1-thiogalactopyranoside
IR	Infa-red
ITC	Isothermal titration calorimetry
KG	Keto glutarate
KLD	Kinase, ligase and Dpn1
KPSI	Kilo pounds per square inch
KR	Ketoreductase
KS	Ketosynthase
LB	Luria-Bertani
LCMS	Liquid chromatography mass spectrometry
LiHMDS	Lithium bis(trimethylsilyl)amide
LRMS	Low resolution mass spectrometry
mCPBA	meta-Chloroperoxybenzoic acid
MDR	Multi-drug resistant

MH	Mueller-Hinton
MIC	Minimum inhibitory concentration
MRSA	Methicillin resistant <i>Staphylococcus aureus</i>
MS	Mass spectrometry
MT	Methyl transferase
MWCO	Molecular weight cut off
NAC	<i>N</i> -Acetyl cysteamine
NADH	$\beta$ -Nicotinamide adenine dinucleotide
NADPH	$\beta$ -Nicotinamide adenine dinucleotide 2'-phosphate
NMO	<i>N</i> -Methyl morpholine <i>N</i> -oxide
NMP	<i>N</i> -Methyl-2-pyrrolidone
NMR	Nuclear magnetic resonance
NRPS	Non ribosomal peptide synthetase
OD	Optical density
PAGE	Polyacrylamide gel electrophoresis
PBP	Penicillin binding protein
PCC	Pyridinium chlorochromate
PCP	Peptidyl carrier protein
PCR	Polymerase chain reaction
PDB	Protein data bank
PKS	Polyketide synthase
ppm	Parts per million
PQQ	Pyrrroloquinoline quinone
PS	Pyran synthase
RCM	Ring closing metathesis
RNA	Ribonucleic acid
rSAP	Shrimp alkaline phosphatase
RT	Room temperature
SAM	<i>S</i> -Adenosyl methionine
SAR	Structure-activity relationship
SDS	Sodium dodecyl sulfate
TBE	Tris-borate-EDTA
TBS	<i>tert</i> -Butyl-dimethylsilyl
TE	Thioesterase
TEA	Triethylamine
THCCA	Trihydroxycyclohexanecarboxylic acid

THF	Tetrahydrofuran
TLC	Thin layer chromatography
TFA	Trifluoroacetic acid
TFAA	Trifluoroacetic acid anhydride
TOF	Time of flight
Tris	Tris(hydroxymethyl)aminomethane
UV	Ultraviolet
UHPLC	Ultra high performance liquid chromatography
Vis	Visible
WHO	World Health Organisation
WT	Wild type



## Abstract

The emergence of antibiotic resistance combined with the decline in the discovery of novel antibiotic scaffolds has led to an urgent need for the development of effective antimicrobial treatments. Recently a Gram-negative genus of bacteria, *Burkholderia*, has been shown to be an untapped source of antimicrobial compounds. Two such compounds produced by *Burkholderia* are gladiolin and enacyloxin IIa (figure 1), which are active against the multi-drug resistant pathogens *Mycobacterium tuberculosis* and *Acinetobacter baumannii* respectively. Both compounds are assembled by polyketide synthases, but there are parts of the biosynthesis of both natural products that are not well understood.

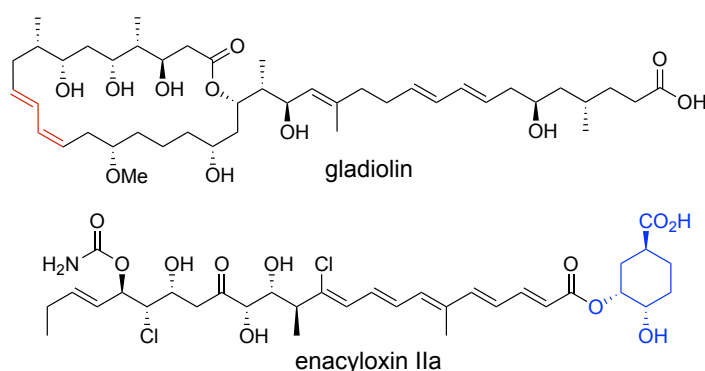


**Figure 1** The structures of gladiolin and enacyloxin IIa.

The installation of the *E,Z*-diene motif in gladiolin (red, figure 1) was investigated using an intact protein MS-based assay with chemically synthesized polyketide intermediate mimics. The diene was shown to be installed by an unprecedented double dehydration, which appears to be conserved for the installation of dienes in some other polyketide natural products based on bioinformatics analyses. The biosynthesis of the dihydroxycyclohexanecarboxylic acid (DHCCA) unit of enacyloxin IIa (blue, figure 1) was also investigated using *in vitro* biochemical assays. The initial hypothesis for the pathway was shown to be incorrect, and the elucidation of the correct pathway also led to the discovery of a new potential biocatalyst.

Using multiple biosynthetic engineering strategies that rely upon a thorough understanding of enacyloxin IIa biosynthesis, a library of enacyloxin IIa analogues was generated. This provided useful structure-activity relationship (SAR) data with regards to the binding of enacyloxin IIa to its target, EF-Tu. Five enacyloxin IIa analogues were also generated which had improved biological activity. These analogues may provide a platform for the rational engineering of improved enacyloxin IIa analogues harboring more complex structural changes.

# **1. Introduction**

## 1.1 Antibiotics

### 1.1.1 Discovery of Natural Products as a Source of Antibiotics

Natural products, or specialized metabolites, are organic compounds produced by an organism which are not essential for growth, development or reproduction, but can often aid the survival of the organism due to antibiotic or other properties.<sup>1</sup> Microbial natural products have long provided a major foundation for the development of antibiotic drugs. Over 20,000 microbial natural products being described over the past several decades.<sup>2</sup>

One of the earliest and most famous discoveries of a natural product with antimicrobial activity, was the serendipitous discovery of the fungal metabolite and  $\beta$ -lactam antibiotic, penicillin G **1**.<sup>3</sup> Sir Alexander Fleming accidentally discovered that a fungal contaminant affected the growth of bacteria in 1928, however it was not until Howard Florey assembled a team including Ernst Chain and Norman Heatley in 1939, that penicillin G was successfully purified and its activity determined.<sup>4</sup> In 1943 Edward Abraham along with Chain proposed the  $\beta$ -lactam structure of penicillin G, which was later confirmed in 1945 by Dorothy Hodgkin using X-ray crystallography.<sup>5</sup> Fleming, along with Chain and Florey, subsequently won the 1945 Nobel prize in physiology and medicine for the discovery and clinical studies of penicillin, which enabled the control of infections caused by Gram-positive pathogens such as *Staphylococcus* and *Streptococcus*, and revolutionized drug discovery research.<sup>6</sup>

Following this discovery, Selman Waksman and H. Boyd Woodruff developed a revolutionary screening technique for the discovery of antimicrobial natural products, often referred to as the 'Waksman platform'.<sup>7,8</sup> This technique consists of the incubation of soil sample suspensions with susceptible test microorganisms, and based on growth inhibition zones, single colonies of soil microbes (largely Actinobacteria) were isolated and screened against specifically targeted pathogens, before the corresponding bioactive metabolite could be isolated.<sup>8,9</sup> This technique propelled antimicrobial natural product discovery into the so-called 'golden age' and resulted in a boom of new discoveries between the 1940s and 1960s.<sup>2,8,10</sup>

Using this technique, the clinically important aminoglycoside antibiotic, streptomycin **2**, was discovered in the Waksman lab by Albert Schatz in 1944, which was the first effective antibiotic for *Mycobacterium tuberculosis*.<sup>11</sup> This was followed by the discovery of tetracycline **3** and its derivatives which exhibit activity against both Gram-positive and Gram-negative pathogens.<sup>12</sup> Many other clinically important antibiotics were discovered shortly thereafter including the macrolide erythromycin **4** which is still commonly administered as a

treatment for skin and respiratory tract infections, as well as the glycopeptide vancomycin **5**, which is used to treat multi-drug resistant (MDR) Gram-positive pathogens (figure **1.1**).<sup>13,14</sup>

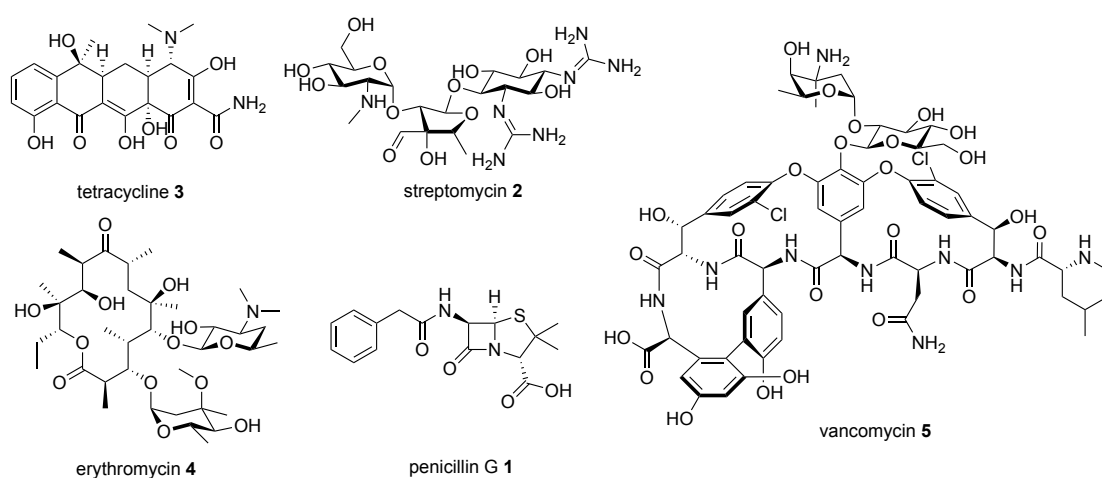


**Figure 1.1** The structures of tetracycline (**3**), streptomycin (**2**), erythromycin (**4**), penicillin G (**1**) and vancomycin (**5**).

### 1.1.2 Emergence of Antimicrobial Resistance

A consequence of the use of the antibiotics discovered in the ‘golden age’ (figure **1.1**) was the emergence of widespread antimicrobial resistance (AMR). Bacteria have developed a variety of resistance mechanisms, including efflux pumps, decreased membrane permeability, target modification and antibiotic modifying enzymes.<sup>15</sup> Despite  $\beta$ -lactam antibiotics, such as penicillin G **1**, constituting greater than 60 % of the antimicrobials used in human medicine, resistance to this class of antibiotics is widespread.<sup>16</sup> Penicillin G **1** was introduced into the clinic in the early 1940s, but penicillin-resistant *Staphylococcus aureus* emerged as soon as 1944.<sup>17</sup> Staphylococcal resistance is mediated by  $\beta$ -lactamases, which inactivate the antibiotic by catalyzing the hydrolysis of the  $\beta$ -lactam core.<sup>17</sup>

The emergence of penicillin-resistant *Staphylococcus aureus* was initially combated by discovering new  $\beta$ -lactam antibiotics, such as cephalosporin C **6**, which was stable to the staphylococcal  $\beta$ -lactamase.<sup>17</sup> Another approach was the development of semi-synthetic  $\beta$ -lactams such as methicillin **7**, which were able to evade the lactamases via the steric protection of the  $\beta$ -lactam ring (figure **1.2**).<sup>18</sup> However methicillin-resistant *Staphylococcus aureus* (MRSA), which exhibits resistance to  $\beta$ -lactam antibiotics via the production of a modified penicillin binding protein (PBP2a, the target of  $\beta$ -lactam antibiotics) emerged. This limits the accessibility of the antibiotic to the active site of the target.<sup>19</sup> As a result,  $\beta$ -lactam antibiotics

alone are not sufficient to treat MRSA infections, but are often used in combination with other antibiotics that act synergistically.<sup>20</sup>

In addition to resistance via the production of a modified penicillin binding protein, extended-spectrum  $\beta$ -lactamases (ESBL) also emerged. This resulted in strains that were resistant to later-generation, semi-synthetic  $\beta$ -lactam antibiotics.<sup>17</sup> To overcome this, a combination of the antibiotic and a  $\beta$ -lactamase inhibitor is administered. An example of a  $\beta$ -lactamase inhibitor is clavulanic acid **8**, a  $\beta$ -lactam natural product that, despite showing poor antibiotic activity, is a potent inhibitor of  $\beta$ -lactamases.<sup>21</sup> Clavulanic acid **8** is administered with the semi-synthetic penicillin analogue, amoxicillin **9**. This treatment, marketed as Augmentin, was the best selling antibiotic treatment in 2001 (figure 1.2).<sup>22</sup> Despite this success, many  $\beta$ -lactamases are not inhibited by current clinically available inhibitors.<sup>23</sup> The emergence and evolution of AMR to  $\beta$ -lactam antibiotics is mirrored by other antibiotics discovered in the ‘golden era’ (figure 1.1), highlighting the importance of identifying new antibiotics, or improving existing ones.

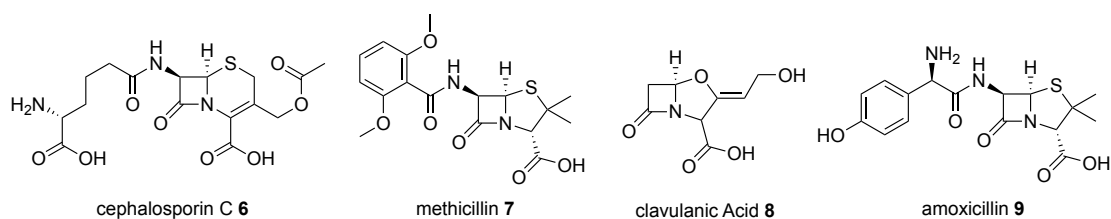


**Figure 1.2** The structures of  $\beta$ -lactams cephalosporin C **6**, methicillin **7**, clavulanic acid **8** and amoxicillin **9** discovered or developed to combat AMR.

### 1.1.3 Strategies for Improving Antibiotics

Some of the strategies used for combating resistance to  $\beta$ -lactam antibiotics discussed in section 1.1.2 have been used to overcome resistance to other antibiotics. New strategies have also been developed. In addition to combating resistance, structural modification of antibiotics can be used to improve potency, spectrum of activity, stability, oral bioavailability and pharmacokinetic properties.

### 1.1.3.1 Semi-synthesis

The semi-synthetic production of antibiotics consists of the synthetic modification of naturally produced antibiotic scaffolds. In addition to the development of semi-synthetic  $\beta$ -lactam antibiotics such as methicillin **7** (figure 1.2), to overcome  $\beta$ -lactamase mediated resistance, many other antibiotic scaffolds have been modified by semi-synthesis to evade a range of resistance mechanisms. A prime example is the recent food and drug administration (FDA)-approved semi-synthetic aminoglycoside antibiotic plazomicin **10** (figure 1.3), which evades the action of multiple inactivating enzymes that reduce the effectiveness of earlier aminoglycosides such as gentamicin and butirosin.<sup>24</sup>

Semi-synthetic antibiotics can also be developed to improve pharmacokinetic properties. For example, the semi-synthetic tetracycline derivative minocycline **11** has increased tissue penetration, a longer half-life and activity against a broader range of pathogens relative to natural tetracyclines, due to its increased lipophilicity.<sup>25</sup> There are also examples of semi-synthetic antibiotic derivatives with increased bioavailability and stability. First generation macrolide antibiotics such as erythromycin **4** have poor bioavailability and low stability at the acidic pH of the stomach, which due to acid-catalyzed hemiketal formation results in the formation of inactive spiroketal derivatives.<sup>13</sup> However, the development of semi-synthetic macrolides, such as clarithromycin **12**, which harbors a modification that prevents hemiketal formation, has resulted in more stable and bioavailable macrolide antibiotics (figure 1.3).<sup>26</sup>

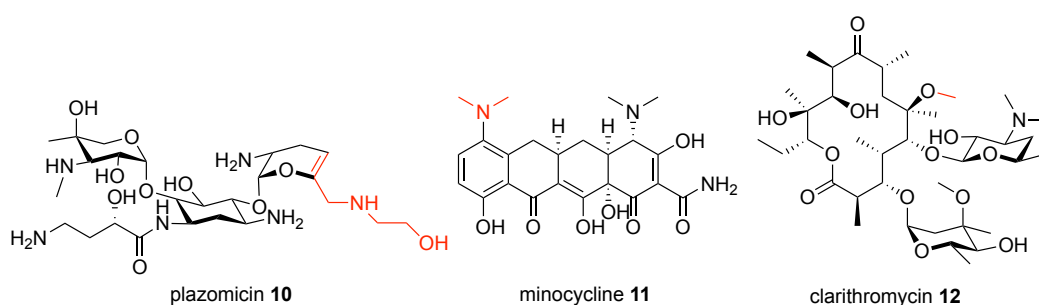


**Figure 1.3** Structures of the semi-synthetic antibiotics plazomicin **10**, minocycline **11** and clarithromycin **12** with the synthetic modifications highlighted in red.

Semi-synthetic approaches continue to be used to produce antibiotic analogues, however this strategy is inherently limited.<sup>27</sup> Modifications can only be made at positions on the antibiotic scaffold that are amenable to functionalization, and due to the often highly functionalized and sensitive structures of natural products, degradation or unwanted byproducts are commonly observed.

### 1.1.3.2 Total Synthesis

The limited scope of semi-synthetic modification can in theory be combated using carefully designed total syntheses, which can be used generate a diverse library of analogues. An excellent example of this is the recently FDA-approved antibiotic eravacycline **13**, which was developed using a synthetic library approach.<sup>28</sup> Eravacycline **13** is an analogue of tetracycline **3**, which harbors several structural modifications, including an *N*-alkyl glycyamido group at the 9-position of the tetracycline core resulting in activity against tetracycline-resistant pathogens.<sup>29</sup> Synthetic analogues of  $\beta$ -lactam antibiotics have also been developed, including the *N*-sulfonated  $\beta$ -lactam, carumonam **14**, which displays greater potency against Gram-negative pathogens such as *Klebsiella pneumonia* and *Enterobacter cloacae* than previous  $\beta$ -lactam antibiotics.<sup>30</sup> Myers and co-workers have also developed a robust synthetic route for the synthesis of macrolide antibiotic analogues, including FSM-100573 **15**, which exhibits enhanced activity against MDR *Streptococcus pneumonia* and *Pseudomonas aeruginosa* (figure 1.4).<sup>31</sup>

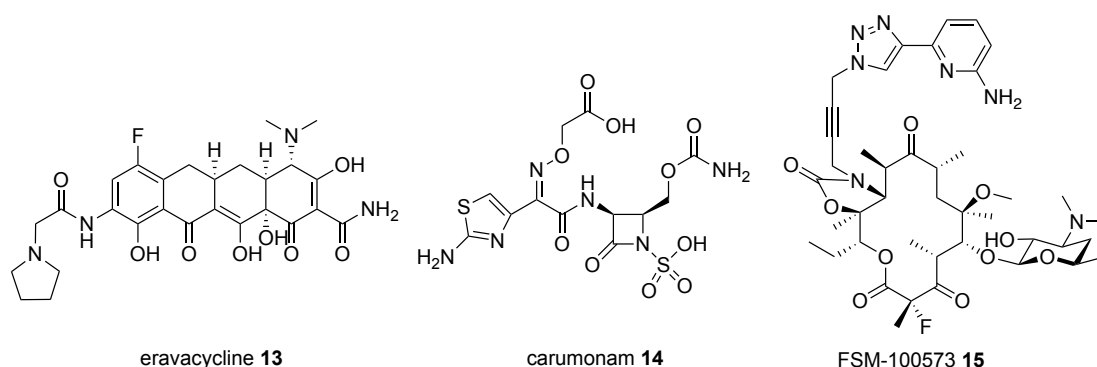


**Figure 1.4** The structures of synthetic antibiotics eravacycline **13**, carumonam **14** and FSM-100573 **15**.

Despite the promise of these approaches, antibiotic scaffolds are often highly complex, harbouring many stereocentres and sensitive functional groups. This makes the synthesis of such molecules challenging and time consuming, and often only modest amounts of material can be produced.

### 1.1.3.3 Genetic Engineering

The discovery that the genes directing the biosynthesis of antimicrobial natural products are clustered, coupled with developments in synthetic biology and mechanistic understanding of biosynthetic pathways, has provided a basis for genetic engineering to produce antibiotic analogues.<sup>32</sup> The biosynthesis of aminoglycoside antibiotic kanamycin A **16** was recently established, facilitating *in vivo* engineering of the pathway to produce amikacin **17**, a semi-synthetic aminoglycoside. The pathway was further manipulated to produce 1-*N*-AHBA-kanamycin **18**, which shows greater antibacterial activity than amikacin **17** (figure 1.5).<sup>33</sup> The gene cluster that directs the biosynthesis of tetracycline antibiotic chelocardin **19** was also identified and engineered to produce a novel tetracycline analogue, 2-carboxamido-2-deacetyl-chelocardin (CDCHD) **20** (figure 1.5).<sup>34</sup> CDCHD **20** is a promising lead because it is active against the full panel of ESKAPE pathogens, a group of problematic, MDR Gram-negative pathogens comprising of *Enterococcus faecium*, *Staphylococcus aureus*, *Klebsiella pneumoniae*, *Acinetobacter baumannii*, *Pseudomonas aeruginosa*, and *Enterobacter* species.<sup>35</sup> A library of glycopeptide antibiotics was also generated using a synthetic biology approach from a minimal teicoplanin scaffold **21**. This resulted in novel analogues, which were active against glycopeptide resistant bacteria (figure 1.5).<sup>36</sup>

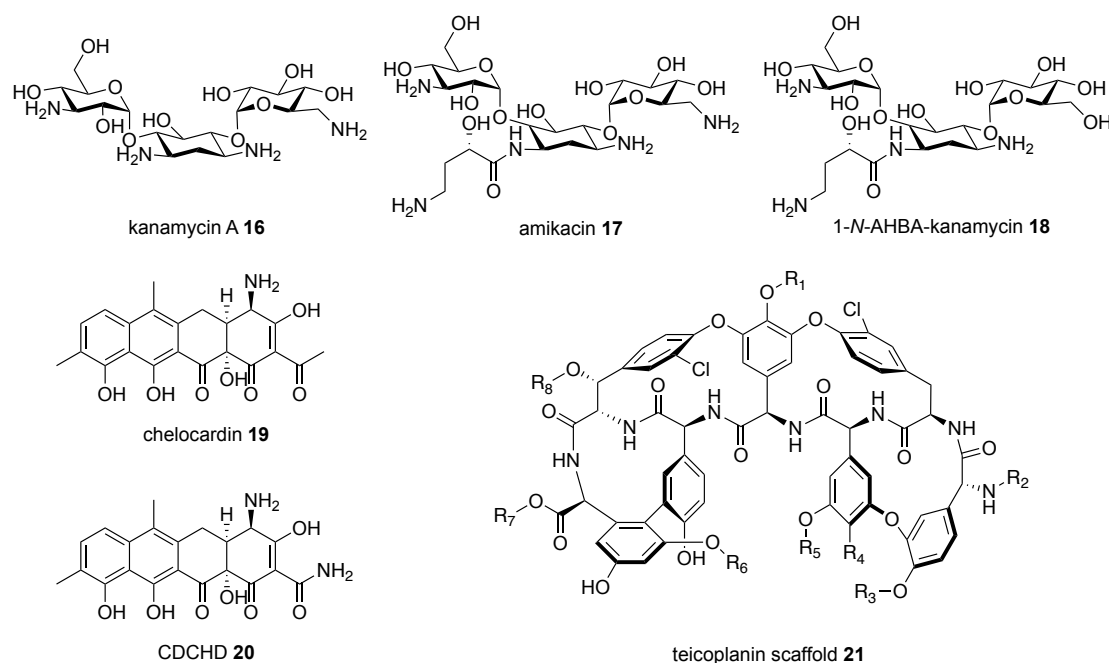


**Figure 1.5** The structures of kanamycin A **16**, amikacin **17**, 1-*N*-AHBA-kanamycin **18**, chelocardin **19**, CDCHD **20** and the teicoplanin scaffold **21** used to generate glycopeptide analogues (with differing R groups).





The majority of antimicrobial natural products in the clinic have been isolated from soil microorganisms (often strains belonging to the *Streptomyces* genus). However it is estimated that less than one per cent of soil microorganisms are culturable using conventional techniques.<sup>41</sup> This implies there is a huge untapped resource of potential antimicrobial natural products, which has prompted the development of methods to access the metabolites of “unculturable” soil microorganisms. The development of a multichannel device, the iChip, which allows the simultaneous isolation and growth of uncultured soil bacteria, allowed Lewis and co-workers to isolate teixobactin **24** (figure 1.6).<sup>42</sup> Teixobactin **24** is an antibiotic that belongs to a novel structural class and is produced by a new species of Gram-negative,  $\beta$ -proteobacteria provisionally named *Eleftheria terrae*.<sup>43</sup> Although the majority of clinically used antimicrobial natural products originate from Gram-positive Actinobacteria, Gram-negative bacteria such as  $\beta$ -proteobacteria are becoming increasingly recognised as a valuable source of novel antimicrobials, particularly for the treatment of problematic Gram-negative pathogens.<sup>44</sup>

## 1.2 *Burkholderia*

*Burkholderia* is also a genus of Gram-negative  $\beta$ -proteobacteria that is an emerging source of bioactive natural products. The genus was defined in 1992 having previously been included in the *Pseudomonas* genus due to phylogenetic similarities. The genus has now expanded to include almost 100 species, which occupy a diverse range of ecological niches, ranging from the rhizosphere of plants, to humans. Several *Burkholderia* species have been shown to have agricultural benefits, including promoting plant growth and degrading pollutants. However, their industrial use is limited, because many species are reported to be opportunistic pathogens of plants and for humans.<sup>45</sup>

One particular group of genetically distinct, but phenotypically similar *Burkholderia* species, known as the *Burkholderia cepacia* complex (Bcc), consists of opportunistic pathogens that can cause severe infections in cystic fibrosis (CF) sufferers and immunocompromised patients. Bcc species in particular have attracted interest from researchers due to their resistance to a range of antibiotics, their broad-spectrum of antimicrobial activity, and their ability to produce a variety of bioactive molecules.<sup>46</sup> Bioactive natural products produced by *Burkholderia* species include the respiratory toxin bongkrekic acid **25**, the polyene antibiotic caryoynencin **26**, the antimetabolic agent rhizoxin **27**, and the antifungal cyclic lipopeptide burkholdine 1215 **28** (figure 1.7).<sup>47-50</sup> The work described in this thesis focuses on two polyketides produced by *Burkholderia* species: gladiolin **29** and enacyloxin IIa **30** (figure 1.7).

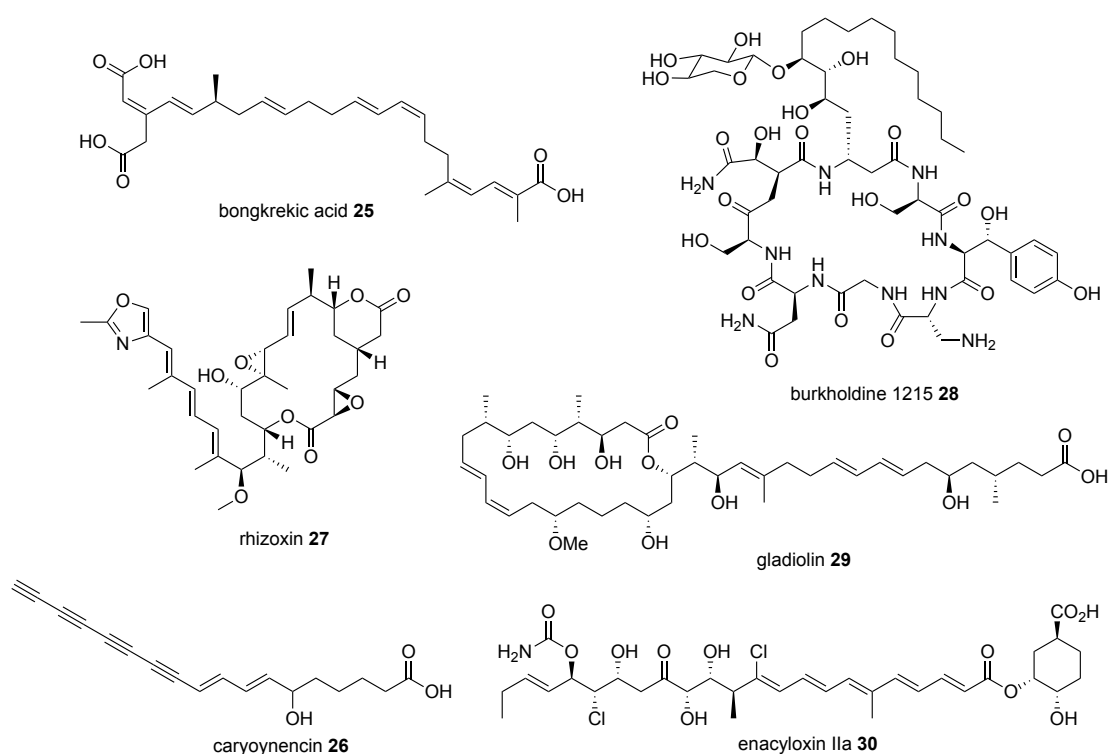


**Figure 1.7** The structures of *Burkholderia* produced natural products bongkreikic acid **25**, burkholdine 1215 **28**, rhizoxin **27**, caryoyneincin **26**, gladiolin **29** and enacyloxin IIa **30**.

### 1.3 Polyketide Synthases

Polyketide synthases (PKSs) are remarkable biosynthetic machines that catalyze the assembly of complex hydrocarbon scaffolds from a series of acyl thioester building blocks.<sup>51</sup> PKSs can be subdivided into three types based on their structural organization and catalytic mechanism. Type I PKSs consist of giant multifunctional polypeptides containing several catalytic domains, whereas type II PKSs consist of several discrete, iteratively-acting enzymes, and type III PKSs employ only a single iterative condensing enzyme.<sup>52</sup>

Type I PKSs can be further categorized depending on whether the multifunctional polypeptides are used in an iterative or modular manner. Type I iterative PKSs harbor one of each of the catalytic domains required for polyketide assembly within a single multifunctional polypeptide. The catalytic domains are used repeatedly in multiple rounds of chain elongation, assembling the polyketide chain in an iterative manner.<sup>53</sup> In contrast, type I modular PKSs consist of multiple modules in which each of the catalytic domains is typically used once during chain assembly. Each module is normally responsible for catalyzing a single round of

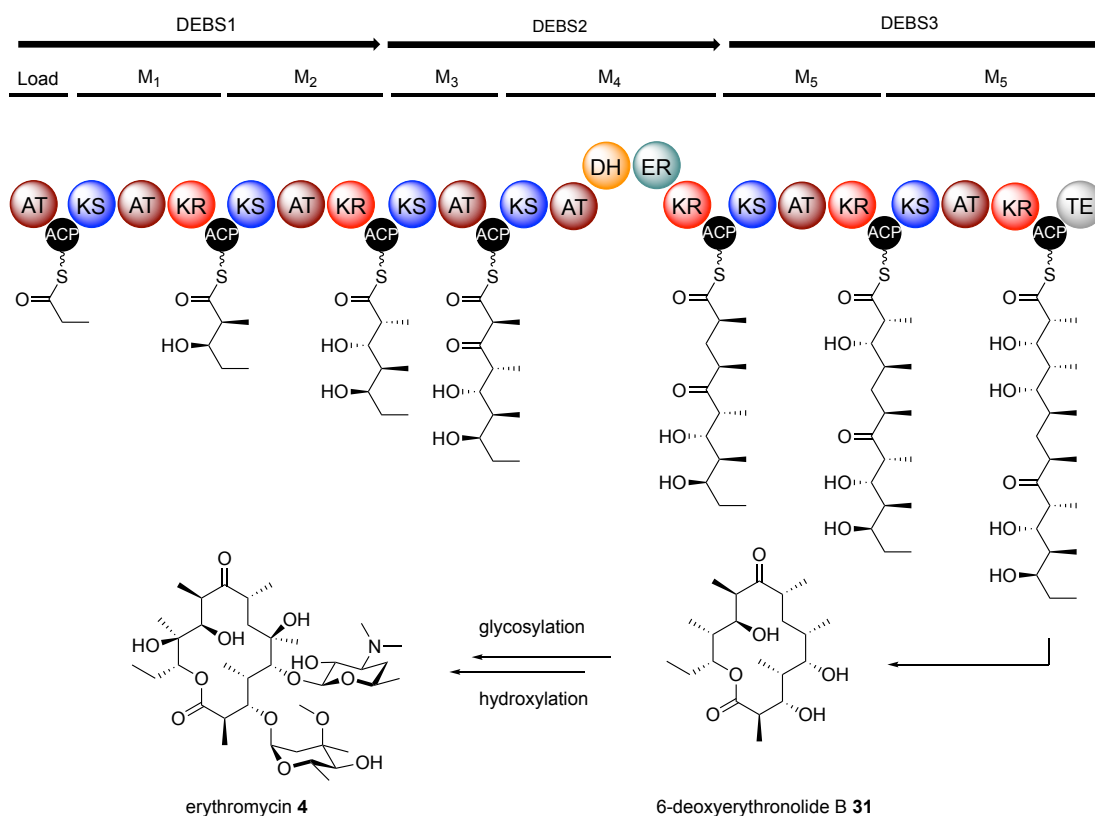
chain elongation. However, there are some examples of iterative module use by type I modular PKSs.<sup>54,55</sup>

### 1.3.1 Type I Modular PKSs

Typically, each chain extension module harbors three minimal catalytic domains: an acyl carrier protein (ACP) domain, an acyltransferase (AT) domain and a ketosynthase (KS) domain. The catalytic activity of these three domains results in the incorporation of one acyl-coenzyme A (CoA) thioester extender unit into the nascent polyketide chain, resulting in a single round of chain elongation (section 1.3.1.1). Many chain extension modules also contain accessory domains, including ketoreductase (KR), dehydratase (DH), methyltransferase (MT) and enoyl reductase (ER) domains, which are responsible for processing the 3-keto thioester resulting from chain elongation (section 1.3.1.2). The release of the assembled polyketide chain is usually catalyzed via a terminal thioesterase (TE) domain, and is usually achieved via macrolactonization, transesterification or hydrolysis.<sup>56</sup>

The polyketide scaffold of macrolide antibiotic erythromycin **4** is assembled by an archetypal example of a type I modular PKS, the 6-deoxyerythronolide B synthase (DEBS). DEBS consists of three polypeptide units (DEBS1-3), which can be split into seven modules responsible for the condensation of one propionyl-CoA starter unit with six methylmalonyl-CoA extender units. The resulting heptaketide acyl chain is then offloaded via lactonization to afford 6-deoxyerythronolide B **31**, which is then glycosylated, hydroxylated and methylated to produce erythromycin **4** (scheme 1.1).<sup>57</sup>

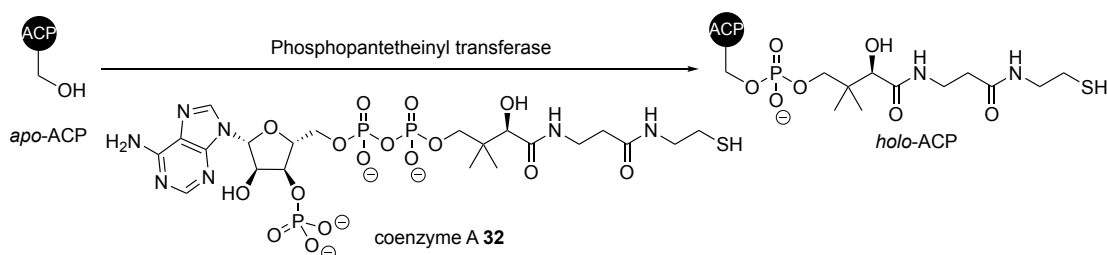
It is important to note that for the purposes of this study, a module can be defined as the combination of domains responsible for catalyzing a single chain extension, starting from an elongating KS domain, and ending at the first downstream ACP domain. This “functional” definition of a module has consistently been used in the literature and originates from the domain architecture of mammalian fatty acid synthase (FAS), which exists as KS-AT-DH-ER-KR-ACP-TE. PKS modules were defined equivalently to begin with KS and end with ACP, with the AT domain and optional processing domains in the middle.<sup>58</sup> Recent work by Abe and co-workers indicated that throughout the evolution of PKSs, the accessory domains appear to migrate with the downstream KS domain, and they propose that modules should be redefined so that the accessory domains are grouped with the downstream KS domain.<sup>59</sup> However this newly proposed “evolutionary” definition of a module complicates the “functional” role of a module, and so will not be used for the systems studied in this thesis.



**Scheme 1.1** The DEBS-catalyzed assembly of 6-deoxyerythronolide **31** followed by post-PKS tailoring steps to afford macrolide antibiotic erythromycin **4**.

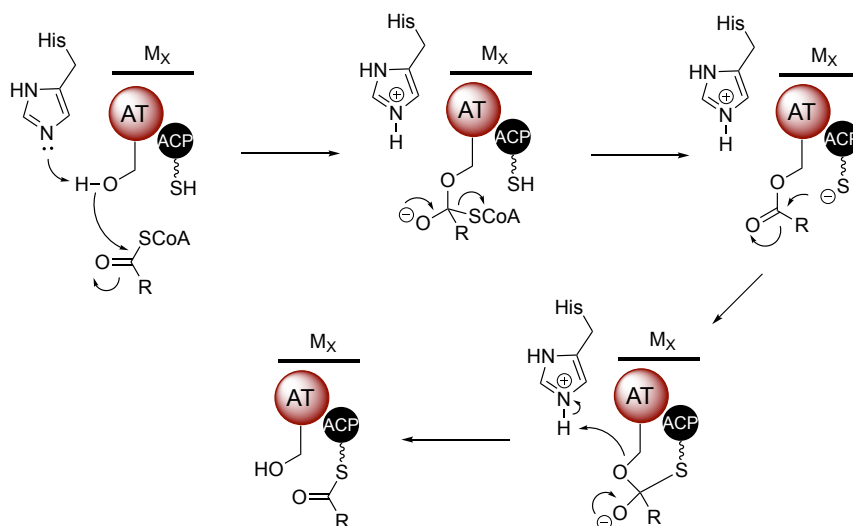
### 1.3.1.1 Minimal catalytic domains

ACP domains are small, four-helical bundles, which tether the growing polyketide chain via a thioester bond, and are responsible for shuttling the biosynthetic intermediates between the catalytic domains of a module. They are post-translationally converted from their inactive *apo*-form to their catalytically active *holo*-form by a phosphopantetheinyl transferase. This enzyme catalyzes the condensation of a conserved serine residue of the ACP domain with CoA **32**, resulting in the addition of a flexible, phosphopantetheinyl arm bearing a terminal thiol (scheme 1.2).<sup>60</sup>



**Scheme 1.2** The post-translational conversion of *apo*-ACP domains to their *holo* form.

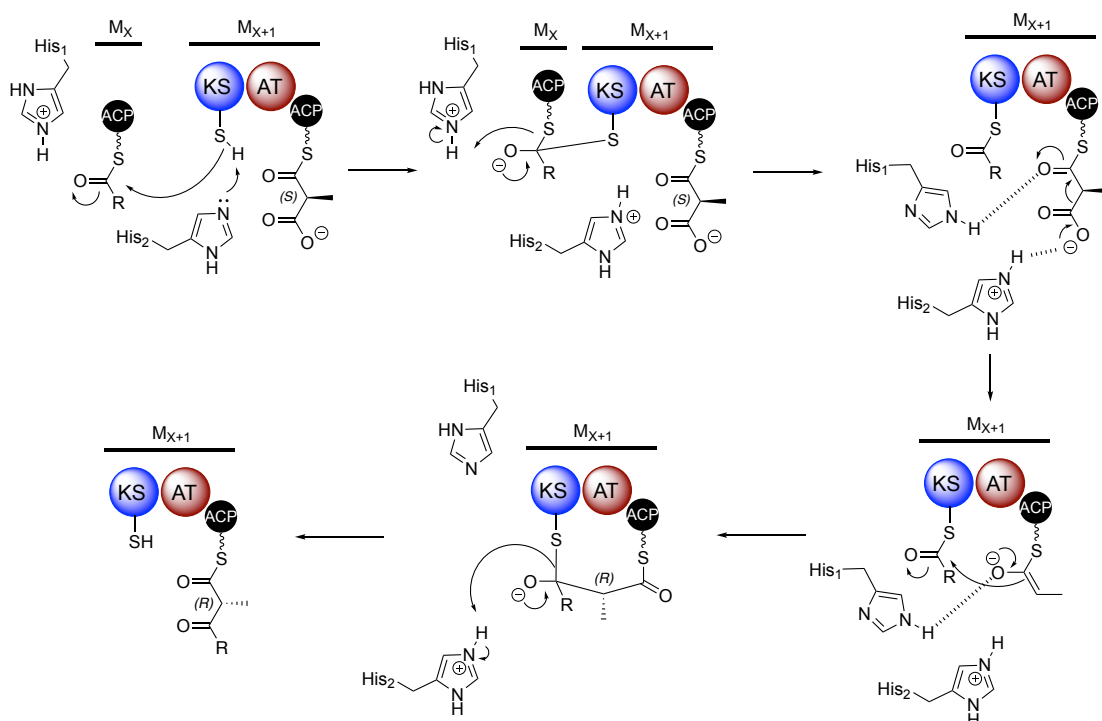
AT domains are responsible for priming downstream *holo*-ACP domains with either a starter unit (in the loading module) or an extender unit (in chain extension modules). Commonly used starter units include acetyl-CoA and propionyl-CoA, whereas extender units are often their respective carboxylated derivatives, malonyl-CoA and methylmalonyl-CoA. However, there are many examples of PKSs using more structurally diverse starter and extender units, and many systems utilize a KS<sup>Q</sup> domain in the loading module, which catalyzes the decarboxylation of a malonated ACP domain (loaded by an AT domain) to generate the starter unit *in situ*.<sup>61,62</sup> The starter/extender unit is first loaded onto a catalytic serine residue of the AT domain, which is activated as a nucleophile by a conserved histidine residue. The resulting AT-tethered acyl group is then translocated onto the phosphopantetheinyl arm of the downstream *holo*-ACP domain (scheme 1.3).<sup>63</sup>



**Scheme 1.3** The transacylation catalyzed by AT domains, which results in the loading of CoA thioesters onto *holo*-ACP domains.

The KS domain is typically responsible for catalyzing the elongation of the polyketide chain via a decarboxylative Claisen condensation. Initially, the ACP-bound polyketide chain generated by the upstream module is translocated onto the conserved active site cysteine residue of the KS domain. The KS domain then catalyzes the condensation between the malonated downstream ACP domain (loaded by the AT domain), and the nascent polyketide chain tethered to the KS domain, resulting in elongation of the chain by two carbons (scheme 1.4). The translocation and Claisen condensation reactions have been reported to be mediated by two conserved histidine residues by Khosla and coworkers.<sup>64</sup> However the mechanism they propose (scheme 1.4) may not be correct, as non-elongating KS domains (KS<sup>0</sup> domains, section 1.3.3.1) lacking one of the conserved histidine residues (His<sub>1</sub>) are still capable of

catalyzing translocation. The extender unit loaded by the AT domains in DEBS is (2*S*)-methylmalonyl-CoA, but the condensation catalyzed by the KS domain occurs with inversion of stereochemistry to generate a (2*R*)-methylmalonyl thioester product (scheme 1.4).<sup>65</sup>

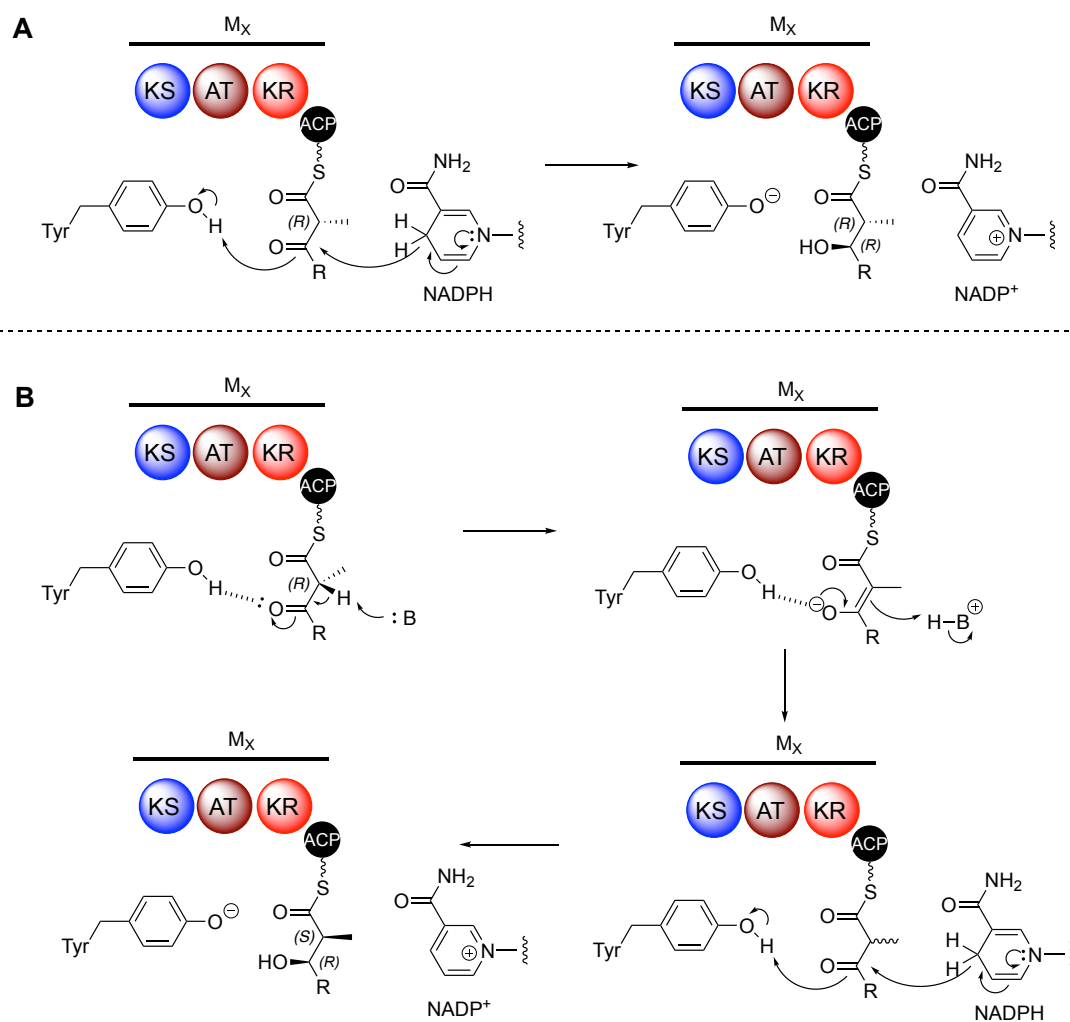


**Scheme 1.4** The KS domain-catalyzed translocation and elongation reactions resulting in chain elongation by two carbon units.

### 1.3.1.2 Accessory catalytic domains

In addition to the minimal catalytic domains described above, PKS chain extension modules usually contain one or more accessory domains, which modify the C-2 and/or C-3 atoms of the 3-keto thioester intermediate produced by the KS domain. KR domains typically reduce the 3-keto thioester to produce a stereodefined 3-hydroxy thioester. The stereochemistry of the 3-hydroxy thioester can be predicted based upon sequence alignments. KR domains that reduce (2*R*)-2-methyl-3-keto thioesters (generated by the KS domain, scheme 1.4) to install (2*R*,3*S*)-2-methyl-3-hydroxy thioesters are often referred to as A1-type KR domains, and those that install (2*R*,3*R*)-2-methyl-3-hydroxy thioesters are B1-type (scheme 1.5A).<sup>65</sup> The B1-type KR domains harbor a conserved aspartate residue which is not present in A1-type KR domains.<sup>66</sup> The reduction is catalyzed using a nicotinamide adenine dinucleotide phosphate (NADPH) cofactor, which delivers a hydride nucleophile to the ketone carbonyl group, whilst the resulting oxyanion is protonated via a conserved tyrosine residue.<sup>67</sup>

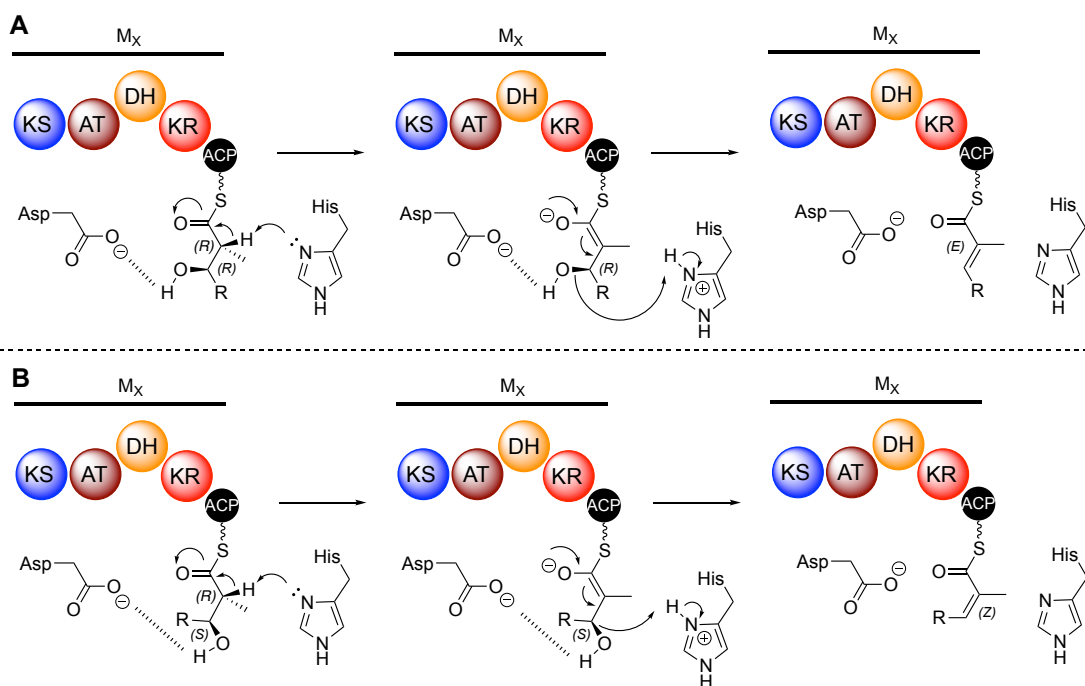
KR domains are also capable of catalyzing the racemization of the C-2 methyl group, followed by subsequent diastereoselective reduction to form (2*S*,3*S*)-2-methyl-3-hydroxy thioesters (A2-type KR domain) or (2*S*,3*R*)-2-methyl-3-hydroxy thioesters (B2-type KR domain).<sup>65</sup> The racemization proceeds via deprotonation at the C-2 position to form an enolate intermediate followed by subsequent reprotonation, the residue responsible for the proton exchange is yet to be determined (scheme **1.5B**).<sup>68</sup> There are also examples of KR domains that lack any catalytic activity (C1-type), and KR domains capable of racemization but not reduction (C2-type), all of which can be identified using sequence alignments.<sup>69</sup> It is important to note that KR domains that reduce 3-keto thioesters (lacking the C-2 methyl group) can simply be referred to as A-type or B-type depending on whether they produce (3*S*)- or (3*R*)-hydroxy thioesters respectively.



**Scheme 1.5** **A** The (B1-type) KR domain-catalyzed reduction to form a (2*R*,3*R*)-2-methyl-3-hydroxy thioester. **B** The (B2-type) KR domain-catalyzed racemization and reduction to form a (2*S*,3*R*)-2-methyl-3-hydroxy thioester.



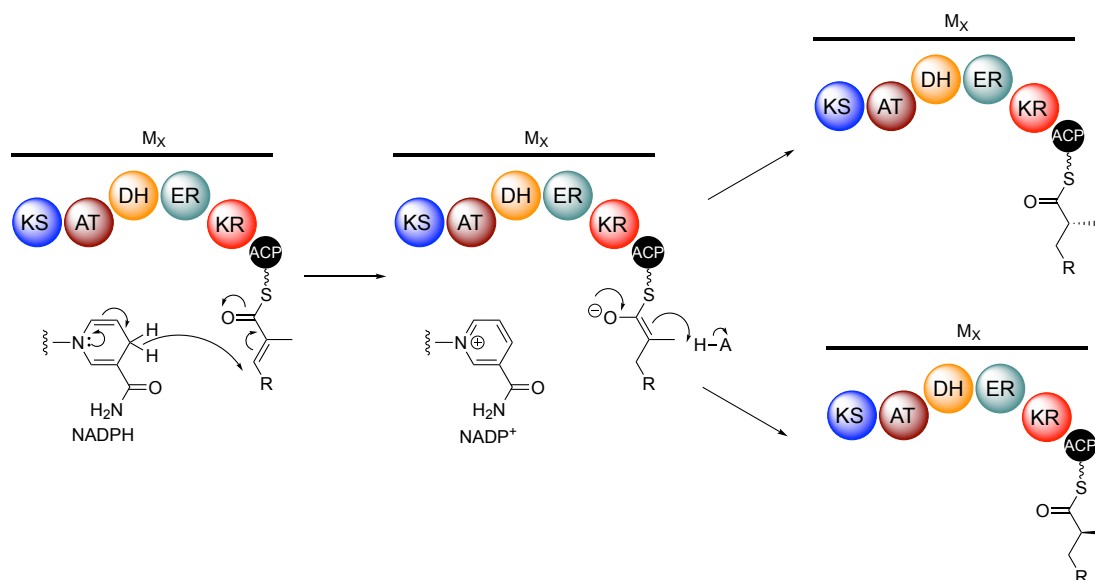
The 3-hydroxy thioester product of the KR domain can then be processed by a DH domain if one is present in the module. DH domains typically catalyze dehydration of the 3-hydroxy thioester to produce the corresponding 2-enoyl thioester via a *syn*-elimination mechanism, using a conserved histidine residue. The *syn*-elimination mechanism results in the dehydration of (*R*)-configured alcohols to afford (*E*)-configured alkenes, and (*S*)-configured alcohols to afford (*Z*)-configured alkenes. The dehydration is believed to proceed via an E1<sub>CB</sub> mechanism involving deprotonation at the C-2 carbon by the histidine residue to form an enolate intermediate, from which the C-3 hydroxyl group is eliminated.<sup>70</sup> The role of a conserved aspartate residue has been the subject of some debate, which is discussed in detail in section 2.1.1.2. Recent work by Cane and coworkers suggests that the histidine residue used to generate the enolate acts as the proton donor, and the aspartate is used to bind and orient the substrate (scheme 1.6).<sup>71</sup>



**Scheme 1.6** **A** The DH-catalyzed dehydration of a (3*R*)-hydroxy thioester intermediate to produce a (2*E*)-enoyl thioester. **B** The dehydration of a (3*S*)-hydroxy thioester intermediate to produce a (2*Z*)-enoyl thioester.

The resulting 2-enoyl thioester can then be reduced by an ER domain, resulting in a saturated acyl thioester intermediate. The ER-catalyzed reduction of 2-methylenoyl thioesters results in the generation of a defined stereocenter at the 2-position. The stereoselectivity of the ER domain can again be predicted using conserved amino acid residues, with the presence of a conserved tyrosine residue usually resulting in the formation of a (2*S*)-configured product.<sup>72</sup>

The catalytic mechanism of ER domains consists of the nucleophilic attack of a hydride (donated by NADPH) at the 3-position of the 2-enoyl thioester. This results in an enolate intermediate, which is protonated at the 2-position to afford the saturated acyl thioester (scheme 1.7). The catalytic residue responsible for the protonation remains to be identified.<sup>73</sup>

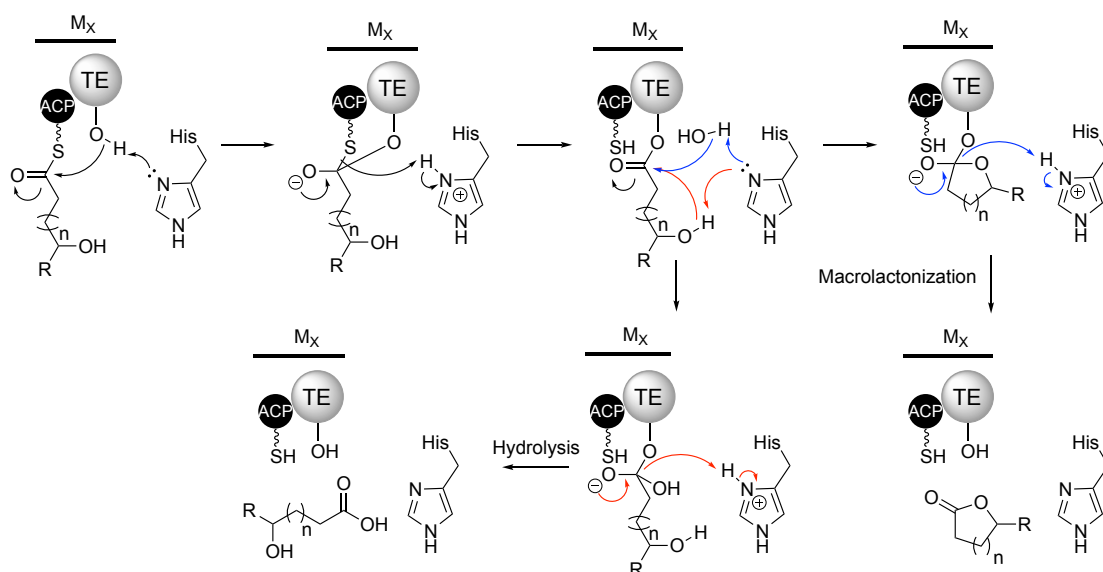


**Scheme 1.7** The ER-catalyzed reduction of a 2-enoyl thioester intermediate to afford stereodefined saturated acyl thioesters.

In addition to the accessory domains described above, some PKS modules harbor methyltransferase (MT) domains. These domains either methylate the 2-position of the 3-keto thioester intermediate (*C*-MTs), or *O*-methylate the 3-hydroxy group resulting from ketoreduction (*O*-MTs) and use a *S*-adenosylmethionine (SAM) cofactor.<sup>74,75</sup>

### 1.3.1.3 Polyketide chain offloading

The offloading of the fully assembled polyketide chain is usually catalyzed by a TE domain located at the *C*-terminus of the PKS. Firstly the ACP-bound polyketide chain is translocated onto a conserved serine residue of the TE domain, which is catalyzed by a conserved histidine residue. The chain is then offloaded from the megasynthase via either intramolecular (macrocyclization, blue) or intermolecular (hydrolysis or transesterification, red) nucleophilic attack, again catalyzed by the conserved histidine residue (scheme 1.8).<sup>76</sup> Many other chain release mechanisms have also been reported, including thioester reduction to produce an aldehyde, which can be further reduced to an alcohol, and tetronate formation via condensation with a glyceryl thioester, mediated by a FabH-like ketosynthase.<sup>77,78</sup>



**Scheme 1.8** The TE-catalyzed offloading of the ACP-bound polyketide chain by macrocyclization (blue arrows) or hydrolysis (red arrows).

### 1.3.2 Post-PKS Tailoring Enzymes

Following the assembly and offloading of the polyketide scaffold, further structural modifications are often introduced via post-PKS tailoring enzymes. These enzymes can catalyze the installation of a variety of functional groups, which often make an important contribution to the bioactivity of the molecule. Tailoring enzymes have commonly been the target of combinatorial biosynthesis approaches for the generation of natural product analogues (section 3.1.1.1), and have also been developed into robust *in vitro* biocatalysts.<sup>79,80</sup> They can be subdivided into several classes based upon their catalytic mechanism and the functionality they install.

#### 1.3.2.1 Oxidoreductases

Oxidoreductases are a broad class of tailoring enzymes, including oxygenases, oxidases, peroxidases, reductases and dehydrogenases. A common class of oxygenase enzymes are heme-dependent cytochrome P450 monooxygenases (CYP450s), which are capable of catalysing hydroxylation, epoxidation and dealkylation, among other reactions.<sup>81</sup> Two CYP450s are encoded by genes in the erythromycin 4 biosynthetic gene cluster (EryF and EryK). These are responsible for post-PKS hydroxylation at the 6- and 12-positions of the macrolide (figure 1.8).<sup>82</sup> Post-PKS hydroxylation can also be catalysed by non-heme iron and  $\alpha$ -ketoglutarate ( $\alpha$ KG)-dependant dioxygenases, such as the enzyme responsible for

introducing the hemiketal hydroxyl group into the antitumour agent FR901464 **33** (figure 1.8).<sup>83</sup> There are also many examples of flavin-dependent oxidoreductases, such as the flavin adenine dinucleotide (FAD)-dependant dehydrogenase involved in the oxidation of a hemiacetal to a lactone during the biosynthesis of antitumour drug gilvocarcin V **34**.<sup>84</sup>

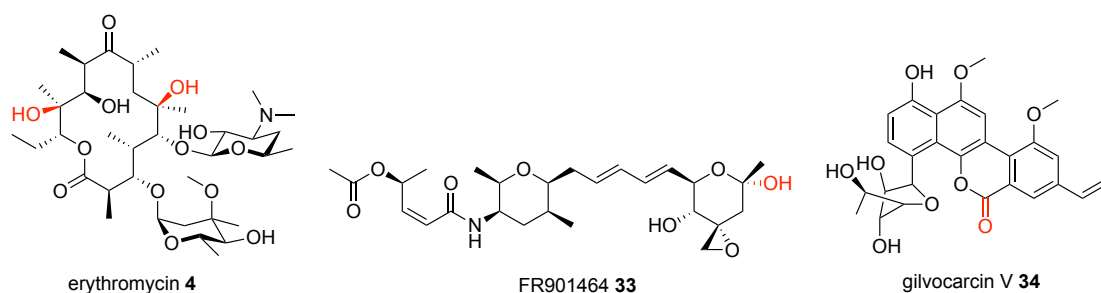


**Figure 1.8** The structures of natural products erythromycin **4**, FR901464 **33** and gilvocarcin **34**. Post-PKS modifications in their biosynthesis are highlighted in red.

### 1.3.2.2 Transferases

Many post-PKS tailoring enzymes catalyze the transfer of functional groups onto heteroatoms of the polyketide scaffold, including glycosyl transferases, methyl transferases, acyl transferases and carbamoyl transferases.<sup>79</sup> Two glycosyl transferase enzymes catalyze the transfer of L-mycarose and D-desosamine onto the erythromycin scaffold, prior to *O*-methylation of the D-desosamine residue by an *O*-MT domain (red/blue, figure 1.9).<sup>85</sup> Both methyl transferase and acyl transferase post-PKS tailoring enzymes are involved in rifamycin B **35** biosynthesis, catalyzing *O*-methylation and *O*-acetylation respectively.<sup>86</sup> The biosynthetic gene cluster of another ansamycin antibiotic, geldanamycin **36**, contains genes encoding a carbamoyl transferase in addition to methyl transferases which are involved in methoxymalonyl precursor biosynthesis (figure 1.9).<sup>87</sup>

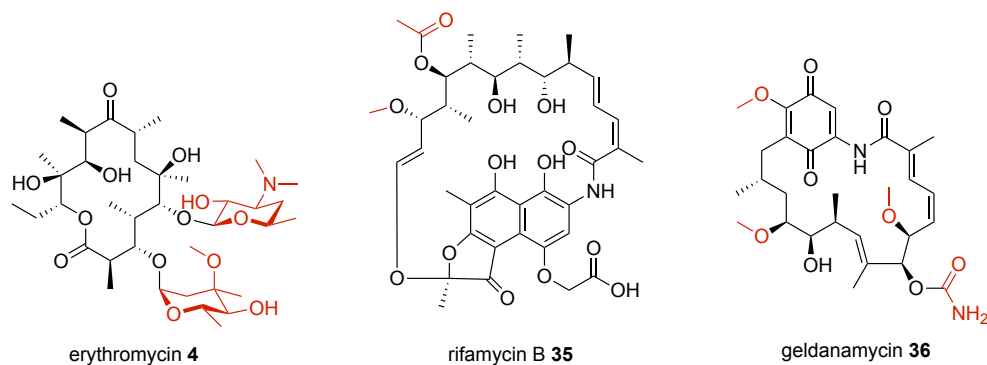


**Figure 1.9** The structures of natural products erythromycin **4**, rifamycin B **35** and geldanamycin **36**, which have undergone post- or pre-PKS modification (red/blue).

### 1.3.2.3 Halogenases

Many polyketide natural products contain halogens that contribute to their bioactivity. Chloride and bromide groups are most commonly observed, but there are examples of fluorinated and iodinated polyketides.<sup>88</sup> The introduction of halogens at electron-rich (often aromatic) positions is usually catalyzed by flavin-dependent halogenases. Examples include post-PKS chlorination during 7-chlortetracycline **37** biosynthesis as well as the biosynthesis of anti-cancer agent radicicol **38** (figure 1.10).<sup>89</sup> Halogenation at aliphatic positions is usually catalyzed by Fe(II) and  $\alpha$ KG-dependent halogenases,<sup>90</sup> which often act during polyketide assembly on ACP-tethered intermediates. A well-studied example is the introduction of the vinyl chloride group in the biosynthesis of jamaicamide A **39** (figure 1.10).<sup>91</sup>

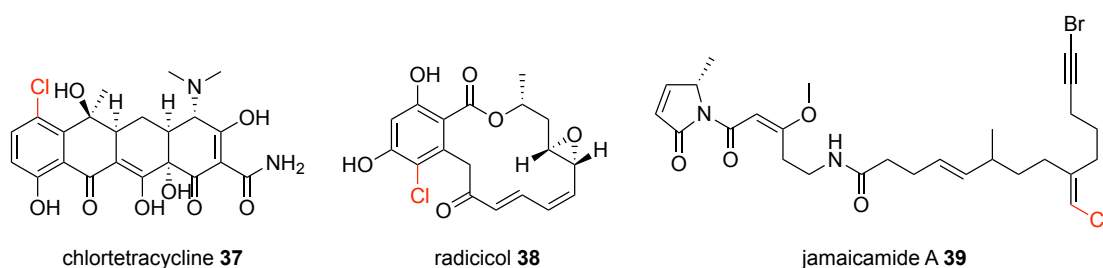


**Figure 1.10** The structures of halogenated polyketide natural products chlortetracycline **37**, radicicol **38** and jamaicamide A **39**. Halogens introduced by tailoring enzymes are highlighted in red.

### 1.3.3 *trans*-AT PKSs

Type I modular PKSs can be subdivided into *cis*- and *trans*-AT types on the basis of phylogenetic analyses. *cis*-AT PKSs such as DEBS (scheme 1.1) have AT domains embedded within each module, which are responsible for priming the adjacent ACP domain with a starter or extender unit. *trans*-AT PKSs have separately encoded AT domains that act in *trans* to prime ACP domains in the assembly line with extender units (figure 1.11).<sup>92</sup> Recent work has suggested that some ACP domains in *trans*-AT PKSs, particularly those directly downstream of KS<sup>0</sup> domains (section 1.3.3.1) avoid malonylation.<sup>93</sup> *trans*-AT PKSs also frequently have *trans*-acting ER domains which catalyse enoyl reduction of unsaturated thioester intermediates in *trans*.

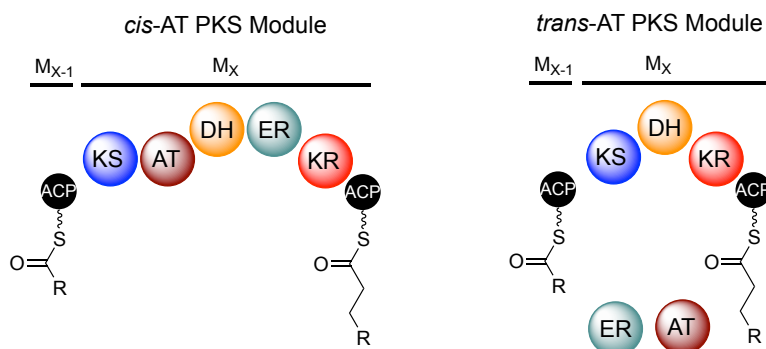


**Figure 1.11** The comparison of a typical *cis*-AT PKS module harboring embedded AT and ER domains, with a *trans*-AT PKS module which has a separately encoded AT and ER domains.

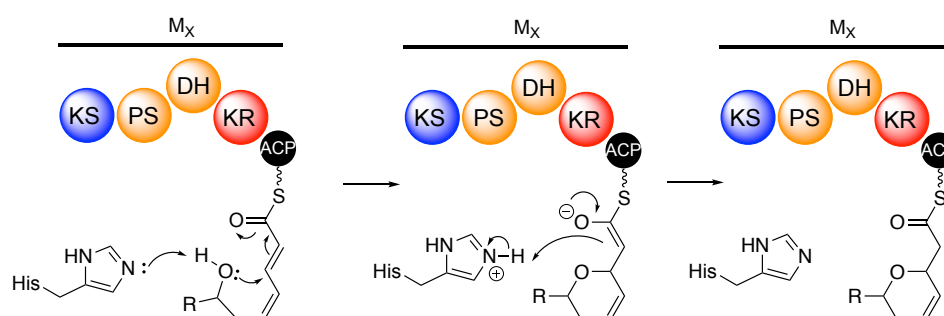
*cis*-AT PKSs typically obey the co-linearity principle, in that the order and function of catalytic modules and domains in the megasynthase generally correlates to the structure of the polyketide product. This makes it possible to predict the structure of putative polyketide products based upon domain architecture alone.<sup>94</sup> Many of the domains discussed in sections **1.3.1.1** and **1.3.1.2** are still present in *trans*-AT PKS systems, however they are often mis-assigned and can have variants that catalyze different reactions to those discussed in the previous sections.<sup>94</sup> *trans*-AT PKS systems can also have great architectural diversity including modules with unusual domain orders and modules split across polypeptide subunits, which often makes the structures of putative polyketide products from *trans*-AT PKSs difficult to predict based on domain and module architecture alone. Some common features of *trans*-AT PKSs are discussed in the following sections (**1.3.3.1-1.3.3.4**).

### 1.3.3.1 KS<sup>0</sup> Domains

A unique feature of *trans*-AT PKSs is KS<sup>0</sup> domains, which are non-elongating variants of KS domains. These domains are structurally similar to KS domains (section **1.3.1.1**), but lack a conserved histidine residue required for the decarboxylative Claisen condensation, and so are not able to catalyze chain elongation. Despite this, KS<sup>0</sup> domains still harbour the conserved cysteine residue required for translocation, and so are capable of facilitating transfer of the acyl chain onto downstream carrier proteins, this is exemplified in the chain release mechanism of enacyloxin biosynthesis (section **1.5**).<sup>93,95</sup>

### 1.3.3.2 Pyran Synthase Domains

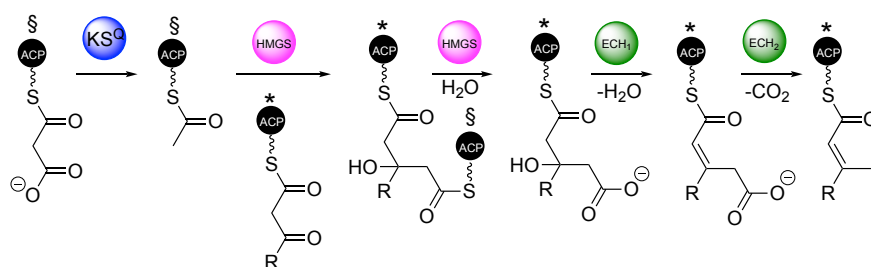
Pyran synthase (PS) domains are variants of DH domains that are exclusive to *trans*-AT PKSs. They catalyse the formation of 5- or 6-membered ether rings via an oxa-Michael addition (scheme 1.9). PS domains resemble DH domains, but contain a deletion within the HxxxGxxxxP active-site motif that is found in canonical DH domains.<sup>94</sup> The mechanism of oxacycle formation is not fully understood, but it is thought that a conserved active site histidine residue catalyzes proton transfer during the Michael addition (scheme 1.9).<sup>96</sup>



**Scheme 1.9** The PS-catalyzed cycloether ring formation observed in *trans*-AT PKSs.

### 1.3.3.3 $\beta$ -Branching Cassette

*trans*-AT PKS gene clusters often encode *trans*-acting  $\beta$ -branching cassettes that are responsible for the introduction of  $\beta$ -branches into the polyketide chain.  $\beta$ -Methyl branching is typically catalyzed by a series of enzymes known as the 3-hydroxy-3-methylglutaryl synthase (HMGS) cassette.<sup>94</sup> This includes a KS<sup>Q</sup> domain, which is responsible for the decarboxylation of a separate malonyl-ACP to form the corresponding-acetyl ACP. The KS<sup>Q</sup> domain cannot catalyse chain elongation because its active site cysteine residue is mutated to a glutamine. A HMGS enzyme catalyzes the aldol addition of the acetyl unit onto the 3-keto thioester bound to an ACP domain of the megasynthase, followed by hydrolysis. The aldol product is then dehydrated and decarboxylated by two enoyl-CoA hydratase-like enzymes (ECH), resulting in the installation of the  $\beta$ -methyl group (scheme 1.10).<sup>97</sup> Variants of  $\beta$ -branching cassettes are also employed for the installation of other functional groups such as cyclopropanes.<sup>98</sup>



**Scheme 1.10** The HMGS cassette responsible for the installation of a  $\beta$ -methyl group. § denotes a separately encoded ACP domain, \* denotes a megasynthase ACP domain.

### 1.3.3.4 Split Modules

Split modules are a good example of the unusual domain architecture that can be found in *trans*-AT PKSs. They are modules that span across polypeptide subunits and harbour an inter-subunit gap (figure 1.12). Split modules harboring a DH domain at the *N*-terminus of the downstream subunit are often referred to as “dehydrating bimodules” of which there are two types, type A and type B.<sup>94</sup> Type A harbour a  $KS^0$  domain at the *C*-terminus of the upstream subunit and are proposed to install an alkene, whereas type B harbour a KS domain at the *C*-terminus of the upstream subunit and are proposed to install a diene. However, there is no biochemical evidence for this.<sup>99</sup> The subunits are brought together during chain assembly by a disordered DH-docking (DHD) domain appended to the *C*-terminus of the upstream subunit, which docks to the surface of the DH domain at the *N*-terminus of the downstream subunit (figure 1.12).<sup>100</sup> Split modules are discussed in more detail in section 2.1.2.

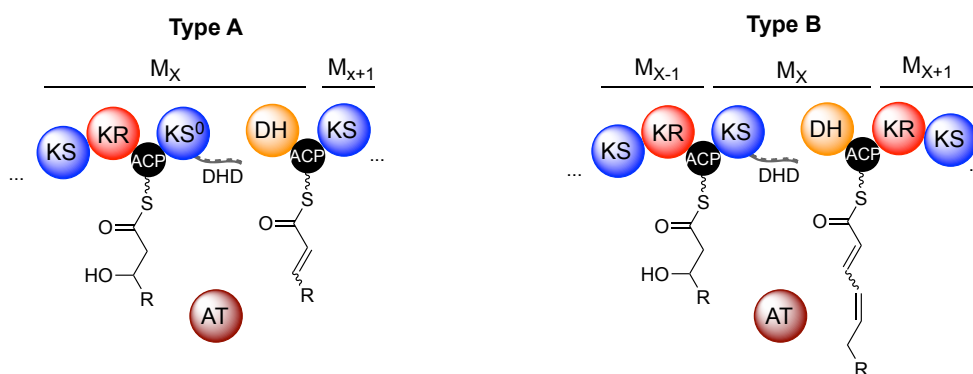


**Figure 1.12** Organisation of type A and type B split modules also known as ‘dehydrating bimodules’ in *trans*-AT PKSs.



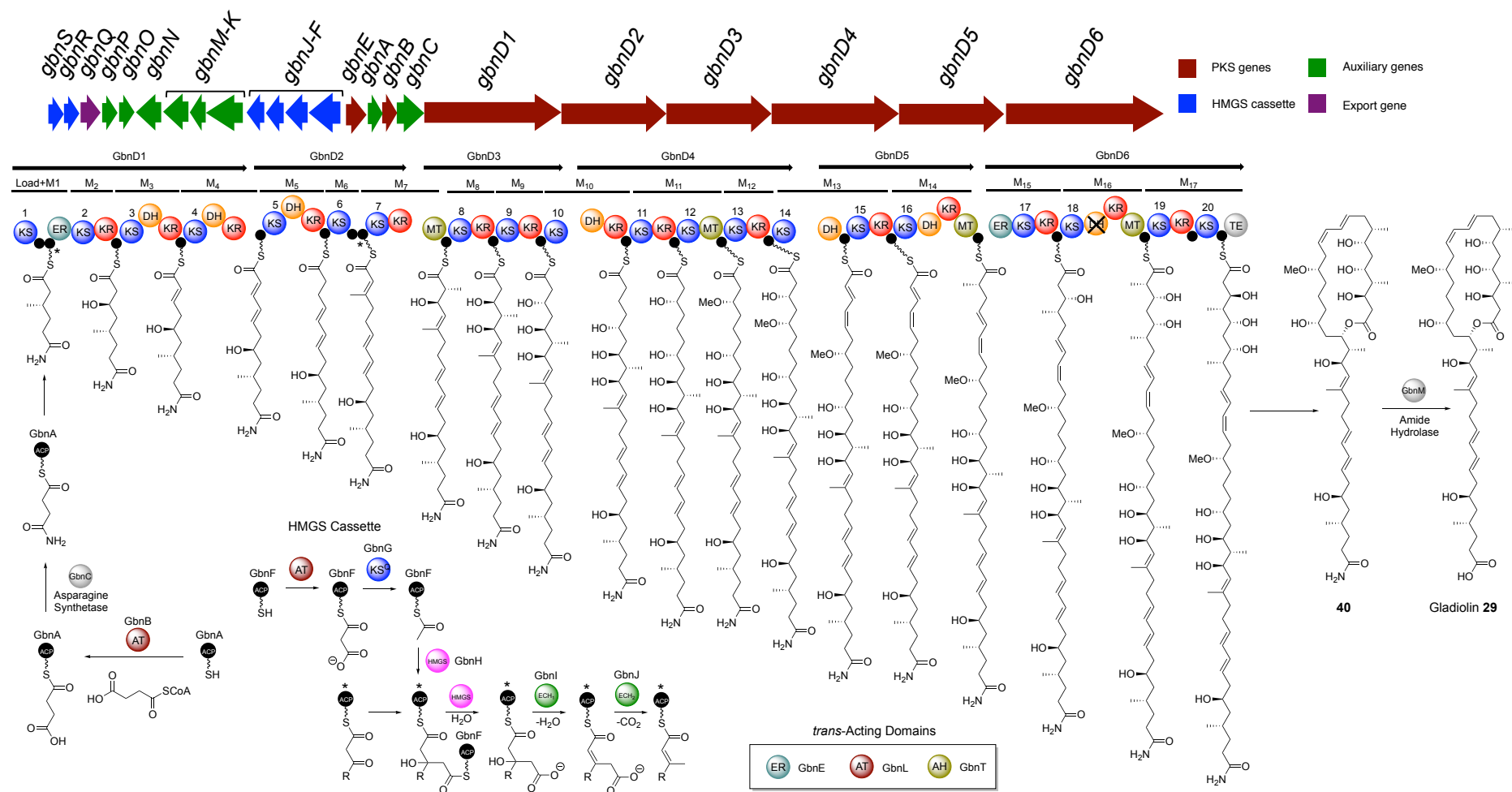
## 1.4 Gladiolin

Gladiolin **29** is a macrolide antibiotic, which has been isolated from *Burkholderia gladioli* BCC0238, a clinical isolate from a CF patient. It shows potent activity against *Mycobacterium tuberculosis*, with a minimum inhibitory concentration (MIC) of 0.4 µg/mL against the H37Rv strain, and has been shown to be active against several antibiotic resistant clinical isolates.<sup>101</sup> The target of gladiolin is RNA polymerase, which is also inhibited by several other antibiotics used to treat tuberculosis, such as rifampicin.<sup>102</sup>

Gladiolin **29** is assembled by a *trans*-AT PKS consisting of 17 modules that is encoded by six genes (GbnD1-GbnD6). Three upstream genes encode two *trans*-acting AT domains (GbnB and GbnL), and an acyl hydrolase (AH) domain (GbnT), which hydrolyzes acylated ACP domains that block polyketide assembly (scheme **1.11**).<sup>101,103</sup> Polyketide assembly is initiated by the GbnB-catalyzed transacylation of a succinyl-CoA starter unit onto a standalone ACP domain (GbnA). The succinyl group is then converted to a succinamide group via an asparagine synthetase (GbnC), before the acyl chain is transferred onto the *N*-terminal KS domain (KS1) of the PKS, which then catalyzes elongation with the malonated downstream ACP domain (scheme **1.11**).

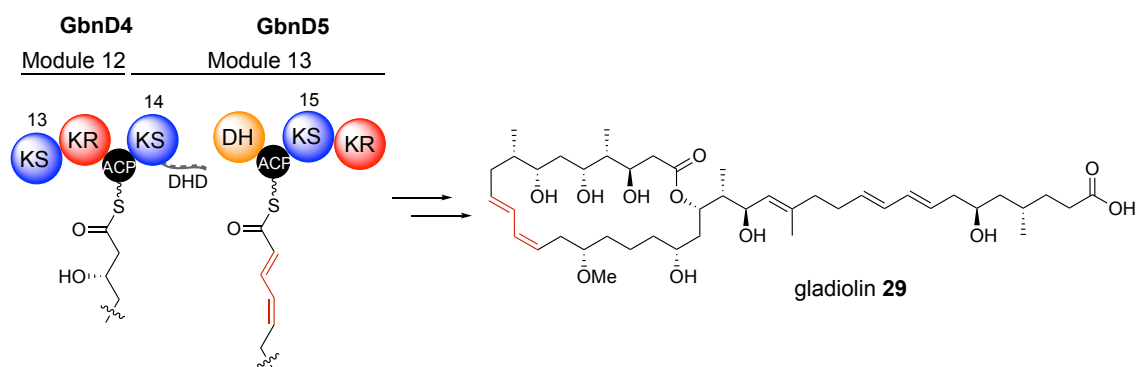
The resulting ACP-bound keto-ester is then converted to a 3-methyl-2-enoyl thioester, catalyzed by the HMGS cassette described in section **1.3.3.3**, which includes a KS<sup>Q</sup> (GbnG), HMGS (GbnH) and two enoyl-CoA hydratase-like enzymes (GbnI and GbnJ, scheme **1.11**). A β-methyl branch is also installed by module 6. In addition, a *trans*-acting ER domain (GbnE) is encoded by the gene cluster. This catalyzes reduction of enoyl thioester intermediates attached to the ACP domains of modules 5 and 10, accounting for the saturation of C-17 and C-27 of gladiolin.<sup>97,101</sup> Once off-loaded from the PKS, the amide variant of gladiolin (**40**) then undergoes hydrolysis catalyzed by an amide hydrolase (GbnM) to produce gladiolin **29**.

The assembly of gladiolin **29** requires 17 chain elongation reactions. However, there appears to be 20 KS domains, each capable of catalyzing chain elongation, embedded within the PKS. This suggests that three KS domains may function as transacylase domains, facilitating the transfer of the growing polyketide chain to a downstream ACP domain without catalyzing elongation. However, it is difficult to identify which three KS domains do not elongate the polyketide chain without experimental data. In addition, there appears to be six functional DH domains within the PKS, yet seven dehydrations are required for the assembly of gladiolin **29**. This suggests that one of the DH domains may catalyze two successive dehydrations.



**Scheme 1.11** Domain and module organization of the gladiolin **29** *trans*-AT PKS, along with putative ACP-bound intermediates resulting from the reactions catalyzed by each module. The  $\beta$ -methyl 2-enoyl thioesters assembled by modules 1 and 6 (\*) are installed by the HMGS cassette.

Module 13 of the gladiolin PKS harbors a type B split module (section 1.3.3.4) which is proposed to result in the installation of the (*E,Z*)-configured diene of gladiolin **29** (scheme 1.12). Given that there is only one DH domain present within the module, this DH domain may catalyze a previously uncharacterized double dehydration.



**Scheme 1.12** The type B split module present in the gladiolin PKS thought to be responsible for the installation of the (*E,Z*)-diene motif (red).

## 1.5 Enacyloxin

Another polyketide that exhibits antimicrobial activity is enacyloxin IIa **30** (figure 1.13), which is produced by *Burkholderia ambifaria* AMMD. This metabolite was identified by screening Bcc isolates against pathogenic bacteria leading to the identification of activity of the *B. ambifaria* strain against *B. multivorans*, a pathogen which commonly causes infections in CF patients.<sup>104,105</sup> Enacyloxin IIa **30** and several congeners were originally isolated from the  $\gamma$ -proteo-bacterium, *Frateriia* sp. W-315 by Watanabe and co-workers (figure 1.13). However the enacyloxin biosynthetic gene cluster has only been identified in *B. ambifaria*.<sup>106–108</sup>

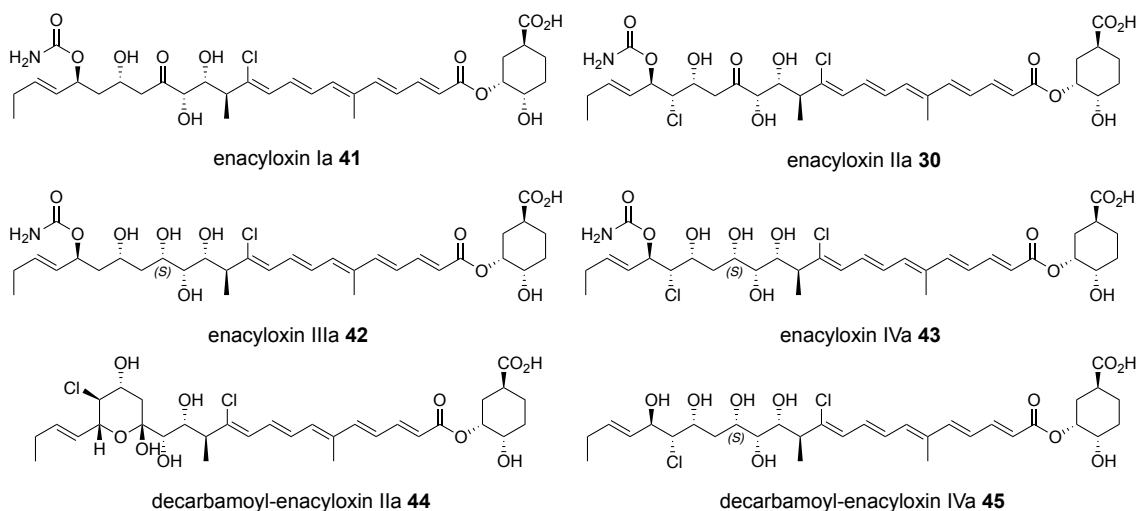


**Figure 1.13** The enacyloxin congeners isolated by Watanabe and co-workers. The stereocenter marked (*S*) is now believed to be (*R*)-configured.

In addition to being active against cystic fibrosis pathogens, enacyloxin IIa **30** shows potent (MIC of 2  $\mu\text{g/mL}$ ), narrow-spectrum activity against *Acinetobacter baumannii*.<sup>104</sup> *A. baumannii* is a Gram-negative MDR pathogen that causes hospital-acquired infections, and is high on the world health organizations (WHOs) priority list of dangerous pathogens.<sup>109</sup> The antibiotic acts by targeting ribosomal elongation factor thermo unstable (EF-Tu). Guanosine 5'-triphosphate (GTP)-bound EF-Tu carries aminoacyl-tRNA to the mRNA-programmed ribosome during bacterial protein synthesis. The codon-anticodon interaction at the ribosome promotes the hydrolysis of the bound GTP, which triggers the release of the EF-Tu-Guanosine 5'-diphosphate (GDP) complex, as well as peptide bond formation during protein synthesis. The binding of enacyloxin IIa hinders the release of the EF-Tu-GDP complex from the ribosome, which inhibits recycling of EF-Tu, peptide bond formation and hence bacterial protein synthesis.

The structure of enacyloxin IIa **30** co-crystallized with the EF-Tu-GDP complex from *E.coli* solved by Parmeggiani and co-workers is shown in figure **1.14**.<sup>110</sup> The dissociation constant ( $K_d$ ) for the EF-Tu-enacyloxin complex could not be determined however due to the poor water solubility of enacyloxin IIa, and so little is known about the affinity of enacyloxin IIa for EF-Tu compared to the derivatives isolated by Watanabe and co-workers (figure **1.13**).<sup>110</sup>

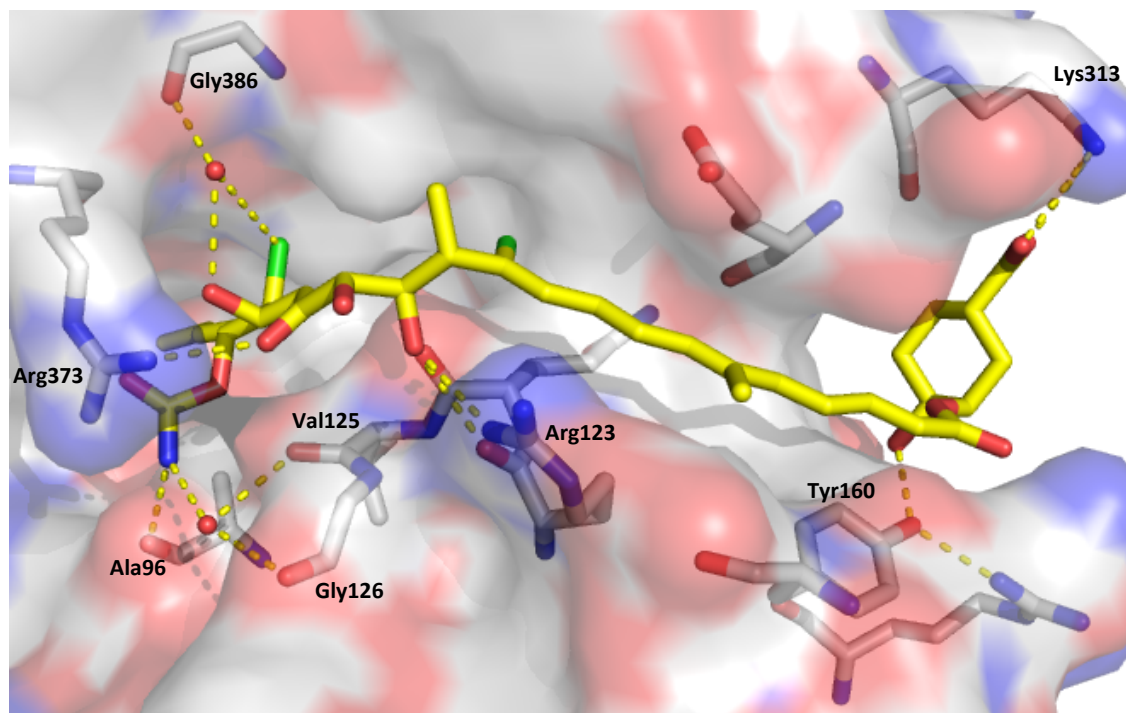


**Figure 1.14** The crystal structure of enacyloxin IIA **30** bound to the EF-Tu-GDP complex.

Based on the binding of enacyloxin IIA **30** to the EF-Tu-GDP complex shown in figure 1.14, the structure of enacyloxin IIA can be split into three sections (figure 1.15). Firstly the dihydroxycyclohexane carboxylic acid (DHCCA) unit (green), which appears to be involved in polar contacts with a lysine (313) and a tyrosine (160) residue in the binding pocket. The polyol region (blue), which appears to make polar contacts with two arginine residues (123 and 373), two ordered water molecules as well as a backbone alanine residue (96). Finally the polyene region (red), which acts as a rigid linker region. In order to determine whether these polar contacts are key to activity, it would be useful to generate a library of enacyloxin analogues harbouring structural changes in both the DHCCA and polyol regions. This would provide useful structure-activity relationship (SAR) data, and potentially more potent analogues.

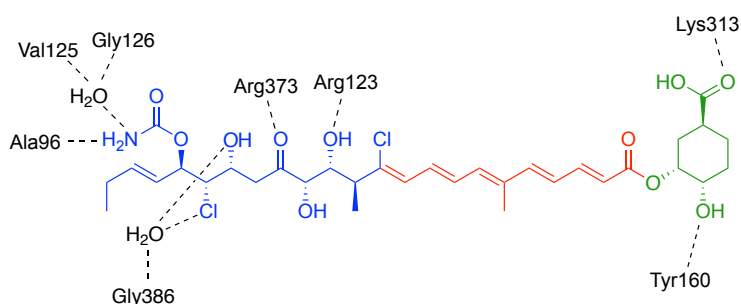
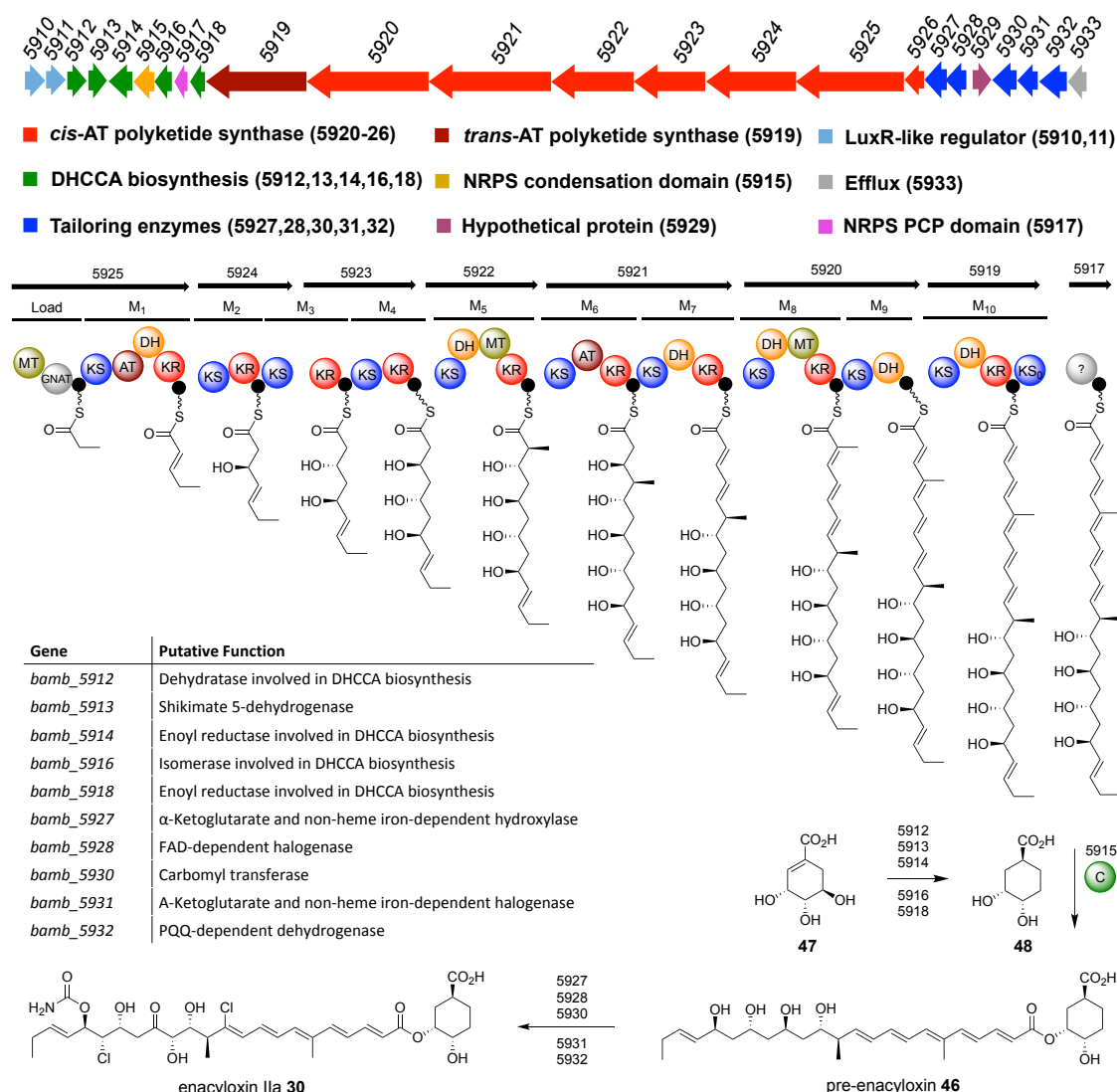


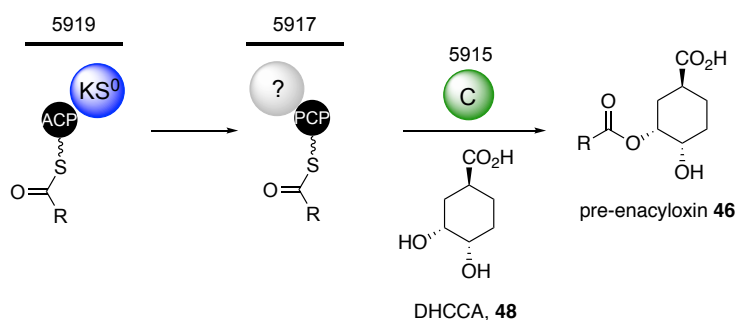
**Figure 1.15** The key polar contacts between enacyloxin and the binding site in EF-Tu.

The enacyloxin biosynthetic gene cluster contains seven PKS genes, encoding a hybrid *cis*-AT/*trans*-AT PKS consisting of ten chain extension modules and a loading module (scheme 1.13). Curiously, no standalone AT domains are encoded within the cluster, suggesting that either the AT domains of modules 1 and 6 may act in *trans* in order to malonate ACP domains of other modules, or there may be a *trans*-acting AT encoded outside of the cluster. Polyketide assembly is initiated by the GCN5-related *N*-acetyltransferase (GNAT) domain which catalyzes the decarboxylation of methylmalonyl-ACP (generated by the MT domain of the loading module from malonyl-ACP) to generate propionyl-ACP. The subsequent domain architecture shows perfect co-linearity with the proposed biosynthetic intermediates, with the exception of a DH domain missing from module 6 and a KR domain from module 9. The functions of these missing domains may be catalysed by *trans*-acting enzymes, or neighbouring modules.<sup>104</sup>



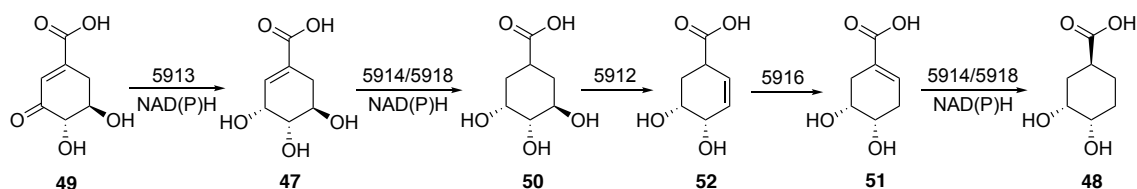
**Scheme 1.13** The enacyloxin gene cluster and proposed biosynthetic pathway. Note that the domain marked ‘?’ in *Bamb\_5917* is of unknown function. The putative functions of all the genes involved in enacyloxin biosynthesis can be found in appendix 8.6.

The PKS chain release mechanism is particularly unusual (scheme 1.14). A  $KS^0$  domain is present at the C-terminus of the final PKS subunit (Bamb\_5919), rather than the TE domain usually responsible for chain release during polyketide assembly. The  $KS^0$  domain catalyses the transfer of the ACP-bound intermediate of module 10 onto a peptidyl carrier protein (PCP) domain (Bamb\_5917).<sup>93</sup> The PCP-bound polyketide chain is then offloaded by a condensation domain (Bamb\_5915) with DHCCA **48**. Condensation reactions of PCP-bound thioesters catalysed by condensation domains are frequently observed in nonribosomal peptide synthetases (NRPSs). However the thioester is typically condensed with an amine to form an amide rather than an alcohol to form an ester.<sup>111</sup>



**Scheme 1.14** The off-loading mechanism from the enacyloxin PKS.

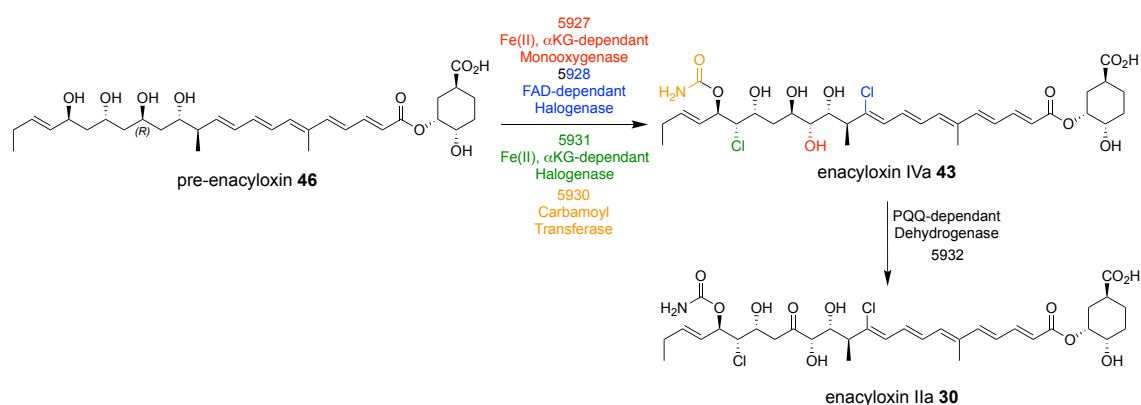
DHCCA **48** is proposed to be derived from shikimate **47**, with five enzymes (Bamb\_5912, 5913, 5914, 5916 and 5918) hypothesized to be involved in the pathway (scheme 1.15). The pathway consists of the reduction of 3-dehydroshikimate **49** to shikimate **47** by a shikimate dehydrogenase (Bamb\_5913), followed by reduction to a trihydroxycyclohexanecarboxylic acid (THCCA) intermediate **50** by one of two enoyl reductases (Bamb\_5914 or 5918). This intermediate is then proposed to be dehydrated by Bamb\_5912 and isomerized by Bamb\_5916 to form unsaturated DHCCA analogue **51**. The final step to form DHCCA **48** is catalyzed by the remaining enoyl reductase (Bamb\_5914 or 5918). However, none of these steps have been confirmed experimentally.



**Scheme 1.15** The proposed pathway for DHCCA (**48**) biosynthesis.

The condensation product, pre-enacyloxin **46**, is then proposed to be elaborated by five tailoring enzymes (Bamb\_5927, 5928, 5930, 5931 and 5932) to form enacyloxin IIa **30** (scheme **1.16**). Pyrroloquinoline quinone (PQQ)-dependent dehydrogenase (Bamb\_5932) has been characterized as an extracellular enzyme responsible for the oxidation of enacyloxin IVa **43** to enacyloxin IIa **30**.<sup>112</sup> Enacyloxin IVa **43** was isolated from *Frateuria* sp. W-315 (figure **1.13**). However, Watanabe and co-workers assigned the C-15 stereocentre as (*S*)-configured, which is not in agreement with the predicted stereoselectivity of the module 4 KR domain encoded by the gene cluster from *B. ambifaria*.<sup>107</sup>

The four remaining tailoring enzymes are putative carbamoyl transferase Bamb\_5930, Fe(II) and  $\alpha$ -KG-dependant dioxygenase Bamb\_5927, FAD-dependant halogenase Bamb\_5928 and Fe(II) and  $\alpha$ -ketoglutarate-dependant halogenase Bamb\_5931. These are proposed to carbamoylate, hydroxylate and halogenate pre-enacyloxin **46**, to form enacyloxin IVa **43**. However the order of these steps, or whether in fact they act on ACP-bound polyketide intermediates rather than pre-enacyloxin **46** post-PKS assembly, is yet to be established.



**Scheme 1.16** The proposed tailoring steps of the enacyloxin biosynthetic pathway leading to the production of enacyloxin IIa **30** from pre-enacyloxin **46**.

## 1.6 Aims of the Project

The overall aim of this project was to develop a better understanding of the gladiolin and enacyloxin biosynthetic pathways with a view to engineered biosynthesis of antibiotic analogues. More specifically, the first aim was to establish the role of the module 13 DH domain in generating the *E,Z*-diene motif of gladiolin **29**. This would provide greater insight into how DH domains function in type B split modules, which are commonly found in *trans*-AT PKS systems but are largely uncharacterized. The second aim was to generate a structurally



diverse library of enacyloxin analogues using established and newly developed strategies, which could provide useful SAR data in addition to analogues with increased potency. The final aim was to confirm the biosynthetic pathway for the DHCCA **48** unit of enacyloxin IIa **30**. This could be achieved using a combination of *in vitro* assays of recombinant proteins putatively involved in the pathway with chemically synthesized substrates, in addition to gene deletion studies.

## **2. Results and Discussion I: Diene-Forming DH Domains**

## 2.1 Introduction

### 2.1.1 Dehydratase (DH) Domains

#### 2.1.1.1 Structure of DH Domains

The structures of many DH domains have been solved, with much of the initial structural work being based upon bacterial (type II) FAS DHs. These discrete proteins (FabA and FabZ) exist as dimers consisting of a structure known as the “hotdog fold” whereby an antiparallel  $\beta$ -sheet “bun” encases a hydrophobic  $\alpha$ -helical “sausage” (figure 2.1A). Each pair of dimers harbors two inter-subunit active sites, which contain a histidine from one monomer and either an aspartate (FabA) or a glutamate (FabZ) from the other monomer (figure 2.1B).<sup>113–116</sup> This culminates in a catalytic dyad that is observed in the active sites of all DH domains and has been shown to be essential to catalytic activity via site-directed mutagenesis experiments.<sup>115</sup>

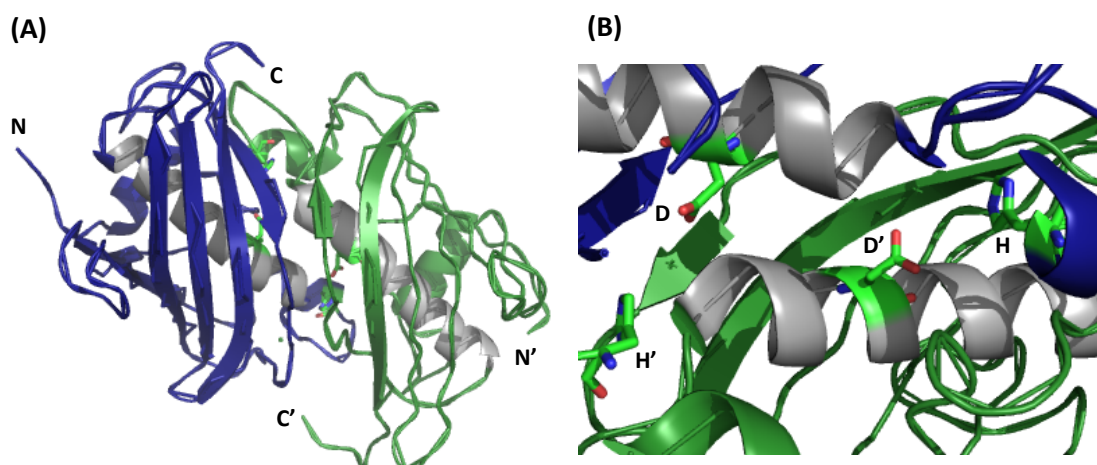


**Figure 2.1** The crystal structure of FabA (PDB: 4B0C) from *Pseudomonas aeruginosa*. **(A)**: The two monomers are shown in blue and green respectively, with the  $\alpha$ -helix of each monomer shown in grey illustrating the “hotdog fold”. **(B)**: The two active sites encompassed by the dimer with aspartate and histidine residues being provided by each monomer (D,H and D', H' respectively).<sup>114</sup>

DH domains from mammalian (type I) FAS and PKSs retain many of the structural features found in bacterial FAS DHs. However, they are no longer standalone enzymes but are incorporated into megasynthases. They still exist as dimers, however one key structural difference is that rather than having inter-subunit active sites, each monomer exists as a “double hotdog fold” in which the catalytic dyad is found (figure 2.2).<sup>99,117–120</sup>

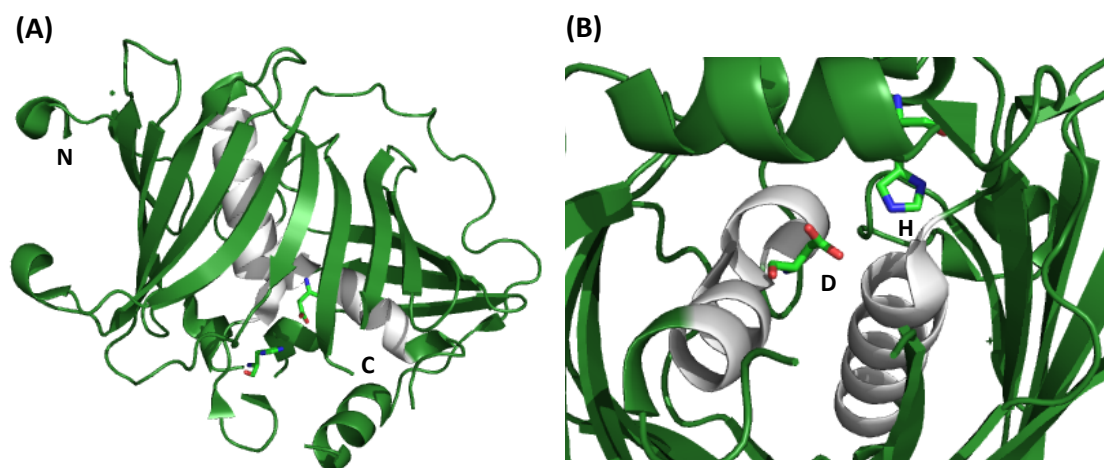
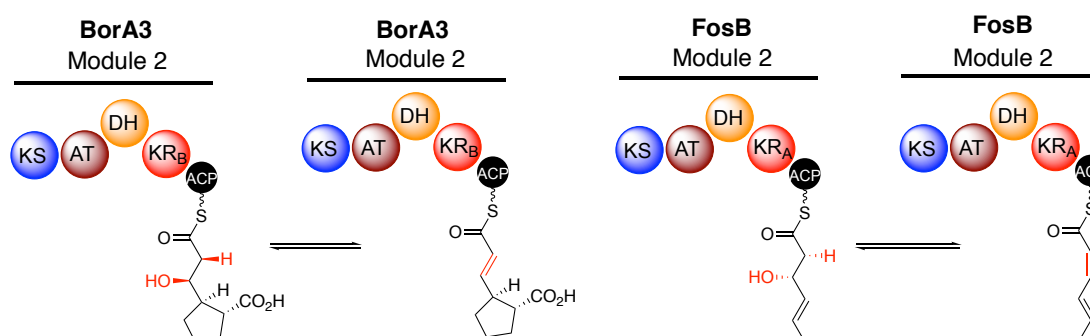


**Figure 2.2** The crystal structure of EryDH4 (PDB: 3EL6). (A): The “double hotdog fold” with the antiparallel  $\beta$ -sheets shown in green and the two  $\alpha$ -helices shown in grey. (B): The active site aspartate and histidine residues (D and H).<sup>118</sup>

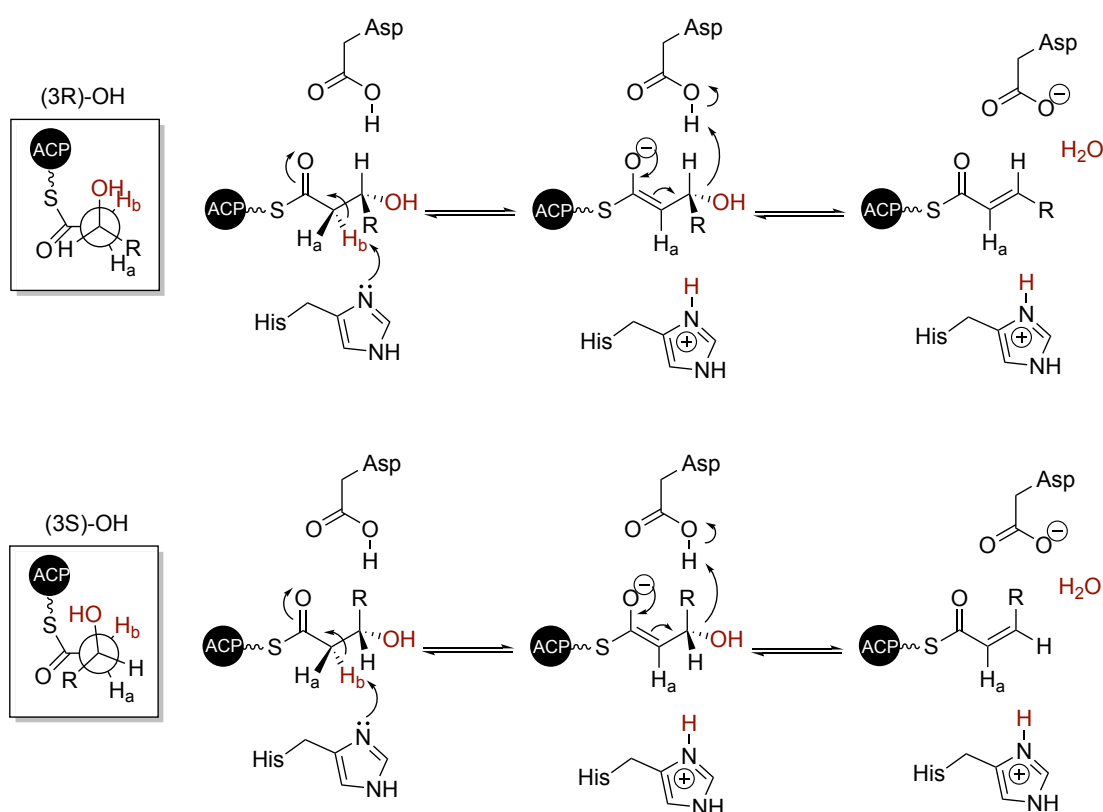
### 2.1.1.2 Mechanism of DH Domains

DH domains have been shown to reversibly catalyze the dehydration of 3-hydroxyacyl thioester intermediates (in both FAS and PKS systems), as well as 2-methyl-3-hydroxyacyl thioester intermediates (in PKS systems), all via a stereoselective *syn* elimination mechanism (section 1.3.1.2).<sup>70,121,122</sup> The stereochemistry of a 3-hydroxyacyl thioester substrate dehydrated by the DH domain can be predicted based upon the amino acid sequence of the upstream KR domain (A-type (KR<sub>A</sub>) installs (*S*)- and B-type (KR<sub>B</sub>) installs (*R*)-configured hydroxyl groups, scheme 2.1).<sup>65,123</sup> The *syn* elimination results in the dehydration of (3*R*)-hydroxyacyl thioesters to form (2*E*)-enoyl thioesters and dehydration (3*S*)-hydroxyacyl thioesters to form (2*Z*)-enoyl thioesters (scheme 2.1).<sup>124–129</sup>



**Scheme 2.1** Biochemically characterized examples of DH domain-catalyzed *syn* eliminations: Dehydration to afford a (2*E*)-enoyl thioester in borrelidin biosynthesis and dehydration to afford a (2*Z*)-enoyl thioester in fostriecin biosynthesis.<sup>125,130</sup>

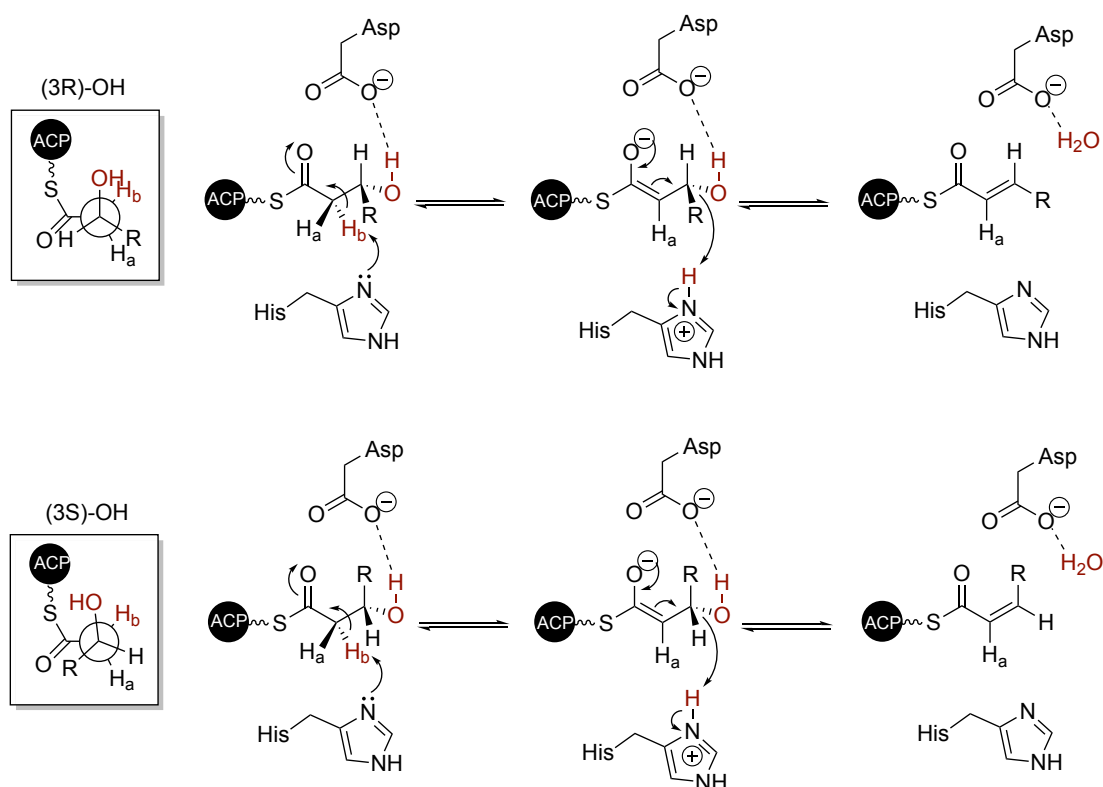
The *syn* elimination mechanism is believed to proceed via deprotonation at the C-2 position by the catalytic histidine residue to form an enolate intermediate, before the elimination of the C-3 hydroxyl group in order to form the resulting alkene. The role of the catalytically important aspartate residue has been the subject of some debate. Many reports suggest that its role is to reprotonate the leaving hydroxyl group, facilitating the required cleavage of the C-O bond in a “two-base” or “base-acid” mechanism (scheme 2.2).<sup>70,99,113–116</sup> The main rationale behind this mechanism is the spatial relationship between the thioester substrate and the catalytic aspartate and histidine dyad.



**Scheme 2.2** The “base-acid” mechanism whereby the histidine deprotonates at the C-2-position and the aspartate reprotonates the C-3 hydroxyl group to form (*E*)- and (*Z*)-configured alkenes.

This mechanism would require the  $pK_a$  of the acidic aspartate residue ( $pK_a \sim 4$ ) to exceed that of the histidine imidazolium ( $pK_a \sim 6$ ) for the aspartate to be protonated whilst the imidazolium is deprotonated at physiological pH. Although the observed  $pK_a$  of an active site amino acid residue can differ from those of the free amino acids,<sup>131</sup> as yet there has been no reported experimental evidence confirming the  $pK_a$  differences required for the “base-acid” mechanism. In fact, one of the only reported studies of the pH dependence of PKS DH domains actually indicated that the active site histidine had a  $pK_a$  of  $\sim 7$ , meaning it is even less likely that the  $pK_a$

of the active site aspartate exceeds that of the histidine, which suggests that the “base-acid” mechanism is not correct.<sup>132</sup> A recent kinetic study by Cane and co-workers provides experimental evidence for a “single-base” mechanism.<sup>71</sup> They propose the histidine residue both deprotonates at the C-2-position and reprotonates the C-3 hydroxyl group on the same face, whilst the aspartate residue is proposed to bind and orient the substrate (scheme 2.3). This provides rationale for the *syn* elimination observed whilst avoiding the  $pK_a$ -associated problems of the “base-acid” mechanism.



**Scheme 2.3** The “single-base” mechanism whereby the histidine both deprotonates at the  $\alpha$ -position and reprotonates the leaving hydroxyl group to form (*E*) and (*Z*)-configured alkenes.

## 2.1.2 Split Modules

### 2.1.2.1 Split Modules in *trans*-AT PKSs

DH domains from *trans*-AT PKS systems have been shown to have variants that catalyze reactions other than dehydration such as enoyl isomerization (enoyl isomerases (EIs)) and pyran formation (PSs, section 1.3.3.2).<sup>133,134</sup> They can also occur in split modules, which are a common feature of *trans*-AT PKSs (section 1.3.3.4).<sup>94,135</sup> Split modules harboring a DH domain at the interface are often referred to as “dehydrating bimodules” and have of a KS-KR-ACP-KS domain architecture at the C-terminus of an upstream PKS subunit, and a DH-ACP didomain motif at the N-terminus of the downstream subunit (figure 2.3). The subunits interact with one another via a DHD domain at the C-terminus of the KS domain and the surface of the downstream DH domain.<sup>100</sup>

These split modules can be categorized into either type A or type B varieties.<sup>136</sup> Type A split modules result in the formation of either a (2*E*)- or (2*Z*)-configured enoyl thioester intermediate and harbor a KS<sup>0</sup> domain (section 1.3.3.1) at the C-terminus of the upstream subunit (figure 2.3). In contrast, type B split modules have a catalytically active KS domain at the interface, as well as an additional KR domain downstream of the DH domain, and are proposed to result in the formation of a 2,4-dienoyl thioester intermediate with either an (*E,E*)- or an (*E,Z*)-configuration (figure 2.3).<sup>94,99,136,137</sup> The structure of a DH domain from a type B split module (module 10 of the difficidin PKS) was recently solved by Keating-Clay and co-workers.<sup>99</sup>

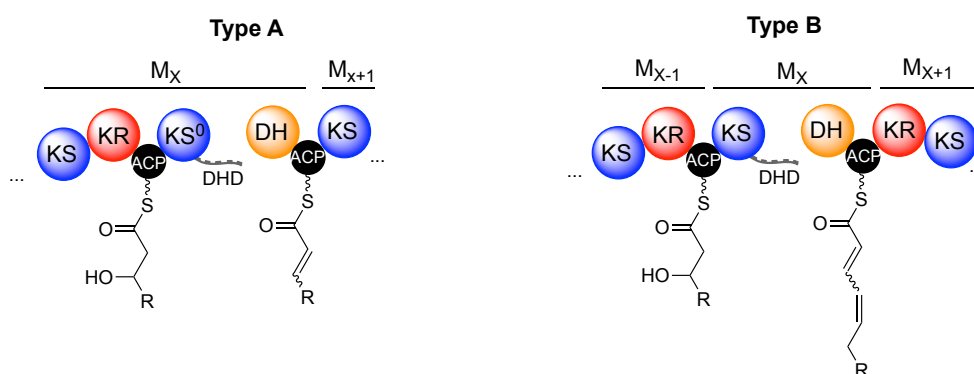
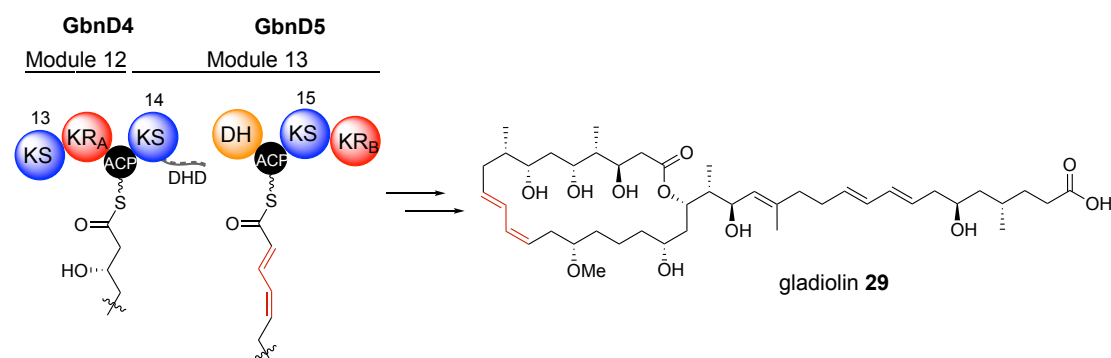


**Figure 2.3** The domain architecture of type A and type B split modules. The KS<sup>0</sup> domain in type A facilitates chain transfer whereas the KS domain in type B is proposed to result in an additional chain elongation.

### 2.1.2.2 Split Module in the Gladiolin PKS

Module 13 of the gladiolin PKS (scheme 2.4) appears to be a split module, which is responsible for the installation of the (*E,Z*)-diene in the macrolide ring of gladiolin **29**. The module has a type B split module architecture, as the KS domain is capable of catalyzing chain elongation provided the relevant ACP domain is malonated. In addition, there are six DH domains in the gladiolin PKS, yet seven dehydrations are required to assemble gladiolin, suggesting at least one DH domain must catalyze more than a single dehydration. It is also important to note that the KR domain upstream of the DH domain is A-type (predicted to install a (*3S*)-configured hydroxyl group), whereas the KR domain downstream of the DH domain is B-type (predicted to install a (*3R*)-configured hydroxyl group).



**Scheme 2.4** The type B split module present in the gladiolin PKS thought to be responsible for the installation of the (*E,Z*)-diene motif (red).

### 2.1.3 Aims

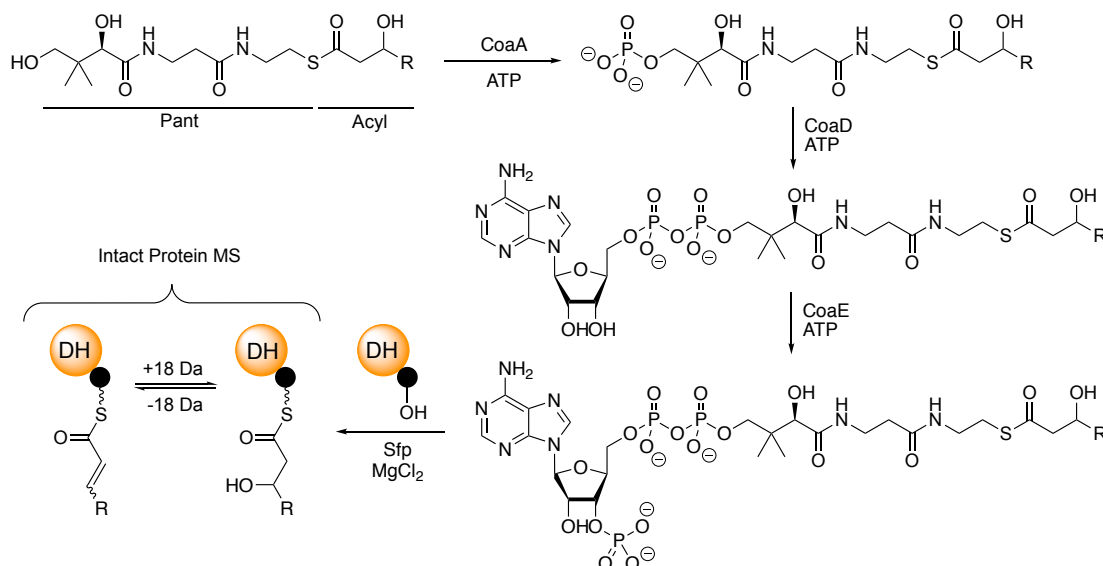
We aimed to biochemically characterize the GbnD5 DH domain found in module 13 of the gladiolin PKS (scheme 2.4). More specifically, using *in vitro* biochemical assays, the role of the DH domain in forming the (*E,Z*)-diene motif found in gladiolin was investigated. A variety of chemically synthesized substrates were used to probe the mechanism and stereospecificity of the domain.



## 2.1.4 *in vitro* Assay used to Probe the DH Domain

Diffusible small molecule probes such as acyl-*N*-acetylcysteamine (SNAC) or acyl-pantetheine substrates have previously been used to investigate the function of individual PKS domains *in vitro*.<sup>71,73,138–143</sup> However this approach has been somewhat less successful when investigating the function of DH domains, potentially due to the slow kinetics of excised DH domains coupled with the reversibility of the reaction.<sup>144</sup> A study by Cane and co-workers even reported an SNAC substrate binding incorrectly in the active site of a DH domain, resulting in reversal of stereospecificity.<sup>127</sup> An alternative approach utilizes ACP-bound substrates.<sup>70,125,127,145</sup>

To probe the catalytic activity of the DH domain from module 13 of the gladiolin PKS, an intact protein mass spectrometry (MS)-based assay was used to detect DH-catalysed dehydration and rehydration. Firstly, the GbnD5 DH-ACP didomain was overproduced (Dr. Matt Jenner) and loaded with chemically synthesized pantetheine thioester substrates.<sup>100</sup> The loading reaction (conditions described in section 6.7.1) consisted of the conversion of the pantetheine thioester to the corresponding acyl-coenzyme A using a cassette of accessory enzymes from *E. coli* (constructs obtained from the group of Dr. Manuela Tosin). This enzymatic approach was used because CoA thioesters can often be challenging to synthesize directly. This is followed by loading onto the ACP domain of the *apo*-DH-ACP didomain using the non-specific 4'-phosphopantethenyl transferase, Sfp (scheme 2.5).<sup>146–148</sup>



**Scheme 2.5** The intact protein MS-based assay used to probe the activity of the GbnD5 DH domain using a representative synthetic pantetheine substrate.

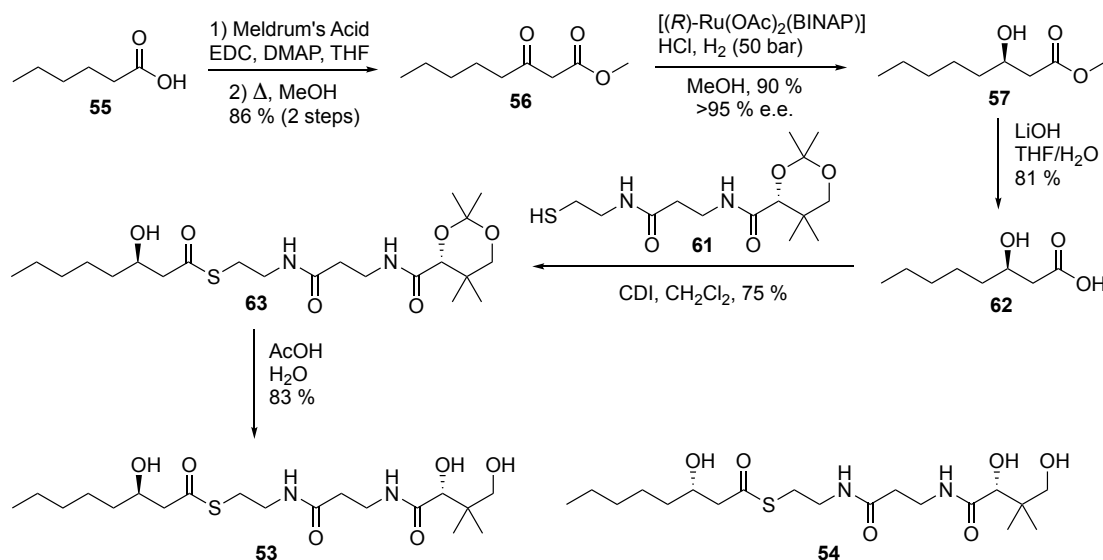
DH-catalysed dehydration or rehydration of loaded substrates could be detected by intact protein MS (section 6.1), as indicated by  $\pm$  18 Da mass shifts (scheme 2.5). It is worth noting that during preliminary experiments the standalone GbnD5 DH domain (overproduced by Dr. Matt Jenner) was found to be unable to dehydrate pantetheine thioesters.

## 2.2 Results and Discussion

### 2.2.1 Catalytic Activity of the GbnD5 DH Domain

#### 2.2.1.1 Dehydration of 3-Hydroxyacyl Thioesters

Firstly, the activity and stereospecificity of the GbnD5 DH domain towards 3-hydroxyacyl thioesters was examined. To do this, both (3*R*)- and (3*S*)-3-hydroxyacyl pantetheine thioesters **53** and **54** were synthesized (scheme 2.6). Commercially available hexanoic acid **55** was converted to  $\beta$ -keto ester **56** via formation of the Meldrum's acid adduct and subsequent thermolysis in methanol. Following this, both (*R*)- and (*S*)-configured 3-hydroxy esters **57** and **58** were prepared via asymmetric reduction under a H<sub>2</sub> atmosphere (50 bar). This was achieved using Noyori's (*R*)- or (*S*)-BINAP ruthenium catalysts, respectively, and afforded the desired alcohols in excellent yield and enantiomeric excess (*e.e.*).<sup>149,150</sup> The stereochemistry of the alcohols were confirmed via comparison of optical rotation values to those in the literature, and the *e.e.* was calculated from NMR shifts after conversion to the Mosher's esters **59** and **60**.<sup>151</sup> Saponification followed by coupling with protected pantetheine **61** using 1'-carbonyldiimidazole (CDI) and removal of the acetonide protecting group using acidic conditions afforded **53** and **54**.<sup>152</sup>



**Scheme 2.6** The synthetic route used to prepare (3*R*)-3-hydroxyacyl pantetheine thioester **53**. **54** was generated in similar yields, using an analogous procedure.

The (3*R*)- and (3*S*)-3-hydroxyacyl pantetheine thioesters, **53** and **54**, were separately loaded onto the GbnD5 DH-ACP didomain using the method described in section 6.7.1 and incubated for 3 h. The deconvoluted spectra from intact protein MS analyses showed that the DH domain can dehydrate the (3*R*)-3-hydroxyacyl thioester (figure 2.4). In contrast, the (3*S*)-3-hydroxyacyl thioester was not significantly dehydrated. The *apo*-DH-ACP didomain was also subjected to intact protein MS analysis without the loaded pantetheine substrate as a negative control (appendix 8.4). No dehydration was observed confirming that the dehydration is occurring at the loaded acyl chain.

To determine the geometry of the unsaturated product resulting from the DH-catalyzed dehydration of the (3*R*)-3-hydroxyacyl thioester, attempts were made to cleave the product from the DH-ACP didomain. However, attempts at both enzymatic and chemical cleavage of the DH-ACP-bound 2-enoyl thioester were unsuccessful. It was thought that this may be due to the DH domain blocking the cleavage of the ACP-bound pantetheine thioester.

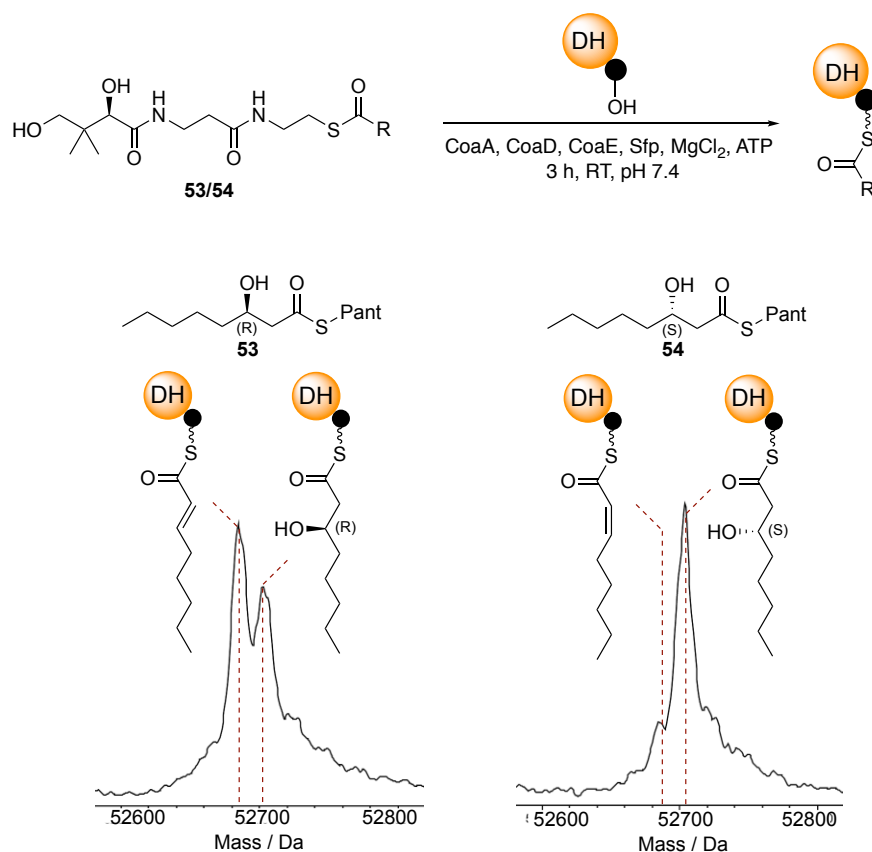
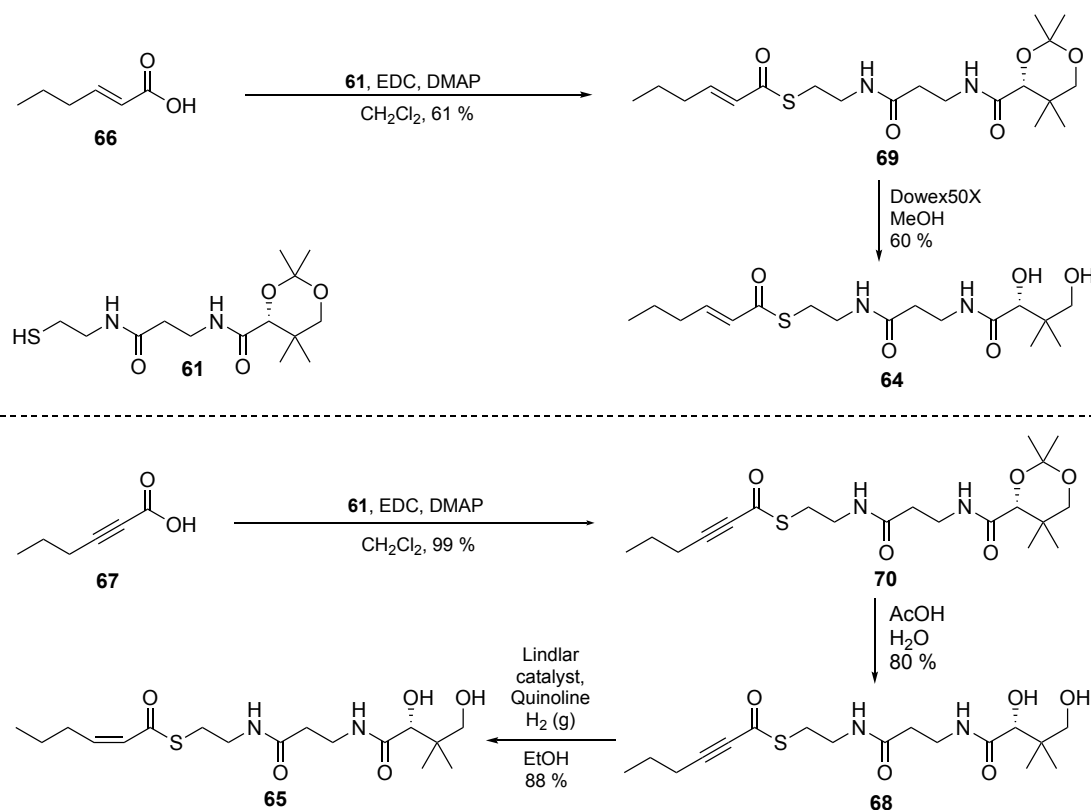


**Figure 2.4** Deconvoluted spectra from intact protein MS analyses of the GbnD5 DH-ACP didomain onto which thioesters **53** and **54** were loaded. The corresponding masses of the dehydrated and rehydrated species can be found in appendix **8.5**.

### 2.2.1.2 Rehydration of *E*- and *Z*-configured 2-Enoyl Thioesters

If dehydration of the (3*R*)-3-hydroxyacyl thioester proceeds via a *syn*-elimination mechanism, the (2*E*)-2-enoyl thioester should be produced.<sup>125,127</sup> Because it was not possible to determine the geometry of the dehydration product directly, the ability of the DH domain to catalyze rehydration of (2*E*)- and (2*Z*)-2-enoyl thioesters was examined. Both (2*E*)- and (2*Z*)-2-enoyl pantetheine thioesters, **64** and **65**, were synthesized according to the route shown in scheme **2.7**. The (2*E*)-2-enoyl pantetheine thioester **64** (synthesized by Dr. Doug Roberts) was prepared via the coupling of commercially available (2*E*)-2-hexenoic acid **66** with protected pantetheine **61**, and subsequent deprotection using an acidic resin.<sup>73</sup> The (2*Z*)-2-enoyl pantetheine thioester **65** was synthesized by coupling of commercially available hexynoic acid **67** to protected pantetheine **61**, acidic deprotection to afford alkyne **68**, and hydrogenation over Lindlar's catalyst. This reaction was slow, presumably because the thioester poisons the palladium catalyst, and additional catalyst had to be added at regular intervals. However after ten days and

addition of almost a stoichiometric amount of catalyst, (2*Z*)-2-enoyl pantetheine thioester **63** was produced. It was necessary for the (*Z*)-configured alkene to be installed in the last step, because the acidic conditions used for removal of the acetonide group promoted the isomerization of the (*Z*)-configured alkene to the (*E*)-configured isomer.



**Scheme 2.7** Synthesis of (2*E*)- and (2*Z*)-2-enoyl pantetheine thioesters, **64** (Dr. Douglas Roberts) and **65**.

The (2*E*)- and (2*Z*)-2-enoyl pantetheine substrates, **64** and **65** were separately loaded onto the GbnD5 DH-ACP didomain (figure 2.5). The deconvoluted spectra from intact protein MS analyses showed that the DH domain rehydrates the (2*E*)-2-enoyl thioester (figure 2.5). In contrast, no rehydration of the (2*Z*)-2-enoyl thioester was observed.

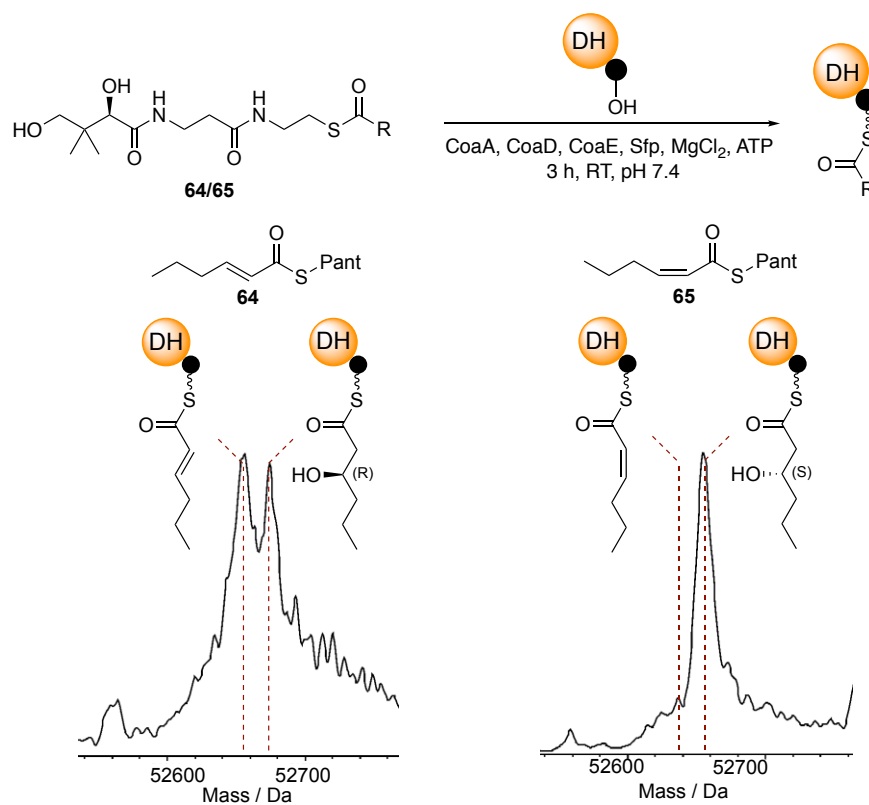
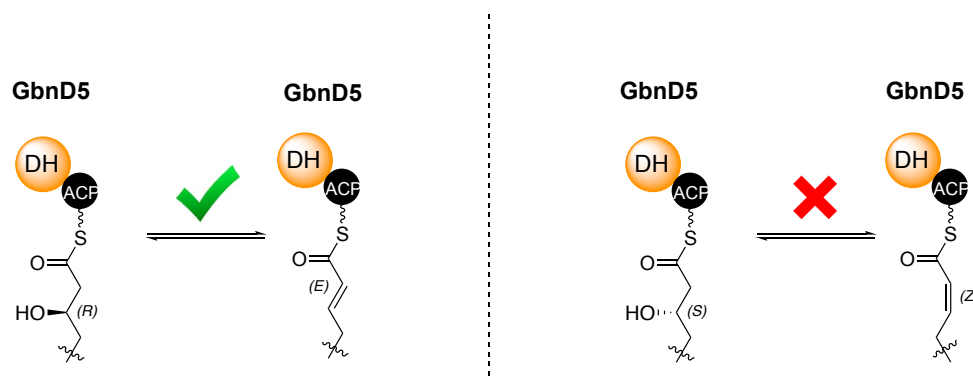


**Figure 2.5** Deconvoluted spectra from intact protein MS analyses of the GbnD5 DH-ACP didomain onto which thioesters **64** and **65** were loaded.

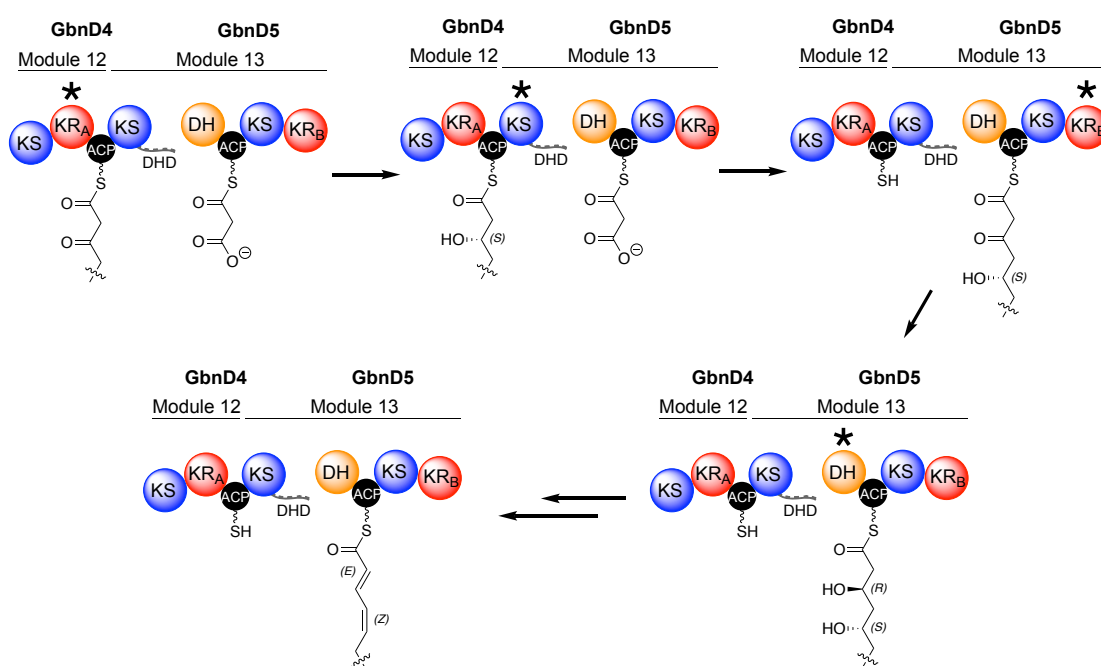
These data indicate that the DH domain catalyzes the interconversion of (3*R*)-3-hydroxyacyl and (2*E*)-2-enoyl thioesters, but cannot interconvert (3*S*)-3-hydroxyacyl and (2*Z*)-2-enoyl thioesters (scheme **2.8**). This behaviour is consistent with the *syn*-elimination of water from (3*R*)-3-hydroxyacyl thioesters observed for other DH domains.



**Scheme 2.8** The GbnD5 DH domain catalyzes the interconversion of (3*R*)-3-hydroxyacyl and (2*E*)-2-enoyl thioesters, but cannot interconvert (3*S*)-3-hydroxyacyl and (2*Z*)-2-enoyl thioesters.

### 2.2.1.3 Dehydration of a (3*R*,5*S*)-3,5-Dihydroxyacyl Thioester Intermediate

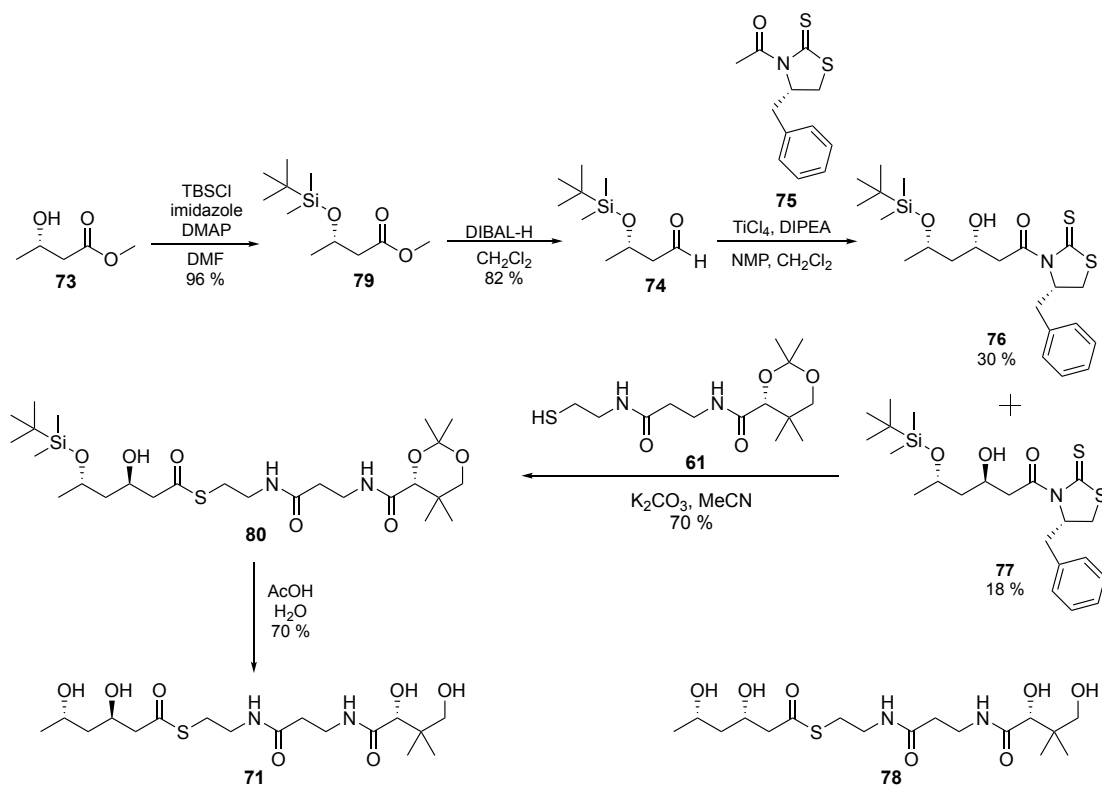
In section 2.2.1.1, it was shown that the DH domain is able to dehydrate a (3*R*)-3-hydroxyacyl thioester. The KR domain predicted to produce a (3*R*)-3-hydroxyacyl thioester (KR<sub>B</sub> domain) is downstream of the DH domain (scheme 2.9). Thus, the role of the KR domain upstream of the DH domain (in module 12) is unclear. Given that this domain is predicted to produce a (3*S*)-3-hydroxyacyl thioester (KR<sub>A</sub> domain), it was proposed that the DH domain converts a (3*R*,5*S*)-3,5-dihydroxyacyl thioester (generated via the steps shown in scheme 2.9) to an (*E*,*Z*)-diene via an unprecedented double dehydration.



**Scheme 2.9** The biosynthetic steps involved in generating the (3*R*,5*S*)-3,5-dihydroxyacyl thioester intermediate proposed to be the substrate for the GbnD5 DH domain. \* Denotes the PKS domain involved in catalyzing each step.

To examine whether the DH domain is able to catalyze double dehydration of a (3*R*,5*S*)-3,5-dihydroxyacyl thioester to an (*E*,*Z*)-diene, the (3*R*,5*S*)-3,5-dihydroxyacyl and (2*E*,4*Z*)-dienoyl pantetheine thioesters, **71** and **72**, were synthesized and loaded onto the GbnD5 DH-ACP didomain to investigate the dehydration and rehydration reactions, respectively.

The (3*R*,5*S*)-3,5-dihydroxyacyl pantetheine thioester, **71**, was synthesized from commercially available methyl (3*S*)-3-hydroxybutanoate **73**. The alcohol was *tert*-butyldimethylsilyl (TBS) protected, followed by reduction of the ester to the corresponding aldehyde **74** using diisobutylaluminium hydride (DIBAL-H). Following the procedure of Vederas *et al.*, the aldehyde **74** was used in a TiCl<sub>4</sub>-catalyzed, non-selective aldol reaction with **75**, this led to the formation of the *syn*- and *anti*-diastereomers, **76** and **77**, which were separable by silica chromatography.<sup>153</sup> The chiral auxiliary was then displaced using protected pantetheine **61** under basic conditions, and both the TBS and acetonide protecting groups were removed under acidic conditions to afford the (3*R*,5*S*)-3,5-dihydroxyacyl pantetheine thioester, **71** (scheme 2.10). (3*S*,5*S*)-3,5-Dihydroxyacyl pantetheine thioester, **78** was also synthesized via this route from the *syn*-diastereomer **76** (section 2.2.3.1).



**Scheme 2.10** Synthesis of the (3*R*,5*S*)-3,5-dihydroxyacyl pantetheine thioester, **71**. The (3*S*,5*S*)-3,5-dihydroxyacyl pantetheine thioester, **78**, was made via the same route.



The relative stereochemistry of the *syn*- and *anti*-diastereomers, **76** and **77**, was confirmed by comparing chemical shift values in the  $^1\text{H}$  NMR spectrum with those reported by Vederas *et. al.*, as well as comparing coupling constants with those reported for similar compounds in the literature (figure 2.6).<sup>153,154</sup>

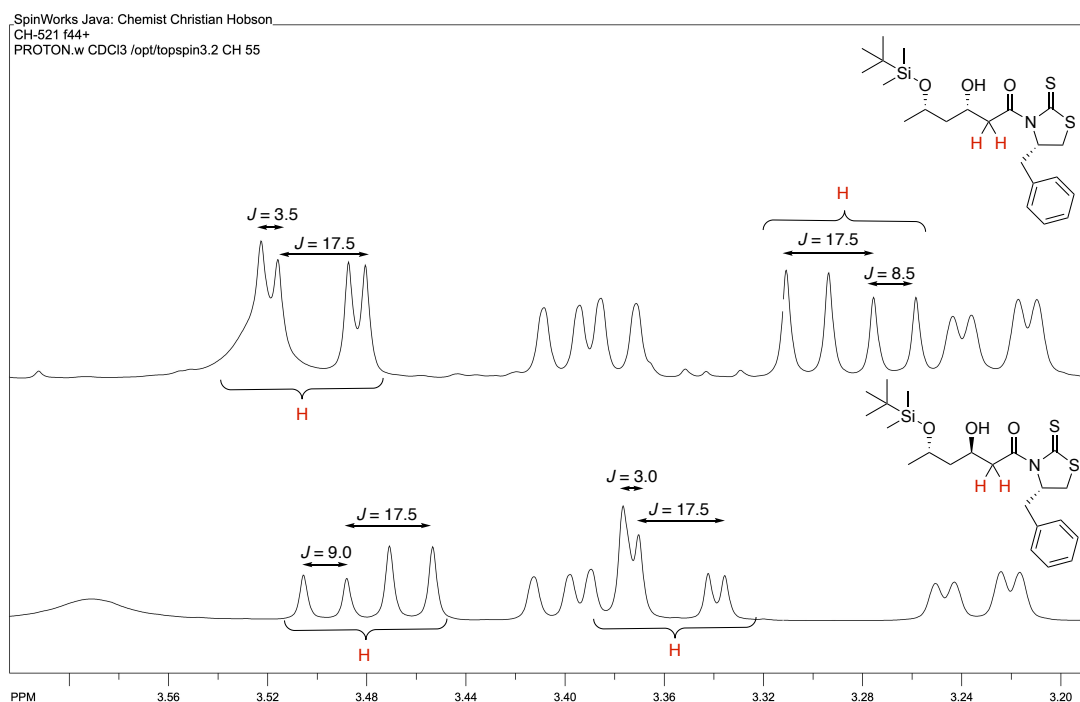
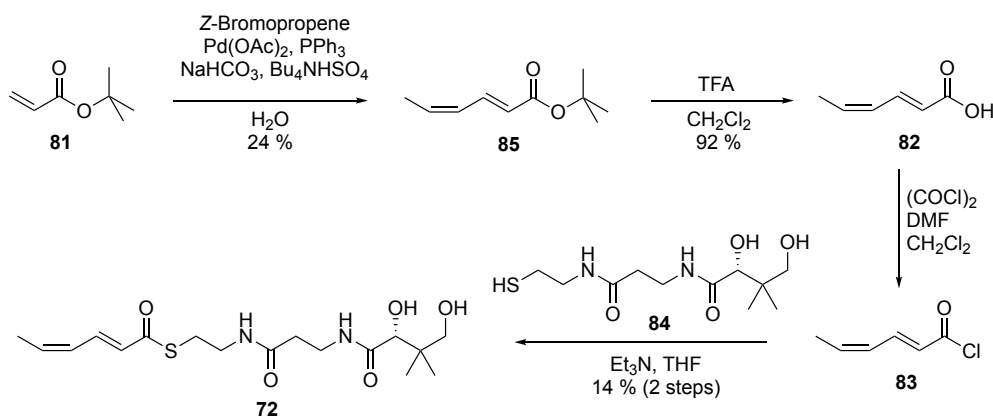


**Figure 2.6** Regions of  $^1\text{H}$  NMR spectra for **76** and **77**. According to a study by Hodge *et. al.*, the  $\alpha$ -protons (red) of *syn*- and *anti*-Evans' aldol products have diagnostic coupling constants, allowing assignment of relative stereochemistry. The upfield  $\alpha$ -proton of the *syn*-product is predicted to have coupling constants of around 17.6 and 2.7 Hz, and the downfield  $\alpha$ -proton 17.6 and 9.5 Hz. The upfield  $\alpha$ -proton of the *anti*-product is predicted to have coupling constants of around 17.5 and 9.5 Hz, and the downfield  $\alpha$ -proton 17.5 and 3.1 Hz. The coupling constants for the  $\alpha$ -protons of both **76** and **77** appear to be in agreement with this study.<sup>154</sup>

(*2E,4Z*)-Dienoyl pantetheine thioester, **72**, was synthesized from commercially available *tert*-butyl acrylate **81**. Following a procedure reported by Davies *et. al.*, *tert*-butyl acrylate **81** was coupled with (*Z*)-bromopropene via a Heck-type coupling reaction, and the *tert*-butyl protecting group was removed under acidic conditions to afford (*2E,4Z*)-2,4-hexadienoic acid **82**.<sup>155</sup> Initially, acid **82** was coupled to protected pantetheine **61** and deprotected using acidic conditions as conducted previously. However, the acidic deprotection conditions caused isomerization of the (*E,Z*)-diene to an (*E,E*)-diene. To overcome this, the acid **82** was converted to the corresponding acid chloride **83** and condensed with pantetheine **84** in a one-pot procedure

to afford the (2*E*,4*Z*)-dienoyl pantetheine thioester, **72**, in a poor yield but with the desired (*E*,*Z*)-diene geometry (scheme 2.11).



**Scheme 2.11** Synthesis of (2*E*,4*Z*)-dienoyl pantetheine thioester, **72**.

The (3*R*,5*S*)-3,5-dihydroxyacyl and (2*E*,4*Z*)-dienoyl pantetheine thioesters, **71** and **72**, were separately loaded onto the GbnD5 DH-ACP didomain and intact protein MS analysis was conducted (figure 2.7). A cluster of three peaks, each separated by 18 Da, was observed for the (3*R*,5*S*)-3,5-dihydroxyacyl pantetheine thioester, **71**. The peak with the greatest mass corresponds to the loaded diol. The central peak is consistent with a (2*E*,5*S*)-5-hydroxy-2-enoyl thioester resulting from elimination of the (3*R*)-configured hydroxyl group, as observed in earlier assays (section 2.2.1.1), however this species could also correspond to a species resulting from elimination of the C-5 hydroxyl group. The remaining peak is consistent with a (2*E*,4*Z*)-2,4-dienoyl thioester, and indicates that the GbnD5 DH domain is able to catalyze a double dehydration. Loading of the (2*E*,4*Z*)-dienoyl pantetheine thioester, **72**, results in the same cluster of three peaks, indicating that the *E*,*Z*-diene can be fully rehydrated back to the diol via a mono-rehydrated intermediate (figure 2.7). These results indicate that the GbnD5 DH domain can reversibly dehydrate a (3*R*,5*S*)-3,5-dihydroxyacyl thioester, to form a (2*E*,4*Z*)-dienoyl thioester, which is predicted to correspond to the *E*,*Z*-diene motif in gladiolin **29**.

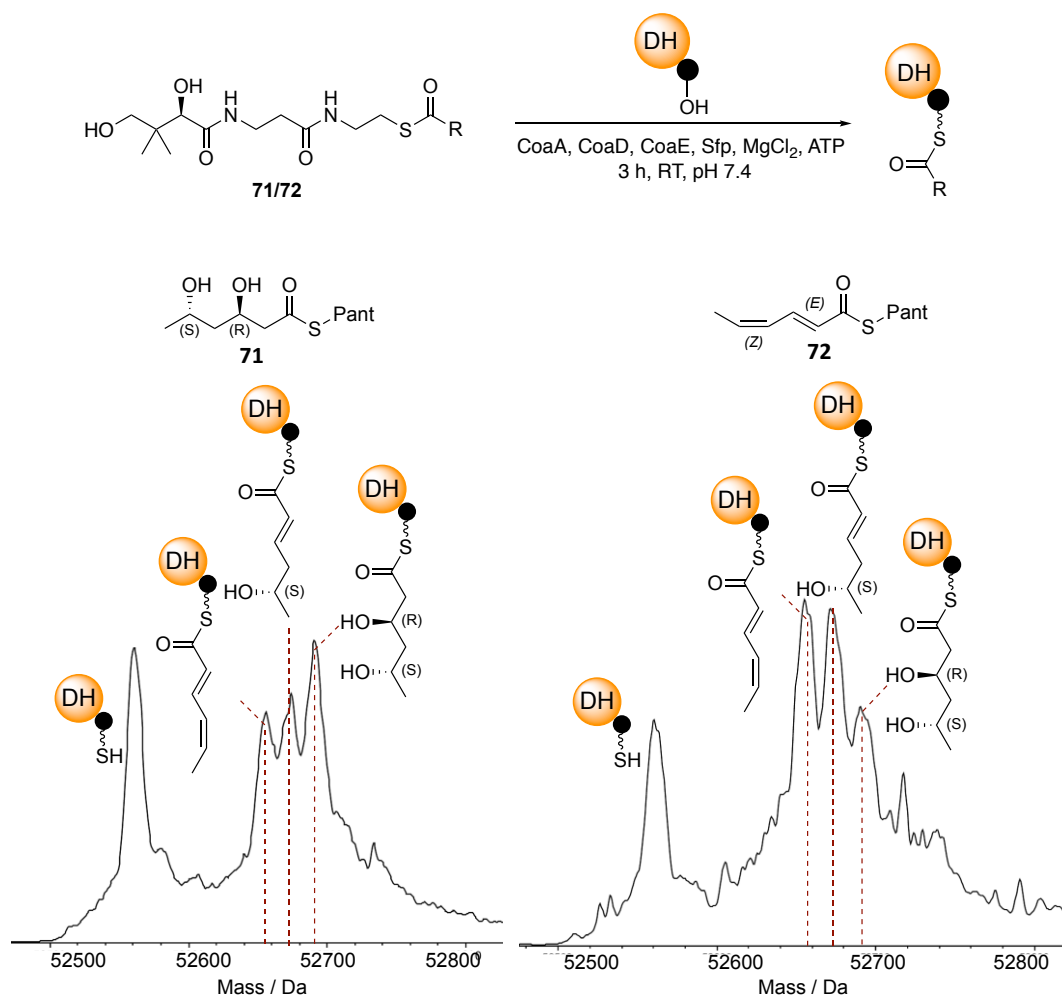


**Figure 2.7** Deconvoluted spectra from intact protein MS analyses of the GbnD5 DH-ACP didomain onto which thioesters **71** and **72** were loaded. Note the presence of a peak in both spectra corresponding to the *holo*-DH-ACP didomain, This presumably arises from spontaneous  $\delta$ -lactonization of the diols.

This is the first biochemical evidence for double dehydration catalyzed by a DH domain. The data obtained are consistent with a *syn*-elimination mechanism in which the (*R*)-configured alcohol is eliminated to form an (*E*)-configured alkene and the (*S*)-configured alcohol yields a (*Z*)-configured alkene. However, the mechanistic details and structural features of the GbnD5 DH domain which enable it to catalyze a double dehydration required further investigation.

## 2.2.2 Catalytic Mechanism of the GbnD5 DH Domain

### 2.2.2.1 Identification of an Additional Active Site Histidine Residue

To better understand the mechanism of the double dehydration reaction catalyzed by the GbnD5 DH domain, the sequences of DH domains from type B split modules (including the GbnD5 DH

domain) were aligned with sequences of well-characterized, *cis*-AT PKS DH domains. (Dr. Matt Jenner, figure 2.8).

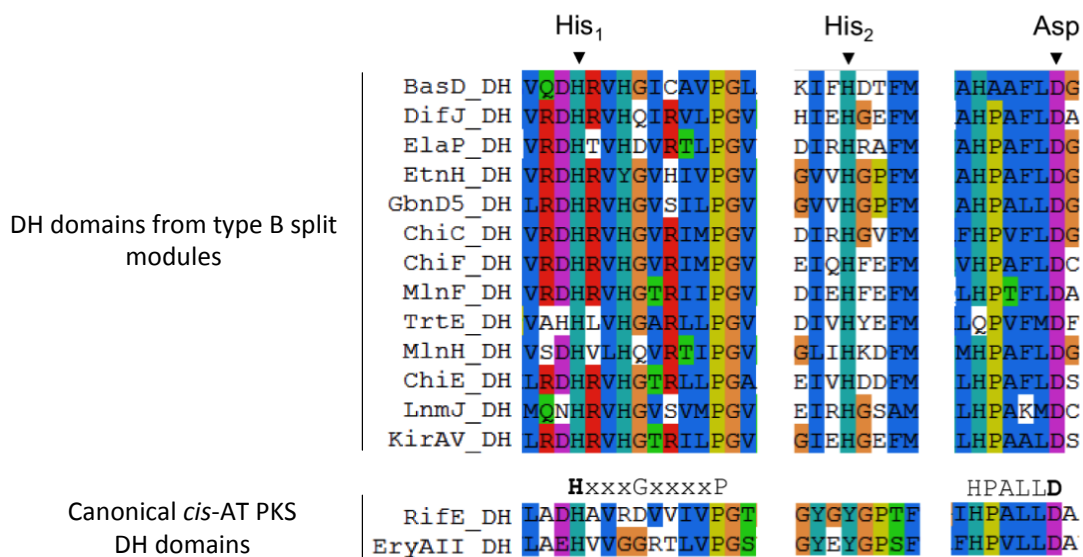


**Figure 2.8** Sequence alignment of DH domains predicted to catalyze double dehydrations with canonical DH domains from *cis*-AT PKSs.

The alignment shows that DH domains from type B split modules contain a histidine residue (His<sub>2</sub>) in place of a conserved tyrosine residue in *cis*-AT PKS DH domains. In light of this, a homology model of the GbnD5 DH domain, based on the crystal structure of a DH domain from a type B split module in the diffidicin PKS, was generated (Dr. Matt Jenner, figure 2.9).<sup>99</sup>

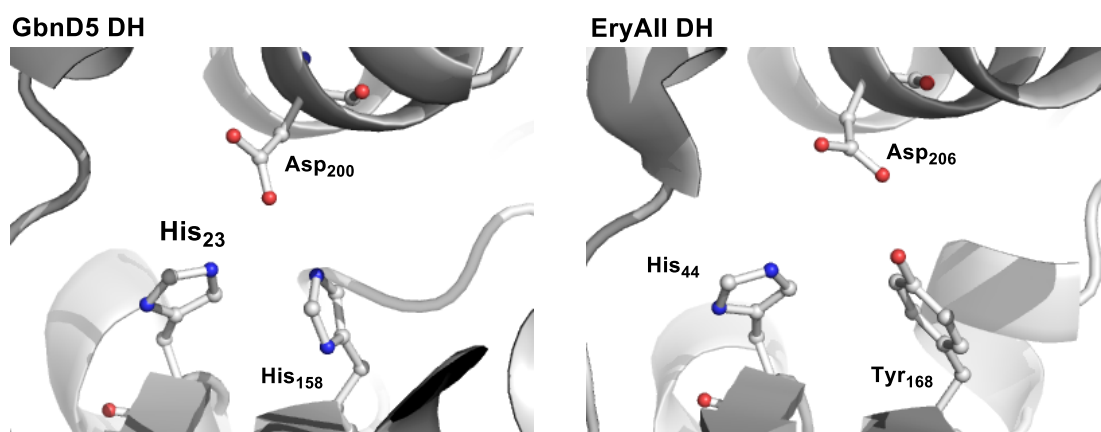
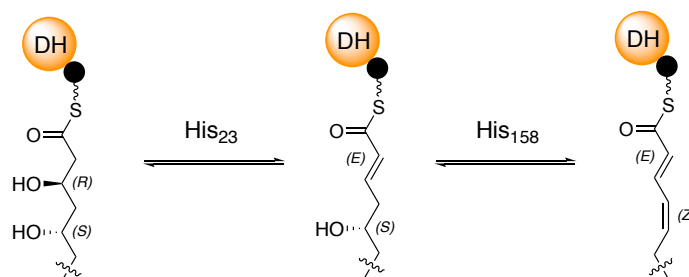


**Figure 2.9** The homology model of the GbnD5 DH domain indicating that it contains an additional active site histidine residue (His<sub>158</sub>) compared with the EryAII DH domain active site.

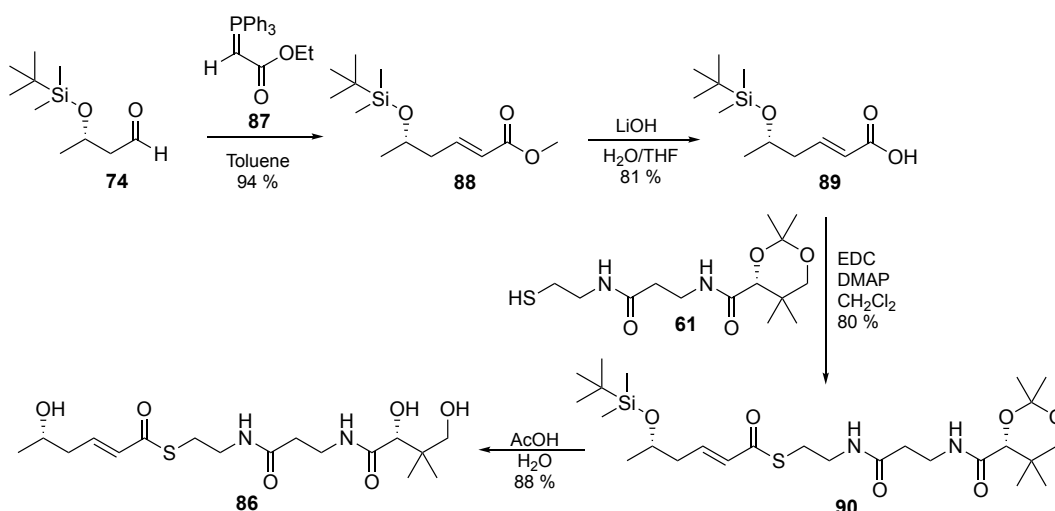
The additional histidine residue appears to be ideally positioned to catalyze dehydration of a (*2E,5S*)-5-hydroxy-2-enoyl thioester (scheme 2.12). Keatinge-Clay and co-workers noticed the presence of this additional active site histidine residue in the DH domain from module 10 of the difficidin PKS. However, they suggested it is unlikely to be involved in catalysis due to the proximity of the residue with respect to the pantetheine-bound acyl chain.<sup>99</sup>



**Scheme 2.12** Proposed roles of His<sub>23</sub> and His<sub>158</sub> in the double dehydration reaction catalyzed by the GbnD5 DH domain.

### 2.2.2.2 The Additional Histidine is Required for a Vinylogous Dehydration

To investigate the role played by the additional histidine residue, (*2E,5S*)-5-hydroxy-2-enoyl pantetheine thioester, **86**, was synthesized (scheme 2.13). The (*E*)-configured double bond was introduced via a Wittig reaction between aldehyde **74** (scheme 2.10) and stabilized phosphorane **87**. Hydrolysis of the ester, followed by coupling with protected pantetheine **61** and removal of both the TBS and acetonide protecting groups under acidic conditions culminated in the formation of (*2E,5S*)-5-hydroxy-2-enoyl pantetheine thioester, **86**.



**Scheme 2.13** Synthesis of (*2E,5S*)-5-hydroxy-2-enoyl pantetheine thioester, **86**.

The (*2E,5S*)-5-hydroxy-2-enoyl pantetheine thioester, **86**, was loaded onto the DH-ACP didomain (figure **2.10**). The same cluster of three peaks was observed in the intact protein MS analysis as for both the diol and diene substrates, **71** and **72**, indicating that the (*2E,5S*)-5-hydroxy-2-enoyl thioester is an intermediate in diene formation. When the (*2E,5S*)-5-hydroxy-2-enoyl pantetheine thioester, **86**, is loaded onto a H158Y mutant (generated by Dr. Matt Jenner) of the DH-ACP didomain, only peaks corresponding to the loaded thioester and the diol resulting from addition of water to the C=C double bond were observed. This confirms that His<sub>158</sub> is involved in diene formation.

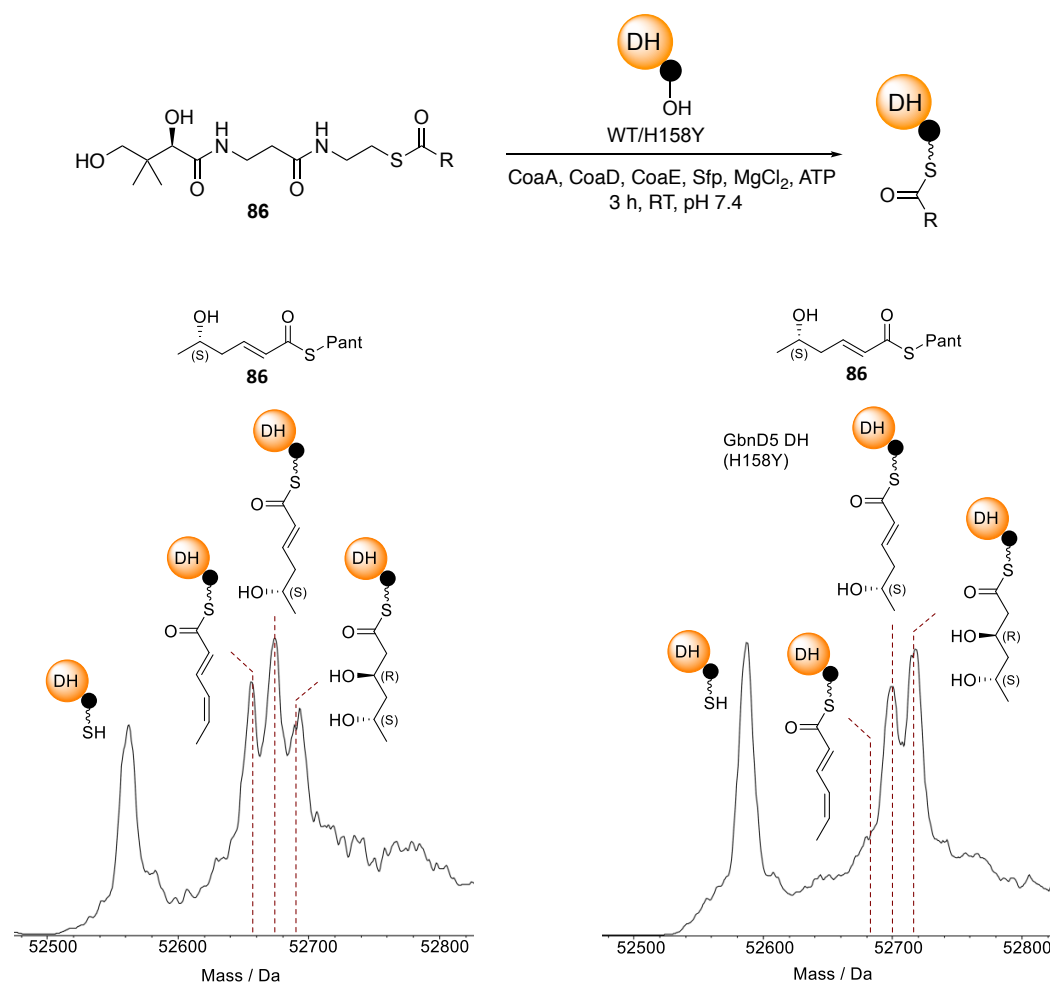
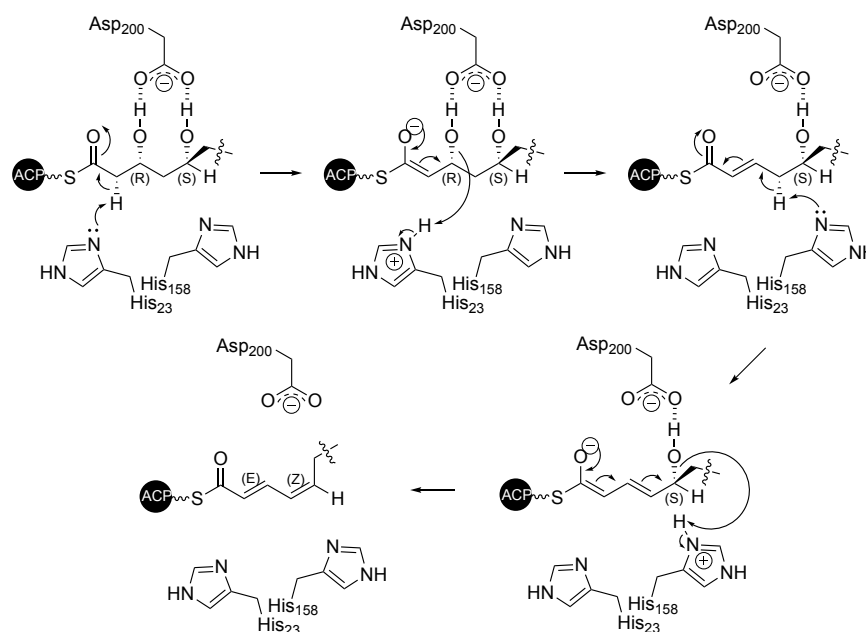


**Figure 2.10** The deconvoluted intact protein MS of the GbnD5 DH-ACP didomain (left) and the H158Y mutant (right) after the loading of pantetheine thioester **86**.

It is proposed that His<sub>158</sub> deprotonates the (*2E,5S*)-5-hydroxy-2-enoyl thioester intermediate at the C-4 position, affording a vinylogous enolate intermediate that eliminates the C-5 hydroxyl group with concomitant proton transfer from the His<sub>158</sub> residue. The aspartate residue is proposed to position the substrate appropriately via hydrogen bonding interactions (scheme

**2.14).** This is analogous to a vinylogous dehydration recently observed in curacin biosynthesis, and is consistent with the “single base” mechanism proposed by Cane and co-workers.<sup>71,132</sup>

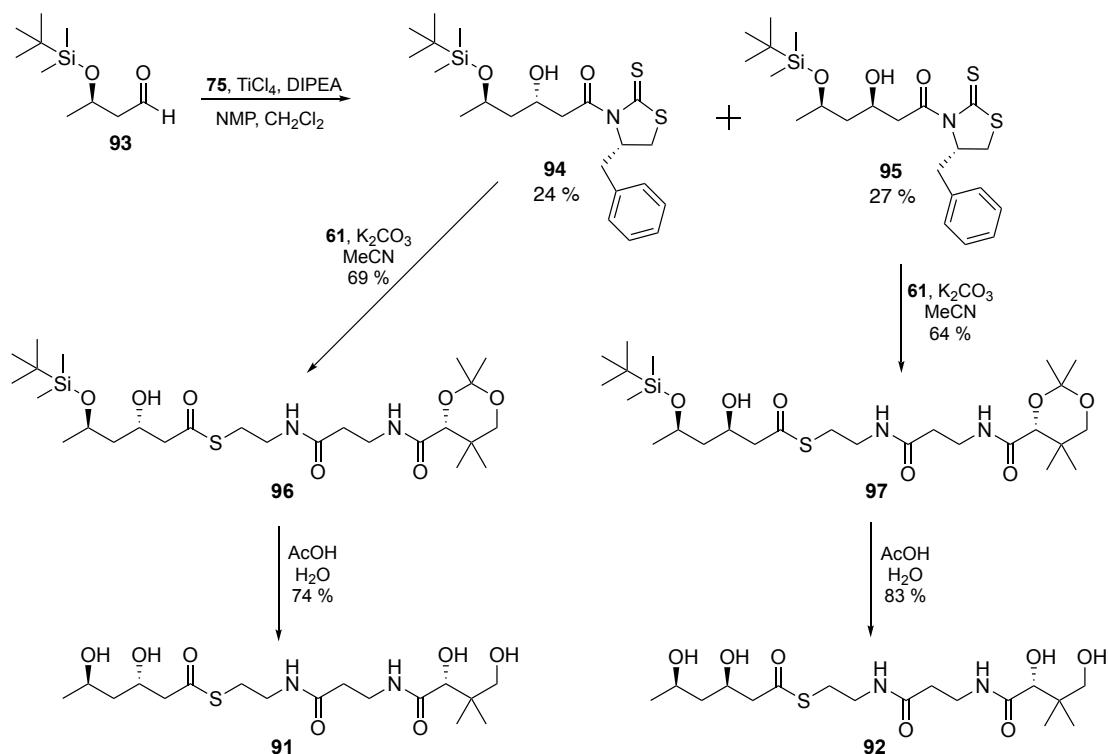


**Scheme 2.14** The proposed mechanism of the double dehydration reaction catalyzed by the GbnD5 DH domain.

## 2.2.3 Substrate Tolerance of the GbnD5 DH Domain

### 2.2.3.1 Dehydration of Stereoisomeric 3,5-Dihydroxyacyl Thioesters

To more fully evaluate the substrate tolerance of the GbnD5 DH domain, the three diastereomers of (3*R*,5*S*)-3,5-dihydroxyacyl pantetheine thioester, **71**, were also synthesized and loaded onto the GbnD5 DH-ACP didomain. (3*S*,5*S*)-3,5-Dihydroxyacyl pantetheine thioester, **78**, was synthesized via the route shown in scheme **2.10**. The (3*S*,5*R*)- and (3*R*,5*R*)-3,5-dihydroxyacyl pantetheine thioesters, **91** and **92** respectively, were synthesized using the route shown in scheme **2.15**. Aldehyde **93** was synthesized via the same route and with similar yields to aldehyde **74** (scheme **2.10**) from commercially available methyl (3*R*)-3-hydroxybutanoate. The aldehyde was then subjected to the same TiCl<sub>4</sub>-catalyzed aldol reaction as used previously, yielding a separable mixture of aldol products. The relative stereochemistry of the products, **94** and **95**, was again confirmed by the analysis of diagnostic coupling constants in the <sup>1</sup>H NMR spectrum, as was conducted for diastereomers **76** and **77** (figure **2.6**). The auxiliary was displaced using protected pantetheine **61**, and acid catalyzed deprotection afforded the desired thioesters.



**Scheme 2.15** Synthesis of 3,5-dihydroxyacyl pantetheine thioesters, **91** and **92**.

Pantetheine thioesters **78**, **91** and **92** were loaded onto GbnD5 DH-ACP didomain and DH-catalyzed activity was examined using intact protein MS analysis (figure **2.11**). As expected, negligible dehydration was observed for thioesters **78** and **91**. This was unsurprising because it had already been shown that the DH domain is not capable of processing (3*S*)-configured substrates (section **2.2.1.1**). Interestingly, peaks corresponding to a mono-dehydrated and a doubly dehydrated species were observed for thioester **92**. The single dehydration was expected because it had already been shown that the DH domain is capable of processing (3*R*)-configured substrates (section **2.2.1.1**). However, the additional dehydration, which is thought to result in the formation of an (*E,E*)-configured diene, suggests that the DH domain may be promiscuous with respect to the stereochemistry of the C-5 hydroxyl group.



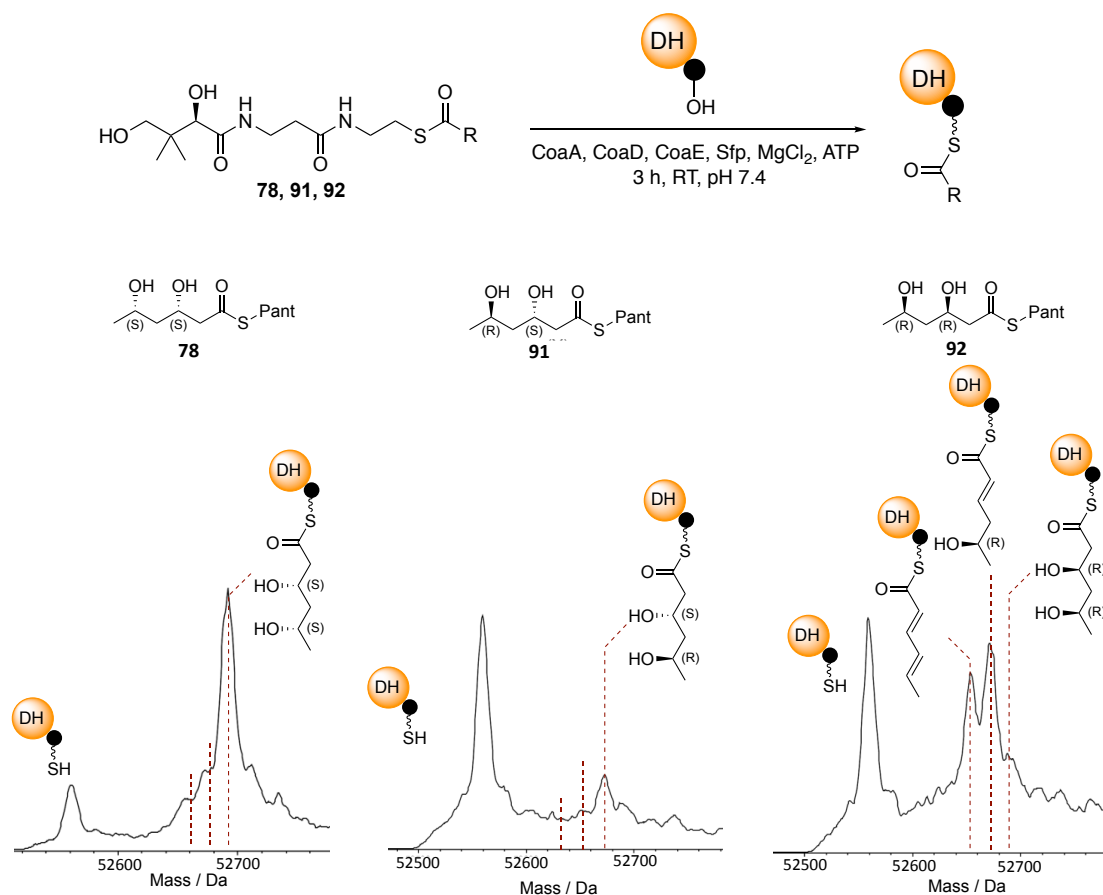
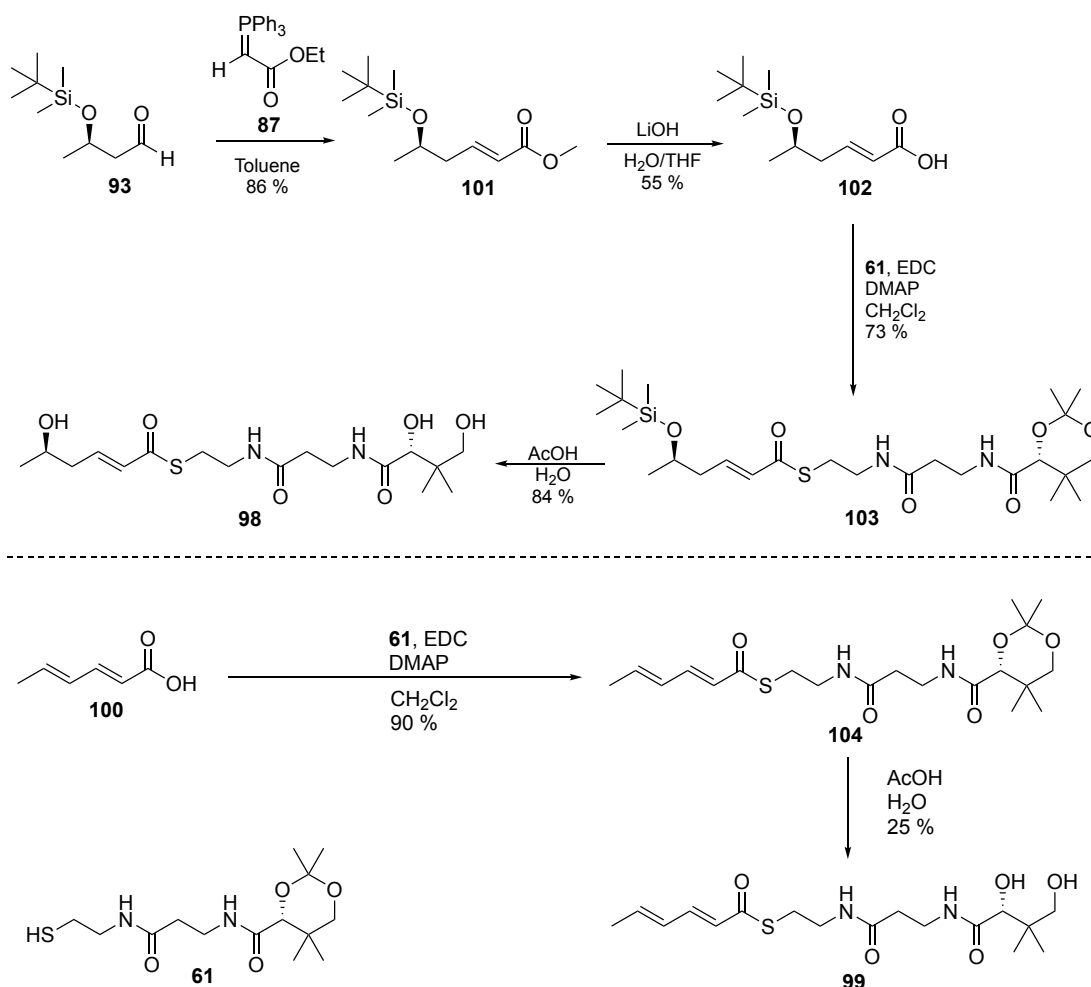


**Figure 2.11** The deconvoluted intact protein MS of the GbnD5 DH-ACP didomain loaded with substrates **78**, **91** and **92**.

### 2.2.3.2 Rehydration of an (*E,E*)-Configured Dienoyl Thioester

To investigate GbnD5 DH-catalysed, (*E,E*)-configured diene formation, (*2E,5R*)-5-hydroxy-2-enoyl and (*2E,4E*)-dienoyl pantetheine thioesters, **98** and **99**, were synthesized using the routes shown in scheme **2.16**. (*2E,5R*)-5-Hydroxy-2-enoyl pantetheine thioester, **98**, was synthesized in the same way as the (*2E,5S*)-5-hydroxy-2-enoyl pantetheine thioester, **86**, using aldehyde **93** as the starting material. The (*2E,4E*)-dienoyl pantetheine thioester, **99**, was synthesized via the coupling of commercially available sorbic acid **100**, to protected pantetheine **61**, followed by acid-catalyzed deprotection. The product, **99**, was isolated in a poor yield. This may be due to polymerization which appears to be promoted by the acidic conditions.



**Scheme 2.16** Syntheses of (2*E*,5*R*)-5-hydroxy-2-enoyl and (2*E*,4*E*)-dienoyl pantetheine substrates, **98** and **99**, respectively.

Both thioester substrates, **98** and **99**, were loaded onto GbnD5 DH-ACP didomain (figure **2.12**). Intact protein MS analysis showed that the (2*E*,5*R*)-5-hydroxy-2-enoyl thioester is converted to a diene, confirming that the DH domain is capable of eliminating a (5*R*)-configured hydroxyl group. However, no significant peak corresponding to rehydration to the diol is observed. A peak corresponding to a mono-rehydrated species is observed for the (2*E*,4*E*)-dienoyl thioester, but there is again no significant peak corresponding to a diol present. This suggests that the GbnD5 DH domain is capable of dehydrating a (3*R*,5*R*)-3,5-dihydroxyacyl thioester to a (2*E*,4*E*)-dienoyl thioester. However, it cannot rehydrate the diene to a diol, perhaps because it is not the native substrate of the DH domain. This is further confirmation that the diene installed by the DH domain has an *E,Z*-geometry, as the (2*E*,4*Z*)-dienoyl thioester was fully rehydrated back to the diol (section **2.2.1.3**), indicating that this is the native geometry installed by the domain.

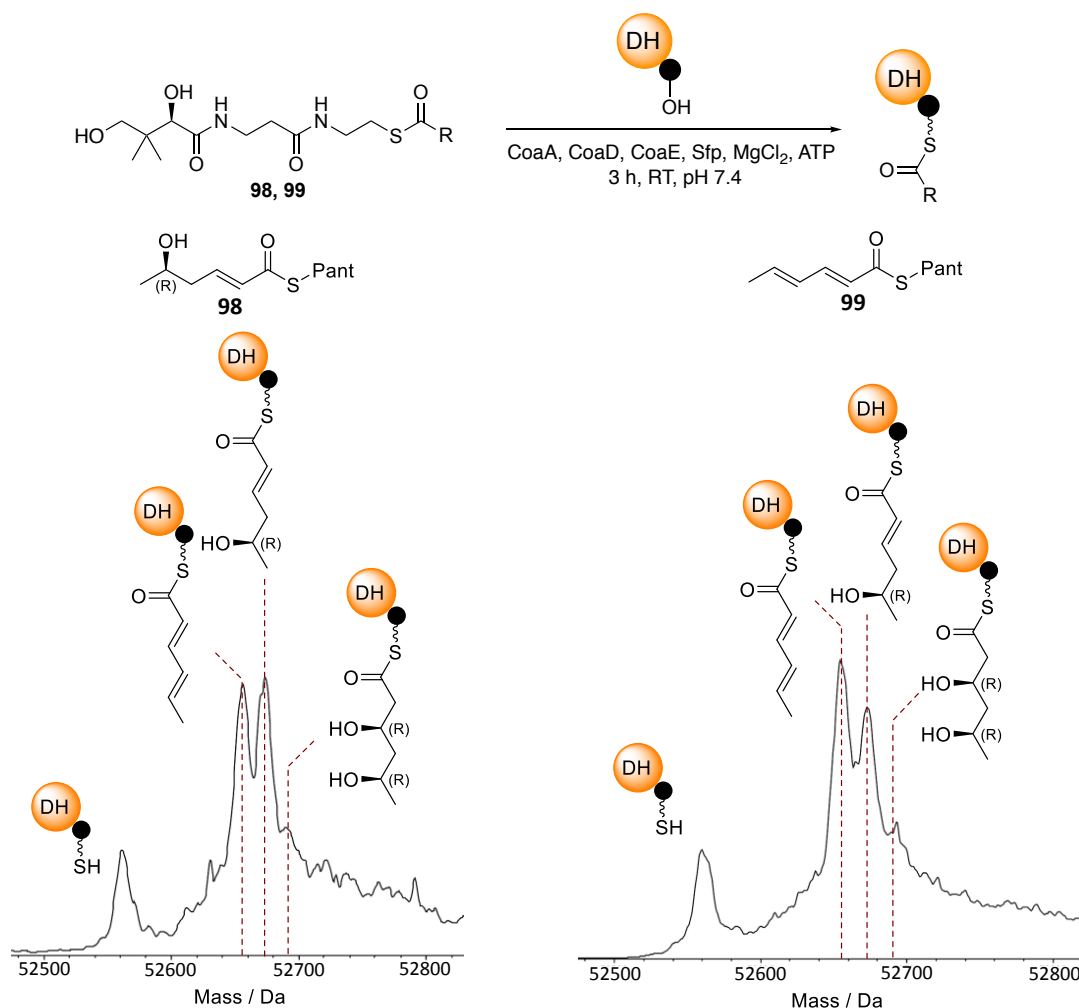


**Figure 2.12** The deconvoluted intact protein MS of the GbnD5 DH-ACP didomain loaded with substrates **98** and **99**.

## 2.3 Conclusions

### 2.3.1 Summary

In this study, the first example of a DH domain capable of catalyzing a double dehydration was discovered. The GbnD5 DH domain has been shown to reversibly dehydrate a (3*R*,5*S*)-3,5-dihydroxyacyl thioester to form a (2*E*,4*Z*)-2,4-dienoyl thioester corresponding to the *E,Z*-diene observed in gladiolin. An additional histidine residue in the active site of the DH domain was identified, and was shown to catalyze dehydration of a (2*E*,5*S*)-5-hydroxy-2-enoyl thioester intermediate. The substrate tolerance of the domain was investigated using a variety of pantetheine thioesters, and it was shown to also be capable of producing an (*E,E*)-diene from a (3*R*,5*R*)-3,5-dihydroxyacyl thioester.

### 2.3.2 Diene Synthase Domains in Other Systems

A phylogenetic analysis (conducted by Dr. Matt Jenner, appendix 8.1) identified several other DH domains that are predicted to install dienes into their respective polyketide products. Most of these are part of dehydrating bimodules, but some are incorporated into conventional modules and some are present in *cis*-AT PKS systems. In most cases they appear to be responsible for (*E,Z*)-diene formation. However, one example (tartrolon) is predicted to form an (*E,E*)-diene, consistent with the observation that the GbnD5 DH domain can convert a (3*R*,5*R*)-3,5-dihydroxyacyl thioester to a diene (section 2.2.3.2). Two examples of systems predicted to harbor DH domains that install dienes (leinamycin 105 and macrolactin A 106 biosynthesis) are shown in figure 2.13, and the domain architectures of more systems with these DH domains can be found in section 5.1.1.

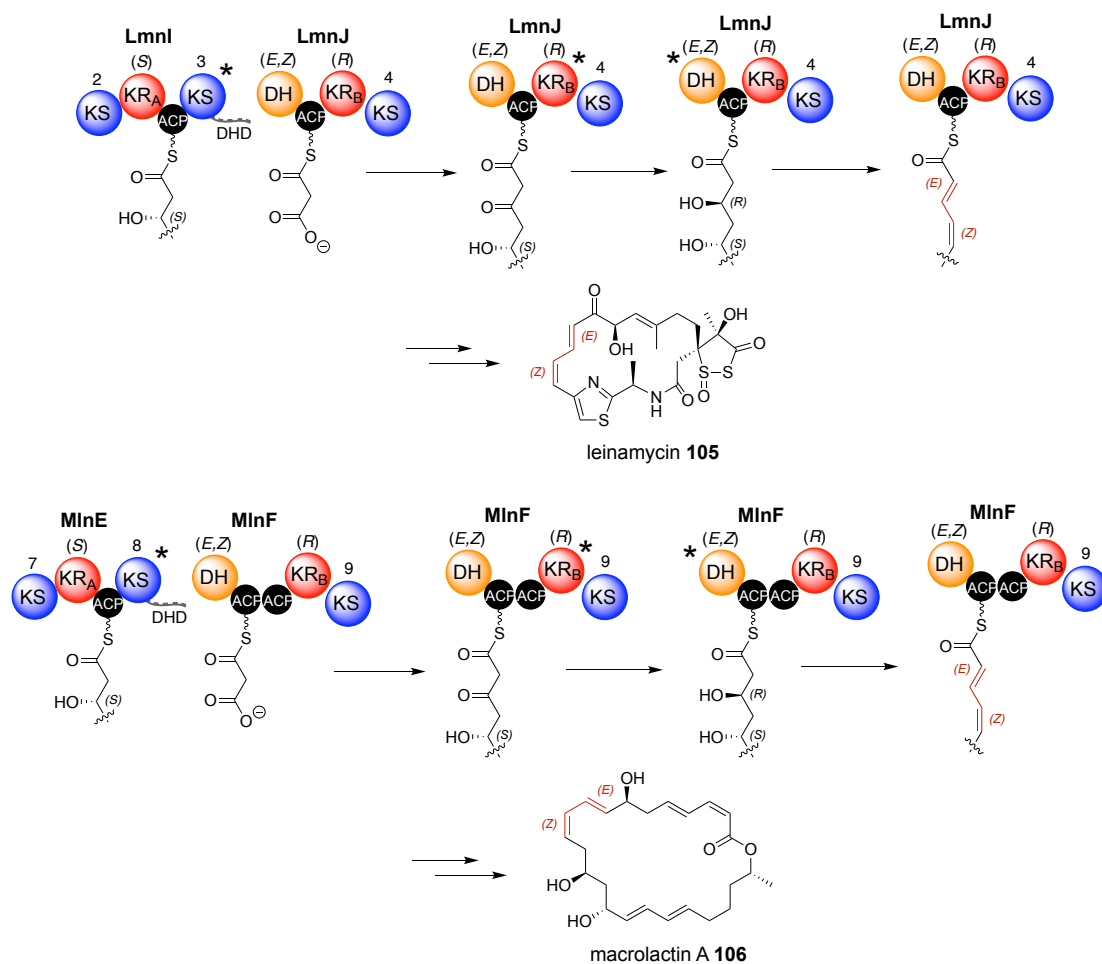


**Figure 2.13** Putative diene-forming DH domains present in leinamycin 105 and macrolactin A 106 biosynthesis.

The presence of previously unrecognized diene-forming DH domains in many systems reinforces the importance of characterizing PKS catalytic domains. The understanding gained from this study has not only shed light upon the biosynthetic mechanism for formation of (*E,Z*)-dienes motifs in many polyketide natural products, but has also led to the discovery of a novel and highly conserved enzyme which could potentially be exploited as a biocatalyst, or for biosynthetic engineering to create novel natural product analogues.

### **3. Results and Discussion II: Enacyloxin IIa Analogues**

## 3.1 Introduction

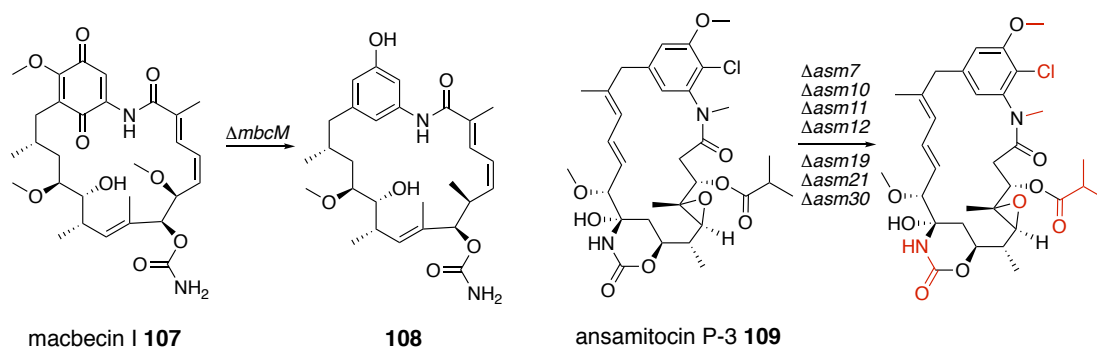
### 3.1.1 Approaches used for the Generation of Natural Product Analogues

As discussed in section 1.1.3, traditional strategies for the generation of natural product analogues have relied upon synthetic and semi-synthetic approaches. However, these strategies can often be challenging as well as time-consuming, particularly for natural products that are highly functionalized and contain multiple stereocentres such as enacyloxin IIa **30** (section 1.5). Despite several reports detailing the synthesis of enacyloxin IIa **30** fragments, there have been no successful reports of the total synthesis.<sup>156–158</sup>

#### 3.1.1.1 Gene Disruption to Generate Natural Product Analogues

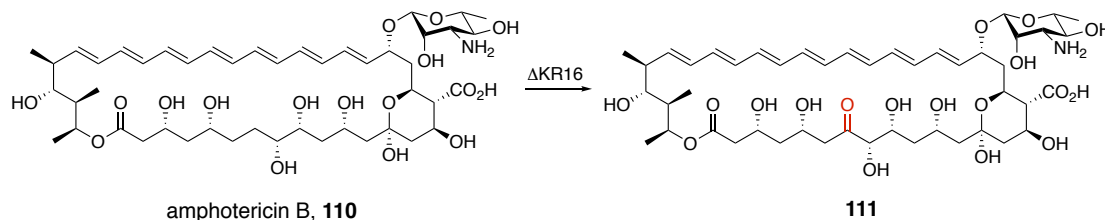
An alternative approach is to use genetic engineering to manipulate the associated gene cluster in order to generate structural analogues. This can be achieved in the native host providing it is genetically tractable, or with the development of cloning and DNA synthesis, the gene cluster can be cloned and expressed into fast growing, genetically tractable heterologous hosts, optimized for genetic engineering. One approach used to generate structural changes in natural products is the disruption of genes that act downstream in a biosynthetic pathway. Tailoring genes are often good candidates for engineering as their role is often to install late stage functionality without being directly involved in the biosynthesis of the core of the molecule. This strategy has been used successfully to generate analogues via the deletion of cytochrome P450 enzymes such as hydroxylases and epoxidases, as well as halogenases, dehydrogenases, carbamoyl transferases and many other tailoring genes.<sup>79,159–164</sup>

This approach was used to generate an analogue of anti-cancer drug macbecin I **107** (scheme 3.1) which had improved activity. The deletion of the gene encoding monooxygenase tailoring enzyme (*mbcM*), resulted in the production of analogue **108**, which has an improved binding affinity for its target, Hsp90, compared with macbecin I ( $K_d$  3 nM vs 240 nM), as well as reduced toxicity.<sup>164</sup> An example of the generation of a library of structural variants using this strategy is the investigation of ansamitocin P-3 (**109**) biosynthesis by Floss and co-workers. They deleted genes encoding various tailoring enzymes in order to determine their function, but in the process generated a library of ansamitocin analogues which lack the groups highlighted in red (scheme 3.1).<sup>163</sup>



**Scheme 3.1** The deletion of tailoring enzymes to generate analogues of macbecin I (**107**) and ansamitocin P-3 (**109**).

As well as the inactivation of tailoring enzymes, the inactivation of individual domains within megasynthases has also been used to generate analogues. This is achieved via site-directed mutagenesis to avoid complete disruption of the megasynthase. Inactivation of KR, DH and ER domains have all been used to generate analogues.<sup>165–171</sup> A good example of this is the antifungal agent amphotericin B **110**. Caffrey and co-workers inactivated a KR domain (KR16) in the PKS, which resulted in the production of oxo-derivative **111**, this analogue had reduced antifungal activity, but showed a decrease in undesirable hemolytic activity (scheme 3.2).<sup>170</sup>



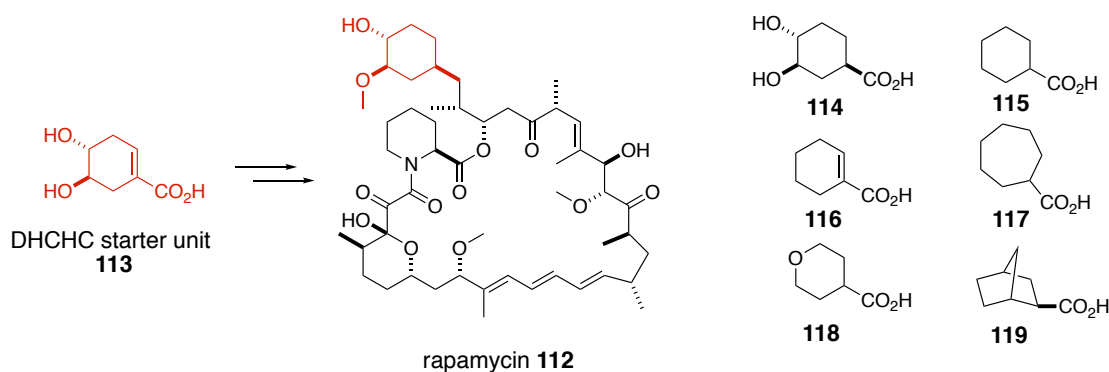
**Scheme 3.2** The inactivation of a KR domain from module 16 of amphotericin biosynthesis resulting in an analogue with an additional ketone group (red).<sup>170</sup>

### 3.1.1.2 Mutasynthesis to Generate Natural Product Analogues

The strategy of inactivating genes can be coupled with the feeding of precursors to generate novel structural analogues in an approach commonly known as mutasynthesis. This often involves the deletion of genes responsible for the biosynthesis of a precursor, followed by the feeding and incorporation of precursor analogues. This exploits the promiscuity of downstream enzymes, and has been used to generate a diverse array of analogues of many classes of natural products including macrolides, aminoglycosides and glycopeptides.<sup>172–177</sup> Starter units are often a common target of this strategy, as highlighted by the engineered biosynthesis of rapamycin

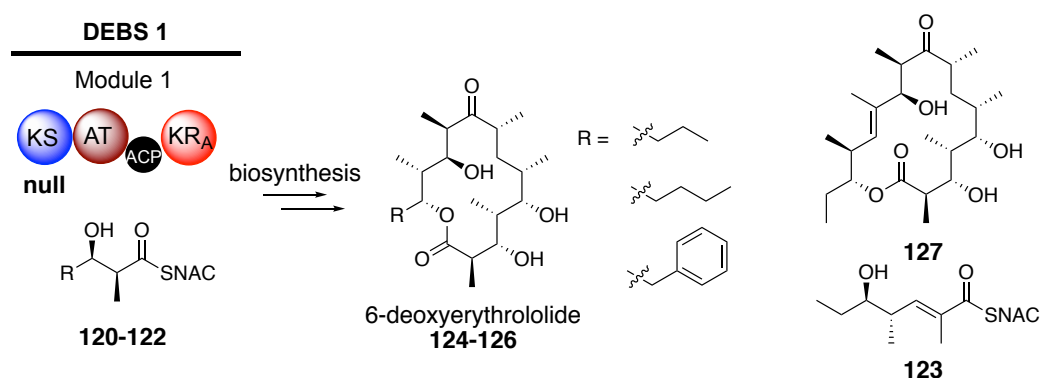


(**112**) analogues (scheme 3.3). A mutant strain lacking the genes responsible for the biosynthesis of the 4,5-dihydroxy-1-cyclohexenecarboxylic acid (DHCHC) starter unit **113**, was fed with DHCHC analogues **114-119** to afford rapamycin analogues with the unnatural starter units incorporated.<sup>173</sup>



**Scheme 3.3** A mutasynthetic approach to generating rapamycin analogues. Starter unit mimics **114-119** were incorporated using a mutant lacking the genes required for the assembly of the DHCHC starter unit (red).<sup>173</sup>

Another common target for the generation of analogues via mutasynthesis is early stage PKS-bound intermediates. Small molecule PKS intermediate mimics can be fed into KS domain-inactivated mutants in order to generate a range of polyketide natural product analogues. This technique has been used extensively to exploit the erythromycin biosynthetic pathway.<sup>178-183</sup> The KS domain of module 1 was inactivated, and the producing strain fed with acyl-*N*-acetylcysteamine thioester (acyl-SNAC) substrates **120-123**. This resulted in the production of erythromycin analogues **124-127** as the inactivated KS domain uses the acyl-SNAC as a starter unit (scheme 3.4).<sup>178</sup>



**Scheme 3.4** A mutasynthesis approach to generate erythromycin analogues **124-127**.<sup>178</sup> Note that the feeding of SNAC **123** resulted in ring-expanded product **127**.

These strategies rely on the ability of downstream enzymes to accept non-native substrates. In some pathways, these enzymes are so promiscuous that simply feeding a precursor at a sufficient concentration is enough to generate analogues without the need for any genetic manipulation. This simple technique is often referred to as ‘precursor directed biosynthesis’ and has been used for many pathways, a prime example being the incorporation of non-proteinogenic amino acid units in the NRPS-generated immunosuppressant cyclosporine **128** (figure 3.1).<sup>184-186</sup> The adenylation domains from the cyclosporine NRPS are sufficiently promiscuous to accept non-proteinogenic amino acid analogues, resulting in the production of cyclosporine analogues **129-132**.<sup>186</sup> However, a common problem with this technique is that a mixture of the desired analogue and the natural product may be produced, making purification of the analogue difficult.

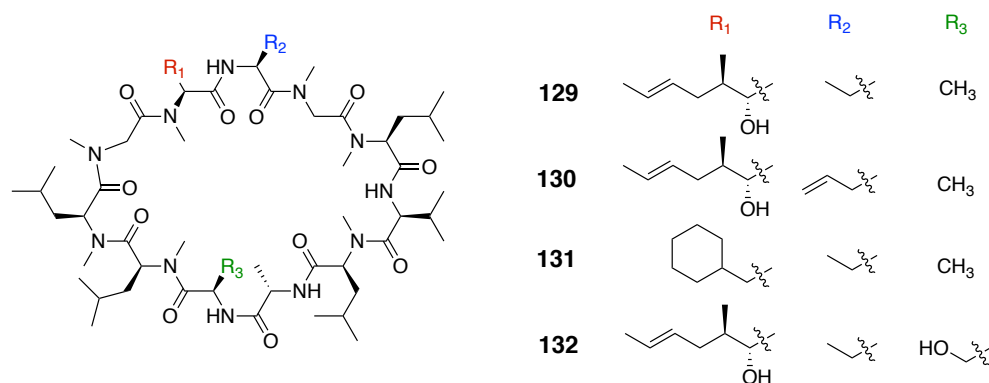
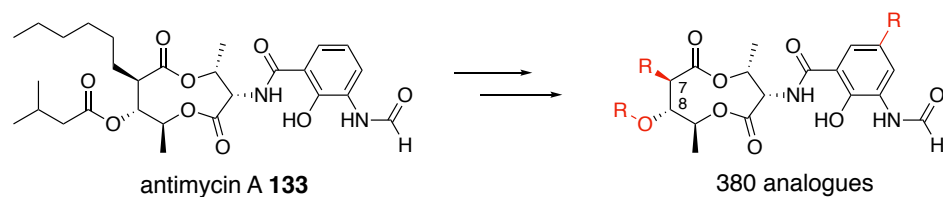


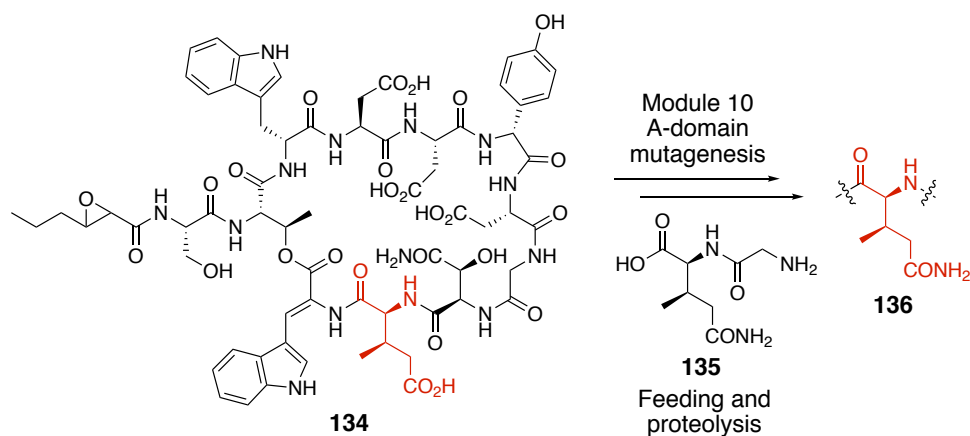
**Figure 3.1** Feeding of non-proteinogenic amino acids into the cyclosporine (**128**) producing strain results in the production of analogues **129-132**.<sup>186</sup>

A combination of the deletion of tailoring genes with precursor directed biosynthesis was used by Liu and co-workers to generate a remarkable 380 antimycin (**133**) analogues. The NRPS/PKS-catalyzed assembly uses a tryptophan-derived starter unit, which could be complimented with 5-fluoro-tryptophan in order to generate a fluorinated starter unit. The AT domain in the PKS module primes an alkylmalonyl-CoA extender unit, but also has sufficient promiscuity to prime a range of synthetic, non-natural extender units, providing diversity at the C-7 position. Once the core structure is assembled, an acyl transferase tailoring enzyme acylates at the C-8 position using CoA acyl donors. This enzyme is also promiscuous in that it can catalyze acylation with a range of alternative CoAs, generating diversity at the C-8 position. This tailoring gene was also deleted in order to generate analogues lacking the acyl group at the C-8 position (scheme 3.5).<sup>187</sup>



**Scheme 3.5** The generation of 380 antimycin (**133**) analogues via multiple strategies.

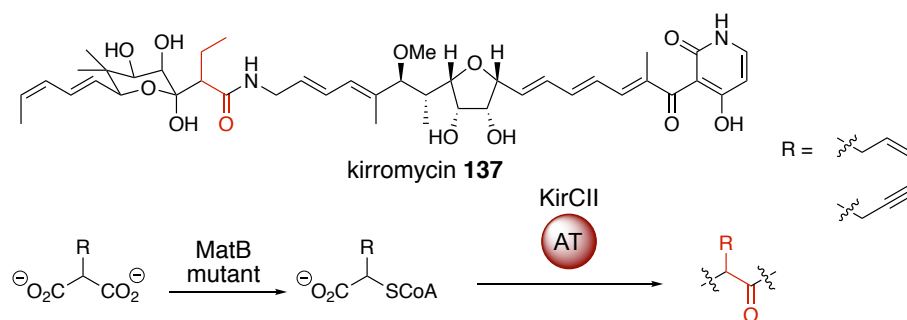
One of the major problems with the mutasynthesis and precursor directed biosynthesis strategies is that the downstream enzymes may not always have the desired promiscuity. In order to address this, approaches have been used whereby domains have been engineered to accept non-native substrates.<sup>185,188–191</sup> This strategy was used successfully when a single mutation in an adenylation domain altered its amino acid specificity, resulting in the isolation of a novel NRPS-generated calcium-dependant antibiotic (CDA) **134**. The adenylation domain of module 10 of the NRPS was engineered to accept methyl glutamine as a substrate, and after the feeding of methyl glutamine derivative **135**, the corresponding methyl glutamine analogue of the antibiotic **136** was isolated (scheme 3.6).<sup>192</sup>



**Scheme 3.6** An A-domain from a NRPS-generated CDA (**134**) was engineered to accept methyl glutamine derivative **135**.<sup>192</sup>

Another example of the use of this strategy is a mutant variant of malonyl-CoA synthetase, MatB. The role of this enzyme is to generate malonyl-CoA, the commonly used extender unit of PKSs, however the mutant variant is capable of generating an array of alternative extender units after feeding of the appropriate acid. The combination of this enzyme with promiscuous AT domains, has resulted in a diverse array of analogues from several systems.<sup>193–196</sup> An example of this is the *trans*-AT PKS kirromycin **137** system (scheme 3.7). The promiscuous KirCII AT domain which acts in *trans*, is capable of priming an ACP domain with unnatural extender units

generated by the MatB mutant to afford kirromycin analogues.<sup>193</sup> One of the analogues harbors an alkyne group, which can act as a synthetic handle for click chemistry.



**Scheme 3.7** The use of an engineered malonyl-CoA synthetase, MatB, to generate unnatural extender units. The promiscuous KirCII AT domain primes the extender units onto the relevant ACP domain before incorporation into kirromycin (**137**).<sup>193</sup>

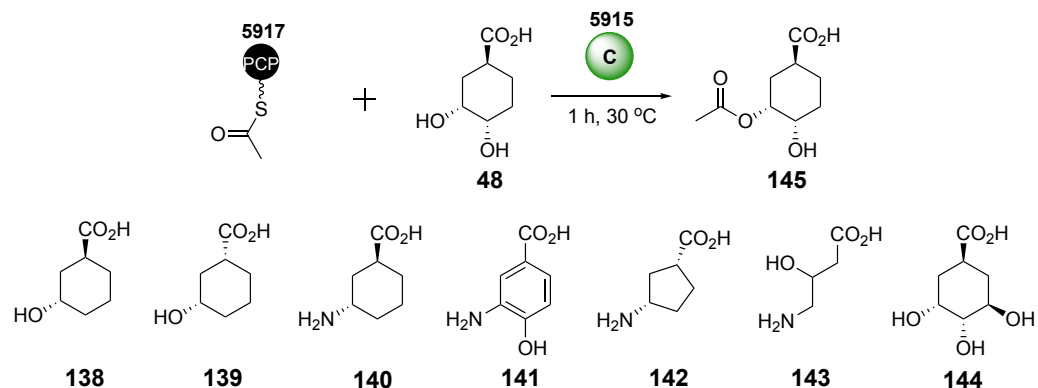
There have been many more complex strategies developed in recent years, including domain swapping, module swapping and the generation of hybrid systems consisting of genes from different pathways.<sup>188,197,198</sup> However, these approaches are beyond the scope of this chapter. Further to this, despite the engineering of megasynthases being used successfully in many cases, it can result in low product yields or completely abolished production, possibly due to the downstream domains in the megasynthase not being able to accept the modified acyl chain. A greater understanding of the molecular architecture, inter-subunit interactions and specificity of natural product assembly lines is required before the engineering of megasynthases can be utilized to its full potential.<sup>59,198–201</sup>

### 3.1.2 Previous Work in the Challis Group

All enacyloxin analogues in this section were generated by Dr. Joleen Masschelein.

#### 3.1.2.1 Enacyloxin as a Target for Genetic Engineering

Recently, the Bamb\_5915 condensation domain responsible for the off-loading of the chain with the DHCCA (**48**) unit has been shown to catalyze the condensation of an acyl chain mimic (acetyl-PCP domain) with a variety of DHCCA analogues *in vitro*.<sup>93</sup> The overproduced Bamb\_5917 PCP domain was loaded with acetyl CoA, before the addition of the Bamb\_5915 condensation domain along with a DHCCA analogue (**138-144**), the production of the condensed acetyl-DHCCA analogue **145** was detected using LC-MS (scheme **3.8**).



**Scheme 3.8** DHCCA (48) analogues 138-144 accepted by the Bamb\_5915 condensation domain during *in vitro* assays.<sup>93</sup> A detailed procedure for the condensation assay is described in section 6.7.2.

As well as the promiscuous condensation domain, the enacyloxin biosynthetic gene cluster encodes tailoring enzymes including two halogenases (Bamb\_5928 and 5931), a dioxygenase (Bamb\_5927), a dehydrogenase (Bamb\_5932) and a carbamoyl transferase (Bamb\_5930) as shown in figure 3.2. Given the presence of these features, it was thought that both the gene disruption and mutasynthesis strategies (sections 3.1.1.1 and 3.1.1.2) could be used to generate a library of enacyloxin IIa (30) derivatives. This would lead to analogues harboring structural changes in both the polyol region and the DHCCA unit, providing useful SAR data associated with the polar contacts observed in the crystal structure (figure 1.14) and potentially analogues with increased potency. More potent analogues may then serve as a platform for making more complex changes to the structure, such as engineering the megasynthase,

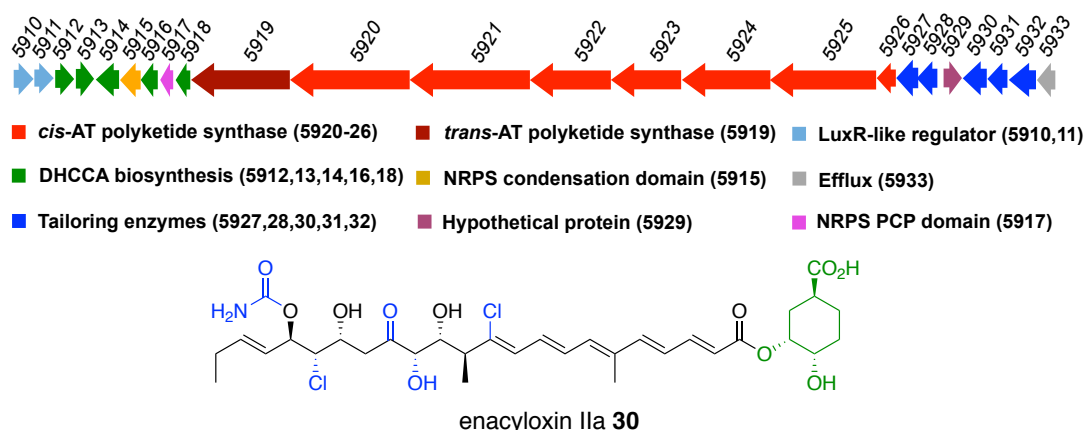


**Figure 3.2** The enacyloxin gene cluster. The groups installed by the tailoring enzymes (blue) as well as the DHCCA unit (green) serve as handles for genetic engineering.

The original producing *B.ambifaria* AMMD strain was found to be intractable, however another producing strain (*B.ambifaria* BCC0203) was identified which is genetically tractable, meaning genetic manipulation can be carried out in a native producer rather than having to heterologously express the gene cluster. The strain is also fast-growing, and produces enacyloxin in a good titre (>10 mg/L), all of which will facilitate the engineering of analogues.

### 3.1.2.2 Targeting the Tailoring Enzymes

Using an in-frame gene deletion approach (section 6.4.1), initial inroads were made into deleting the tailoring genes in order to generate analogues. Vectors for the deletion of genes encoding the Fe(II)  $\alpha$ -KG-dependent dioxygenase (Bamb\_5927), the Fe(II)  $\alpha$ -KG-dependent chlorinase (Bamb\_5931) and the carbamoyl transferase (Bamb\_5930) were constructed and used to make the respective gene deletions in the *B.ambifaria* BCC0203 wild-type strain. The corresponding analogues were isolated and characterized, and their activity against *A. baumannii* was determined (figure 3.3). The deletion of the gene encoding carbomyl transferase (Bamb\_5930) resulted in cyclic ether analogue **44**, this results from hemiketal formation between the de-carbamoylated hydroxyl group and the keto group. Both cyclic ether and des-chloro analogues **44** and **41** were isolated from *Frateruria* sp. W-315 by Watanabe and co-workers as before the biosynthetic gene cluster was identified in *B. ambifaria* (section 1.5).<sup>158</sup>

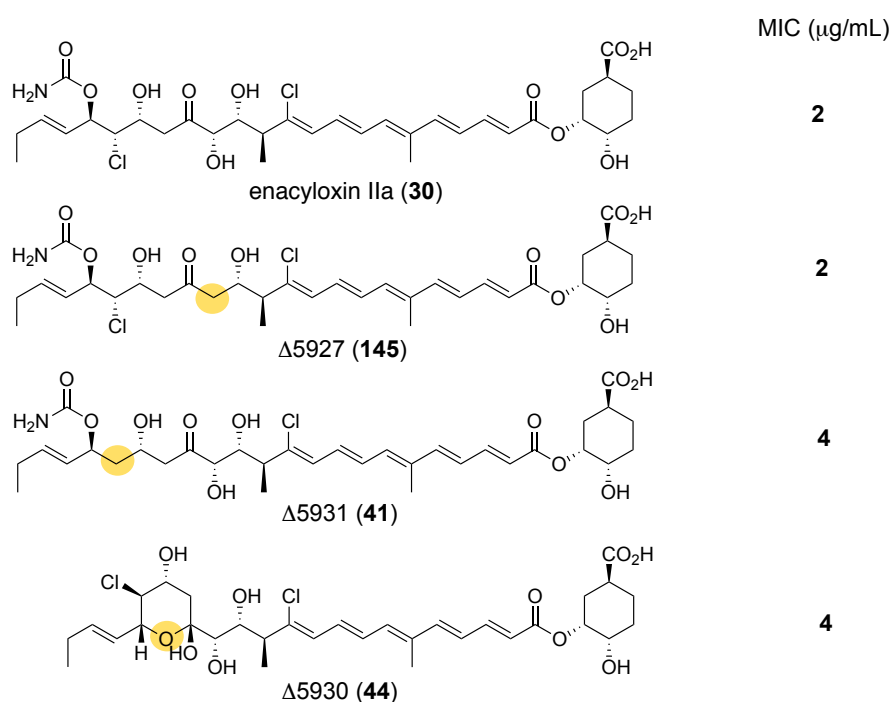


**Figure 3.3** The enacyloxin analogues isolated from *B.ambifaria* BCC0203  $\Delta 5927$ ,  $\Delta 5931$  and  $\Delta 5930$  mutant strains along with their respective activities (Dr. Joleen Masschelein).

As well as deleting the tailoring genes individually, mutants were generated in which multiple genes were deleted to produce a more diverse array of analogues. Two double knock-out mutants were generated, one lacking the dioxygenase and halogenase enzymes ( $\Delta 5927 + 5931$  mutant strain), and the other lacking the dioxygenase and carbonyl transferase ( $\Delta 5927 + 5930$  mutant strain). The resulting analogues are shown in figure 3.4.

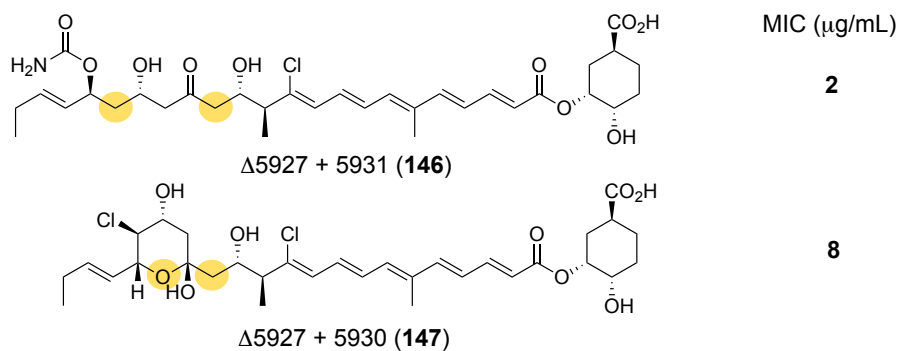


**Figure 3.4** The enacyloxin analogues isolated from *B.ambifaria* BCC0203  $\Delta 5927 + 5931$  and  $\Delta 5927 + 5930$  double knock-out mutant strains along with their respective activities (Dr. Joleen Masschelein).

### 3.1.2.3 Generating Enacyloxin Analogues via a Mutasynthesis Approach

To utilize the aforementioned promiscuity of the condensation domain demonstrated *in vitro* (section 3.1.2.1), a mutant was generated in which some of the genes involved in DHCCA biosynthesis (*bamb\_5912-bamb\_5914*) were deleted. This abolished the production of the DHCCA unit, and hence enacyloxin IIa. This mutant was then fed with synthetic and commercially available DHCCA analogues (**138**, **140** and **143**) to generate enacyloxin derivatives **148-150** (figure 3.5).

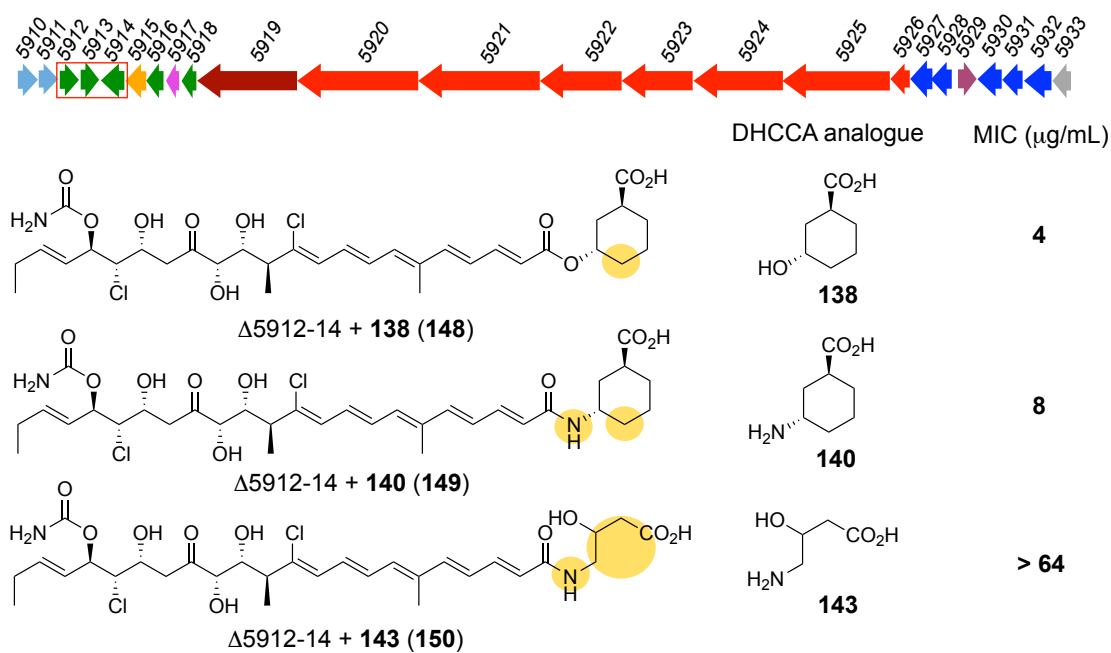


**Figure 3.5** The enacyloxin analogues isolated from feeding the *B. ambifaria* BCC0203  $\Delta 5912-14$  mutant strain with DHCCA analogues **138**, **140** and **143**, along with their activity (Dr. Joleen Masschelein).

One potential limitation of enacyloxin IIa as a viable drug candidate is that the ester linkage from the DHCCA unit to the linear acyl chain may be susceptible to *in vivo* hydrolysis. However, it appears that the mutasynthesis strategy can be used to generate analogues that harbor a more stable amide group in place of the ester (**149** and **150**). Despite the increased stability, both of these analogues have lost potency relative to enacyloxin IIa, and so further structural modifications may need to be made to restore the activity. It is also clear that the DHCCA unit is very important with regards to the activity of the compound, as when it is replaced with an acyclic unit (**143**) the activity is lost.

### 3.1.2.4 Discovery of Vibroxin

A gene cluster homologous to the enacyloxin biosynthetic gene cluster was identified in the genome of a *Vibrio rhizosphaerae* strain using genome mining. *V. rhizosphaerae* was grown on the enacyloxin-producing basal salts medium (BSM), and the metabolite associated with the newly identified gene cluster was isolated and characterized as vibroxin **151** (figure 3.6). Vibroxin retains many of the structural features of enacyloxin IIa **30**, but has an alternative starter unit, an additional alkene (installed by an additional DH domain in the PKS) and lacks some of the functional groups introduced by tailoring enzymes, all changes that occur in the



polyol region of the molecule. Vibroxin **151** is more potent than enacyloxin IIa **30**, which validates the strategy of generating enacyloxin analogues harboring structural changes in the polyol region of the molecule. It would also be useful to generate analogues of vibroxin using the previously described strategies, however the *V. rhizosphaerae* producing strain is not genetically tractable, and so the heterologous expression of this gene cluster to enable genetic engineering is required.

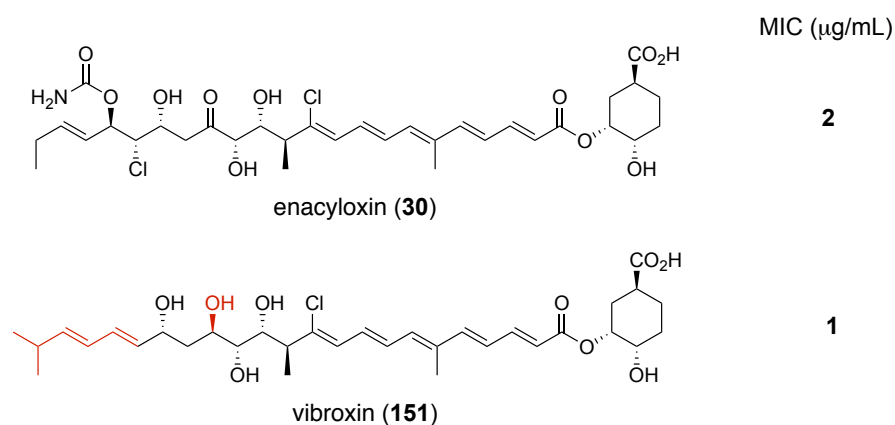


**Figure 3.6** The structure of vibroxin **151** compared to enacyloxin IIa **30**.

### 3.1.3 Aims

The overall aim of this project was to generate a more complete library of enacyloxin IIa analogues using multiple strategies. This would include deleting the genes encoding the remaining tailoring enzymes, as well as making various combinations of these knock-out mutants. In addition to this, the mutasynthesis strategy would be used alongside chemically synthesized DHCCA mimics in order to generate a more diverse array of analogues. It was hoped that this would lead to derivatives harboring structural changes in both the polyol region and the DHCCA unit in order to determine the importance of the polar contacts between enacyloxin IIa and EF-Tu (see section 1.5). This would provide useful SAR data and potentially deliver analogues with increased potency, which may then provide a platform for the rational design of improved analogues and eventually making more complex changes to the structure.

## 3.2 Results and Discussion

### 3.2.1 Generation of Analogues via Deletion of Genes Encoding Tailoring Enzymes

The analogues in this section were generated in collaboration with Dr. Xinyun Jian.

#### 3.2.1.1 Producing the Mutant Strains

Gene deletions were generated using a double homologous recombination approach (section 6.4.1).<sup>202</sup> This involved the cloning of the two flanking regions (500-1000 base pairs) of the gene to be deleted, into a suicide plasmid (pGPI). This plasmid has two important features required for the gene deletion: a trimethoprim resistance marker, as well as a *SceI* endonuclease restriction site.

The plasmid was introduced into *E. coli* SY327 by electroporation, after the ligation of the two flanking arms into the plasmid. The transformants were selected on LB agar plates supplemented with trimethoprim before the construct was verified by sequencing. The plasmid could then be introduced into the *B. ambifaria* BCC0203 wild-type strain via triparental conjugation using the *E. coli* SY327 (pGPI) donor strain along with an *E. coli* HB101 (pRK2013) helper strain. Transconjugants were then selected for using trimethoprim and gentamicin. The trimethoprim forces the first recombination event to occur; the wild-type *B. ambifaria* strain is not resistant to trimethoprim, and so needs to integrate the pGPI plasmid into its genomic DNA in order to survive. Gentamicin is used to select against *E. coli* strains, leaving only the gentamicin and trimethoprim resistant single crossover *B. ambifaria* strain. The single crossover event was confirmed using colony PCR.

Another plasmid (pDAI) was then introduced into the mutant; this plasmid has the gene encoding the *SceI* endonuclease as well as tetracycline resistance. Using *E. coli* SY327 (pDAI) as the donor strain, the plasmid was introduced into the *B. ambifaria* BCC0203 single crossover mutant via the same triparental conjugation, using the *E. coli* HB101 (pRK2013) helper strain. Transconjugants were then selected for using tetracycline and gentamicin. The introduction of the pDAI plasmid forces the second recombination event to occur; the *SceI* endonuclease encoded by the pDAI plasmid makes a clean cut at the *SceI* restriction site, which is now incorporated into the genomic DNA. To repair this cut, a second homologous recombination event occurs to eliminate the pGPI plasmid, resulting in a mixture of wild-type and deletion strains, which were discriminated using colony PCR (figure 3.7).

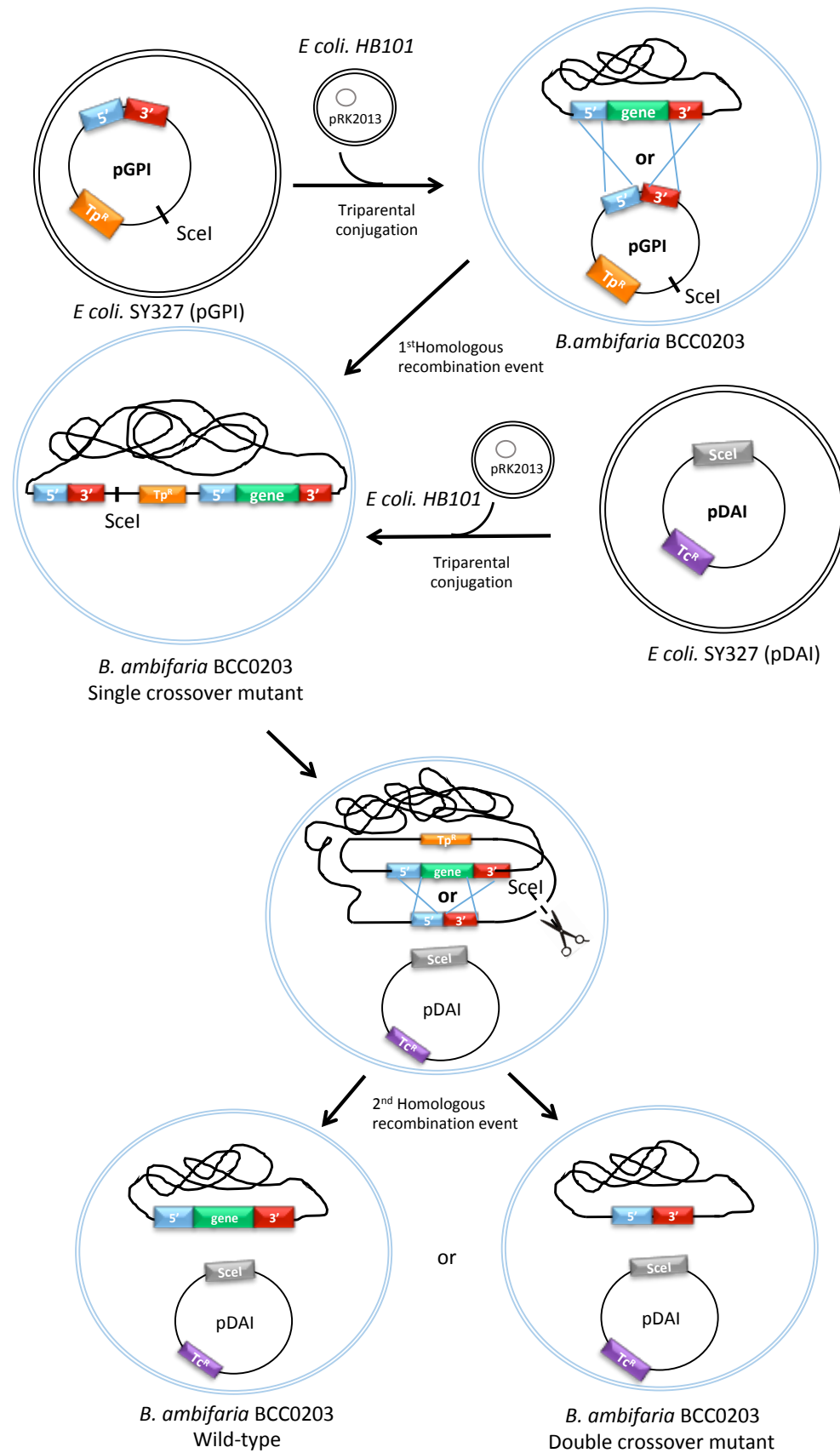


**Figure 3.7** The construction of in-frame gene deletions in *B. ambifaria* BCC0203.

The PCR used to confirm the gene deletion was conducted using either the forward primer of the 5' flanking arm and the reverse primer of the 3' flanking arm, or a newly designed set of primers if the melting temperature or GC content of the primers were not compatible. The mutant is clearly distinguishable from the wild-type as the region amplified is significantly shorter in the mutant because the gene is no longer present between the flanking arms (figure 3.8). The genetic evidence confirming the mutants constructed in this chapter can be found in section 6.4.2.

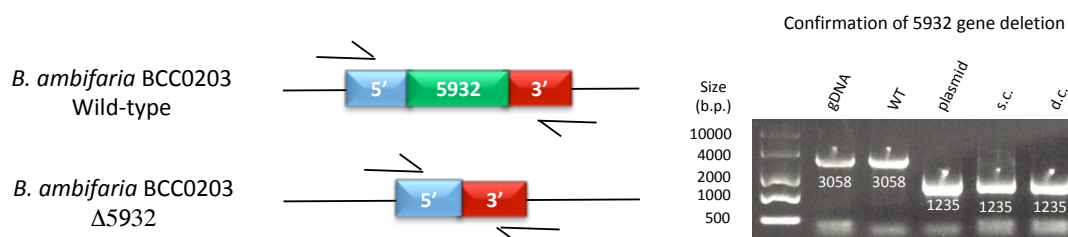


**Figure 3.8** PCR screening to identify in-frame deletion mutants. The agarose gel corresponds to the deletion of the gene encoding PQQ-dependent dehydrogenase Bamb\_5932. The lanes correspond to the PCR of wild-type *B.ambifaria* BCC0203 genomic DNA (gDNA), wild-type *B.ambifaria* BCC0203 (WT), pGPI plasmid (plasmid), single crossover mutant (s.c.) and double crossover mutant (d.c.) respectively.

To detect the production of enacyloxin analogues by the mutant strains, they were grown on a single plate of BSM before extraction and UHPLC-ESI-Q-TOF-MS analysis (section 6.1). After production of the desired analogue was confirmed, the strain was grown on a larger scale (1 L of BSM) before extraction and preparative HPLC purification (section 6.1). The analogue was then characterized using NMR spectroscopy before its activity against *A.baumannii* determined using whole cell (MIC) assays (section 6.5.4).

All of the enacyloxin analogues generated during this project were tested against two strains of *A. baumannii* in order to validate the observed activity. The analogues were tested against both *A. baumannii* ATCC17978 – a genome sequenced strain isolated in 1951, and *A. baumannii* DSM25645 – a recent clinical isolate from a soldier injured in the 2008 Georgian-Russian war that is resistant to many classes of antibiotics.<sup>104</sup> All of the analogues showed the same activity against both strains and, so only a single MIC value is shown for each compound.

### 3.2.1.2 Deletion of the Genes Encoding the Remaining Tailoring Enzymes

Among the genes encoding tailoring enzymes, those encoding the PQQ-dependent dehydrogenase (Bamb\_5932), responsible for the installation of the ketone, and flavin-dependent halogenase (Bamb\_5928), responsible for the chlorination of the polyene, had yet to be deleted (figure 3.9).

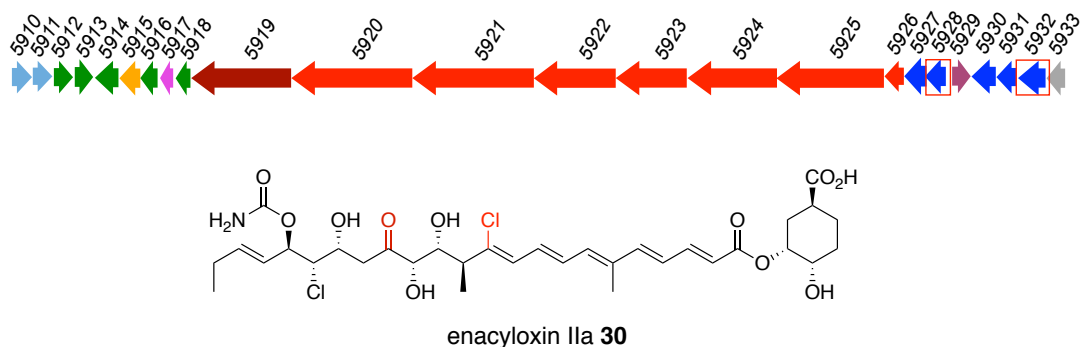


**Figure 3.9** Genes encoding the PQQ-dependent dehydrogenase (Bamb\_5932), responsible for the installation of the ketone, and flavin-dependent halogenase (Bamb\_5928), responsible for the chlorination of the polyene.

The deletion of *bamb\_5932* resulted in the production of expected enacyloxin analogue **43** (figure 3.10). The structure of **43** was confirmed by the addition of 2 Da in the HRMS relative to enacyloxin IIa, as well as the disappearance of the diagnostic ketone carbon shift in the  $^{13}\text{C}$ -NMR spectrum. This analogue was also isolated from *Frateuria* sp. W-315 by Watanabe and co-workers and was named enacyloxin IVa, however the configuration of the additional stereocenter was assigned incorrectly (section 1.5).<sup>104,112</sup> The correct configuration of the additional stereocenter generated by the gene deletion was confirmed using Kishi's NMR database for contiguous polyols (section 3.2.1.4).<sup>203</sup>

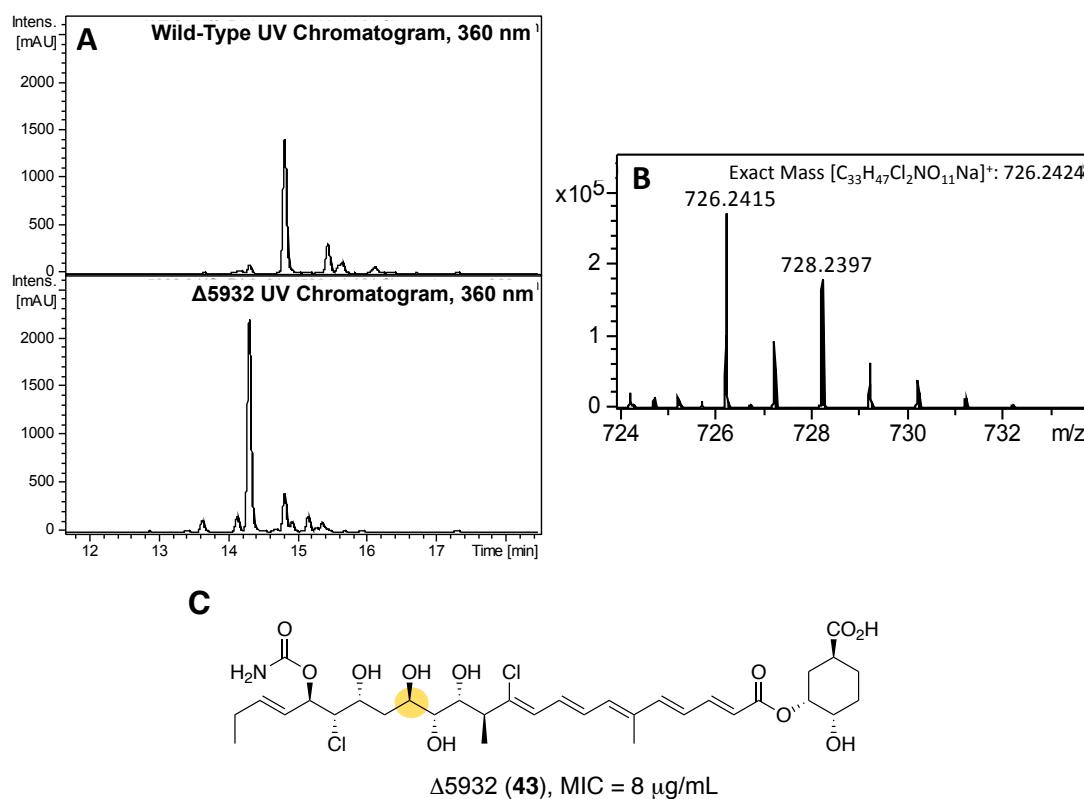


**Figure 3.10** **A** UV chromatograms (360 nm) from LC-MS analyses of *B. ambifaria* wild-type and  $\Delta 5930$  mutant extracts. **B** The HRMS for the species eluting at 14.15 min from the  $\Delta 5930$  mutant extract. **C** The structure assigned by NMR spectroscopy and the activity of the analogue against *A. baumannii*.

The deletion of *bamb\_5928* resulted in the production of expected enacyloxin analogue **152** (figure 3.11). The structure of **152** was confirmed by the loss of 34 Da in the HRMS relative to enacyloxin IIa as well as the change in isotope distribution. The appearance of an additional proton in the vinyl region of the <sup>1</sup>H NMR spectrum (5.86 ppm) also confirmed that the vinyl chloride group was no longer present.

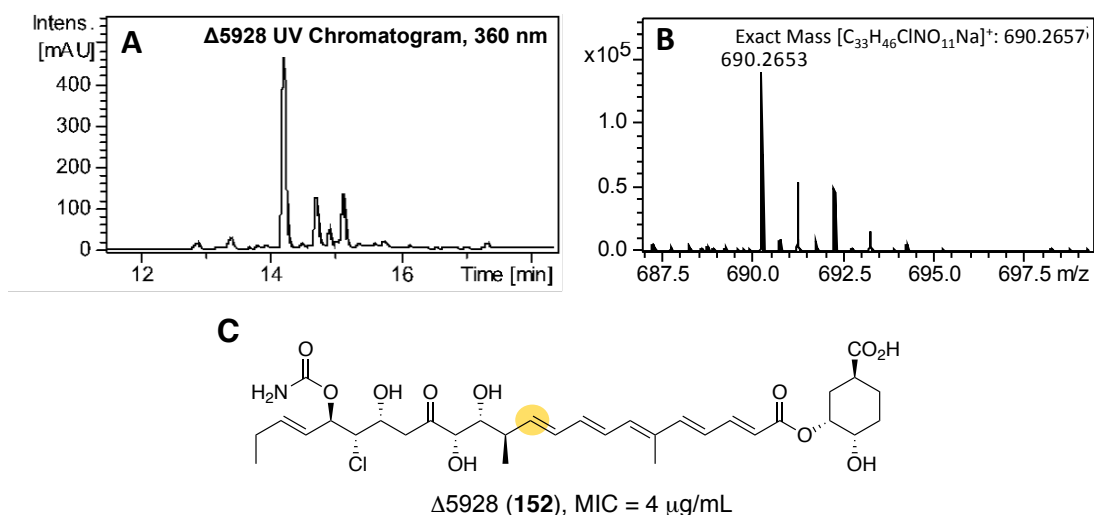


**Figure 3.11** **A** UV chromatogram (360 nm) from LC-MS analyses of *B. ambifaria* ( $\Delta 5928$ ) extracts. **B** The HRMS for the species eluting at 14.1 min. **C** The structure assigned by NMR spectroscopy and the activity of the analogue against *A. baumannii*.

### 3.2.1.3 Generation of Multiple Knock-out Mutants

In order to produce a greater diversity of analogues, mutant strains with multiple gene deletions were generated. This was accomplished via two routes: either new deletion constructs were designed to eliminate multiple genes that were adjacent in the gene cluster, or the deletion constructs were used in combination to delete genes not adjacent in the cluster. To do this, the single knock-out mutant strains were cured on M9 minimal medium (section 6.2.2) to remove the pDAI plasmid. The same procedure was then employed using the appropriate mutant strain in place of the wild-type *B. ambifaria* BCC0203 strain.

Firstly, a double knock-out mutant strain was generated in which the genes encoding both the carbamoyl transferase (Bamb\_5930) and the PQQ-dependent dehydrogenase (Bamb\_5932) were deleted in order to generate a linear de-carbamoylated analogue. As these genes are not adjacent in the cluster, the *B. ambifaria* BCC0203  $\Delta 5930$  mutant was cured and treated with the *bamb\_5932* deletion construct to generate the double knock-out mutant. This resulted in the production of the expected linear enacyloxin analogue **45** (figure 3.12). The structure of **45** was confirmed by the loss of 41 Da in the HRMS relative to enacyloxin IIa, as well as the disappearance of both the carbamoyl and ketone carbons in the  $^{13}\text{C}$ -NMR spectrum. This analogue was also isolated by Watanabe and co-workers as decarbomyl enacyloxin IVa (section 1.5).

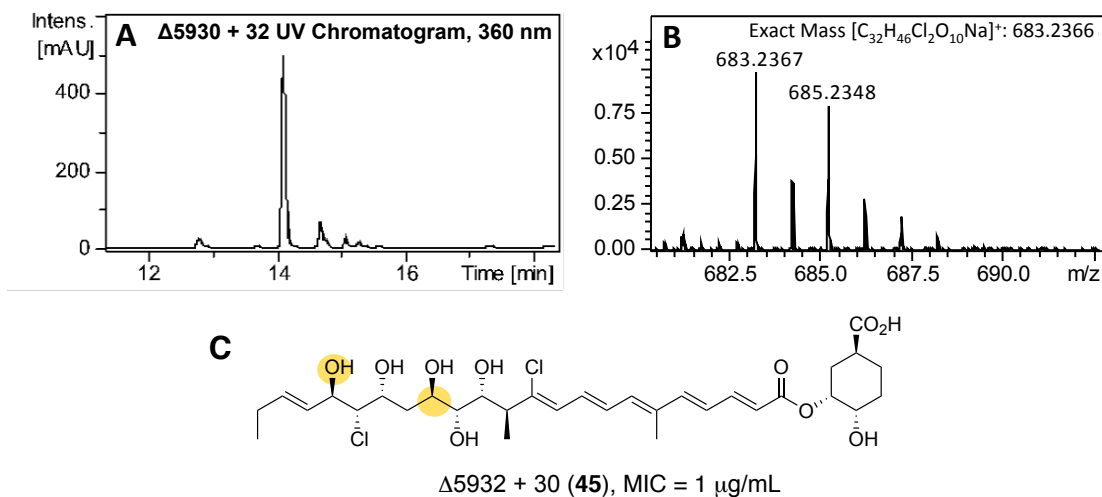


**Figure 3.12** **A** UV chromatogram (360 nm) from LC-MS analyses of *B. ambifaria* ( $\Delta 5930 + 32$ ) extracts. **B** The HRMS for the species eluting at 14.0 min. **C** The structure assigned by NMR spectroscopy and the activity of the analogue against *A. baumannii*.

Next, a double knock-out mutant strain was generated in which the genes encoding both carbamoyl transferase (Bamb\_5930) and the Fe(II)  $\alpha$ -KG-dependent halogenase (Bamb\_5931) were deleted. As these genes are adjacent in the cluster, a pGPI construct could be generated in which the flanking regions used encompass both genes. This resulted in the production of unexpected enacyloxin analogue **153** (figure 3.13). Both the carbamoyl group and the C-18 chloride group are not present as expected. However, an additional keto group is also present at C-19. This is thought to be due to the PQQ-dependent dehydrogenase (Bamb\_5932) being able to oxidize the de-carbamoylated hydroxyl group now that the sterically hindering adjacent chloride group is no longer present. The structure of **153** was confirmed by the loss of 74 Da in the HRMS relative to enacyloxin IIa as well as the change in the isotope distribution. The appearance of an additional ketone carbon in the  $^{13}\text{C}$ -NMR spectrum (201.3 ppm) as well as the change in the chemical shifts of the adjacent protons in the  $^1\text{H}$  NMR spectrum (proton bonded to C-20 shifts from 5.57 ppm to 6.14 ppm) further confirmed the structure.



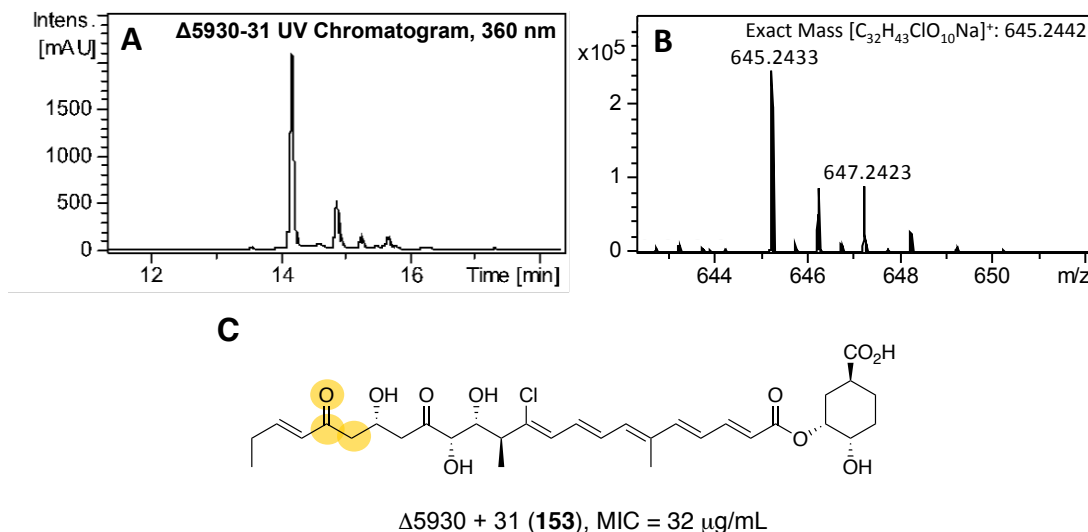


**Figure 3.13** **A** UV chromatogram (360 nm) from LC-MS analyses of *B. ambifaria* ( $\Delta 5930 + 31$ ) extracts. **B** The HRMS for the species eluting at 14.0 min. **C** The structure assigned by NMR spectroscopy and the activity of the analogue against *A. baumannii*.

A triple knock-out mutant was also constructed in which the genes encoding the carbamoyl transferase (Bamb\_5930), the Fe(II)  $\alpha$ -KG-dependent halogenase (Bamb\_5931) and the PQQ-dependent dehydrogenase (Bamb\_5932) were all deleted. This was achieved using both the Bamb\_5932 and Bamb\_5930 + 5931 deletion constructs. The mutant strain produced the expected enacyloxin analogue **154** (figure 3.14). The structure of **154** was confirmed by the loss of 70 Da in the HRMS as well as the change in the isotope distribution. The disappearance of the C-15 ketone carbon in the  $^{13}\text{C}$  NMR spectrum (no longer present at 211.7 ppm) as well as the appearance of additional aliphatic protons bonded to C-18 in the  $^1\text{H}$  NMR spectrum (1.62 ppm) further confirmed the structure.

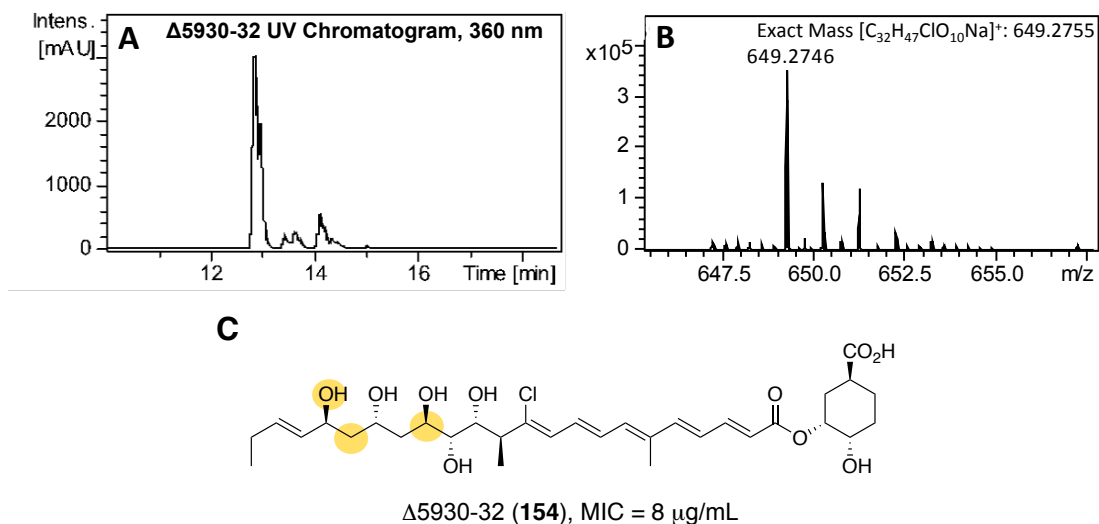


**Figure 3.14** **A** UV chromatogram (360 nm) from LC-MS analyses of *B. ambifaria* ( $\Delta 5930\text{-}32$ ) extracts. **B** The HRMS for the species eluting at 13.0 min. **C** The structure assigned by NMR spectroscopy and the activity of the analogue against *A. baumannii*

Finally, a mutant was generated where all five tailoring genes were deleted. This was achieved using a pGPI construct in which the flanking regions used encompassed all of the tailoring genes (*bamb\_5927-32*). This also included the gene encoding a hypothetical protein (*bamb\_5929*), the role of which is unclear. The mutant strain produced expected analogue **155**, albeit in a reduced yield compared with previous analogues. The structure of **155** was confirmed by the loss of 125 Da in the HRMS relative to enacyloxin IIa as well as the change in the isotope distribution (figure 3.15). The loss of all functional groups introduced by the tailoring enzymes could be accounted for in the NMR spectra, in particular the loss of the carbamoyl and ketone carbons in the  $^{13}\text{C}$  NMR spectrum (158.7 and 211.7 ppm respectively) and the presence of additional aliphatic and vinyl protons in the  $^1\text{H}$  NMR spectrum (1.57, 1.48 and 5.83 ppm respectively).

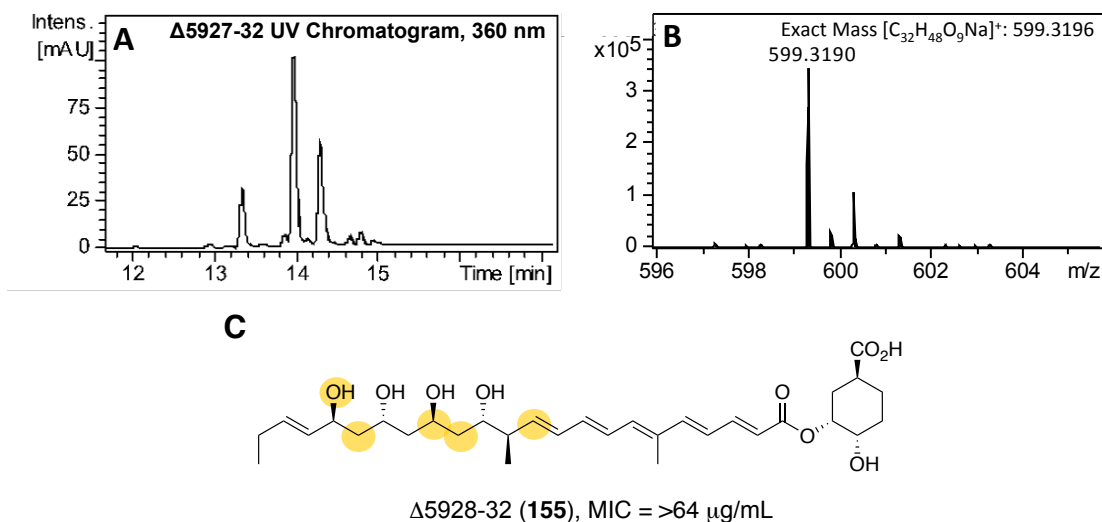


**Figure 3.15** **A** UV chromatogram (360 nm) from LC-MS analyses of *B. ambifaria* ( $\Delta 5927-32$ ) extracts. **B** The HRMS for the species eluting at 14.0 min. **C** The structure assigned by NMR spectroscopy and the activity of the analogue against *A. baumannii*

When more significant changes are made to the structure of the molecule, a greater variation in activity is observed. When all the functional groups introduced by the tailoring enzymes are removed the activity decreases significantly, confirming the importance of these groups for biological activity. Analogue **45** has improved activity compared with enacyloxin IIa, confirming that this strategy can be used to generate analogues with increased potency.

#### 3.2.1.4 Confirmation of the Stereochemistry of the Additional Stereocentre

The deletion of the gene encoding the PQQ-dependent dehydrogenase (Bamb\_5932) results in an additional stereocentre, which is present in analogues **43**, **45**, **154** and **155**. The configuration of this stereocenter was confirmed using Kishi's NMR database for contiguous polyols.<sup>203</sup> The <sup>13</sup>C-NMR chemical shifts of enacyloxin analogue **155** appear to be consistent with those predicted by the database. The shifts are consistent with that of linearmycin A **156**, a natural product harboring the same polyol region, the stereochemistry of which was also solved using the database (figure 3.16).<sup>204</sup> Furthermore, the predicted configuration of the stereocentre is consistent with that predicted using KR domain sequence alignments.<sup>123</sup>

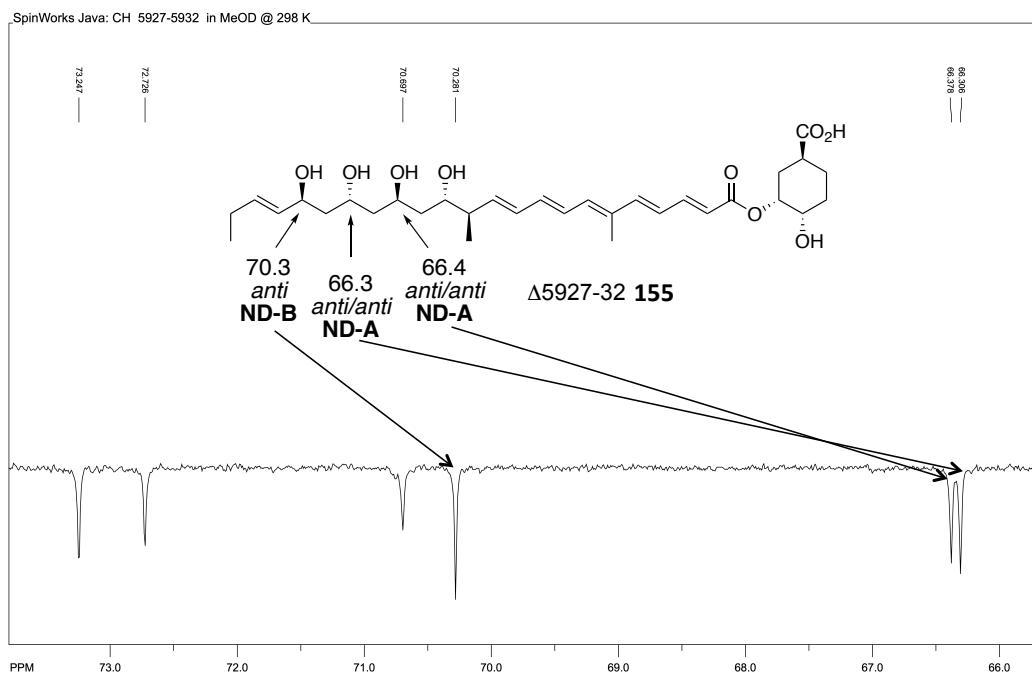
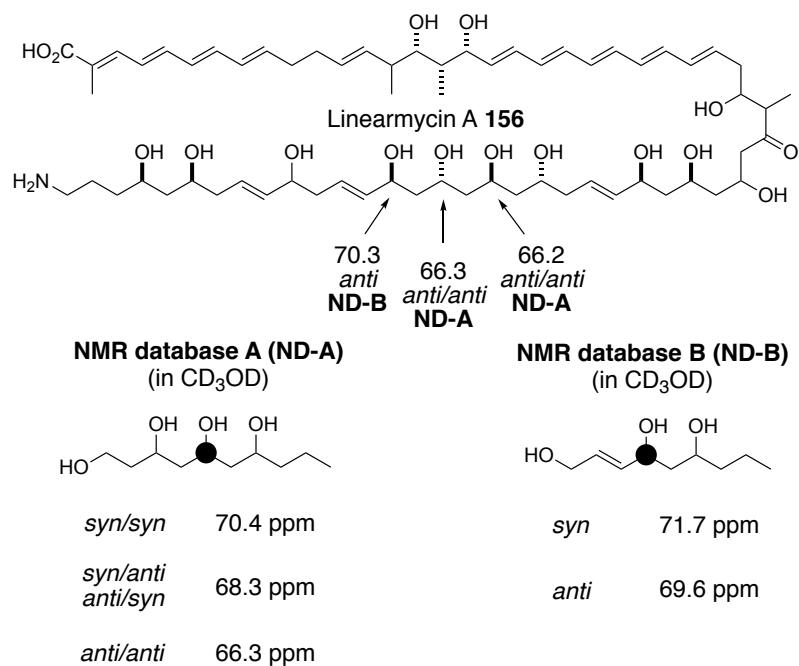
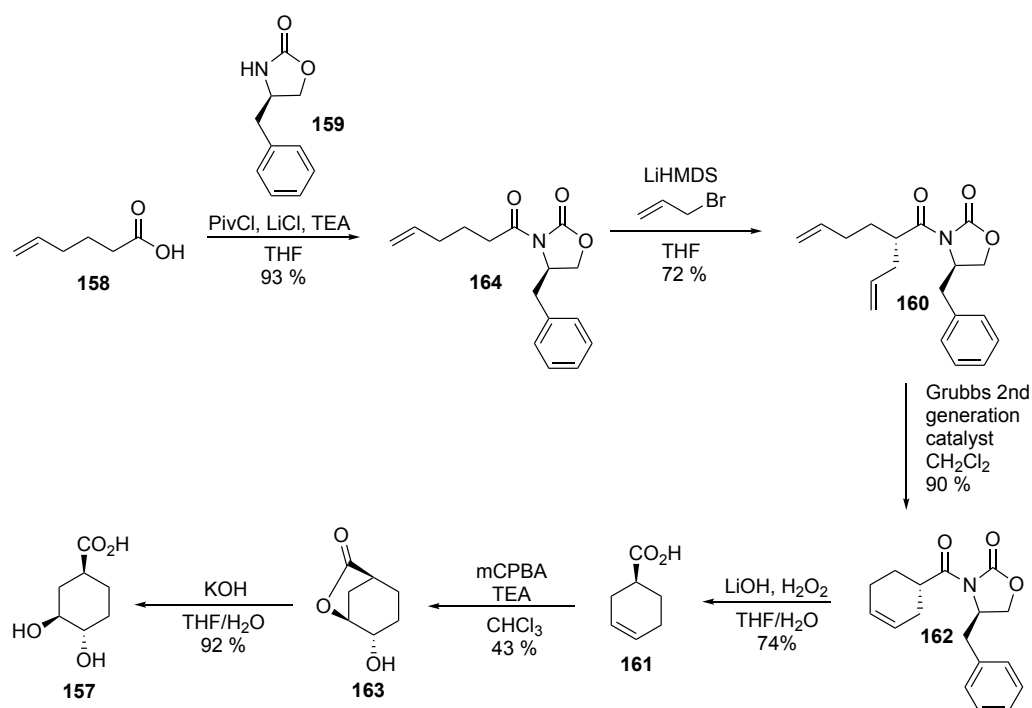


**Figure 3.16** The assignment of the relative stereochemistry of linearmycin A **156** using Kishi's NMR database.<sup>203</sup> The <sup>13</sup>C chemical shifts of enacyloxin analogue **155** appear to be consistent with those of linearmycin A **156** as well as those in the NMR database.

### 3.2.1.5 Generation of Analogues using Mutasynthesis

Using the *B. ambifaria* BCC0203  $\Delta$ 5912-14 mutant strain generated previously (section 3.1.2.3), the production medium was supplemented with synthetic DHCCA analogues. A DHCCA analogue harboring alternative stereochemistry (**157**) to that observed in enacyloxin IIa was synthesized in order to examine what affect this change would have on activity. DHCCA analogue **157** was synthesized according to the route shown in scheme 3.9. Commercially available 5-hexenoic acid **158** was condensed with (*R*)-4-(phenylmethyl)-2-oxazolidinone **159**, and asymmetric alkylation with allyl bromide afforded compound **160**. Ring closing metathesis (RCM) using Grubbs' 2<sup>nd</sup> generation catalyst, followed by removal of the auxiliary in basic conditions gave chiral cyclohexenoic acid **161**. The configuration of acid **161** was confirmed by the comparison of optical rotation values to those in the literature. The enantiomeric purity of the acid was confirmed by <sup>13</sup>C NMR analyses of the precursor **162** (figure 3.17). The treatment of acid **161** with mCPBA under basic conditions resulted in the formation of lactone **163**. Hydrolysis of the lactone resulted in the formation of the desired DHCCA analogue **157**.



**Scheme 3.9** The route used for the synthesis of DHCCA analogue **157**.

The enantiopurity of cyclohexenoic acid **161** was determined by calculating the *d.e.* of auxiliary-bound precursor **162**. The *d.e.* could be calculated by the comparison of  $^{13}\text{C}$  NMR shifts of compound **162** with those of diastereomeric mixture **165** which was generated via the acylation of auxiliary **159** with commercially available racemic 3-cyclohexene carboxylic acid. The *d.e.* of compound **162** is greater than 95 % as determined by NMR, confirming the enantiopurity of cyclohexene carboxylic acid **161** (figure 3.17).

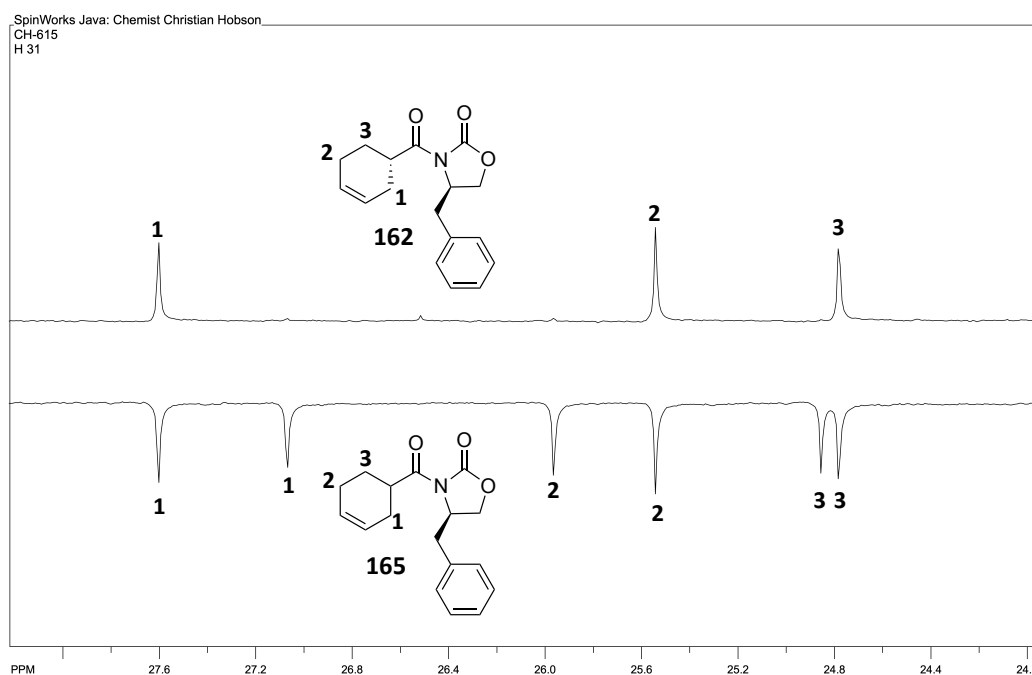


**Figure 3.17** The  $^{13}\text{C}$  NMR shifts of **162** compared with a mixture of diastereomers **165**.

Supplementing the production medium with DHCCA analogue **157** resulted in the  $\Delta 5912-14$  mutant strain producing the expected enacyloxin analogue **166** (figure 3.18). The structure of **166** was confirmed by the chemical shift in the  $^1\text{H}$  NMR spectrum of the proton highlighted in structure **166** (4.68 ppm), which is attached to a carbon atom with the opposite absolute stereochemistry to the natural product. The activity of the analogue against *A. baumannii* is the same as enacyloxin IIa (MIC 2  $\mu\text{g}/\text{mL}$ ).

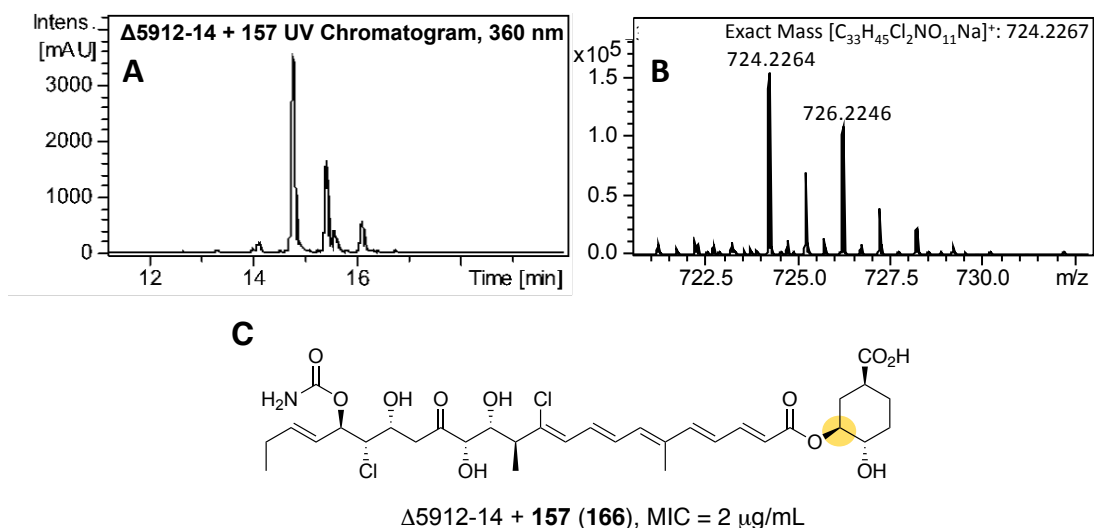
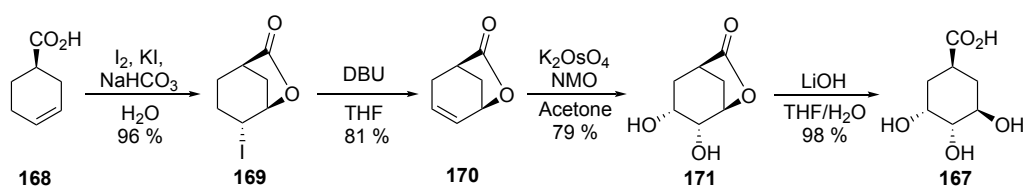


**Figure 3.18** **A** UV chromatogram (360 nm) from LC-MS analyses of extracts of *B. ambifaria* ( $\Delta 5912-14$ ) supplemented with DHCCA analogue **157**. **B** The HRMS for the species eluting at 14.4 min. **C** The structure assigned by NMR spectroscopy and the activity of the analogue against *A. baumannii*.

As well as altering the stereochemistry of the DHCCA unit, the activity of an analogue with an additional substituent on the ring was also tested. DHCCA analogue **167** harboring an additional hydroxyl group was synthesized (scheme 3.10) to investigate this. (*S*)-Configured cyclohexene carboxylic acid **168** was synthesized via the same route as **161**, using (*S*)-4-(phenylmethyl)-2-oxazolidinone (scheme 3.9). Cyclohexene carboxylic acid **168** was converted to iodolactone **169** via treatment with iodine and potassium iodide under basic conditions. Iodolactone **169** was then treated with DBU to afford alkene **170**, which was dihydroxylated to form the *anti*-diastereomer of lactone **171** selectively, as reported by Fukuyama and co-workers.<sup>205</sup> Hydrolysis of the lactone afforded DHCCA analogue **167** (scheme 3.10).



**Scheme 3.10** The synthetic route to DHCCA analogue **167**.

Supplementing the production medium with DHCCA analogue **167** resulted in the  $\Delta 5912-14$  mutant strain producing enacyloxin derivative **172** (figure 3.19). The structure of **172** was confirmed by the increase of 16 Da in the HRMS relative to enacyloxin as well as the disappearance of a proton from the DHCCA unit in the  $^1\text{H}$  NMR spectrum. The analogue is significantly less potent than enacyloxin IIa, suggesting that additional substituents on the DHCCA unit adversely effect activity of the molecule.

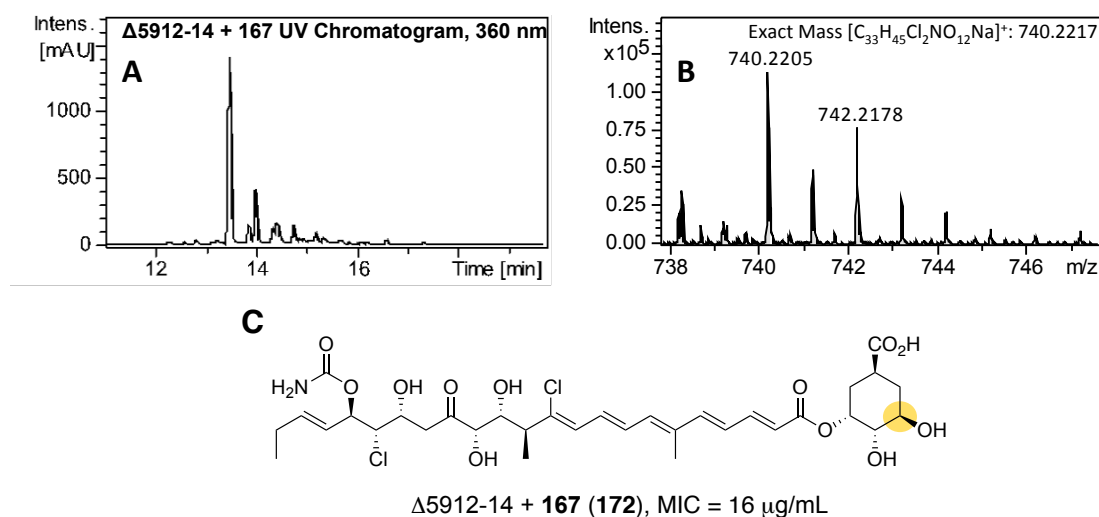
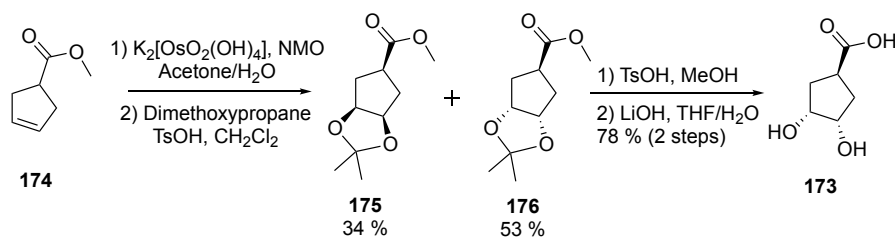


**Figure 3.19** **A** UV chromatogram (360 nm) from LC-MS analyses of extracts of *B. ambifaria* ( $\Delta 5912-14$ ) supplemented with DHCCA analogue **167**. **B** The HRMS for the species eluting at 13.4 min. **C** The structure assigned by NMR spectroscopy and the activity of the analogue against *A. baumannii*

As well as investigating the effect of substituents on the DHCCA ring, the effect of ring size on the activity of the compound was also tested. DHCCA analogue **173** harboring a cyclopentane ring was synthesized (scheme 3.11) to investigate this. Commercially available ester **174** was dihydroxylated and acetonide protected to allow the separation of the resulting *syn*- and *anti*-diastereomers, **175** and **176**.<sup>206</sup> The *anti*-diastereomer **176** was deprotected and hydrolysed to afford DHCCA analogue **173**.



**Scheme 3.11** The synthetic route used to DHCCA analogue **173**.



Supplementing the production medium with DHCCA analogue **173** resulted in the  $\Delta 5912-14$  mutant strain producing a mixture of diastereomers, **177** and **178** (figure 3.20). The production of this mixture is unavoidable, because although DHCCA analogue **173** is a *meso*-compound (achiral), the condensation domain is able to acylate both hydroxyl groups, producing a mixture of analogues where the DHCCA unit is no longer achiral. The analogues were separated using preparative HPLC. However, it was not possible to distinguish between the analogues using NMR spectroscopy. Interestingly, one analogue was slightly more potent (MIC 2  $\mu\text{g}/\text{mL}$  vs 4  $\mu\text{g}/\text{mL}$ ), although both had very similar activity to enacyloxin IIa.

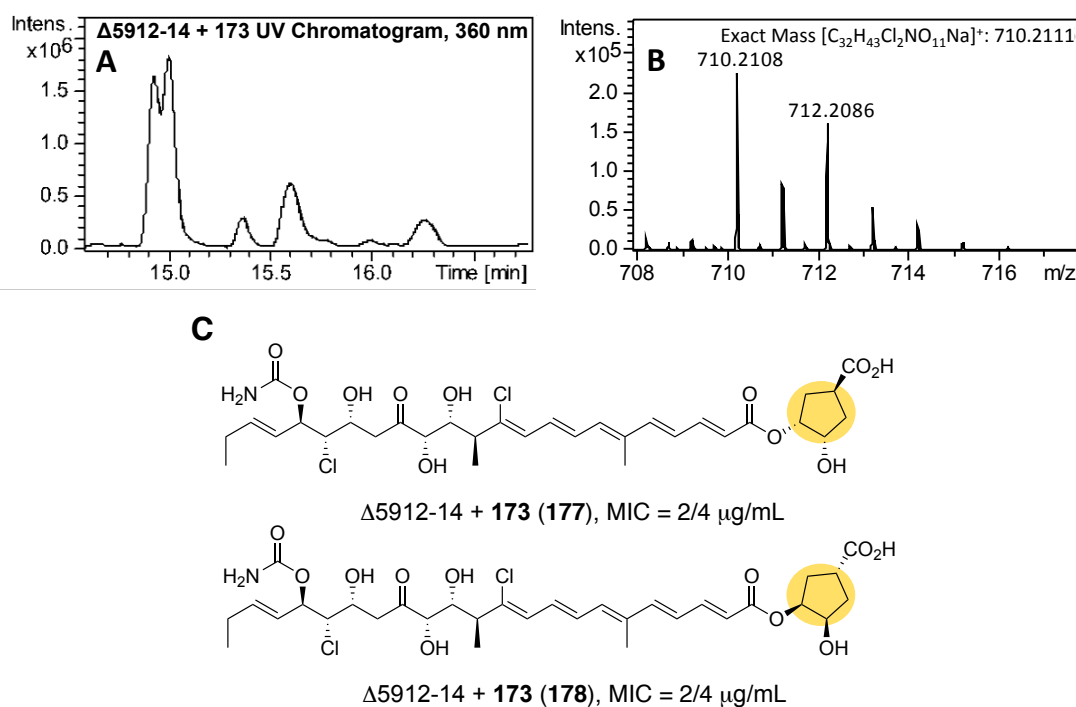
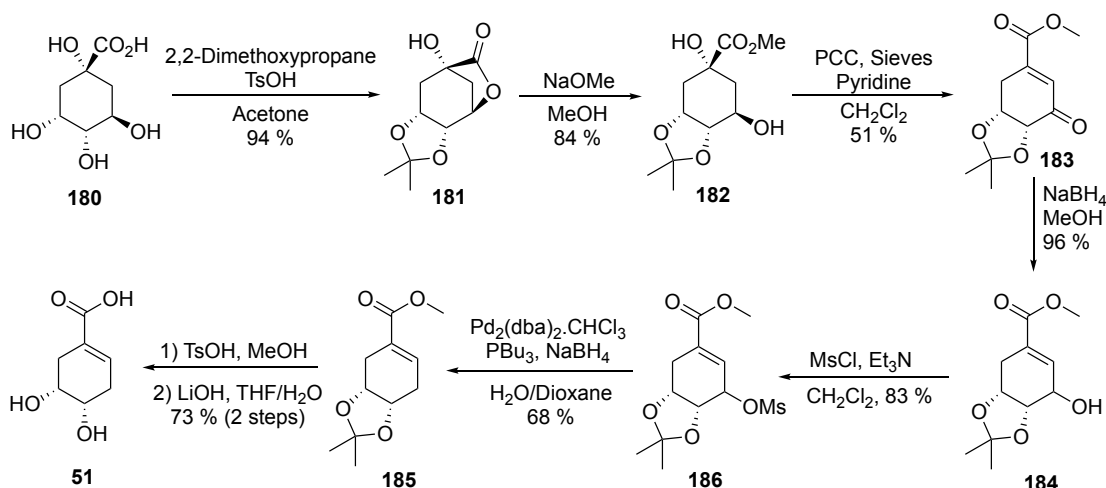


**Figure 3.20** **A** UV chromatogram (360 nm) from LC-MS analyses of extracts of *B. ambifaria* ( $\Delta 5912-14$ ) supplemented with DHCCA analogue **173**. **B** The HRMS for the species eluting at 14.9 and 15.0 min. **C** The structures assigned by NMR spectroscopy and the activity of the analogues against *A. baumannii*. Note it was not possible to distinguish between **177** and **178**.

Finally, the effect on activity of introducing a double bond into the ring was investigated using DHCCA analogue **51** (scheme 3.12). Commercially available quinic acid **180** was acetonide protected and esterified to afford lactone **181**, which was converted to methyl ester **182** using sodium methoxide. Ketone **183** was generated using an oxidation-elimination reaction followed by reduction to alcohol **184**. The alcohol was mesylated, then subjected to palladium-catalyzed elimination to afford ester **185**. The acetonide group was removed and the ester was hydrolyzed to produce DHCCA analogue **51**.



**Scheme 3.12** The synthetic route to DHCCA analogue **51**.

Supplementing the production medium with DHCCA analogue **51** resulted in the production of expected enacyloxin analogue **187** (figure 3.21). The structure of **187** was confirmed by the loss of 2 Da in the HRMS relative to enacyloxin IIa as well as the appearance of an additional vinyl proton from the DHCCA unit in the  $^1\text{H}$  NMR spectrum. The analogue is more potent than enacyloxin IIa, and more potent than any other analogue produced, confirming that the mutasynthesis strategy can be used to create analogues with increased potency.

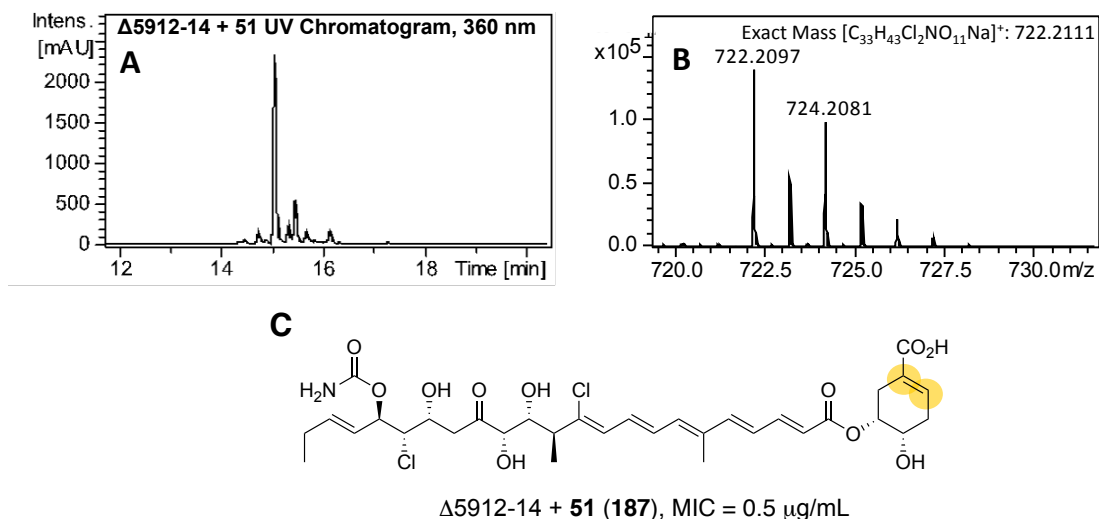
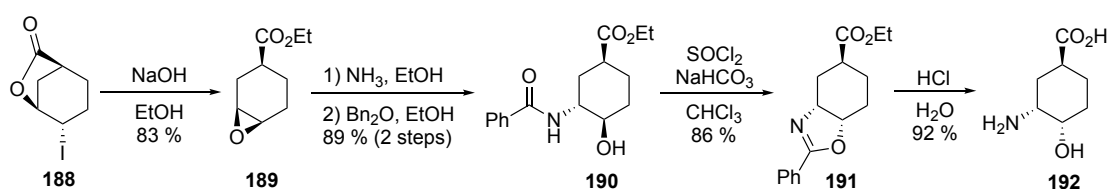


**Figure 3.21** **A** UV chromatogram (360 nm) from LC-MS analyses of extracts of *B. ambifaria* ( $\Delta 5912-14$ ) supplemented with DHCCA analogue **51**. **B** The HRMS for the species eluting at 15.0 min. **C** The structure assigned by NMR spectroscopy and the activity of the analogue against *A. baumannii*

It had already been shown that the mutasynthesis strategy could be used to produce an enacyloxin analogue **149**, with an amide in place of the ester (section 3.1.2.3). Although this analogue **149** is less potent than enacyloxin IIa **30** (MIC 8 µg/mL), the amide group is likely to be more stable than the ester linkage in enacyloxin IIa **30**. In an effort to produce a more potent amide derivative, a 3-amino analogue of DHCCA, aminohydroxy-cyclohexanecarboxylic acid (AHCCA, **192**) was synthesized (scheme 3.13). Iodolactone **188** was prepared via the same route used for iodolactone **169**, from (*R*)-cyclohexene carboxylic acid **161**. The iodolactone was treated with hydroxide in ethanol to form epoxide **189**, which was selectively ring-opened using aqueous ammonia and the resulting amine was benzoylated to afford amide **190**. Using thionyl chloride, the hydroxyl group of **190** was activated and displaced to form oxazoline **191**, which was hydrolysed in acidic conditions to afford AHCCA **192**.



**Scheme 3.13** The synthetic route to DHCCA analogue **192**.

Using the same feeding procedure as for previous DHCCA analogues, the enacyloxin derivative could not be detected. It was unclear if this was because AHCCA **192** is not a substrate for the Bamb\_5915 condensation domain, or due to a problem with the uptake of the derivative. The ability of the condensation domain to accept AHCCA **192** as a substrate was tested *in vitro* (figure 3.22). The acetylated Bamb\_5917 PCP domain was incubated with Bamb\_5915 (both overproduced and purified by Dr. Joleen Masschelein), and AHCCA **192**. The production of the corresponding amide **193** was detected by LC-MS, by comparison with a synthetic standard **193** which was prepared by acetylation of AHCCA **192**.<sup>93</sup> From the results of the assay, it is clear that Bamb\_5915 is able to use AHCCA analogue **192** as a substrate, suggesting that the lack of production of the corresponding enacyloxin derivative may be due to poor cell uptake, potentially due to its high polarity.

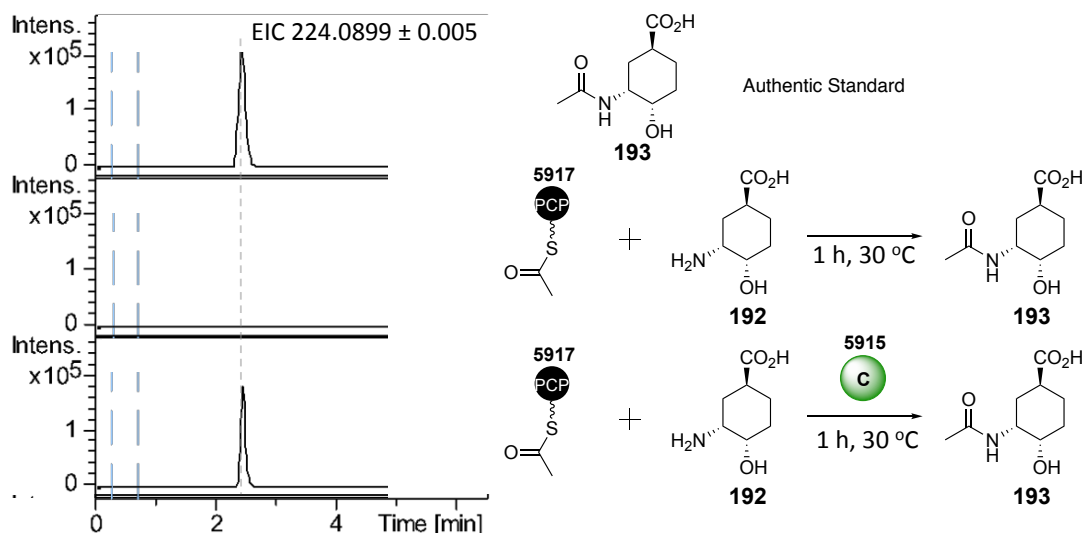
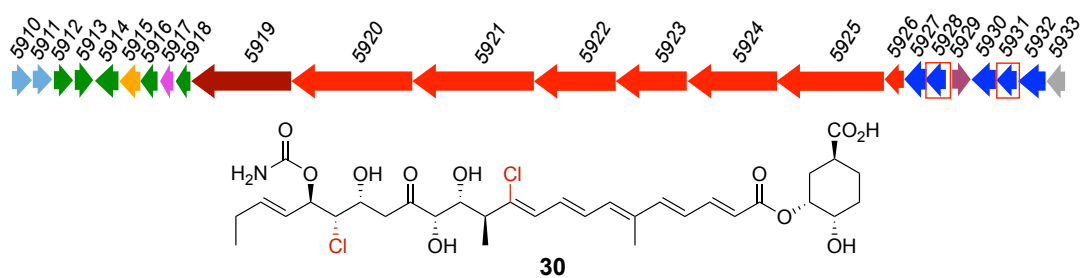


**Figure 3.22** The results of the *in vitro* assay confirming that AHCCA **192** is a substrate for the condensation domain. A detailed procedure for this assay can be found in section **6.7.2**.

### 3.2.1.6 Production of Brominated Analogues

Analogues in this section were purified in collaboration with Jake Sergeant.

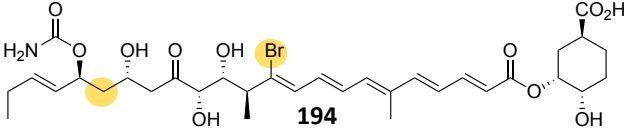
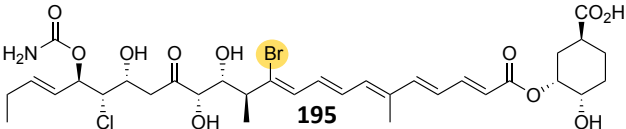
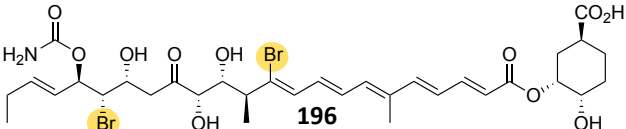
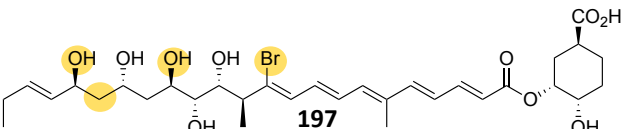
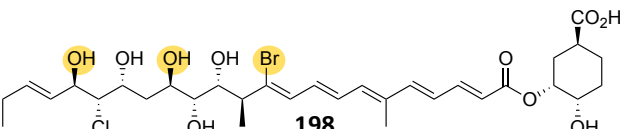
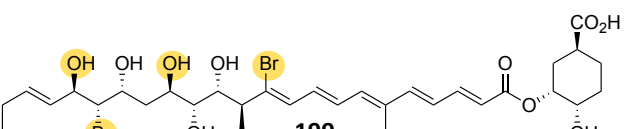
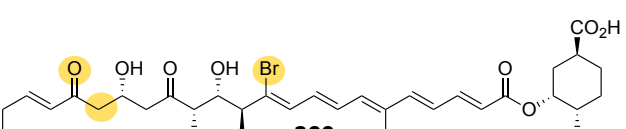
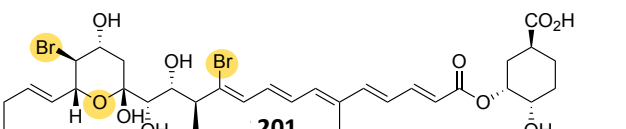
There are many examples of halogenase enzymes catalyzing bromination as well chlorination.<sup>207,208</sup> Given the presence of genes encoding the flavin-dependent halogenase (Bamb\_5928) and the Fe(II)  $\alpha$ -KG-dependant halogenase (Bamb\_5931) in the enacyloxin gene cluster, it was hoped that these enzymes could be utilized in order to generate brominated derivatives of enacyloxin (figure **3.23**). A bromide analogue of enacyloxin was generated by Watanabe and co-workers by adding a source of bromide into the production medium, a similar strategy was employed here.<sup>209</sup>

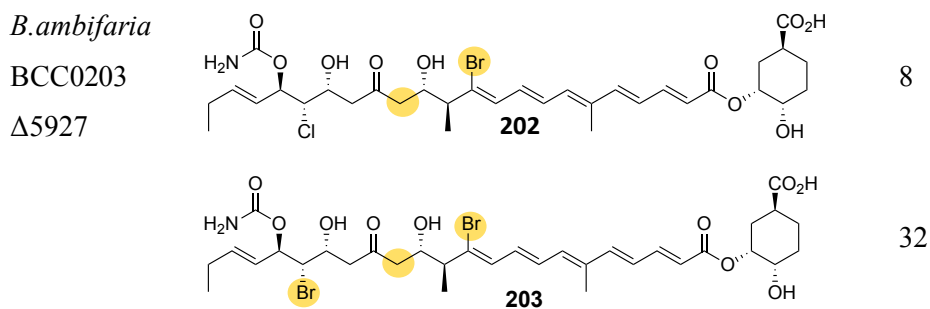


**Figure 3.23** The halogenase enzymes in the enacyloxin cluster (Bamb\_5928 and 5931).

To generate brominated enacyloxin derivatives, the source of chloride in the BSM production media (ammonium chloride) was replaced by a source of bromide (ammonium bromide). The wild-type *B.ambifaria* BCC0203 strain was then grown on the brominated media and any brominated analogues were detected using LC-MS (appendix 8.2), before being purified by HPLC. This resulted in the production of mono-brominated, chloro-brominated and di-brominated analogues. This procedure was repeated using several of the mutant strains created in section 3.2.1.2 to generate a library of brominated analogues (table 3.1).

**Table 3.1:** Brominated Enacyloxin Derivatives

Strain	Structure (Determined by NMR and HRMS)	MIC ( $\mu\text{g/mL}$ )
<i>B.ambifaria</i> BCC0203 WT	 <b>194</b>	16
	 <b>195</b>	2
	 <b>196</b>	1
<i>B.ambifaria</i> BCC0203 $\Delta 5930 + 32$	 <b>197</b>	32
	 <b>198</b>	2
	 <b>199</b>	1
<i>B.ambifaria</i> BCC0203 $\Delta 5930$	 <b>200</b>	8
	 <b>201</b>	32



Using this strategy, a variety of brominated analogues could be generated, some with increased potency relative to the corresponding chlorinated enacyloxin derivatives. All of these analogues harbor a vinyl bromide functional group, which can serve as a handle for synthetic modification via metal catalyzed coupling reactions.<sup>210,211</sup> These reactions typically result in the formation of new carbon-carbon bonds, and so the generation of brominated analogues provides scope for semi-synthetic derivatives of enacyloxin harboring an additional carbon skeleton at the C-11 position. This represents a more facile method for the modification of the carbon skeleton of enacyloxin, compared with engineering of the megasynthase (section 3.1.1).

### 3.2.1.7 Rational Design of a Potent Enacyloxin Derivative

The SAR data resulting from the library of enacyloxin analogues were exploited to try to rationally design an analogue with even greater potency. The structures of analogues with increased potency relative to enacyloxin IIa were compared to identify changes likely to be responsible (figure 3.24). Analogue **187**, harboring the unsaturated DHCCA unit, and analogues **45** and **199**, lacking both the ketone and carbamoyl functional groups, are both more potent than enacyloxin IIa. Thus, a mutant lacking the genes encoding the carbamoyl transferase (Bamb\_5930), the PQQ dependent dehydrogenase (Bamb\_5932) and the DHCCA biosynthesis enzymes (Bamb\_5912-14) was constructed. This mutant was made by introducing the  $\Delta$ 5912-14 deletion construct (provided by Dr. Joleen Masschelein) into the cured  $\Delta$ 5930 + 32 deletion mutant. The resulting strain was then grown on production medium supplemented with DHCCA analogue **51**, and analogue **204** was purified and characterized by NMR spectroscopy (figure 3.25).

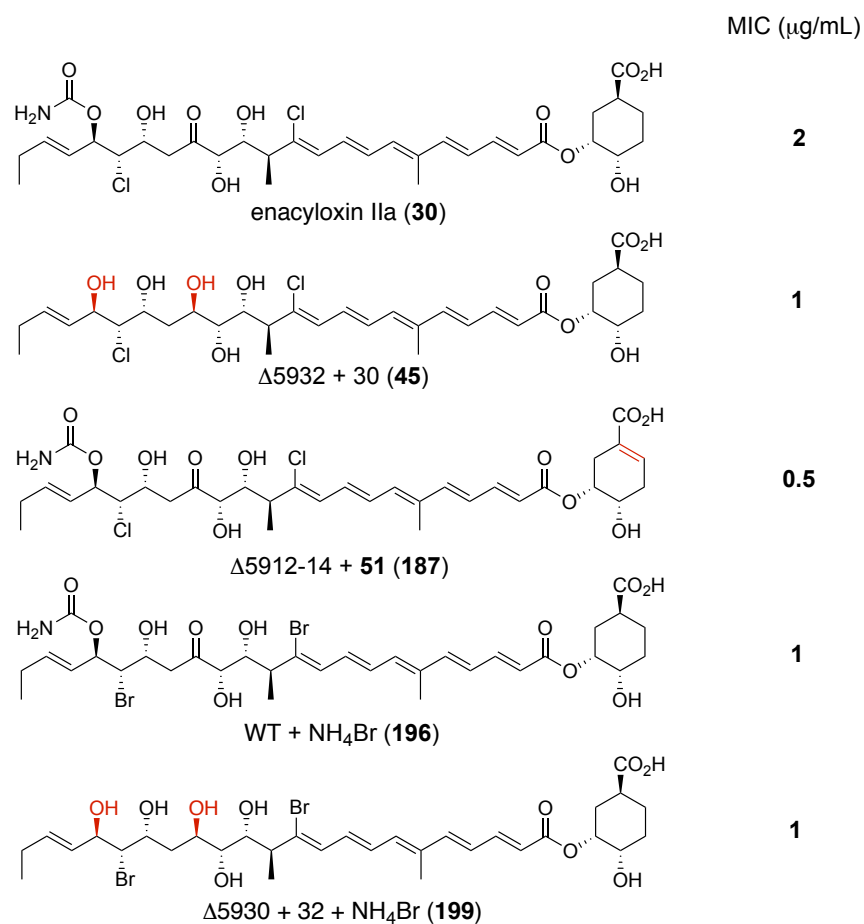


**Figure 3.24** The enacyloxin analogues with increased potency relative to enacyloxin IIa, the features identified as influencing the activity are highlighted in red.

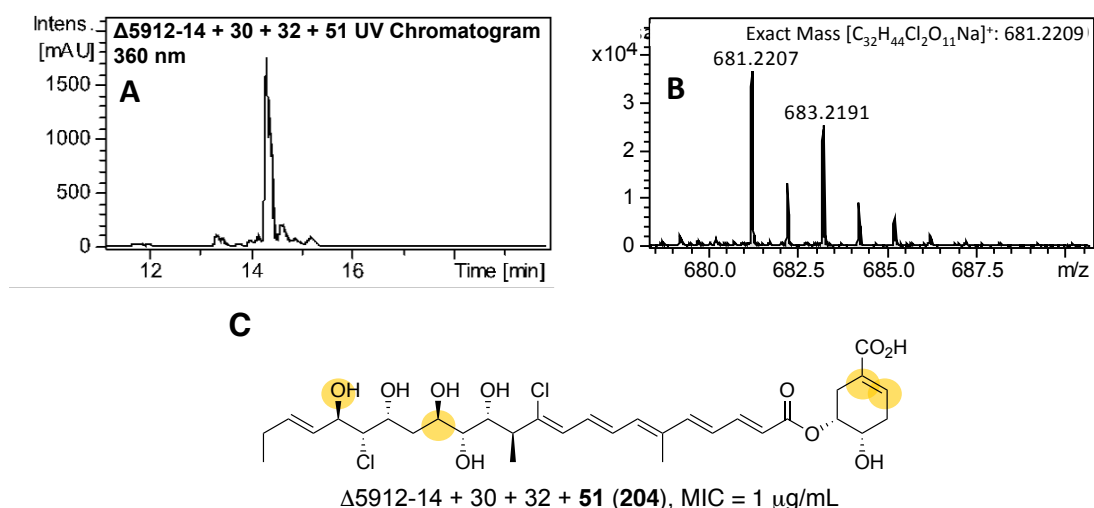


**Figure 3.25** **A** UV chromatogram (360 nm) from LC-MS analyses of extracts of *B. ambifaria* ( $\Delta 5912-14+30+32$ ) supplemented with DHCCA analogue **51**. **B** The HRMS for the species eluting at 14.3 min. **C** The structure assigned by NMR spectroscopy and the activity of the analogue against *A. baumannii*

Surprisingly, analogue **204** had the same potency as analogue **45**. The reason for this is unclear. However, this result suggests that changes made to the structure of enacyloxin IIa may affect the activity of analogues against *A. baumannii* in ways other than target binding. The changes in polarity of the analogues may result in changes in the ability of the derivatives to cross cell membranes, which may influence the changes in MIC observed. The derivatives may also be more susceptible to efflux and degradation, making the rational design of derivatives based on MIC values alone more challenging.

### **3.3 Conclusions**

#### **3.3.1 Summary**

Three biosynthetic engineering strategies have been used to generate a library of enacyloxin IIa analogues, which harbor structural changes in both the DHCCA unit and the polyol region (green and blue regions respectively, figure **3.26**). This has resulted in the production of five enacyloxin analogues that are more potent than enacyloxin IIa **30** (figure **3.26**). These five analogues may provide a starting point for more complex changes to the structure, which may be necessary to further improve the activity and the stability of the molecule.



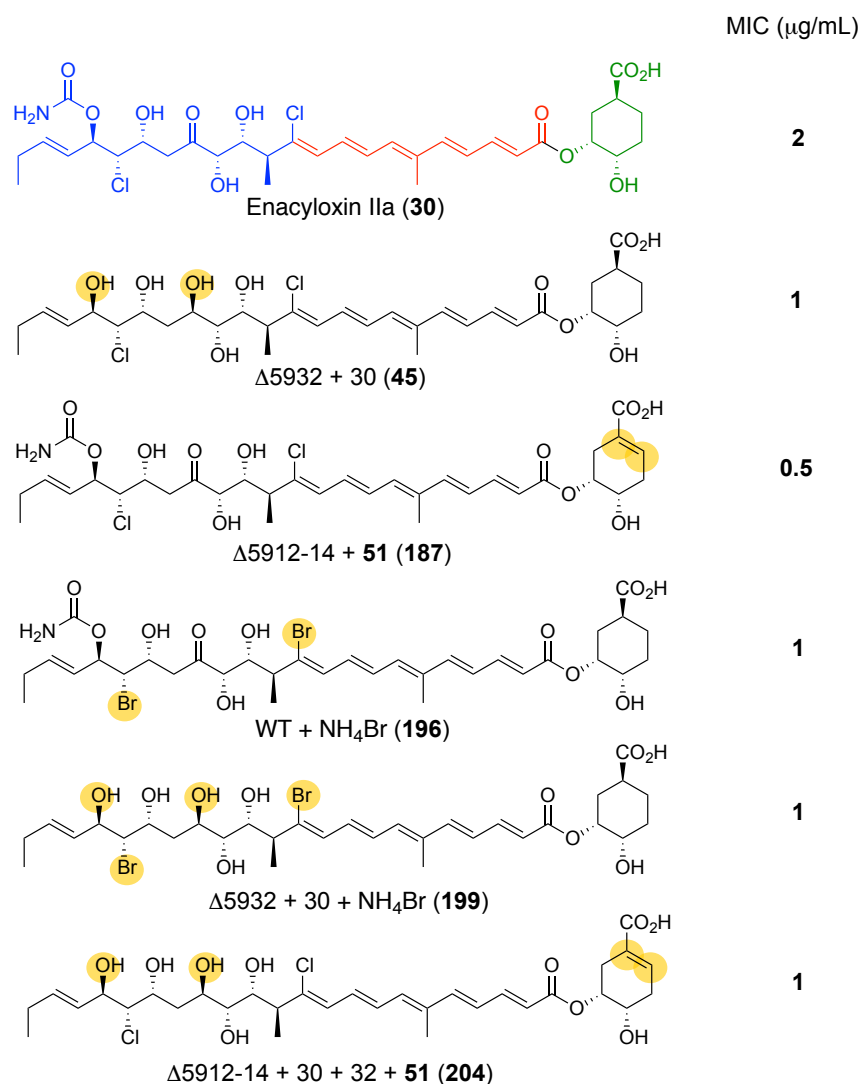


**Figure 3.26** The five enacyloxin analogue with increased potency relative to enacyloxin IIa **30**.

### 3.3.2 Rationalizing Changes in Activity

One of the aims of this project was to probe the importance of the polar contacts between enacyloxin IIa **30** and EF-Tu, highlighted in the crystal structure (figure 3.27).<sup>110</sup> Many analogues were generated that harbor structural changes predicted to influence the polar contacts. The changes in activity of the analogues were rationalized in relation to the structure.

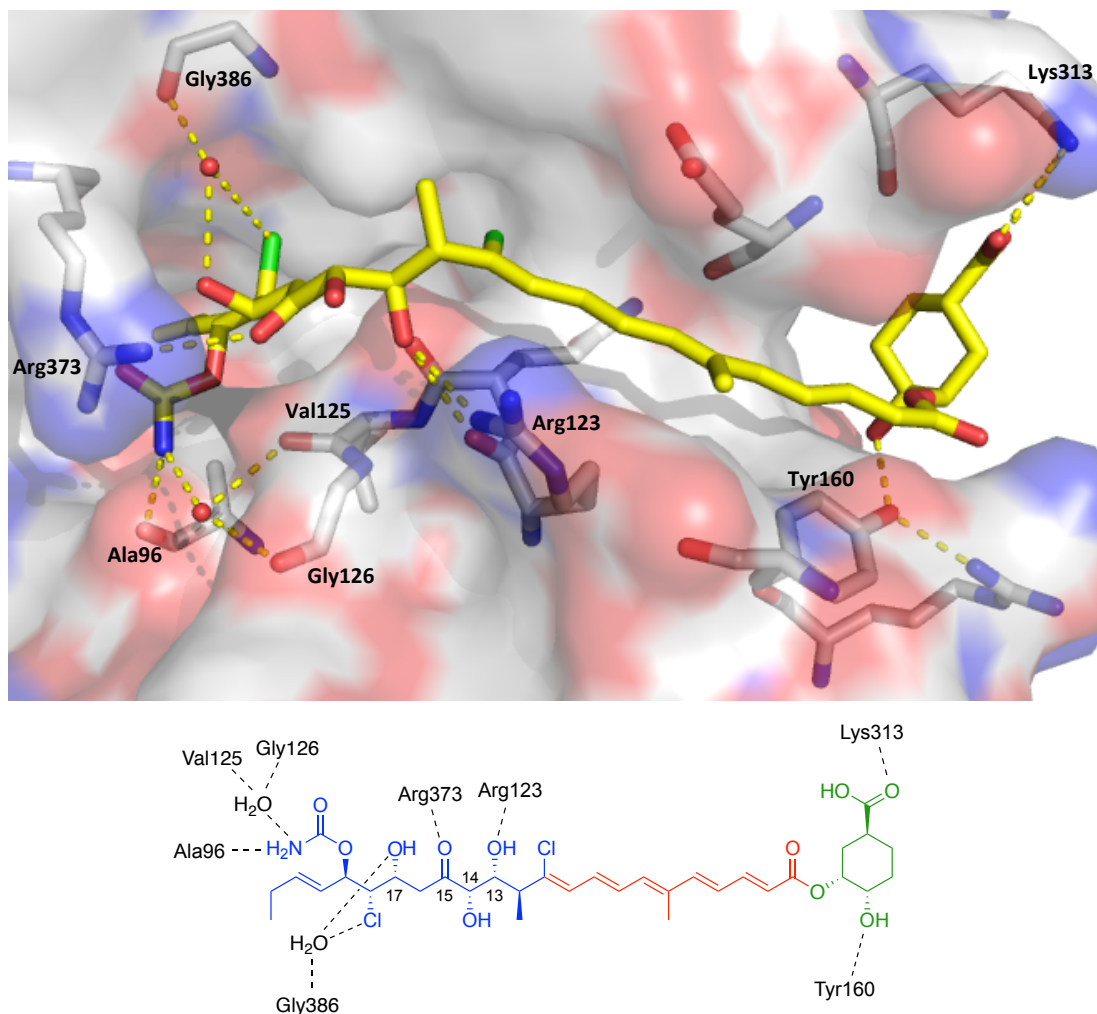


**Figure 3.27** The crystal structure of enacyloxin IIa bound to *E. coli* EF-Tu. The polar contacts between the protein and the antibiotic are highlighted.

Based on the key polar interactions identified in the structure (figure 3.27), the activity of some of the analogues produced in this chapter, as well as some of those created previously could be explained (figure 3.28). When the C-14 hydroxyl group (installed by the Fe(II)  $\alpha$ -KG-dependent dioxygenase (Bamb\_5927)) is removed, the activity does not change. This is in accordance with the observation that this hydroxyl group does not make any polar contacts with the protein. Removal of the carbamoyl group results in reduced activity. This could be due to the formation of the cyclic hemiacetal at the C-15 position, but the analogue is likely to be in equilibrium with the acyclic ketone form. Given that the carbamoyl group appears to make several polar contacts with the protein, the decrease in activity is more likely due to reduced binding affinity of the acyclic form. When the C-15 keto group was converted to a hydroxyl group, the activity was significantly reduced. The keto also makes contacts with EF-Tu and the change in hybridization of the C-15 carbon may weaken these interactions.

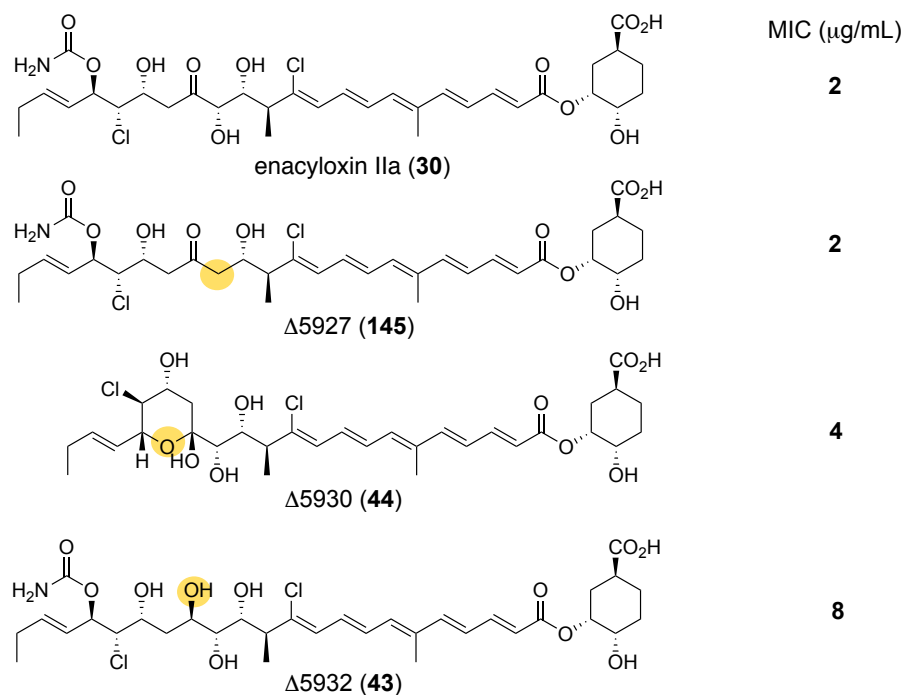


**Figure 3.28** The activity of three enacyloxin analogues relative to enacyloxin IIa **30**, which can be explained on the basis of polar contacts observed in the crystal structure.

However, when both the carbamoyl and keto groups are missing (analogue **45**), the activity increases relative to enacyloxin IIa. This cannot be explained on the basis of the crystal structure, because both of these groups make polar contacts (figure 3.29). In addition, when both of these groups are removed individually (analogues **43** and **44**), the activity is reduced. The increase in potency may be due to the chain binding in a different orientation, or changes in cell permeability. The most potent analogue generated (analogue **187**) harbors an unsaturated DHCCA unit. Based on the crystal structure, there are no obvious interactions that could explain the increase in activity. The increase may again be due to changes in cell permeability, or due to the reduced entropic cost of binding the more rigid unsaturated DHCCA moiety in analogue **187**, relative to the more flexible DHCCA unit of enacyloxin IIa. This indicates that not all of the changes in activity observed for the analogues can be rationalized solely on the basis the polar contacts, and other factors such as changes in conformation, entropic costs and cell permeability need to be considered.

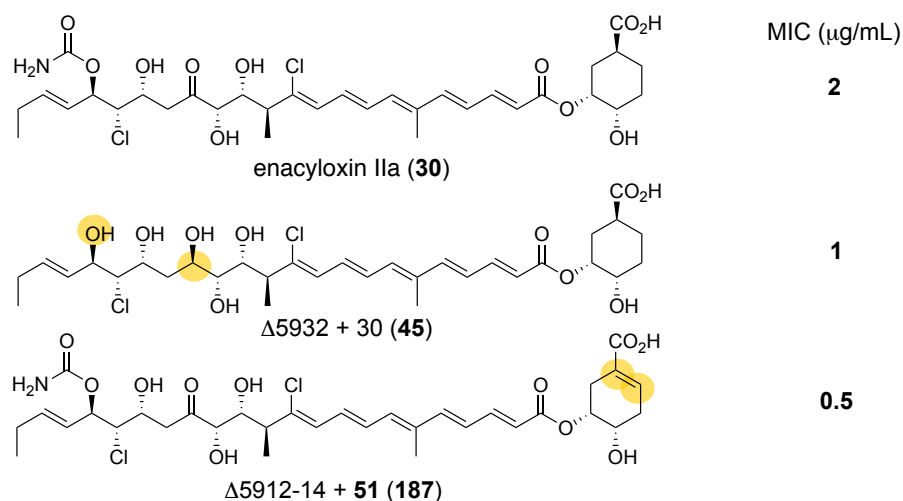


**Figure 3.29** The activity of two enacyloxin analogues relative to enacyloxin IIa **30**, which cannot be explained solely on the basis of polar contacts observed in the crystal structure

This makes it difficult to determine the importance of the polar contacts based on the results of whole cell assays alone. To eliminate factors such as cell permeability, the interaction between EF-Tu and the analogues needs to be investigated *in vitro*. This could be achieved using isothermal titration calorimetry (ITC), which allows the determination of the dissociation constant ( $K_d$ ) for the interaction.

### 3.3.3 Future Work

Another limitation of enacyloxin IIa as a viable drug candidate is light-induced isomerization. The presence of the C-6 methyl group in the polyene region, coupled with the extent of conjugation, promotes light-induced isomerization to a less active analogue due to steric clashing (figure 3.30). This stability problem cannot be addressed directly using the library of analogues generated in this study.

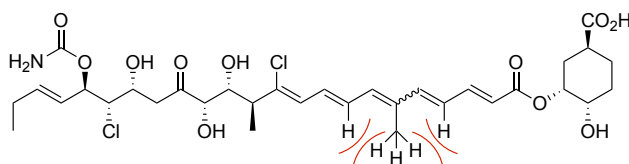


**Figure 3.30** The light-induced isomerization promoted by the C-6 methyl group.

In an effort to address this problem, a mutant was generated by Helen Smith, another PhD student in the group, in which the MT domain responsible for the installation of the methyl group in the polyene region was inactivated using site-directed mutagenesis. This resulted in the production of an enacyloxin analogue **205** lacking the C-6 methyl group thought to promote isomerization (figure 3.31).

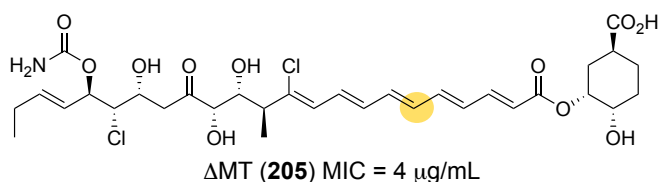


**Figure 3.31** The enacyloxin analogue lacking the methyl group thought to promote isomerization.

The activity of this analogue is reduced compared to that of enacyloxin IIa **30**. This is where the platform of potent enacyloxin analogues generated in this chapter could be used. The features identified in this chapter that increase potency, could be combined with the deletion of the methyl group, to produce more stable enacyloxin analogues, with similar potency to the natural product (figure 3.32).

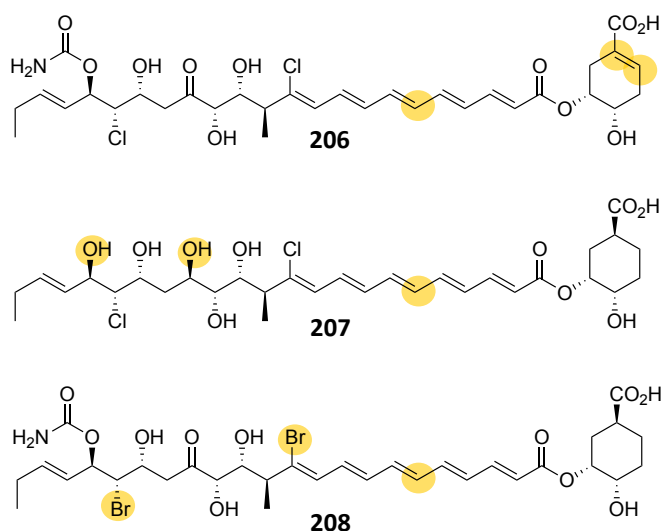


**Figure 3.32** Potential enacyloxin analogues that may have increased stability whilst retaining potency.

Another way in which the platform of potent analogues generated in this chapter could be used, is to address the instability of the labile ester linkage in enacyloxin IIa. It has already been shown that a simplified amide derivative can be generated using the mutasynthesis strategy (section 3.1.2.3). This is likely to be more stable to hydrolysis, but the activity of this analogue was reduced (MIC of 4  $\mu\text{g/mL}$ ) compared with enacyloxin IIa. The features identified in this chapter that increase potency, could be combined with an amide linkage, to produce more hydrolytically resistant enacyloxin analogues that retain potency (figure 3.33).

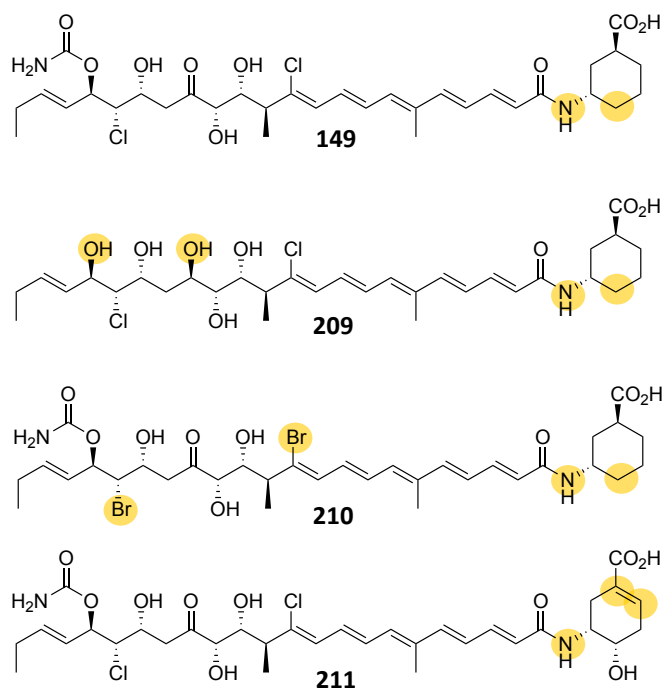
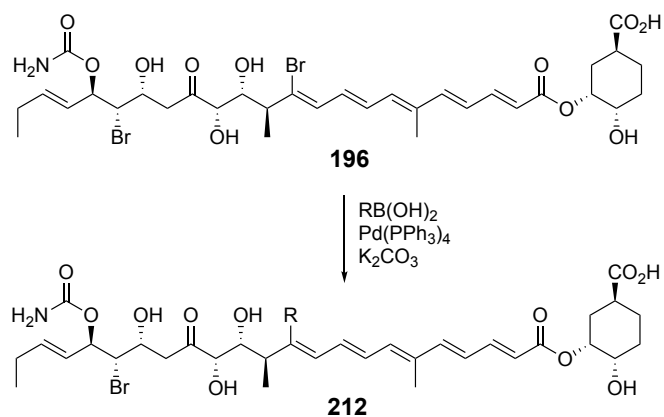


**Figure 3.33** The simplified amide analogue (**149**) generated in section 3.1.2.3, along with potential additional amide enacyloxin analogues (**209-211**), which are likely to have enhanced potency.

As well as using the library generated in this chapter as a platform for more stable analogues, the brominated derivatives could be used to generate analogues with more diverse structures. This could be achieved using Suzuki coupling reactions (scheme 3.14).<sup>210,211</sup>



**Scheme 3.14** The use of a palladium-catalyzed coupling reaction to derivatize brominated enacyloxin analogue **196**.

Overall, the library of enacyloxin analogues created in this chapter can be used both as a platform for the generation of more stable enacyloxin analogues, as well as a basis for a more diverse library of derivatives harboring more complex structural changes. The analogues produced could also be tested in animal infection models to establish whether they are viable drug candidates.

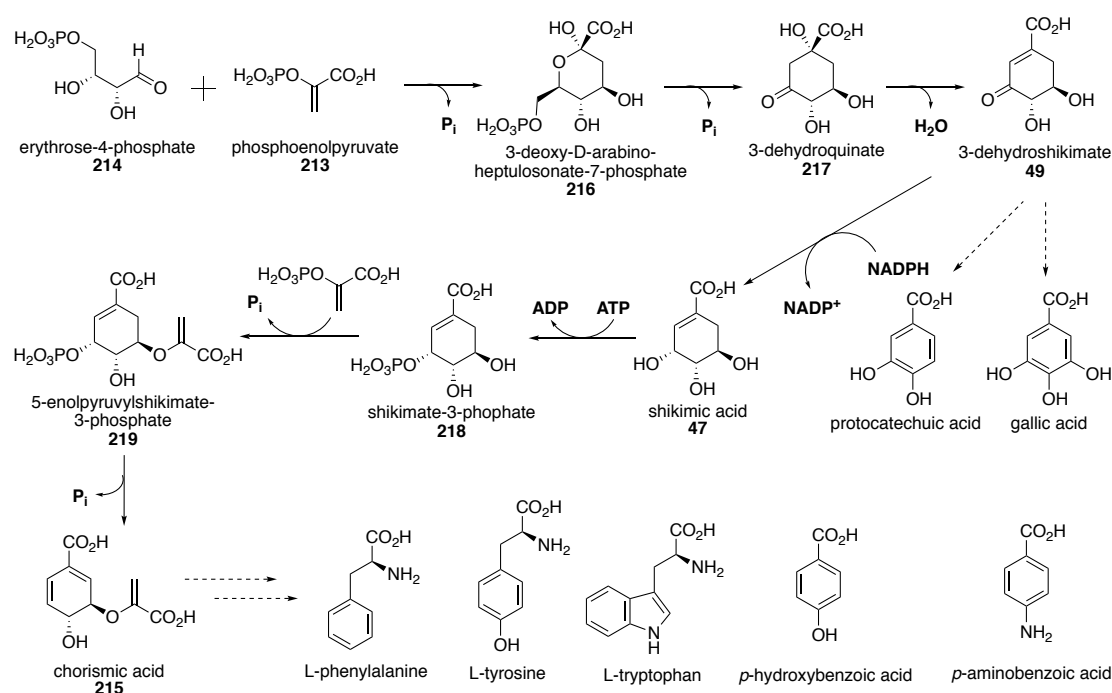
## **4. Results and Discussion III: DHCCA Biosynthesis**



## 4.1 Introduction

### 4.1.1 Shikimate Derived Natural Products

The shikimate pathway is a primary metabolic route used by plants and microorganisms for the biosynthesis of aromatic amino acids tryptophan, tyrosine and phenylalanine, as well as other aromatic primary metabolites essential for survival of the organism. The pathway starts with the condensation of phosphoenolpyruvate **213** and erythrose-4-phosphate **214** and leads to the formation of chorismic acid **215** via shikimic acid **47**, with various branch points along the pathway leading to the formation of essential primary metabolites (scheme 4.1).<sup>212,213</sup>



**Scheme 4.1** The shikimate pathway in plants and microorganisms. Dotted arrows indicated branch points where essential primary metabolites are formed.

As well as being important for the production of essential primary amino acids, the shikimate pathway is also utilized for the biosynthesis of many secondary metabolites.<sup>214</sup> Often these metabolites are comprised of the end products of the shikimate pathway, for example aromatic amino acids are found in many NRPS assembled natural products, and there are many phenylalanine-derived phenylpropanoid natural products found in plants.<sup>215</sup> In bacteria, there are many examples of shikimate-derived natural products that utilize variants of the shikimate pathway by branching off at earlier steps.<sup>214</sup> Examples include ansatrienin A (**220**), rapamycin (**112**) and ansamitocin P-3 (**109**) (figure 4.1).<sup>57,216,217</sup>

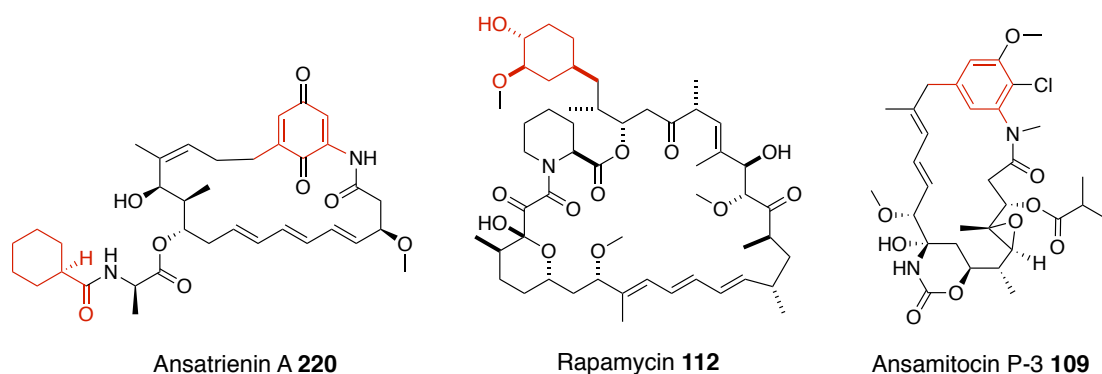
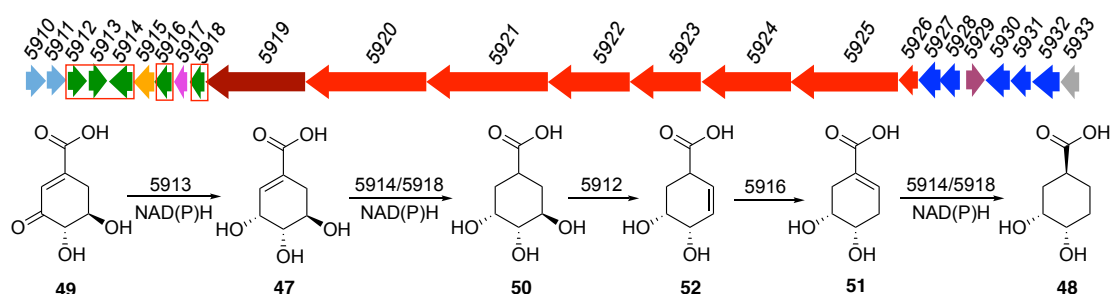


**Figure 4.1** Shikimate-derived natural products, the unit incorporated from the shikimate pathway is highlighted in red.<sup>57,216,217</sup>

#### 4.1.2 Proposal for DHCCA Biosynthesis

The DHCCA unit of enacyloxin IIa was shown to be essential to biological activity in section 3.1.2.3. DHCCA **48** is proposed to be derived from shikimate **47**, with five enzymes (Bamb\_5912, 5913, 5914, 5916 and 5918) hypothesized to be involved in the biosynthetic pathway (scheme 4.2).<sup>104</sup> The pathway consists of the reduction of 3-dehydroshikimate **49** to shikimate **47** by a shikimate dehydrogenase (Bamb\_5913). This is followed by reduction to a trihydroxycyclohexanecarboxylic acid (THCCA) intermediate **50** by one of two enoyl reductases (Bamb\_5914 or 5918). This intermediate is then dehydrated via a dehydratase (Bamb\_5912), which is followed by isomerization via an enoyl isomerase (Bamb\_5916) to form unsaturated DHCCA analogue **51**. The final step to form DHCCA **48** is catalyzed by the remaining enoyl reductase enzyme (Bamb\_5914 or 5918). The reduction of shikimate **47** is a key step in the pathway as this is the branch point away from the shikimate pathway (scheme 4.1).



**Scheme 4.2** The proposed pathway for the biosynthesis of DHCCA **48**.<sup>104</sup> The putative functions of all the genes involved in enacyloxin biosynthesis can be found in appendix

**8.6.**

### 4.1.3 Aims

The aim of this project was to confirm the biosynthetic pathway of the DHCCA unit of enacyloxin IIa using both *in vivo* gene deletions and *in vitro* biochemical assays. As well as providing insight into biosynthesis of this key unit of enacyloxin IIa, it was hoped that this investigation would lead to the identification more genes that could be targeted for further engineering of enacyloxin IIa analogues.

## 4.2 Results and Discussion

### 4.2.1 Investigation of the Proposed Pathway using Gene Deletions

The five genes proposed to be involved in DHCCA biosynthesis (scheme 4.2) were deleted using the same gene deletion methodology described in section 3.2.1.1 to try to confirm their respective roles in the pathway (figure 4.2). The deletion of *bamb\_5912* (performed by Dr. Joleen Masschelein) resulted in the production of enacyloxin analogue 172. This is in agreement with the proposed pathway, as the Bamb\_5912-catalyzed dehydration of 50 cannot take place, resulting in the incorporation of 50 (scheme 4.2). The deletion of *bamb\_5913* resulted in wild-type levels of enacyloxin IIa 30 production as well as a small amount of analogue 172. The production of enacyloxin IIa 30 can be explained, as despite Bamb\_5913 no longer being present to reduce 3-dehydroshikimate 49, there may still be enough shikimic acid 47 present in the cell from primary metabolism in order for DHCCA biosynthesis to still proceed. The presence of analogue 172 cannot be explained based on the proposed pathway.

The deletion of *bamb\_5914* abolished the production of enacyloxin IIa 30. This can be rationalized based on the proposed pathway if this enzyme is responsible for the reduction of shikimate 47. The deletion of *bamb\_5916* also abolished production. If the pathway is correct, this suggests that alkene intermediate 52 is not a substrate for the Bamb\_5915 condensation domain. Finally, the deletion of *bamb\_5918* resulted in wild-type levels of enacyloxin IIa 30 production as well as a small amount of analogue 172. This cannot be explained based on the proposed pathway, as if Bamb\_5918 catalyzes the final reduction step, the incorporation of unsaturated intermediate 51 into the structure of enacyloxin should be observed, as chemically synthesized 51 has already been shown to be incorporated (section 3.2.1.5). Alternatively, if Bamb\_5918 catalyzed the reduction of shikimate 47, enacyloxin IIa 30 production would be abolished, as the reduction of shikimate 30 would not take place. Overall, the results of these deletions are not congruent with the proposed pathway.

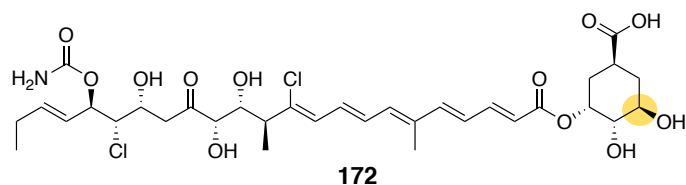
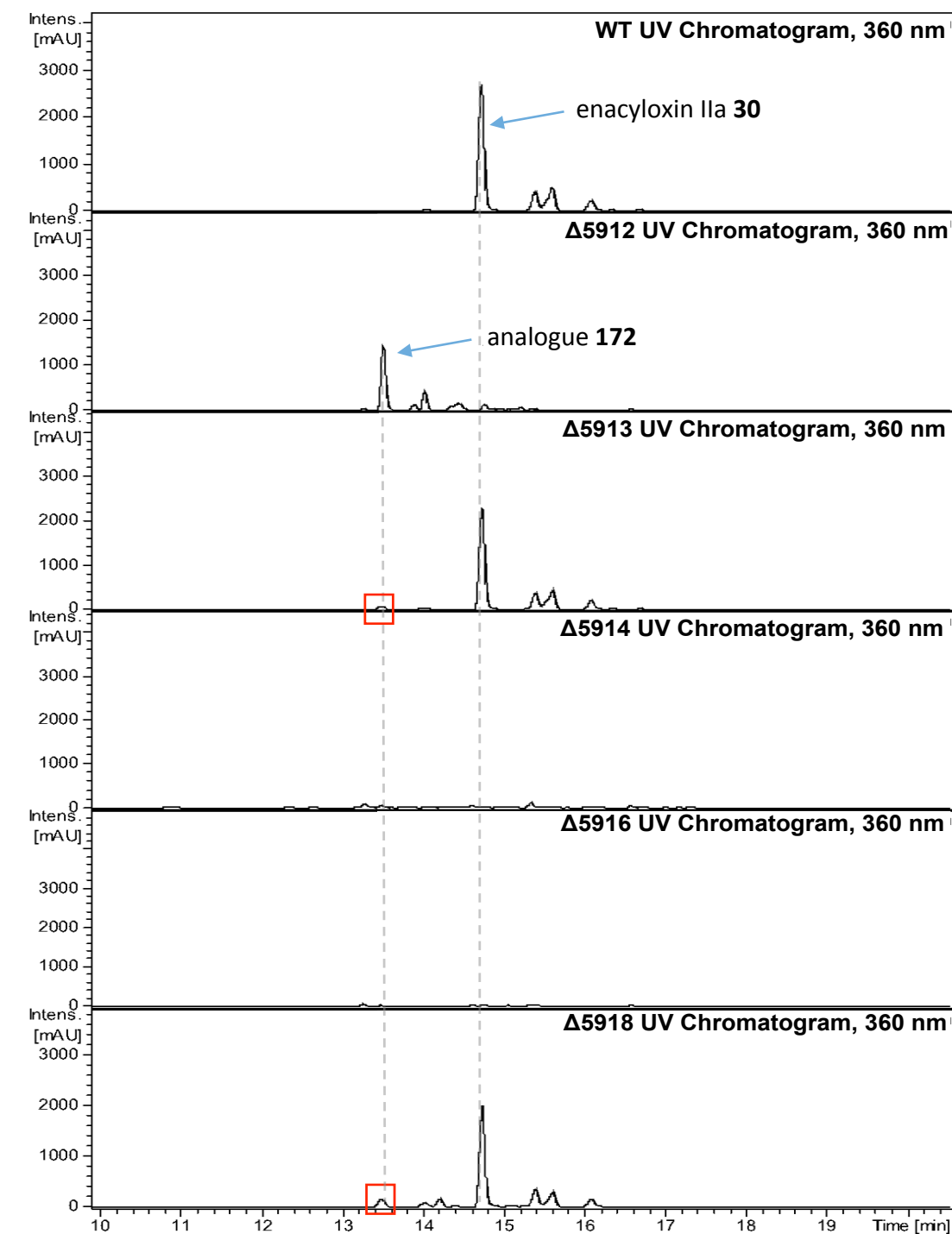


**Figure 4.2** The UV chromatograms corresponding to the deletion of the five genes involved in DHCCA biosynthesis. The presence of the proposed compounds was confirmed by HRMS and analogue **172** was characterized by NMR.

#### 4.2.2 Investigation of the Proposed Pathway using *in vitro* Biochemistry

To investigate the proposed pathway *in vitro*, the five proposed DHCCA biosynthesis genes were cloned into an appropriate expression vector, before overproduction and purification of the corresponding proteins for *in vitro* biochemical assays. The five genes were amplified using primers designed with a CACC overhang on the forward primer in order to facilitate TOPO cloning into the pET151 expression vector (section 6.3.6.3). This vector has an IPTG-inducible T7 promoter and encodes a *N*-terminal His<sub>6</sub>-tag allowing for IPTG-induced expression and purification by metal-affinity chromatography (section 6.6.3). Both the *bamb\_5914* and *bamb\_5916* genes were cloned into pET151 as verified by sequencing. However neither of the corresponding proteins were successfully overproduced in either *E.coli* BL21(DE3) or *E.coli* C43(DE3) expression cell lines (figure 4.3). It was thought that this could be due to the high GC content (73 %) of the genes from the enacyloxin gene cluster not being compatible with the low GC content of the DNA of *E.coli* expression strains.

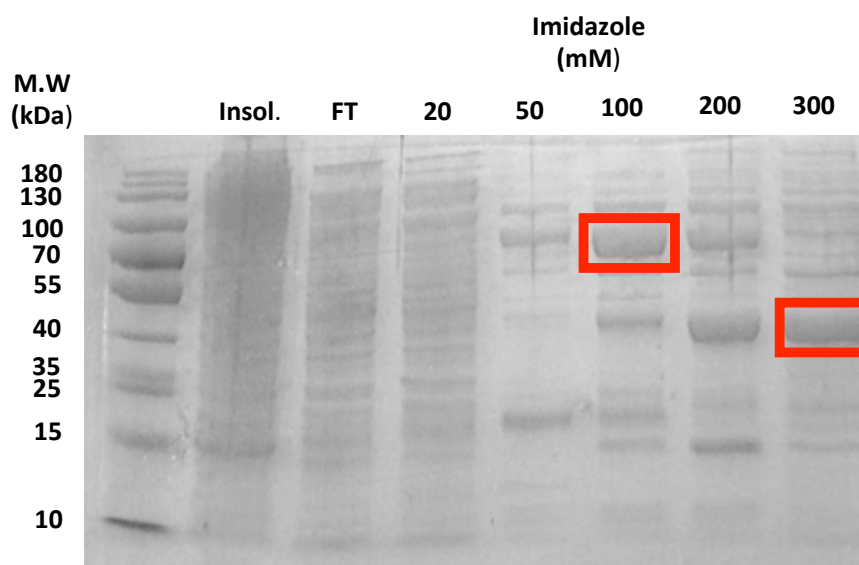


**Figure 4.3** The 10 % SDS-PAGE gel corresponding to the unsuccessful overproduction and purification of Bamb\_5914 (38.4 KDa) in *E.coli* BL21(DE3) cells. The bands observed from the elution fractions (red) correspond to background *E.coli* proteins binding non-specifically to the metal-affinity column.

The DHCCA unit and homologues of the same five enzymes thought to be responsible for its biosynthesis are also found in the vibroxin (151) gene cluster (figure 4.4). The vibroxin gene cluster has a much lower GC content than the enacyloxin cluster, and so it was thought that these genes would be more compatible with the *E.coli* expression strains.

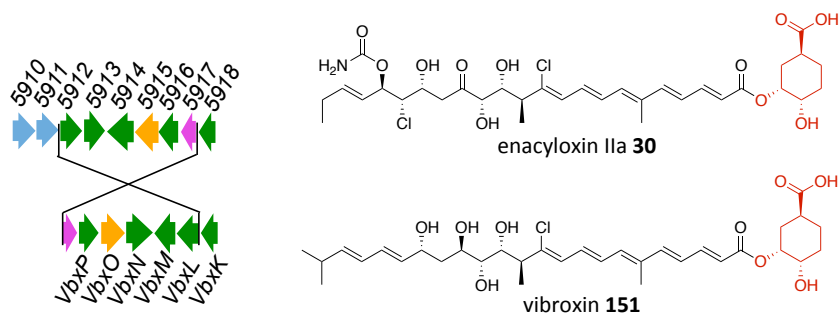


**Figure 4.4** The DHCCA biosynthesis genes present in both the enacyloxin and vibroxin gene clusters. *bamb\_5912*, *5913*, *5914*, *5916* and *5918* are equivalent to *VbxL*, *VbxM*, *VbxN*, *VbxP* and *VbxK* respectively.

The five DHCCA biosynthesis genes from the vibroxin cluster were cloned into pET151 (TOPO cloning, ampicillin marker) as confirmed by sequencing. Only *VbxM* and *VbxL* were successfully overproduced and purified from *E.coli* BL21(DE3) cells (figure 4.5). Switching cell line to *E.coli* C43(DE3) resulted in the overproduction and purification of *VbxL* and *VbxP* (figure 4.5), however no expression of *VbxN* was observed. The *VbxN* gene was cloned into an alternative expression vector, pET28a (restriction cloning, kanamycin marker). After confirmation by sequencing, the protein was overproduced and purified from *E.coli* BL21(DE3) cells (figure 4.5). The production of each protein was confirmed by protein HRMS (appendix 8.3).

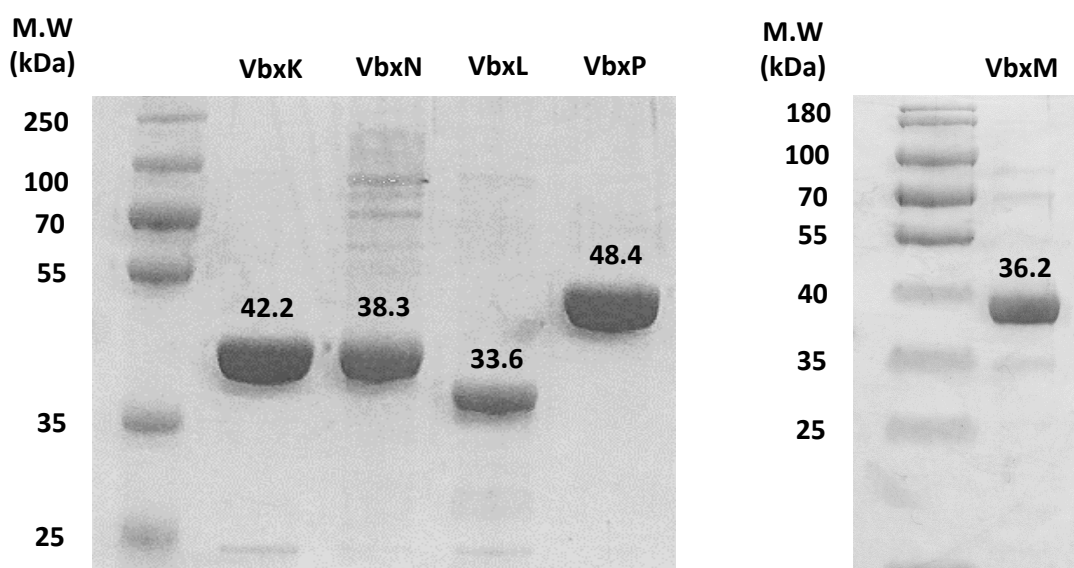
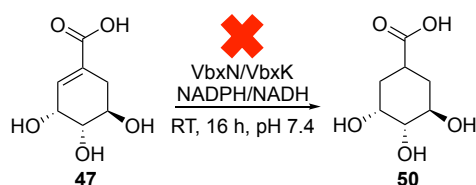


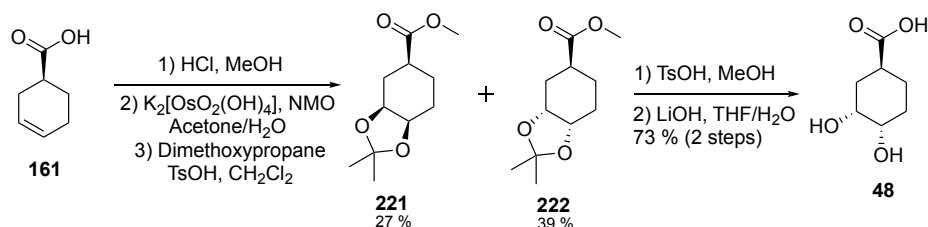
**Figure 4.5** The 10 % SDS-PAGE gels corresponding to the production of *VbxK*, *VbxN*, *VbxL*, *VbxP* and *VbxM* from the vibroxin gene cluster.

Now that all five enzymes had been successfully overproduced, the proposed pathway (scheme 4.2) could be probed using *in vitro* assays. Firstly, the reduction of shikimic acid **47** to THCCA intermediate **50** was tested using both proposed enoyl reductase enzymes (VbxN and VbxK). Commercially available shikimic acid **47** was incubated with either VbxN or VbxK and NADH or NADPH in storage buffer (section 6.7.6/6.7.9). The production of the THCCA intermediate **50** was monitored by LCMS along with a boiled enzyme negative control reaction and the previously synthesized THCCA standard (scheme 3.10). The THCCA reduction product **50** could not be detected using any combination of enzyme or cofactor (scheme 4.3).



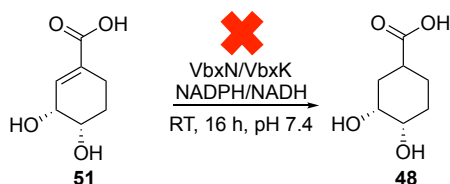
**Scheme 4.3** The unsuccessful reduction of shikimic acid **47** using both enoyl reductases, VbxN and VbxK, as well as NADPH and NADH cofactors.

The second enoyl reduction step in the pathway (scheme 4.2) was also investigated. The unsaturated intermediate **51** was synthesized previously (section 3.2.1.5), but the DHCCA product **48** needed to be synthesized as an LCMS standard (scheme 4.4). Cyclohexene carboxylic acid **161** was esterified before being dihydroxylated and acetonide protected to facilitate the separation of the resulting *syn*- and *anti*-diastereomers, **221** and **222**. Diastereomers **221** and **222** had been synthesized and separated previously in the literature, and so the comparison of diagnostic  $^1\text{H}$  NMR shifts were used in order to confirm their respective stereochemistry.<sup>218</sup> The *anti*-diastereomer **222** was then deprotected and hydrolysed to afford DHCCA **48**.



**Scheme 4.4** The route used for the synthesis of the DHCCA standard **48**.

Unsaturated acid **51** was incubated with either VbxN or VbxK and NADH or NADPH in storage buffer (section 6.7.6/6.7.9). The production of DHCCA **48** was monitored by LCMS along with a boiled enzyme negative control reaction and the DHCCA standard. The DHCCA product **48** could again not be detected using any combination of enzyme or cofactor (scheme 4.5).



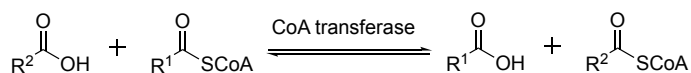
**Scheme 4.5** The unsuccessful reduction of unsaturated acid **51** using both enoyl reductases, VbxN and VbxK, as well as NADPH and NADH cofactors.

These results, combined with the results from the gene deletions, strongly suggest that the initially proposed pathway (scheme 4.2) is not correct. In light of this, the sequences of the five proteins were subjected to basic local alignment search tool (BLAST) analyses. This tool uses sequence alignments and generates a conserved domain search, which allows prediction of the function of a protein by comparison to homologues.<sup>219</sup> It was hoped that this would provide an insight into the true function of the five enzymes (VbxP, VbxN, VbxM, VbxL and VbxK).

#### 4.2.2.1 Shikimate CoA Formation Catalyzed by VbxP

From the conserved domain search generated by the protein BLAST of VbxP, it appears that the enzyme may function as a type III CoA transferase (figure 4.6). CoA transferases catalyze the reversible transfer of CoA between carboxylic acids, and can be classified into three subgroups (types I–III) based on differences in their protein sequences and reaction mechanisms.<sup>220</sup>





CoA transferase [Vibrio rhizosphaerae]

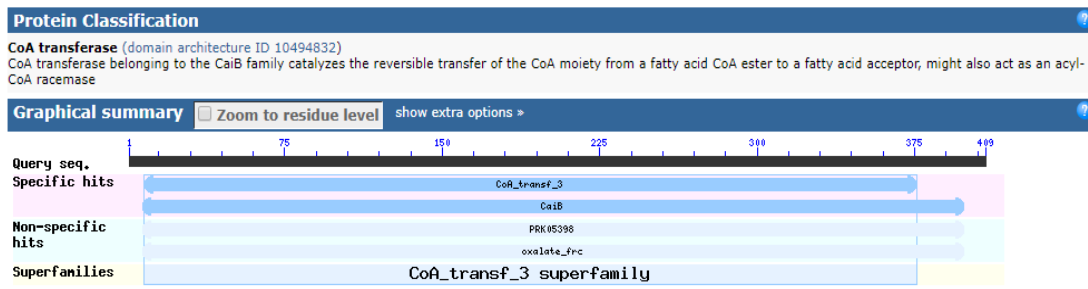
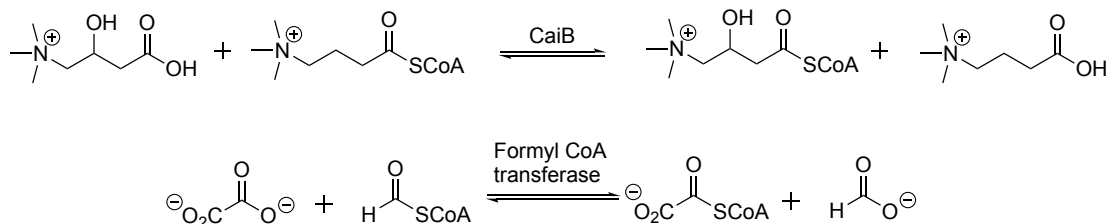


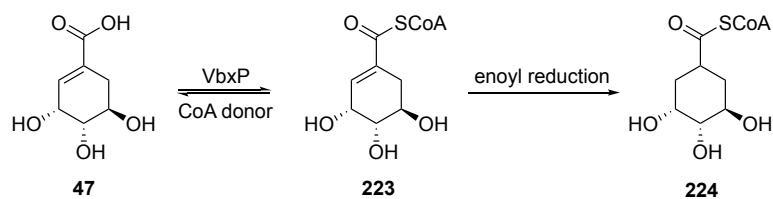
**Figure 4.6** The conserved domain search generated from protein BLAST analysis of VbxP, and the reaction catalyzed by CoA transferase domains.

The protein is homologous to CaiB (59.9 % sequence similarity), a type III CoA transferase involved in carnitine metabolism, as well as a formyl-CoA transferase involved in oxalate degradation (scheme 4.6).<sup>221,222</sup> These enzymes are commonly used in primary metabolic processes, and have recently been shown to be involved in the biosynthesis of thiocarboxylic acid-containing natural products.<sup>223</sup>



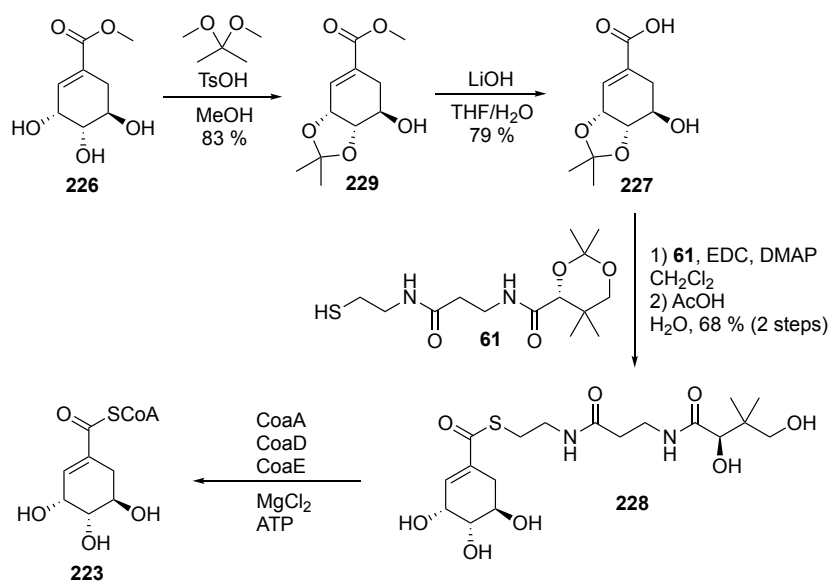
**Scheme 4.6** The reactions catalyzed by VbxK homologues, CaiB and formyl CoA transferase respectively.

Based on the results of the BLAST analysis, it was hypothesized that VbxP may be responsible for the formation of shikimate CoA **223** from shikimic acid **47** (scheme 4.7). This would then facilitate downstream reduction of the shikimate unit, which was unsuccessful for the free acid **47** (section 4.2.2). The reduction of an enoyl thioester is energetically more favourable than the enoyl acid due to the enoyl thioester being significantly more electrophilic.



**Scheme 4.7** The proposed role of VbxP followed by downstream reduction.

To investigate this hypothesis, an assay was conducted whereby shikimic acid **47** was incubated with VbxP and acetyl CoA **225** as a CoA donor. The production of shikimate CoA **223** was then detected using LC-MS analysis. A shikimate CoA standard **223** was synthesized to confirm its formation (scheme **4.8**). Commercially available methyl shikimate **226** was acetonide protected, before hydrolysis to form acid **227**. Acid **227** was then coupled to protected pantetheine **61** before removal of both acetonide protecting groups afforded shikimate pantetheine **228**. This was then used in order to generate shikimate CoA **223** *in situ* using the cassette of accessory enzymes described in section **2.1.4**.



**Scheme 4.8** The synthesis of shikimate pantetheine **228** followed by the formation of shikimate CoA **223** *in situ*.

The results of the incubation of shikimic acid **47** with VbxP and acetyl CoA for 16 h are shown in figure **4.7**. The chromatograms indicate that VbxP catalyzes the formation of shikimate CoA **223**, as a peak with the correct mass and same retention time as the shikimate CoA standard is observed from the assay, but not from the boiled enzyme control. The assay was initially conducted using a 1 : 1 ratio of acetyl CoA to shikimate **47**, this resulted in a 1 : 1 ratio of

shikimate CoA **223** to acetyl CoA due to the reversibility of the reaction. In order to achieve full conversion to shikimate CoA **223**, 10 equivalents of shikimic acid **47** relative to acetyl CoA were used.

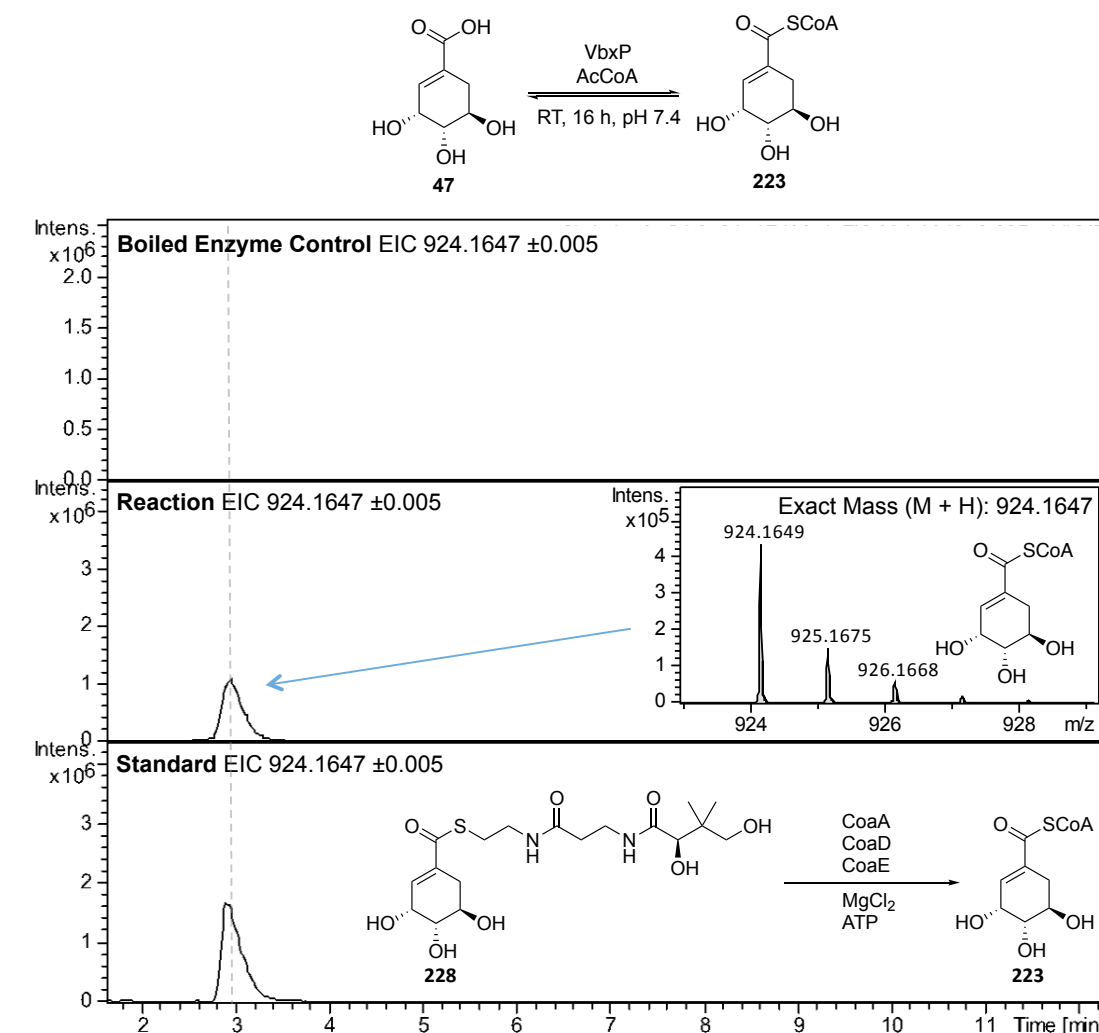


**Figure 4.7** The extracted ion chromatograms and HRMS corresponding to the VbxP catalyzed formation of shikimate CoA **223** from shikimate **47** and acetyl CoA.

Type III CoA transferases are proposed to harbor a conserved aspartate residue which forms a mixed anhydride intermediate with the acyl group of the acyl CoA donor (acetyl CoA **225** in this case). The resulting CoA thiolate is then proposed to attack the anhydride to form a covalent CoA thioester with the aspartate residue. The acceptor acid (shikimic acid **47** in this case) is proposed to attack the thioester and form another mixed anhydride with the aspartate residue. The CoA thiolate can then attack the anhydride to form the new acyl CoA species (shikimate CoA **223** in this case) and regenerate the aspartate residue (scheme **4.9**).<sup>220,224</sup>



The VbxP assay used to generate shikimate CoA **223** was repeated using the D171S mutant. From the chromatogram shown in figure **4.9**, it's clear that the aspartate residue plays a key role in catalysis as shikimate CoA **223** is no longer produced.

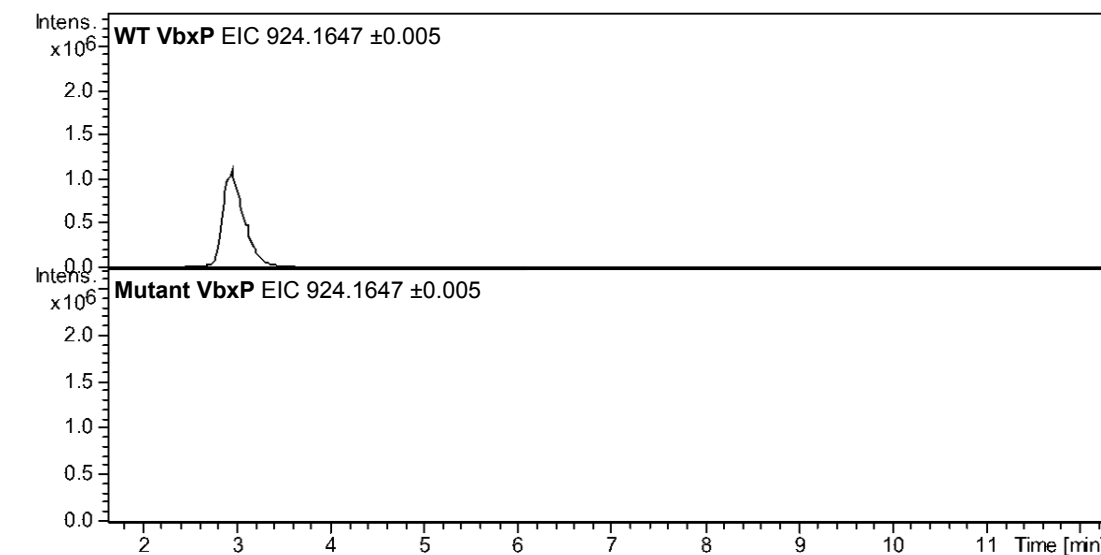


**Figure 4.9** The extracted ion chromatograms corresponding to the VbxP catalyzed formation of shikimate CoA **223** with wild-type VbxP and the D171S mutant.

To confirm the exact role of the aspartate residue during catalysis, the assay was probed using intact protein MS. VbxP was incubated with acetyl CoA for 1 h, and intact protein MS was used to detect the formation of either of the proposed covalent anhydride or CoA thioester intermediates (scheme **4.9**). Acetyl CoA was omitted as a negative control assay, and the assay was repeated with the D171S mutant to confirm any observed intermediates are due to the aspartate residue. From the deconvoluted spectra shown in figure **4.10**, it's clear that the aspartate residue of VbxP forms a covalent adduct with acetyl CoA, as the adduct is not observed with the D171S mutant. When the assay is left for 4 h, the protein fully converts to the covalent adduct. The adduct is 745 Da larger than the wild-type VbxP protein, and corresponds to the covalent CoA thioester adduct (scheme **4.9**), indicating that VbxP catalysis does proceed via the proposed mechanism.

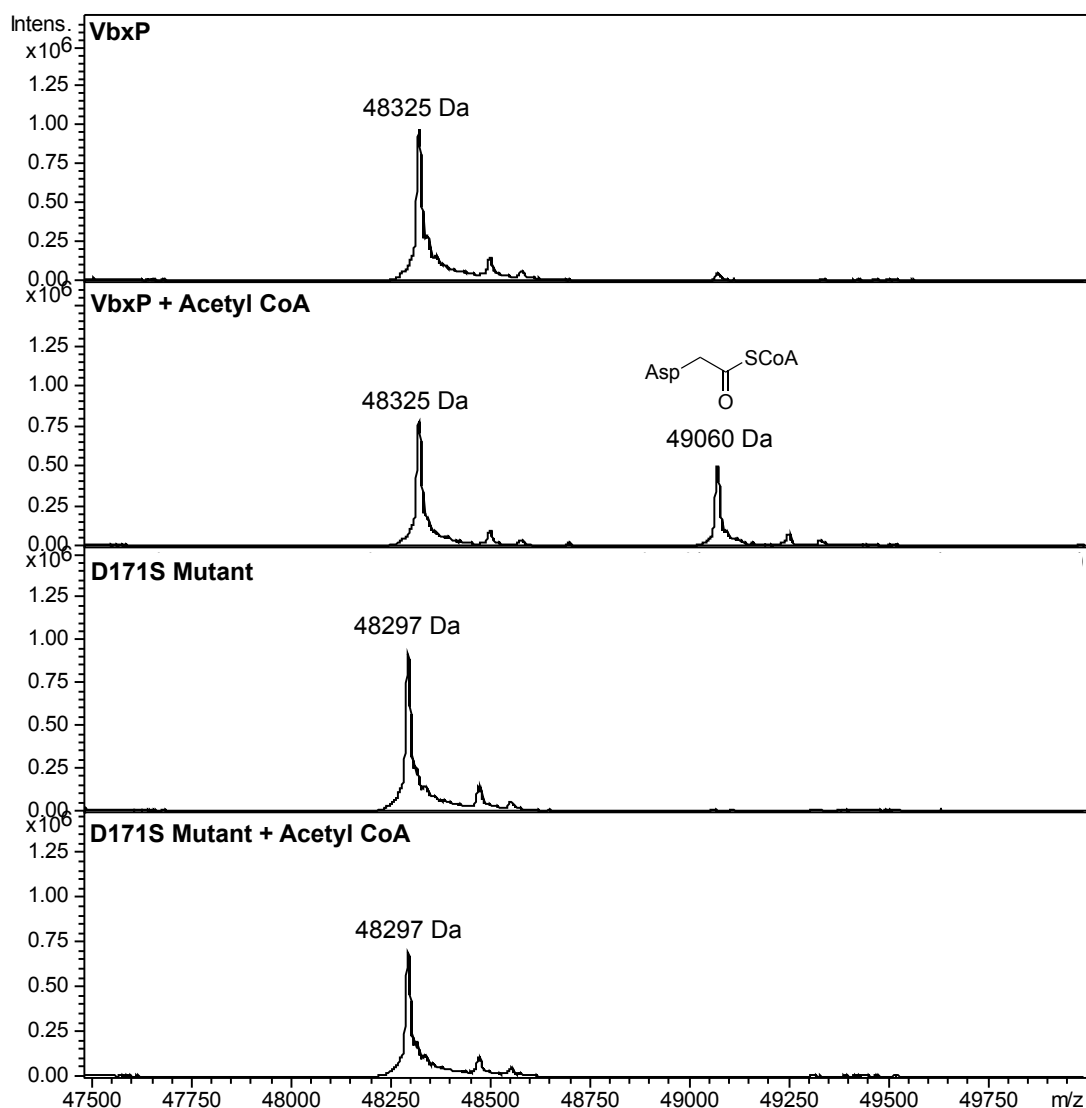


**Figure 4.10** The deconvoluted spectra corresponding to the incubation of VbxP with acetyl CoA for 1 h. The CoA adduct (49060 Da) is not observed for the D171S mutant.

CoA thioesters can be used as probes for the *in vitro* investigation of biosynthetic mechanism, but can often be challenging to synthesize and only a limited range are commercially available. As an alternative, VbxP could be used as a biocatalyst for the production of CoA thioesters *in situ*. The substrate tolerance of VbxP was explored and the enzyme was shown to catalyze the formation of CoA thioesters of a variety of organic acid substrates. Organic acids harboring heteroatoms at the C-2 position appear to be poor substrates for the CoA transferase however (figure 4.11).

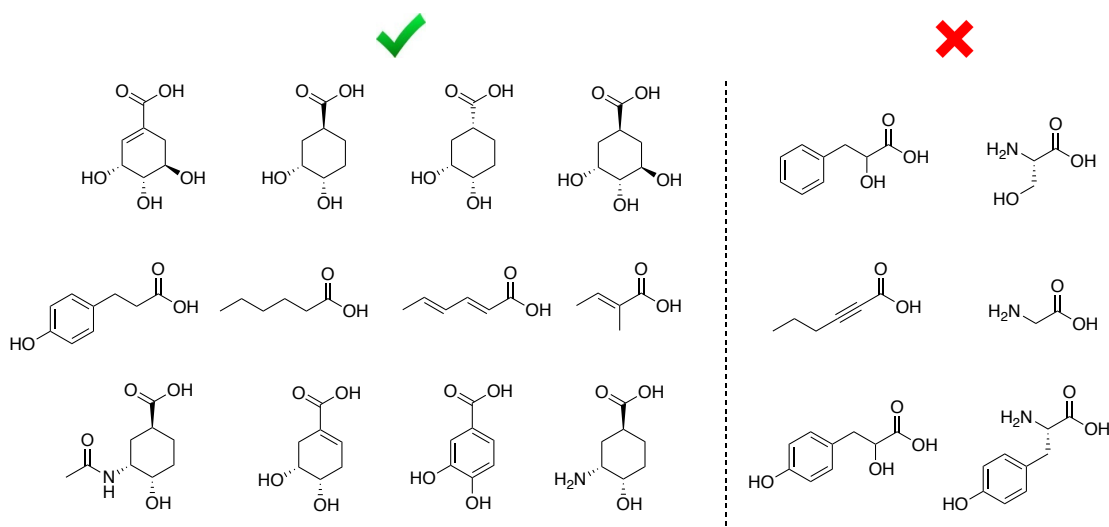


**Figure 4.11** The organic acid substrate tolerance of the VbxP CoA transferase. MS data for the corresponding CoAs generated can be found in appendix 8.7.

One way in which CoA thioesters can be used for *in vitro* assays is for the loading of carrier proteins. It was thought that as an alternative to chemically synthesizing a pantetheine substrate and using a cassette of accessory enzymes, VbxP could be used in order to generate the CoA from a CoA donor and appropriate organic acid *in situ*. In order to test this, VbxP was incubated with acetyl CoA and 10 equivalents of shikimate in order to generate shikimate CoA **223**. An *apo*-ACP domain (GbnD5-ACP from module 13 of gladiolin biosynthesis, section 6.6.1), Sfp and magnesium chloride were then added, and the loading of generated CoA was detected using intact protein MS (figure 4.12). From the deconvoluted spectra, it appears that the *apo*-ACP domain has been successfully loaded with the shikimate CoA **223** generated by VbxP. However peaks corresponding to the *holo*-ACP domain as well as loaded acetyl CoA are also present, indicating a small amount of hydrolysis has taken place, and the acetyl CoA hasn't fully converted to shikimate CoA **223**. Despite this, the results are promising and suggest that with optimization, VbxP can be used as a biocatalyst in order to generate acyl CoAs for *in vitro* assays.

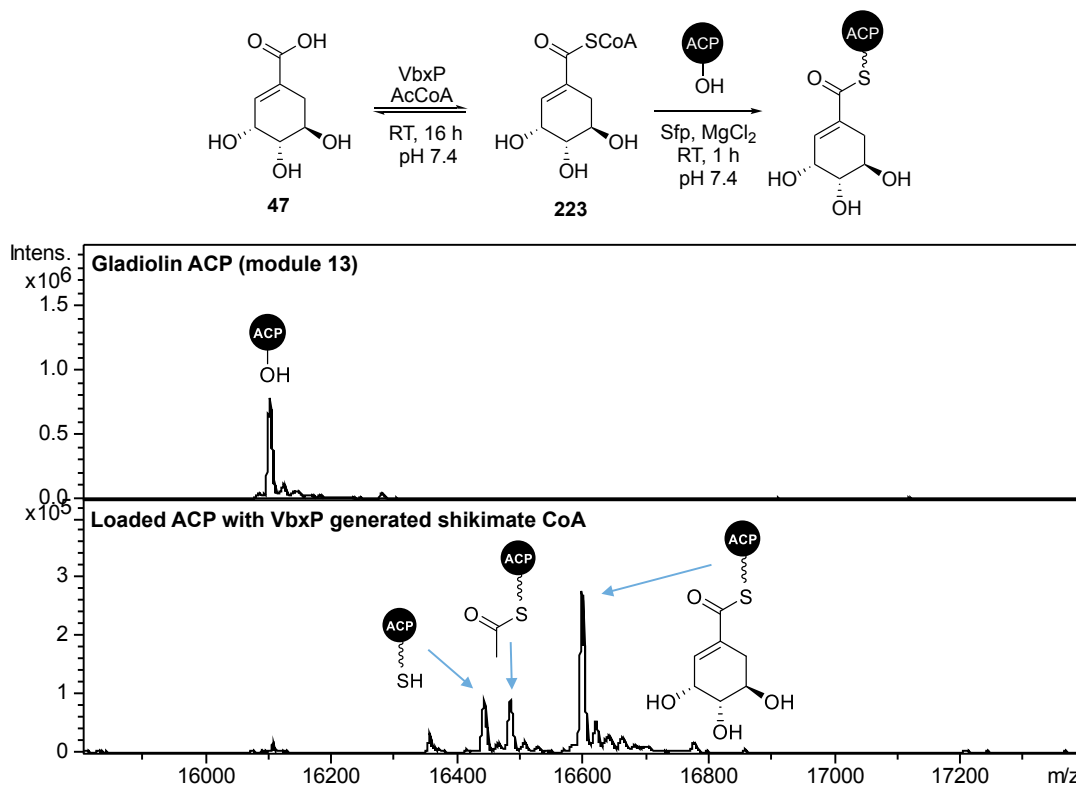


**Figure 4.12** The spectra corresponding to the loading of VbxP generated shikimate CoA **223** onto gladiolin module 13 *apo*-ACP domain.

#### 4.2.2.2 Enoyl Reduction catalyzed by VbxN

Having established the role of VbxP as generating shikimate CoA **223**, the next step in the biosynthetic pathway was investigated. It was thought that the formation of the thioester would facilitate downstream enoyl reduction (scheme 4.7), but the corresponding enoyl reductase had not yet been identified. The protein BLAST results of VbxN suggested that the protein has a conserved NAD(P)H binding site, and is similar to both quinone oxidoreductase and PKS ER domains (figure 4.13). These results suggest that VbxN is a good candidate for the enzyme that the enoyl reduction of shikimate CoA **223**.



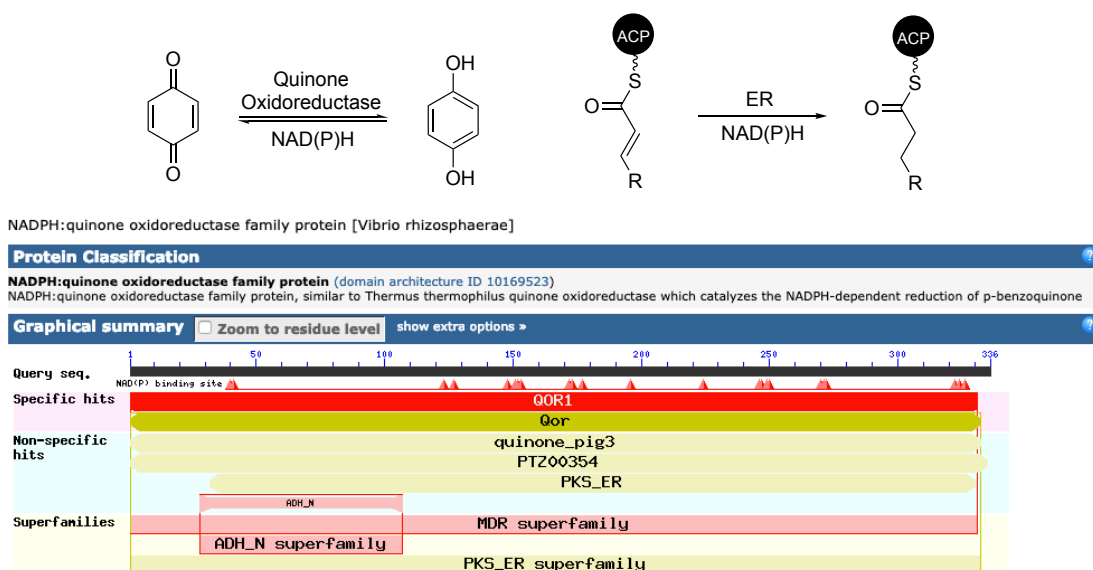


**Figure 4.13** The conserved domain search generated from protein BLAST analysis of VbxN and the reactions catalyzed by quinone oxidoreductase and PKS ER domains.

To test if VbxN was capable of the reduction, an *in vitro* assay was conducted whereby shikimate CoA **223** was generated *in situ* using VbxP. VbxN and NADPH were then added and the presence of the reduced shikimate CoA product **224** was detected using LCMS analysis. This was conducted alongside a boiled VbxN control and a standard generated by the incubation of previously synthesized THCCA **167** (section 3.2.1.5) with VbxP and acetyl CoA. The chromatograms shown in figure 4.14 indicate that VbxN is catalyzing the reduction of shikimate CoA **223**, as the peak corresponding to the reduced product is not present in the boiled enzyme control, and has the same retention time as the reduced shikimate CoA product standard **224**. The assay was conducted with both NADPH and NADH cofactors, the reaction only proceeded when NADPH was used.

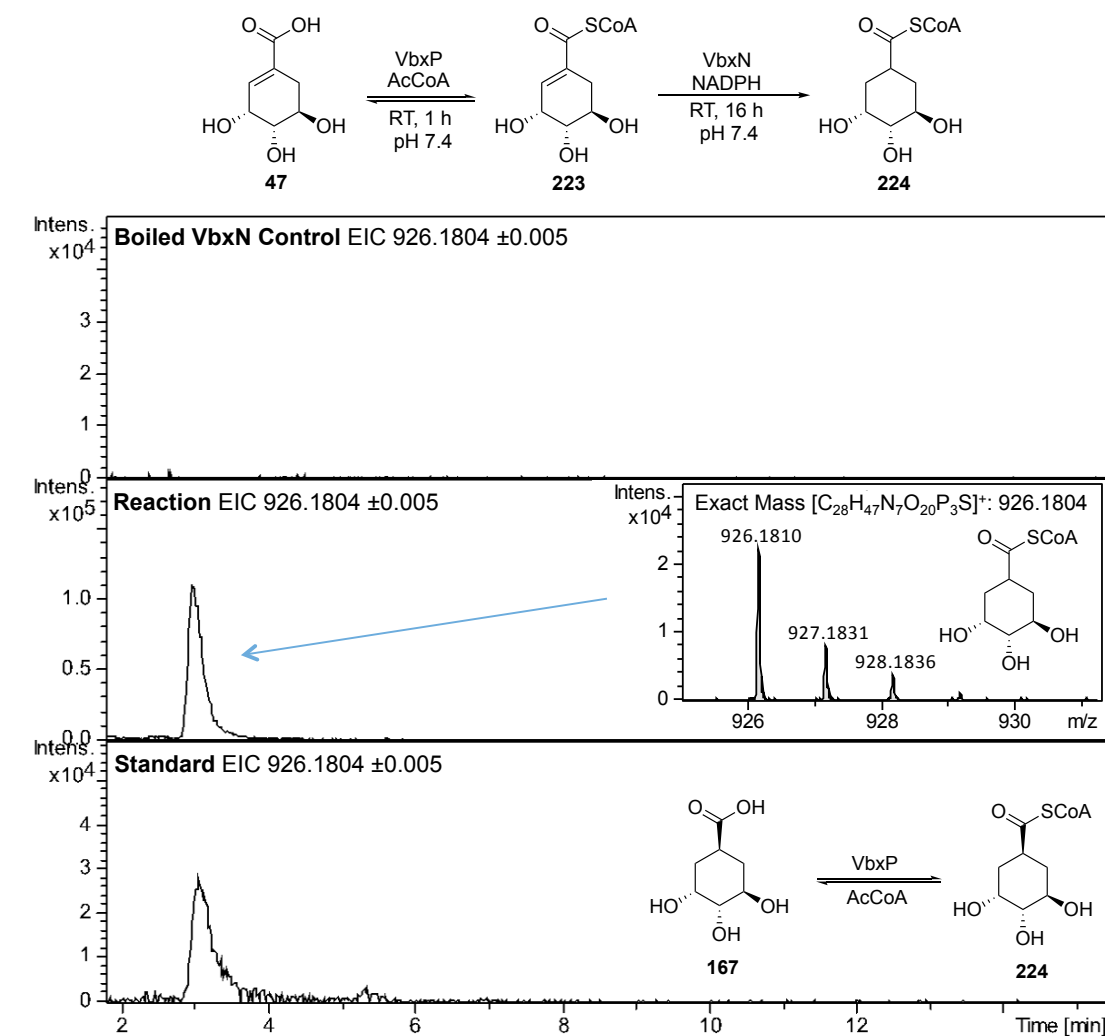
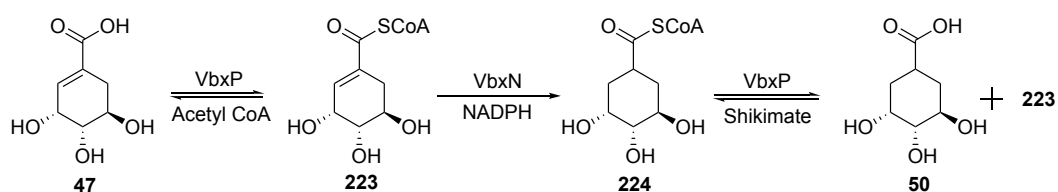


**Figure 4.14** The extracted ion chromatograms and HRMS corresponding to the VbxN catalyzed reduction of shikimate CoA **223** to form reduced shikimate CoA **224**.

Having established that VbxN can catalyze the reduction of shikimate CoA **223**, it was thought that VbxP may then catalyze the production of the THCCA **50**. This may occur by VbxP using the reduced shikimate CoA **224** as a donor CoA, to generate another molecule of shikimate CoA **223** and form the THCCA intermediate **50** in the process (scheme 4.10).



**Scheme 4.10** The proposed sequence of events leading to the formation of THCCA intermediate **50**.

To test if VbxP catalyzes the production of the THCCA intermediate **50**, the same VbxN catalyzed reduction assay can be used, as because VbxP is present in the reaction, THCCA **50** should be formed and can be detected. This also presents an opportunity to investigate the stereoselectivity of the VbxN catalyzed reduction. The retention time of the THCCA formed in the reaction can be compared with that of synthetic, enantiomerically pure THCCA **167**, as well as a mixture of diastereomers generated via hydrogenation (figure 4.15).

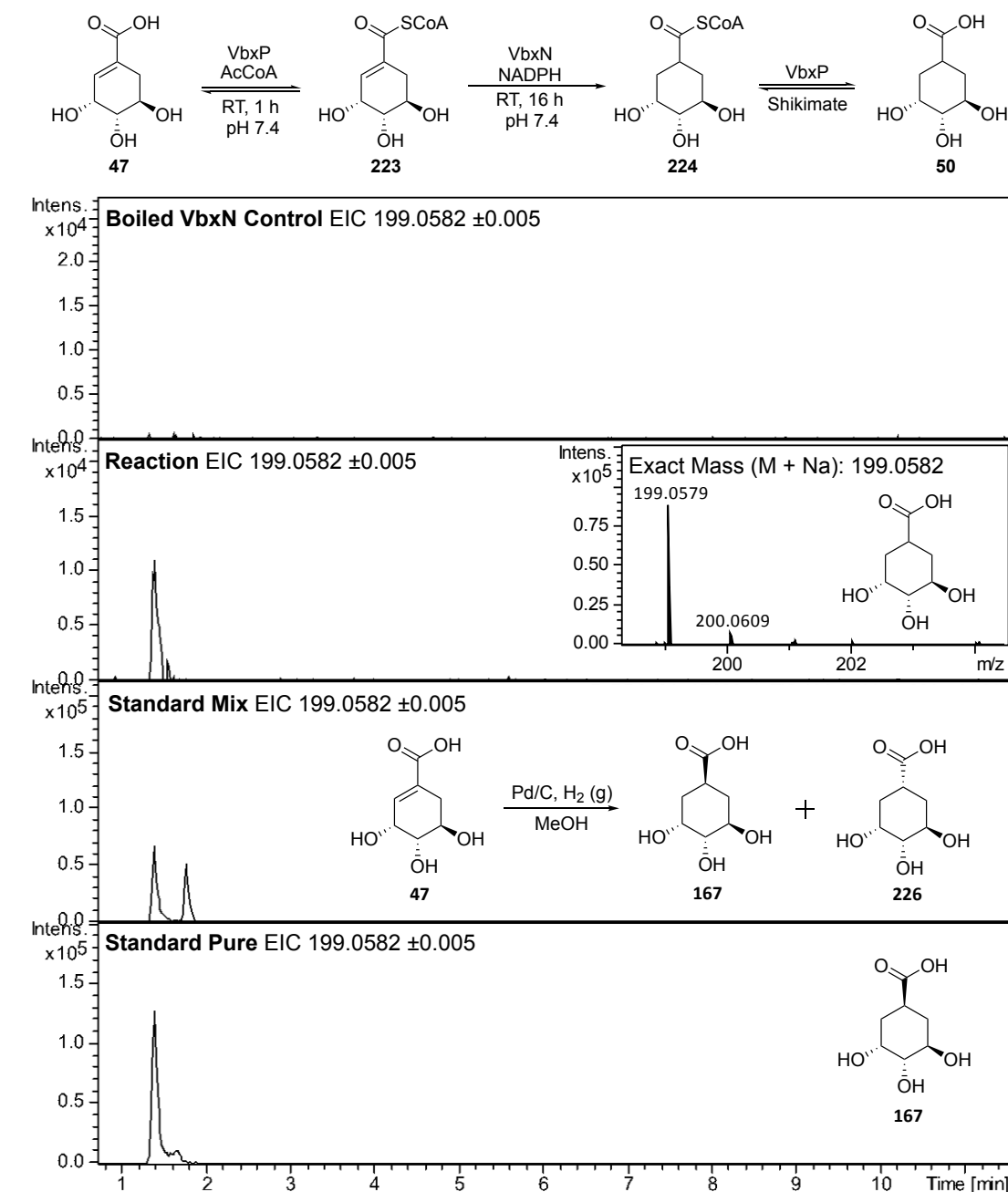


**Figure 4.15** The extracted ion chromatograms and HRMS corresponding to the VbxN catalyzed reduction and VbxP catalyzed formation of THCCA intermediate **50**.

The chromatograms shown in figure 4.15 indicate that VbxP catalyzes the formation of the THCCA intermediate **167** due to the peak observed corresponding to the correct mass from the reaction but not the boiled enzyme control. The peak has the same retention time as enantiomerically pure THCCA standard **167**, confirming the stereoselectivity of the VbxN catalyzed reduction. Furthermore, the stereochemistry of the resulting THCCA intermediate **167**, is the same stereochemistry observed in the enacyloxin analogue **172** isolated from the *bamb\_5912* gene deletion (section 4.2.1). To further confirm this, analogue **172** was hydrolyzed and the retention time of the resulting THCCA compared with that of the synthetic standards. The chromatograms shown in figure 4.16 confirm that the stereochemistry of the THCCA reduction product **167** is the same as the stereochemistry of the THCCA unit observed in enacyloxin analogue **172**.

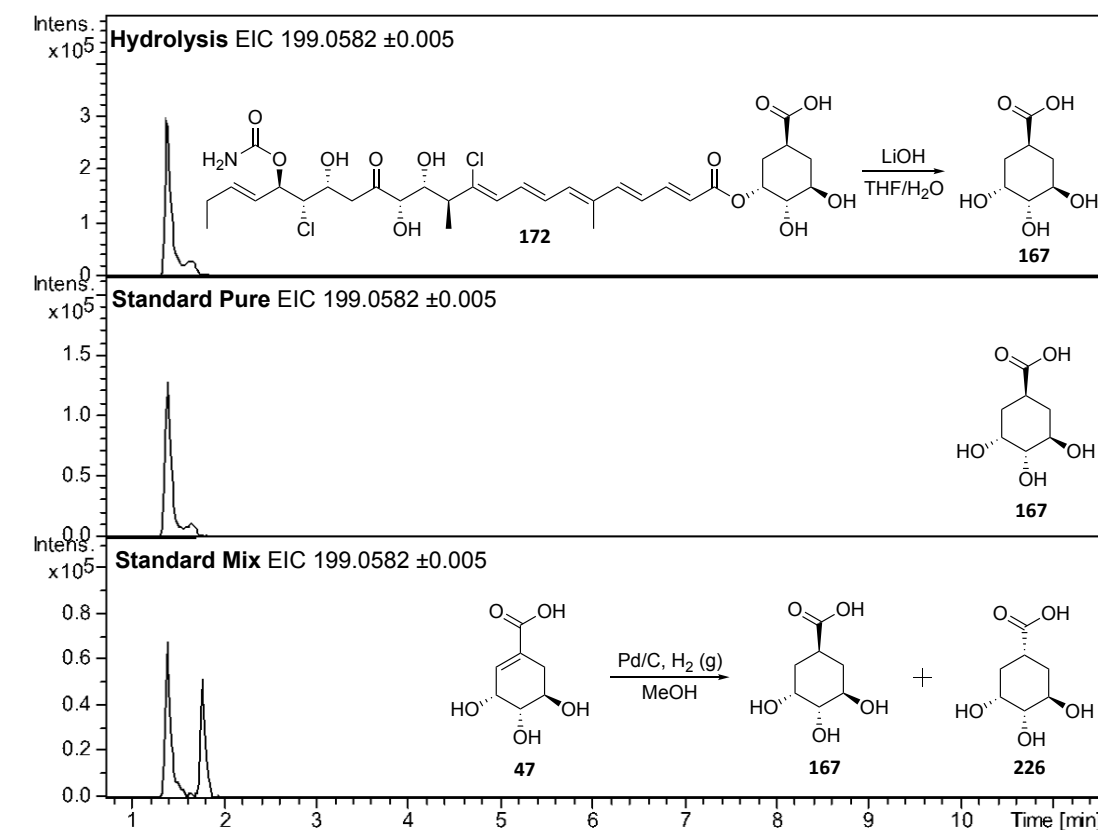
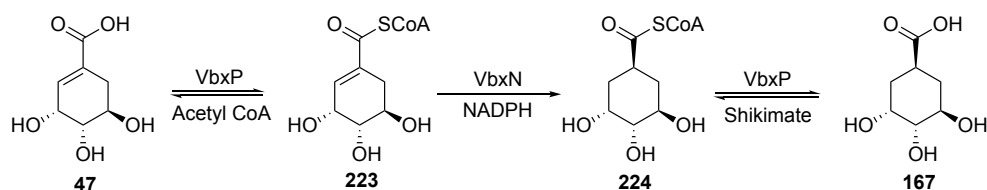


**Figure 4.16** The extracted ion chromatograms corresponding to the hydrolysis of enacyloxin analogue **172** and synthetic THCCA standards.

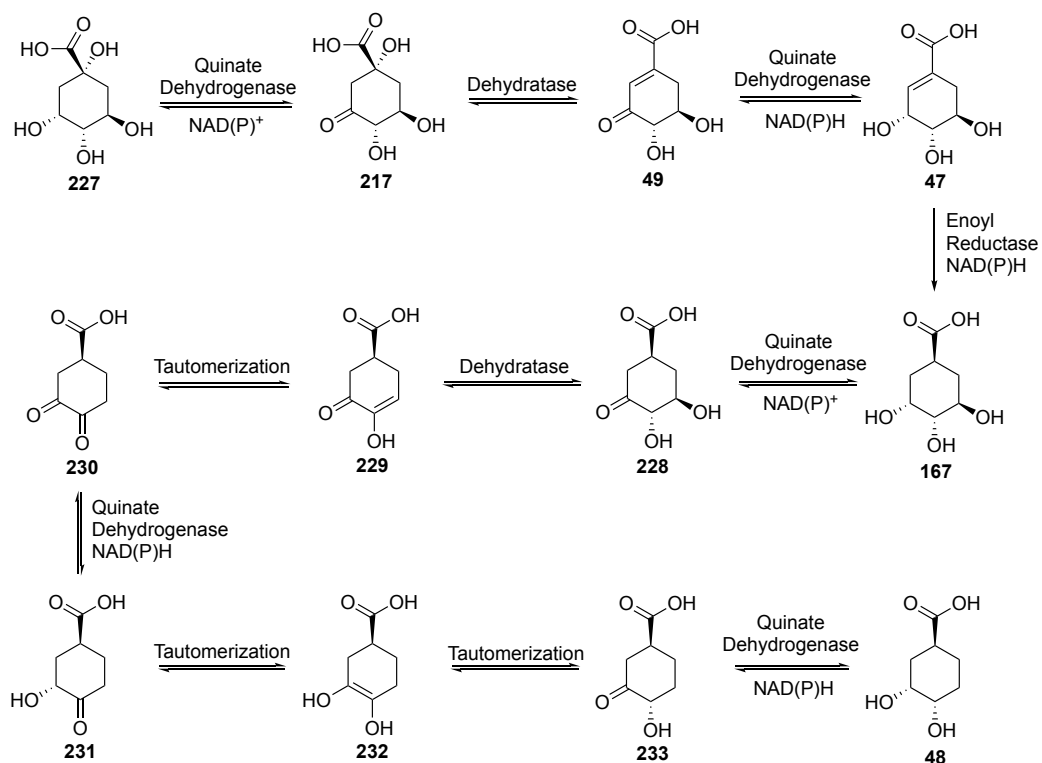
Overall, the first three steps of the pathway have been characterized *in vitro*. The pathway consists of formation of a transient CoA thioester of shikimic acid by VbxP, followed a stereoselective enoyl reduction catalyzed by VbxN. The resulting reduced shikimate CoA product **224** is then used as a CoA donor by VbxP, resulting in the production of THCCA intermediate **167** (scheme 4.11).



**Scheme 4.11** The first three steps of DHCCA biosynthesis resulting in THCCA intermediate **167**.

#### 4.2.2.3 Oxidation Catalyzed by VbxM

Now that THCCA **167** had been established as an intermediate in the pathway, the biosynthetic steps from THCCA **167** to DHCCA **48** could be investigated. Coggins and co-workers previously isolated DHCCA **48** during the early 1970s, as a quinate metabolite of *Lactobacillus plantarum*.<sup>225</sup> They proposed a pathway for the biosynthesis of DHCCA **48** from quinic acid **227** via THCCA intermediate **167** based upon lysate assays (scheme 4.12).<sup>226</sup> They proposed that a single quinate dehydrogenase enzyme catalyzes five steps in the pathway, including the oxidation of THCCA intermediate **167** to form ketone **228**, before dehydration. Cain and co-workers have since confirmed that a quinate dehydrogenase is capable of oxidizing THCCA intermediate **167** as well as some of the other intermediates in the proposed pathway.<sup>227</sup>



**Scheme 4.12** The proposed biosynthetic pathway from quinic acid **227** to DHCCA **48**.

The results of the protein BLAST search for VbxM suggested that the protein functions as a shikimate dehydrogenase. It was thought that this enzyme may catalyze the same oxidation of the THCCA intermediate **167** as proposed by Coggins and co-workers (figure 4.17).

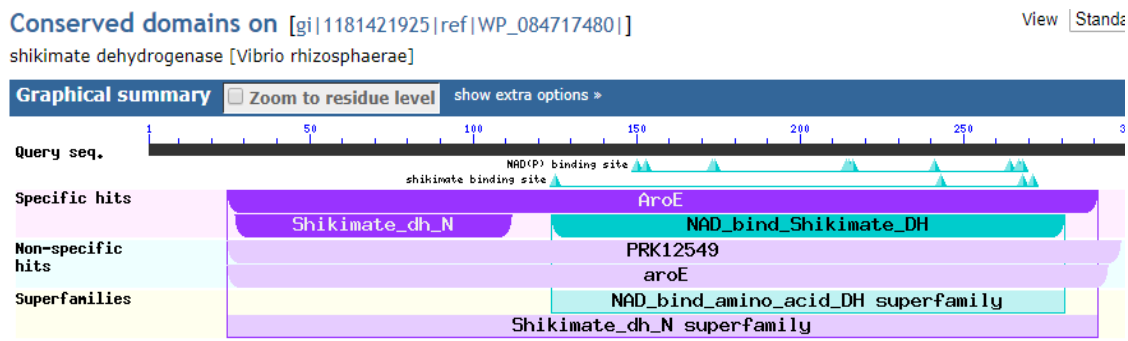
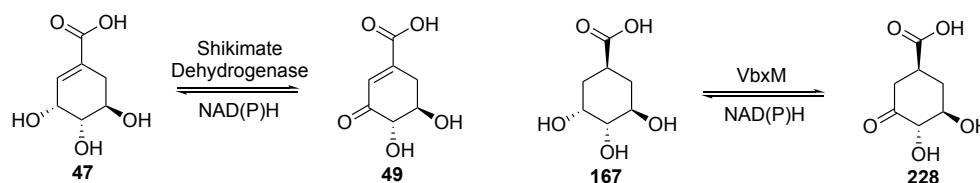


**Figure 4.17** The conserved domain search generated from protein BLAST analysis of VbxM, the reaction catalyzed by shikimate dehydrogenase and the proposed oxidation catalyzed by VbxM.

To determine if VbxM was capable of catalyzing the oxidation of THCCA **167**, an *in vitro* assay was conducted whereby synthetic THCCA **167** was incubated with VbxM, along with NADP<sup>+</sup> or NAD<sup>+</sup> for 16 h, and the production of ketone **228** monitored by LC-MS. The ketone product **228** could not be detected by LC-MS from assays using either cofactor. It was thought that this could be due to the poor ionization of ketone product **228**, or instability. Another way to monitor the reaction was to use UV-Vis spectroscopy, NAD(P)H has a characteristic absorption at 340 nm, and so by monitoring absorption at this wavelength the conversion of NAD(P)<sup>+</sup> to NAD(P)H can be detected (figure 4.18). When THCCA **167** was incubated with VbxM and NAD<sup>+</sup>, the absorption at 340 nm increases, indicating that the oxidation of THCCA **167** is taking place. No change in absorbance was observed when NADP<sup>+</sup> was used.

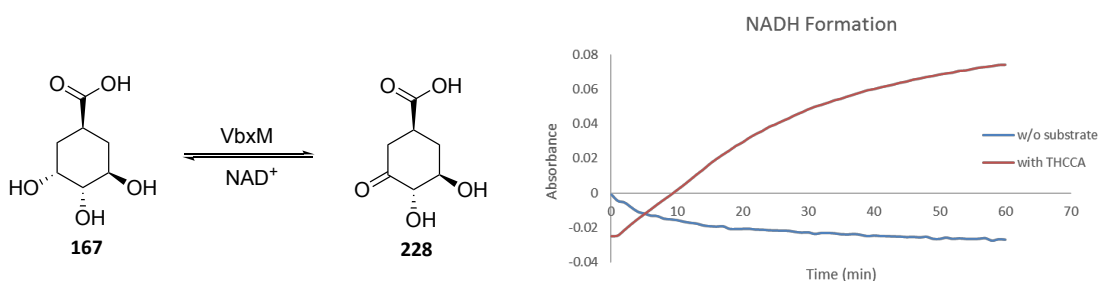
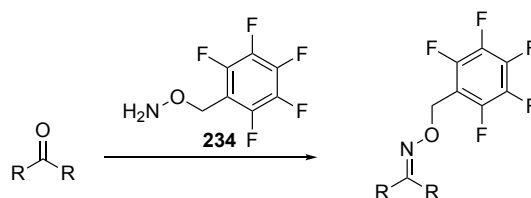


**Figure 4.18** The absorption at 340 nm for the VbxM catalyzed oxidation of THCCA **167** with and without the THCCA substrate.

In order to confirm that the ketone product **228** is being produced in the reaction, pentafluorobenzylhydroxylamine derivatizing agent **234** was used to generate a product that could be detected by LCMS. This derivatizing agent reacts with ketones and aldehydes to rapidly form ionizable oxime products (scheme 4.13).



**Scheme 4.13** The formation of ionizable oxime products from ketones using derivatizing agent **234**.

The VbxM catalyzed oxidation of THCCA **167** was repeated with addition of derivatizing agent **234** for 1 h at the end of the reaction. A standard **237** was generated for the derivatized product via the hydrogenation of commercially available 3-dehydroshikimate **49** to form ketone **236**, before the addition of the derivatizing agent **234**. From the chromatograms shown in figure **4.19**, a peak corresponding to the mass of the derivatized product **235** is observed from the reaction, which has the same retention time as the standard **237** and is not present in the boiled enzyme control. This is strong evidence to suggest that VbxM catalyzes the oxidation of THCCA **167** to form ketone product **228**.

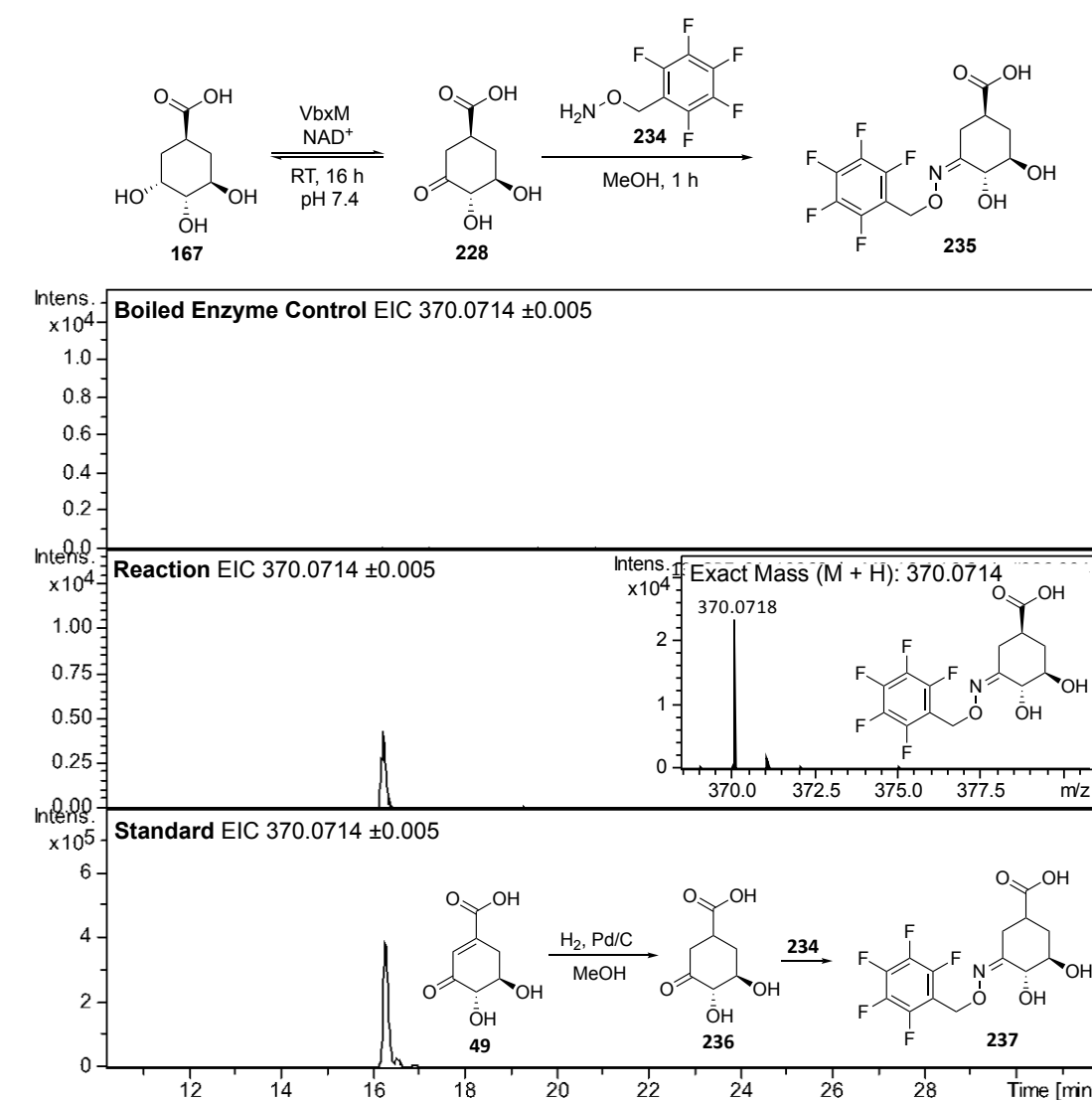


**Figure 4.19** The extracted ion chromatograms and HRMS corresponding to the VbxM catalyzed oxidation and derivatization of THCCA intermediate **167**.



#### 4.2.2.4 Dehydration catalyzed by VbxL

According to the pathway proposed by Coggins and co-workers, the step following the oxidation of THCCA **167** is dehydration to form unsaturated ketone **229** (scheme 4.12). From the gene deletions in section 4.2.1, the deletion of *bamb\_5912* (homologue of VbxL) resulted in enacyloxin analogue **172**, which harbors the THCCA unit. This suggests that VbxL may be responsible for the elimination of the hydroxyl group on the THCCA unit, and may act as a dehydratase responsible for the dehydration of ketone **228** (figure 4.20). The results of the protein BLAST analysis of VbxL suggest that the protein functions as a sugar phosphate isomerase (figure 4.20). The isomerization reaction requires the deprotonation of an  $\alpha$ -hydroxycarbonyl species, similar to what is required in an E<sub>1CB</sub>-type dehydration, indicating that VbxL may well catalyze a dehydration.

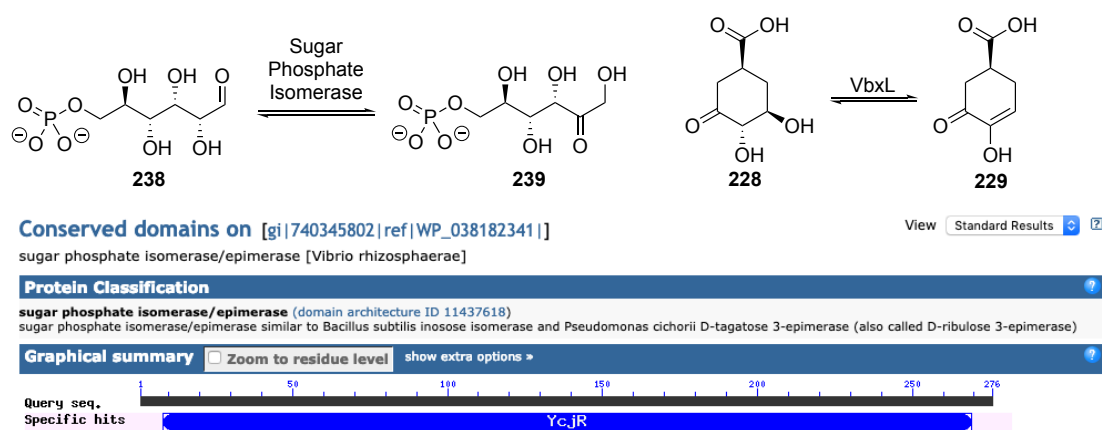


**Figure 4.20** The conserved domain search generated from protein BLAST analysis of VbxL, the reaction catalyzed by a sugar phosphate isomerase and the proposed dehydration catalyzed by VbxL.

In order to test if VbxL is capable of the dehydration of ketone **228**, the ketone substrate **236** that is generated by hydrogenation of 3-dehydroshikimate **49**, was incubated with VbxL, before the addition of derivatizing agent **234**. The dehydrated product **240** can tautomerize to diketone **241**, and so the expected derivatized product should be dioxime **242**. From the chromatograms shown in figure 4.21, a peak corresponding to the correct mass of the dioxime product **242** is observed from the reaction but not in the boiled enzyme control. This suggests that VbxL catalyzes the dehydration of ketone **228** as the next step in the pathway to afford unsaturated ketone **229**.

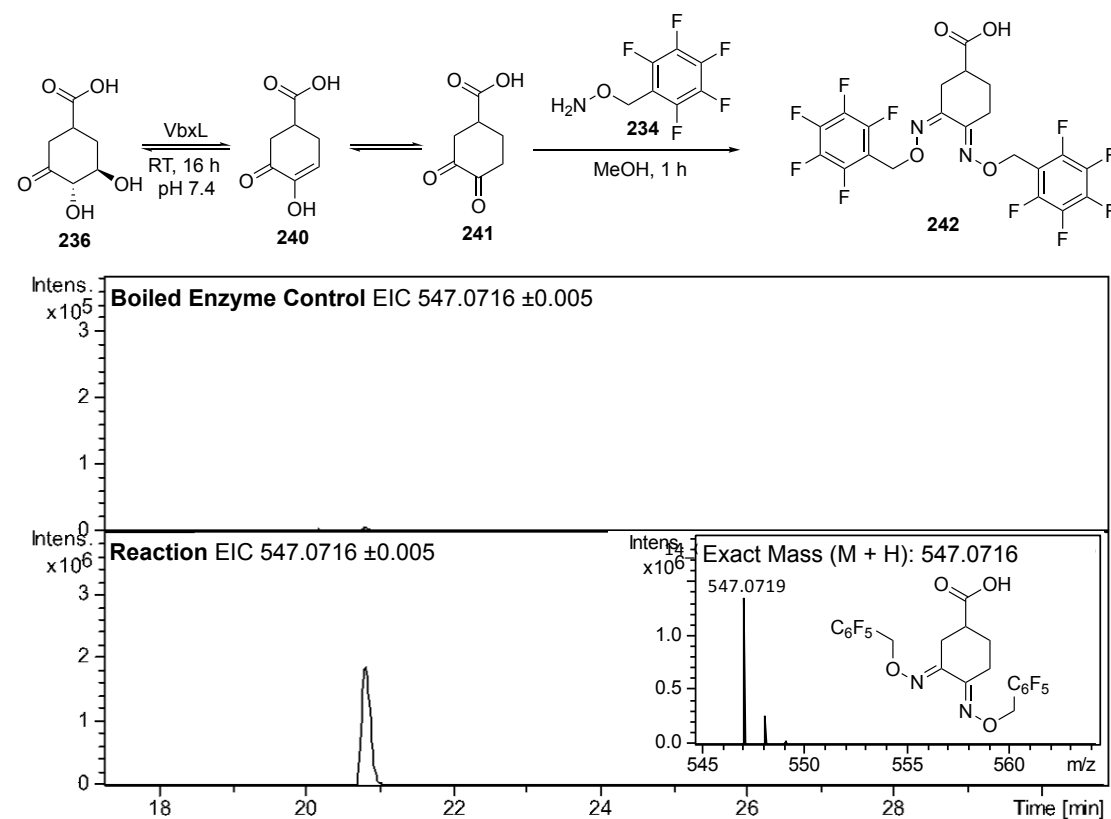
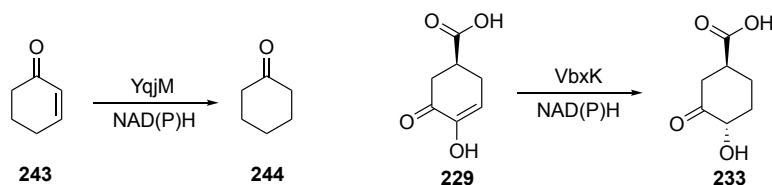


**Figure 4.21** The extracted ion chromatograms and HRMS corresponding to the VbxL catalyzed dehydration and derivatization of ketone **236**.

#### 4.2.2.5 Enone Reduction Catalyzed by VbxK

The remaining enzyme proposed to be involved in the biosynthesis of the DHCCA is VbxK. The results from the protein BLAST analysis of VbxK (figure **4.22**) suggest that the protein functions as a flavin mononucleotide (FMN)-dependent enone reductase. The protein is a closely related homologue of YqjM, a well-characterized FMN-dependent enone reductase which has been shown to reduce a variety of  $\alpha,\beta$ -unsaturated ketones.<sup>228</sup> Given the function of YqjM, it was thought that VbxK may be capable of the enoyl reduction of unsaturated ketone **229** (figure **4.22**).



Conserved domains on [gi|740345805|ref|WP\_038182344|]

View [Standard](#)

NADH:flavin oxidoreductase/NADH oxidase [Vibrio rhizosphaerae]

#### Protein Classification

NADH:flavin oxidoreductase/NADH oxidase (domain architecture ID 10121205)

NADH:flavin oxidoreductase/NADH oxidase similar to Aspergillus flavus NADPH dehydrogenase Aflavarin synthesis protein A (AfvA), which is part of the gene d mediates the biosynthesis of aflavarin, a bicoumarin that exhibits anti-insectan activity against the fungivorous beetle C.hemipterus

#### Graphical summary

Zoom to residue level

[show extra options >](#)

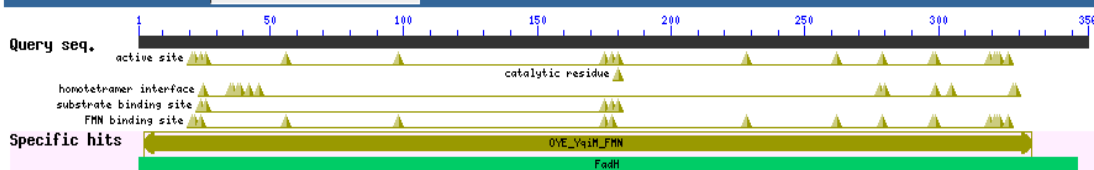
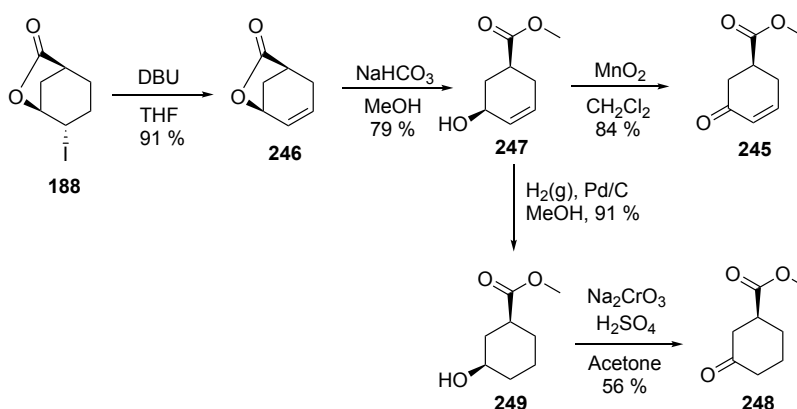


**Figure 4.22** The conserved domain search generated from protein BLAST analysis of VbxK, a reduction catalyzed by YqjM and the proposed reduction catalyzed by VbxK.

Unsaturated ketone **229** is a difficult substrate to synthesize and is also prone to aromatization, making a direct reduction assay with this intermediate difficult. In light of this, substrate mimic **245** was synthesized (scheme 4.14) in order to probe the activity of VbxK. Lactone **246** was generated from iodolactone **188** (section 3.2.1.5) using DBU, before being ring-opened with methanol in basic conditions to afford alcohol **247**. Oxidation using manganese dioxide then afforded unsaturated ketone substrate mimic **245**. To generate saturated ketone standard **248**, alcohol **247** was hydrogenated before oxidation using Jones' reagent.



**Scheme 4.14** The route used for the synthesis of the unsaturated ketone mimic **245** as well as saturated ketone standard **248**.

In order to probe the activity of VbxK, substrate mimic **245** was incubated with VbxK and NADPH, and the presence of reduced product **248** detected by LC-MS analysis (figure 4.23). The presence of the peak corresponding to the correct mass of product **248** from the reaction, with the same retention time as standard **248**, but not present in the boiled enzyme control confirms that VbxK is capable of reducing the substrate mimic **245**. The reaction also proceeded when NADH was used as cofactor.

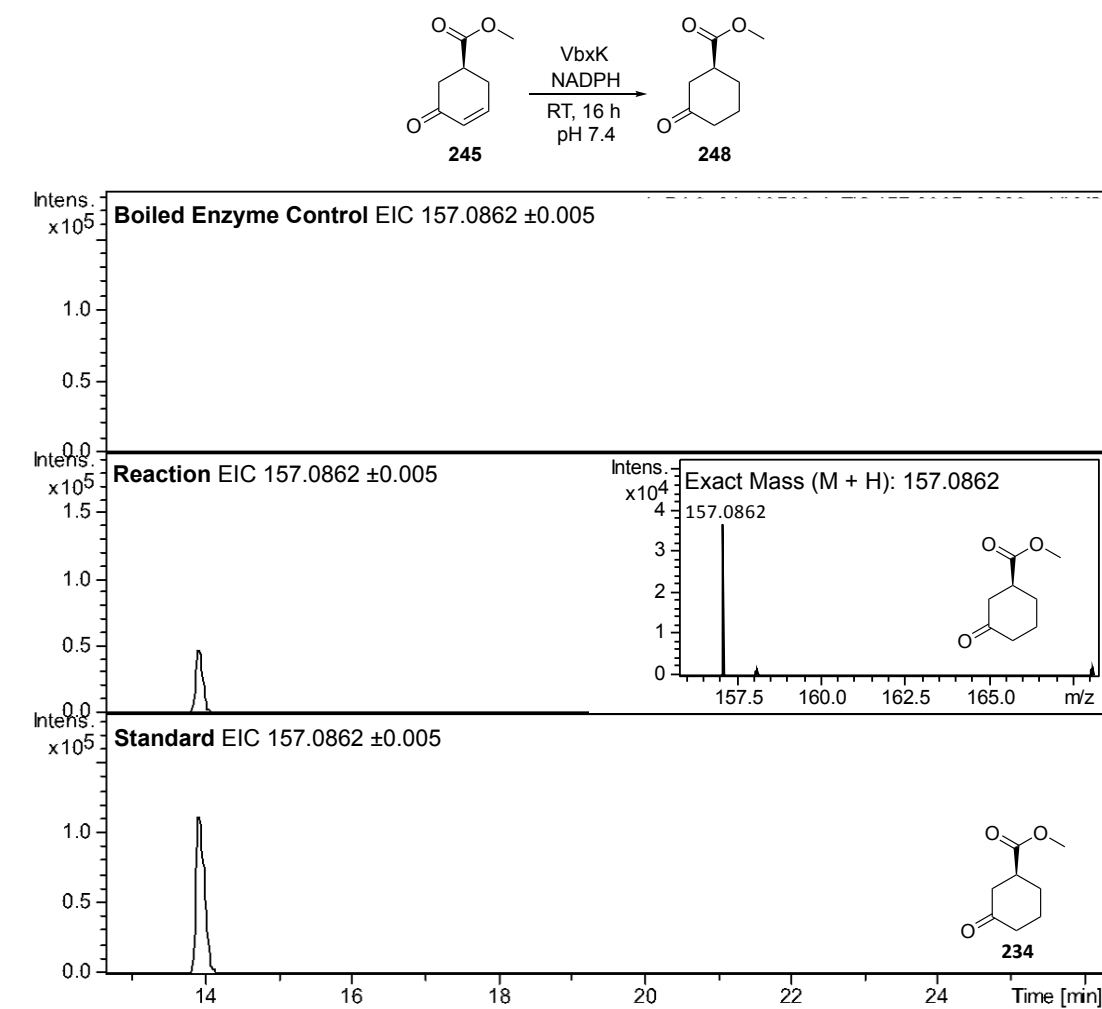


**Figure 4.23** The extracted ion chromatograms and HRMS corresponding to the VbxK catalyzed reduction of substrate mimic **245**.

To confirm that VbxK is capable of reducing the keto-enol group present in unsaturated ketone **229**, another substrate mimic, keto-enol **250**, was synthesized (figure 4.24). Substrate **250** was synthesized from commercially available diol **251** via a Swern oxidation, and was incubated with VbxK and NADPH, before derivatization with **234**. The presence of derivatized product **252** was detected by LC-MS analysis along with derivatized standard **252** (formed from commercially available ketone **253**). The presence of the peak corresponding to the correct mass of the derivatized product **252** from the reaction, with the same retention time as derivatized

standard **252**, but not present in the boiled enzyme control, confirms that VbxK is capable of reducing keto-enol substrate **250**.

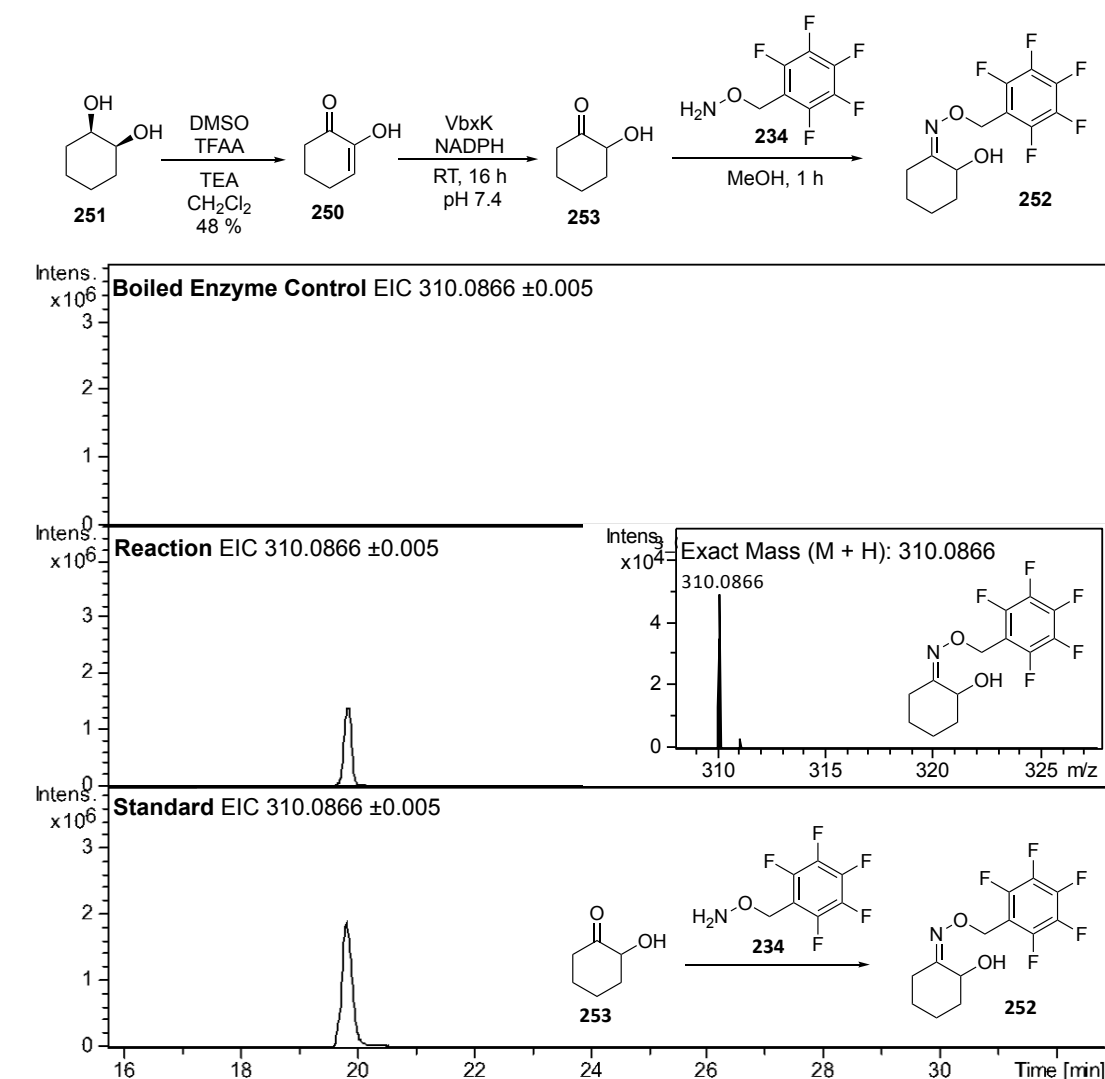


**Figure 4.24** The extracted ion chromatograms and HRMS corresponding to the VbxK catalyzed reduction of keto-enol substrate **250**.

In order to further confirm that the role of VbxK is to reduce unsaturated ketone intermediate **229**, a coupled assay was used. VbxL was used to generate substrate **240** *in situ* via the dehydration of ketone **239**, VbxK and NADPH were then added followed by derivatizing agent **234**. The production of derivatized product **254** was monitored by LC-MS (figure 4.25). The presence of the peak corresponding to the correct mass of the derivatized product **254** from the reaction, but not present in either of the boiled enzyme controls is further confirmation that the role of VbxK is to reduce unsaturated ketone substrate **229**.

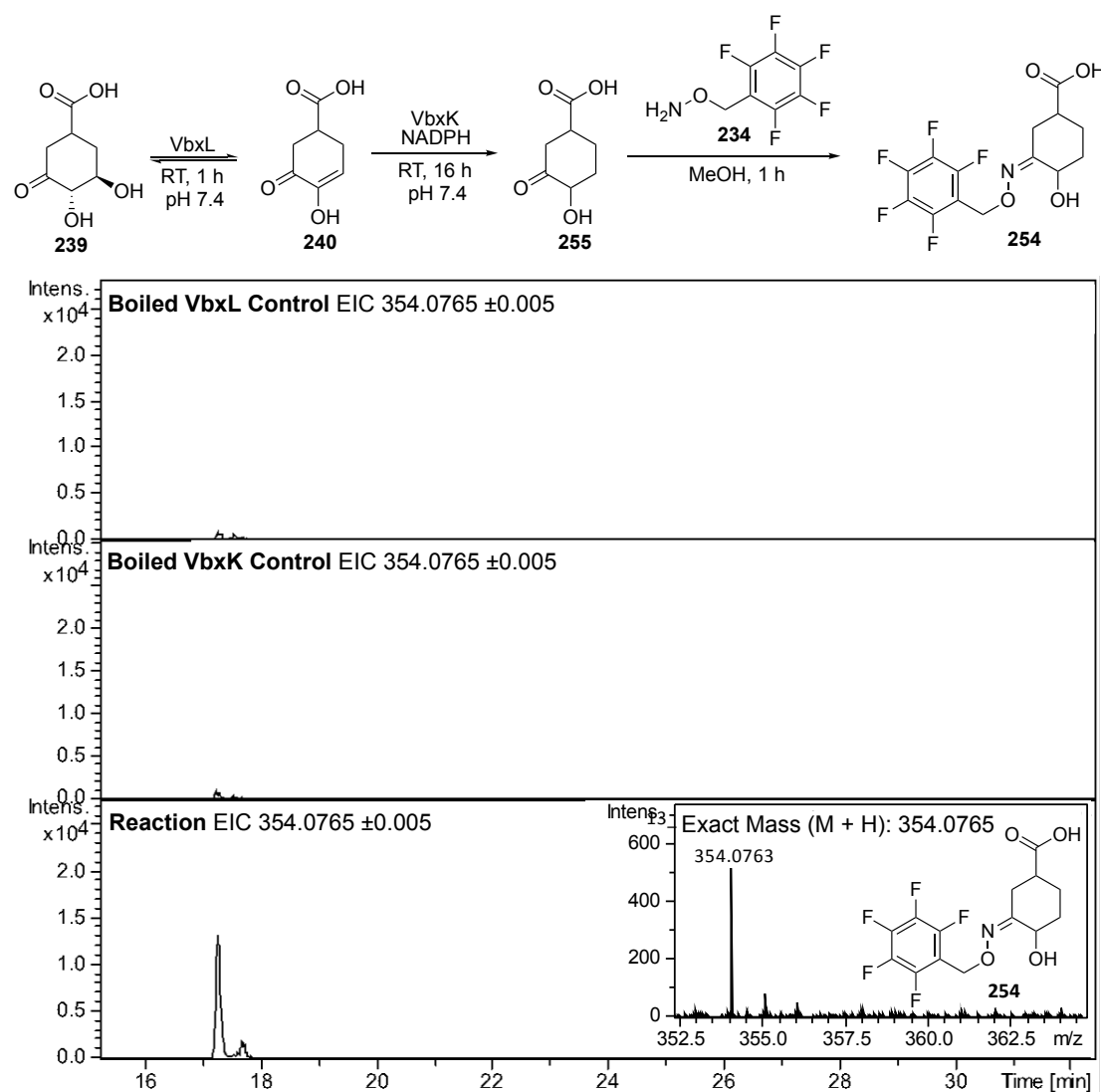
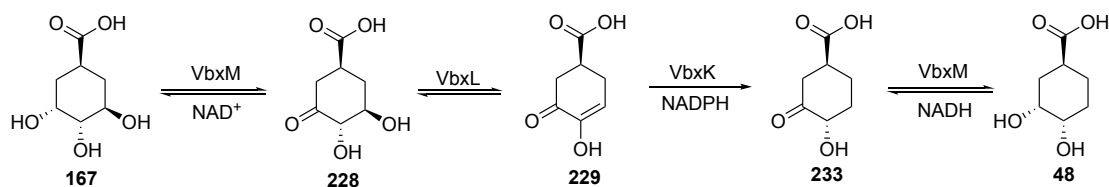


**Figure 4.25** The extracted ion chromatograms and HRMS corresponding to the VbxK catalyzed reduction of VbxL-generated unsaturated ketone **240**.

#### 4.2.2.6 Reduction Catalyzed by VbxM

Now that the enone reduction step catalyzed by VbxK had been confirmed, it was proposed that a single reduction step remained in order to generate DHCCA **48** from ketone **233** (scheme **4.15**). From the pathway proposed by Coggins and co-workers, the proposed final reduction step is also catalyzed by the quinate dehydrogenase.<sup>226</sup> These enzymes are well known to catalyze reversible reductions, and so it was thought that VbxM may catalyze the final reduction step in the DHCCA biosynthetic pathway in addition to its previous role of oxidizing THCCA **167**.<sup>227</sup>



**Scheme 4.15** The steps confirmed from THCCA **167** to form ketone **233**, and the final reduction step to form DHCCA **48** predicted to be catalyzed by VbxM.

Ketone **233** is a difficult substrate to synthesize, however DHCCA **48** had been synthesized previously (scheme **4.4**). As this reaction is predicted to be reversible, the reverse reaction which consists of the oxidation of DHCCA **48** to generated ketone **233** could be probed.<sup>227,229</sup> DHCCA **48** was incubated with VbxM and  $\text{NAD}^+$ , followed by the addition of derivatizing agent **234** and the presence of the derivatized ketone product **256** detected by LC-MS. The derivatized product of the enone reduction catalyzed by VbxK (section **4.2.2.5**) was used as a product standard (**254**). From the chromatograms shown in figure **4.26**, the presence of the peak corresponding to the correct mass of derivatized product **256**, with the same retention time as the enzymatically generated standard **254**, but not present in the boiled enzyme control reaction, indicates that VbxM is catalyzing the oxidation. Due to the reversibility of these enzymes, this is evidence to suggest that VbxM can catalyze the final reduction step of the pathway (scheme **4.15**).

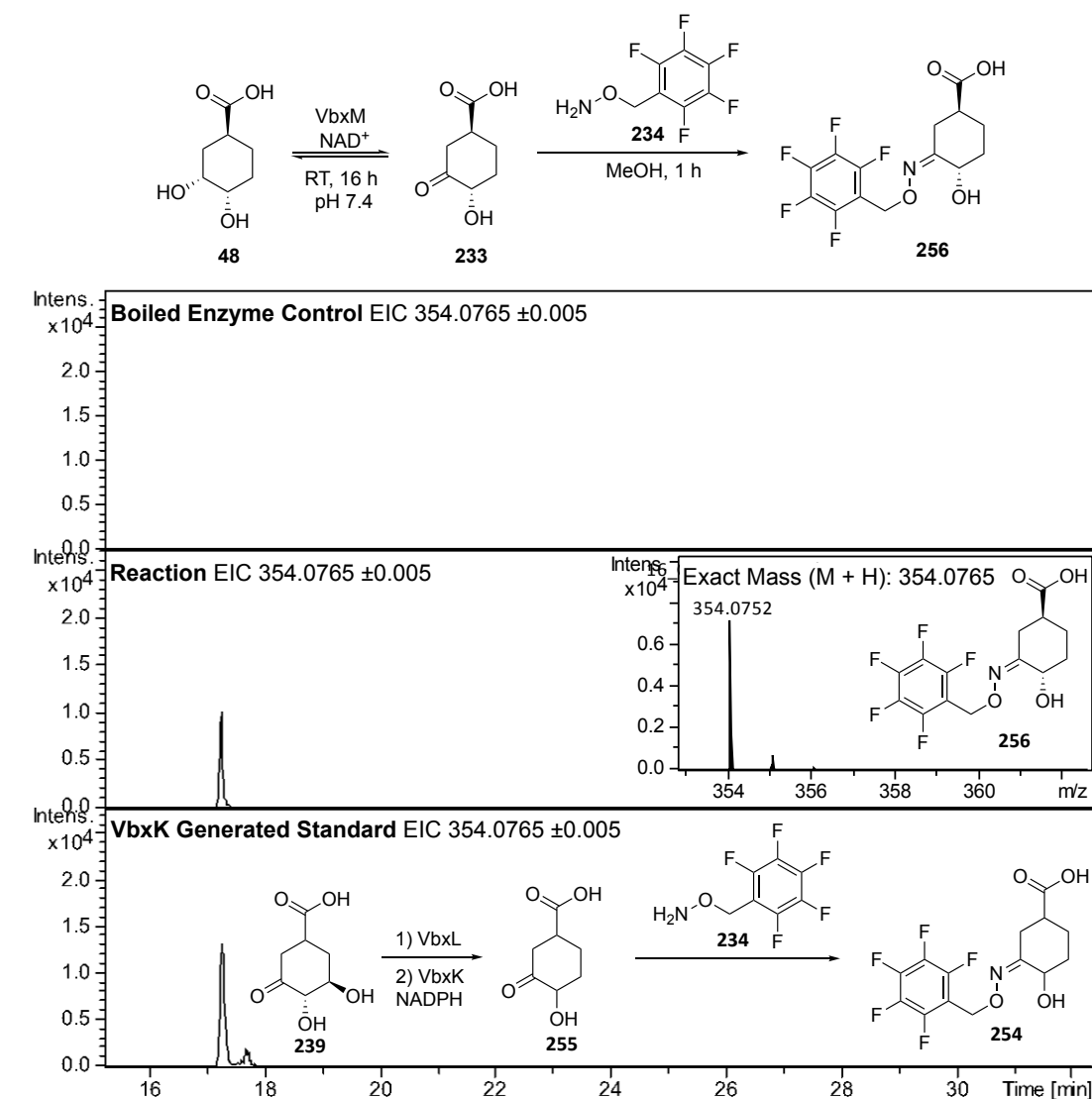
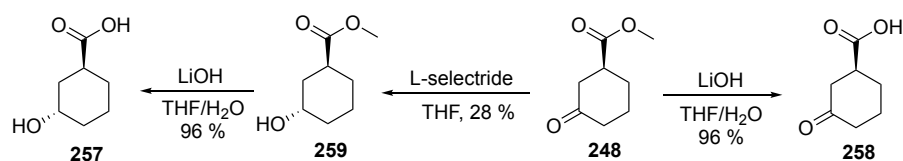


**Figure 4.26** The extracted ion chromatograms and HRMS corresponding to the VbxM catalyzed oxidation of DHCCA **48**.

The results of the oxidation assay with VbxM indicate that the oxidation is taking place, however the assay does not confirm which of the two hydroxyl groups from DHCCA **48** undergoes oxidation. In order to probe this, alcohol **257** and ketone standard **258** were synthesized (scheme **4.16**) via asymmetric reduction and hydrolysis of chiral keto-ester **248**.



**Scheme 4.16** The route used for the synthesis of alcohol **257** and ketone **258**.



Alcohol **257** was incubated with VbxM and  $\text{NAD}^+$ , followed by the addition of derivatizing agent **234**. The presence of the derivatized ketone product **260** was detected by LC-MS alongside derivatized ketone standard **260**. From the chromatograms shown in figure 4.27, the presence of the peak corresponding to the correct mass of derivatized product **260**, with the same retention time as the derivatized ketone standard **260**, but not present in the boiled enzyme control reaction, indicates that VbxM is catalyzing the oxidation at the C-3 position.

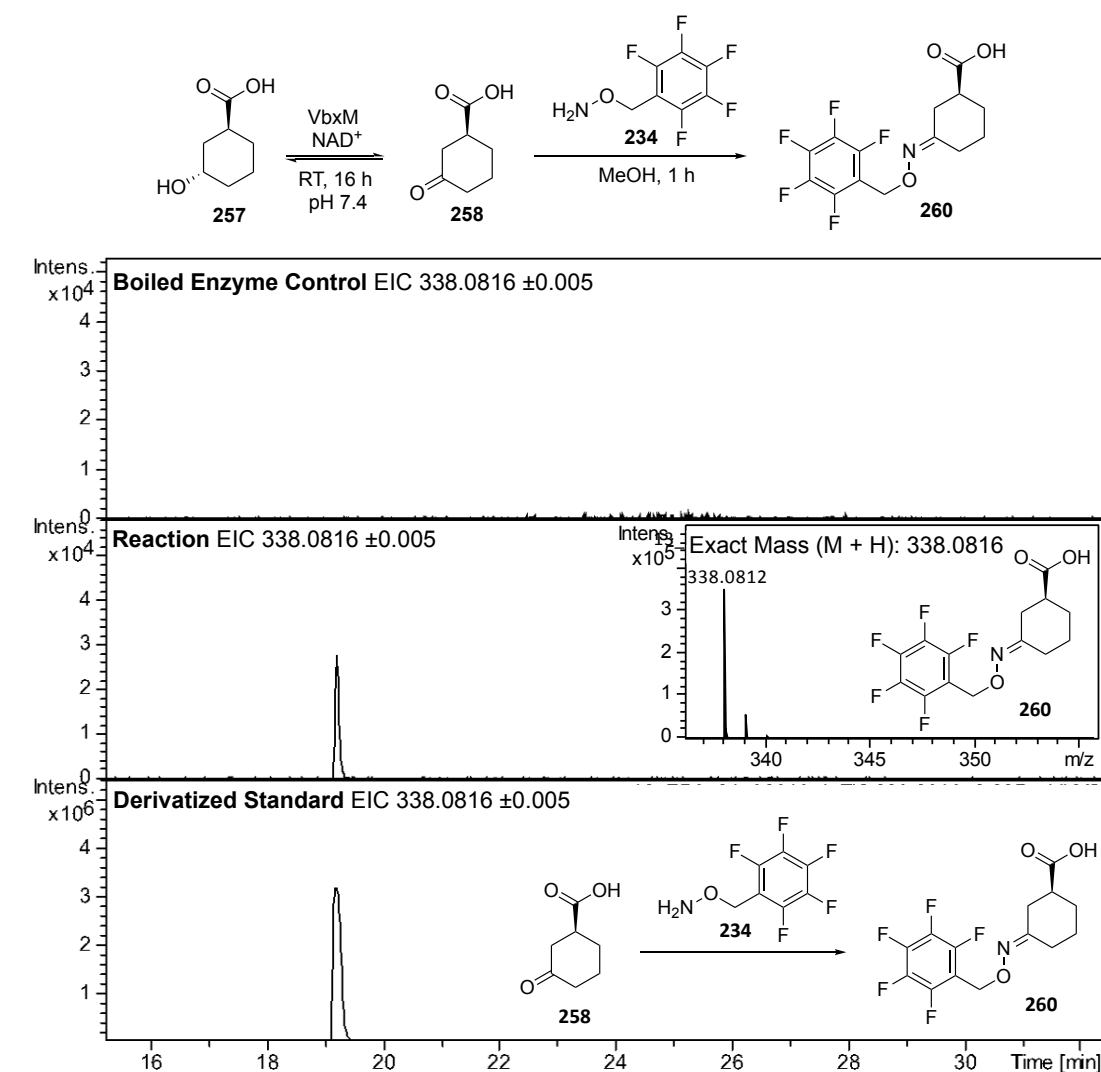
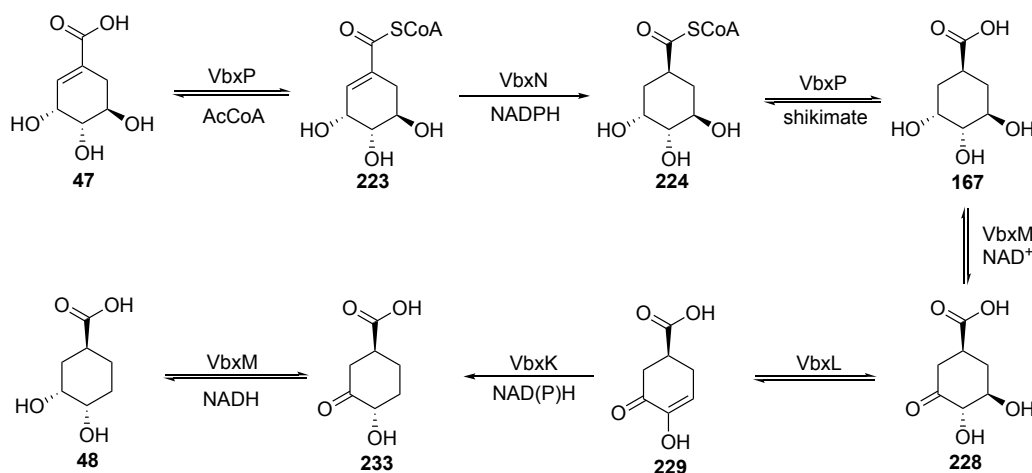


**Figure 4.27** The extracted ion chromatograms and HRMS corresponding to the VbxM catalyzed oxidation of alcohol **257**.

## 4.3 Conclusions

### 4.3.1 DHCCA Biosynthesis as Determined *in vitro*

From the *in vitro* experiments conducted in this study, DHCCA biosynthesis is predicted to proceed via the pathway shown in scheme 4.17. CoA transferase domain, VbxP, catalyzes the generation of shikimate CoA **223**, before VbxN catalyzes enoyl reduction to afford the reduced product **224**. VbxP can then use reduced product **224** as a CoA donor in order to generate another molecule of shikimate CoA **223**, and generating THCCA intermediate **167** in the process. VbxM then catalyzes the oxidation of THCCA **167** to afford ketone **228**, before dehydration catalyzed by VbxL generates unsaturated ketone intermediate **229**. VbxK then catalyzes enoyl reduction to produce ketone **233** before VbxM catalyzes the final reduction yielding DHCCA **48**.



**Scheme 4.17** The DHCCA biosynthetic pathway as determined using *in vitro* assays.

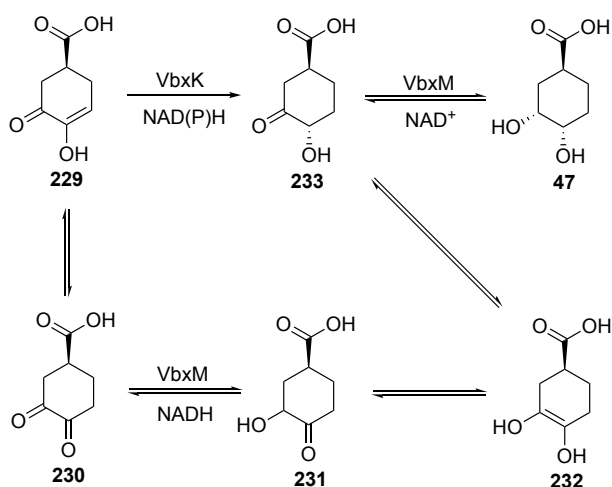
### 4.3.2 New Pathway Compared with *in vivo* Gene Deletions

Now that a new pathway has been established using *in vitro* assays, the results of gene deletions in the enacyloxin cluster (section 4.2.1, figure 4.2) were analyzed to see if they were in agreement with the new pathway. When *bamb\_5916* was deleted (gene encoding the homologue of VbxP), enacyloxin IIa production was abolished. This is in agreement with the new pathway as shikimate CoA **223** cannot be generated, which is essential for the following reduction step, and so DHCCA biosynthesis cannot proceed. When *bamb\_5914* was deleted (gene encoding the homologue of VbxN), enacyloxin IIa production was also abolished, which is again in agreement with the pathway, as the key reduction step can no longer proceed. When *bamb\_5912*

was deleted (gene encoding the homologue of VbxL), enacyloxin analogue **172** harboring the THCCA unit was produced. This is again consistent with the pathway, as the dehydration of ketone **228** can no longer proceed, and the oxidation step catalyzed by VbxM to form ketone **228** from THCCA **167** is reversible. This explains the incorporation of the THCCA **167**, which has already been shown to be a substrate for the condensation domain (section **3.2.1.5**).

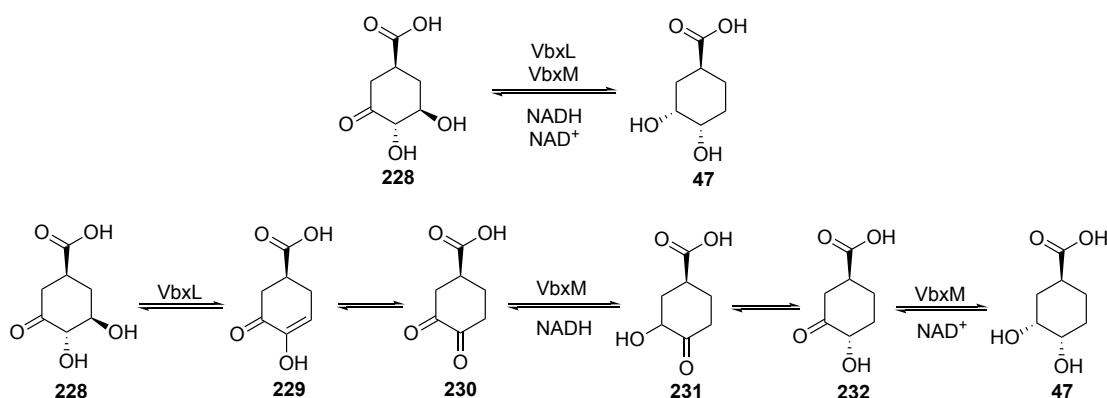
The deletion of *bamb\_5913* (gene encoding the homologue of VbxM) resulted in a small amount of analogue **172** but mostly wild-type levels of enacyloxin IIa production. The small amount of analogue **172** can be explained based on the pathway as if the VbxM-catalyzed oxidation of THCCA **167** cannot take place, THCCA **167** would be incorporated. The presence of mostly enacyloxin IIa suggests that there may be another enzyme complimenting the role of VbxM, which is not an unreasonable explanation as quinate dehydrogenase enzymes are present in primary metabolic pathways. Finally the deletion of *bamb\_5918* (gene encoding the homologue of VbxK), also resulted in a small amount of analogue **172** but mostly wild-type levels of enacyloxin IIa production. Again, the small amount of analogue **172** can be explained based on the pathway, as if the VbxK-catalyzed reduction of unsaturated ketone intermediate **229** cannot proceed, the reversibility of the preceding steps can result in the incorporation of THCCA **167**. The presence of enacyloxin IIa again suggests that another enzyme (possibly from primary metabolism) may be complimenting the role of VbxK.

An alternative explanation is that the step catalyzed by VbxK can proceed via an alternative route, whereby only VbxM is required (scheme **4.18**) as suggested by Coggins and co-workers.<sup>226</sup> This involves the tautomerization of unsaturated ketone **229** to diketone **230**, which can then be reduced by VbxM. The resulting keto-alcohol **231** can then further tautomerize to ketone **232** which can be reduced to DHCCA **48**.



**Scheme 4.18** An alternative pathway where VbxK is no longer required.

A preliminary assay was attempted in order to investigate this alternative pathway, whereby ketone **228** was incubated with VbxL, as well as VbxM, NAD<sup>+</sup> and NADH and the production of DHCCA **47** monitored by LC-MS (scheme 4.19). However the DHCCA product **47** could not be detected, so it remains unclear whether this is a true alternative pathway.



**Scheme 4.19** The preliminary assay used to investigate the alternative pathway along with the proposed sequence of steps.

### 4.3.3 Future Work

Despite the reconstitution of the DHCCA biosynthetic pathway *in vitro*, most of the enzymes involved have only been characterized at a functional level. With the exception of VbxP (CoA transferase, section 4.2.2.1), the mechanistic details of the enzyme-catalyzed steps of the pathway requires further investigation. One way in which this can be achieved is by protein crystallography. The FMN-dependent enone reductase VbxK (section 4.2.2.5) was crystallized (figure 4.28), and a 2.3 Å data set was collected. However, solving of the structure by molecular replacement is currently ongoing.

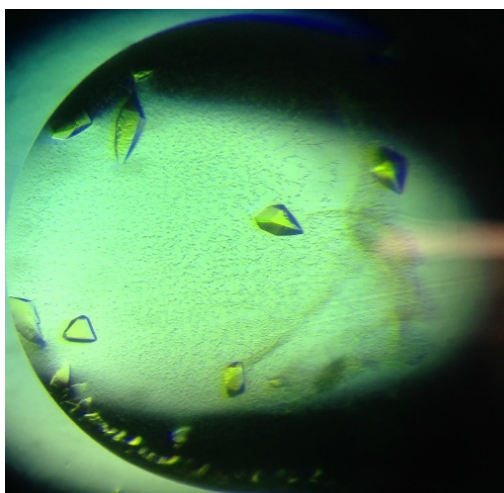


**Figure 4.28** The crystals obtained for FMN-dependent enone reductase, VbxK.

#### 4.3.4 Summary

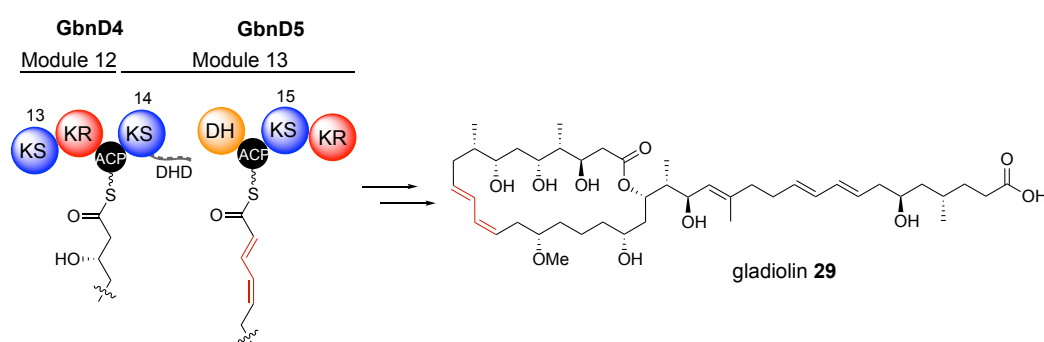
Here, the biosynthesis of the DHCCA unit of enacyloxin, which has been shown to be key to the activity of the molecule, has been fully reconstituted *in vitro*. This led to the discovery of a promiscuous CoA transferase domain, which has the potential to be utilized as a biocatalyst for the generation of CoAs. The pathway utilizes the transient formation of a CoA thioester (shikimate CoA **223**) in order to facilitate the otherwise chemically unfavorable reduction of an enoyl acid, as well as the formation of a transient ketone (ketone **228**) in order to facilitate the otherwise chemically unfavorable elimination of a hydroxyl group. The pathway proceeds via a significantly different route to what was initially predicted, which reinforces the value of investigating biosynthetic pathways using *in vitro* biochemistry.

## **5. Conclusions**

## 5.1 Elucidation of Biosynthetic Pathways

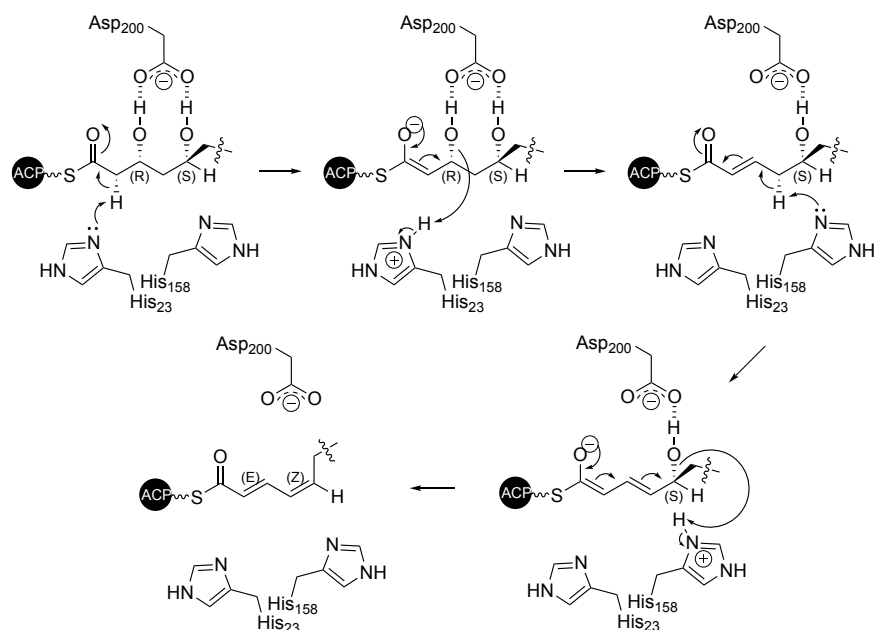
### 5.1.1 Diene-Forming DH Domains

The first aim of this project was to investigate the role of a DH domain in the installation of an *E,Z*-diene motif in the macrolide antibiotic, gladiolin **29**. The DH domain is embedded in module 13 of the gladiolin PKS, which has a type B split module architecture (scheme 5.1). Type B split modules are a common feature of *trans*-AT PKSs, and are proposed to install diene motifs in a number of polyketide natural products, yet the mechanism by which the diene is formed by a single module had not previously been characterized.<sup>94</sup>



**Scheme 5.1** The type B split module present in the gladiolin **29** PKS thought to be responsible for the installation of the (*E,Z*)-diene motif (red).

Using an intact protein MS-based assay with chemically synthesized polyketide intermediate mimics loaded onto the overproduced DH-ACP didomain of module 13, the DH domain was shown to dehydrate a (3*R*,5*S*)-3,5-dihydroxyacyl thioester to form an (*E,Z*)-diene. This is the first biochemical evidence of a DH domain catalyzing more than a single dehydration. Using sequence alignments, an additional histidine residue in the active site of the DH domain was identified, which was shown to be involved in the vinylogous dehydration of a (2*E*,5*S*)-5-hydroxy-2-enoyl thioester intermediate to form the *E,Z*-diene. The mechanism of DH catalyzed diene formation is proposed to proceed via firstly the canonical *syn*-elimination of the (3*R*)-configured hydroxyl group to install the (2*E*)-configured alkene. The additional histidine residue then catalyzes the vinylogous dehydration of the (5*S*)-configured hydroxyl group in order to generate the *E,Z*-diene (scheme 5.2). The substrate tolerance of the domain was also investigated, and the DH was shown to also be capable of the dehydration of a (3*R*,5*R*)-3,5-dihydroxyacyl thioester substrate, which was thought to result in an (*E,E*)-diene.



**Scheme 5.2** The proposed mechanism of double dehydration catalyzed by the GbnD5 DH domain.

To confirm if diene-forming DH domains are present in other systems, the sequence of the GbnD5 DH domain was aligned with the sequences of other known DH domains, and a phylogenetic tree was generated (Dr. Matt Jenner, appendix 8.1). The phylogenetic analysis identified several other diene-forming DH domains (figure 5.1). The domains appear to occur mostly within type B dehydrating bimodules, but some occur as part of conventional modules (such as in chivosazol biosynthesis) as well as in *cis*-AT PKS systems (such as in thuggacin biosynthesis). There is also an example where the DH domain is predicted to install an (*E,E*)-configured diene (tartrolon), consistent with what was observed for the GbnD5 DH domain when provided with a (*3R,5R*)-3,5-dihydroxyacyl thioester. From the biochemical investigation of the GbnD5 DH domain, not only has a better understanding of gladiolin biosynthesis been obtained, but due to the conserved nature of these DH domains, the biosynthetic pathways of many other diene-containing polyketides can now be better understood.



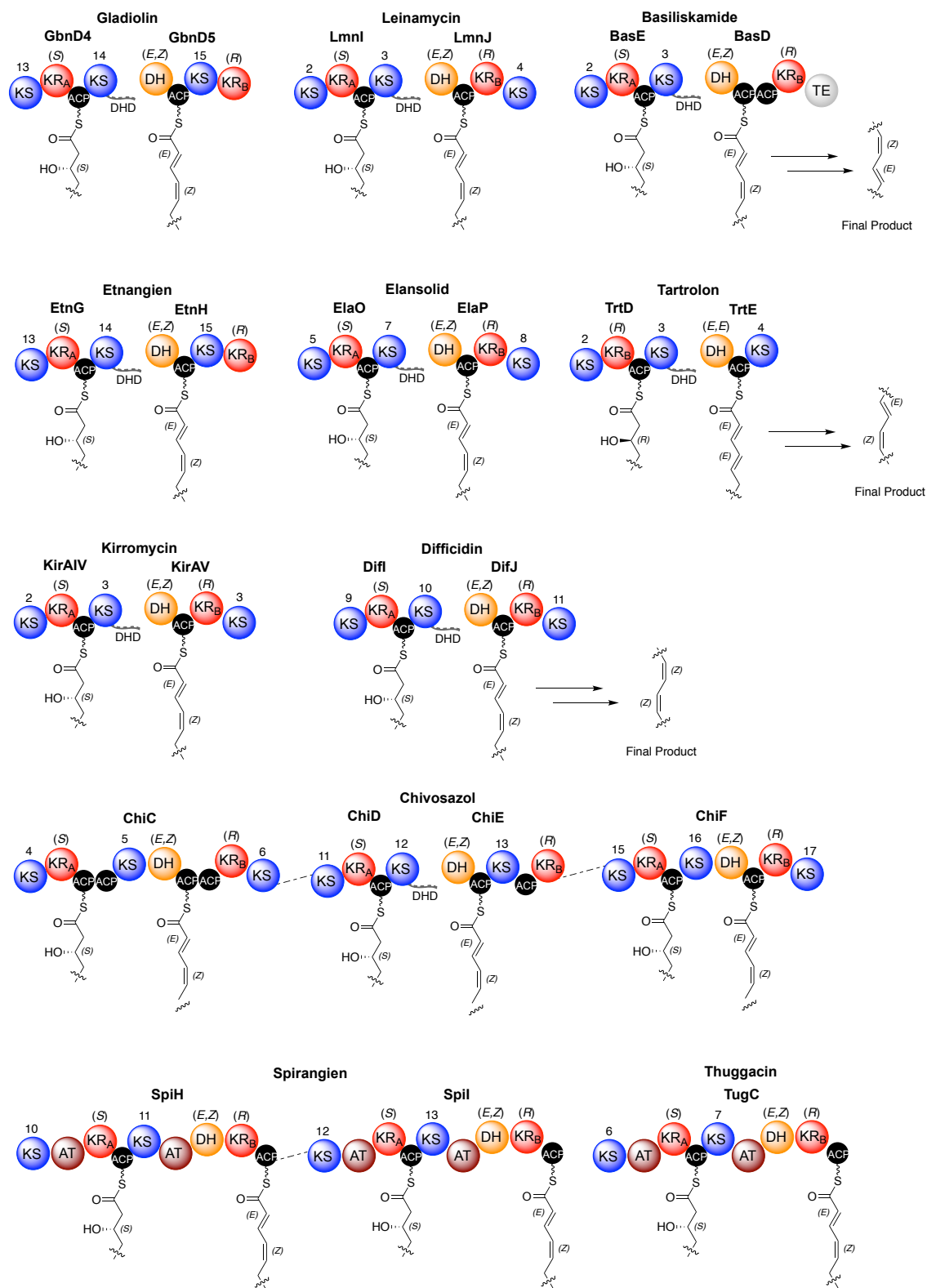
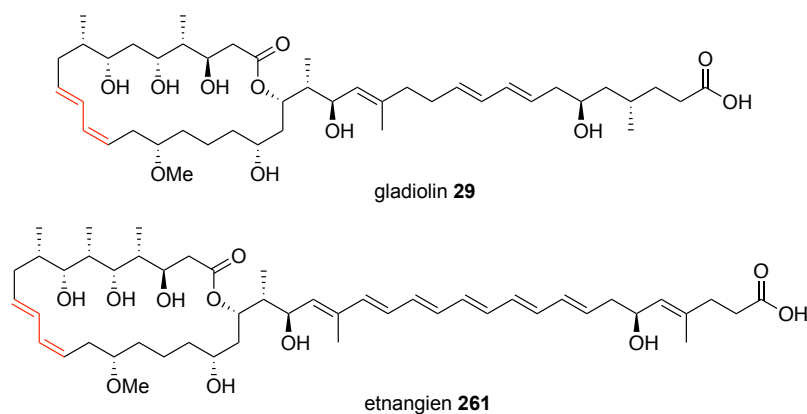


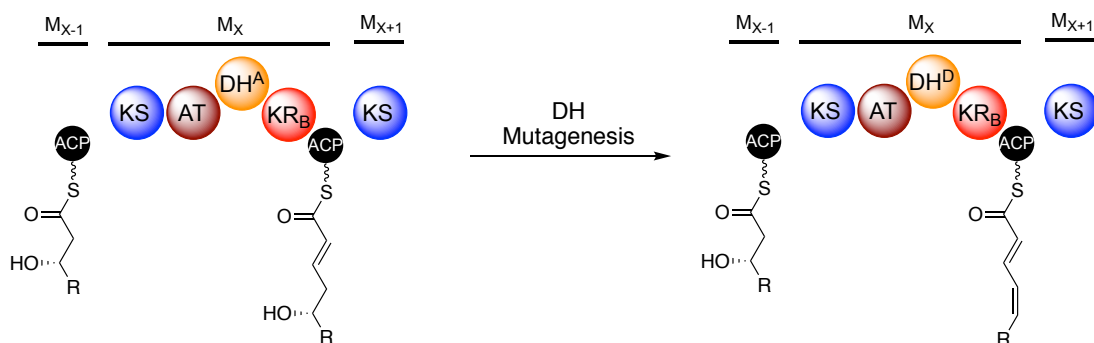
Figure 5.1 Examples of diene-forming DH domains identified in other PKS systems.

The *E,Z*-diene motif of gladiolin **29** is also present in the closely related polyketide antibiotic etnangien **261** (figure 5.2). Both molecules are very similar in structure and act by binding to RNA polymerase.<sup>230</sup> The *E,Z*-diene motif may be required in order for the macrolide ring to bind to its target in the correct conformation.



**Figure 5.2** The structures of gladiolin **29** and etnangien **261**.

The discovery and mechanistic understanding of diene-forming DH domains provides scope for the introduction of *E,Z*- or *E,E*-dienes into polyketide scaffolds via genetic engineering approaches. This could conceivably be achieved via the *in vivo* mutagenesis of a canonical DH domain, embedded within a module that processes an appropriate 3,5-dihydroxyacyl intermediate, to a diene-forming DH domain, resulting in the formation of the corresponding diene (scheme 5.3). This approach results in minimal disruption to the PKS assembly line, however is dependent on the ability of the downstream KS domain to accept the resulting dienoyl thioester as a substrate for further elongation of the chain and continued polyketide assembly.

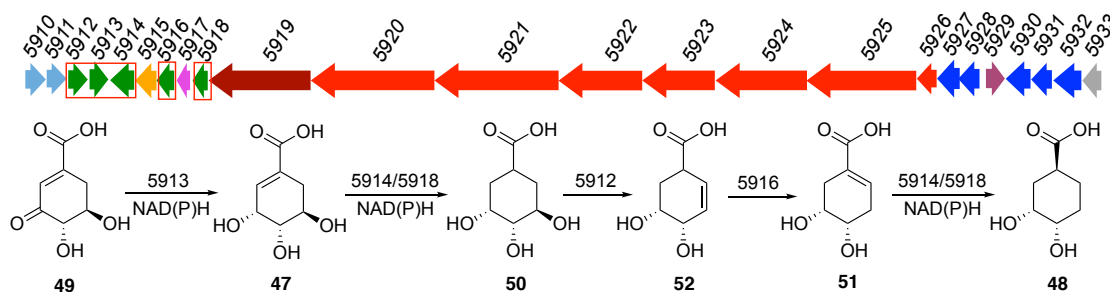


**Scheme 5.3** The engineering of a diene-forming DH domain into a canonical *cis*-AT PKS module. DH<sup>A</sup> = canonical alkenyl-forming DH domain, DH<sup>D</sup> = diene-forming DH domain.

There is also scope for diene-forming DH domains to be developed into *in vitro* biocatalysts. *E,Z*-Dienes are often generated synthetically using organometallic coupling reactions, which can involve the use of expensive metal catalysts as well as harsh reaction conditions.<sup>231</sup> These reaction conditions are typically avoided when it comes to industrial scale synthesis, so the development of a biocatalyst capable of *E,Z*-diene production would be beneficial. The diene-forming DH domain in this study has not yet been shown to process small molecule substrates, and so may need to be optimized via directed evolution, a technique that has been used successfully for the generation of many robust biocatalysts.<sup>232</sup>

### 5.1.2 DHCCA Biosynthesis

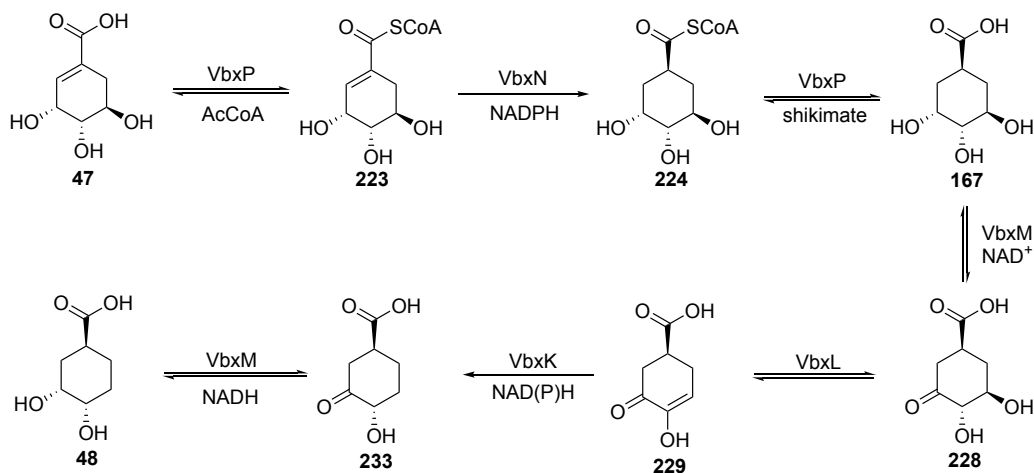
The shikimate-derived DHCCA unit of enacyloxin IIa **30** is key to the biological activity of the antibiotic (section 3.1.2.3). When the enacyloxin IIa gene cluster was reported in 2011, DHCCA **48** was proposed to be biosynthesized from shikimate **47** using five enzymes (encoded by *bamb\_5912*, *5913*, *5914*, *5916* and *5918*) and an initial pathway was postulated (scheme 5.4).<sup>104</sup> Given the importance of the DHCCA unit to the activity of enacyloxin IIa **30**, the predicted pathway was investigated using both *in vivo* gene deletions and *in vitro* biochemical assays.



**Scheme 5.4** The proposed pathway for the biosynthesis of DHCCA **48**.<sup>104</sup>

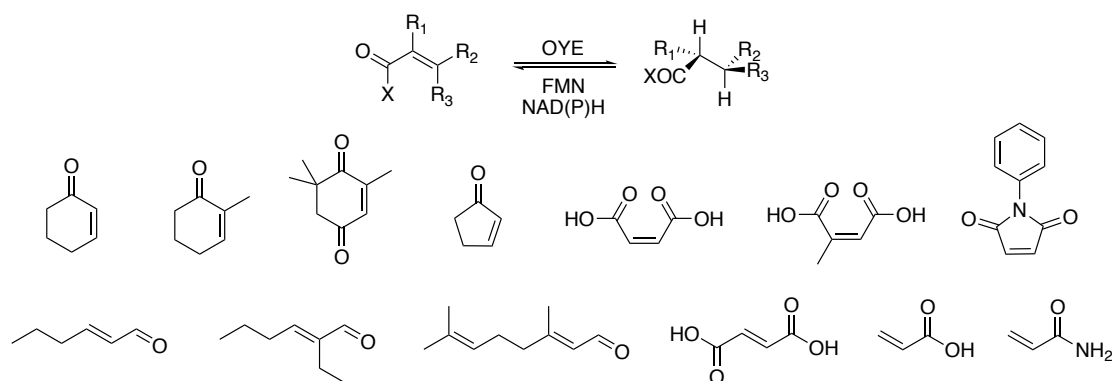
From the results of *in vivo* gene deletions and initial *in vitro* assays, it was clear that the initially proposed pathway was incorrect. After the BLAST analysis of the five enzymes involved, it became apparent that several of the enzymes had different roles to what was initially predicted. A new pathway was proposed based on these new roles, which was confirmed using *in vitro* assays (scheme 5.5) and was more consistent with the *in vivo* results. The pathway utilizes the transient formation of a CoA thioester in order to facilitate the otherwise chemically unfavorable enoyl reduction of shikimic acid **47**, as well as the formation of a transient ketone in order to facilitate the otherwise chemically unfavorable elimination of a hydroxyl group (from THCCA **167**). The pathway proceeds via a significantly different route to the initially

predicted pathway, reinforcing the value of investigating biosynthetic pathways using *in vitro* biochemistry.



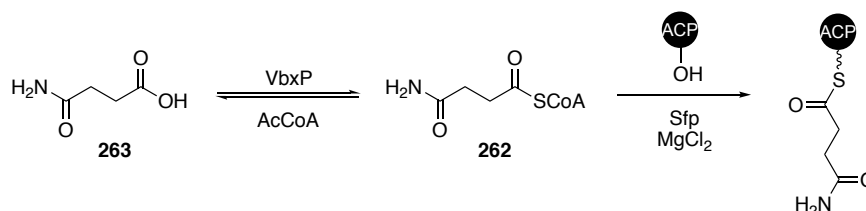
**Scheme 5.5** The DHCCA biosynthetic pathway as determined using *in vitro* assays.

The discovery and characterization of the enzymes from the DHCCA biosynthetic pathway leads to the potential of new biocatalysts. Both enoyl reductase enzymes, VbxN and VbxK, catalyze reactions resulting in the installation of stereocenters, which can be challenging to install synthetically. Asymmetric synthesis often involves the use of expensive chiral metal complexes as catalysts, such as Noyori's ruthenium-based reduction catalyst, which was used in section 2.2.1.1 during the asymmetric synthesis of chiral pantetheines.<sup>233</sup> As well as being expensive, asymmetric reduction catalysts also often require high-pressure hydrogen atmospheres typically avoided during industrial scale synthesis, meaning alternative methods of installing stereocenters are of great value.<sup>234</sup> The enone-reductase, VbxK is a member of the old yellow enzyme (OYE) family, a group of flavin-dependant reductase enzymes, which have already been extensively developed into robust biocatalysts for the stereoselective *trans* hydrogenation of conjugated C=C double bonds (scheme 5.6).<sup>235</sup>



**Scheme 5.6** The stereospecific enoyl reduction catalyzed by OYEs along with some representative substrates.

Another enzyme from the DHCCA biosynthetic pathway, VbxP, also has the potential to be developed into a useful biocatalyst. VbxP is a CoA transferase responsible for the generation of shikimate CoA **223** in the pathway (scheme 5.5), but was also shown to be capable of generating a range of other CoA thioesters when supplied with the appropriate acid substrate (section 4.2.2.1). CoA thioesters are often used during the *in vitro* investigation of biosynthetic mechanism, but can often be challenging to synthesize due to their high functionality and polarity, and only a limited range are commercially available. Another approach is to synthesize the corresponding acyl-pantetheine and use the enzymatic loading cassette utilized in section 2.4.1, however pantetheine substrates are often also challenging to synthesize depending on the required acyl group. VbxP may provide an alternative to these routes, eliminating the need for challenging chemical synthesis. Since the discovery and characterization of VbxP, the enzyme has been used to generate a required CoA substrate, succinamide-CoA **262**, which was then successfully loaded onto an *apo*-ACP domain *in situ* for a biochemical assay, demonstrating the applicability of VbxP (scheme 5.7).



**Scheme 5.7** The *in situ* generation of succinamide-CoA **262** via VbxP and loading of an *apo*-ACP domain.

Overall, the investigation of biosynthetic mechanism in both the gladiolin **29** and enacyloxin IIa **30** biosynthetic pathways has provided valuable insights into how key motifs are installed in both of these polyketide antibiotics as well as other polyketide natural products. The greater understanding of these pathways provides more scope for the engineering of antibiotic analogues and has led to the discovery of potential biocatalysts.

## 5.2 Engineering Antibiotic Analogues

The long-term goal of this study was to establish a greater understanding of biosynthetic pathways to facilitate the engineering of improved antibiotic analogues. This concept is exemplified with the strategies used in order to generate enacyloxin IIa analogues as they rely on a thorough understanding of the enacyloxin IIa biosynthetic pathway. The *in vitro* characterization of the unusual chain release mechanism and substrate tolerance of the enacyloxin condensation domain (Bamb\_5915), led to the design and implementation of a strategy for the generation of analogues harbouring alternative DHCCA units (green, figure 5.3). This strategy consisted of the deletion of several of the DHCCA biosynthesis genes (*bamb\_5912-14*) and feeding of simple DHCCA analogues, which had been accepted by the condensation domain *in vitro* (Dr. Joleen Masschelein). This strategy was then expanded to include the incorporation of a range of chemically synthesized DHCCA analogues, which resulted in the production of an enacyloxin analogue (**187**, figure 5.3) harbouring an unsaturated DHCCA derivative **51** which had increased potency relative to enacyloxin IIa **30**.

In addition to the chain release mechanism, the tailoring enzymes involved in enacyloxin IIa biosynthesis were also targeted for the engineering of analogues. The tailoring enzymes were deleted individually as well as in combination with each other in order to generate an array of enacyloxin analogues harbouring changes in the polyol region (blue, figure 5.3). This resulted in the production of a more potent enacyloxin analogue lacking the carbamoyl and keto tailoring groups (**45**, figure 5.3). As well as deleting the tailoring enzymes, the ability of the two halogenase enzymes (Bamb\_5928 and 5931) to catalyse bromination as well as chlorination was used to generate bromide analogues, two of which (**196** and **199**, figure 5.3) were again more potent than enacyloxin IIa **30**. In an attempt to rationally design an analogue with even greater potency, a mutant was generated harbouring both changes in the polyol region and the unsaturated DHCCA derivative **51**, which had resulted in more potent analogues (**45** and **187**), however the resulting analogue (**204**) did not display the desired increase in potency.

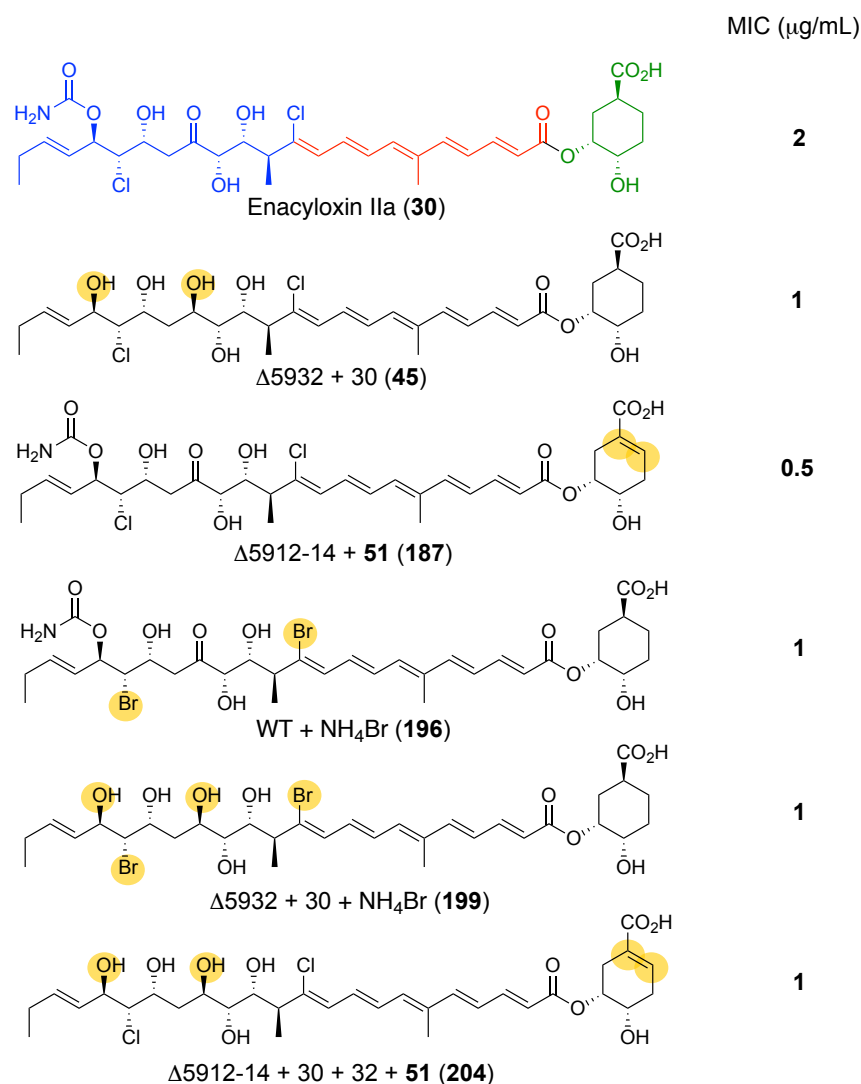


**Figure 5.3** Engineered enacyloxin analogues with increased potency.

From the crystal structure of enacyloxin Ila **30** bound to its target, EF-Tu (figure 3.27, section 3.3.2), there appears to be key polar contacts between residues of EF-Tu and functional groups in both the polyol and DHCCA regions of enacyloxin Ila.<sup>110</sup> One of the aims of generating the library of enacyloxin analogues was to examine the affect on activity of altering the structure of enacyloxin Ila in both the polyol and DHCCA regions of the molecule. The SAR data generated could then potentially be used as a basis for the rational engineering of more potent analogues. From the SAR data, it was difficult to correlate the changes in activity observed to the key polar contacts identified from the crystal structure. This suggests that data other than MIC assays, such as *in vitro* EF-Tu binding assays or testing in animal infection models, may be required in order to form a more reliable basis for the engineering of analogues. However it is clear that the removal of many of the tailoring groups, as well as replacing the DHCCA unit with a linear analogue, results in reduced potency.

Five analogues were still generated which were more potent than enacyloxin IIa, and could be used as a platform for the engineering of analogues harboring more complex changes. The platform could potentially be used to combat the inherent stability problems associated with enacyloxin IIa. The light-induced isomerization believed to be promoted by the methyl group of the polyene region has been addressed via the generation of an MT domain-inactive mutant (figure 5.4). However the resulting des-methyl analogue **205** loses potency relative to enacyloxin IIa (MIC 2  $\mu\text{g/mL}$ ). The combination of the MT domain-inactive mutant with some of the structural features identified in this study as being key to lowering MIC may result in des-methyl analogues which retain potent activity (figure 5.4).

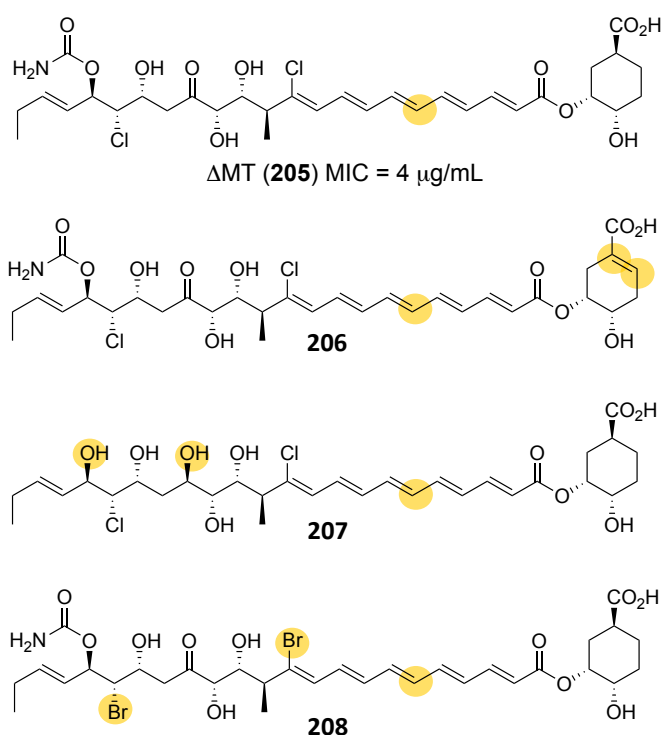


**Figure 5.4** The des-methyl enacyloxin IIa analogue **205** and potential des-methyl enacyloxin analogues (**206-208**) that may retain potency.

The other potential stability problem associated with enacyloxin IIa, is the labile ester linkage between the DHCCA unit and the linear acyl chain. This was addressed via the incorporation of a simplified amine DHCCA derivative (**140**), however the resulting amide enacyloxin analogue **149** again displayed reduced potency (section 3.1.2.3). The platform of potent analogues established in this study could again be used in order to generate amide analogues which may retain activity (figure 5.5).



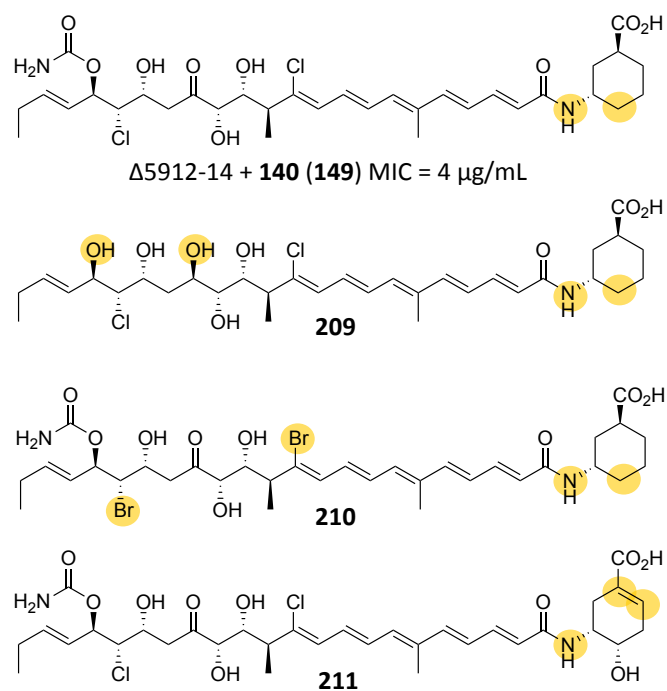


**Figure 5.5** The simplified amide analogue (**149**) and potential amide enacyloxin analogues (**209-211**), which are more likely to retain potency.

In addition to the improved analogues generated in this study, vibroxin **151** (figure 5.6) may also be considered as a platform for the generation of potent derivatives. Vibroxin **151** is more potent than enacyloxin IIa **30**. However, it is produced by a genetically intractable *Vibrio rhizosphaerae* strain. The heterologous expression of the vibroxin **151** gene cluster would facilitate the engineering of improved vibroxin analogues, and allow the introduction of the MIC-lowering features identified in this study (figure 5.6).

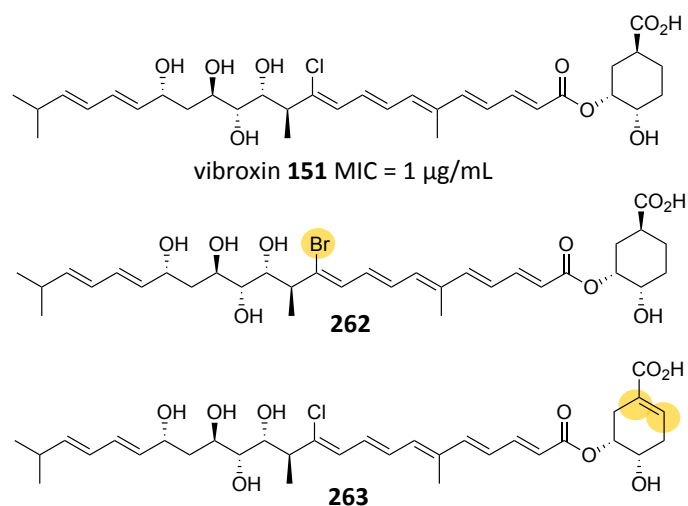


**Figure 5.6** The structure of vibroxin **151** and the structures of potential improved vibroxin analogues (**262** and **263**)

Overall, several enacyloxin IIa analogues have been generated in this study, which display greater potency than enacyloxin IIa itself. These analogues were generated using multiple strategies, which were designed based upon a thorough understanding of the enacyloxin IIa biosynthetic pathway. This reaffirms the importance of the role that the elucidation of biosynthetic pathways has to play in the production of improved antibiotics, which are urgently required for the treatment of rapidly emerging, life-threatening MDR pathogens.

## **6. Experimental**

## 6.1 Instruments and Equipment

All media was autoclaved was at at 121 °C and 1 bar for 10 min. Sterile filtering was conducted using Minisart syringe filters (Sartorius). Liquid and solid cultures were incubated using New Brunswick Scientific Innova shakers or Thermo Scientific Heraeus static incubators respectively. Centrifugations were conducted using Eppendorf models 5415D, 5424, 5804R and 5810R, or a Thermo Scientific Sorvall RC 6 Plus equipped with an SS34 or SLA3000 rotor. *Burkholderia* and *Acinetobacter* strains were handled in a category 2 laboratory equipped with a Bassaire laminar flow hood. Optical densities were measured using a Thermo Scientific BioMate 3 spectrophotometer. Electroporations were conducted with a BioRad Gene Pulser® II (200  $\Omega$ , 25  $\mu$ F, 1.7 kV) in combination with a BioRad Pulse Controller Plus. DNA and protein concentrations were determined using a Thermo Scientific NanoDrop Lite spectrophotometer. PCR was conducted using an Eppendorf Mastercycler Gradient. Agarose gel electrophoresis was performed using a BioRad tank in combination with either a PowerPac Basic or a PowerPac 300. Visualisation of agarose gels was conducted with a UVP BioDoc-It Imaging System 2UV Transilluminator. Cell lysis was conducted using a Constant Systems Ltd TS-Series Cabinet cell disruptor (One-Shot mode, 20 KPSI). Proteins were analysed by SDS-PAGE gel electrophoresis using a BioRad Mini-PROTEAN Tetra cell. UV-Vis readings of solutions in 3 mm path length sub-micro quartz cuvettes (Starna scientific) were attained using a Varian Cary 50 Bio UV-Visible Spectrophotometer (single wavelength) or a Perkin Elmer Lambda 3S UV/Vis Spectrophotometer (multiple wavelengths).

Room temperature (RT) refers to ambient temperature (20-22 °C), 5 °C refers to a cold water bath and 0 °C refers to an ice slush bath. Heated experiments were conducted using thermostatically controlled oil baths. All commercially available solvents and chemicals were used without any further purification. Anhydrous solvents were obtained by distillation under argon using calcium hydride as drying reagent and stored over 4 Å molecular sieves. Solvents were evaporated using a BUCHI Rotavapor R-200 or R-210 connected to a BUCHI Vacuum Pump V-700. NMR spectra were recorded on Bruker Advance AV-300, HD-400 and HD-500 MHz spectrometers at RT. Chemical shifts are reported in parts per million (ppm) referenced from  $\text{CDCl}_3$  ( $\delta_{\text{H}}$ : 7.26 ppm and  $\delta_{\text{C}}$ : 77.2 ppm) or MeOD ( $\delta_{\text{H}}$ : 3.31 ppm and  $\delta_{\text{C}}$ : 49.0 ppm). Coupling constants ( $J$ ) are rounded to the nearest 0.5 Hertz (Hz). Multiplicities are given as multiplet (m), singlet (s), doublet (d), triplet (t), quartet (q), quintet (quin.), sextet (sext.), septet (sept.), octet (oct.) and nonet (non.).  $C_{\text{quart}}$  donates a quaternary carbon.  $^1\text{H}$  and  $^{13}\text{C}$  assignments were established on the basis of COSY,  $^{13}\text{C}$ -DEPT, HMQC and HMBC

correlations. Infra-red (IR,  $\nu_{\max}$ ) spectra were recorded using either a Perkin Elmer Spectrum 100 FT-IR spectrometer or an Alpha Bruker Platinum ATR single reflection diamond ATR module. Optical rotations were measured using an Optical Activity Ltd AA-1000 millidegree auto-ranging polarimeter (589 nm). Specific rotations are given in units of  $10^{-1} \text{ deg cm}^2 \text{ g}^{-1}$ . Melting points were recorded on a Stuart scientific melting point apparatus and are uncorrected. Silica column chromatography was performed on 40-60 Å silica gel (Sigma Aldrich). Thin layer chromatography (TLC) was carried out aluminum sheets coated with 0.2 mm silica gel (Fisher Scientific) F<sub>254</sub>. Visualisation was effected by UV light (254 nm) or by potassium permanganate solution followed by heating. Low resolution mass spectra (LRMS) were recorded using an Agilent 6130B single Quad (ESI). High resolution mass spectra (HRMS) were obtained by either Dr Lijiang Song or Mr Philip Aston using a Bruker micro-TOF ESI spectrometer.

Small molecules were analyzed using a Dionex UltiMate 3000 UHPLC connected to a Zorbax Eclipse Plus column (C<sub>18</sub>, 100 × 2.1 mm, 1.8 mm) coupled to a Bruker maXis impact mass spectrometer. Mobile phases consisted of water (A) and acetonitrile (B), each supplemented with 0.1% formic acid. The column was eluted with a linear gradient of 5 - 100% B over 35 min, employing a flow rate of 0.2 mL/min. The mass spectrometer was operated in positive ion mode with a scan range of 50-3000 *m/z*. Source conditions were: end plate offset at -500 V; capillary at -4500 V; nebulizer gas (N<sub>2</sub>) at 1.6 bar; dry gas (N<sub>2</sub>) at 8 L min<sup>-1</sup>; dry temperature at 180 °C. Ion transfer conditions were: ion funnel RF at 200 Vpp; multiple RF at 200 Vpp; quadrupole low mass at 55 *m/z*; collision energy at 5.0 eV; collision RF at 600 Vpp; ion cooler RF at 50-350 Vpp; transfer time at 121 ms; pre-pulse storage time at 1 ms. Calibration was performed with 1 mM sodium formate through a loop injection of 20 µL at the start of each run.

UHPLC-ESI-Q-TOF-MS analyses of intact proteins were conducted using a Dionex UltiMate 3000 RS UHPLC connected to an ACE 3 C<sub>4</sub>-300 reverse phase column (Advanced Chromatography Technologies, Aberdeen, UK; 100 × 2.1 mm, 5 µM, 30 °C) coupled to a Bruker maXis II mass spectrometer. Proteins were eluted with a linear gradient of 5 - 100% MeCN containing 0.1% formic acid over 30 min. The mass spectrometer was operated in positive ion mode with a scan range of 200-3000 *m/z*. Source conditions were: end plate offset at -500 V; capillary at -4500 V; nebulizer gas (N<sub>2</sub>) at 1.8 bar; dry gas (N<sub>2</sub>) at 9.0 Lmin<sup>-1</sup>; dry temperature at 200 °C. Ion transfer conditions were: ion funnel RF at 400 Vpp; multiple RF at 200 Vpp; quadrupole low mass at 200 *m/z*; collision energy at 8.0 eV; collision RF at 2000 Vpp; transfer time at 110.0 µs; pre-pulse storage time at 10.0 µs.

Preparative HPLC was conducted using an Agilent 1260 instrument equipped with a Zorbax SB-C<sub>18</sub> column (21.2 x 100 mm, 5 µm), monitoring absorbance at 360 nm. Mobile phases consisted of H<sub>2</sub>O and MeOH, with the H<sub>2</sub>O supplemented with 0.1% formic acid. A gradient of 30% MeOH to 100% MeOH over 40 minutes was employed at a flow rate of 10 mL/min.

## 6.2 Materials

### 6.2.1 General

Bacto casamino acids, Bacto yeast extract and Bacto agar were purchased from Becton Dickinson Microbiology. Luria-Bertani (LB) broth powder and Mueller-Hinton (MH) broth powder were purchased from Sigma Aldrich. GelRed Nucleic Acid Gel Stain and Instant Blue were purchased from Cambridge Bioscience (UK) and Expedeon (UK) respectively. All chemical reagents and solvents were purchased from Sigma Aldrich (USA), Thermo Fisher Scientific (UK), Fisher Scientific (UK), Alfa Aesar (USA) or VWR (UK).

### 6.2.2 Growth and Production Media

**Luria-Bertani medium (LB):** LB broth powder was dissolved in deionised H<sub>2</sub>O (25 g/L) and was sterilized by autoclaving. LB agar was prepared using the same procedure with Bacto agar (15 g/L) added prior to sterilization.

**Basal salts medium (BSM):** K<sub>2</sub>HPO<sub>4</sub>·3H<sub>2</sub>O (4.3 g/L), NaH<sub>2</sub>PO<sub>4</sub> (1.0 g/L), NH<sub>4</sub>Cl (2.0 g/L), MgSO<sub>4</sub>·7H<sub>2</sub>O (0.2 g/L), FeSO<sub>4</sub>·7H<sub>2</sub>O (0.01 g/L), MnSO<sub>4</sub>·H<sub>2</sub>O (0.003 g/L), ZnSO<sub>4</sub>·H<sub>2</sub>O (0.003 g/L), CoSO<sub>4</sub>·7H<sub>2</sub>O (0.001 g/L), nitrioloacetic acid (0.1 g/L), Bacto yeast extract (0.5 g/L), Bacto casamino acids (0.5 g/L) and glycerol (4.0 g/L) were dissolved in deionised H<sub>2</sub>O and the pH adjusted to 7.2. Bacto agar (15 g/L) was then added prior to sterilization.<sup>236</sup>

**M9 minimal medium:** Na<sub>2</sub>HPO<sub>4</sub> (6.0 g/L), KH<sub>2</sub>PO<sub>4</sub> (3.0 g/L), NaCl (0.5 g/L), NH<sub>4</sub>Cl (1.0 g/L), sucrose (10.0 g/L), MgSO<sub>4</sub> (0.1 g/L) and CaCl<sub>2</sub> (0.01 g/L) were dissolved in deionised H<sub>2</sub>O and the pH adjusted to 7.4. Bacto agar (15 g/L) was then added prior to sterilization.

**Mueller-Hinton medium (MH):** MH broth powder was dissolved in deionised H<sub>2</sub>O (22 g/L) and was sterilized by autoclaving.

### 6.2.3 Buffers

**Tris/Borate/EDTA (TBE) buffer (10x):** Tris-HCl (890 mM), boric acid (890 mM) and EDTA (20 mM) were dissolved in deionised H<sub>2</sub>O. The solution was diluted to 1 x before use.

**Loading Buffer:** NaCl (100 mM), Tris base (20 mM) and imidazole (20 mM) were dissolved in deionised H<sub>2</sub>O and the pH was adjusted to 8.0, before the solution was sterile filtered.

**Elution Buffers:** NaCl (100 mM), Tris base (20 mM) and imidazole (50-300 mM) were dissolved in deionised H<sub>2</sub>O and the pH was adjusted to 8.0, before the solution was sterile filtered.

**Storage Buffer:** NaCl (100 mM) and Tris base (20 mM) were dissolved in deionised H<sub>2</sub>O and the pH was adjusted to 7.4, before the solution was sterile filtered. 10 % glycerol was added before flash freezing.

**SDS-PAGE sample buffer (5 ×):** SDS (10 % w/v), 2-mercaptoethanol (10 mM), glycerol (20 % w/v), Tris base (0.2 M) and bromophenol blue (0.05 %, w/v) was dissolved in deionised H<sub>2</sub>O and the pH adjusted to 6.8. The solution was diluted to 1 × with protein sample when used.

**SDS-PAGE running buffer (10 ×):** Tris base (250 mM), glycine (2 M) and SDS (1 % w/v) were dissolved in deionised H<sub>2</sub>O and the pH adjusted to 8.0. The solution was diluted to 1 × with protein sample when used.

**Chemically competent cell preparation buffer I (CCCI):** Potassium acetate (30 mM) and CaCl<sub>2</sub> (80 mM) were dissolved in deionised H<sub>2</sub>O and the pH adjusted to 5.8 before sterilization.

**Chemically competent cell preparation buffer II (CCCI):** Potassium acetate (30 mM), CaCl<sub>2</sub> (80 mM) and glycerol (15 % w/v) were dissolved in deionised H<sub>2</sub>O and the pH adjusted to 5.8 before sterilization.

## 6.2.4 Kits

GeneJET Gel Extraction Kit, GeneJET PCR Purification kit, MagJET Genomic DNA Kit, GeneJET Plasmid Miniprep Kit and Champion™ pET151 Directional TOPO® Expression Kit were all purchased from Thermo Fisher Scientific (UK). Restriction enzymes, corresponding buffers and OneTaq Hot Start quick-load polymerase master mix were also purchased from the same supplier. T4 DNA ligase, Q5® Site-Directed Mutagenesis Kit and Q5® Hot Start High-Fidelity Master Mix were obtained from New England Biolabs (USA).

## 6.2.5 Antibiotics

**Table 6.1:** Antibiotics used within this project.

Antibiotic	Working conc.	Solvent	Supplier	Strain to be applied
Ampicillin	100 µg/mL	H <sub>2</sub> O	Melford (UK)	<i>E.coli</i> carrying recombinant pET151
Kanamycin	50 µg/mL	H <sub>2</sub> O	Melford (UK)	<i>E.coli</i> carrying recombinant pET28a(+)
Trimethoprim	50 µg/mL	DMSO	Sigma Aldrich (UK)	<i>E.coli</i> carrying recombinant pGPI-SceI
	150 µg/mL	DMSO	Sigma Aldrich (UK)	<i>Burkholderia</i> carrying recombinant pGPI-SceI
Tetracycline	20 µg/mL	70 % EtOH	Sigma Aldrich (UK)	<i>E.coli</i> carrying pDAI-SceI
	200 µg/mL	70 % EtOH	Sigma Aldrich (UK)	<i>Burkholderia</i> carrying pDAI-SceI
Gentamicin	50 µg/mL	H <sub>2</sub> O	Sigma Aldrich (UK)	<i>Burkholderia</i> carrying recombinant pGPI-SceI, <i>Burkholderia</i> carrying pDAI-SceI

## 6.2.6 Bacterial Strains

**Table 6.2:** Bacterial strains used within this project.

Strain	Use	Supplier
<i>Escherichia coli</i>		
<i>E.coli</i> TOP10	Host for general cloning and plasmid storage	Thermo Fisher Scientific (UK)



<i>E. coli</i> BL21 Star™ (DE3)	High level recombinant protein expression	Thermo Fisher Scientific (UK)
<i>E. coli</i> C43(DE3)	High level recombinant protein expression	Challis lab stock
<i>E. coli</i> SY327	Donor strain for conjugation between <i>E. coli</i> and <i>Burkholderia</i>	Challis lab stock
<i>E. coli</i> HB101/ <b><i>Burkholderia</i></b>	Helper strain for conjugation between	Challis lab stock
<i>B. ambifaria</i> BCC0203	Enacyloxin producing strain	Mahenthiralingam/ Challis lab stock
<b><i>Acinetobacter</i></b>		
<i>A. baumannii</i> ATCC17978	Strain used for determining MIC of Enacyloxin derivatives	Mahenthiralingam/ Challis lab stock
<i>A. baumannii</i> DSM25645	Strain used for determining MIC of Enacyloxin derivatives	Mahenthiralingam/ Challis lab stock
<b><i>Vibrio</i></b>		
<i>V. rhizosphaerae</i> DSM18581	Genomic DNA extracted for the cloning of enzymes from the vibroxin cluster	Challis lab stock

### 6.2.7 Vectors

**Table 6.3:** Vectors used within this project

Vector	Use	Resistance	Supplier
pET151- TOPO®	Recombinant protein expression in <i>E. coli</i> ( <i>N</i> -terminal His tag)	Ampicillin	Thermo Fisher Scientific (UK)
pET28a (+)	Recombinant protein expression in <i>E. coli</i> ( <i>N</i> -terminal His tag)	Kanamycin	Novagen
pGPI-SceI	Gene deletion in <i>Burkholderia</i>	Trimethoprim	Mahenthiralingam/ Challis lab stock
pDAI-SceI	Gene deletion in <i>Burkholderia</i>	Tetracycline	Mahenthiralingam/ Challis lab stock

## 6.3 General DNA Manipulation

### 6.3.1 Genomic DNA Isolation

Genomic DNA for PCR was extracted using the MagJET Genomic DNA Kit. The DNA concentration was measured using a NanoDrop™ Lite spectrophotometer.

### 6.3.2 Isolation of Plasmid DNA

Plasmid DNA was isolated from an *E.coli* overnight culture (5 mL) using the GeneJET Plasmid Miniprep kit. The concentration of the purified plasmid DNA was measured using a NanoDrop™ Lite spectrophotometer.

### 6.3.3 Polymerase Chain Reaction (PCR)

Q5® Hot Start High-Fidelity DNA polymerase was used for the amplification of DNA fragments for cloning and OneTaq® Hot Start DNA polymerase was used for colony PCR screening. Typical reaction conditions are shown in table 6.4.

**Table 6.4:** Typical PCR reaction components

Reaction composition for PCR with Q5® Hot Start High-Fidelity DNA polymerase		Reaction composition for PCR with OneTaq® Hot Start DNA polymerase	
Component	Volume / $\mu\text{L}$	Component	Volume / $\mu\text{L}$
Template DNA (purified DNA)	0.5	Template DNA (culture)	1
Q5® Hot Start High-Fidelity	12.5	OneTaq® Hot Start	12.5
Master Mix (2x)		Quick-Load Master Mix (2x)	
Forward primer (10 $\mu\text{M}$ )	1.5	Forward primer (10 $\mu\text{M}$ )	1.5
Reverse primer (10 $\mu\text{M}$ )	1.5	Reverse primer (10 $\mu\text{M}$ )	1.5
DMSO*	0-2	DMSO*	0-2
Nuclease-free water	up to 25	Nuclease-free water	up to 25

\*Increased volumes (between 0-2  $\mu\text{L}$ ) of DMSO were often used depending on GC content

Typical thermocycling conditions for routine PCR reactions are shown in table 6.5.

**Table 6.5:** Typical thermocycling conditions for routine PCR reactions

Step		Temperature / °C	Duration
Initial Denaturation		98	1 min*
Denaturation		98	30 s
Annealing	30 cycles	58-70**	30 s
Extension		72	30 s/kb***
Final Extension		72	10 min
Hold		4	

\*Initial denaturation step was extended to 10 min for colony PCR

\*\*Annealing temperatures were approximately 5 °C below the melting temperature of the primers used

\*\*\*When OneTaq<sup>®</sup> Hot Start DNA polymerase was used the extension time was extended to 1 min/kb

#### 6.3.4 Agarose Gel Electrophoresis

To 1 × TBE buffer solution (100 mL) was added agarose (0.7 g) and the mixture heated until the agarose had fully dissolved. The solution was then allowed to cool to RT before GelRed (0.5 µL) was added. The solution was then poured into the appropriate mould and the appropriate comb was added. Once set, the gel was placed into a gel tank filled with 1 × TBE buffer and the DNA samples were loaded, each containing 1 × DNA loading dye, along with the appropriate DNA size marker (Thermo Scientific GeneRuler 1 kb or FastRuler Middle Range). The gel was then electrophoresed at 120 V for 40-60 min depending on the size of the DNA fragments.

#### 6.3.5 Fragment DNA Purification

Following agarose gel electrophoresis, the DNA fragments were visualised using a UV-transilluminator and the desired fragments were purified using the GeneJET PCR Purification kit. If required, the fragments were excised and purified from the gel using a GeneJET Gel Extraction kit. The concentration of the resulting purified DNA fragment was determined using a NanoDrop<sup>™</sup> Lite spectrophotometer.

## **6.3.6 Restriction Digests and Ligations**

### **6.3.6.1 Restriction digests for analysis of recombinant vectors**

To the recombinant vector (3  $\mu\text{L}$ ) was added the appropriate restriction enzyme(s) (1-3  $\mu\text{L}$ ), the appropriate 10x buffer(s) (2  $\mu\text{L}$ ) and  $\text{H}_2\text{O}$  (up to 20  $\mu\text{L}$ ). The buffer was chosen according to supplier recommendation (single digests) or using the Thermo Scientific DoubleDigest Calculator (double digests). The reactions were then incubated at 37  $^\circ\text{C}$  for 90 min, followed by 65  $^\circ\text{C}$  for 5 min in order to inactivate the enzymes. The resulting fragments were then analyzed by agarose gel electrophoresis.

### **6.3.6.2 Restriction digests and subsequent ligation into pET28a(+)**

To the appropriate purified PCR product (48  $\mu\text{L}$ ) were added the appropriate restriction enzymes (1-3  $\mu\text{L}$ ), the appropriate 10x buffer(s) (6  $\mu\text{L}$ ) and  $\text{H}_2\text{O}$  (up to 60  $\mu\text{L}$ ). The reactions were then incubated at 37  $^\circ\text{C}$  for 90 min, followed by 65  $^\circ\text{C}$  for 5 min in order to inactivate the enzymes. The resulting digested DNA was then purified using the GeneJET PCR Purification kit.

At the same time, to the empty pET28a vector (48  $\mu\text{L}$ ) was added the appropriate restriction enzyme(s) (1-3  $\mu\text{L}$ ), the appropriate 10x buffer(s) (6  $\mu\text{L}$ ) and  $\text{H}_2\text{O}$  (up to 60  $\mu\text{L}$ ). The reaction was then incubated at 37  $^\circ\text{C}$  for 90 min, before the addition of shrimp alkaline phosphatase (rSAP) (2  $\mu\text{L}$ ) and the mixture was incubated at 37  $^\circ\text{C}$  for a further 30 min. The mixture was then heated to 65  $^\circ\text{C}$  for 5 min in order to inactivate the enzymes and the resulting digested DNA was purified using the GeneJET PCR Purification kit.

The purified digested DNA fragment and the digested linearized vector were ligated using T4 DNA ligase. To the linearized vector (50 ng) was added the insert (150 ng) followed by the 10x T4 DNA ligase buffer (4  $\mu\text{L}$ ), T4 DNA ligase (1.5  $\mu\text{L}$ ) and  $\text{H}_2\text{O}$  (up to 20  $\mu\text{L}$ ). The reaction was incubated at 15  $^\circ\text{C}$  overnight before transformation into *E.coli* TOP10 chemically competent cells.

### **6.3.6.3 TOPO<sup>®</sup> Cloning**

TOPO cloning into pET151 was conducted using Champion<sup>™</sup> pET151 Directional TOPO<sup>®</sup> Expression Kit. A four nucleotide CACC- overhang was included at the 5' end of the forward

primer in order to allow directional cloning of the insert into the pET151 vector. Q5<sup>®</sup> Hot Start High-Fidelity DNA polymerase was used to amplify the insert from template DNA.

To the purified fragment DNA (0.5-4  $\mu\text{L}$ , 2 : 1 ratio of insert : vector) was added salt solution (1  $\mu\text{L}$ ), TOPO<sup>®</sup> vector (1  $\mu\text{L}$ ) and H<sub>2</sub>O (to 6  $\mu\text{L}$ ). The reaction was mixed gently and incubated at RT for 1 h before being transformed into *E.coli* TOP10 chemically competent cells.

#### **6.3.6.4 Restriction digests and subsequent ligation into pGPI**

To the appropriate purified PCR products (48  $\mu\text{L}$ ) were added the appropriate restriction enzymes (1-3  $\mu\text{L}$ ), the appropriate 10  $\times$  buffer(s) (6  $\mu\text{L}$ ) and H<sub>2</sub>O (up to 60  $\mu\text{L}$ ). The reactions were then incubated at 37 °C for 90 min, followed by 65 °C for 5 min in order to inactivate the enzymes. The resulting digested DNA was then purified using the GeneJET PCR Purification kit.

At the same time, to the empty pGPI vector (48  $\mu\text{L}$ ) was added the appropriate restriction enzyme(s) (1-3  $\mu\text{L}$ ), the appropriate 10x buffer(s) (6  $\mu\text{L}$ ) and H<sub>2</sub>O (up to 60  $\mu\text{L}$ ). The reaction was then incubated at 37 °C for 90 min, before the addition of shrimp alkaline phosphatase (rSAP) (2  $\mu\text{L}$ ) and the mixture was incubated at 37 °C for a further 30 min. The mixture was then heated to 65 °C for 5 min in order to inactivate the enzymes and the resulting digested DNA was purified using the GeneJET PCR Purification kit.

The purified digested DNA fragments and the digested linearized vector were ligated using T4 DNA ligase. To the linearized vector (50 ng) was added both inserts (2 x 150 ng) followed by the 10  $\times$  T4 DNA ligase buffer (4  $\mu\text{l}$ ), T4 DNA ligase (1.5  $\mu\text{L}$ ) and H<sub>2</sub>O (up to 20  $\mu\text{L}$ ). The reaction was incubated at 15 °C overnight.

The DNA was then purified by the addition of 3 M sodium acetate (2  $\mu\text{L}$ ) followed by 95 % EtOH (50  $\mu\text{L}$ ) and the reaction was left at -20 °C for 5 min. The mixture was then centrifuged (13000 rpm) at 4 °C for 20 min. The supernatant was carefully removed and the pellet washed with 70 % EtOH and dried. The purified DNA was then dissolved in H<sub>2</sub>O (10  $\mu\text{L}$ ) before transformation into *E.coli* SY327 electrocompetent cells.

## **6.3.7 Transformation and Electroporation**

### **6.3.7.1 Preparation of competent cells**

Chemically competent *E.coli* BI21(DE3), C43(DE3) and TOP10 were required during this project. A single colony of the required *E.coli* strain was picked and grown overnight in LB (5 mL) with shaking (180 rpm). From the overnight culture 0.5 mL was taken and diluted with LB (50 mL). The resulting culture was shaken (180 rpm) at 37 °C in a 250 mL flask for around 3.5 h until an OD<sub>600</sub> of 0.4-0.6 was reached. The culture was then cooled on ice and the cells harvested by centrifuging for 10 min at 4000 rpm at 4 °C. The supernatant was discarded and the cell pellet was resuspended in CCCI buffer (30 mL) and kept on ice for 1 h. Cells were then harvested by centrifuging for 10 min at 4000 rpm at 4 °C and the supernatant discarded. The cell pellet was washed with CCCI (30 mL) again and resuspended in CCCII (1.5 mL) before being divided into 50 µl aliquots, flash frozen and stored at -80 °C.

Electrocompetent *E.coli* SY327 cells were also required during this project. Electrocompetent cells were prepared using the same procedure but with the use of sterile 10 % glycerol solution in place of CCC1 and CCC2.

### **6.3.7.2 Transformation of chemically competent *E.coli* cells**

To an aliquot of thawed chemically competent cells (50 µL) was added plasmid DNA (0.5-2 µL) or ligation mixture (2-8 µL) and the components gently mixed. The mixture was left on ice for 30 min before being heat shocked at 42 °C for 60 s and then cooled on ice for 1 min. LB (250 µL) was then added and the mixture was shaken (180 rpm) horizontally at 37 °C for 1 h. Different volumes of the transformation mixture were then spread onto pre-warmed LB agar plates supplemented with the appropriate antibiotic and the plates incubated at 37 °C overnight.

### **6.3.7.3 Transformation of electrocompetent *E.coli* cells**

To an aliquot of thawed electrocompetent cells (50 µL) was added plasmid DNA (0.5-2 µL) or ligation mixture (2-8 µL) and the components gently mixed. The mixture was left on ice for 5 min before being transferred to a pre-cooled 1 mm gap electroporation cuvette (Bio-Rad). The electroporation was conducted with a BioRad Gene Pulser® II (200 Ω, 25 µF, 1.7 kV) in combination with a BioRad Pulse Controller Plus. Immediately after the electroporation LB

(950  $\mu$ L) was then added and the mixture was shaken (180 rpm) horizontally at 37 °C for 1 h. Different volumes of the transformation mixture were then spread onto pre-warmed LB agar plates supplemented with the appropriate antibiotic and the plates incubated at 37 °C overnight.

## 6.4 Genetic Manipulation of *Burkholderia*

### 6.4.1 Gene Deletions in *Burkholderia*

In-frame deletions of genes from *Burkholderia ambifaria* BCC0203 were introduced via a double homologous recombination strategy using the suicide plasmid pGPI and the *SceI* expression plasmid pDAI.<sup>202</sup> Firstly, the sequences of regions (500-1000 bp) flanking the gene targeted for deletion were amplified from *B. ambifaria* BCC0203 genomic DNA using Q5<sup>®</sup> Hot Start High-Fidelity DNA polymerase. Restriction sites were introduced at the 5'-end of the primers to allow for directional cloning of the PCR products into the pGPI vector. Constructs were introduced into *E. coli* SY327 by electroporation and transformants were selected on LB agar plates supplemented with trimethoprim (50  $\mu$ g/mL). Plasmids were purified from trimethoprim-resistant colonies using the GeneJET Plasmid Miniprep kit and correct assembly of the construct was confirmed by Sanger sequencing (GATC Biotech). Validated constructs were introduced into *B. ambifaria* BCC0203 via triparental mating using *E. coli* SY327 (pGPI) and *E. coli* HB101 (pRK2013) as the donor and helper strain, respectively, and transconjugants were selected using trimethoprim (200  $\mu$ g/ml) and gentamicin (50  $\mu$ g/ml). Single *B. ambifaria* mutants were selected and correct integration of the mutagenesis plasmids into the genome was confirmed by colony PCR. Next, the pDAI plasmid was introduced into the *B. ambifaria* single crossover mutants by triparental mating using *E. coli* SY327 (pDAI) and *E. coli* HB101 (pRK2013) as the donor and helper strain, respectively. Transconjugants were selected on LB agar plates containing tetracycline (200  $\mu$ g/ml) and gentamicin (50  $\mu$ g/ml). Single *B. ambifaria* mutants were selected and correct gene deletion was confirmed by colony PCR. The mutant strain was then grown on M9 minimal media in order to remove the pDAI plasmid which was confirmed by the loss of tetracycline resistance. In order to generate multi-gene deletion strains the same procedure was employed using the appropriate mutant strain in place of the wild-type *B. ambifaria* BCC0203 strain. The constructs generated for gene deletions in *Burkholderia* along with the associated primers are shown in table 6.6.

**Table 6.6:** The constructs generated for gene deletions in *Burkholderia* along with associated primers

<b>Construct (use)</b>	<b>Primer</b>
pGPI-Δ5932-5'3' (deletion of PQQ-dependant dehydrogenase (5932))	5'F: GGCTCTAGACGAGGTGATAGGACGAGGCATC 5'R: GTCAAGCTTACGCTGCTCGAACTGCCAATG 3'F: GCCAAGCTTGACGCCGAACAGGGCAAG 3'R: GCCGAATTCGTTGCTGGTGTATCCCGATCGT
pGPI-Δ5928-5'3' (deletion of Flavin-dependant halogenase (5928))	5'F: GACTCTAGAGCGTGCAGTCGGCATCGA 5'R: GTCAAGCTTGGAACCGGCCTGAGAGGAAC 3'F: CAGAAGCTTCCGAGCTTGGGCAACTGC 3'R: TCGGAATTCGGGCGATTGCGGATGAAACC
pGPI-Δ5930-31-5'3' (deletion of carbamoyl transferase (5930) and non-heme iron-dependent halogenase (5931))	5'F: AGCTCTAGACGGATCGGAACACCTACT 5'R: GCGAAGCTTTACGAGGCGGATACGTC 3'F: GGCAAGCTTCCGCGTCATCTTCGTGTAC 3'R: CAGGAATTCGACCCCGCAGCTTCTTCAT
pGPI-Δ5927-32-5'3' (deletion of all five tailoring enzymes: 5927, 5928, 5930, 5931 and 5932)	5'F: GCATCTAGACGAAATCGGCACGGATCT 5'R: GCAAAGCTTATTACCGATTGGGGCACG 3'F: GCCAAGCTTGACGCCGAACAGGGCAAG 3'R: GCCGAATTCGTTGCTGGTGTATCCCGATCGT
pGPI-Δ5912-5'3' (deletion of dehydratase involved in DHCCA biosynthesis (5912))	5'F: CGCTCTAGACGATGCTCGGCCTGCTCATCTGA 5'R: CACAAGCTTGGCGGCGGCAGATCGAGT 3'F: CACAAGCTTGACGGTGCCTCATGACG 3'R: CTCGAATTCTGCTCGGGTGCCTCGATG
pGPI-Δ5913-5'3' (deletion of dehydrogenase involved in DHCCA biosynthesis (5913))	5'F: CGGTCTAGACGAACTCGAATTCATGGC 5'R: AGCAAGCTTGAGCGGCGTAACGAACGA 3'F: GAGAAGCTTTTCGAGCTGTTACCG 3'R: AGAGAATTCCAAGGCCTTCAAGGACG
pGPI-Δ5914-5'3' (deletion of enoyl reductase involved in DHCCA biosynthesis (5914))	5'F: CGCTCTAGACTACTCGAACTCGGGGCAAC 5'R: CTGAAGCTTGATCCGGCCGTTTCATCTCG 3'F: GATAAGCTTGCGACGGTGTGAGTATGGCT 3'R: CATGAATTCGCTGCAGACCTCGCTCTTC
pGPI-Δ5916-5'3' (deletion of CoA transferase involved in DHCCA biosynthesis (5916))	5'F: CACTCTAGACGGCCGTCCTTTCATGGA 5'R: CACAAGCTTGCCAGCACAATCGCGAGA 3'F: CCGAAGCTTGGCTTGACATGTCGATCTCCA 3'R: CACGAATTCGAGAACCTCGCGCTGATCTG



pGPI- $\Delta$ 5918-5'3' (deletion of enone reductase involved in DHCCA biosynthesis (5918))	5'F: CGCTCTAGACAGATCAGCGCGAGGTTCTC 5'R: TACAAGCTTGATGCCGACCTGGTGCTG 3'F: CGCAAGCTTCGGGGAGAACAGTGACATGA 3'R: GTGGAATCCCGAGATCGTGGTGCTGT
--	---

## 6.4.2 Agarose Gels Confirming Gene Deletions

Colony PCR was used to confirm the presence of the gene deletions. Shown in figure 6.1 are agarose gels confirming the gene deletions along with the appropriate positive (pGPI construct) and negative (*B. ambifaria* BCC0203 wild-type) controls.

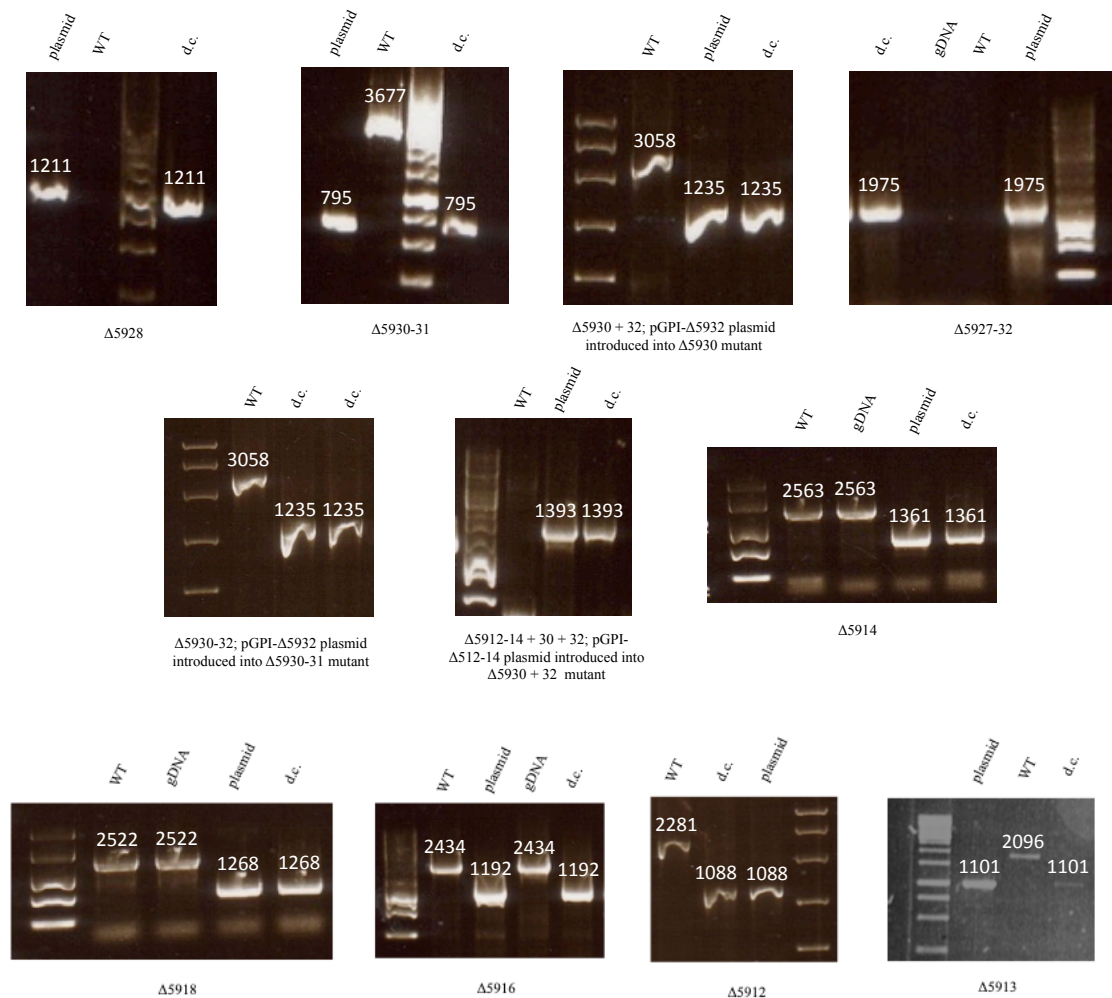


**Figure 6.1** Agarose gels confirming the gene deletions in *B.ambifaria* BCC0203 (d.c. : double crossover, fragment sizes are shown in base pairs)

## 6.5 *Burkholderia* Metabolite Production and Analysis

### 6.5.1 Small-scale Metabolite Production

In order to investigate the effect of the gene deletions on enacyloxin biosynthesis, *B. ambifaria* BCC0203 deletion mutants were grown overnight in LB (5 mL). The cells were harvested and resuspended in NaCl (0.9 %) solution, before being spread on a single plate of solid basal salts medium (BSM, section 6.2.2). Following incubation for 3 days at 30 °C in the dark, the cells were removed, the agar cut into small cubes and extracted with EtOAc (10 mL). The resulting extract was concentrated *in vacuo*, resuspended in MeOH and subjected to UHPLC-ESI-Q-TOF-MS analysis (see section 6.1), UV absorbance was monitored at 360 nm.

### 6.5.2 Production and Purification of Enacyloxin Derivatives

For the production of enacyloxin derivatives, the small-scale culture was scaled up to 750 mL BSM. Following incubation for 3 days, the cells were scraped off and the agar was extracted twice using EtOAc (2 x 500 mL). The combined extracts were concentrated *in vacuo* and the resulting residue was re-dissolved in MeOH for purification by preparative HPLC (see section 6.1). Enacyloxin derivative-containing fractions were pooled, concentrated *in vacuo*, and subsequently lyophilized. To avoid photo-induced isomerization of the compounds, exposure to light was minimized throughout the entire purification process.

Bromide derivatives were generated using the same procedure, however the ammonium chloride in the BSM minimal media was replaced with two equivalents of ammonium bromide. For the mutasynthetic production of enacyloxin derivatives, *B. ambifaria* BCC0203 wildtype or the relevant mutant strain was grown on BSM supplemented with 10 mM of the appropriate DHCCA analogue.

### 6.5.3 Characterization of Enacyloxin Analogues

Structure elucidation of the enacyloxin derivatives was achieved using a combination of UHPLC-ESI-Q-TOF-MS and 1- and 2-D NMR experiments. For NMR analysis, purified enacyloxin derivatives were dissolved in CD<sub>3</sub>OD and <sup>1</sup>H, <sup>13</sup>C, COSY, HSQC and HMBC spectra were recorded on a Bruker Avance 500MHz spectrometer equipped with a DCH

cryoprobe at 25 °C. Assignments of enacyloxin analogues produced in section 3.2 are shown below in tables 6.7-6.27.

**15-hydroxy-enacyloxin IIa (43) (CD<sub>3</sub>OD), <sup>1</sup>H 500 MHz, <sup>13</sup>C 125 MHz.**

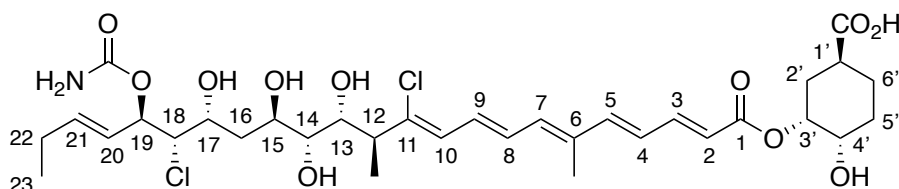


**Table 6.7:** <sup>1</sup>H and <sup>13</sup>C assignments for enacyloxin analogue 43

Position	<sup>1</sup> H (ppm)	<sup>13</sup> C (ppm)
1'-COOH		179.5
1'	2.55 (br. t, <i>J</i> 11.5)	38.8
2'	1.74/2.20-2.14 (br. t, <i>J</i> 8.0/m)	32.4
3'	5.22-5.18 (m)	73.1
4'	3.74-3.70 (m)	70.5
5'	1.85-1.77 (2H) (m)	26.3
6'	1.61-1.52/2.07-2.01 (m/m)	27.6
1		168.5
2	6.02 (d, <i>J</i> 15.0)	121.3
3	7.43 (dd, <i>J</i> 15.0, 11.0)	146.8
4	6.52 (dd, <i>J</i> 15.0, 11.5)	127.8
5	6.76 (d, <i>J</i> 15.0)	146.6
6		137.2
6-Me	1.96 (s)	12.7
7	6.45-6.40 (m)	137.1
8	6.76-6.72 (m)	131.7
9	6.76-6.72 (m)	131.3
10	6.45-6.40 (m)	127.1
11		142.0
12	2.87 (dq, <i>J</i> 9.5, 6.5)	47.4
12-Me	1.13 (d, <i>J</i> 6.5)	16.2
13	3.97-3.93 (m)	72.2
14	3.36 (d, <i>J</i> 8.0)	74.1
15	3.90 (ddd, <i>J</i> 10.1, 8.0, 2.0)	69.6
16	2.20/1.48 (ddd, <i>J</i> 14.5, 10.5, 1.8/ddd, <i>J</i> 14.0, 10.0, 2.0)	40.3
17	4.24 (dt, <i>J</i> 10.0, 2.5)	67.6
18	3.97-93 (m)	72.2
19	5.29 (t, <i>J</i> 7.5)	75.7
19-carbamate		158.7
20	5.57 (ddt, <i>J</i> 15.5, 7.5, 1.5)	126.1
21	5.89 (dt, <i>J</i> 15.5, 6.5)	139.0
22	2.10 (qdd, <i>J</i> 7.5, 6.5, 1.5)	26.3
23	1.01 (t, <i>J</i> 7.5)	13.6

11-deschloro-enacyloxin IIa (152) (CD<sub>3</sub>OD), <sup>1</sup>H 500 MHz, <sup>13</sup>C 125 MHz.

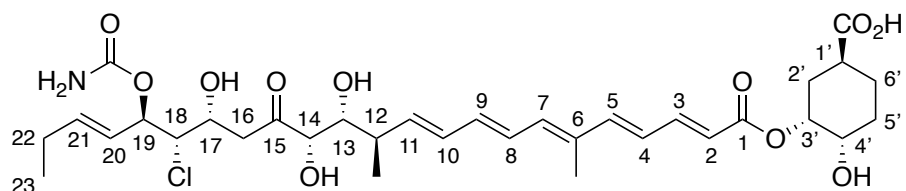


**Table 6.8:** <sup>1</sup>H and <sup>13</sup>C assignments for enacyloxin analogue **152**

Position	<sup>1</sup> H (ppm)	<sup>13</sup> C (ppm)
1'-COOH		179.4
1'	2.54 (br. t, <i>J</i> 11.0)	39.7
2'	1.72/2.19-2.13 (br. t, <i>J</i> 12.0/m)	32.7
3'	5.22-5.18 (m)	73.3
4'	3.75-3.69 (m)	70.7
5'	1.84-1.77 (2H) (m)	29.6
6'	1.60-51/2.05-1.99 (m/m)	27.9
1		168.7
2	5.99 (d, <i>J</i> 15.5)	120.9
3	7.42 (dd, <i>J</i> 15.0, 11.0)	147.0
4	6.48 (dd, <i>J</i> 15.0, 11.0)	128.6
5	6.73 (d, <i>J</i> 15.0)	146.9
6		135.7
6-Me	1.94 (s)	12.6
7	6.35 (d, <i>J</i> 11.0)	137.6
8	6.41 (dd, <i>J</i> 15.0, 10.5)	137.4
9	6.48 (dd, <i>J</i> 15.0, 11.5)	126.4
10	6.29 (dd, <i>J</i> 15.0, 11.0)	132.8
11	5.86 (dd, <i>J</i> 15.0, 8.5)	140.2
12	2.60 (tq, <i>J</i> 8.5, 7.5)	41.4
12-Me	1.10 (d, <i>J</i> 7.0)	17.3
13	3.73 (dd, <i>J</i> 8.5, 2.5)	76.7
14	4.22 (d, <i>J</i> 2.5)	79.4
15		211.7
16	3.02/2.83 (dd, <i>J</i> 17.0, 8.0/dd, <i>J</i> 17.0, 5.0)	44.7
17	4.49 (ddd, <i>J</i> 7.5, 4.5, 2.5)	66.7
18	4.02 (dd, <i>J</i> 8.0, 2.5)	68.0
19	5.26 (t, <i>J</i> 8.0)	75.5
19-carbamate		158.6
20	5.54 (ddt, <i>J</i> 15.5, 7.5, 1.5)	126.1
21	5.89 (dt, <i>J</i> 15.5, 6.5)	139.2
22	2.09 (qdd, <i>J</i> 7.5, 6.5, 1.5)	26.3
23	1.01 (t, <i>J</i> 7.5)	13.6

15-hydroxy-decarbamoyle-encycloxin IIa (45) (CD<sub>3</sub>OD), <sup>1</sup>H 500 MHz, <sup>13</sup>C 125 MHz.

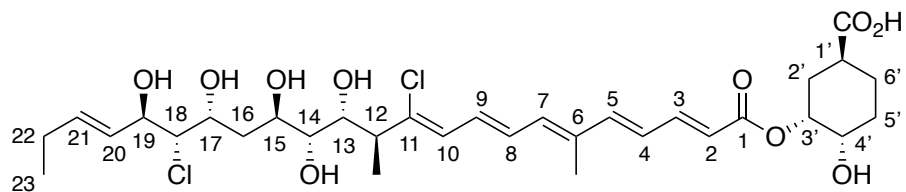


**Table 6.9:** <sup>1</sup>H and <sup>13</sup>C assignments for encyloxin analogue 45

Position	<sup>1</sup> H (ppm)	<sup>13</sup> C (ppm)
1'-COOH		179.1
1'	2.55 (tt, <i>J</i> 11.0, 3.5)	38.6
2'	1.74/2.19-2.14 (ddd, <i>J</i> 14.0, 11.5, 2.0/m)	32.3
3'	5.22-5.18 (m)	73.1
4'	3.74-3.70 (m)	71.1
5'	1.85-1.77 (2H) (m)	29.4
6'	1.61-52/2.07-2.01 (m/m)	27.5
1		168.5
2	6.02 (d, <i>J</i> 15.0)	121.2
3	7.43 (dd, <i>J</i> 15.0, 11.0)	146.9
4	6.52 (dd, <i>J</i> 15.0, 11.0)	127.4
5	6.76 (d, <i>J</i> 15.0)	147.0
6		137.2
6-Me	1.96 (s)	12.7
7	6.44-6.40 (m)	137.0
8	6.75-6.72 (m)	131.7
9	6.75-6.72 (m)	131.2
10	6.44-6.40 (m)	127.1
11		142.0
12	2.87 (dq, <i>J</i> 9.5, 6.5)	47.5
12-Me	1.13 (d, <i>J</i> 6.5)	16.1
13	3.96 (d, <i>J</i> 9.5)	72.2
14	3.37 (d, <i>J</i> 8.0)	74.1
15	3.91 (ddd, <i>J</i> 10.0, 8.0, 2.0)	69.5
16	2.21/1.47 (ddd, <i>J</i> 14.0, 10.0, 2.0/ddd, <i>J</i> 14.0, 10.0, 2.5)	40.4
17	4.45 (dt, <i>J</i> 10.0, 2.5)	67.7
18	3.75 (dd, <i>J</i> 7.5, 2.0)	70.5
19	4.27 (t, <i>J</i> 7.5)	74.4
20	5.59 (ddt, <i>J</i> 15.5, 7.0, 1.5)	126.5
21	5.82 (dtd, <i>J</i> 15.5, 6.5, 0.5)	136.6
22	2.10 (qdd, <i>J</i> 7.5, 6.5, 1.0)	26.3
23	1.02 (t, <i>J</i> 7.5)	13.8

18-deschloro-decarbamoyle-encyloxin IIa (153) (CD<sub>3</sub>OD), <sup>1</sup>H 500 MHz, <sup>13</sup>C 125 MHz.

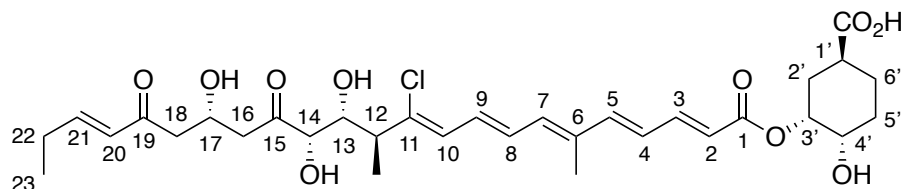


**Table 6.10:** <sup>1</sup>H and <sup>13</sup>C assignments for encyloxin analogue **153**

Position	<sup>1</sup> H (ppm)	<sup>13</sup> C (ppm)
1'-COOH		179.8
1'	2.54 (tt, <i>J</i> 11.5, 3.5)	39.9
2'	1.73/2.20-2.13 (ddd, <i>J</i> 14.0, 11.5, 2.0/m)	32.4
3'	5.22-5.18 (m)	73.2
4'	3.73 (ddd, <i>J</i> 9.5, 5.5, 3.0)	70.6
5'	1.85-1.77 (2H) (m)	29.5
6'	1.56/2.07-2.00 (dtd, <i>J</i> 13.0, 11.0, 6.0/m)	27.7
1		168.5
2	6.02 (d, <i>J</i> 15.0)	121.4
3	7.43 (dd, <i>J</i> 15.0, 11.0)	146.8
4	6.53 (dd, <i>J</i> 15.0, 11.0)	127.2
5	6.79-6.71 (m)	146.6
6		137.4
6-Me	1.96 (s)	12.5
7	6.41 (d, <i>J</i> 10.0)	136.9
8	6.79-6.71 (m)	131.5
9	6.79-6.71 (m)	131.5
10	6.43 (d, <i>J</i> 10.0)	128.4
11		140.7
12	2.94 (dq, <i>J</i> 9.5, 6.5)	47.5
12-Me	1.18 (d, <i>J</i> 7.0)	16.2
13	4.06 (dd, <i>J</i> 9.5, 1.5)	74.1
14	4.23 (d, <i>J</i> 1.5)	78.9
15		212.1
16	2.87/2.76 (dd, <i>J</i> 16.5, 7.5/dd, <i>J</i> 16.5, 5.0)	46.6
17	4.58 (tt, <i>J</i> 7.0, 5.5)	66.5
18	2.79-2.82 (2H) (m)	47.6
19		201.3
20	6.14 (dt, <i>J</i> 16.0, 1.5)	130.8
21	7.01 (dt, <i>J</i> 16.0, 6.5)	151.8
22	2.28 (qdd, <i>J</i> 7.5, 6.5, 1.5)	26.6
23	1.09 (t, <i>J</i> 7.5)	12.6

15-hydroxy-18-deschloro-decarbamoyl-enacyloxin IIa (**154**) (CD<sub>3</sub>OD), <sup>1</sup>H 500 MHz, <sup>13</sup>C 125 MHz.

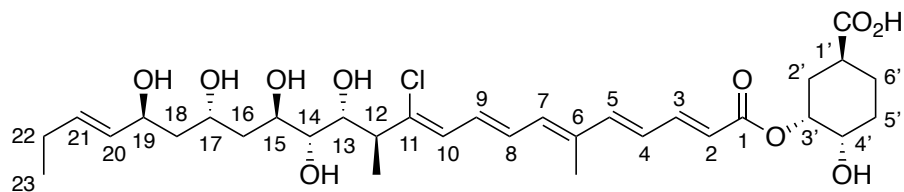


**Table 6.11:** <sup>1</sup>H and <sup>13</sup>C assignments for enacyloxin analogue **154**

Position	<sup>1</sup> H (ppm)	<sup>13</sup> C (ppm)
1'-COOH		179.3
1'	2.58-2.51 (m)	38.7
2'	1.74/2.19-2.14 (ddd, <i>J</i> 14.5, 12.0, 2.5/m)	32.3
3'	5.20 (dt, <i>J</i> 4.5, 2.5)	73.1
4'	3.73 (ddd, <i>J</i> 9.5, 5.5, 3.0)	70.5
5'	1.84-1.78 (2H) (m)	29.4
6'	1.59-52/2.08-2.01 (m/m)	27.5
1		168.6
2	6.02 (d, <i>J</i> 15.0)	121.2
3	7.43 (dd, <i>J</i> 15.0, 11.0)	146.7
4	6.53 (dd, <i>J</i> 15.0, 11.0)	127.8
5	6.76 (d, <i>J</i> 15.0)	146.9
6		137.2
6-Me	1.96 (s)	12.6
7	6.44-6.40 (m)	137.1
8	6.75-6.72 (m)	131.7
9	6.75-6.72 (m)	131.2
10	6.44-6.40 (m)	127.1
11		142.0
12	2.87 (dq, <i>J</i> 9.5, 6.5)	47.4
12-Me	1.12 (d, <i>J</i> 6.5)	16.2
13	3.96 (d, <i>J</i> 10.0)	72.2
14	3.37 (d, <i>J</i> 8.0)	74.1
15	3.92 (ddd, <i>J</i> 10.5, 8.0, 2.5)	69.8
16	2.90/1.52 (ddd, <i>J</i> 14.5, 10.0, 2.5/ddd, 14.5, 10.0, 3.0)	42.6
17	4.15-4.09 (m)	66.3
18	1.62 (dd, <i>J</i> 7.5, 6.5)	46.5
19	4.28 (q, <i>J</i> 6.5)	70.3
20	5.49 (ddt, <i>J</i> 15.5, 6.5, 1.5)	133.5
21	5.71 (dtd, <i>J</i> 15.5, 6.5, 1.0)	133.4
22	2.08-2.01 (m)	26.3
23	1.00 (t, <i>J</i> 7.5)	13.9

11-deschloro-14-deshydroxy-15-hydroxy-18-deschloro-decarbamoylenacyloxin IIa (155)

(CD<sub>3</sub>OD), <sup>1</sup>H 500 MHz, <sup>13</sup>C 125 MHz.

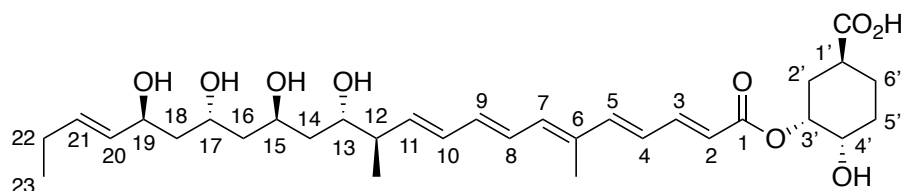


Table 6.12: <sup>1</sup>H and <sup>13</sup>C assignments for enacyloxin analogue 155

Position	<sup>1</sup> H (ppm)	<sup>13</sup> C (ppm)
1'-COOH		179.6
1'	2.52 (tt, <i>J</i> 11.5, 3.5)	39.4
2'	1.73/2.19-2.13 (ddd, <i>J</i> 14.0, 12.0, 2.0/m)	32.7
3'	5.20 (dt, <i>J</i> 4.5, 2.5)	73.2
4'	3.72 (ddd, <i>J</i> 9.5, 6.0, 3.0)	70.7
5'	1.84-1.77 (2H) (m)	29.5
6'	1.59-51/2.08-1.96 (m/m)	27.9
1		168.7
2	6.00 (d, <i>J</i> 15.0)	120.8
3	7.42 (dd, <i>J</i> 15.0, 11.0)	146.9
4	6.48 (dd, <i>J</i> 15.0, 11.0)	126.4
5	6.73 (d, <i>J</i> 15.0)	147.0
6		135.6
6-Me	1.94 (s)	12.5
7	6.34 (d, <i>J</i> 11.5)	137.4
8	6.57 (dd, <i>J</i> 14.5, 11.5)	128.5
9	6.40 (dd, <i>J</i> 14.5, 10.5)	137.6
10	6.25 (dd, <i>J</i> 15.0, 10.5)	132.6
11	5.83 (dd, <i>J</i> 15.0, 8.5)	139.7
12	2.34-2.27 (m)	45.0
12-Me	1.08 (d, <i>J</i> 7.0)	16.9
13	3.79 (dt, <i>J</i> 9.0, 4.0)	72.7
14	1.48 (td, <i>J</i> 8.5, 3.5)	43.4
15	4.09-4.03 (m)	66.4
16	1.53 (dd, <i>J</i> 6.0, 4.0)	46.6
17	4.09-4.03 (m)	66.3
18	1.57 (t, <i>J</i> 6.5)	46.3
19	4.25 (q, <i>J</i> 6.5)	70.3
20	5.48 (ddt, <i>J</i> 15.5, 6.5, 1.5)	133.3
21	5.69 (dtd, <i>J</i> 15.5, 6.5, 0.5)	133.6
22	2.08-2.01 (m)	26.2
23	1.00 (t, <i>J</i> 7.5)	14.0



3'-*epi*-enacyloxin IIa (166) (CD<sub>3</sub>OD), <sup>1</sup>H 500 MHz, <sup>13</sup>C 125 MHz.

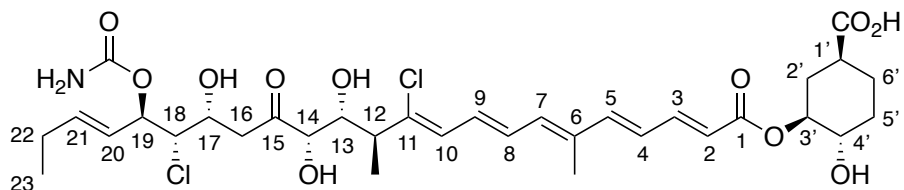
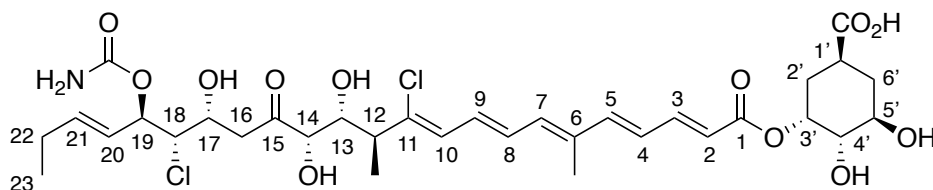


Table 6.13: <sup>1</sup>H and <sup>13</sup>C assignments for enacyloxin analogue 166

Position	<sup>1</sup> H (ppm)	<sup>13</sup> C (ppm)
1'-COOH		179.4
1'	2.45 (br. t, <i>J</i> 11.5)	42.5
2'	1.54-1.42 (2H) (m)	33.8
3'	4.68 (ddd, <i>J</i> 11.0, 9.0, 4.5)	74.1
4'	3.58 (td, <i>J</i> 10.0, 4.5)	72.5
5'	2.28-2.22/1.54-1.42 (m/m)	33.1
6'	2.02-1.98/1.54-1.42 (m/m)	28.1
1		168.6
2	5.98 (d, <i>J</i> 15.5)	121.3
3	7.41 (dd, <i>J</i> 15.0, 11.0)	146.6
4	6.52 (dd, <i>J</i> 15.0, 11.5)	128.4
5	6.78-6.70 (1H) (m)	146.8
6		137.4
6-Me	1.95 (s)	12.6
7	6.45-6.39 (1H) (m)	136.9
8	6.78-6.70 (1H) (m)	131.6
9	6.78-6.70 (1H) (m)	131.5
10	6.45-6.39 (1H) (m)	127.2
11		140.7
12	2.94 (dq, <i>J</i> 9.5, 7.0)	47.6
12-Me	1.19 (d, <i>J</i> 6.5)	16.2
13	4.06-4.02 (1H) (m)	77.7
14	4.23 (d, <i>J</i> 1.5)	78.9
15		211.4
16	3.04/2.83 (dd, <i>J</i> 17.0, 8.0/dd, <i>J</i> 17.0, 5.0)	44.5
17	4.51 (ddd, <i>J</i> 7.5, 4.5, 2.5)	66.8
18	4.06-4.02 (1H) (m)	67.9
19	5.27 (t, <i>J</i> 8.0)	75.5
19-carbamate		158.6
20	5.55 (ddt, <i>J</i> 15.5, 7.5, 1.5)	126.2
21	5.89 (dt, <i>J</i> 15.5, 6.5)	139.2
22	2.13-2.06 (m)	26.3
23	1.01 (t, <i>J</i> 7.5)	13.6

5'-hydroxy-enacyloxin IIa (167) (CD<sub>3</sub>OD), <sup>1</sup>H 500 MHz, <sup>13</sup>C 125 MHz.



**Table 6.14:** <sup>1</sup>H and <sup>13</sup>C assignments for enacyloxin analogue **167**

Position	<sup>1</sup> H (ppm)	<sup>13</sup> C (ppm)
1'-COOH		178.5
1'	2.68-2.64 (m)	38.8
2'	1.72-1.67/2.11-2.06 (m/m)	32.9
3'	5.30 (q, <i>J</i> 3.0)	73.7
4'	3.45 (dd, <i>J</i> 9.5, 3.0)	74.4
5'	3.82 (ddd, <i>J</i> 11.5, 9.5, 5.0)	69.9
6'	1.51-1.46/2.25-2.21 (m/m)	35.7
1		168.4
2	6.00 (d, <i>J</i> 15.0)	121.2
3	7.40 (dd, <i>J</i> 15.0, 11.0)	147.0
4	6.52 (dd, <i>J</i> 15.0, 11.0)	127.4
5	6.74 (d, <i>J</i> 15.0)	146.6
6		137.5
6-Me	1.95 (br, s)	12.6
7	6.41 (br. d, <i>J</i> 10.0)	137.5
8	6.75 (dd, <i>J</i> 15.0, 10.0)	132.2
9	6.72 (dd, <i>J</i> 15.0, 10.0)	131.5
10	6.43 (d, <i>J</i> 10.0)	128.4
11		140.7
12	2.93 (dq, <i>J</i> 9.5, 6.5)	47.6
12-Me	1.19 (d, <i>J</i> 6.5)	16.3
13	4.04 (br. d, <i>J</i> 9.5)	74.2
14	4.22 (d, <i>J</i> 1.5)	79.0
15		211.5
16	2.82/3.03 (dd, <i>J</i> 17.0, 4.5/dd, <i>J</i> 17.0, 8.0)	44.6
17	4.52-4.47 (m)	66.8
18	4.07-4.00 (m)	68.0
19	5.26 (dd, <i>J</i> 8.0, 7.5)	75.9
19-carbamate		158.7
20	5.54 (ddt, <i>J</i> 15.5, 7.5, 1.5)	126.2
21	5.88 (dt, <i>J</i> 15.0, 6.5)	139.2
22	2.09 (qdd, <i>J</i> 8.0, 6.5, 1.5)	26.4
23	1.01 (t, <i>J</i> 7.5)	13.7

cyclopentyl-enacyloxin IIa (177) (CD<sub>3</sub>OD), <sup>1</sup>H 500 MHz, <sup>13</sup>C 125 MHz.

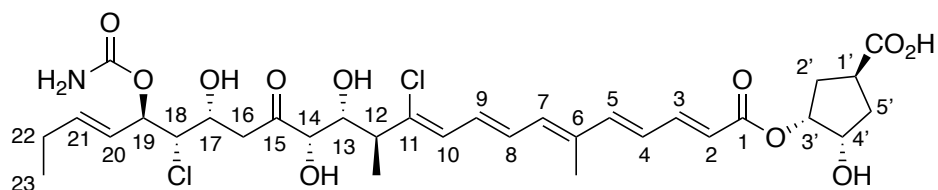


**Table 6.15:** <sup>1</sup>H and <sup>13</sup>C assignments for enacyloxin analogue 177

Position	<sup>1</sup> H (ppm)	<sup>13</sup> C (ppm)
1'-COOH		180.8
1'	2.25 (dt, <i>J</i> 13.0, 6.0)	40.2
2'	2.14-2.01 (2H) (m)	35.8
3'	5.13-5.08 (m)	74.1
4'	4.30 (q, <i>J</i> 5.0)	73.2
5'	2.14-2.01 (m/m)	33.0
1		168.5
2	6.00 (d, <i>J</i> 15.0)	121.1
3	7.43 (dd, <i>J</i> 15.0, 11.0)	146.6
4	6.52 (dd, <i>J</i> 15.0, 11.5)	128.4
5	6.79-6.70 (1H) (m)	146.9
6		137.4
6-Me	1.95 (s)	12.6
7	6.45-6.39 (1H) (m)	137.0
8	6.79-6.70 (1H) (m)	131.6
9	6.79-6.70 (1H) (m)	131.6
10	6.45-6.39 (1H) (m)	127.2
11		140.7
12	2.94 (dq, <i>J</i> 9.5, 7.0)	47.5
12-Me	1.19 (d, <i>J</i> 6.5)	16.2
13	4.06-4.02 (1H) (m)	77.4
14	4.24 (d, <i>J</i> 1.5)	78.9
15		211.5
16	3.05/2.83 (dd, <i>J</i> 17.0, 8.0/dd, <i>J</i> 17.0, 4.5)	44.5
17	4.51 (ddd, <i>J</i> 7.5, 4.5, 2.5)	66.8
18	4.07-4.03 (1H) (m)	67.9
19	5.27 (t, <i>J</i> 7.5)	75.5
19-carbamate		158.6
20	5.55 (ddt, <i>J</i> 15.5, 7.5, 1.5)	126.2
21	5.89 (dt, <i>J</i> 15.0, 6.5)	139.2
22	2.14-2.05 (m)	26.3
23	1.01 (t, <i>J</i> 7.5)	13.6

Identical spectra was obtained for epi-cyclopentyl-enacyloxin IIa (178).

1',6'-dehydro-enacyloxin IIa (187) (CD<sub>3</sub>OD), <sup>1</sup>H 500 MHz, <sup>13</sup>C 125 MHz.

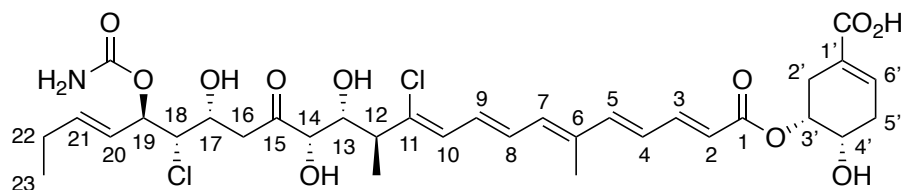
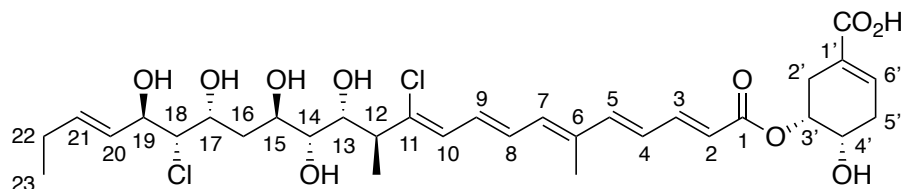


Table 6.16: <sup>1</sup>H and <sup>13</sup>C assignments for enacyloxin analogue 187

Position	<sup>1</sup> H (ppm)	<sup>13</sup> C (ppm)
1'-COOH		171.2
1'		130.1
2'	2.74-2.55 (2H) (m)	32.6
3'	5.15-5.09 (m)	72.8
4'	4.08-4.02 (m)	66.9
5'	2.74-2.55 (2H) (m)	28.6
6'	6.88 (br. s)	136.9
1		168.5
2	5.99 (d, <i>J</i> 16.0)	121.0
3	7.42 (dd, <i>J</i> 15.0, 11.0)	146.6
4	6.51 (dd, <i>J</i> 15.0, 11.5)	128.3
5	6.77-6.67 (1H) (m)	146.9
6		137.3
6-Me	1.95 (s)	12.6
7	6.45-6.48 (1H) (m)	136.9
8	6.77-6.67 (1H) (m)	131.5
9	6.77-6.67 (1H) (m)	131.5
10	6.45-6.48 (1H) (m)	127.0
11		140.6
12	2.93 (dq, <i>J</i> 9.5, 6.5)	47.4
12-Me	1.18 (d, <i>J</i> 6.0)	16.2
13	4.08-4.02 (m)	74.0
14	4.23 (br. s)	78.8
15		211.4
16	3.04/2.83 (dd, <i>J</i> 17.0, 8.0, 2.1/dd, <i>J</i> 17.5, 4.5)	44.4
17	4.53-4.48 (m)	66.7
18	4.05 (dd, <i>J</i> 4.5, 1.5)	67.8
19	5.27 (t, <i>J</i> 7.5)	75.4
20	5.55 (dd, <i>J</i> 15.5, 7.5)	126.0
21	5.89 (dt, <i>J</i> 15.0, 6.5)	139.1
22	2.09 (dt, <i>J</i> 14.0, 7.0)	26.2
23	1.02 (t, <i>J</i> 7.5)	13.5

**1',6'-dehydro-15-hydroxy-decarbamoylenacyloxin IIa (204) (CD<sub>3</sub>OD), <sup>1</sup>H 500 MHz, <sup>13</sup>C 125 MHz.**



**Table 6.17:** <sup>1</sup>H and <sup>13</sup>C assignments for enacyloxin analogue **204**

Position	<sup>1</sup> H (ppm)	<sup>13</sup> C (ppm)
1'-COOH		170.4
1'		129.1
2'	2.65-2.53 (2H) (m)	32.6
3'	5.14-5.10 (m)	72.9
4'	4.07-4.03 (m)	66.9
5'	2.49-2.42 (1H) (m), 2.65-2.53 (1H) (m)	28.6
6'	6.88 (br. s)	137.1
1		168.6
2	5.98 (d, <i>J</i> 15.0)	121.1
3	7.42 (dd, <i>J</i> 15.0, 11.0)	146.7
4	6.51 (dd, <i>J</i> 15.5, 11.5)	127.8
5	6.77-6.71 (1H) (m)	147.0
6		137.2
6-Me	1.95 (s)	12.6
7	6.45-6.40 (1H) (m)	137.1
8	6.77-6.71 (1H) (m)	131.8
9	6.77-6.71 (1H) (m)	131.2
10	6.45-6.40 (1H) (m)	127.1
11		142.1
12	2.87 (dq, <i>J</i> 9.5, 6.5)	47.5
12-Me	1.12 (d, <i>J</i> 6.5)	16.1
13	3.96 (dd, <i>J</i> 9.5, 0.5)	72.2
14	3.36 (dd, <i>J</i> 8.0, 0.5)	74.1
15	3.90 (ddd, <i>J</i> 10.0, 8.0, 2.0)	69.5
16	2.21/1.46 (ddd, <i>J</i> 14.0, 10.0, 2.1/ddd, <i>J</i> 14.0, 10.0, 2.5)	40.4
17	4.44 (dt, <i>J</i> 10.0, 2.5)	67.7
18	3.74 (dd, <i>J</i> 7.5, 2.0)	70.1
19	4.27 (t, 7.5)	74.4
20	5.58 (ddt, <i>J</i> 15.5, 7.0, 1.5)	130.1
21	5.81 (dtd, <i>J</i> 15.5, 6.5, 0.5)	136.6
22	2.13-2.06 (m)	26.4
23	1.02 (t, <i>J</i> 7.5)	13.8

11-bromo-18-deschloroenacyloxin IIa (194) (CD<sub>3</sub>OD), <sup>1</sup>H 500 MHz, <sup>13</sup>C 125 MHz.

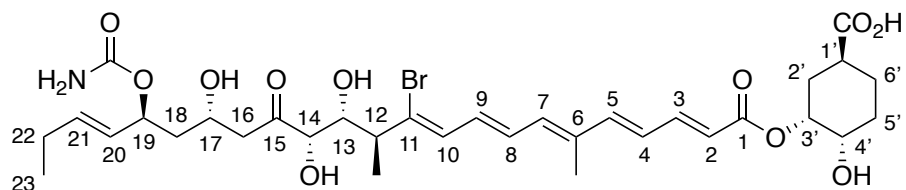


Table 6.18: <sup>1</sup>H and <sup>13</sup>C assignments for enacyloxin analogue 194

Position	<sup>1</sup> H (ppm)	<sup>13</sup> C (ppm)
1'-COOH		179.4
1'	2.58-2.47 (m)	39.1
2'	1.75-1.71/2.19-2.13 (m/m)	32.6
3'	5.22-5.19 (m)	73.3
4'	3.73 (ddd, <i>J</i> 8.5, 6.0, 3.0)	70.7
5'	1.84-1.79 (m)	29.5
6'	1.57-1.50/2.03-2.00 (m/m)	27.8
1		168.6
2	6.03 (d, <i>J</i> 15.5)	121.5
3	7.43 (dd, <i>J</i> 15.0, 11.5)	146.8
4	6.55 (dd, <i>J</i> 15.0, 11.0)	127.4
5	6.76 (d, <i>J</i> 15.0)	146.6
6		137.7
6-Me	1.95 (s)	12.7
7	6.41 (d, <i>J</i> 12.0)	136.8
8	6.82 (dd, <i>J</i> 13.6, 11.0)	132.2
9	6.70-6.63 (m)	133.7
10	6.35 (d, <i>J</i> 11.5)	136.6
11		136.1
12	2.89-2.84 (m)	49.6
12-Me	1.17 (d, <i>J</i> 7.0)	17.3
13	4.05 (dd, <i>J</i> 10.0, 1.5)	74.6
14	4.23 (d, <i>J</i> 1.5)	78.9
15		212.0
16	2.83/2.66 (dd, <i>J</i> 16.5, 8.5/dd, <i>J</i> 16.5, 4.0)	47.2
17	4.20 (tt, <i>J</i> 8.5, 3.5)	65.2
18	1.80/1.65 (ddd, <i>J</i> 14.0, 10.0/ ddd, <i>J</i> 14.0, 9.5, 3.5)	43.8
19	5.23 (ddd, <i>J</i> 10.0, 7.0, 3.5)	73.0
19-carbamate		159.7
20	5.45 (ddt, <i>J</i> 15.5, 7.5, 1.5)	129.3
21	5.78 (dt, <i>J</i> 15.5, 6.5)	135.8
22	2.05 (dq, <i>J</i> 7.5, 1.0)	26.2
23	0.99 (t, <i>J</i> 7.5)	13.7

11-bromo-enacyloxin IIa (195) (CD<sub>3</sub>OD), <sup>1</sup>H 500 MHz, <sup>13</sup>C 125 MHz.

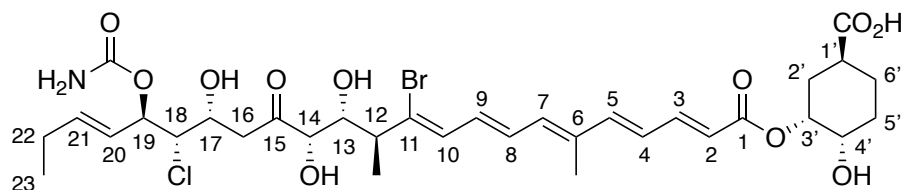


Table 6.19: <sup>1</sup>H and <sup>13</sup>C assignments for enacyloxin analogue 195

Position	<sup>1</sup> H (ppm)	<sup>13</sup> C (ppm)
1'-COOH		179.5
1'	2.58-2.48 (m)	39.0
2'	1.76-1.70/2.19-2.14 (m/m)	32.5
3'	5.23-5.18 (m)	73.2
4'	3.76-3.70 (m)	70.6
5'	1.84-1.79 (m)	29.5
6'	1.62-1.50/2.06-2.01 (m/m)	27.7
1		168.6
2	6.03 (d, <i>J</i> 15.5)	121.4
3	7.43 (dd, <i>J</i> 15.0, 11.0)	146.8
4	6.55 (dd, <i>J</i> 15.0, 11.0)	127.4
5	6.76 (d, <i>J</i> 15.0)	146.6
6		137.7
6-Me	1.96 (s)	12.7
7	6.41 (d, <i>J</i> 11.5)	136.8
8	6.82 (dd, <i>J</i> 13.5, 11.5)	132.3
9	6.70-6.65 (m)	133.7
10	6.34 (d, <i>J</i> 11.5)	136.6
11		136.0
12	2.90-2.84 (m)	47.7
12-Me	1.17 (d, <i>J</i> 6.5)	17.3
13	4.04 (dd, <i>J</i> 8.0, 2.0)	74.7
14	4.24 (d, <i>J</i> 1.5)	78.9
15		211.5
16	2.84/3.04 (dd, <i>J</i> 17.0, 4.0/dd, <i>J</i> 17.0, 8.5)	44.6
17	4.51 (ddd, <i>J</i> 7.0, 4.5, 2.5)	66.8
18	4.07-4.05 (m)	67.9
19	5.27 (t, <i>J</i> 8.0)	75.5
19-carbamate		158.6
20	5.55 (ddt, <i>J</i> 15.0, 7.5, 1.5)	126.2
21	5.90 (dt, <i>J</i> 15.5, 6.5)	139.3
22	2.13-2.06 (m)	26.3
23	1.02 (t, <i>J</i> 7.5)	13.6

11,18-dibromo-enacyloxin IIa (196) (CD<sub>3</sub>OD), <sup>1</sup>H 500 MHz, <sup>13</sup>C 125 MHz.

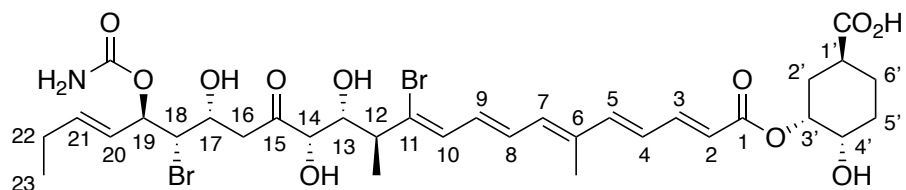
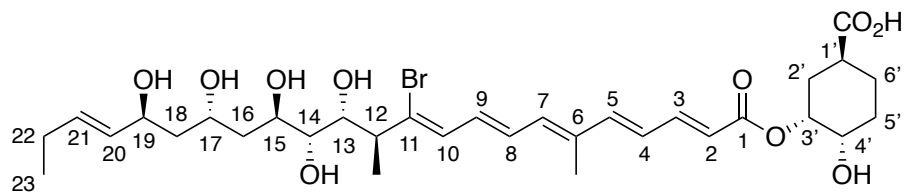


Table 6.20: <sup>1</sup>H and <sup>13</sup>C assignments for enacyloxin analogue 196

Position	<sup>1</sup> H (ppm)	<sup>13</sup> C (ppm)
1'-COOH		179.5
1'	2.58-2.47 (m)	39.0
2'	1.76-1.70/2.19-2.13 (m/m)	32.5
3'	5.23-5.18 (m)	73.2
4'	3.73 (ddd, <i>J</i> 8.5, 6.0, 3.0)	70.6
5'	1.85-1.78 (m)	29.5
6'	1.61-1.51/2.04-2.00 (m/m)	27.7
1		168.5
2	6.03 (d, <i>J</i> 15.0)	121.5
3	7.43 (dd, <i>J</i> 15.0, 11.0)	146.8
4	6.55 (dd, <i>J</i> 15.0, 11.0)	127.4
5	6.76 (d, <i>J</i> 15.0)	146.6
6		137.7
6-Me	1.96 (s)	12.7
7	6.41 (d, <i>J</i> 11.5)	136.8
8	6.82 (dd, <i>J</i> 13.5, 11.5)	132.3
9	6.63 (dd, <i>J</i> 13.5, 11.5)	133.7
10	6.35 (d, <i>J</i> 11.5)	136.6
11		136.0
12	2.90-2.86 (m)	49.6
12-Me	1.17, (d, <i>J</i> 7.0)	17.3
13	4.04 (dd, <i>J</i> 10.0, 1.5)	74.7
14	4.23 (d, <i>J</i> 1.5)	78.9
15		211.4
16	2.84/3.04 (dd, <i>J</i> 14.0, 4.5/dd <i>J</i> 17.0, 8.0)	45.9
17	4.40-4.36 (m)	66.5
18	4.17 (dd, <i>J</i> 8.0, 2.5)	62.7
19	5.31 (t, <i>J</i> 8.0)	75.7
19-carbamate		158.6
20	5.55 (ddt, <i>J</i> 15.5, 7.5, 1.5)	126.9
21	5.89 (dt, <i>J</i> 15.5, 6.5)	139.2
22	2.10 (dq, <i>J</i> 7.5, 1.0)	26.3
23	1.02 (t, <i>J</i> 7.5)	13.6



**11-bromo-15-hydroxy-18-deschloro-decarbamoylenacyloxin IIa (197) (CD<sub>3</sub>OD), <sup>1</sup>H 500 MHz, <sup>13</sup>C 125 MHz.**



**Table 6.21:** <sup>1</sup>H and <sup>13</sup>C assignments for enacyloxin analogue **197**

Position	<sup>1</sup> H (ppm)	<sup>13</sup> C (ppm)
1'-COOH		179.4
1'	2.59-2.48 (m)	38.8
2'	1.76-1.70/2.20-2.13 (m/m)	32.4
3'	5.22-5.18 (m)	73.1
4'	3.75-3.70 (m)	70.5
5'	1.84-1.79 (m)	29.5
6'	1.63-1.57/2.03-2.00 (m/m)	27.6
1		168.5
2	6.03 (d, <i>J</i> 15.0)	121.4
3	7.43 (dd, <i>J</i> 15.0, 11.0)	146.8
4	6.54 (dd, <i>J</i> 15.0, 11.0)	127.2
5	6.76 (d, <i>J</i> 15.0)	146.6
6		137.5
6-Me	1.96 (s)	12.7
7	6.41 (d, <i>J</i> 11.5)	137.0
8	6.81 (dd, <i>J</i> 14.0, 11.5)	131.9
9	6.72-6.63 (m)	133.6
10	6.35 (d, <i>J</i> 11.5)	136.7
11		137.5
12	2.80 (dq, <i>J</i> 10.0, 6.5)	49.6
12-Me	1.11 (d, <i>J</i> 6.5)	17.2
13	3.95 (d, <i>J</i> 9.5)	72.8
14	3.36 (d, <i>J</i> 8.0)	74.0
15	3.93-3.89 (m)	69.9
16	1.52/1.90 (ddd, <i>J</i> 14.0, 10.0, 2.5)/ddd, <i>J</i> 14.0, 10.0, 2.5)	42.7
17	4.12 (tt, <i>J</i> 10.0, 3.0)	66.3
18	1.57-1.66 (m)	46.5
19	4.28 (dt, <i>J</i> 6.5, 6.0)	70.3
20	5.50 (ddt, <i>J</i> 15.5, 7.0, 1.5)	133.4
21	5.71 (dt, <i>J</i> 15.5, 6.5)	134.0
22	2.06 (dq, <i>J</i> 7.5, 1.0)	26.3
23	1.01 (t, <i>J</i> 7.5)	14.0

11-bromo-15-hydroxy-decarbamoylenacyloxin IIa (198) (CD<sub>3</sub>OD), <sup>1</sup>H 500 MHz, <sup>13</sup>C 125 MHz.

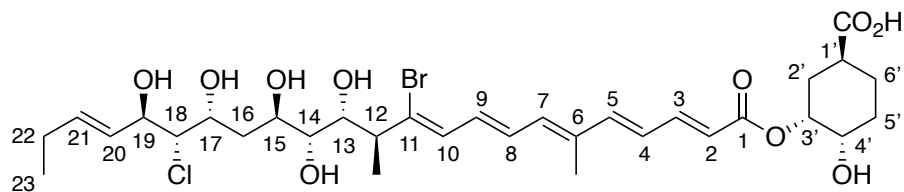
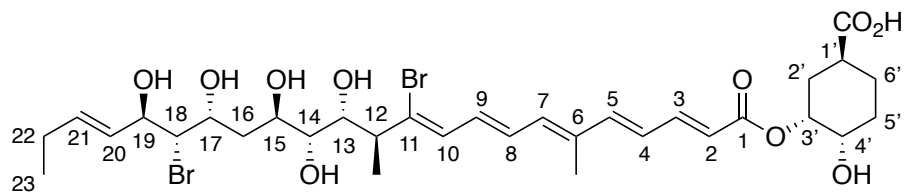


Table 6.22: <sup>1</sup>H and <sup>13</sup>C assignments for enacyloxin analogue 198

Position	<sup>1</sup> H (ppm)	<sup>13</sup> C (ppm)
1'-COOH		179.4
1'	2.59-2.47 (m)	38.9
2'	1.76-1.70/2.19-2.16 (m/m)	32.5
3'	5.22-5.18 (m)	73.2
4'	3.74-3.70 (m)	70.6
5'	1.85-1.79 (m)	29.5
6'	1.61-1.54/2.05-2.01 (m/m)	27.7
1		168.5
2	6.03 (d, <i>J</i> 15.0)	121.4
3	7.43 (dd, <i>J</i> 15.0, 11.0)	146.8
4	6.55 (dd, <i>J</i> 15.0, 11.5)	127.3
5	6.76 (d, <i>J</i> 15.0)	146.6
6		137.5
6-Me	1.96 (s)	12.7
7	6.42 (d, <i>J</i> 11.5)	137.0
8	6.81 (dd, <i>J</i> 14.5, 11.5)	131.9
9	6.73-6.65 (m)	134.0
10	6.35 (d, <i>J</i> 11.5)	136.7
11		137.4
12	2.80 (dq, <i>J</i> 9.5, 6.5)	49.6
12-Me	1.11 (d, <i>J</i> 6.5)	17.2
13	3.95 (d, <i>J</i> 9.5)	72.9
14	3.36 (d, <i>J</i> 8.5)	74.1
15	3.93-3.88 (m)	69.6
16	1.46/2.24-2.20 (ddd, <i>J</i> 14.0, 10.0, 2.5/m)	40.5
17	4.27 (t, <i>J</i> 7.5)	74.4
18	3.74 (dd, <i>J</i> 7.5, 2.5)	71.1
19	4.47-4.43 (m)	67.8
20	5.59 (ddt, <i>J</i> 15.5, 7.0, 1.5)	130.6
21	5.82 (dt, <i>J</i> 15.5, 6.5)	136.6
22	2.10 (dq, <i>J</i> 7.5, 1.5)	26.4
23	1.03 (t, <i>J</i> 7.5)	13.8

**11,18-dibromo-15-hydroxy-decarbamoylenacyloxin IIa (199)** (CD<sub>3</sub>OD), <sup>1</sup>H 500 MHz, <sup>13</sup>C 125 MHz.



**Table 6.23:** <sup>1</sup>H and <sup>13</sup>C assignments for enacyloxin analogue **199**

Position	<sup>1</sup> H (ppm)	<sup>13</sup> C (ppm)
1'-COOH		179.4
1'	2.61-2.48 (m)	38.8
2'	1.76-1.69/2.17-2.14 (m/m)	32.4
3'	5.24-5.18 (m)	73.2
4'	3.73 (ddd, <i>J</i> 8.5, 6.0, 3.0)	70.6
5'	1.85-1.78 (m)	29.5
6'	1.62-1.52/2.06-2.01 (m/m)	27.6
1		168.5
2	6.03 (d, <i>J</i> 15.5)	121.4
3	7.43 (dd, <i>J</i> 15.0, 11.0)	146.8
4	6.55 (dd, <i>J</i> 15.0, 11.0)	127.3
5	6.76 (d, <i>J</i> 15.0)	146.6
6		137.5
6-Me	1.96 (s)	12.7
7	6.42 (d, <i>J</i> 11.5)	137.0
8	6.81 (dd, <i>J</i> 14.5, 11.5)	131.9
9	6.65-6.72 (m)	134.0
10	6.35 (d, <i>J</i> 11.5)	136.7
11		137.3
12	2.80 (dq, <i>J</i> 9.5, 6.5)	49.6
12-Me	1.11 (d, <i>J</i> 6.5)	17.2
13	3.95 (d, <i>J</i> 9.5)	72.9
14	3.36 (d, <i>J</i> 8.0)	74.1
15	3.90-3.88 (m)	69.5
16	1.46/2.21 (ddd, <i>J</i> 14.0, 10.0, 2.5)/ddd, <i>J</i> 14.0, 10.0, 2.5)	41.8
17	4.35-4.29 (m)	67.6
18	3.92 (dd, <i>J</i> 7.5, 2.5)	66.7
19	4.35-4.29 (m)	74.7
20	5.59 (ddt, <i>J</i> 15.5, 7.0, 1.5)	130.7
21	5.81 (dt, <i>J</i> 15.5, 6.5)	136.6
22	2.10 (dq, <i>J</i> 7.5, 1.5)	26.3
23	1.03 (t, <i>J</i> 7.5)	13.8

11-bromo-18-deschloro-decarbamyloxyenacyloxin IIa (**200**) (CD<sub>3</sub>OD), <sup>1</sup>H 500 MHz, <sup>13</sup>C 125 MHz.

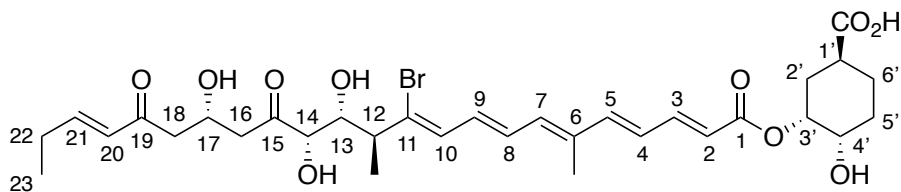


Table 6.24: <sup>1</sup>H and <sup>13</sup>C assignments for enacyloxin analogue **200**

Position	<sup>1</sup> H (ppm)	<sup>13</sup> C (ppm)
1'-COOH		179.4
1'	2.58-2.46 (m)	38.9
2'	1.79-1.69/2.19-2.13 (m/m)	32.8
3'	5.23-5.18 (m)	73.4
4'	3.72 (ddd, <i>J</i> 8.5, 6.0, 3.0)	70.8
5'	1.83-1.78 (m)	29.6
6'	1.63-1.49/2.06-1.99 (m/m)	26.6
1		168.6
2	6.03 (d, <i>J</i> 15.5)	121.5
3	7.43 (dd, <i>J</i> 15.0, 11.0)	146.7
4	6.55 (dd, <i>J</i> 15.0, 11.0)	127.4
5	6.76 (d, <i>J</i> 15.0)	146.5
6		137.7
6-Me	1.96 (s)	12.6
7	6.41 (d, <i>J</i> 11.5)	136.8
8	6.82 (dd, <i>J</i> 14.0, 11.5)	132.2
9	6.65-6.62 (m)	133.7
10	6.35 (d, <i>J</i> 11.5)	136.6
11		136.0
12	2.81-2.79 (m)	46.6
12-Me	1.17 (d, <i>J</i> 6.5)	17.3
13	4.05 (dd, <i>J</i> 10.0, 2.0)	74.7
14	4.23 (d, <i>J</i> 1.5)	78.9
15		212.1
16	2.87 (dd, <i>J</i> 16.5, 7.0)	47.6
17	2.82-2.79 (m)	47.5
18	4.61-4.55 (m)	65.5
19		201.3
20	6.14 (dt, <i>J</i> 16.0, 1.5)	130.8
21	7.01 (dt, <i>J</i> 16.0, 6.5)	151.8
22	2.28 (dq, <i>J</i> 7.5, 1.5)	26.6
23	1.10 (t, <i>J</i> 7.5)	12.7

11,18-dibromo-decarbamoylenacyloxin IIa (201) (CD<sub>3</sub>OD), <sup>1</sup>H 500 MHz, <sup>13</sup>C 125 MHz.

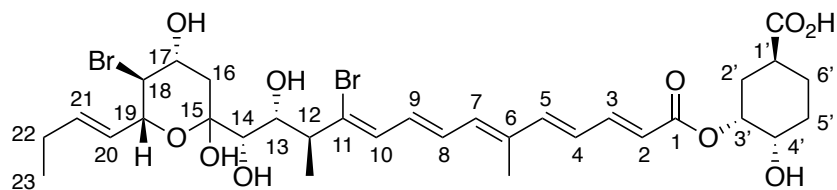
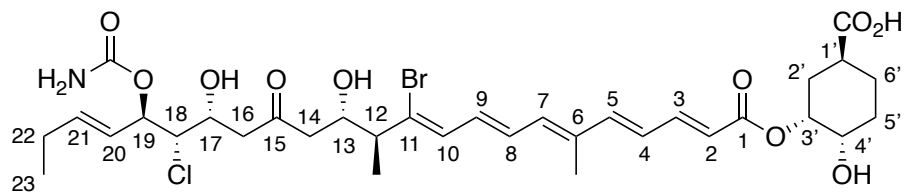


Table 6.25: <sup>1</sup>H and <sup>13</sup>C assignments for enacyloxin analogue 201

Position	<sup>1</sup> H (ppm)	<sup>13</sup> C (ppm)
1'-COOH		179.4
1'	2.58-2.49 (m)	38.9
2'	1.77-1.69/2.20-2.16 (m, m)	32.5
3'	5.22-5.18 (m)	73.2
4'	3.73 (ddd, <i>J</i> 8.5, 6.0, 3.0)	70.6
5'	1.85-1.78 (m)	29.5
6'	1.61-1.52/2.06-2.00 (m/m)	27.7
1		168.5
2	6.03 (d, <i>J</i> 15.0)	121.4
3	7.43 (dd, <i>J</i> 15.0, 11.0)	146.8
4	6.55 (dd, <i>J</i> 15.0, 11.0)	127.3
5	6.76 (d, <i>J</i> 15.0)	146.6
6		137.6
6-Me	1.95 (s)	12.7
7	6.41 (d, <i>J</i> 11.5)	136.9
8	6.81 (dd, <i>J</i> 14.2, 11.5)	132.1
9	6.71-6.64 (m)	133.8
10	6.35 (d, <i>J</i> 11.5)	136.6
11		137.3
12	2.82 (dq, <i>J</i> 9.5, 6.5)	49.6
12-Me	1.10 (d, <i>J</i> 6.5)	17.1
13	4.16 (d, <i>J</i> 9.5)	73.3
14	3.45 (d, <i>J</i> 1.0)	73.4
15		100.5
16	2.44/1.54 (dd, <i>J</i> 13.0, 5.0, dd, <i>J</i> 13.0, 1.5)	43.0
17	3.49 (t, <i>J</i> 10.0)	61.5
18	4.08-4.01 (m)	70.9
19	4.46 (dd, <i>J</i> 10.0, 7.0)	74.9
20	5.54 (ddt, <i>J</i> 15.5, 7.0, 1.5)	128.0
21	5.83 (dt, <i>J</i> 15.5, 6.5)	137.8
22	2.10 (dq, <i>J</i> 7.5, 1.5)	26.4
23	1.02 (t, <i>J</i> 7.5)	13.8

11-bromo-14-deshydroxydecarbamoylenacyloxin IIa (**202**) (CD<sub>3</sub>OD), <sup>1</sup>H 500 MHz, <sup>13</sup>C 125 MHz.



**Table 6.26:** <sup>1</sup>H and <sup>13</sup>C assignments for enacyloxin analogue **202**

Position	<sup>1</sup> H (ppm)	<sup>13</sup> C (ppm)
1'-COOH		179.4
1'	2.55-2.46 (m)	38.9
2'	1.76-1.69/2.19-2.14 (m/m)	32.6
3'	5.23-5.18 (m)	73.3
4'	3.73 (ddd, <i>J</i> 8.5, 6.0, 3.0)	70.8
5'	1.83-1.79 (m)	29.6
6'	1.64-1.47/2.06-1.99 (m/m)	26.3
1		168.5
2	6.03 (d, <i>J</i> 15.5)	121.5
3	7.43 (dd, <i>J</i> 15.0 11.0)	146.7
4	6.55 (dd, <i>J</i> 15.0, 11.0)	127.4
5	6.76 (d, <i>J</i> 15.0)	146.5
6		137.8
6-Me	1.96 (s)	12.7
7	6.41 (d, <i>J</i> 11.5)	136.8
8	6.83 (dd, <i>J</i> 14.0, 11.5)	132.4
9	6.65-6.60 (m)	133.7
10	6.35 (d, <i>J</i> 11.5)	136.5
11		134.6
12	2.70-2.58 (m)	51.8
12-Me	1.13 (d, <i>J</i> 7.0)	16.5
13	4.24 (td, <i>J</i> 8.0, 3.5)	70.7
14	2.70-2.58 (m)	49.1
15		209.6
16	2.90/2.78 (dd, <i>J</i> 17.0, 8.0/dd, <i>J</i> 17.0, 5.0)	50.5
17	4.48-4.44 (m)	66.6
18	3.99 (dd, <i>J</i> 8.0, 2.5)	67.8
19	5.26 (t, <i>J</i> 8.0)	75.5
19-carbamate		158.6
20	5.54 (ddt, <i>J</i> 15.5, 7.5, 1.5)	126.2
21	5.89 (dt, <i>J</i> 15.5, 6.5)	139.2
22	2.10 (dq, <i>J</i> 7.5, 1.0)	26.3
23	1.01 (t, <i>J</i> 7.5)	13.6

**11,18-dibromo-14-deshydroxydecarbamoylenacyloxin IIa (203)** (CD<sub>3</sub>OD), <sup>1</sup>H 500 MHz,  
<sup>13</sup>C 125 MHz.

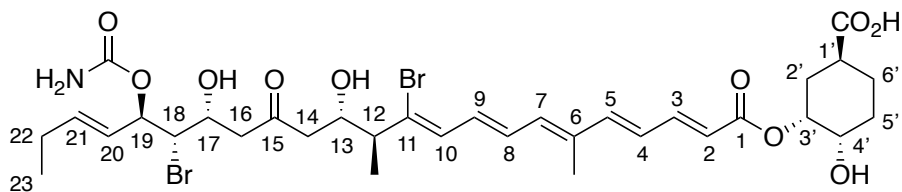


**Table 6.27:** <sup>1</sup>H and <sup>13</sup>C assignments for enacyloxin analogue **203**

Position	<sup>1</sup> H (ppm)	<sup>13</sup> C (ppm)
1'-COOH		179.3
1'	2.58-2.49	38.8
2'	1.77-1.69/2.20-2.13 (m/m)	32.4
3'	5.24-5.17 (m)	73.1
4'	3.73 (ddd, <i>J</i> 8.5, 6.0, 3.0)	70.7
5'	1.85-1.78 (m)	29.5
6'	1.62-1.51/2.07-2.00 (m/m)	27.6
1		168.5
2	6.03 (d, <i>J</i> 15.0)	121.5
3	7.43 (dd, <i>J</i> 15.0, 11.0)	146.9
4	6.55 (dd, <i>J</i> 15.0, 11.0)	127.4
5	6.76 (d, <i>J</i> 15.0)	146.6
6		137.8
6-Me	1.96 (s)	12.7
7	6.41 (d, <i>J</i> 11.5)	136.8
8	6.83 (dd, <i>J</i> 13.5, 11.5)	132.4
9	6.68-6.61 (m)	133.8
10	6.35 (d, <i>J</i> 11.5)	136.5
11		134.7
12	2.71-2.58 (m)	51.8
12-Me	1.13 (d, <i>J</i> 7.0)	16.5
13	4.24 (td, <i>J</i> 8.0, 3.5)	70.5
14	2.71-2.58 (m)	49.0
15		209.5
16	2.90/2.78 (dd, <i>J</i> 17.0, 8.0/dd, <i>J</i> 17.0, 4.5)	50.4
17	4.31-4.35 (m)	66.3
18	4.12 (dd, <i>J</i> 8.0, 2.5)	62.6
19	5.30 (t, <i>J</i> 8.0)	75.7
19-carbamate		158.6
20	5.54 (ddt, <i>J</i> 15.5, 7.5, 1.5)	126.9
21	5.89 (dt, <i>J</i> 15.5, 6.5)	139.2
22	2.10 (dq, <i>J</i> 7.5, 1.0)	26.3
23	1.01 (t, <i>J</i> 7.5)	13.6

#### 6.5.4 Minimum Inhibitory Concentration (MIC) Assays

MIC values were determined using the broth microdilution method according to the official CLSI guidelines. Briefly, *Acinetobacter baumannii* test strains (ATCC17978 and DSM25645) were grown overnight in MH broth at 37 °C. In a 96-well microtiter plate, 50 µL of serial twofold dilutions of an enacyloxin derivative in MH broth were mixed with 50 µL of bacterial suspension, diluted to a concentration of 10<sup>6</sup> cell-forming units (CFU)/ml in MH broth. The desired inoculum density was achieved using a 0.5 McFarland turbidity standard. Following incubation for 18 h at 37°C, MICs were defined as the lowest concentrations that visibly inhibited bacterial growth. All MIC determinations were performed in triplicate.

### 6.6 Recombinant Protein Overproduction and Purification

#### 6.6.1 Recombinant Protein Expression Constructs

The constructs used for recombinant protein overproduction in *E.coli* are shown in tables 6.28 and 6.29 along with the primers used for cloning and the cell line employed for overproduction. All DNA inserts were either amplified from the genomic DNA of *Burkholderia ambifaria* BCC0203, *Burkholderia gladioli* BCC0238 or *Vibrio rhizosphaerae*. Correct assembly of each construct was confirmed by Sanger sequencing (GATC Biotech). Constructs GbnD5-DH-ACP and GbnD5-ACP were generated by Dr. Matt Jenner.

**Table 6.28:** The primers used to generate constructs (Dr. Matt Jenner) for recombinant protein overproduction in *E.coli* in order to investigate the functionality of the diene synthase and VbxP (Sections 2.1.4/4.2.2.1).

Construct	Cell Line	Primer
GbnD5-DH-ACP	BL21(DE3)	F: CACCATGACTCATCGCCATGCA
		R: TCATGCAGCCACCGATTTCGCT
GbnD5-ACP	BL21(DE3)	F: CACCGTGGCGGCCGGGTACGA
		R: TCATGCAGCCACCGATTTCGCT



**Table 6.29:** The primers used to generate constructs for recombinant protein overproduction in *E.coli* in order to investigate DHCCA biosynthesis (Section 4.2).

Construct	Cell Line	Primer
pET-151-5914	BL21(DE3)	F: CACCATGAAAGCCATACTCAGCACC
	C43(DE3)	R: CTCAGACCAGCGCCTCGT
pET-151-5916	BL21(DE3)	F: CACCATGTCAAGCCAAGCACAGT
	C43(DE3)	R: CTCACAGGCTTGCCGCTT
pET-151-VbxP	C43(DE3)	F: CACCCTAAAACAACCGCCCCCTCTA
		R: TCAGTTAGTTTCATCTTTAAGGGGGACTTG
pET-151-VbxK	C43(DE3)	F: CACCTCGCTTTTTTCATCATTTGAACTTGG
		R: TCTAAGTGGCAGACGACCAAG
pET-151-VbxN	BL21(DE3)	F: CACCAGAGCTTTACTAAGTAAAACAACGGGA
	C43(DE3)	R: CCTAAAGGGCATCGATTGAGTGTTTTA
pET-151-VbxL	BL21(DE3)	F: CACCAATTTATCAAATATACCGAGTTTGGCA
		R: TTAAAGACATAGACTTTCCTCTACCCGA
pET-151-VbxM	BL21(DE3)	F: CACCTCTTTAAATGATTTGCAAGTTCCTG
		R: GACGCATCAGTTAAGTATTCTATGC
pET-28a-VbxN	BL21(DE3)	F: GAGCATATGAGAGCTTTACTAAGTAAAACAACGG
		R: ATAGTCCACGGCATCGATTGAGTGTTTTAAT

### 6.6.2 Site-Directed Mutagenesis

Site-directed mutagenesis was conducted using the Q5<sup>®</sup> Site-Directed Mutagenesis Kit. Mutant plasmids were first amplified from the wild-type construct using Q5<sup>®</sup> hot start high fidelity polymerase and the resulting linear plasmid was purified using the GeneJET PCR Purification kit. The PCR product (1 µl) was then incubated with the kinase, ligase and DpnI (KLD) mix (1 µL) along with the KLD buffer (5 µL) and H<sub>2</sub>O (3 µL). The reaction was left at RT for 5 min before transformation (*E.coli* TOP10). Mutagenesis constructs, primers used for cloning and the cell line employed for overproduction are shown in table 6.30. The GbnD5-DH-ACP (H158Y) construct was generated by Dr. Matt Jenner.

**Table 6.30:** The constructs generated for site-directed mutagenesis (codon change underlined).

Construct	Cell Line	Primer
pET-151-VbxP (D171S)	BL21(DE3)	F: GCCTGTCGCT <u>TCT</u> ATGTATGCG R: ATTCTCATCAGTGGTGGC
GbnD5-DH-ACP (H158Y)	BL21(DE3)	F: CGGCGTGGT <u>TAT</u> ATGGCCCGTTCATGC R: AGCTCGCGCACGCCGCGA

### 6.6.3 Recombinant Protein Overproduction

Sterile LB supplemented with the appropriate antibiotic (10 mL) was inoculated with single transformants of *E.coli* BL21(DE3) or C43(DE3) and the culture was shaken (180 rpm) at 37 °C overnight. The following day, sterile LB (1 L) was inoculated with the overnight culture (10 mL) and shaken (180 rpm) at 37 °C until OD<sub>600</sub> 0.6-0.8 was reached. The culture was then cooled to 4 °C before the addition of sterile isopropyl-β-thiogalactopyranoside (IPTG) (0.5 mL of 1 M stock) was added (0.5 mM in final culture). The culture was then shaken (180 rpm) at 15 °C overnight in order to induce protein overproduction.

### 6.6.4 Recombinant Protein Purification

Cells were harvested by centrifugation (4000 rpm, 4 °C, 30 min), resuspended in loading buffer (10 mL/L of culture) and kept on ice. Cells were then lysed using a cell disrupter before centrifugation (17000 rpm, 4 °C, 45 min). The supernatant was then passed through a 0.45 μm syringe filter (GE Healthcare) and loaded onto a 1 mL HiTrap™ HP chelating column (GE Healthcare) pre-charged with NiSO<sub>4</sub> solution (100 mM, 5 mL) and equilibrated with loading buffer (5 mL). The loaded column was then washed with loading buffer (15 mL) in order to remove any non-specific binding proteins. The protein was then eluted using elution buffers containing 50 mM (5 mL), 100 mM (5 mL), 200 mM (3 mL) and 300 mM (3 mL) imidazole (see section 6.2.3 for composition of buffers). Fractions containing the overproduced protein (as determined by SDS-PAGE analysis, see section 6.6.5) were collected and concentrated (4000 rpm, 4 °C) using a Viva-spin concentrator (GE Healthcare) with a 10 kDa molecular weight cut-off filter. Once concentrated to 1 mL, the protein was exchanged into storage buffer (2 × 15 mL) and concentrated again before a desired concentration was attained (as determined by nanodrop). Glycerol (25 % of final solution) was then added, the protein was aliquoted, flash frozen in liquid N<sub>2</sub> and stored at -80 °C.

### 6.6.5 SDS-PAGE Gel Electrophoresis

SDS-PAGE gel electrophoresis was used in order to determine the size and the purity of overproduced proteins. 10 % acrylamide SDS-PAGE gels were used in this project (for 20-80 kDa proteins) and were prepared as detailed in table 6.31.

**Table 6.31:** The reagents and volumes used for the preparation of 10 % acrylamide SDS-PAGE gels

Resolving gel		Stacking gel	
Reagent	Volume (mL)	Reagent	Volume (mL)
H <sub>2</sub> O	3.8	H <sub>2</sub> O	1.4
30 % acrylamide mix	3.4	30 % acrylamide mix	0.33
1.5 M Tris-HCl (pH 8.8)	2.5	1.5 M Tris-HCl (pH 6.8)	0.25
10 % SDS	0.1	10 % SDS	0.02
10 % ammonium persulfate	0.1	10 % ammonium persulfate	0.02
TEMED	0.005	TEMED	0.002

Protein samples containing 1 x SDS-PAGE loading dye (10  $\mu$ L) were then loaded along with a protein molecular weight ladder (Thermo Scientific PageRuler) (6  $\mu$ L). The gel was electrophoresed at 200 V for 40-60 min. Gels were then stained with InstantBlue and destained with H<sub>2</sub>O and EtOH in order to visualise the proteins.

### 6.7 *In vitro* Biochemical Assays

All concentrations shown in this section are concentrations in the final reaction volume unless specified otherwise.

#### 6.7.1 Pantetheine Substrate Loading and Dehydration Assay

GbnD5 DH-ACP and GbnD5 DH-ACP(H158Y) didomains were cloned and overproduced by Dr. Matt Jenner. Constructs for the loading enzymes (Sfp, CoaA, CoaD and CoaE) were taken from the lab of Dr. Manuela Tosin.

Typically, loading reactions were carried out using DH-ACP or DH-ACP(H158Y) didomain (200  $\mu$ M) in storage buffer (final volume 50  $\mu$ L). The loading reaction was initiated by addition of Sfp (2  $\mu$ M), CoaA (1  $\mu$ M), CoaD (1  $\mu$ M), CoaE (1  $\mu$ M), MgCl<sub>2</sub> (10 mM), ATP (10 mM) and pantetheine substrate (500  $\mu$ M), and the reaction was incubated at RT for 3 h. The

reaction was diluted to 20  $\mu\text{M}$  with deionised  $\text{H}_2\text{O}$  prior to UHPLC-ESI-Q-TOF-MS analysis (see section 6.1).<sup>135</sup> All assays were conducted in triplicate.

### 6.7.2 Condensation Assay with AHCCA

5915 condensation domain and 5919 PCP domain were cloned and overproduced by Dr. Joleen Masschelein.

*apo*-PCP Domain (Bamb\_5919) (200  $\mu\text{M}$ ) was incubated with  $\text{MgCl}_2$  (12.5 mM), Sfp (10  $\mu\text{M}$ ) and acetyl-CoA (0.5 mM) in storage buffer (final volume 200  $\mu\text{L}$ ) at 30  $^\circ\text{C}$  for 45 min. Excess acetyl-CoA was then removed using Amicon Ultra centrifugal filters with a 5 kDa MWCO membrane (Millipore). Conversion of the protein to the acetylated *holo*-form was verified by UHPLC-ESI-Q-TOF-MS analysis (see Section 6.1). The loaded PCP domain (200  $\mu\text{M}$ ) was then incubated with the Bamb\_5915 condensation domain (20  $\mu\text{M}$ ) and AHCCA 192 (1 mM), in storage buffer (final volume 100  $\mu\text{L}$ ). The condensation domain was omitted from negative control reactions. Following incubation for 1 h at 30  $^\circ\text{C}$ , the reaction was quenched via the addition of MeOH (200  $\mu\text{L}$ ). Precipitates were removed by centrifugation (13000 g, 10 min) and the supernatants were analysed by UHPLC-ESI-Q-TOF-MS (see section 6.1).<sup>93</sup> All assays were conducted in triplicate.

### 6.7.3 CoA Transferase Assay with VbxP

To a solution of carboxylic acid (1 mM or 10 mM) and VbxP or VbxP (D171S) (50  $\mu\text{M}$ ) in storage buffer (final volume 100  $\mu\text{L}$ ) was added acetyl CoA (1 mM) and the reaction incubated at RT for 16 h. Boiled VbxP was used for negative control reactions. The reaction was quenched via the addition of MeOH (200  $\mu\text{L}$ ). Precipitates were removed by centrifugation (13000 g, 10 min) and the supernatants were analysed by UHPLC-ESI-Q-TOF-MS (see section 6.1). All assays were conducted in triplicate.

### 6.7.4 Intact Analysis of VbxP

To a solution of VbxP (50  $\mu\text{M}$ ) in storage buffer (final volume 100  $\mu\text{L}$ ) was added acetyl CoA (1 mM) and the reaction incubated at RT. UHPLC-ESI-QTOF-MS analysis was then conducted at various time points (see section 6.1).

### 6.7.5 ACP Loading using VbxP

To a solution of carboxylic acid (10 mM) and VbxP (50  $\mu$ M) in storage buffer (final volume 100  $\mu$ L) was added acetyl CoA (1 mM) and the reaction incubated at RT overnight. The Acyl CoA generated *in situ* (50  $\mu$ L) was then added to GbnD5 ACP domain (200  $\mu$ M) in storage buffer (50  $\mu$ L) before the addition of Sfp (2  $\mu$ M), the resulting solution was incubated at RT for 1 h before UHPLC-ESI-Q-TOF-MS analysis (see section 6.1).

### 6.7.6 Enoyl Reductase Assays with VbxN

To a solution of shikimic acid (1 mM) and VbxP (50  $\mu$ M) in storage buffer (final volume 85  $\mu$ L) was added acetyl CoA (1 mM) and the reaction incubated at RT for 1 h. VbxN (50  $\mu$ M) and NADPH (1 mM) was then added and the reaction incubated at RT for 16 h. Boiled VbxN was used for negative control reactions. The reaction was quenched via the addition of MeOH (200  $\mu$ L). Precipitates were removed by centrifugation (13000 g, 10 min) and the supernatants were analysed by UHPLC-ESI-Q-TOF-MS (see section 6.1). All assays were conducted in triplicate.

For the attempted enoyl reduction of free carboxylic acids (Section 4.2.2) the reaction was set up as follows: To a solution of carboxylic acid (1 mM) and VbxN (50  $\mu$ M) in storage buffer (final volume 85  $\mu$ L) was added NADPH (1 mM) and the reaction incubated at RT for 16 h. Boiled VbxN was used for negative control reactions. The reaction was quenched via the addition of MeOH (200  $\mu$ L). Precipitates were removed by centrifugation (13000 g, 10 min) and the supernatants were analysed by UHPLC-ESI-Q-TOF-MS (see section 6.1).

### 6.7.7 Dehydrogenation Assays with VbxM

To a solution of alcohol (1 mM) and VbxM (50  $\mu$ M) in storage buffer (final volume 100  $\mu$ L) was added NADP<sup>+</sup> (1 mM) and the reaction incubated at RT for 16 h. Boiled VbxM was used for negative control reactions. The reaction was quenched via the addition of MeOH (200  $\mu$ L) followed by the addition of *O*-((perfluorophenyl)methyl)hydroxylamine **234** (30  $\mu$ L of 100 mg/mL solution) and the solution left at RT for 1 h. Precipitates were removed by centrifugation (13000 g, 10 min) and the supernatants were analysed by UHPLC-ESI-Q-TOF-MS (see section 6.1). All assays were conducted in triplicate.

### 6.7.8 Dehydration Assays with VbxL

To a solution of alcohol (1 mM) in storage buffer (final volume 100  $\mu$ L) was added and VbxL (50  $\mu$ M) and the reaction incubated at RT for 16 h. Boiled VbxL was used for negative control reactions. The reaction was quenched via the addition of MeOH (200  $\mu$ L) and when required was followed by the addition of *O*-((perfluorophenyl)methyl)hydroxylamine **234** (30  $\mu$ L of 100 mg/mL solution) and the solution left at RT for 1 h. Precipitates were removed by centrifugation (13000 g, 10 min) and the supernatants were analysed by UHPLC-ESI-QTOF-MS (see section 6.1). All assays were conducted in triplicate.

### 6.7.9 Enoyl Reduction Assays with VbxK

To a solution of unsaturated ketone (1 mM) and VbxK (50  $\mu$ L) in storage buffer (final volume 100  $\mu$ L) was added and NADPH or NADH (1 mM) and the reaction incubated at RT for 16 h. Boiled VbxK was used for negative control reactions. The reaction was quenched via the addition of MeOH (200  $\mu$ L) and when required was followed by the addition of *O*-((perfluorophenyl)methyl)hydroxylamine **234** (30  $\mu$ L of 100 mg/mL solution) and the solution left at RT for 1 h. Precipitates were removed by centrifugation (13000 g, 10 min) and the supernatants were analysed by UHPLC-ESI-QTOF-MS (see section 6.1). All assays were conducted in triplicate.

For coupled assays, the unsaturated ketone was generated *in situ* using VbxL, the reaction was conducted as follows: To a solution of (1*S*,3*R*,4*S*)-3,4-dihydroxy-5-oxocyclohexane-1-carboxylic acid **228** (1 mM) in storage buffer (final volume 100  $\mu$ L) was added and VbxL (50  $\mu$ M) and the reaction incubated at RT for 1 h. VbxK (50  $\mu$ M) was then added followed by NADPH or NADH (1 mM) and the reaction incubated at RT for 16 h. Boiled VbxK and boiled VbxL were used for separate negative control reactions. The reaction was quenched via the addition of MeOH (200  $\mu$ L) followed by the addition of *O*-((perfluorophenyl)methyl)hydroxylamine (30  $\mu$ L of 100 mg/mL solution) and the solution left at RT for 1 h. Precipitates were removed by centrifugation (13000 g, 10 min) and the supernatants were analysed by UHPLC-ESI-Q-TOF-MS (see section 6.1). The assay was conducted in triplicate.

For the attempted enoyl reduction of free carboxylic acids (Section 4.2.2) the reaction was set up as follows the reaction was set up as follows: To a solution of carboxylic acid (1 mM) and VbxK (50  $\mu$ M) in storage buffer (final volume 85  $\mu$ L) was added NADPH (1 mM) and the

reaction incubated at RT for 16 h. Boiled VbxK was used for negative control reactions. The reaction was quenched via the addition of MeOH (200  $\mu$ L). Precipitates were removed by centrifugation (13000 g, 10 min) and the supernatants were analysed by UHPLC-ESI-Q-TOF-MS (see Section 6.1).

## **6.8 Homology Modelling and Bioinformatic Analysis**

### **6.8.1 Homology Modelling of GbnD5 DH Domain**

Homology model of GbnD5 DH domain generated by Dr. Matt Jenner.

Homology modelling of GbnD5 DH domain (figure 2.9) (using entry 5KKU from the PDB as a template) was conducted using the I-TASSER server, and further refinement of the model was achieved using the MolProbity server.<sup>237-239</sup>

### **6.8.2 Phylogenetic Analysis of DH Domains**

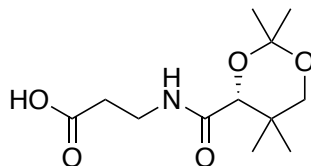
Generation of sequence alignment (figure 2.8) and phylogenetic tree (appendix 8.1) carried out by Dr. Matt Jenner.

Sequences of DH domains were collected from MIBiG. Multiple sequence alignment of DH domains was achieved using ClustalX. Phylogenetic tree was generated using the sequence alignment and FigTree.<sup>240,241</sup>

## 6.9 Chemical Synthesis of Substrates

### 6.9.1 Diene Synthase Substrates

#### (*R*)-3-(2,2,5,5-tetramethyl-1,3-dioxane-4-carboxamido)propanoic acid (264)

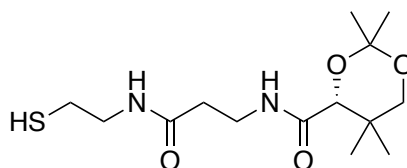


Procedure taken from Gaudelli *et al.*<sup>152</sup> To a 500 mL round-bottomed flask, equipped with a magnetic stir bar, *D*-pantothenic acid hemicalcium salt (5.0 g, 21.0 mmol, 1.0 equiv.), *p*-toluenesulfonic acid monohydrate (4.80 g, 25.2 mmol, 1.2 equiv.), and 3.0 Å molecular sieves (5.0 g) were suspended in acetone (250 mL). The flask was capped, and the suspension was stirred at RT for 12 h. The slurry was filtered through Celite<sup>®</sup> and washed with acetone (3 × 100 mL), and the filtrate was concentrated to a viscous oil. The oil was dissolved in EtOAc (200 mL), washed with brine (2 × 100 mL), dried (MgSO<sub>4</sub>) and concentrated *in vacuo*. The product was recrystallized from boiling EtOAc to afford the product as white crystals (4.68 g, 83 %, 17.4 mmol).

$\delta_{\text{H}}$  (500 MHz; CDCl<sub>3</sub>) 7.02 (1H, br. t, *J* 6.0, NH), 4.10 (1H, s, CH), 3.69 (1H, d, *J* 11.5, CH<sub>2</sub>OC(CH<sub>3</sub>)<sub>2</sub>), 3.60 (1H, dq, *J* 12.5 and 6 NHCH<sub>2</sub>), 3.50 (1H, dq, *J* 12.5 and 6 NHCH<sub>2</sub>), 3.28 (1H, d, *J* 11.5, CH<sub>2</sub>OC(CH<sub>3</sub>)<sub>2</sub>), 2.63 (2H, t, *J* 6.5, CH<sub>2</sub>CO<sub>2</sub>H), 1.46 (3H, s, OC(CH<sub>3</sub>)<sub>2</sub>), 1.43 (3H, s, OC(CH<sub>3</sub>)<sub>2</sub>), 1.04 (3H, s, CH<sub>2</sub>C(CH<sub>3</sub>)<sub>2</sub>), 0.98 (3H, s, CH<sub>2</sub>C(CH<sub>3</sub>)<sub>2</sub>);  $\delta_{\text{C}}$  (125 MHz, CDCl<sub>3</sub>) 176.4 (CO<sub>2</sub>H), 170.4 (CONH), 99.4 (OC(CH<sub>3</sub>)<sub>2</sub>), 77.4 (CH), 71.7 (CH<sub>2</sub>OC(CH<sub>3</sub>)<sub>2</sub>), 34.3 (CH<sub>2</sub>NH), 34.1 (CH<sub>2</sub>CO<sub>2</sub>H), 33.3 (CH<sub>2</sub>C(CH<sub>3</sub>)<sub>2</sub>), 29.7 (OC(CH<sub>3</sub>)<sub>2</sub>), 22.4 (CH<sub>2</sub>C(CH<sub>3</sub>)<sub>2</sub>), 19.1 (CH<sub>2</sub>C(CH<sub>3</sub>)<sub>2</sub>), 19.0 (OC(CH<sub>3</sub>)<sub>2</sub>); HRMS (ESI) cald. for C<sub>12</sub>H<sub>20</sub>NO<sub>5</sub> (M - H<sup>+</sup>) requires 258.1347, found 258.1348. Spectroscopic data consistent with that previously reported in the literature.<sup>152</sup>



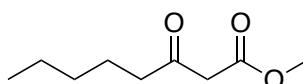
**(R)-N-(3-((2-mercaptoethyl)amino)-3-oxopropyl)-2,2,5,5-tetramethyl-1,3-dioxane-4-carboxamide (61)**



Procedure taken from Gaudelli *et al.*<sup>152</sup>. To a 250 mL round-bottomed flask equipped with a magnetic stir bar, (*R*)-3-(2,2,5,5-tetramethyl-1,3-dioxane-4-carboxamido)propanoic acid **264** (4.18 g, 16.1 mmol, 1.1 equiv.) was dissolved in dry THF (100 mL), and treated with 1',1'-carbonyldiimidazole (2.61 g, 16.1 mmol, 1.1 equiv.) and stirred for 1 h at RT. To this solution was added cysteamine hydrochloride (1.13 g, 14.6 mmol, 1.0 equiv.) and stirred at RT for 12 h. The THF was concentrated *in vacuo*, and CH<sub>2</sub>Cl<sub>2</sub> (100 mL) was added. The organic solution was washed with saturated NH<sub>4</sub>Cl (1 × 50 mL), brine (1 × 50 mL), dried (MgSO<sub>4</sub>) and concentrated to afford colourless oil. The crude mixture was purified by silica chromatography (EtOAc) to afford the product product as a white solid (3.61 g, 78 %, 11.4 mmol).

$\delta_{\text{H}}$  (500 MHz; CDCl<sub>3</sub>) 7.00 (1H, br. t, *J* 6.0, *NH*), 6.32 (1H, br. t, *J* 6.0, *NHCH*<sub>2</sub>CH<sub>2</sub>SH), 4.07 (1H, s, *CH*), 3.67 (1H, d, *J* 11.5, *CH*<sub>2</sub>OC(CH<sub>3</sub>)<sub>2</sub>), 3.58 (1H, dq, *J* 13.5 and 6.0, *NHCH*<sub>2</sub>), 3.52 (1H, dq, *J* 13.5 and 6.0, *NHCH*<sub>2</sub>), 3.46 (1H, dq, *J* 13.0 and 6.5, *CH*<sub>2</sub>CH<sub>2</sub>SH), 3.39 (1H, dq, *J* 13.0 and 6.5, *CH*<sub>2</sub>CH<sub>2</sub>SH), 3.27 (1H, d, *J* 11.5, *CH*<sub>2</sub>OC(CH<sub>3</sub>)<sub>2</sub>), 2.65 (2H, dtd, *J* 8.5, 6.5 and 2.0, *CH*<sub>2</sub>SH), 2.46 (2H, td, *J* 6.0 and 1.5, *CH*<sub>2</sub>CONH), 1.45 (3H, s, OC(CH<sub>3</sub>)<sub>2</sub>), 1.41 (3H, s, OC(CH<sub>3</sub>)<sub>2</sub>), 1.36 (1H, t, *J* 8.5, *SH*), 1.03 (3H, s, CH<sub>2</sub>C(CH<sub>3</sub>)<sub>2</sub>), 0.96 (3H, s, CH<sub>2</sub>C(CH<sub>3</sub>)<sub>2</sub>);  $\delta_{\text{C}}$  (125 MHz, CDCl<sub>3</sub>) 171.3 (CH<sub>2</sub>CONH), 170.5 (CHCONH), 99.4 (OC(CH<sub>3</sub>)<sub>2</sub>), 77.4 (CH), 71.7 (CH<sub>2</sub>OC(CH<sub>3</sub>)<sub>2</sub>), 42.7 (CH<sub>2</sub>CH<sub>2</sub>SH), 36.4 (CH<sub>2</sub>CONH), 35.1 (CH<sub>2</sub>NH), 33.2 (CH<sub>2</sub>C(CH<sub>3</sub>)<sub>2</sub>), 29.8 (OC(CH<sub>3</sub>)<sub>2</sub>), 24.8 (CH<sub>2</sub>SH), 22.4 (CH<sub>2</sub>C(CH<sub>3</sub>)<sub>2</sub>), 19.2 (CH<sub>2</sub>C(CH<sub>3</sub>)<sub>2</sub>), 19.0 (OC(CH<sub>3</sub>)<sub>2</sub>); HRMS (ESI) cald. for C<sub>14</sub>H<sub>26</sub>N<sub>2</sub>NaO<sub>4</sub>S (M + Na<sup>+</sup>) requires 341.1505, found 341.1507. Spectroscopic data consistent with that previously reported in the literature.<sup>152</sup>

**Methyl 3-oxooctanoate (56)**

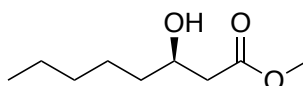


Procedure modified from Riva *et al.*<sup>242</sup> To a solution of hexanoic acid (1.0 g, 8.5 mmol, 1.0 equiv.), Meldrum's acid (1.2 g, 8.5 mmol, 1.0 equiv.) and DMAP (1.28 g, 10.5 mmol, 1.24 equiv.) in dry THF (100 mL), was added EDC.HCl (1.8 g, 9.4 mmol, 1.1 equiv.) at 0 °C

under an Argon atmosphere. The reaction was stirred at RT for 16 hours. The reaction was then concentrated *in vacuo*, the residue dissolved in CH<sub>2</sub>Cl<sub>2</sub> (50 mL), washed with 1 M HCl (50 mL), brine (50 mL), dried (MgSO<sub>4</sub>) and concentrated *in vacuo* to give the Meldrum's adduct as a yellow oil (1.9 g). The oil was then dissolved in MeOH and heated to reflux for 16 hours. The reaction was then concentrated *in vacuo* and subjected to column chromatography (1 : 4 diethyl ether : petroleum ether) to afford the product as a yellow oil (keto:enol = 15:1, 1.26 g, 86 %, 7.31 mmol).

$\delta_{\text{H}}$  (500 MHz; CDCl<sub>3</sub>) 3.73 (3H, s, COOCH<sub>3</sub>), 3.44 (2H, s, CH<sub>2</sub>CO<sub>2</sub>Me), 2.52 (2H, t, *J* 7.5, CH<sub>2</sub>CO), 1.59 (2H, quin., *J* 7.5, CH<sub>2</sub>CH<sub>2</sub>CO), 1.35-1.23 (4H, m, CH<sub>3</sub>CH<sub>2</sub>CH<sub>2</sub>), 0.88 (3H, t, *J* 7.0, CH<sub>2</sub>CH<sub>3</sub>);  $\delta_{\text{C}}$  (125 MHz, CDCl<sub>3</sub>) 203.0 (CH<sub>2</sub>COCH<sub>2</sub>), 167.8 (COOCH<sub>3</sub>), 52.5 (COOCH<sub>3</sub>), 49.1 (COCH<sub>2</sub>CO), 43.2 (CH<sub>2</sub>CO), 31.3 (CH<sub>2</sub>CH<sub>2</sub>CO), 23.3 (CH<sub>3</sub>CH<sub>2</sub>CH<sub>2</sub>), 22.5 (CH<sub>3</sub>CH<sub>2</sub>) 14.0 (CH<sub>3</sub>); HRMS (ESI) calcd. for C<sub>9</sub>H<sub>16</sub>NaO<sub>3</sub> (M + Na<sup>+</sup>) requires 195.0997, found 195.0993. Spectroscopic data consistent with that previously reported in the literature.<sup>243</sup>

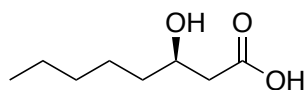
### Methyl (*R*)-3-hydroxyoctanoate (**57**)



The following procedure was modified from Ratovelomanana-Vidal *et al.*<sup>150</sup> To a solution of [(*R*)-Ru(OAc)<sub>2</sub>(BINAP)] (14.5 mg, 0.02 mmol, 0.01 equiv.) and 1 M HCl in MeOH (20  $\mu$ L, 20  $\mu$ mol, 0.01 equiv.) in MeOH (2 mL) was added methyl 3-oxooctanoate **56** (300 mg, 1.70 mmol, 1.0 equiv.) in a 10 mL test tube containing a magnetic stirring bar. The reaction was heated to 60 °C at 50 bar hydrogen pressure using hydrogenation apparatus for 16 h. The mixture was then filtered through Celite<sup>®</sup> and concentrated *in vacuo* to afford the product as a yellow oil (> 95 % e.e. as confirmed by derivatization to the Mosher's ester, 272 mg, 90 %, 1.5 mmol, [ $\alpha$ ]<sub>D</sub><sup>28</sup> (c 1.0, CHCl<sub>3</sub>): -19.4).

$\delta_{\text{H}}$  (500 MHz; CDCl<sub>3</sub>) 4.05-3.95 (1H, m, CHOH), 3.71 (3H, s, COOCH<sub>3</sub>), 2.84 (1H, d, *J* 4.0, OH), 2.52 (1H, dd, *J* 16.5 and 3.5 CH<sub>2</sub>CO<sub>2</sub>Me), 2.41 (1H, dd, *J* 16.5 and 9.0, CH<sub>2</sub>CO<sub>2</sub>Me), 1.56-1.22 (8H, m, CH<sub>3</sub>CH<sub>2</sub>CH<sub>2</sub>CH<sub>2</sub>CH<sub>2</sub>), 0.89 (3H, d, *J* 7.0, CH<sub>2</sub>CH<sub>3</sub>);  $\delta_{\text{C}}$  (125 MHz, CDCl<sub>3</sub>) 173.7 (COOCH<sub>3</sub>), 68.2 (CHOH), 51.9 (COOCH<sub>3</sub>), 42.2 (CH<sub>2</sub>CO<sub>2</sub>Me), 36.6 (CHCH<sub>2</sub>), 31.8 (CHCH<sub>2</sub>CH<sub>2</sub>), 25.3 (CHCH<sub>2</sub>CH<sub>2</sub>CH<sub>2</sub>), 22.7 (CH<sub>2</sub>CH<sub>3</sub>), 14.1 (CH<sub>2</sub>CH<sub>3</sub>); HRMS (ESI) calcd. for C<sub>9</sub>H<sub>18</sub>NaO<sub>3</sub> (M + Na<sup>+</sup>) requires 197.1148, found 197.1150. Spectroscopic data consistent with that previously reported in the literature.<sup>244</sup>

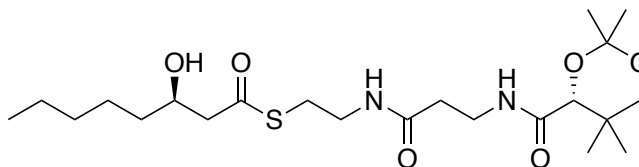
**(R)-3-Hydroxyoctanoic acid (62)**



To a solution of methyl (*R*)-3-hydroxyoctanoate **57** (250 mg, 1.4 mmol, 1.0 equiv.) in a 2 : 1 mixture of THF (4 mL) and water (2 mL), was added LiOH (56 mg, 2.9 mmol, 2.0 equiv.) and the reaction stirred for 16 h. THF was removed *in vacuo* and the resulting solution acidified to pH 2.0 using 1 M HCl. The mixture was then extracted with CH<sub>2</sub>Cl<sub>2</sub> (3 × 10 mL), the combined organics washed with brine (20 mL), dried (MgSO<sub>4</sub>) and concentrated *in vacuo* to afford the product as a colourless oil (178 mg, 81 %).

$\delta_{\text{H}}$  (500 MHz; CDCl<sub>3</sub>) 4.03 (1H, dddd, *J* 9.0, 7.5, 4.5 and 3.0, CHOH), 2.57 (1H, dd, *J* 16.5 and 3.0, CH<sub>2</sub>CO<sub>2</sub>H), 2.47 (1H, dd, *J* 16.5 and 9.0, CH<sub>2</sub>CO<sub>2</sub>H), 1.59-1.24 (8H, m, CH<sub>3</sub>CH<sub>2</sub>CH<sub>2</sub>CH<sub>2</sub>CH<sub>2</sub>), 0.89 (3H, t, *J* 7.0, CH<sub>2</sub>CH<sub>3</sub>);  $\delta_{\text{C}}$  (125 MHz, CDCl<sub>3</sub>) 177.9 (COOH), 68.2 (CHOH), 41.2 (CH<sub>2</sub>CO<sub>2</sub>H), 36.6 (CHCH<sub>2</sub>), 31.8 (CHCH<sub>2</sub>CH<sub>2</sub>), 25.3 (CHCH<sub>2</sub>CH<sub>2</sub>CH<sub>2</sub>), 22.7 (CH<sub>2</sub>CH<sub>3</sub>), 14.2 (CH<sub>2</sub>CH<sub>3</sub>); HRMS (ESI) cald. for C<sub>8</sub>H<sub>15</sub>O<sub>3</sub> [M – H]<sup>–</sup> requires 159.1027, found 159.1028. Spectroscopic data consistent with that previously reported in the literature.<sup>245</sup>

**S-(2-(3-((*R*)-2,2,5,5-tetramethyl-1,3-dioxane-4-carboxamido)propanamido) ethyl)(*R*)-3-hydroxyoctanethioate (63)**

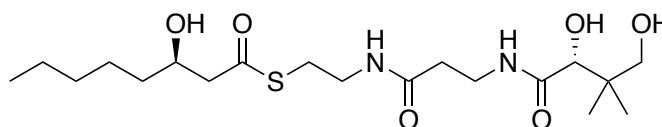


To a solution of (*R*)-3-hydroxyoctanoic acid **62** (100 mg, 0.63 mmol, 1.1 equiv.) in CH<sub>2</sub>Cl<sub>2</sub> (10 mL) was added CDI (102 mg, 0.63 mmol, 1.1 equiv.) and the reaction was stirred at RT for 1 h. (*R*)-*N*-(3-((2-mercaptoethyl)amino)-3-oxopropyl)-2,2,5,5-tetramethyl-1,3-dioxane-4-carboxamide **61** (180 mg, 0.57 mmol, 1.0 equiv.) was then added and the reaction stirred at RT for 16 h. 1 M HCl (5 mL) was then added and the mixture was extracted with CH<sub>2</sub>Cl<sub>2</sub> (3 x 5 mL), the combined organics were then washed with saturated NaHCO<sub>3</sub> (10 mL), brine (10 mL), dried (MgSO<sub>4</sub>) and concentrated *in vacuo* to give a yellow oil which was purified by silica chromatography (19 : 1 CH<sub>2</sub>Cl<sub>2</sub> : MeOH) to afford the product as a colourless oil (196 mg, 75 %, 0.43 mmol).

$\nu_{\text{max}}/\text{cm}^{-1}$  (neat) 3417 (OH), 2931 (NH), 1656, 1529 (C=O), 1160 (C-O);  $\delta_{\text{H}}$  (500 MHz; CDCl<sub>3</sub>) 6.99 (1H, br. t, *J* 6.0, NH), 6.38 (1H, br. s, NHCH<sub>2</sub>CH<sub>2</sub>S), 4.12-4.06 (1H, m, CHOH),

4.07 (1H, s, CHCONH), 3.67 (1H, d  $J$  11.5, CH<sub>2</sub>OC(CH<sub>3</sub>)<sub>2</sub>), 3.59-3.33 (5H, m, NHCH<sub>2</sub>, CH<sub>2</sub>CH<sub>2</sub>S, OH), 3.27 (1H, d  $J$  11.5, CH<sub>2</sub>OC(CH<sub>3</sub>)<sub>2</sub>), 3.12 (1H, ddd,  $J$  14.0, 7.0 and 5.5, CH<sub>2</sub>S), 2.98 (1H, ddd,  $J$  14.0, 6.5 and 5.5, CH<sub>2</sub>S), 2.72 (1H, dd,  $J$  15.0 and 4.0, CH<sub>2</sub>COS), 2.68 (1H, dd,  $J$  15.0 and 8.5, CH<sub>2</sub>COS), 2.41 (2H, td  $J$  6.5 and 1.5, CH<sub>2</sub>CONH), 1.55-1.40 (3H, m, CHOHCH<sub>2</sub>CH<sub>2</sub>), 1.46 (3H, s, OC(CH<sub>3</sub>)<sub>2</sub>), 1.42 (3H, s, OC(CH<sub>3</sub>)<sub>2</sub>), 1.37-1.23 (5H, m, CH<sub>2</sub>CH<sub>2</sub>CH<sub>2</sub>CH<sub>3</sub>), 1.03 (3H, s, CH<sub>2</sub>C(CH<sub>3</sub>)<sub>2</sub>), 0.95 (3H, s, CH<sub>2</sub>C(CH<sub>3</sub>)<sub>2</sub>), 0.88 (3H, t,  $J$  7.0, CH<sub>2</sub>CH<sub>3</sub>);  $\delta_c$  (125 MHz, CDCl<sub>3</sub>) 199.4 (COS), 171.3 (CH<sub>2</sub>CONH), 170.7 (CHCONH), 99.3 (OC(CH<sub>3</sub>)<sub>2</sub>), 77.3 (CH), 71.6 (CH<sub>2</sub>OC(CH<sub>3</sub>)<sub>2</sub>), 69.0 (CHOH), 51.4 (CH<sub>2</sub>COS), 39.3 (CH<sub>2</sub>CH<sub>2</sub>S), 37.2 (CH<sub>2</sub>CHOH), 36.4 (CH<sub>2</sub>CONH), 35.4 (CH<sub>2</sub>NH), 33.1 (CH<sub>2</sub>C(CH<sub>3</sub>)<sub>2</sub>), 31.9 (CHOHCH<sub>2</sub>CH<sub>2</sub>), 29.6 ((OC(CH<sub>3</sub>)<sub>2</sub>), 28.8 (CH<sub>2</sub>S), 25.3 (CH<sub>3</sub>CH<sub>2</sub>CH<sub>2</sub>), 22.7 (CH<sub>3</sub>CH<sub>2</sub>), 22.3 (CH<sub>2</sub>C(CH<sub>3</sub>)<sub>2</sub>), 19.0 (CH<sub>2</sub>C(CH<sub>3</sub>)<sub>2</sub>), 18.9 (OC(CH<sub>3</sub>)<sub>2</sub>), 14.2 (CH<sub>2</sub>CH<sub>3</sub>); HRMS (ESI) cald. for C<sub>22</sub>H<sub>40</sub>N<sub>2</sub>NaO<sub>6</sub>S (M + Na<sup>+</sup>) requires 483.2499, found 483.2500;  $[\alpha]_D^{26}$  (c 0.2, CHCl<sub>3</sub>): +17.5.

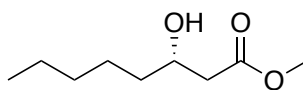
***S*-(2-(3-((*R*)-2,4-dihydroxy-3,3-dimethylbutanamido)propanamido)ethyl)(*R*)-3-hydroxyoctanethioate (53)**



*S*-(2-(3-((*R*)-2,2,5,5-tetramethyl-1,3-dioxane-4-carboxamido)propanamido)ethyl) (*R*)-3-hydroxyoctanethioate **63** (100 mg, 0.22 mmol, 1.0 equiv.) was stirred in AcOH : H<sub>2</sub>O (2 : 1, 3 mL), for 16 h at RT. The reaction was then concentrated *in vacuo* and purified using silica chromatography (17 : 3 CH<sub>2</sub>Cl<sub>2</sub> : MeOH) to afford the product as a colourless oil (76 mg, 83 %, 0.18 mmol).

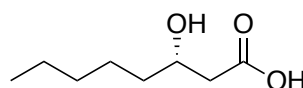
$\nu_{\max}/\text{cm}^{-1}$  (neat) 3405 (OH), 2871 (NH), 1642, 1529 (C=O), 1076 (C-O);  $\delta_H$  (500 MHz; CD<sub>3</sub>OD) 4.05-3.99 (1H, m, CHOH), 3.89 (1H, s, CH), 3.53-3.32 (6H, m, NHCH<sub>2</sub>, CH<sub>2</sub>CH<sub>2</sub>S, CH<sub>2</sub>CHOH), 3.02 (2H, t,  $J$  6.5, CH<sub>2</sub>S), 2.71 (1H, dd,  $J$  15.0 and 5.0, CH<sub>2</sub>COS), 2.68 (1H, dd,  $J$  15.0 and 7.5, CH<sub>2</sub>COS), 2.41 (2H, t,  $J$  6.5, CH<sub>2</sub>CONH), 1.50-1.25 (8H, m, CH<sub>3</sub>CH<sub>2</sub>CH<sub>2</sub>CH<sub>2</sub>CH<sub>2</sub>), 0.92 (6H, s, CH<sub>2</sub>C(CH<sub>3</sub>)<sub>2</sub>), 0.91 (3H, t,  $J$  7.5, CH<sub>2</sub>CH<sub>3</sub>);  $\delta_c$  (125 MHz, CD<sub>3</sub>OD) 198.9 (COS), 176.0 (CHCONH), 173.9 (CH<sub>2</sub>CONH), 77.3 (CH), 70.3 (CH<sub>2</sub>OH), 69.6 (CHOH), 52.6 (CH<sub>2</sub>COS), 40.3 (CH<sub>2</sub>C(CH<sub>3</sub>)<sub>2</sub>), 40.0 (CH<sub>2</sub>CH<sub>2</sub>S), 38.1 (CH<sub>2</sub>CONH), 36.4 (CH<sub>2</sub>OH), 36.3 (CH<sub>2</sub>NH), 32.8 (CH<sub>3</sub>CH<sub>2</sub>CH<sub>2</sub>CH<sub>2</sub>), 29.3 (CH<sub>2</sub>S), 26.3 (CH<sub>3</sub>CH<sub>2</sub>CH<sub>2</sub>), 23.6 (CH<sub>3</sub>CH<sub>2</sub>), 21.3 (CH<sub>2</sub>C(CH<sub>3</sub>)<sub>2</sub>), 20.9 (CH<sub>2</sub>C(CH<sub>3</sub>)<sub>2</sub>), 14.4 (CH<sub>3</sub>CH<sub>2</sub>); HRMS (ESI) cald. for C<sub>19</sub>H<sub>36</sub>N<sub>2</sub>NaO<sub>6</sub>S (M + Na<sup>+</sup>) requires 443.2186, found 443.2189;  $[\alpha]_D^{26}$  (c 0.1, CHCl<sub>3</sub>): +16.5.

### Methyl (*S*)-3-hydroxyoctanoate (**265**)



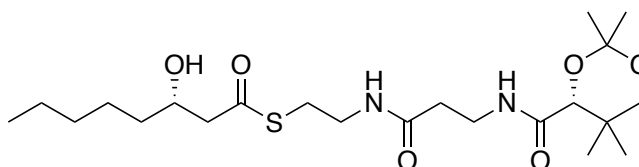
Methyl (*S*)-3-hydroxyoctanoate **265** was synthesized using the same procedure as for the synthesis of methyl (*R*)-3-hydroxyoctanoate **57** using methyl 3-oxooctanoate **56** (300 mg, 1.70 mmol, 1.0 equiv.) and [(*S*)-Ru(OAc)<sub>2</sub>(BINAP)] (14.5 mg, 0.02 mmol, 0.01 equiv.) to afford the product as a yellow oil (268 mg, 88 %, 1.56 mmol, >95 % e.e. as confirmed by derivatization to the Mosher's ester,  $[\alpha]_D^{28}$  (c 1.0, CHCl<sub>3</sub>): +20.5). Spectroscopic data was identical to that of methyl (*R*)-3-hydroxyoctanoate **57** and consistent with that previously reported in the literature.<sup>246</sup>

### (*S*)-3-Hydroxyoctanoic acid (**266**)



(*S*)-3-hydroxyoctanoic acid **266** was synthesized using the same procedure as for the synthesis of (*R*)-3-hydroxyoctanoic acid **62** using methyl (*S*)-3-hydroxyoctanoate **265** (220 mg, 1.26 mmol, 1.0 equiv.) to give the product as a colourless oil (139 mg, 69 %, 0.87 mmol). Spectroscopic data was identical to that of (*R*)-3-hydroxyoctanoic acid and consistent with that previously reported in the literature.<sup>247</sup>

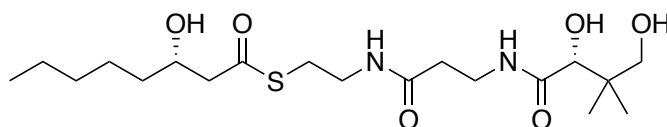
### *S*-(2-(3-((*R*)-2,2,5,5-tetramethyl-1,3-dioxane-4-carboxamido)propan-amido) ethyl) (*S*)-3-hydroxyoctanethioate (**267**)



*S*-(2-(3-((*R*)-2,2,5,5-tetramethyl-1,3-dioxane-4-carboxamido)propanamido)ethyl) (*S*)-3-hydroxyoctanethioate **267** was synthesized using the same procedure as for the synthesis of *S*-(2-(3-((*R*)-2,2,5,5-tetramethyl-1,3-dioxane-4-carboxamido) propanamido)ethyl) (*R*)-3-hydroxyoctanethioate **63** using (*S*)-3-hydroxyoctanoic acid **266** (100 mg, 0.63 mmol, 1.1 equiv.) to give the product as a colourless oil (202 mg, 77 %, 0.44 mmol).

$\nu_{\max}/\text{cm}^{-1}$  (neat) 3324 (OH), 2930 (NH), 1666, 1542 (C=O), 1159 (C-O);  $\delta_{\text{H}}$  (500 MHz;  $\text{CDCl}_3$ ) 6.99 (1H, br. t,  $J$  6.5, NH), 6.38 (1H, br. t,  $J$  5.5,  $\text{NHCH}_2\text{CH}_2\text{S}$ ), 4.11-4.05 (1H, m,  $\text{CHOH}$ ), 4.06 (1H, s,  $\text{CHCONH}$ ), 3.67 (1H, d  $J$  11.5,  $\text{CH}_2\text{OC}(\text{CH}_3)_2$ ), 3.59-3.39 (5H, m,  $\text{NHCH}_2$ ,  $\text{CH}_2\text{CH}_2\text{S}$ , OH), 3.27 (1H, d,  $J$  11.5,  $\text{CH}_2\text{OC}(\text{CH}_3)_2$ ), 3.09 (1H, dt,  $J$  14.0 and 6.0,  $\text{CH}_2\text{S}$ ), 3.00 (1H, dt,  $J$  14.0 and 6.0,  $\text{CH}_2\text{S}$ ), 2.72 (1H, dd,  $J$  15.0 and 3.5,  $\text{CH}_2\text{COS}$ ), 2.67 (1H, dd,  $J$  15.0 and 9.0,  $\text{CH}_2\text{COS}$ ), 2.40 (2H, td,  $J$  7.0 and 2.5,  $\text{CH}_2\text{CONH}$ ), 1.55-1.39 (3H, m,  $\text{CHOHCH}_2\text{CH}_2$ ), 1.45 (3H, s,  $\text{OC}(\text{CH}_3)_2$ ), 1.41 (3H, s,  $\text{OC}(\text{CH}_3)_2$ ), 1.37-1.21 (5H, m,  $\text{CH}_2\text{CH}_2\text{CH}_2\text{CH}_3$ ), 1.02 (3H, s,  $\text{CH}_2\text{C}(\text{CH}_3)_2$ ), 0.96 (3H, s,  $\text{CH}_2\text{C}(\text{CH}_3)_2$ ), 0.88 (3H, t,  $J$  7.0,  $\text{CH}_2\text{CH}_3$ );  $\delta_{\text{C}}$  (125 MHz,  $\text{CDCl}_3$ ) 199.4 (COS), 171.3 ( $\text{CH}_2\text{CONH}$ ), 170.7 ( $\text{CHCONH}$ ), 99.3 ( $\text{OC}(\text{CH}_3)_2$ ), 77.3 (CH), 71.5 ( $\text{CH}_2\text{OC}(\text{CH}_3)_2$ ), 69.2 ( $\text{CHOH}$ ), 51.4 ( $\text{CH}_2\text{COS}$ ), 39.4 ( $\text{CH}_2\text{CH}_2\text{S}$ ), 37.3 ( $\text{CH}_2\text{CHOH}$ ), 36.5 ( $\text{CH}_2\text{CONH}$ ), 35.3 ( $\text{CH}_2\text{NH}$ ), 33.1 ( $\text{CH}_2\text{C}(\text{CH}_3)_2$ ), 31.9 ( $\text{CHOHCH}_2\text{CH}_2$ ), 29.6 ( $\text{OC}(\text{CH}_3)_2$ ), 28.8 ( $\text{CH}_2\text{S}$ ), 25.3 ( $\text{CH}_3\text{CH}_2\text{CH}_2$ ), 22.7 ( $\text{CH}_3\text{CH}_2$ ), 22.3 ( $\text{CH}_2\text{C}(\text{CH}_3)_2$ ), 19.0 ( $\text{CH}_2\text{C}(\text{CH}_3)_2$ ), 18.8 ( $\text{OC}(\text{CH}_3)_2$ ), 14.2 ( $\text{CH}_2\text{CH}_3$ ); HRMS (ESI) cald. for  $\text{C}_{22}\text{H}_{40}\text{N}_2\text{NaO}_6\text{S}$  ( $\text{M} + \text{Na}^+$ ) requires 483.2499, found 483.2498;  $[\alpha]_{\text{D}}^{26}$  (c 0.075,  $\text{CHCl}_3$ ): +34.

***S*-(2-(3-((*R*)-2,4-dihydroxy-3,3-dimethylbutanamido)propanamido)ethyl) (S)-3-hydroxyoctanethioate (54)**

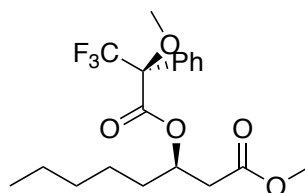


*S*-(2-(3-((*R*)-2,4-dihydroxy-3,3-dimethylbutanamido)propanamido)ethyl) (S)-3-hydroxyoctanethioate **54** was synthesized using the same procedure as for the synthesis of *S*-(2-(3-((*R*)-2,4-dihydroxy-3,3-dimethylbutanamido)propanamido)ethyl) (R)-3-hydroxyoctanethioate **53** using *S*-(2-(3-((*R*)-2,2,5,5-tetramethyl-1,3-dioxane-4-carboxamido)propanamido)ethyl) (S)-3-hydroxyoctanethioate **267** (100 mg, 0.22 mmol, 1.0 equiv.) to give the product as a colourless oil (78 mg, 85 %, 0.19 mmol).

$\nu_{\max}/\text{cm}^{-1}$  (neat) 3293 (OH), 2870 (NH), 1642, 1529 (C=O), 1076 (C-O);  $\delta_{\text{H}}$  (500 MHz;  $\text{CD}_3\text{OD}$ ) 4.05-3.99 (1H, m,  $\text{CHOH}$ ), 3.89 (1H, s, CH), 3.53-3.32 (6H, m,  $\text{NHCH}_2$ ,  $\text{CH}_2\text{CH}_2\text{S}$ ,  $\text{CH}_2\text{CHOH}$ ), 3.02 (2H, t,  $J$  6.5,  $\text{CH}_2\text{S}$ ), 2.71 (1H, dd,  $J$  15.0 and 5.0,  $\text{CH}_2\text{COS}$ ), 2.68 (1H, dd,  $J$  15.0 and 7.5,  $\text{CH}_2\text{COS}$ ), 2.41 (2H, t,  $J$  6.5,  $\text{CH}_2\text{CONH}$ ), 1.49-1.26 (8H, m,  $\text{CH}_3\text{CH}_2\text{CH}_2\text{CH}_2\text{CH}_2$ ), 0.92 (6H, s,  $\text{CH}_2\text{C}(\text{CH}_3)_2$ ), 0.91 (3H, t,  $J$  7.5,  $\text{CH}_2\text{CH}_3$ );  $\delta_{\text{C}}$  (125 MHz,  $\text{CD}_3\text{OD}$ ) 198.9 (COS), 176.0 ( $\text{CHCONH}$ ), 173.9 ( $\text{CH}_2\text{CONH}$ ), 77.3 (CH), 70.4 ( $\text{CH}_2\text{OH}$ ), 69.6 ( $\text{CHOH}$ ), 52.6 ( $\text{CH}_2\text{COS}$ ), 40.4 ( $\text{CH}_2\text{C}(\text{CH}_3)_2$ ), 40.0 ( $\text{CH}_2\text{CH}_2\text{S}$ ), 38.1 ( $\text{CH}_2\text{CONH}$ ), 36.4 ( $\text{CH}_2\text{OH}$ ), 36.3 ( $\text{CH}_2\text{NH}$ ), 32.9 ( $\text{CH}_3\text{CH}_2\text{CH}_2\text{CH}_2$ ), 29.3 ( $\text{CH}_2\text{S}$ ), 26.3 ( $\text{CH}_3\text{CH}_2\text{CH}_2$ ), 23.7

(CH<sub>3</sub>CH<sub>2</sub>), 21.3 (CH<sub>2</sub>C(CH<sub>3</sub>)<sub>2</sub>), 20.9 (CH<sub>2</sub>C(CH<sub>3</sub>)<sub>2</sub>), 14.4 (CH<sub>3</sub>CH<sub>2</sub>); HRMS (ESI) cald. for C<sub>22</sub>H<sub>40</sub>N<sub>2</sub>NaO<sub>6</sub>S (M + Na<sup>+</sup>) requires 483.2499, found 483.2500; [α]<sub>D</sub><sup>26</sup> (c 0.15, CHCl<sub>3</sub>): +10.3.

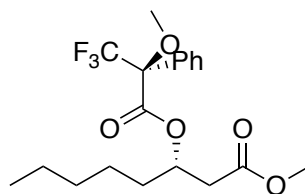
**Methyl (*R*)-3-(((*S*)-3,3,3-trifluoro-2-methoxy-2-phenylpropanoyl)oxy)octanoate (268)**



To a solution of methyl (*R*)-3-hydroxyoctanoate **57** (10 mg, 0.06 mmol, 1.0 equiv.), (*S*)-3,3,3-trifluoro-2-methoxy-2-phenylpropanoic acid (28 mg, 0.12 mmol, 2.0 equiv.) and DMAP (15 mg, 0.12 mmol, 2.0 equiv.) in CH<sub>2</sub>Cl<sub>2</sub> (5 mL), was added EDC.HCl (19 mg, 0.12 mmol, 2.0 equiv.) at 0 °C. The reaction was stirred at RT for 17 h, and was quenched by the addition of 2 M HCl. The mixture was extracted with CH<sub>2</sub>Cl<sub>2</sub> (3 × 10 mL), washed with brine (10 mL), dried (MgSO<sub>4</sub>), filtered and concentrated *in vacuo*. The resulting was purified by silica chromatography (EtOAc) to afford the product as a colourless oil (13 mg, 56 %, 0.03 mmol).

δ<sub>H</sub> (500 MHz; CDCl<sub>3</sub>) 7.54-7.50 (2H, m, ArH), 7.41-7.37 (3H, m, ArH), 5.48 (1H, tt, *J* 7.5 and 5.5 CHOCH<sub>2</sub>), 3.59 (3H, s, COOCH<sub>3</sub>), 3.52 (3H, s, OCH<sub>3</sub>), 2.65 (1H, dd, *J* 16.0 and 8.0 CH<sub>2</sub>CO<sub>2</sub>Me), 2.58 (1H, dd, *J* 16.0 and 5.0, CH<sub>2</sub>CO<sub>2</sub>Me), 1.79-1.62 (2H, m, CH<sub>2</sub>CHO), 1.38-1.21 (6H, m, CH<sub>3</sub>CH<sub>2</sub>CH<sub>2</sub>CH<sub>2</sub>), 0.88 (3H, t, *J* 6.5, CH<sub>2</sub>CH<sub>3</sub>); δ<sub>C</sub> (125 MHz, CDCl<sub>3</sub>) 170.5 (COOCH<sub>3</sub>), 166.0 (COOCH), 132.3 (ArC<sub>quart</sub>), 129.7 (ArC), 128.5 (ArC), 127.6 (ArC), 124.6 (CF<sub>3</sub>), 122.3 (COCH<sub>3</sub>), 73.6 (CHOCO), 55.5 (OCH<sub>3</sub>) 51.9 (COOCH<sub>3</sub>), 38.6 (CH<sub>2</sub>CO<sub>2</sub>Me), 33.8 (CHOCH<sub>2</sub>), 31.5 (CHCH<sub>2</sub>CH<sub>2</sub>), 24.8 (CHCH<sub>2</sub>CH<sub>2</sub>CH<sub>2</sub>), 22.6 (CH<sub>2</sub>CH<sub>3</sub>), 14.1 (CH<sub>2</sub>CH<sub>3</sub>); HRMS (ESI) cald. for C<sub>19</sub>H<sub>25</sub>F<sub>3</sub>NaO<sub>5</sub> (M + Na<sup>+</sup>) requires 413.1552, found 413.1543.

**Methyl (*S*)-3-(((*S*)-3,3,3-trifluoro-2-methoxy-2-phenylpropanoyl)oxy)octanoate (269)**

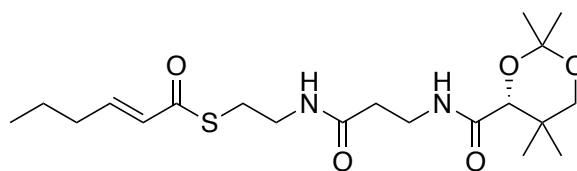


Methyl (*S*)-3-(((*S*)-3,3,3-trifluoro-2-methoxy-2-phenylpropanoyl)oxy)octanoate **269** was synthesized using the same procedure as for the synthesis of methyl (*R*)-3-(((*S*)-3,3,3-trifluoro-2-methoxy-2-phenylpropanoyl)oxy)octanoate **268** using methyl (*S*)-3-hydroxyoctanoate **265**

(10 mg, 0.06 mmol, 1.0 equiv.) to give the product as a colourless oil (11 mg, 47 %, 0.03 mmol).

$\delta_{\text{H}}$  (500 MHz;  $\text{CDCl}_3$ ) 7.55-7.51 (2H, m, ArH), 7.41-7.37 (3H, m, ArH), 5.48 (1H, tt,  $J$  7.5 and 5.0  $\text{CHOCH}_2$ ), 3.66 (3H, s,  $\text{COOCH}_3$ ), 3.55 (3H, s,  $\text{OCH}_3$ ), 2.70 (1H, dd,  $J$  16.0 and 8.5  $\text{CH}_2\text{CO}_2\text{Me}$ ), 2.61 (1H, dd,  $J$  16.0 and 5.0,  $\text{CH}_2\text{CO}_2\text{Me}$ ), 1.70-1.52 (2H, m,  $\text{CH}_2\text{CHO}$ ), 1.34-1.12 (6H, m,  $\text{CH}_3\text{CH}_2\text{CH}_2\text{CH}_2$ ), 0.86 (3H, t,  $J$  7.0,  $\text{CH}_2\text{CH}_3$ );  $\delta_{\text{C}}$  (125 MHz,  $\text{CDCl}_3$ ) 170.7 ( $\text{COOCH}_3$ ), 166.1 ( $\text{COOCH}$ ), 132.4 ( $\text{ArC}_{\text{quart}}$ ), 129.7 (ArC), 128.4 (ArC), 127.5 (ArC), 124.6 ( $\text{CF}_3$ ), 122.3 ( $\text{COCH}_3$ ), 73.5 ( $\text{CHOCO}$ ), 55.6 ( $\text{OCH}_3$ ) 52.1 ( $\text{COOCH}_3$ ), 38.7 ( $\text{CH}_2\text{CO}_2\text{Me}$ ), 33.7 ( $\text{CHOCH}_2$ ), 31.5 ( $\text{CHCH}_2\text{CH}_2$ ), 24.4 ( $\text{CHCH}_2\text{CH}_2\text{CH}_2$ ), 22.5 ( $\text{CH}_2\text{CH}_3$ ), 14.0 ( $\text{CH}_2\text{CH}_3$ ); HRMS (ESI) cald. for  $\text{C}_{19}\text{H}_{25}\text{F}_3\text{NaO}_5$  ( $\text{M} + \text{Na}^+$ ) requires 413.1552, found 413.1550.

**(R)-S-(2-(3-(2,2,5,5-tetramethyl-1,3-dioxane-4-carboxamido)propanamido) ethyl) (E)-hex-2-enethioate (69) (made by Dr. Doug Roberts)**



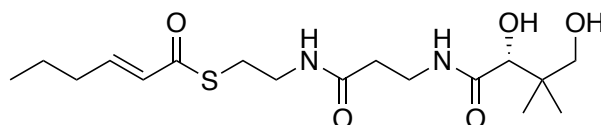
Procedure modified from Roberts *et al.*<sup>73</sup> To a solution of hex-2-enoic acid (76 mg, 0.67 mmol, 1.3 equiv.), (*R*)-*N*-(3-((2-mercaptoethyl)amino)-3-oxopropyl)-2,2,5,5-tetramethyl-1,3-dioxane-4-carboxamide **61** (235 mg, 0.74 mmol, 1.4 equiv.) and DMAP (18 mg, 0.16 mmol, 0.3 equiv.) in  $\text{CH}_2\text{Cl}_2$  (5 mL), was added EDC.HCl (141 mg, 0.75 mmol, 1.4 equiv.) at 0 °C. The reaction was stirred at RT for 17 h, and was quenched by the addition of 2 M HCl. The mixture was extracted with  $\text{CH}_2\text{Cl}_2$  (3  $\times$  10 mL), washed with brine (10 mL), dried ( $\text{MgSO}_4$ ), filtered and concentrated *in vacuo*. The resulting was purified by silica chromatography (EtOAc) to afford the product as a colourless oil (167 mg, 61 %, 0.33 mmol).

$\nu_{\text{max}}/\text{cm}^{-1}$  (neat) 2914 (NH), 1618 (C=O), 1520 (C=O), 1159 (C-O);  $\delta_{\text{H}}$  (300 MHz;  $\text{CDCl}_3$ ) 7.01 (1H, br. t,  $J$  6.0, NH), 6.92 (1H, dt,  $J$  15.5 and 7.0,  $\text{CHCHCOS}$ ), 6.18-6.07 (2H, m,  $\text{NHCH}_2\text{CH}_2\text{S}$ ,  $\text{CHCOS}$ ), 4.07 (1H, s, CH), 3.67 (1H, d,  $J$  12.0,  $\text{CH}_2\text{OC}(\text{CH}_3)_2$ ), 3.62-3.40 (4H, m,  $\text{NHCH}_2$ ,  $\text{CH}_2\text{CH}_2\text{S}$ ), 3.27 (1H, d,  $J$  12.0,  $\text{CH}_2\text{OC}(\text{CH}_3)_2$ ), 3.07 (2H, t,  $J$  6.0,  $\text{CH}_2\text{S}$ ), 2.40 (2H, t,  $J$  6.0,  $\text{CH}_2\text{CONH}$ ), 2.17 (2H, q,  $J$  7.0,  $\text{CH}_3\text{CH}_2\text{CH}_2$ ), 1.50-1.44 (2H, m,  $\text{CH}_3\text{CH}_2$ ), 1.44 (3H, s,  $\text{OC}(\text{CH}_3)_2$ ), 1.40 (3H, s,  $\text{OC}(\text{CH}_3)_2$ ), 1.03 (3H, s,  $\text{CH}_2\text{C}(\text{CH}_3)_2$ ), 0.97-0.89 (6H, m,  $\text{CH}_2\text{CH}_3$ ,  $\text{CH}_2\text{C}(\text{CH}_3)_2$ );  $\delta_{\text{C}}$  (75 MHz,  $\text{CDCl}_3$ ) 190.1 (COS), 171.6 ( $\text{CH}_2\text{CONH}$ ), 170.1 ( $\text{CHCONH}$ ), 146.7 ( $\text{CHCHCOS}$ ), 128.5 ( $\text{CHCOS}$ ), 99.2 ( $\text{OC}(\text{CH}_3)_2$ ), 77.2 (CH), 71.5 ( $\text{CH}_2\text{OC}(\text{CH}_3)_2$ ), 39.8 ( $\text{CH}_2\text{CH}_2\text{S}$ ), 36.0 ( $\text{CH}_2\text{CONH}$ ), 34.8 ( $\text{CH}_2\text{NH}$ ), 34.2 ( $\text{CH}_2\text{S}$ ), 33.0 ( $\text{CH}_2\text{C}(\text{CH}_3)_2$ ), 29.5 ( $\text{OC}(\text{CH}_3)_2$ ), 22.2 ( $\text{CH}_2\text{C}(\text{CH}_3)_2$ ), 21.2 ( $\text{CH}_3\text{CH}_2\text{CH}_2$ ), 21.1 ( $\text{CH}_3\text{CH}_2$ ),



19.0 (CH<sub>2</sub>C(CH<sub>3</sub>)<sub>2</sub>), 18.8 (OC(CH<sub>3</sub>)<sub>2</sub>), 13.6 (CH<sub>3</sub>CH<sub>2</sub>); HRMS (ESI) calcd. for C<sub>20</sub>H<sub>34</sub>N<sub>2</sub>NaO<sub>5</sub>S (M + Na<sup>+</sup>) requires 437.2086, found 437.2088; [α]<sub>D</sub><sup>26</sup> (c 0.2, CHCl<sub>3</sub>): +6.5.

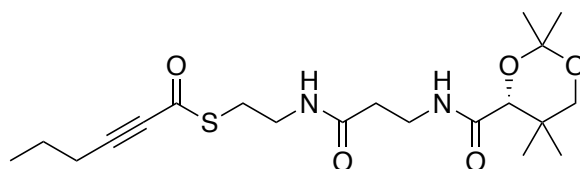
**(R)-S-(2-(3-(2,4-dihydroxy-3,3-dimethylbutanamido)propanamido)ethyl)(E)-hex-2-enethioate (64) (made by Dr. Doug Roberts)**



Procedure modified from Roberts *et al.*<sup>73</sup> To a solution of (R)-S-(2-(3-(2,2,5,5-tetramethyl-1,3-dioxane-4-carboxamido)propanamido)ethyl) (E)-hex-2-enethioate **69** (167 mg, 0.40 mmol, 1.0 equiv.) in MeOH (2 mL) was added Dowex 50w resin (85 mg) and the reaction stirred at RT for two days. The reaction mixture was then filtered and concentrated *in vacuo* to afford the product as a colourless oil (91 mg, 60 %, 0.24 mmol).

$\nu_{\max}/\text{cm}^{-1}$  (neat) 3301 (OH), 2946 (NH), 1642, 1530 (C=O), 1099 (C-O);  $\delta_{\text{H}}$  (400 MHz; CDCl<sub>3</sub>) 7.59 (1H, br. t, *J* 6.5, NH), 7.06 (1H, br. s, NHCH<sub>2</sub>CH<sub>2</sub>S), 6.89 (1H, dt, *J* 15.5 and 6.5, CHCHCOS), 6.08 (1H, dt, *J* 15.5 and 1.5, CHCOS), 3.98 (1H, s, CH), 3.56-3.35 (6H, m, NHCH<sub>2</sub>, CH<sub>2</sub>CH<sub>2</sub>S, CH<sub>2</sub>CHOH), 3.06-3.00 (2H, m, CH<sub>2</sub>S), 2.45 (2H, t, *J* 6.0, CH<sub>2</sub>CONH), 2.15 (2H, qd, *J* 7.0 and 1.5, CH<sub>3</sub>CH<sub>2</sub>CH<sub>2</sub>), 1.51-1.42 (2H, m, CH<sub>3</sub>CH<sub>2</sub>), 0.94-0.87 (9H, m, CH<sub>2</sub>CH<sub>3</sub>, CH<sub>2</sub>C(CH<sub>3</sub>)<sub>2</sub>);  $\delta_{\text{C}}$  (100 MHz, CDCl<sub>3</sub>) 190.5 (COS), 174.2 (CHCONH), 172.0 (CH<sub>2</sub>CONH), 146.8 (CHCHCOS), 128.5 (CHCOS), 77.1 (CH), 70.6 (CH<sub>2</sub>OH), 39.7 (CH<sub>2</sub>CH<sub>2</sub>S), 39.4 (CH<sub>2</sub>CONH), 35.8 (CH<sub>2</sub>NH), 35.5 (CH<sub>2</sub>S), 34.3 (CH<sub>3</sub>CH<sub>2</sub>CH<sub>2</sub>), 28.1 (CH<sub>2</sub>C(CH<sub>3</sub>)<sub>2</sub>), 23.1 (CH<sub>3</sub>CH<sub>2</sub>), 20.7 (CH<sub>2</sub>C(CH<sub>3</sub>)<sub>2</sub>), 13.7 (CH<sub>3</sub>CH<sub>2</sub>); HRMS (ESI) calcd. for C<sub>17</sub>H<sub>30</sub>N<sub>2</sub>NaO<sub>5</sub>S (M + Na<sup>+</sup>) requires 397.1768, found 397.1770; [α]<sub>D</sub><sup>26</sup> (c 0.2, CHCl<sub>3</sub>): +8.3.

**(R)-S-(2-(3-(2,2,5,5-tetramethyl-1,3-dioxane-4-carboxamido)propanamido) ethyl) hex-2-ynethioate (70)**

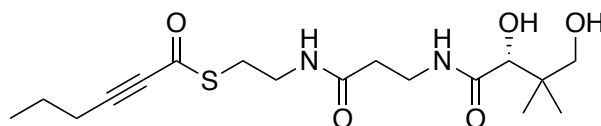


To a solution of hex-2-ynoic acid (0.12 mL, 0.75 mmol, 1.0 equiv.), (R)-N-(3-((2-mercaptoethyl)amino)-3-oxopropyl)-2,2,5,5-tetramethyl-1,3-dioxane-4-carboxamide **61** (255 mg, 0.80 mmol, 1.1 equiv.) and DMAP (21 mg, 0.23 mmol, 0.2 equiv.) in CH<sub>2</sub>Cl<sub>2</sub> (10 mL), was added EDC.HCl (156 mg, 0.80 mmol, 1.1 equiv.) at 0 °C. The reaction was

stirred at RT for 16 h, and was quenched by the addition of 1 M HCl. The mixture was extracted with CH<sub>2</sub>Cl<sub>2</sub> (3 × 10 mL), washed with saturated NaHCO<sub>3</sub> solution (10 mL), dried (MgSO<sub>4</sub>), filtered and concentrated *in vacuo* to give a viscous oil which was purified by silica chromatography (EtOAc) to give the product as a colourless oil (305 mg, 99 %, 0.75 mmol).

$\nu_{\max}/\text{cm}^{-1}$  (neat) 3309 (OH), 2939 (NH), 1649 (C=O), 1529 (C=O), 1158 (C-O);  $\delta_{\text{H}}$  (500 MHz; CDCl<sub>3</sub>) 7.01 (1H, br. t, *J* 6.0, NH), 6.20 (1H, br. s, NHCH<sub>2</sub>CH<sub>2</sub>S), 4.07 (1H, s, CH), 3.67 (1H, d, *J* 11.5, CH<sub>2</sub>OC(CH<sub>3</sub>)<sub>2</sub>), 3.61-3.39 (4H, m, NHCH<sub>2</sub>, CH<sub>2</sub>CH<sub>2</sub>S), 3.27 (1H, d, *J* 11.5, CH<sub>2</sub>OC(CH<sub>3</sub>)<sub>2</sub>), 3.09 (2H, t, *J* 6.5, CH<sub>2</sub>S), 2.43 (2H, t, *J* 6.0, CH<sub>2</sub>CONH), 2.37 (2H, t, *J* 7.0, CH<sub>3</sub>CH<sub>2</sub>CH<sub>2</sub>), 1.62 (2H, sext., *J* 7.5, CH<sub>3</sub>CH<sub>2</sub>), 1.46 (3H, s, OC(CH<sub>3</sub>)<sub>2</sub>), 1.42 (3H, s, OC(CH<sub>3</sub>)<sub>2</sub>), 1.03 (3H, s, CH<sub>2</sub>C(CH<sub>3</sub>)<sub>2</sub>), 1.02 (3H, t, *J* 7.5, CH<sub>2</sub>CH<sub>3</sub>), 0.96 (3H, s, CH<sub>2</sub>C(CH<sub>3</sub>)<sub>2</sub>);  $\delta_{\text{C}}$  (125 MHz, CDCl<sub>3</sub>) 176.4 (COS), 171.4 (CH<sub>2</sub>CONH), 170.3 (CHCONH), 99.2 (OC(CH<sub>3</sub>)<sub>2</sub>), 96.7 (CCCOS), 78.9 (CCCOS), 77.3 (CH), 71.6 (CH<sub>2</sub>OC(CH<sub>3</sub>)<sub>2</sub>), 42.6 (CH<sub>2</sub>CH<sub>2</sub>S), 36.1 (CH<sub>2</sub>CONH), 34.9 (CH<sub>2</sub>NH), 33.1 (CH<sub>2</sub>C(CH<sub>3</sub>)<sub>2</sub>), 29.6 (OC(CH<sub>3</sub>)<sub>2</sub>), 29.5 (CH<sub>2</sub>S), 22.3 (CH<sub>2</sub>C(CH<sub>3</sub>)<sub>2</sub>), 21.2 (CH<sub>3</sub>CH<sub>2</sub>CH<sub>2</sub>), 21.1 (CH<sub>3</sub>CH<sub>2</sub>), 19.0 (CH<sub>2</sub>C(CH<sub>3</sub>)<sub>2</sub>), 18.8 (OC(CH<sub>3</sub>)<sub>2</sub>), 13.6 (CH<sub>3</sub>CH<sub>2</sub>); HRMS (ESI) cald. for C<sub>20</sub>H<sub>32</sub>N<sub>2</sub>NaO<sub>5</sub>S (M + Na<sup>+</sup>) requires 435.1924, found 435.1926;  $[\alpha]_{\text{D}}^{26}$  (c 0.3, CHCl<sub>3</sub>): +4.8.

**(*R*)-*S*-(2-(3-(2,4-dihydroxy-3,3-dimethylbutanamido)propanamido)ethyl) hex-2-ynethioate (68)**

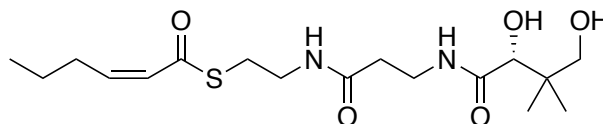


(*R*)-*S*-(2-(3-(2,2,5,5-tetramethyl-1,3-dioxane-4-carboxamido)propanamido)ethyl) hex-2-ynethioate **70** (300 mg, 0.73 mmol, 1.0 equiv.) was stirred in AcOH (4 mL) and water (2 mL) for 16 h and RT. The mixture was then concentrated *in vacuo* and purified using silica chromatography (1 : 10 MeOH : EtOAc) to give the product as a colourless oil (216 mg, 80 %, 0.58 mmol).

$\nu_{\max}/\text{cm}^{-1}$  (neat) 3299 (OH), 2964 (NH), 1643 (C=O), 1533 (COS), 1037 (C-O);  $\delta_{\text{H}}$  (500 MHz; CD<sub>3</sub>OD) 3.89 (1H, s, CH), 3.61-3.39 (6H, m, NHCH<sub>2</sub>, CH<sub>2</sub>CH<sub>2</sub>S, CH<sub>2</sub>CHOH), 3.09 (2H, t, *J* 6.5, CH<sub>2</sub>S), 2.42 (2H, t, *J* 7.0, CH<sub>3</sub>CH<sub>2</sub>CH<sub>2</sub>), 2.41 (2H, t, *J* 6.5, CH<sub>2</sub>CONH), 1.62 (2H, sext., *J* 7.5, CH<sub>3</sub>CH<sub>2</sub>), 1.03 (3H, t, *J* 7.5, CH<sub>2</sub>CH<sub>3</sub>), 0.92 (6H, s, CH<sub>2</sub>C(CH<sub>3</sub>)<sub>2</sub>);  $\delta_{\text{C}}$  (125 MHz, CD<sub>3</sub>OD) 177.2 (COS), 176.1 (CHCONH), 174.0 (CH<sub>2</sub>CONH), 96.9 (CCCOS), 79.6 (CCCOS), 77.3 (CH), 70.4 (CH<sub>2</sub>OH), 40.4 (CH<sub>2</sub>C(CH<sub>3</sub>)<sub>2</sub>), 39.8 (CH<sub>2</sub>CH<sub>2</sub>S), 36.4 (CH<sub>2</sub>CONH), 36.3 (CH<sub>2</sub>NH), 30.1 (CH<sub>2</sub>S), 22.2 (CH<sub>3</sub>CH<sub>2</sub>CH<sub>2</sub>), 21.4 (CH<sub>3</sub>CH<sub>2</sub>), 21.2 (CH<sub>2</sub>C(CH<sub>3</sub>)<sub>2</sub>), 19.0 (CH<sub>2</sub>C(CH<sub>3</sub>)<sub>2</sub>),

13.7 (CH<sub>3</sub>CH<sub>2</sub>); HRMS (ESI) cald. for C<sub>17</sub>H<sub>28</sub>N<sub>2</sub>NaO<sub>5</sub>S (M + Na<sup>+</sup>) requires 395.1611, found 395.1615; [α]<sub>D</sub><sup>26</sup> (c 0.4, CHCl<sub>3</sub>): +15.4.

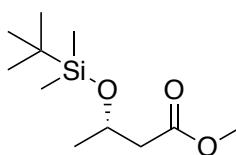
**(R)-S-(2-(3-(2,4-dihydroxy-3,3-dimethylbutanamido)propanamido)ethyl) (Z)-hex-2-enethioate (65)**



Procedure modified from Alhamadsheh *et al.*<sup>248</sup> A mixture of Lindlar catalyst (10 mg, 5 wt% of Pd on CaCO<sub>3</sub>, poisoned with Pb) and quinoline (5.0 μL, 0.05 mmol, 0.1 equiv.) in anhydrous ethanol (5 ml) was stirred at RT for 20 min. A solution of (R)-S-(2-(3-(2,4-dihydroxy-3,3-dimethylbutanamido)propanamido)ethyl) hex-2-ynethioate **68** (200 mg, 0.51 mmol, 1.0 equiv.) in ethanol (5 ml) was added and the mixture was stirred for an additional 20 min at RT. The reaction mixture was placed under hydrogen atmosphere (balloon) and stirred for additional 4 hr. After analysis via mass spectrometry, the reaction appeared to have not yet reached completion. More catalyst was added (10 mg), and this process was repeated until the reaction was complete (8 days, 100 mg total catalyst). The catalyst was removed by filtration through Celite<sup>®</sup> and the filtrate was concentrated *in vacuo* to afford a yellow oil which was purified by silica chromatography (1 : 10 MeOH : EtOAc) to afford the product as a colourless oil (168 mg, 88 % 0.45 mmol, 95 : 5, Z : E).

$\nu_{\max}/\text{cm}^{-1}$  (neat) 3287 (OH), 2951 (NH), 1640 (C=O), 1539 (COS), 1070 (C-O);  $\delta_{\text{H}}$  (500 MHz; CD<sub>3</sub>OD) 6.14-6.06 (2H, m, CHCHCOS, CHCHCOS), 3.89 (1H, s, CH), 3.53-3.33 (6H, m, NHCH<sub>2</sub>, CH<sub>2</sub>CH<sub>2</sub>S, CH<sub>2</sub>CHOH), 3.05 (2H, t, *J* 7.0, CH<sub>2</sub>S), 2.59 (2H, q, *J* 7.0, CH<sub>3</sub>CH<sub>2</sub>CH<sub>2</sub>), 2.41 (2H, t, *J* 6.5, CH<sub>2</sub>CONH), 1.48 (2H, sext., *J* 7.5, CH<sub>3</sub>CH<sub>2</sub>), 0.94 (3H, t, *J* 7.5, CH<sub>2</sub>CH<sub>3</sub>), 0.92 (6H, s, CH<sub>2</sub>C(CH<sub>3</sub>)<sub>2</sub>);  $\delta_{\text{C}}$  (125 MHz, CD<sub>3</sub>OD) 190.4 (COS), 176.1 (CHCONH), 173.9 (CH<sub>2</sub>CONH), 148.5 (CHCHCOS), 127.2 (CHCHCOS), 77.3 (CH), 70.3 (CH<sub>2</sub>OH), 40.4 (CH<sub>2</sub>C(CH<sub>3</sub>)<sub>2</sub>), 40.2 (CH<sub>2</sub>CH<sub>2</sub>S), 36.4 (CH<sub>2</sub>CONH), 36.3 (CH<sub>2</sub>NH), 32.9 (CH<sub>2</sub>S), 29.1 (CH<sub>3</sub>CH<sub>2</sub>CH<sub>2</sub>), 23.3 (CH<sub>3</sub>CH<sub>2</sub>), 21.3 (CH<sub>2</sub>C(CH<sub>3</sub>)<sub>2</sub>), 20.9 (CH<sub>2</sub>C(CH<sub>3</sub>)<sub>2</sub>), 14.1 (CH<sub>3</sub>CH<sub>2</sub>); HRMS (ESI) cald. for C<sub>17</sub>H<sub>30</sub>N<sub>2</sub>NaO<sub>5</sub>S (M + Na<sup>+</sup>) requires 397.1768, found 397.1767; [α]<sub>D</sub><sup>26</sup> (c 0.1, CHCl<sub>3</sub>): +7.

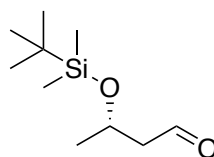
### Methyl (*S*)-3-((*tert*-butyldimethylsilyl)oxy)butanoate (**79**)



Procedure taken from Sugimoto *et al.*<sup>249</sup> Under an Argon atmosphere, TBSCl (3.35 g, 22.2 mmol, 1.05 equiv.) was added to a solution of methyl (*S*)-3-hydroxybutanoate (2.50 g, 21.2 mmol, 1.00 equiv.), imidazole (2.16 g, 31.8 mmol, 1.50 equiv.) and DMAP (1.30 g, 10.6 mmol, 0.50 equiv.) in DMF (60 mL) at 0 °C, and the mixture was stirred for 3 hours at RT. The reaction mixture was then diluted with Et<sub>2</sub>O, successively washed with HCl solution (10 %, 50 mL), saturated NaHCO<sub>3</sub> (50 mL), dried (MgSO<sub>4</sub>) and concentrated *in vacuo* to afford the product as a colourless oil (4.72 g, 96 %, 20.3 mmol).

$\delta_{\text{H}}$  (500 MHz; CDCl<sub>3</sub>) 4.27 (1H, dqd, *J* 7.5, 6 and 5.5, CH), 3.66 (3H, s, OCH<sub>3</sub>), 2.48 (1H, dd, *J* 14.5 and 7.5, CH<sub>2</sub>), 2.37 (1H, dd, *J* 14.5 and 5.5, CH<sub>2</sub>), 1.19 (3H, d, *J* 6.0, CH<sub>3</sub>), 0.86 (9H, s, C(CH<sub>3</sub>)<sub>3</sub>), 0.06 (3H, s, SiCH<sub>3</sub>), 0.04 (3H, s, SiCH<sub>3</sub>);  $\delta_{\text{C}}$  (125 MHz, CDCl<sub>3</sub>) 172.4 (CO<sub>2</sub>Me), 66.1 (CH), 51.7 (OCH<sub>3</sub>), 45.1 (CH<sub>2</sub>), 26.0 (C(CH<sub>3</sub>)<sub>3</sub>), 24.2 (CH<sub>3</sub>), 18.2 (C(CH<sub>3</sub>)<sub>3</sub>), -4.2 (SiCH<sub>3</sub>), -4.8 (SiCH<sub>3</sub>); HRMS (ESI) cald. for C<sub>11</sub>H<sub>24</sub>NaO<sub>3</sub>Si (M + Na<sup>+</sup>) requires 255.1387, found 255.1387. Spectroscopic data consistent with that previously reported in the literature.<sup>249</sup>

### (*S*)-3-((*tert*-butyldimethylsilyl)oxy)butanal (**74**)

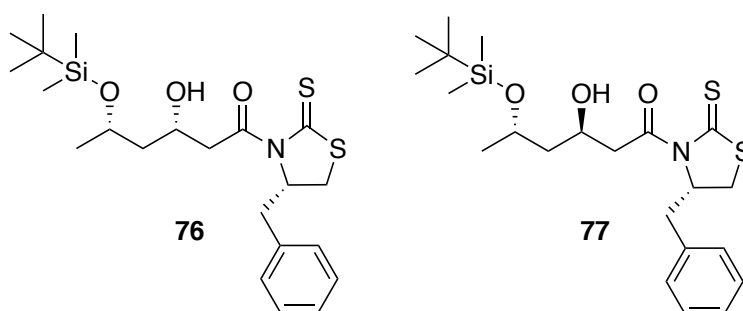


Procedure modified from Fernandes *et al.*<sup>250</sup> To a stirred solution of methyl (*S*)-3-((*tert*-butyldimethylsilyl)oxy)butanoate **79** (1.23 g, 5.00 mmol, 1.0 equiv.) in CH<sub>2</sub>Cl<sub>2</sub> (50 mL) was added a 1 M solution DIBAL-H in hexane (5.50 mL, 5.50 mmol, 1.1 equiv.) dropwise at -78 °C under an argon atmosphere. After being stirred for 30 minutes at this temperature, MeOH (10 mL) was added, and the reaction was warmed to RT. A saturated solution of sodium potassium tartrate was then added (50 mL), and the mixture stirred until clear separation was observed. The organic layer was removed, and the aqueous layer further extracted with CH<sub>2</sub>Cl<sub>2</sub> (2 × 50 mL), the combined organics were washed with brine (50 mL), dried (MgSO<sub>4</sub>) and concentrated *in vacuo*. The resulting oil was then purified by silica

chromatography (3:100 Et<sub>2</sub>O : Petroleum ether) to afford the product as a colourless oil (891 mg, 82 %, 4.5 mmol).

$\delta_{\text{H}}$  (500 MHz; CDCl<sub>3</sub>) 9.79 (1H, dd, *J* 3.0 and 2.0, CHO), 4.35 (1H, dqd, *J* 7.0, 6.0 and 5.0, CH), 2.55 (1H, ddd, *J* 15.5, 7.0 and 3.0, CH<sub>2</sub>), 2.46 (1H, dd, *J* 15.5, 5.0 and 2.0, CH<sub>2</sub>), 1.23 (3H, d, *J* 6.0, CH<sub>3</sub>), 0.87 (9H, s, C(CH<sub>3</sub>)<sub>3</sub>), 0.07 (3H, s, SiCH<sub>3</sub>), 0.06 (3H, s, SiCH<sub>3</sub>);  $\delta_{\text{C}}$  (125 MHz, CDCl<sub>3</sub>) 202.6 (CHO), 64.9 (CH), 53.4 (CH<sub>2</sub>), 26.1 (C(CH<sub>3</sub>)<sub>3</sub>), 24.6 (CH<sub>3</sub>), 18.3 (C(CH<sub>3</sub>)<sub>3</sub>), -4.0 (SiCH<sub>3</sub>), -4.6 (SiCH<sub>3</sub>)<sub>3</sub>; HRMS (ESI) calcd. for C<sub>11</sub>H<sub>26</sub>NaO<sub>3</sub>Si (M + MeOH + Na<sup>+</sup>) requires 257.1543, found 257.1543. Spectroscopic data consistent with that previously reported in the literature.<sup>250</sup>

**(3*R*,5*S*)-1-((*S*)-4-benzyl-2-thioxothiazolidin-3-yl)-5-((*tert*-butyldimethylsilyl)oxy)-3-hydroxyhexan-1-one and (3*S*,5*S*)-1-((*S*)-4-benzyl-2-thioxothiazolidin-3-yl)-5-((*tert*-butyldimethylsilyl)oxy)-3-hydroxyhexan-1-one (76 and 77)**



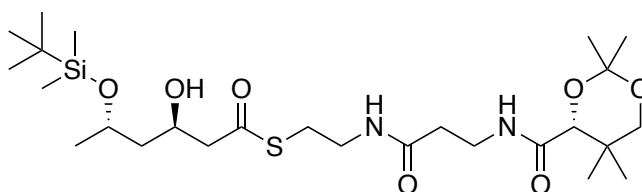
Procedure taken from Gao *et al.*<sup>251</sup> To a solution of (*S*)-1-(4-benzyl-2-thioxothiazolidin-3-yl)ethan-1-one **75** (600 mg, 2.39 mmol, 1.00 equiv.) in dry CH<sub>2</sub>Cl<sub>2</sub> (20 mL) under an Ar atmosphere was added a 1 M solution of TiCl<sub>4</sub> in CH<sub>2</sub>Cl<sub>2</sub> (2.55 mL, 2.51 mmol, 1.05 equiv.) dropwise at 0 °C. The orange suspension was allowed to stir for 15 minutes at the same temperature before diisopropylethylamine (0.46 mL, 2.63 mmol, 1.10 equiv.) was added dropwise, the resulting purple solution was allowed to stir for a further 40 min at 0 °C. 1-Methyl-2-pyrrolidinone (0.46 mL, 4.78 mmol, 2.00 equiv.) was then added at the same temperature and the reaction stirred for an additional 10 min before a solution of (*S*)-3-((*tert*-butyldimethylsilyl)oxy)butanal **74** (965 mg, 4.78 mmol, 2.00 equiv.) in dry CH<sub>2</sub>Cl<sub>2</sub> (5 mL) was added. The reaction was left to stir for 2 h at 0 °C before the addition of saturated NH<sub>4</sub>Cl (10 mL), the organic layer was separated and the aqueous layer extracted with CH<sub>2</sub>Cl<sub>2</sub> (2 × 20 mL). The combined organics were dried (MgSO<sub>4</sub>), filtered and concentrated *in vacuo* to give the crude product, which was purified by silica chromatography (1 : 9 EtOAc : Petroleum ether) to give (3*R*,5*S*)-1-((*S*)-4-benzyl-2-thioxothiazolidin-3-yl)-5-((*tert*-butyldimethylsilyl)oxy)-3-hydroxyhexan-1-one **77** (196 mg, 18 %, 0.43 mmol) and (3*S*,5*S*)-1-((*S*)-4-benzyl-2-

thioxothiazolidin-3-yl)-5-((*tert*-butyldimethylsilyl)oxy)-3-hydroxyhexan-1-one **76** (326 mg, 30 %, 0.7 mmol) as yellow oils respectively.

(3*R*,5*S*)-1-((*S*)-4-benzyl-2-thioxothiazolidin-3-yl)-5-((*tert*-butyldimethylsilyl)oxy)-3-hydroxyhexan-1-one **77**:  $\delta_{\text{H}}$  (500 MHz; CDCl<sub>3</sub>) 7.36-7.27 (5H, m, ArH), 5.41 (1H, ddd, *J* 10.5, 7.0 and 4.0, CHN), 4.38 (1H, tt, *J* 9.5 and 3.0, CHOH), 4.18 (1H, quin.d, *J* 6.5 and 3.5, CHOSi), 3.59 (1H, br. s, OH), 3.48 (1H, dd, *J* 17.5 and 9.0, CH<sub>2</sub>CON), 3.39 (1H, dd, *J* 11.5 and 7.5, CH<sub>2</sub>S), 3.36 (1H, dd, *J* 17.5 and 3.5, CH<sub>2</sub>CON), 3.23 (1H, dd, *J* 13.0 and 4.0, CH<sub>2</sub>Ar), 3.04 (1H, dd, *J* 13.0 and 10.5, CH<sub>2</sub>Ar), 2.89 (1H, d, *J* 11.5, CH<sub>2</sub>S), 1.68 (1H, ddd, *J* 14.0, 10.0 and 3.0, CHCH<sub>2</sub>CHOH), 1.53 (1H, ddd, *J* 14.0, 7.5 and 2.5, CHCH<sub>2</sub>CHOH), 1.21 (3H, d, *J* 6.5, CH<sub>3</sub>CH), 0.89 (9H, s, C(CH<sub>3</sub>)<sub>3</sub>), 0.10 (3H, s, SiCH<sub>3</sub>), 0.09 (3H, s, SiCH<sub>3</sub>);  $\delta_{\text{C}}$  (125 MHz, CDCl<sub>3</sub>) 201.5 (CS<sub>2</sub>), 173.3 (CON), 136.6 (ArC<sub>quat</sub>), 129.6 (ArC), 129.1 (ArC), 127.4 (ArC), 68.5 (CHN), 66.4 (CHOSi), 65.3 (CHOH), 46.4 (CH<sub>2</sub>CON), 45.0 (CHCH<sub>2</sub>CHOH), 37.0 (CH<sub>2</sub>Ar), 32.1 (CH<sub>2</sub>S), 26.1 (C(CH<sub>3</sub>)<sub>3</sub>), 23.8 (CHCH<sub>3</sub>), 18.2 (C(CH<sub>3</sub>)<sub>3</sub>), -4.3 (SiCH<sub>3</sub>), -4.7 (SiCH<sub>3</sub>); HRMS (ESI) cald. for C<sub>22</sub>H<sub>36</sub>NO<sub>3</sub>S<sub>2</sub>Si (M + H<sup>+</sup>) requires 454.1900, found 454.1905.

(3*S*,5*S*)-1-((*S*)-4-benzyl-2-thioxothiazolidin-3-yl)-5-((*tert*-butyldimethylsilyl)oxy)-3-hydroxyhexan-1-one **76**:  $\delta_{\text{H}}$  (500 MHz; CDCl<sub>3</sub>) 7.36-7.25 (5H, m, ArH), 5.40 (1H, ddd, *J* 11.0, 7.0 and 4.0, CHN), 4.36 (1H, tt, *J* 8.5 and 3.5, CHOH), 4.12 (1H, dqd., *J* 8.5, 6.0 and 4.5, CHOSi), 3.52 (1H, br. s, OH), 3.50 (1H, dd, *J* 17.5 and 3.5, CH<sub>2</sub>CON), 3.39 (1H, dd, *J* 11.5 and 7.0, CH<sub>2</sub>S), 3.28 (1H, dd, *J* 17.5 and 8.5, CH<sub>2</sub>CON), 3.23 (1H, dd, *J* 13.5 and 4.0, CH<sub>2</sub>Ar), 3.04 (1H, dd, *J* 13.5 and 10.5, CH<sub>2</sub>Ar), 2.88 (1H, d, *J* 11.5, CH<sub>2</sub>S), 1.73 (1H, dt, *J* 14.0 and 9.0, CHCH<sub>2</sub>CHOH), 1.62 (1H, dt, *J* 14.0 and 4.0, CHCH<sub>2</sub>CHOH), 1.21 (3H, d, *J* 6.5, CH<sub>3</sub>CH), 0.89 (9H, s, C(CH<sub>3</sub>)<sub>3</sub>), 0.12 (3H, s, SiCH<sub>3</sub>), 0.10 (3H, s, SiCH<sub>3</sub>);  $\delta_{\text{C}}$  (125 MHz, CDCl<sub>3</sub>) 201.5 (CS<sub>2</sub>), 172.6 (CON), 136.7 (ArC<sub>quat</sub>), 129.6 (ArC), 129.1 (ArC), 127.4 (ArC), 68.8 (CHOSi), 68.6 (CHN), 67.2 (CHOH), 46.3 (CH<sub>2</sub>CON), 45.6 (CHCH<sub>2</sub>CHOH), 36.9 (CH<sub>2</sub>Ar), 32.2 (CH<sub>2</sub>S), 26.0 (C(CH<sub>3</sub>)<sub>3</sub>), 24.4 (CHCH<sub>3</sub>), 18.1 (C(CH<sub>3</sub>)<sub>3</sub>), -3.8 (SiCH<sub>3</sub>), -4.6 (SiCH<sub>3</sub>); HRMS (ESI) cald. for C<sub>22</sub>H<sub>35</sub>NNaO<sub>3</sub>S<sub>2</sub>Si (M + Na<sup>+</sup>) requires 476.1720, found 476.1724. Spectroscopic data for both compounds was consistent with that previously reported in the literature.<sup>251</sup> The relative stereochemistry of each aldol product was further confirmed by comparison of diagnostic proton shifts to those described previously in the literature.<sup>154</sup>

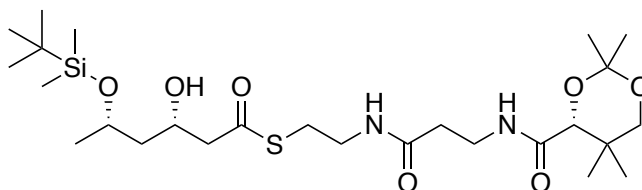
***S*-(2-(3-((*R*)-2,2,5,5-tetramethyl-1,3-dioxane-4-carboxamido)propanamido) ethyl) (3*R*,5*S*)-5-((*tert*-butyldimethylsilyl)oxy)-3-hydroxyhexanethioate (80)**



Procedure modified from Gao *et al.*<sup>251</sup> To a stirred solution of (3*R*,5*S*)-1-((*S*)-4-benzyl-2-thioxothiazolidin-3-yl)-5-((*tert*-butyldimethylsilyl)oxy)-3-hydroxyhexan-1-one **77** (150 mg, 0.33 mmol, 1.0 equiv.) in acetonitrile (5 mL), was added K<sub>2</sub>CO<sub>3</sub> (63 mg, 0.33 mmol, 1.0 equiv.) and (3*R*)-*N*-(3-((2-mercaptoethyl)amino)-3-oxopropyl)-2,2,5,5-tetramethyl-1,3-dioxane-4-carboxamide **61** (106 mg, 0.33 mmol, 1.0 equiv.). The mixture was stirred at RT for 1 h before being quenched by the addition of saturated NH<sub>4</sub>Cl solution (1 mL). The acetonitrile was then removed *in vacuo* and the resulting solution extracted with EtOAc (3 × 10 mL). The combined organics were washed with brine, dried (MgSO<sub>4</sub>), filtered and concentrated *in vacuo* to give a crude oil which was purified by silica chromatography (1 : 10 MeOH : CH<sub>2</sub>Cl<sub>2</sub>) to give the product as a colourless oil (128 mg, 70 %, 0.23 mmol).

$\nu_{\max}/\text{cm}^{-1}$  (neat) 3323 (OH), 2956 (NH), 1656 (C=O), 1530 (C=O), 1099 (C-O);  $\delta_{\text{H}}$  (500 MHz; CDCl<sub>3</sub>) 7.02 (1H, br. t, *J* 6.0, CHCONH), 6.32 (1H, br. s, NHCH<sub>2</sub>CH<sub>2</sub>S), 4.43-4.38 (1H, m, CHOH), 4.17 (1H, quin.d, *J* 6.0 and 3.5, CHOSi), 4.06 (1H, s, CHCONH), 3.83 (1H, br. s, OH), 3.67 (1H, d, *J* 11.5, CH<sub>2</sub>OC(CH<sub>3</sub>)<sub>2</sub>), 3.60-3.35 (4H, m, NHCH<sub>2</sub>, CH<sub>2</sub>CH<sub>2</sub>S), 3.27 (1H, d, *J* 11.5, CH<sub>2</sub>OC(CH<sub>3</sub>)<sub>2</sub>), 3.05 (1H, dt, *J* 14.0 and 6.5, CH<sub>2</sub>S), 3.01 (1H, dt, *J* 14.0 and 6.5, CH<sub>2</sub>S), 2.75 (1H, dd, *J* 15.0 and 8.5, CH<sub>2</sub>COS), 2.65 (1H, dd, *J* 15.0 and 4.0, CH<sub>2</sub>COS), 2.40 (2H, t, *J* 6.5, CH<sub>2</sub>CONH), 1.65 (1H, ddd, *J* 14.0, 9.5 and 4.0, CH<sub>2</sub>CHOSi), 1.50 (1H, ddd, *J* 14.0, 6.5 and 2.5, CH<sub>2</sub>CHOSi), 1.45 (3H, s, OC(CH<sub>3</sub>)<sub>2</sub>), 1.41 (3H, s, OC(CH<sub>3</sub>)<sub>2</sub>), 1.21 (3H, d, *J* 6.0, CHCH<sub>3</sub>), 1.02 (3H, s, CH<sub>2</sub>C(CH<sub>3</sub>)<sub>2</sub>), 0.96 (3H, s, CH<sub>2</sub>C(CH<sub>3</sub>)<sub>2</sub>), 0.88 (9H, s, C(CH<sub>3</sub>)<sub>3</sub>), 0.08 (3H, s, SiCH<sub>3</sub>), 0.07 (3H, s, SiCH<sub>3</sub>);  $\delta_{\text{C}}$  (125 MHz, CDCl<sub>3</sub>) 198.5 (CO<sub>2</sub>S), 171.4 (CH<sub>2</sub>CONH), 170.4 (CHCONH), 99.3 (OC(CH<sub>3</sub>)<sub>2</sub>), 77.3 (CH), 71.6 (CH<sub>2</sub>OC(CH<sub>3</sub>)<sub>2</sub>), 70.0 (CHOSi), 66.0 (CHOH), 51.9 (CH<sub>2</sub>COS), 44.4 (CH<sub>2</sub>CHOSi), 39.4 (CH<sub>2</sub>CH<sub>2</sub>S), 36.2 (CH<sub>2</sub>CONH), 35.0 (CH<sub>2</sub>NH), 33.1 (CH<sub>2</sub>C(CH<sub>3</sub>)<sub>2</sub>), 29.6 (OC(CH<sub>3</sub>)<sub>2</sub>), 28.9 (CH<sub>2</sub>S), 26.0 (C(CH<sub>3</sub>)<sub>3</sub>), 23.3 (CHCH<sub>3</sub>), 22.3 (CH<sub>2</sub>C(CH<sub>3</sub>)<sub>2</sub>), 19.1 (CH<sub>2</sub>C(CH<sub>3</sub>)<sub>2</sub>), 18.9 (OC(CH<sub>3</sub>)<sub>2</sub>), 18.1 (C(CH<sub>3</sub>)<sub>3</sub>), -4.3 (SiCH<sub>3</sub>), -4.8 (SiCH<sub>3</sub>); HRMS (ESI) cald. for C<sub>26</sub>H<sub>50</sub>N<sub>2</sub>NaO<sub>7</sub>SSi (M + Na<sup>+</sup>) requires 585.3000, found 585.3004;  $[\alpha]_{\text{D}}^{26}$  (c 0.3, CHCl<sub>3</sub>): +40.

***S*-(2-(3-((*R*)-2,2,5,5-tetramethyl-1,3-dioxane-4-carboxamido)propanamido)ethyl) (3*S*,5*S*)-5-((*tert*-butyldimethylsilyl)oxy)-3-hydroxyhexanethioate (270)**



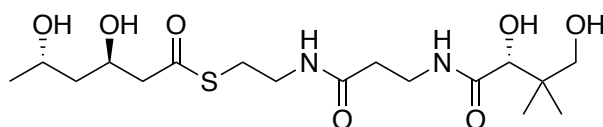
*S*-(2-(3-((*R*)-2,2,5,5-tetramethyl-1,3-dioxane-4-carboxamido)propanamido)ethyl) (3*S*,5*S*)-5-((*tert*-butyldimethylsilyl)oxy)-3-hydroxyhexanethioate **270** was synthesized using the same procedure as that used for the synthesis of *S*-(2-(3-((*R*)-2,2,5,5-tetramethyl-1,3-dioxane-4-carboxamido)propanamido)ethyl) (3*R*,5*S*)-5-((*tert*-butyldimethylsilyl)oxy)-3-hydroxyhexanethioate **80** using (3*S*,5*S*)-1-((*S*)-4-benzyl-2-thioxothiazolidin-3-yl)-5-((*tert*-butyldimethylsilyl)oxy)-3-hydroxyhexan-1-one **76** (200 mg, 0.44 mmol), to afford the product as a colourless oil (179 mg, 78 %, 0.38 mmol).

$\nu_{\max}/\text{cm}^{-1}$  (neat) 3320 (OH), 2953 (NH), 1655 (C=O), 1529 (C=O), 1098 (C=O);  $\delta_{\text{H}}$  (500 MHz;  $\text{CDCl}_3$ ) 7.01 (1H, br. t,  $J$  6.0, CHCONH), 6.20 (1H, br. t,  $J$  6.0, NHCH<sub>2</sub>CH<sub>2</sub>S), 4.25 (1H, tt,  $J$  8.0 and 4.0, CHOH), 4.11-4.04 (2H, m, CHOSi, CHCONH), 3.86 (1H, br. s, OH), 3.67 (1H, d,  $J$  11.5, CH<sub>2</sub>OC(CH<sub>3</sub>)<sub>2</sub>), 3.60-3.41 (4H, m, NHCH<sub>2</sub>, CH<sub>2</sub>CH<sub>2</sub>S), 3.28 (1H, d,  $J$  11.5, CH<sub>2</sub>OC(CH<sub>3</sub>)<sub>2</sub>), 3.07 (1H, dt,  $J$  14.0 and 6.0, CH<sub>2</sub>S), 3.02 (1H, dt,  $J$  14.0 and 6.0, CH<sub>2</sub>S), 2.75 (1H, dd,  $J$  15.0 and 8.0, CH<sub>2</sub>COS), 2.68 (1H, dd,  $J$  15.0 and 4.5, CH<sub>2</sub>COS) 2.42 (1H, dt,  $J$  15.0 and 6.5, CH<sub>2</sub>CONH), 2.39 (1H, dt,  $J$  15.0 and 6.5, CH<sub>2</sub>CONH), 1.67 (1H, dt,  $J$  14 and 9, CH<sub>2</sub>CHOSi), 1.58 (1H, dt,  $J$  14.0 and 4.0, CH<sub>2</sub>CHOSi), 1.46 (3H, s, OC(CH<sub>3</sub>)<sub>2</sub>), 1.42 (3H, s, OC(CH<sub>3</sub>)<sub>2</sub>), 1.18 (3H, d,  $J$  6.0, CHCH<sub>3</sub>), 1.04 (3H, s, CH<sub>2</sub>C(CH<sub>3</sub>)<sub>2</sub>), 0.97 (3H, s, CH<sub>2</sub>C(CH<sub>3</sub>)<sub>2</sub>), 0.89 (9H, s, C(CH<sub>3</sub>)<sub>3</sub>), 0.11 (3H, s, SiCH<sub>3</sub>), 0.10 (3H, s, SiCH<sub>3</sub>);  $\delta_{\text{C}}$  (125 MHz,  $\text{CDCl}_3$ ) 198.4 (CO<sub>2</sub>S), 171.3 (CH<sub>2</sub>CONH), 170.4 (CHCONH), 99.3 (OC(CH<sub>3</sub>)<sub>2</sub>), 77.3 (CH), 71.6 (CH<sub>2</sub>OC(CH<sub>3</sub>)<sub>2</sub>), 69.0 (CHOSi), 68.2 (CHOH), 51.6 (CH<sub>2</sub>COS), 45.6 (CH<sub>2</sub>CHOSi), 39.5 (CH<sub>2</sub>CH<sub>2</sub>S), 36.2 (CH<sub>2</sub>CONH), 35.1 (CH<sub>2</sub>NH), 33.1 (CH<sub>2</sub>C(CH<sub>3</sub>)<sub>2</sub>), 29.7 (OC(CH<sub>3</sub>)<sub>2</sub>), 28.9 (CH<sub>2</sub>S), 26.0 (C(CH<sub>3</sub>)<sub>3</sub>), 24.5 (CHCH<sub>3</sub>), 22.4 (CH<sub>2</sub>C(CH<sub>3</sub>)<sub>2</sub>), 19.1 (CH<sub>2</sub>C(CH<sub>3</sub>)<sub>2</sub>), 18.9 (OC(CH<sub>3</sub>)<sub>2</sub>), 18.1 (C(CH<sub>3</sub>)<sub>3</sub>), -3.8 (SiCH<sub>3</sub>), -4.6 (SiCH<sub>3</sub>); HRMS (ESI) cald. for C<sub>26</sub>H<sub>50</sub>N<sub>2</sub>NaO<sub>7</sub>SSi (M + Na<sup>+</sup>) requires 585.3000, found 585.3004;  $[\alpha]_{\text{D}}^{26}$  (c 0.1,  $\text{CHCl}_3$ ): +64.



**(2-(3-((*R*)-2,4-dihydroxy-3,3-dimethylbutanamido)propanamido)ethyl)**  
**dihydroxyhexanethioate (71)**

**(3*R*,5*S*)-3,5-**

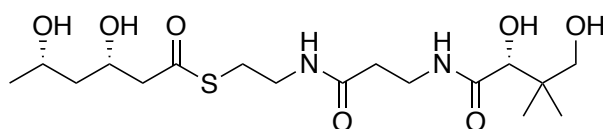


*S*-(2-(3-((*R*)-2,2,5,5-tetramethyl-1,3-dioxane-4-carboxamido)propanamido)ethyl) (3*R*,5*S*)-5-((*tert*-butyldimethylsilyl)oxy)-3-hydroxyhexanethioate **80** (100 mg, 0.18 mmol, 1.0 equiv.) was stirred in a 2:1 ratio of AcOH/H<sub>2</sub>O (3 mL) at RT for 16 h. The reaction was then concentrated *in vacuo* and purified by silica chromatography (15 : 85 MeOH : CH<sub>2</sub>Cl<sub>2</sub>) to afford the desired product as a colourless oil (51 mg, 70 %, 0.13 mmol).

$\nu_{\max}/\text{cm}^{-1}$  (neat) 3380 (OH), 2960 (NH), 1654 (C=O), 1528 (C=O);  $\delta_{\text{H}}$  (500 MHz; CD<sub>3</sub>OD) 4.28 (1H, quin., *J* 6.5, CH<sub>2</sub>CHOHCH<sub>2</sub>), 3.97 (1H, sext., *J* 6.0, CH<sub>3</sub>CHOH), 3.89 (1H, s, CHCONH), 3.54-3.30 (6H, m, NHCH<sub>2</sub>, CH<sub>2</sub>CH<sub>2</sub>S, CH<sub>2</sub>OH), 3.02 (2H, t, *J* 6.5, CH<sub>2</sub>S), 2.74 (1H, dd, *J* 15.0 and 7.5, CH<sub>2</sub>COS), 2.71 (1H, dd, *J* 15.0 and 6.0, CH<sub>2</sub>COS) 2.41 (2H, t, *J* 7.0, CH<sub>2</sub>CONH), 1.53 (2H, dd, *J* 7.0 and 5.5, CH<sub>3</sub>CH<sub>2</sub>CHOH), 1.18 (3H, d, *J* 6.5, CHCH<sub>3</sub>), 0.92 (6H, s, C(CH<sub>3</sub>)<sub>2</sub>);  $\delta_{\text{C}}$  (125 MHz, CD<sub>3</sub>OD) 198.7 (CO<sub>2</sub>S), 176.1 (CH<sub>2</sub>CONH), 174.0 (CHCONH), 77.3 (CHOHC(CH<sub>3</sub>)<sub>2</sub>), 70.4 (CH<sub>2</sub>OH), 66.9 (CH<sub>2</sub>CHOHCH<sub>2</sub>), 65.1 (CH<sub>3</sub>CHOH), 53.1 (CH<sub>2</sub>COS), 46.8 (CHOHCH<sub>2</sub>CHOH), 40.4 (CH<sub>2</sub>C(CH<sub>3</sub>)<sub>2</sub>), 40.0 (CH<sub>2</sub>CH<sub>2</sub>S), 36.4 (CH<sub>2</sub>CONH), 36.3 (CH<sub>2</sub>NH), 29.3 (CH<sub>2</sub>S), 24.3 (CHCH<sub>3</sub>), 21.3 (CH<sub>2</sub>C(CH<sub>3</sub>)<sub>2</sub>), 20.9 (CH<sub>2</sub>C(CH<sub>3</sub>)<sub>2</sub>); HRMS (ESI) cald. for C<sub>17</sub>H<sub>32</sub>N<sub>2</sub>NaO<sub>7</sub>S (M + Na<sup>+</sup>) requires 431.1822, found 431.1824;  $[\alpha]_{\text{D}}^{26}$  (c 0.3, CHCl<sub>3</sub>): +8.2.

***S*-(2-(3-((*R*)-2,4-dihydroxy-3,3-dimethylbutanamido)propanamido)ethyl)**  
**dihydroxyhexanethioate (78)**

**(3*S*,5*S*)-3,5-**

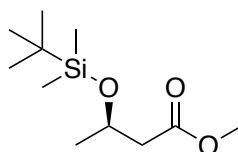


*S*-(2-(3-((*R*)-2,4-dihydroxy-3,3-dimethylbutanamido)propanamido)ethyl) (3*S*,5*S*)-3,5-dihydroxyhexanethioate **78** was synthesized using the same procedure as that used for the synthesis of (2-(3-((*R*)-2,4-dihydroxy-3,3-dimethylbutanamido)propanamido)ethyl) (3*R*,5*S*)-3,5-dihydroxyhexanethioate **71** using *S*-(2-(3-((*R*)-2,2,5,5-tetramethyl-1,3-dioxane-4-carboxamido)propanamido)ethyl) (3*S*,5*S*)-5-((*tert*-butyldimethylsilyl)oxy)-3-

hydroxyhexanethioate **270** (100 mg, 0.18 mmol), to afford the product as a colourless oil (70 mg, 96 %, 0.17 mmol).

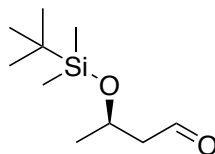
$\nu_{\text{max}}/\text{cm}^{-1}$  (neat) 3326 (OH), 2966 (NH), 1647 (C=O), 1560 (C=O);  $\delta_{\text{H}}$  (500 MHz; CD<sub>3</sub>OD) 4.21 (1H, tt,  $J$  8.5 and 5.5, CH<sub>2</sub>CHOHCH<sub>2</sub>), 3.93 (1H, dqin.,  $J$  7.5 and 6.0, CH<sub>3</sub>CHOH), 3.89 (1H, s, CHCONH), 3.53-3.33 (6H, m, NHCH<sub>2</sub>, CH<sub>2</sub>CH<sub>2</sub>S, CH<sub>2</sub>OH), 3.04 (1H, dt,  $J$  13.5 and 6.5, CH<sub>2</sub>S), 3.01 (1H, dt,  $J$  13.5 and 6.5, CH<sub>2</sub>S), 2.76 (1H, dd,  $J$  15.0 and 5.0, CH<sub>2</sub>COS), 2.72 (1H, dd,  $J$  15.0 and 7.5, CH<sub>2</sub>COS) 2.41 (2H, t,  $J$  7.0, CH<sub>2</sub>CONH), 1.66 (1H, dt,  $J$  14.0 and 8.0, CHOHC<sub>2</sub>CHOH), 1.55 (1H, dt,  $J$  14.0 and 5.0, CHOHC<sub>2</sub>CHOH), 1.18 (3H, d,  $J$  6.0, CHCH<sub>3</sub>), 0.92 (6H, s, C(CH<sub>3</sub>)<sub>2</sub>);  $\delta_{\text{C}}$  (125 MHz, CD<sub>3</sub>OD) 198.7 (CO<sub>2</sub>S), 176.1 (CH<sub>2</sub>CONH), 174.0 (CHCONH), 77.3 (CHOHC(CH<sub>3</sub>)<sub>2</sub>), 70.3 (CH<sub>2</sub>OH), 68.2 (CH<sub>2</sub>CHOHCH<sub>2</sub>), 66.8 (CH<sub>3</sub>CHOH), 52.6 (CH<sub>2</sub>COS), 46.3 (CHOHC<sub>2</sub>CHOH), 40.4 (CH<sub>2</sub>C(CH<sub>3</sub>)<sub>2</sub>), 40.0 (CH<sub>2</sub>CH<sub>2</sub>S), 36.4 (CH<sub>2</sub>CONH), 36.3 (CH<sub>2</sub>NH), 29.3 (CH<sub>2</sub>S), 23.5 (CHCH<sub>3</sub>), 21.3 (CH<sub>2</sub>C(CH<sub>3</sub>)<sub>2</sub>), 20.9 (CH<sub>2</sub>C(CH<sub>3</sub>)<sub>2</sub>); HRMS (ESI) cald. for C<sub>17</sub>H<sub>32</sub>N<sub>2</sub>NaO<sub>7</sub>S (M + Na<sup>+</sup>) requires 431.1822, found 431.1821;  $[\alpha]_{\text{D}}^{26}$  (c 0.35, CHCl<sub>3</sub>): +17.7.

#### Methyl (*R*)-3-((*tert*-butyldimethylsilyl)oxy)butanoate (**271**)



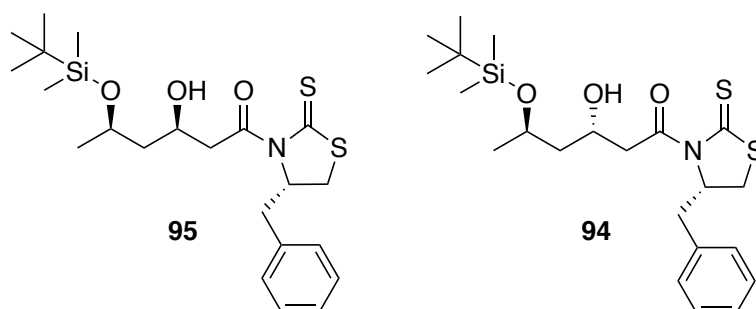
Methyl (*R*)-3-((*tert*-butyldimethylsilyl)oxy)butanoate **271** was synthesized using the same procedure as that used for the synthesis of Methyl (*S*)-3-((*tert*-butyldimethylsilyl)oxy)butanoate **79** using (*R*)-3-hydroxybutanoate (2.50 g, 21.2 mmol). The product was observed as a colourless oil (4.01 g, 82 %, 17.3 mmol). Spectroscopic data was identical to that of Methyl (*S*)-3-((*tert*-butyldimethylsilyl)oxy)butanoate **79** and consistent with that previously reported in the literature.<sup>252</sup>

**(*R*)-3-((*tert*-butyldimethylsilyl)oxy)butanal (**93**)**



(*R*)-3-((*tert*-butyldimethylsilyl)oxy)butanal **93** was synthesized using the same procedure as that used for the synthesis of (*S*)-3-((*tert*-butyldimethylsilyl)oxy)butanal **74** using methyl (*R*)-3-((*tert*-butyldimethylsilyl)oxy)butanoate **271** (1.84 g, 7.5 mmol). The product was observed as a colourless oil (1.32 g, 82 %, 6.15 mmol). Spectroscopic data was identical to that of (*S*)-3-((*tert*-butyldimethylsilyl)oxy)butanal **74** and consistent with that previously reported in the literature.<sup>253</sup>

**(3*R*,5*R*)-1-((*S*)-4-benzyl-2-thioxothiazolidin-3-yl)-5-((*tert*-butyldimethylsilyl)oxy)-3-hydroxyhexan-1-one and (3*S*,5*R*)-1-((*S*)-4-benzyl-2-thioxothiazolidin-3-yl)-5-((*tert*-butyldimethylsilyl)oxy)-3-hydroxyhexan-1-one (**95** and **94**)**

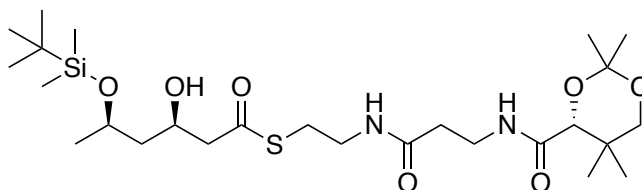


(3*R*,5*R*)-1-((*S*)-4-benzyl-2-thioxothiazolidin-3-yl)-5-((*tert*-butyldimethylsilyl)oxy)-3-hydroxyhexan-1-one **95** and (3*S*,5*R*)-1-((*S*)-4-benzyl-2-thioxothiazolidin-3-yl)-5-((*tert*-butyldimethylsilyl)oxy)-3-hydroxyhexan-1-one **94** were synthesized using the same procedure as that used for the synthesis of (3*R*,5*S*)-1-((*S*)-4-benzyl-2-thioxothiazolidin-3-yl)-5-((*tert*-butyldimethylsilyl)oxy)-3-hydroxyhexan-1-one **77** and (3*S*,5*S*)-1-((*S*)-4-benzyl-2-thioxothiazolidin-3-yl)-5-((*tert*-butyldimethylsilyl)oxy)-3-hydroxyhexan-1-one **76**, using (*R*)-3-((*tert*-butyldimethylsilyl)oxy)butanal **93** (900 mg, 4.4 mmol) to afford the products (3*R*,5*R*)-1-((*S*)-4-benzyl-2-thioxothiazolidin-3-yl)-5-((*tert*-butyldimethylsilyl)oxy)-3-hydroxyhexan-1-one **95** (488 mg, 27 %, 1.2 mmol) and (3*S*,5*R*)-1-((*S*)-4-benzyl-2-thioxothiazolidin-3-yl)-5-((*tert*-butyldimethylsilyl)oxy)-3-hydroxyhexan-1-one **94** (436 mg, 24 %, 1.05 mmol).

(3*R*,5*R*)-1-((*S*)-4-benzyl-2-thioxothiazolidin-3-yl)-5-((*tert*-butyldimethylsilyl)oxy)-3-hydroxy hexan-1-one **95**:  $\nu_{\max}/\text{cm}^{-1}$  (neat) 3498 (OH), 2955 (ArH), 1689 (C=O);  $\delta_{\text{H}}$  (500 MHz; CDCl<sub>3</sub>) 7.37-7.27 (5H, m, ArH), 5.38 (1H, ddd, *J* 11.0, 7.5 and 4.0, CHN), 4.26 (1H, dddd, *J* 9.5, 6.5, 6.0 and 4.0, CHOH), 4.10 (1H, dquin., *J* 8.5 and 6.0, CHOSi), 3.63 (1H, br. d, *J* 2.5, OH), 3.47 (1H, dd, *J* 17.5 and 7.0, CH<sub>2</sub>CON), 3.43 (1H, dd, *J* 17.5 and 5.5, CH<sub>2</sub>CON), 3.38 (1H, dd, *J* 11.5 and 7.5, CH<sub>2</sub>S), 3.24 (1H, dd, *J* 13.5 and 3.5, CH<sub>2</sub>Ar), 3.04 (1H, dd, *J* 13.5 and 10.5, CH<sub>2</sub>Ar), 2.89 (1H, d, *J* 11.5, CH<sub>2</sub>S), 1.74 (1H, dt, *J* 14.0 and 8.5, CHCH<sub>2</sub>CHOH), 1.61 (1H, ddd, *J* 14.0, 4.5 and 3.5, CHCH<sub>2</sub>CHOH), 1.19 (3H, d, *J* 6.0, CH<sub>3</sub>CH), 0.89 (9H, s, C(CH<sub>3</sub>)<sub>3</sub>), 0.10 (3H, s, SiCH<sub>3</sub>), 0.07 (3H, s, SiCH<sub>3</sub>);  $\delta_{\text{C}}$  (125 MHz, CDCl<sub>3</sub>) 201.6 (CS<sub>2</sub>), 173.2 (CON), 136.8 (ArC<sub>quat</sub>), 129.8 (ArC), 129.3 (ArC), 127.6 (ArC), 68.8 (CHN), 68.6 (CHOSi), 67.2 (CHOH), 46.1 (CH<sub>2</sub>CON), 45.8 (CHCH<sub>2</sub>CHOH), 37.1 (CH<sub>2</sub>Ar), 32.3 (CH<sub>2</sub>S), 26.2 (C(CH<sub>3</sub>)<sub>3</sub>), 24.4 (CHCH<sub>3</sub>), 18.3 (C(CH<sub>3</sub>)<sub>3</sub>), -3.7 (SiCH<sub>3</sub>), -4.6 (SiCH<sub>3</sub>); HRMS (ESI) cald. for C<sub>22</sub>H<sub>35</sub>NNaO<sub>3</sub>S<sub>2</sub>Si (M + Na<sup>+</sup>) requires 476.1720, found 476.1723;  $[\alpha]_{\text{D}}^{26}$  (c 0.15, CHCl<sub>3</sub>): +101.

(3*S*,5*R*)-1-((*S*)-4-benzyl-2-thioxothiazolidin-3-yl)-5-((*tert*-butyldimethylsilyl)oxy)-3-hydroxyhexan-1-one **94**:  $\nu_{\max}/\text{cm}^{-1}$  (neat) 3501 (OH), 2954 (ArH), 1689 (C=O);  $\delta_{\text{H}}$  (500 MHz; CDCl<sub>3</sub>) 7.36-7.25 (5H, m, ArH), 5.39 (1H, ddd, *J* 11.0, 7.0 and 4.0, CHN), 4.54 (1H, tt, *J* 10.0 and 2.5, CHOH), 4.21 (1H, quin.d, *J* 6.5 and 3.5, CHOSi), 3.63 (1H, br. s, OH), 3.42 (1H, dd, *J* 17.5 and 3.0, CH<sub>2</sub>CON), 3.39 (1H, dd, *J* 11.5 and 7.0, CH<sub>2</sub>S), 3.30 (1H, dd, *J* 17.5 and 9.0, CH<sub>2</sub>CON), 3.25 (1H, dd, *J* 13.0 and 3.5, CH<sub>2</sub>Ar), 3.04 (1H, dd, *J* 13.0 and 10.5, CH<sub>2</sub>Ar), 2.88 (1H, d, *J* 11.5, CH<sub>2</sub>S), 1.73 (1H, ddd, *J* 14.0, 10.0 and 3.5, CHCH<sub>2</sub>CHOH), 1.57 (1H, ddd, *J* 14.0, 6.5 and 2.0, CHCH<sub>2</sub>CHOH), 1.25 (3H, d, *J* 6.5, CH<sub>3</sub>CH), 0.89 (9H, s, C(CH<sub>3</sub>)<sub>3</sub>), 0.11 (3H, s, SiCH<sub>3</sub>), 0.09 (3H, s, SiCH<sub>3</sub>);  $\delta_{\text{C}}$  (125 MHz, CDCl<sub>3</sub>) 201.4 (CS<sub>2</sub>), 172.6 (CON), 136.6 (ArC<sub>quat</sub>), 129.6 (ArC), 129.0 (ArC), 127.3 (ArC), 68.7 (CHN), 67.0 (CHOSi), 64.9 (CHOH), 46.7 (CH<sub>2</sub>CON), 44.2 (CHCH<sub>2</sub>CHOH), 36.8 (CH<sub>2</sub>Ar), 32.2 (CH<sub>2</sub>S), 26.0 (C(CH<sub>3</sub>)<sub>3</sub>), 23.3 (CHCH<sub>3</sub>), 18.1 (C(CH<sub>3</sub>)<sub>3</sub>), -4.3 (SiCH<sub>3</sub>), -4.8 (SiCH<sub>3</sub>); HRMS (ESI) cald. for C<sub>22</sub>H<sub>35</sub>NNaO<sub>3</sub>S<sub>2</sub>Si (M + Na<sup>+</sup>) requires 476.1720, found 476.1722;  $[\alpha]_{\text{D}}^{26}$  (c 0.1, CHCl<sub>3</sub>): +110.5.

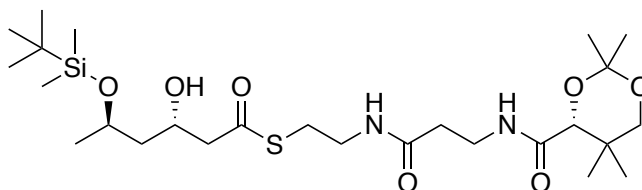
***S*-2-(3-((*R*)-2,2,5,5-tetramethyl-1,3-dioxane-4-carboxamido)propanamido)ethyl) (3*R*,5*R*)-5-((*tert*-butyldimethylsilyl)oxy)-3-hydroxyhexanethioate (**97**)**



*S*-2-(3-((*R*)-2,2,5,5-tetramethyl-1,3-dioxane-4-carboxamido)propanamido)ethyl) (3*R*,5*R*)-5-((*tert*-butyldimethylsilyl)oxy)-3-hydroxyhexanethioate **97** was synthesized using the same procedure as that used for the synthesis of *S*-2-(3-((*R*)-2,2,5,5-tetramethyl-1,3-dioxane-4-carboxamido)propanamido)ethyl) (3*R*,5*S*)-5-((*tert*-butyldimethylsilyl)oxy)-3-hydroxyhexanethioate **80** using (3*R*,5*R*)-1-((*S*)-4-benzyl-2-thioxothiazolidin-3-yl)-5-((*tert*-butyldimethylsilyl)oxy)-3-hydroxyhexan-1-one **95** (310 mg, 0.68 mmol), to afford the product as a colourless oil (243 mg, 64 %, 0.43 mmol).

$\nu_{\max}/\text{cm}^{-1}$  (neat) 3310 (OH), 2953 (NH), 1655 (C=O), 1527 (C=O);  $\delta_{\text{H}}$  (500 MHz;  $\text{CDCl}_3$ ) 7.02 (1H, br. t,  $J$  6.0, CHCONH), 6.19 (1H, br. t,  $J$  6.0, NHCH<sub>2</sub>CH<sub>2</sub>S), 4.28 (1H, tt,  $J$  8.5 and 3.5, CHOH), 4.12-4.04 (2H, m, CHOSi, CHCONH), 3.68 (1H, d  $J$  11.5, CH<sub>2</sub>OC(CH<sub>3</sub>)<sub>2</sub>), 3.60-3.40 (4H, m, NHCH<sub>2</sub>, CH<sub>2</sub>CH<sub>2</sub>S), 3.28 (1H, d  $J$  11.5, CH<sub>2</sub>OC(CH<sub>3</sub>)<sub>2</sub>), 3.07 (1H, dt,  $J$  14.0 and 6.0, CH<sub>2</sub>S), 3.02 (1H, dt,  $J$  14.0 and 6.0, CH<sub>2</sub>S), 2.75 (1H, dd,  $J$  15.0 and 8.5, CH<sub>2</sub>COS), 2.67 (1H, dd,  $J$  15.0 and 4.0, CH<sub>2</sub>COS) 2.42 (1H, dt,  $J$  15.0 and 6.5, CH<sub>2</sub>CONH), 2.40 (1H, dt,  $J$  15.0 and 6.5, CH<sub>2</sub>CONH), 1.67 (1H, dt,  $J$  14.0 and 8.5, CH<sub>2</sub>CHOSi), 1.57 (1H, dt,  $J$  14.0 and 3.5, CH<sub>2</sub>CHOSi), 1.46 (3H, s, OC(CH<sub>3</sub>)<sub>2</sub>), 1.42 (3H, s, OC(CH<sub>3</sub>)<sub>2</sub>), 1.18 (3H, d,  $J$  6.0, CHCH<sub>3</sub>), 1.04 (3H, s, CH<sub>2</sub>C(CH<sub>3</sub>)<sub>2</sub>), 0.97 (3H, s, CH<sub>2</sub>C(CH<sub>3</sub>)<sub>2</sub>), 0.89 (9H, s, C(CH<sub>3</sub>)<sub>3</sub>), 0.11 (3H, s, SiCH<sub>3</sub>), 0.10 (3H, s, SiCH<sub>3</sub>);  $\delta_{\text{C}}$  (125 MHz,  $\text{CDCl}_3$ ) 198.5 (CO<sub>2</sub>S), 171.3 (CH<sub>2</sub>CONH), 170.3 (CHCONH), 99.3 (OC(CH<sub>3</sub>)<sub>2</sub>), 77.4 (CH), 71.5 (CH<sub>2</sub>OC(CH<sub>3</sub>)<sub>2</sub>), 69.0 (CHOSi), 68.2 (CHOH), 51.6 (CH<sub>2</sub>COS), 45.7 (CH<sub>2</sub>CHOSi), 39.4 (CH<sub>2</sub>CH<sub>2</sub>S), 36.2 (CH<sub>2</sub>CONH), 35.0 (CH<sub>2</sub>NH), 33.1 (CH<sub>2</sub>C(CH<sub>3</sub>)<sub>2</sub>), 29.8 (OC(CH<sub>3</sub>)<sub>2</sub>), 28.9 (CH<sub>2</sub>S), 26.0 (C(CH<sub>3</sub>)<sub>3</sub>), 24.5 (CHCH<sub>3</sub>), 22.4 (CH<sub>2</sub>C(CH<sub>3</sub>)<sub>2</sub>), 19.1 (CH<sub>2</sub>C(CH<sub>3</sub>)<sub>2</sub>), 18.9 (OC(CH<sub>3</sub>)<sub>2</sub>), 18.1 (C(CH<sub>3</sub>)<sub>3</sub>), -3.8 (SiCH<sub>3</sub>), -4.6 (SiCH<sub>3</sub>); HRMS (ESI) cald. for C<sub>26</sub>H<sub>50</sub>N<sub>2</sub>NaO<sub>7</sub>SSi (M + Na<sup>+</sup>) requires 585.3000, found 585.3003;  $[\alpha]_{\text{D}}^{26}$  (c 0.1,  $\text{CHCl}_3$ ): +45.5.

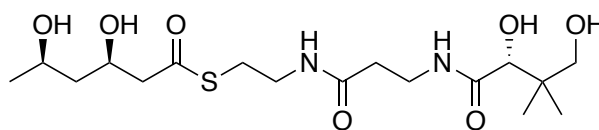
***S*-(2-(3-((*R*)-2,2,5,5-tetramethyl-1,3-dioxane-4-carboxamido)propanamido)ethyl) (3*S*,5*R*)-5-((*tert*-butyldimethylsilyl)oxy)-3-hydroxyhexanethioate (96)**



*S*-(2-(3-((*R*)-2,2,5,5-tetramethyl-1,3-dioxane-4-carboxamido)propanamido)ethyl) (3*S*,5*R*)-5-((*tert*-butyldimethylsilyl)oxy)-3-hydroxyhexanethioate **96** was synthesized using the same procedure as that used for the synthesis of *S*-(2-(3-((*R*)-2,2,5,5-tetramethyl-1,3-dioxane-4-carboxamido)propanamido)ethyl) (3*R*,5*S*)-5-((*tert*-butyldimethylsilyl)oxy)-3-hydroxyhexanethioate **80** using (3*S*,5*R*)-1-((*S*)-4-benzyl-2-thioxothiazolidin-3-yl)-5-((*tert*-butyldimethylsilyl)oxy)-3-hydroxyhexan-1-one **94** (185 mg, 0.41 mmol), to afford the product as a colourless oil (158 mg, 69 %, 0.28 mmol).

$\nu_{\max}/\text{cm}^{-1}$  (neat) 3310 (OH), 2954 (NH), 1655 (C=O), 1529 (C=O);  $\delta_{\text{H}}$  (500 MHz;  $\text{CDCl}_3$ ) 7.02 (1H, br. t,  $J$  6.5, CHCONH), 6.33 (1H, br. t,  $J$  6.0, NHCH<sub>2</sub>CH<sub>2</sub>S), 4.40 (1H, dddd,  $J$  10.0, 8.5, 4.5 and 2.5 CHOH), 4.17 (1H, quin.d,  $J$  6.5 and 3.5, CHOSi), 4.06 (1H, s, CHCONH), 3.81 (1H, br. s, OH), 3.67 (1H, d,  $J$  11.5, CH<sub>2</sub>OC(CH<sub>3</sub>)<sub>2</sub>), 3.60-3.35 (4H, m, NHCH<sub>2</sub>, CH<sub>2</sub>CH<sub>2</sub>S), 3.26 (1H, d,  $J$  11.5, CH<sub>2</sub>OC(CH<sub>3</sub>)<sub>2</sub>), 3.05 (1H, dt,  $J$  14.0 and 6.0, CH<sub>2</sub>S), 3.01 (1H, dt,  $J$  14.0 and 6.5, CH<sub>2</sub>S), 2.74 (1H, dd,  $J$  15.0 and 8.5, CH<sub>2</sub>COS), 2.66 (1H, dd,  $J$  15.0 and 4.0, CH<sub>2</sub>COS), 2.42 (1H, dt,  $J$  15.0 and 5.5, CH<sub>2</sub>CONH), 2.38 (1H, dt,  $J$  15.0 and 6.0, CH<sub>2</sub>CONH), 1.65 (1H, ddd,  $J$  14.0, 10.0 and 3.5, CH<sub>2</sub>CHOSi), 1.51 (1H, ddd,  $J$  14.0, 6.5 and 2.5, CH<sub>2</sub>CHOSi), 1.45 (3H, s, OC(CH<sub>3</sub>)<sub>2</sub>), 1.41 (3H, s, OC(CH<sub>3</sub>)<sub>2</sub>), 1.20 (3H, d,  $J$  6.5, CHCH<sub>3</sub>), 1.02 (3H, s, CH<sub>2</sub>C(CH<sub>3</sub>)<sub>2</sub>), 0.95 (3H, s, CH<sub>2</sub>C(CH<sub>3</sub>)<sub>2</sub>), 0.88 (9H, s, C(CH<sub>3</sub>)<sub>3</sub>), 0.08 (3H, s, SiCH<sub>3</sub>), 0.07 (3H, s, SiCH<sub>3</sub>);  $\delta_{\text{C}}$  (125 MHz,  $\text{CDCl}_3$ ) 198.5 (CO<sub>2</sub>S), 171.4 (CH<sub>2</sub>CONH), 170.4 (CHCONH), 99.3 (OC(CH<sub>3</sub>)<sub>2</sub>), 77.3 (CH), 71.6 (CH<sub>2</sub>OC(CH<sub>3</sub>)<sub>2</sub>), 66.9 (CHOSi), 66.0 (CHOH), 52.0 (CH<sub>2</sub>COS), 44.5 (CH<sub>2</sub>CHOSi), 39.4 (CH<sub>2</sub>CH<sub>2</sub>S), 36.2 (CH<sub>2</sub>CONH), 35.1 (CH<sub>2</sub>NH), 33.1 (CH<sub>2</sub>C(CH<sub>3</sub>)<sub>2</sub>), 29.6 (OC(CH<sub>3</sub>)<sub>2</sub>), 28.9 (CH<sub>2</sub>S), 26.0 (C(CH<sub>3</sub>)<sub>3</sub>), 23.3 (CHCH<sub>3</sub>), 22.3 (CH<sub>2</sub>C(CH<sub>3</sub>)<sub>2</sub>), 19.1 (CH<sub>2</sub>C(CH<sub>3</sub>)<sub>2</sub>), 18.9 (OC(CH<sub>3</sub>)<sub>2</sub>), 18.1 (C(CH<sub>3</sub>)<sub>3</sub>), -4.3 (SiCH<sub>3</sub>), -4.8 (SiCH<sub>3</sub>); HRMS (ESI) calcd. for C<sub>26</sub>H<sub>50</sub>N<sub>2</sub>NaO<sub>7</sub>SSi (M + Na<sup>+</sup>) requires 585.3000, found 585.3007;  $[\alpha]_{\text{D}}^{26}$  (c 0.15,  $\text{CHCl}_3$ ): +27.7.

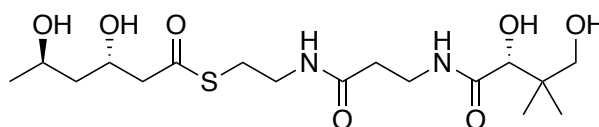
***S*-(2-(3-((*R*)-2,4-dihydroxy-3,3-dimethylbutanamido)propanamido)ethyl) (3*R*,5*R*)-3,5-dihydroxyhexanethioate (92)**



*S*-(2-(3-((*R*)-2,4-dihydroxy-3,3-dimethylbutanamido)propanamido)ethyl) (3*R*,5*R*)-3,5-dihydroxyhexanethioate **92** was synthesized using the same procedure as that used for the synthesis of (2-(3-((*R*)-2,4-dihydroxy-3,3-dimethylbutanamido)propanamido) ethyl) (3*R*,5*S*)-3,5-dihydroxyhexanethioate **71** using *S*-(2-(3-((*R*)-2,2,5,5-tetramethyl-1,3-dioxane-4-carboxamido)propanamido)ethyl) (3*R*,5*R*)-5-((*tert*-butyldimethylsilyl)oxy)-3-hydroxyhexanethioate **97** (100 mg, 0.18 mmol), to afford the product as a colourless oil (61 mg, 83 %, 0.15 mmol).

$\nu_{\max}/\text{cm}^{-1}$  (neat) 3344 (OH), 2960 (NH), 1647 (C=O), 1560 (C=O);  $\delta_{\text{H}}$  (500 MHz; CD<sub>3</sub>OD) 4.21 (1H, tt, *J* 8.5 and 5.0, CH<sub>2</sub>CHOHCH<sub>2</sub>), 3.93 (1H, dqin., *J* 8.0 and 6.0, CH<sub>3</sub>CHOH), 3.89 (1H, s, CHCONH), 3.53-3.32 (6H, m, NHCH<sub>2</sub>, CH<sub>2</sub>CH<sub>2</sub>S, CH<sub>2</sub>OH), 3.02 (2H, t, *J* 6.5, CH<sub>2</sub>S), 2.76 (1H, dd, *J* 15.0 and 5.0, CH<sub>2</sub>COS), 2.72 (1H, dd, *J* 15.0 and 7.5, CH<sub>2</sub>COS), 2.41 (2H, t, *J* 6.5, CH<sub>2</sub>CONH), 1.66 (1H, dt, *J* 14.0 and 8.0, CH<sub>3</sub>CH<sub>2</sub>CHOH), 1.55 (1H, dt, *J* 14.0 and 5.0, CH<sub>3</sub>CH<sub>2</sub>CHOH), 1.18 (3H, d, *J* 6.0, CHCH<sub>3</sub>), 0.92 (6H, s, C(CH<sub>3</sub>)<sub>2</sub>);  $\delta_{\text{C}}$  (125 MHz, CD<sub>3</sub>OD) 198.7 (CO<sub>2</sub>S), 176.1 (CH<sub>2</sub>CONH), 174.0 (CHCONH), 77.3 (CHOHC(CH<sub>3</sub>)<sub>2</sub>), 70.3 (CH<sub>2</sub>OH), 68.2 (CH<sub>2</sub>CHOHCH<sub>2</sub>), 66.8 (CH<sub>3</sub>CHOH), 52.6 (CH<sub>2</sub>COS), 46.3 (CHOHCH<sub>2</sub>CHOH), 40.4 (CH<sub>2</sub>C(CH<sub>3</sub>)<sub>2</sub>), 40.0 (CH<sub>2</sub>CH<sub>2</sub>S), 36.4 (CH<sub>2</sub>CONH), 36.3 (CH<sub>2</sub>NH), 29.3 (CH<sub>2</sub>S), 23.6 (CHCH<sub>3</sub>), 21.3 (CH<sub>2</sub>C(CH<sub>3</sub>)<sub>2</sub>), 20.9 (CH<sub>2</sub>C(CH<sub>3</sub>)<sub>2</sub>); HRMS (ESI) cald. for C<sub>17</sub>H<sub>32</sub>N<sub>2</sub>NaO<sub>7</sub>S (M + Na<sup>+</sup>) requires 431.1822, found 431.1822;  $[\alpha]_{\text{D}}^{26}$  (c 0.45, CHCl<sub>3</sub>): +3.9.

***S*-(2-(3-((*R*)-2,4-dihydroxy-3,3-dimethylbutanamido)propanamido)ethyl) (3*S*,5*R*)-3,5-dihydroxyhexanethioate (91)**

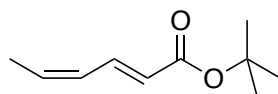


*S*-(2-(3-((*R*)-2,4-dihydroxy-3,3-dimethylbutanamido)propanamido)ethyl) (3*S*,5*R*)-3,5-dihydroxyhexanethioate **91** was synthesized using the same procedure as that used for the synthesis of (2-(3-((*R*)-2,4-dihydroxy-3,3-dimethylbutanamido)propanamido) ethyl) (3*R*,5*S*)-3,5-dihydroxyhexanethioate **71** using *S*-(2-(3-((*R*)-2,2,5,5-tetramethyl-1,3-dioxane-4-

carboxamido)propanamido)ethyl)(3*S*,5*R*)-5-((*tert*-butyldimethylsilyl)oxy)-3-hydroxyhexanethioate **96** (100 mg, 0.18 mmol), to afford the product as a colourless oil (54 mg, 74 %, 0.13 mmol).

$\nu_{\text{max}}/\text{cm}^{-1}$  (neat) 3328 (OH), 2964 (NH), 1648 (C=O), 1543 (C=O);  $\delta_{\text{H}}$  (500 MHz; CD<sub>3</sub>OD) 4.28 (1H, quintet, *J* 6.5, CH<sub>2</sub>CHOHCH<sub>2</sub>), 3.97 (1H, sextet, *J* 6.0, CH<sub>3</sub>CHOH), 3.89 (1H, s, CHCONH), 3.53-3.32 (6H, m, NHCH<sub>2</sub>, CH<sub>2</sub>CH<sub>2</sub>S, CH<sub>2</sub>OH), 3.02 (2H, t, *J* 6.5, CH<sub>2</sub>S), 2.74 (1H, dd, *J* 15.0 and 7.5, CH<sub>2</sub>COS), 2.71 (1H, dd, *J* 15.0 and 5.5, CH<sub>2</sub>COS) 2.41 (2H, t, *J* 7.0, CH<sub>2</sub>CONH), 1.53 (2H, dd, *J* 6.5 and 5.5, CH<sub>3</sub>CH<sub>2</sub>CHOH), 1.18 (3H, d, *J* 6.5, CHCH<sub>3</sub>), 0.92 (6H, s, C(CH<sub>3</sub>)<sub>2</sub>);  $\delta_{\text{C}}$  (125 MHz, CD<sub>3</sub>OD) 198.6 (CO<sub>2</sub>S), 176.1 (CH<sub>2</sub>CONH), 173.9 (CHCONH), 77.3 (CHOHC(CH<sub>3</sub>)<sub>2</sub>), 70.3 (CH<sub>2</sub>OH), 66.8 (CH<sub>2</sub>CHOHCH<sub>2</sub>), 65.1 (CH<sub>3</sub>CHOH), 53.1 (CH<sub>2</sub>COS), 46.8 (CHOHCH<sub>2</sub>CHOH), 40.4 (CH<sub>2</sub>C(CH<sub>3</sub>)<sub>2</sub>), 40.0 (CH<sub>2</sub>CH<sub>2</sub>S), 36.4 (CH<sub>2</sub>CONH), 36.3 (CH<sub>2</sub>NH), 29.3 (CH<sub>2</sub>S), 24.3 (CHCH<sub>3</sub>), 21.3 (CH<sub>2</sub>C(CH<sub>3</sub>)<sub>2</sub>), 20.9 (CH<sub>2</sub>C(CH<sub>3</sub>)<sub>2</sub>); HRMS (ESI) cald. for C<sub>17</sub>H<sub>32</sub>N<sub>2</sub>NaO<sub>7</sub>S (M + Na<sup>+</sup>) requires 431.1822, found 431.1822;  $[\alpha]_{\text{D}}^{26}$  (c 0.5, CHCl<sub>3</sub>): +5.3.

#### ***tert*-butyl (2*E*,4*Z*)-hexa-2,4-dienoate (85)**

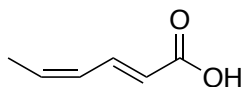


Procedure modified from Davies *et al.*<sup>155</sup> To a stirred solution of *tert*-butyl acrylate (16.9 g, 18.9 mL, 132 mmol, 2.0 equiv.), *cis*-bromopropene (8.0 g, 5.6 mL, 66 mmol, 1.0 equiv.), K<sub>2</sub>CO<sub>3</sub> (22.8 g, 165 mmol, 2.5 equiv.), triphenylphosphine (1.73 g, 6.6 mmol, 0.1 equiv.) and Bu<sub>4</sub>NHSO<sub>4</sub> (22.4 g, 66 mmol, 1.0 equiv.) in MeCN/H<sub>2</sub>O (10 : 1, 100 mL) under an Ar atmosphere was added palladium acetate (739 mg, 3.3 mmol, 0.05 equiv.). The mixture was heated to 50 °C for 48 h, then allowed to cool to RT and filtered through Celite<sup>®</sup>, eluting with ether (250 mL). The resulting organic solution was washed with H<sub>2</sub>O (150 mL) then brine (150 mL), dried (MgSO<sub>4</sub>), filtered and concentrated *in vacuo*. The crude material was purified by silica chromatography (1 : 200 Et<sub>2</sub>O : petroleum ether) to afford the products as a colourless oil (2.70 g, 24 %, 16 mmol).

$\delta_{\text{H}}$  (500 MHz; CDCl<sub>3</sub>) 7.55 (1H, ddd, *J* 15.0, 11.5 and 0.5, CHCHCO), 6.15-6.09 (1H, m, CH<sub>3</sub>CHCH), 5.88 (1H, dqt, *J* 11.0, 7.0 and 1.0, CH<sub>3</sub>CH), 5.80 (1H, d, *J* 15.5, CHCO), 1.87 (3H, dd, *J* 7.0 and 1.5, CH<sub>3</sub>CH), 1.50 (9H, s, C(CH<sub>3</sub>)<sub>3</sub>);  $\delta_{\text{C}}$  (125 MHz, CDCl<sub>3</sub>) 166.9 (CO), 138.3 (CHCHCO), 135.2 (CH<sub>3</sub>CH), 127.6 (CH<sub>3</sub>CHCH), 123.1 (CHCO), 80.4 (C(CH<sub>3</sub>)<sub>3</sub>), 28.3 (C(CH<sub>3</sub>)<sub>3</sub>), 14.1 (CH<sub>3</sub>CH); HRMS (ESI) cald. for C<sub>10</sub>H<sub>16</sub>NaO<sub>2</sub> (M + Na<sup>+</sup>) requires 191.1048, found 191.1050. Spectroscopic data consistent with that previously reported in the literature.<sup>155</sup>



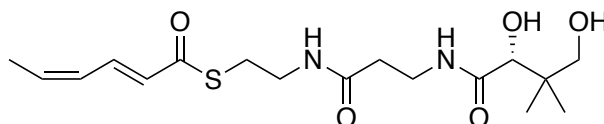
**(2E,4Z)-hexa-2,4-dienoic acid (82)**



Procedure modified from Davies *et al.*<sup>155</sup> To a stirred solution of (2E,4Z)-*tert*-butyl hex-2,4-dienoate **85** (2.50 g, 14.9 mmol, 1.0 equiv.) in CH<sub>2</sub>Cl<sub>2</sub> (25 mL) at 0 °C was added TFA (25 mL) dropwise. The mixture was stirred for 30 min at RT and the volatile material removed *in vacuo*. Purification via silica chromatography (3 : 1 EtO : petroleum ether) afforded the product as a yellow oil (1.53 g, 92 %, 13.7 mmol, 94 : 6 dr).

$\delta_{\text{H}}$  (500 MHz; CDCl<sub>3</sub>) 7.74 (1H, ddd, J 15.0, 12.0 and 0.5, CHCHCO), 6.22-6.16 (1H, m, CH<sub>3</sub>CHCH), 6.00 (1H, dqt, J 11.0, 7.0 and 0.5, CH<sub>3</sub>CH), 5.80 (1H, d, J 15.0, CHCO), 1.91 (3H, dd, J 7.0 and 1.5, CH<sub>3</sub>CH);  $\delta_{\text{C}}$  (125 MHz, CDCl<sub>3</sub>) 172.8 (CO), 141.7 (CHCHCO), 137.4 (CH<sub>3</sub>CH), 127.4 (CH<sub>3</sub>CHCH), 120.2 (CHCO), 14.3 (CH<sub>3</sub>CH). Spectroscopic data consistent with that previously reported in the literature.<sup>155</sup>

**S-(2-(3-((R)-2,4-dihydroxy-3,3-dimethylbutanamido)propanamido)ethyl) (2E,4Z)-hexa-2,4-dienethioate (72)**

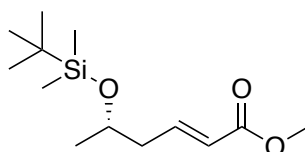


To a stirred solution of (2E,4Z)-hex-2,4-dienoic acid **82** (50 mg, 0.45 mmol, 1.0 equiv.) in CH<sub>2</sub>Cl<sub>2</sub> (5 mL) was added oxalyl chloride (40  $\mu$ L, 0.45 mmol, 1.0 equiv.) drop-wise, followed by 2 drops of DMF. The reaction was stirred for 2 h after which time the reaction was added drop-wise to a pre-stirred mixture of (*R*)-2,4-dihydroxy-*N*-(3-((2-mercaptoethyl)amino)-3-oxopropyl)-3,3-dimethylbutanamide **84** (125 mg, 0.45 mmol, 1.0 equiv.) and TEA (0.06 mL, 0.45 mmol, 1.0 equiv.) in dry THF (1 mL). The reaction was then stirred at RT for 1 h under an inert atmosphere before being concentrated *in vacuo*. The resulting orange oil was purified by silica chromatography (1 : 10 MeOH ; EtOAc) to afford the product as a yellow oil (23 mg, 14 %, 0.06 mmol 4 : 1 *E,Z* : *E,E*).

$\nu_{\text{max}}/\text{cm}^{-1}$  (neat) 3355 (OH), 2976 (NH), 2921 (C=C-H), 1636, 1543 (C=O);  $\delta_{\text{H}}$  (500 MHz; CD<sub>3</sub>OD) 7.61 (1H, dd, J 15.0 and 11.5, CHCHCOS), 6.17 (1H, t, J 11.0, CH<sub>3</sub>CHCH), 6.15 (1H, d, J 15.0, CHCOS), 6.07 (1H, dq, J 11.0 and 7.0 CH<sub>3</sub>CH), 3.89 (1H, s, CHCONH), 3.53-3.33 (6H, m, NHCH<sub>2</sub>, CH<sub>2</sub>CH<sub>2</sub>S, CH<sub>2</sub>OH), 3.10 (2H, t, J 7.0, CH<sub>2</sub>S), 2.41 (2H, t, J 6.5,

CH<sub>2</sub>CONH), 1.90 (3H, dd, *J* 7.0 and 1.5, CHCH<sub>3</sub>), 0.92 (6H, s, C(CH<sub>3</sub>)<sub>2</sub>); δ<sub>C</sub> (125 MHz, CD<sub>3</sub>OD) 191.3 (CO<sub>2</sub>S), 176.1 (CH<sub>2</sub>CONH), 173.9 (CHCONH), 138.9 (CHCHCOS), 136.5 (CH<sub>3</sub>CH), 128.8 (CH<sub>3</sub>CHCH), 128.3 (CHCOS), 77.3 (CH), 70.4 (CH<sub>2</sub>OH), 40.4 (CH<sub>2</sub>C(CH<sub>3</sub>)<sub>2</sub>), 40.2 (CH<sub>2</sub>CH<sub>2</sub>S), 36.4 (CH<sub>2</sub>CONH), 36.3 (CH<sub>2</sub>NH), 29.1 (CH<sub>2</sub>S), 21.3 (CH<sub>2</sub>C(CH<sub>3</sub>)<sub>2</sub>), 20.9 (CH<sub>2</sub>C(CH<sub>3</sub>)<sub>2</sub>), 14.2 (CHCH<sub>3</sub>); HRMS (ESI) cald. for C<sub>17</sub>H<sub>28</sub>N<sub>2</sub>NaO<sub>5</sub>S (M + Na<sup>+</sup>) requires 395.1611, found 395.1613; [α]<sub>D</sub><sup>28</sup> (c 0.3, CHCl<sub>3</sub>): +28.9.

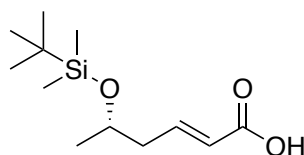
**Methyl (*S,E*)-5-((*tert*-butyldimethylsilyl)oxy)hex-2-enoate (88)**



Procedure modified from Ohta *et al.*<sup>254</sup> To a solution of (*S*)-3-((*tert*-butyldimethylsilyl)oxy)butanal **74** (610 mg, 3.0 mmol, 1.0 equiv.) in dry toluene (25 mL) was added methoxycarbonylmethylenetriphenylphosphorane (1.10 g, 3.3 mmol, 1.1 equiv.) and the mixture heated to reflux for 16 hours. The precipitate was removed by filtration and the filtrate concentrated *in vacuo* to afford a colourless oil, which was purified by silica chromatography (3:10 Et<sub>2</sub>O:Petroleum ether) to afford the desired product as a colourless oil (723 mg, 94 %, 2.82 mmol).

δ<sub>H</sub> (500 MHz; CDCl<sub>3</sub>) 6.96 (1H, dt, *J* 15.5 and 7.5, CH<sub>2</sub>CHCH), 5.84 (1H, dt, *J* 15.5 and 1.5, CH<sub>2</sub>CHCH), 4.35 (1H, sext., *J* 6.0, CH), 3.72 (3H, s, OCH<sub>3</sub>), 2.37-2.27 (2H, m, CH<sub>2</sub>), 1.15 (3H, d, *J* 6.0, CH<sub>3</sub>), 0.88 (9H, s, C(CH<sub>3</sub>)<sub>3</sub>), 0.04 (3H, s, SiCH<sub>3</sub>), 0.04 (3H, s, SiCH<sub>3</sub>); δ<sub>C</sub> (125 MHz, CDCl<sub>3</sub>) 167.3 (COOCH<sub>3</sub>), 146.7 (CH<sub>2</sub>CHCH), 123.2 (CH<sub>2</sub>CHCH), 68.0 (CH), 51.8 (OCH<sub>3</sub>), 42.8 (CH<sub>2</sub>), 26.2 (C(CH<sub>3</sub>)<sub>3</sub>), 24.1 (CH<sub>3</sub>), 18.5 (C(CH<sub>3</sub>)<sub>3</sub>), -4.2 (SiCH<sub>3</sub>), -4.4 (SiCH<sub>3</sub>)<sub>3</sub>; HRMS (ESI) cald. for C<sub>13</sub>H<sub>26</sub>NaO<sub>3</sub>Si (M + Na<sup>+</sup>) requires 281.1543, found 281.1543. Spectroscopic data consistent with that previously reported in the literature.<sup>254</sup>

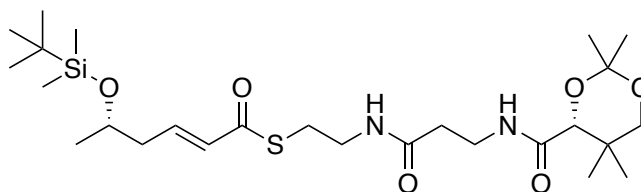
**(*S,E*)-5-((*tert*-butyldimethylsilyl)oxy)hex-2-enoic acid (**89**)**



To a solution of methyl (*S,E*)-5-((*tert*-butyldimethylsilyl)oxy)hex-2-enoate **88** (510 mg, 2.0 mmol, 1.0 equiv.) in a 5:3 mixture of THF (10 mL) and water (6 mL), was added LiOH (80 mg, 4.0 mmol, 2.0 equiv.) and the reaction stirred for 16 hours. THF was removed *in vacuo* and the resulting solution acidified to pH 2.0 using 1 M HCl. The mixture was then extracted with CH<sub>2</sub>Cl<sub>2</sub> (3 x 10 mL), the combined organics washed with brine (10 mL), dried (MgSO<sub>4</sub>) and concentrated *in vacuo* to afford the product as a colourless oil (391 mg, 81 %, 1.62 mmol).

$\delta_{\text{H}}$  (500 MHz; CDCl<sub>3</sub>) 7.07 (1H, dt, *J* 15.5 and 7.5, CH<sub>2</sub>CHCH), 5.84 (1H, dt, *J* 15.5 and 1.5, CH<sub>2</sub>CHCH), 3.94 (1H, sext., *J* 6.0, CH), 2.40-2.30 (2H, m, CH<sub>2</sub>), 1.17 (3H, d, *J* 6.0, CH<sub>3</sub>), 0.88 (9H, s, C(CH<sub>3</sub>)<sub>3</sub>), 0.05 (3H, s, SiCH<sub>3</sub>), 0.04 (3H, s, SiCH<sub>3</sub>);  $\delta_{\text{C}}$  (125 MHz, CDCl<sub>3</sub>) 171.4 (COOH), 149.4 (CH<sub>2</sub>CHCH), 122.8 (CH<sub>2</sub>CHCH), 67.9 (CH), 42.9 (CH<sub>2</sub>), 26.2 (C(CH<sub>3</sub>)<sub>3</sub>), 24.2 (CH<sub>3</sub>), 18.5 (C(CH<sub>3</sub>)<sub>3</sub>), -4.2 (SiCH<sub>3</sub>), -4.4 (SiCH<sub>3</sub>); HRMS (ESI) cald. for C<sub>12</sub>H<sub>23</sub>O<sub>3</sub>Si (M - H<sup>+</sup>) requires 243.1422, found 243.1420. Spectroscopic data consistent with that previously reported in the literature.<sup>254</sup>

***S*-(2-(3-((*R*)-2,2,5,5-tetramethyl-1,3-dioxane-4-carboxamido)propanamido) ethyl) (*S,E*)-5-((*tert*-butyldimethylsilyl)oxy)hex-2-enethioate (**90**)**

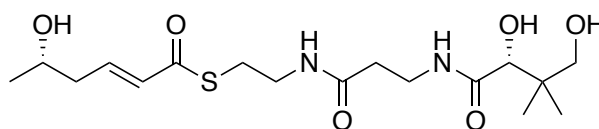


To a solution of (*S,E*)-5-((*tert*-butyldimethylsilyl)oxy)hex-2-enoic acid **89** (60 mg, 0.25 mmol, 1.3 equiv.), (*R*)-*N*-(3-((2-mercaptoethyl)amino)-3-oxopropyl)-2,2,5,5-tetramethyl-1,3-dioxane-4-carboxamide **61** (85 mg, 0.27 mmol, 1.4 equiv.) and DMAP (7 mg, 0.06 mmol, 0.3 equiv.) in CH<sub>2</sub>Cl<sub>2</sub> (4 mL) was added EDC.HCl (52 mg, 0.27 mmol, 1.4 equiv.) at 0 °C, and the mixture allowed to stir at RT for 16 hours. The mixture was then diluted with CH<sub>2</sub>Cl<sub>2</sub> (10 mL), washed with 1 M HCl (10 mL), saturated NaHCO<sub>3</sub> solution (10 mL), dried (MgSO<sub>4</sub>) and concentrated *in*

*vacuo* to give a colourless oil which was purified by silica chromatography (1:99 MeOH:CH<sub>2</sub>Cl<sub>2</sub>) to afford the desired product as a colourless oil (108 mg, 80 %, 0.15 mmol).

$\nu_{\max}/\text{cm}^{-1}$  (neat) 3304 (NH), 2953 (C=C-H), 1664 (C=O), 1525 (C=O);  $\delta_{\text{H}}$  (500 MHz; CDCl<sub>3</sub>) 7.03 (1H, br. t, *J* 5.5, NH), 6.92 (1H, dt, *J* 15.5 and 7.5, CHCHCOS), 6.14 (1H, br. s, NHCH<sub>2</sub>CH<sub>2</sub>S), 6.13 (1H, dt, *J* 15.5 and 1.5, CHCHCOS), 4.07 (1H, s, CHCONH), 3.93 (1H, sext., *J* 6.0, CHOSi), 3.68 (1H, d *J* 11.5, CH<sub>2</sub>OC(CH<sub>3</sub>)<sub>2</sub>), 3.61-3.39 (4H, m, NHCH<sub>2</sub>, CH<sub>2</sub>CH<sub>2</sub>S), 3.27 (1H, d *J* 11.5, CH<sub>2</sub>OC(CH<sub>3</sub>)<sub>2</sub>), 3.08 (2H, t, *J* 6.5, CH<sub>2</sub>S), 2.42 (2H, t, *J* 6.5, CH<sub>2</sub>CONH), 2.32 (2H, td, *J* 6.5 and 0.5, CH<sub>2</sub>CHOSi), 1.46 (3H, s, OC(CH<sub>3</sub>)<sub>2</sub>), 1.41 (3H, s, OC(CH<sub>3</sub>)<sub>2</sub>), 1.16 (3H, d, *J* 6.0, CHCH<sub>3</sub>), 1.03 (3H, s, CH<sub>2</sub>C(CH<sub>3</sub>)<sub>2</sub>), 0.97 (3H, s, CH<sub>2</sub>C(CH<sub>3</sub>)<sub>2</sub>), 0.88 (9H, s, C(CH<sub>3</sub>)<sub>3</sub>), 0.05 (3H, s, SiCH<sub>3</sub>), 0.04 (3H, s, SiCH<sub>3</sub>);  $\delta_{\text{C}}$  (125 MHz, CDCl<sub>3</sub>) 190.3 (CO<sub>2</sub>S), 171.6 (CH<sub>2</sub>CONH), 170.5 (CHCONH), 144.0 (CHCHCOS), 130.5 (CHCHCOS), 99.5 (OC(CH<sub>3</sub>)<sub>2</sub>), 77.5 (CH), 71.9 (CH<sub>2</sub>OC(CH<sub>3</sub>)<sub>2</sub>), 67.9 (CHOSi), 42.8 (CH<sub>2</sub>CHOSi), 40.1 (CH<sub>2</sub>CH<sub>2</sub>S), 36.3 (CH<sub>2</sub>CONH), 35.1 (CH<sub>2</sub>NH), 33.4 (CH<sub>2</sub>C(CH<sub>3</sub>)<sub>2</sub>), 29.9 (OC(CH<sub>3</sub>)<sub>2</sub>), 28.6 (CH<sub>2</sub>S), 26.2 (C(CH<sub>3</sub>)<sub>3</sub>), 24.3 (CHCH<sub>3</sub>), 22.5 (CH<sub>2</sub>C(CH<sub>3</sub>)<sub>2</sub>), 19.3 (CH<sub>2</sub>C(CH<sub>3</sub>)<sub>2</sub>), 19.1 (OC(CH<sub>3</sub>)<sub>2</sub>), 18.4 (C(CH<sub>3</sub>)<sub>3</sub>), -4.1 (SiCH<sub>3</sub>), -4.4 (SiCH<sub>3</sub>); HRMS (ESI) cald. for C<sub>26</sub>H<sub>48</sub>N<sub>2</sub>NaO<sub>6</sub>SSi (M + Na<sup>+</sup>) requires 567.2895, found 567.2901;  $[\alpha]_{\text{D}}^{26}$  (c 0.2, CHCl<sub>3</sub>): +37.5.

***S*-(2-(3-((*R*)-2,4-dihydroxy-3,3-dimethylbutanamido)propanamido)ethyl) (*S,E*)-5-hydroxyhex-2-enethioate (86)**

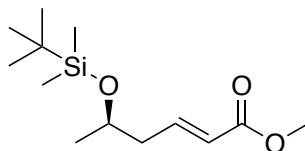


*S*-(2-(3-((*R*)-2,2,5,5-tetramethyl-1,3-dioxane-4-carboxamido)propanamido)ethyl) (*S,E*)-5-((*tert*-butyldimethylsilyloxy)hex-2-enethioate **90** (100 mg, 0.18 mmol, 1.0 equiv.) was stirred in a 2:1 ratio of AcOH/H<sub>2</sub>O (3 mL) at RT for 16 h. The reaction was then concentrated in *vacuo* and purified by silica chromatography (1 : 9 MeOH : CH<sub>2</sub>Cl<sub>2</sub>) to afford the desired product as a colourless oil (63 mg, 88 %, 0.16 mmol).

$\nu_{\max}/\text{cm}^{-1}$  (neat) 3310 (OH), 2967 (C=C-H), 1644 (C=O), 1534 (C=O);  $\delta_{\text{H}}$  (500 MHz; CD<sub>3</sub>OD) 6.96 (1H, dt, *J* 15.5 and 7.5, CHCHCOS), 6.23 (1H, dt, *J* 15.5 and 1.5, CHCHCOS), 3.91 (1H, sextet, *J* 6.5, CHOH), 3.91 (1H, s, CHCONH), 3.55-3.32 (6H, m, CH<sub>2</sub>OH, NHCH<sub>2</sub>, CH<sub>2</sub>CH<sub>2</sub>S), 3.09 (2H, t, *J* 6.5, CH<sub>2</sub>S), 2.43 (2H, t, *J* 6.5, CH<sub>2</sub>CONH), 2.38-2.34 (2H, m, CH<sub>2</sub>CHOH), 1.16 (3H, d, *J* 6.0, CHCH<sub>3</sub>), 1.03 (3H, s, CH<sub>2</sub>C(CH<sub>3</sub>)<sub>2</sub>), 0.94 (6H, s, CH<sub>2</sub>C(CH<sub>3</sub>)<sub>2</sub>);  $\delta_{\text{C}}$  (125 MHz, CDCl<sub>3</sub>) 191.3 (CO<sub>2</sub>S), 176.4 (CHCONH), 174.2 (CH<sub>2</sub>CONH), 144.3 (CHCHCOS), 131.6 (CHCHCOS), 77.6 (CHONH), 70.6 (CH<sub>2</sub>OC(CH<sub>3</sub>)<sub>2</sub>), 67.8 (CHOH), 42.9 (CH<sub>2</sub>CHOH), 40.7

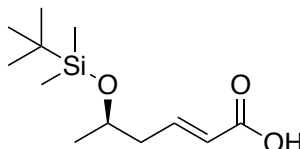
(CH<sub>2</sub>C(CH<sub>3</sub>)<sub>2</sub>), 40.5 (CH<sub>2</sub>CH<sub>2</sub>S), 36.7 (CH<sub>2</sub>NH), 36.6 (CH<sub>2</sub>CONH), 29.2 (CH<sub>2</sub>S), 23.7 (CHCH<sub>3</sub>), 21.6 (CH<sub>2</sub>C(CH<sub>3</sub>)<sub>2</sub>), 21.2 (CH<sub>2</sub>C(CH<sub>3</sub>)<sub>2</sub>); HRMS (ESI) calcd. for C<sub>17</sub>H<sub>30</sub>N<sub>2</sub>NaO<sub>6</sub>S (M + Na<sup>+</sup>) requires 413.1717, found 413.1717; [α]<sub>D</sub><sup>26</sup> (c 0.2, CHCl<sub>3</sub>): +8.5.

**Methyl (*R,E*)-5-((*tert*-butyldimethylsilyl)oxy)hex-2-enoate (**101**)**



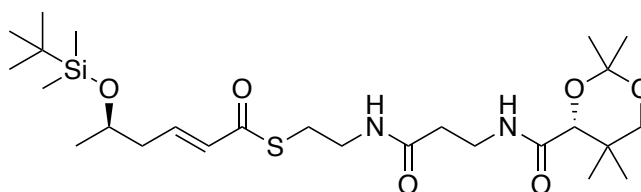
Methyl (*R,E*)-5-((*tert*-butyldimethylsilyl)oxy)hex-2-enoate **101** was synthesized using the same procedure as that used for the synthesis of methyl (*S,E*)-5-((*tert*-butyldimethylsilyl)oxy)hex-2-enoate **88** using (*R*)-3-((*tert*-butyldimethylsilyl)oxy)butanal **93** (1.22 g, 5.98 mmol) to afford the desired product as a colourless oil (1.32 g, 86 %, 5.14 mmol). Spectroscopic data was identical to that of methyl (*S,E*)-5-((*tert*-butyldimethylsilyl)oxy)hex-2-enoate **88** and consistent with that previously reported in the literature.<sup>254</sup>

**(*R,E*)-5-((*tert*-butyldimethylsilyl)oxy)hex-2-enoic acid (**102**)**



(*R,E*)-5-((*tert*-butyldimethylsilyl)oxy)hex-2-enoic acid **102** was synthesized using the same procedure as that used for the synthesis of (*S,E*)-5-((*tert*-butyldimethylsilyl)oxy)hex-2-enoic acid **89** using methyl (*R,E*)-5-((*tert*-butyldimethylsilyl)oxy)hex-2-enoate **101** (170 mg, 0.66 mmol) to afford the product as a colourless oil (88 mg, 55 %, 0.36 mmol). Spectroscopic data was identical to that of (*S,E*)-5-((*tert*-butyldimethylsilyl)oxy)hex-2-enoic acid **89** and consistent with that previously reported in the literature.<sup>254</sup>

***S*-(2-(3-((*R*)-2,2,5,5-tetramethyl-1,3-dioxane-4-carboxamido)propanamido)ethyl) (*R,E*)-5-((*tert*-butyldimethylsilyl)oxy)hex-2-enethioate (**103**)**

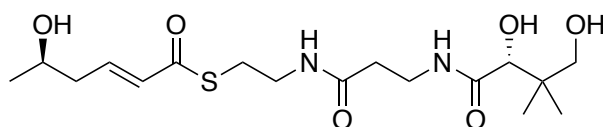


*S*-(2-(3-((*R*)-2,2,5,5-tetramethyl-1,3-dioxane-4-carboxamido)propanamido)ethyl) (*R,E*)-5-((*tert*-butyldimethylsilyl)oxy)hex-2-enethioate **103** was synthesized using the same procedure as that used for the synthesis of *S*-(2-(3-((*R*)-2,2,5,5-tetramethyl-1,3-dioxane-4-carboxamido)propanamido)ethyl)(*S,E*)-5-((*tert*-butyldimethylsilyl)oxy) hex-2-enethioate **90** using (*R,E*)-5-((*tert*-butyldimethylsilyl)oxy)hex-2-enoic acid **102** (180 mg, 0.74 mmol), to afford the product as a colourless oil (296 mg, 73 %, 0.54 mmol).

$\nu_{\text{max}}/\text{cm}^{-1}$  (neat) 3339 (NH), 2953 (C=C-H), 1660 (C=O);  $\delta_{\text{H}}$  (500 MHz;  $\text{CDCl}_3$ ) 7.03 (1H, br. t,  $J$  5.5, NH), 6.94 (1H, dt,  $J$  15.5 and 7.5, CHCHCOS), 6.14 (1H, br. s, NHCH<sub>2</sub>CH<sub>2</sub>S), 6.12 (1H, dt,  $J$  15.5 and 1.5, CHCHCOS), 4.07 (1H, s, CHCONH), 3.93 (1H, sext.,  $J$  6.0, CHOSi), 3.68 (1H, d,  $J$  11.5, CH<sub>2</sub>OC(CH<sub>3</sub>)<sub>2</sub>), 3.60-3.39 (4H, m, NHCH<sub>2</sub>, CH<sub>2</sub>CH<sub>2</sub>S), 3.29 (1H, d,  $J$  11.5, CH<sub>2</sub>OC(CH<sub>3</sub>)<sub>2</sub>), 3.08 (2H, t,  $J$  6.5, CH<sub>2</sub>S), 2.40 (2H, t,  $J$  6.5, CH<sub>2</sub>CONH), 2.32 (2H, td,  $J$  6.5 and 0.5, CH<sub>2</sub>CHOSi), 1.46 (3H, s, OC(CH<sub>3</sub>)<sub>2</sub>), 1.41 (3H, s, OC(CH<sub>3</sub>)<sub>2</sub>), 1.16 (3H, d,  $J$  6.0, CHCH<sub>3</sub>), 1.03 (3H, s, CH<sub>2</sub>C(CH<sub>3</sub>)<sub>2</sub>), 0.97 (3H, s, CH<sub>2</sub>C(CH<sub>3</sub>)<sub>2</sub>), 0.88 (9H, s, C(CH<sub>3</sub>)<sub>3</sub>), 0.04 (3H, s, SiCH<sub>3</sub>), 0.04 (3H, s, SiCH<sub>3</sub>);  $\delta_{\text{C}}$  (125 MHz,  $\text{CDCl}_3$ ) 190.2 (CO<sub>2</sub>S), 171.6 (CH<sub>2</sub>CONH), 170.4 (CHCONH), 144.0 (CHCHCOS), 130.5 (CHCHCOS), 99.5 (OC(CH<sub>3</sub>)<sub>2</sub>), 77.4 (CH), 71.9 (CH<sub>2</sub>OC(CH<sub>3</sub>)<sub>2</sub>), 67.9 (CHOSi), 42.8 (CH<sub>2</sub>CHOSi), 40.0 (CH<sub>2</sub>CH<sub>2</sub>S), 36.3 (CH<sub>2</sub>CONH), 35.1 (CH<sub>2</sub>NH), 33.6 (CH<sub>2</sub>C(CH<sub>3</sub>)<sub>2</sub>), 29.9 (OC(CH<sub>3</sub>)<sub>2</sub>), 28.6 (CH<sub>2</sub>S), 26.2 (C(CH<sub>3</sub>)<sub>3</sub>), 24.3 (CHCH<sub>3</sub>), 22.5 (CH<sub>2</sub>C(CH<sub>3</sub>)<sub>2</sub>), 19.2 (CH<sub>2</sub>C(CH<sub>3</sub>)<sub>2</sub>), 19.1 (OC(CH<sub>3</sub>)<sub>2</sub>), 18.4 (C(CH<sub>3</sub>)<sub>3</sub>), -4.1 (SiCH<sub>3</sub>), -4.3 (SiCH<sub>3</sub>); HRMS (ESI) cald. for C<sub>26</sub>H<sub>48</sub>N<sub>2</sub>NaO<sub>6</sub>SSi (M + Na<sup>+</sup>) requires 567.2895, found 567.2896;  $[\alpha]_{\text{D}}^{26}$  (c 0.2, CHCl<sub>3</sub>): +17.5.

***S*-(2-(3-((*R*)-2,4-dihydroxy-3,3-dimethylbutanamido)propanamido)ethyl) hydroxyhex-2-enethioate (**98**)**

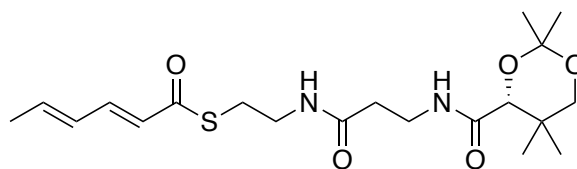
**(*R,E*)-5-**



*S*-(2-(3-((*R*)-2,4-dihydroxy-3,3-dimethylbutanamido)propanamido)ethyl) (*R,E*)-5-hydroxyhex-2-enethioate **98** was synthesized using the same procedure as that used for the synthesis of *S*-(2-(3-((*R*)-2,4-dihydroxy-3,3-dimethylbutanamido)propanamido)ethyl)(*S,E*)-5-hydroxyhex-2-enethioate **86** using *S*-(2-(3-((*R*)-2,2,5,5-tetramethyl-1,3-dioxane-4-carboxamido)propanamido)ethyl) (*R,E*)-5-((*tert*-butyldimethylsilyl)oxy) hex-2-enethioate **103** (100 mg, 0.18 mmol), to afford the product as a colourless oil (60 mg, 84 %, 0.15 mmol).

$\nu_{\max}/\text{cm}^{-1}$  (neat) 3327 (OH), 2966 (C=C-H), 1655 (C=O), 1561 (C=O);  $\delta_{\text{H}}$  (500 MHz; CD<sub>3</sub>OD) 6.96 (1H, dt, *J* 15.5 and 7.5, CHCHCOS), 6.23 (1H, dt, *J* 15.5 and 1.5, CHCHCOS), 3.89 (1H, sext., *J* 6.5, CHOH), 3.91 (1H, s, CHCONH), 3.53-3.33 (6H, m, CH<sub>2</sub>OH, NHCH<sub>2</sub>, CH<sub>2</sub>CH<sub>2</sub>S), 3.07 (2H, t, *J* 6.5, CH<sub>2</sub>S), 2.41 (2H, t, *J* 6.5, CH<sub>2</sub>CONH), 2.36-2.32 (2H, m, CH<sub>2</sub>CHOH), 1.18 (3H, d, *J* 6.5, CHCH<sub>3</sub>), 1.03 (3H, s, CH<sub>2</sub>C(CH<sub>3</sub>)<sub>2</sub>), 0.92 (6H, s, CH<sub>2</sub>C(CH<sub>3</sub>)<sub>2</sub>);  $\delta_{\text{C}}$  (125 MHz, CDCl<sub>3</sub>) 190.9 (CO<sub>2</sub>S), 176.1 (CHCONH), 173.9 (CH<sub>2</sub>CONH), 143.9 (CHCHCOS), 131.3 (CHCHCOS), 77.3 (CHONH), 70.3 (CH<sub>2</sub>OC(CH<sub>3</sub>)<sub>2</sub>), 67.4 (CHOH), 42.6 (CH<sub>2</sub>CHOH), 40.4 (CH<sub>2</sub>C(CH<sub>3</sub>)<sub>2</sub>), 40.1 (CH<sub>2</sub>CH<sub>2</sub>S), 36.4 (CH<sub>2</sub>NH), 36.3 (CH<sub>2</sub>CONH), 28.9 (CH<sub>2</sub>S), 23.4 (CHCH<sub>3</sub>), 21.3 (CH<sub>2</sub>C(CH<sub>3</sub>)<sub>2</sub>), 20.9 (CH<sub>2</sub>C(CH<sub>3</sub>)<sub>2</sub>); HRMS (ESI) cald. for C<sub>17</sub>H<sub>30</sub>N<sub>2</sub>NaO<sub>6</sub>S (M + Na<sup>+</sup>) requires 413.1717, found 413.1719;  $[\alpha]_{\text{D}}^{26}$  (c 0.55, CHCl<sub>3</sub>): +12.7.

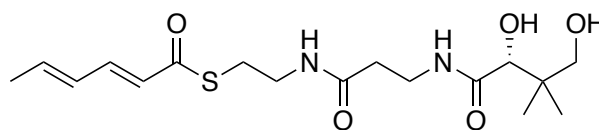
***S*-(2-(3-((*R*)-2,2,5,5-tetramethyl-1,3-dioxane-4-carboxamido)propanamido)ethyl) (*2E,4E*)-hexa-2,4-dienethioate (**104**)**



*S*-(2-(3-((*R*)-2,2,5,5-tetramethyl-1,3-dioxane-4-carboxamido)propanamido)ethyl) (*2E,4E*)-hexa-2,4-dienethioate **104** was synthesized using the same procedure as that used for the synthesis of *S*-(2-(3-((*R*)-2,2,5,5-tetramethyl-1,3-dioxane-4-carboxamido)propanamido)ethyl)(*S,E*)-5-((*tert*-butyldimethylsilyl)oxy) hex-2-enethioate **90** using sorbic acid (61 mg, 0.54 mmol, 1.30 equiv.), to afford the product as a colourless oil (199 mg, 90 %, 0.49 mmol).

$\nu_{\max}/\text{cm}^{-1}$  (neat) 3328 (NH), 2940 (C=C-H), 1671 (C=O), 1512 (C=O);  $\delta_{\text{H}}$  (500 MHz;  $\text{CDCl}_3$ ) 7.19 (1H, dd,  $J$  15.0 and 10.5, CHCHCOS), 7.03 (1H, br. t,  $J$  6.0, NH), 6.24 (1H, dq,  $J$  15.0 and 7.0,  $\text{CH}_3\text{CH}$ ), 6.23 (1H, m,  $\text{NHCH}_2\text{CH}_2\text{S}$ ), 6.15 (1H, ddd,  $J$  15.0, 11.0 and 1.0,  $\text{CH}_3\text{CHCH}$ ), 6.06 (1H, d,  $J$  15.0, CHCOS), 4.06 (1H, s, CHCONH), 3.67 (1H, d,  $J$  11.5,  $\text{CH}_2\text{OC}(\text{CH}_3)_2$ ), 3.60-3.40 (4H, m,  $\text{NHCH}_2$ ,  $\text{CH}_2\text{CH}_2\text{S}$ ), 3.26 (1H, d,  $J$  11.5,  $\text{CH}_2\text{OC}(\text{CH}_3)_2$ ), 3.08 (2H, t,  $J$  6.5,  $\text{CH}_2\text{S}$ ), 2.41 (2H, t,  $J$  6.5,  $\text{CH}_2\text{CONH}$ ), 1.87 (3H, d,  $J$  7.0,  $\text{CHCH}_3$ ), 1.45 (3H, s,  $\text{OC}(\text{CH}_3)_2$ ), 1.41 (3H, s,  $\text{OC}(\text{CH}_3)_2$ ), 1.02 (3H, s,  $\text{CH}_2\text{C}(\text{CH}_3)_2$ ), 0.96 (3H, s,  $\text{CH}_2\text{C}(\text{CH}_3)_2$ );  $\delta_{\text{C}}$  (125 MHz,  $\text{CDCl}_3$ ) 190.3 ( $\text{CO}_2\text{S}$ ), 171.4 ( $\text{CH}_2\text{CONH}$ ), 170.2 (CHCONH), 142.1 ( $\text{CH}_3\text{CH}$ ), 142.0 (CHCHCOS), 129.7 ( $\text{CH}_3\text{CHCH}$ ), 125.8 (CHCHCOS), 99.2 ( $\text{OC}(\text{CH}_3)_2$ ), 77.3 (CH), 71.6 ( $\text{CH}_2\text{OC}(\text{CH}_3)_2$ ), 40.0 ( $\text{CH}_2\text{CH}_2\text{S}$ ), 36.1 ( $\text{CH}_2\text{CONH}$ ), 34.9 ( $\text{CH}_2\text{NH}$ ), 33.1 ( $\text{CH}_2\text{C}(\text{CH}_3)_2$ ), 29.7 ( $\text{OC}(\text{CH}_3)_2$ ), 28.5 ( $\text{CH}_2\text{S}$ ), 22.3 ( $\text{CH}_2\text{C}(\text{CH}_3)_2$ ), 19.1 ( $\text{OC}(\text{CH}_3)_2$ ), 18.9 ( $\text{CH}_2\text{C}(\text{CH}_3)_2$ ), 14.1 ( $\text{CHCH}_3$ ); HRMS (ESI) cald. for  $\text{C}_{20}\text{H}_{32}\text{N}_2\text{NaO}_5\text{S}$  ( $\text{M} + \text{Na}^+$ ) requires 435.1924, found 435.1923;  $[\alpha]_{\text{D}}^{28}$  (c 0.1,  $\text{CHCl}_3$ ): +21.2.

***S*-(2-(3-((*R*)-2,4-dihydroxy-3,3-dimethylbutanamido)propanamido)ethyl) (2*E*,4*E*)-hexa-2,4-dienethioate (99)**



*S*-(2-(3-((*R*)-2,4-dihydroxy-3,3-dimethylbutanamido)propanamido)ethyl) (2*E*,4*E*)-hexa-2,4-dienethioate **99** was synthesized using the same procedure as that used for the synthesis of *S*-(2-(3-((*R*)-2,4-dihydroxy-3,3-dimethylbutanamido)propanamido)ethyl)(*S*,*E*)-5-hydroxyhex-2-enethioate **86** using *S*-(2-(3-((*R*)-2,2,5,5-tetramethyl-1,3-dioxane-4-carboxamido)propanamido)ethyl) (2*E*,4*E*)-hexa-2,4-dienethioate **104** (180 mg, 0.45 mmol) to afford the product as a colourless oil (42 mg, 25 %, 0.11 mmol).

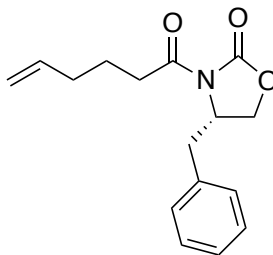
$\nu_{\max}/\text{cm}^{-1}$  (neat) 3340 (OH), 2969 (NH), 2940 (C=C-H), 1651 (C=O), 1540 (C=O);  $\delta_{\text{H}}$  (500 MHz;  $\text{CD}_3\text{OD}$ ) 7.21 (1H, dd,  $J$  15.0 and 10.0, CHCHCOS), 6.30 (1H, dq,  $J$  15.0 and 6.5,  $\text{CH}_3\text{CH}$ ), 6.24 (1H, dd,  $J$  15.0 and 10.0,  $\text{CH}_3\text{CHCH}$ ), 6.15 (1H, d,  $J$  15.0, CHCOS), 3.89 (1H, s, CHCONH), 3.53-3.33 (6H, m,  $\text{NHCH}_2$ ,  $\text{CH}_2\text{CH}_2\text{S}$ ,  $\text{CH}_2\text{OH}$ ), 3.08 (2H, t,  $J$  7.0,  $\text{CH}_2\text{S}$ ), 2.41 (2H, t,  $J$  6.5,  $\text{CH}_2\text{CONH}$ ), 1.87 (3H, d,  $J$  6.0,  $\text{CHCH}_3$ ), 0.92 (6H, s,  $\text{C}(\text{CH}_3)_2$ );  $\delta_{\text{C}}$  (125 MHz,  $\text{CD}_3\text{OD}$ ) 191.2 ( $\text{CO}_2\text{S}$ ), 176.1 ( $\text{CH}_2\text{CONH}$ ), 173.9 (CHCONH), 142.8 ( $\text{CH}_3\text{CH}$ ), 142.8 (CHCHCOS), 130.8 ( $\text{CH}_3\text{CHCH}$ ), 126.9 (CHCHCOS), 77.3 (CH), 70.3 ( $\text{CH}_2\text{OH}$ ), 40.4 ( $\text{CH}_2\text{C}(\text{CH}_3)_2$ ), 40.2 ( $\text{CH}_2\text{CH}_2\text{S}$ ), 36.4 ( $\text{CH}_2\text{CONH}$ ), 36.3 ( $\text{CH}_2\text{NH}$ ), 29.0 ( $\text{CH}_2\text{S}$ ), 21.3



(CH<sub>2</sub>C(CH<sub>3</sub>)<sub>2</sub>), 20.9 (CH<sub>2</sub>C(CH<sub>3</sub>)<sub>2</sub>), 14.2 (CHCH<sub>3</sub>); HRMS (ESI) calcd. for C<sub>17</sub>H<sub>28</sub>N<sub>2</sub>NaO<sub>5</sub>S (M + Na<sup>+</sup>) requires 395.1611, found 395.1605; [ $\alpha$ ]<sub>D</sub><sup>28</sup> (c 0.5, CHCl<sub>3</sub>): +40.4.

## 6.9.2 Synthesis of DHCCA analogues

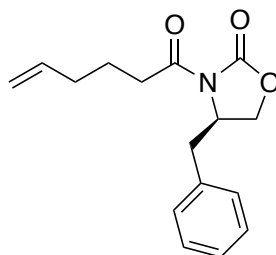
### (S)-4-Benzyl-3-(hex-5-enoyl)oxazolidin-2-one (272)



The following procedure was modified from Steele *et al.*<sup>255</sup> To a solution of 5-hexenoic acid **158** (3.50 ml, 29.6 mmol, 1.05 equiv.) and triethylamine (10.8 mL, 77.4 mmol, 2.75 equiv.) in anhydrous THF (150 mL) at -10°C was added pivaloyl chloride (3.64 mL, 29.6 mmol, 1.05 equiv.) dropwise, the mixture was then stirred at this temperature for 1 h. LiCl (1.37 g, 32.4 mmol, 1.10 equiv.) and (*S*)-4-(phenylmethyl)-2-oxazolidinone (5.00 g, 28.2 mmol, 1.00 equiv.) were then quickly added in one portion, and reaction was allowed to warm to RT and stirred for 16 h. The reaction was quenched with saturated NH<sub>4</sub>Cl (50 mL) and extracted with EtOAc (3 × 50 mL). The combined organics were then washed with saturated NaHCO<sub>3</sub> (50 mL), brine (50 mL), dried (MgSO<sub>4</sub>), concentrated *in vacuo* and purified by silica chromatography (1:5 EtOAc:Petroleum ether) to afford the product as a colourless oil (7.03 g, 91%, 25.7 mmol).

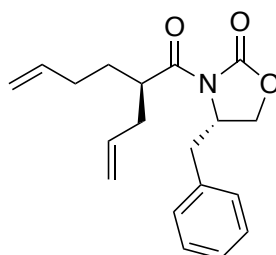
$\delta_H$  (500 MHz; CDCl<sub>3</sub>) 7.35-7.31 (2H, m, ArH), 7.30-7.27 (1H, m, ArH), 7.23-7.19 (2H, m, ArH), 5.82 (1H, ddt, *J* 17.0, 10.0 and 6.5, CH<sub>2</sub>CHCH<sub>2</sub>), 5.06 (1H, dq, *J* 17.0 and 1.5, CH<sub>2</sub>CHCH<sub>2</sub>), 5.00 (1H, d, *J* 10.0, CH<sub>2</sub>CHCH<sub>2</sub>), 4.67 (1H, ddt, *J* 9.5, 7.5 and 3.0, CHCH<sub>2</sub>Ph), 4.20 (1H, dd, *J* 9.0 and 7.5, CH<sub>2</sub>Ph), 4.16 (1H, dd, *J* 9.0 and 3.0, CH<sub>2</sub>Ph), 3.30 (1H, dd, *J* 13.0 and 3.0, OCH<sub>2</sub>CH), 2.98 (1H, ddd, *J* 17.0, 8.0 and 6.5, CH<sub>2</sub>CHCH<sub>2</sub>), 2.91 (1H, ddd, *J* 17.0, 8.0 and 7.0, CH<sub>2</sub>CHCH<sub>2</sub>), 2.77 (1H, dd, *J* 13.5 and 9.5, OCH<sub>2</sub>CH), 2.16 (2H, q, *J* 7.0, COCH<sub>2</sub>), 1.87-1.75 (2H, m, COCH<sub>2</sub>CH<sub>2</sub>);  $\delta_C$  (125 MHz, CDCl<sub>3</sub>) 173.3 (CON), 153.6 (NCOO), 137.9 (CH<sub>2</sub>CHCH<sub>2</sub>), 135.4 (ArC<sub>quart</sub>), 129.5 (ArC), 129.1 (ArC), 127.5 (ArC), 115.5 (CH<sub>2</sub>CHCH<sub>2</sub>), 66.3 (CH<sub>2</sub>Ph), 55.3 (CHCH<sub>2</sub>Ph), 38.0 (OCH<sub>2</sub>CH), 35.0 (CH<sub>2</sub>CHCH<sub>2</sub>), 33.1 (COCH<sub>2</sub>), 23.5 (COCH<sub>2</sub>CH<sub>2</sub>); HRMS (ESI) calcd. for C<sub>16</sub>H<sub>19</sub>NNaO<sub>3</sub> (M + Na<sup>+</sup>) requires 296.1257, found 296.1259. Spectroscopic data consistent with that previously reported in the literature.<sup>255</sup>

**(R)-4-Benzyl-3-(hex-5-enoyl)oxazolidin-2-one (164)**



(R)-4-benzyl-3-(hex-5-enoyl)oxazolidin-2-one **164** was synthesized using the same procedure as for the synthesis of (S)-4-benzyl-3-(hex-5-enoyl)oxazolidin-2-one **272** using (R)-4-(phenylmethyl)-2-oxazolidinone to afford the product as a colourless oil (7.18 g, 93 %, 26.2 mmol). Spectroscopic data was identical to that of (S)-4-benzyl-3-(hex-5-enoyl)oxazolidin-2-one **272** and consistent with that previously reported in the literature.<sup>255</sup>

**(S)-3-((R)-2-Allylhex-5-enoyl)-4-benzyl-oxazolidin-2-one (273)**

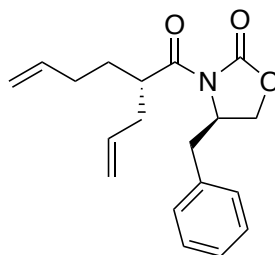


To a stirred solution of (S)-4-benzyl-3-(hex-5-enoyl)oxazolidin-2-one **272** (7.0 g, 25.6 mmol, 1.0 equiv.) in THF (100 mL), under an atmosphere of argon at -78 °C, was added LiHMDS (30.7 mL, 1 M in THF, 30.7 mmol, 1.2 equiv.) and the resulting mixture stirred at -78 °C for 30 min. Allyl bromide (4.53 mL, 51.2 mmol, 2.0 equiv.) was added dropwise, the reaction mixture allowed to warm to RT and stirred for 22 h. Saturated aqueous NH<sub>4</sub>Cl (50 mL) was added and extracted with CH<sub>2</sub>Cl<sub>2</sub> (3 × 50 mL). The organic extracts were combined, washed with brine (20 mL) and dried (MgSO<sub>4</sub>). Solvent was removed *in vacuo* and the crude product purified by silica chromatography (1:9 EtOAc:Petroleum ether) to afford the product as a colourless oil (6.25 g, 78 %).

$\nu_{\max}/\text{cm}^{-1}$  (neat) 3075 (ArCH), 1774 (NH), 1773 (CO), 1693 (CO);  $\delta_{\text{H}}$  (500 MHz; CDCl<sub>3</sub>) 7.35-7.31 (2H, m, ArH), 7.29-7.27 (1H, m, ArH), 7.24-7.21 (2H, m, ArH), 5.83 (1H, ddt, *J* 17.0, 10.0 and 7.0, CHCH<sub>2</sub>CHCH<sub>2</sub>), 5.78 (1H, ddt, *J* 17.0, 10.0 and 6.5, CHCH<sub>2</sub>CH<sub>2</sub>CHCH<sub>2</sub>), 5.09 (1H, dq, *J* 17.0 and 1.5, CHCH<sub>2</sub>CHCH<sub>2</sub>), 5.05 (1H, d, *J* 10.0, CHCH<sub>2</sub>CHCH<sub>2</sub>), 5.00 (1H,

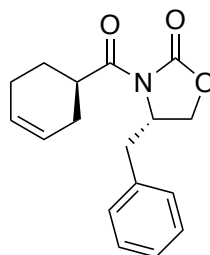
dq,  $J$  17.0 and 1.5, CHCH<sub>2</sub>CH<sub>2</sub>CHCH<sub>2</sub>), 4.95 (1H, d,  $J$  10.0, CHCH<sub>2</sub>CH<sub>2</sub>CHCH<sub>2</sub>), 4.68 (1H, ddt,  $J$  10.0, 7.0 and 3.5, CHCH<sub>2</sub>Ph), 4.17 (1H, d,  $J$  9.0, CH<sub>2</sub>Ph), 4.14 (1H, dd,  $J$  9.0 and 3.5, CH<sub>2</sub>Ph), 3.94 (1H, tt,  $J$  7.5 and 5.5, CHCO), 3.30 (1H, dd,  $J$  13.0 and 3.0, OCH<sub>2</sub>CH), 2.66 (1H, dd,  $J$  13.5 and 10.0, OCH<sub>2</sub>CH), 2.48 (1H, dt,  $J$  14.0 and 7.5, CHCH<sub>2</sub>CHCH<sub>2</sub>), 2.33 (1H, dt,  $J$  13.5 and 6.5, CHCH<sub>2</sub>CHCH<sub>2</sub>), 2.08 (2H, q,  $J$  7.5, CHCH<sub>2</sub>CH<sub>2</sub>CHCH<sub>2</sub>) 1.87 (1H, dq,  $J$  14.0 and 8.0, CHCH<sub>2</sub>CH<sub>2</sub>CHCH<sub>2</sub>), 1.61 (1H, dtd,  $J$  13.5, 7.5 and 5.5, CHCH<sub>2</sub>CH<sub>2</sub>CHCH<sub>2</sub>);  $\delta_c$  (125 MHz, CDCl<sub>3</sub>) 176.0 (CON), 153.3 (NCOO), 138.2 (CHCH<sub>2</sub>CH<sub>2</sub>CHCH<sub>2</sub>), 135.5 (ArC<sub>quart</sub>), 135.2 (CHCH<sub>2</sub>CHCH<sub>2</sub>), 129.6 (ArC), 129.1 (ArC), 127.5 (ArC), 117.5 (CHCH<sub>2</sub>CHCH<sub>2</sub>), 115.1 (CHCH<sub>2</sub>CH<sub>2</sub>CHCH<sub>2</sub>), 66.1 (CH<sub>2</sub>Ph), 55.6 (CHCH<sub>2</sub>Ph), 41.9 (COCH), 38.2 (OCH<sub>2</sub>CH), 37.0 (CHCH<sub>2</sub>CHCH<sub>2</sub>), 31.7 (CHCH<sub>2</sub>CH<sub>2</sub>CHCH<sub>2</sub>), 30.7 (CHCH<sub>2</sub>CH<sub>2</sub>CHCH<sub>2</sub>); HRMS (ESI) cald. for C<sub>19</sub>H<sub>23</sub>NNaO<sub>3</sub> (M + Na<sup>+</sup>) requires 336.1576, found 336.1573;  $[\alpha]_D^{25}$  (c 0.7, MeOH): +41.3.

**(R)-3-((S)-2-Allylhex-5-enoyl)-4-benzyloxazolidin-2-one (160)**



(R)-3-((S)-2-Allylhex-5-enoyl)-4-benzyloxazolidin-2-one **160** was synthesized using the same procedure as for the synthesis of (S)-3-((R)-2-allylhex-5-enoyl)-4-benzyloxazolidin-2-one **273** using (R)-4-benzyl-3-(hex-5-enoyl)oxazolidin-2-one **164** to afford the product as a colourless oil (5.77 g, 72 %, 16.5 mmol). Spectroscopic data was identical to that of (S)-3-((R)-2-Allylhex-5-enoyl)-4-benzyloxazolidin-2-one **273**.

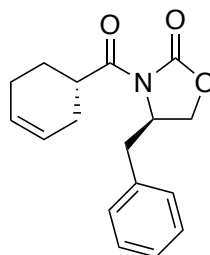
**(S)-4-Benzyl-3-((R)-cyclohex-3-ene-1-carbonyl)oxazolidin-2-one (274)**



The following procedure was modified from Fu *et al.*<sup>256</sup> To a sparged solution of (*S*)-3-((*R*)-2-allylhex-5-enoyl)-4-benzyloxazolidin-2-one **273** (6.0 g, 19.2 mmol, 1.0 equiv.) in anhydrous CH<sub>2</sub>Cl<sub>2</sub> (50 mL), under an argon atmosphere was added Grubbs Catalyst<sup>TM</sup> 2<sup>nd</sup> Generation (85 mg, 0.10 mmol, 0.005 equiv.). The reaction was then heated to reflux for 5 h before being concentrated *in vacuo* and purified by silica chromatography (1:9 EtOAc:Petroleum ether) to afford the product as a white solid (5.20 g, 95 %, 18.2 mmol).

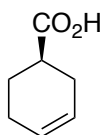
$\delta_{\text{H}}$  (500 MHz; CDCl<sub>3</sub>) 7.36-7.31 (2H, m, ArH), 7.29-7.27 (1H, m, ArH), 7.22-7.19 (2H, m, ArH), 5.75-5.69 (2H, m, CHCH<sub>2</sub>CHCH), 4.68 (1H, ddt, *J* 9.5, 7.5 and 3.0, CHCH<sub>2</sub>Ph), 4.21 (1H, t, *J* 9.0, CH<sub>2</sub>Ph), 4.17 (1H, dd, *J* 9.0 and 3.0, CH<sub>2</sub>Ph), 3.75 (1H, dddd, *J* 11.5, 9.5, 6.5 and 2.5, CHCO), 3.28 (1H, dd, *J* 13.5 and 3.0, OCH<sub>2</sub>CH), 2.78 (1H, dd, *J* 13.5 and 9.5, OCH<sub>2</sub>CH), 2.36-2.27 (2H, m, CHCH<sub>2</sub>CH), 2.21-2.10 (2H, m, CHCH<sub>2</sub>CH<sub>2</sub>CH), 1.97-1.91 (1H, m, CHCH<sub>2</sub>CH<sub>2</sub>CH), 1.72 (1H, qd, *J* 11.5 and 7.0, CHCH<sub>2</sub>CH<sub>2</sub>CH);  $\delta_{\text{C}}$  (125 MHz, CDCl<sub>3</sub>) 176.5 (CON), 153.2 (NCOO), 135.4 (ArC<sub>quart</sub>), 129.5 (ArC), 129.0 (ArC), 127.5 (ArC), 126.8 (CHCH<sub>2</sub>CHCH), 125.2 (CHCH<sub>2</sub>CHCH), 66.2 (CH<sub>2</sub>Ph), 55.5 (CHCH<sub>2</sub>Ph), 38.6 (COCH), 38.0 (OCH<sub>2</sub>CH), 27.6 (CHCH<sub>2</sub>CHCH), 25.5 (CHCH<sub>2</sub>CH<sub>2</sub>CHCH), 24.8 (CHCH<sub>2</sub>CH<sub>2</sub>CHCH); HRMS (ESI) calcd. for C<sub>17</sub>H<sub>19</sub>NNaO<sub>3</sub> (M + Na<sup>+</sup>) requires 308.1257, found 308.1260. Spectroscopic data consistent with that previously reported in the literature.<sup>257</sup>

**(R)-4-Benzyl-3-((S)-cyclohex-3-ene-1-carbonyl)oxazolidin-2-one (162)**



(R)-4-Benzyl-3-((S)-cyclohex-3-ene-1-carbonyl)oxazolidin-2-one **162** was synthesized using the same procedure as for the synthesis of (S)-4-benzyl-3-((R)-cyclohex-3-ene-1-carbonyl)oxazolidin-2-one **274** using (R)-3-((S)-2-allylhex-5-enoyl)-4-benzylloxazolidin-2-one **160** to afford the product as a white solid (4.93 g, 90 %, 17.3 mmol). Spectroscopic data was identical to that of (S)-4-benzyl-3-((R)-cyclohex-3-ene-1-carbonyl)oxazolidin-2-one **274** and consistent with that previously reported in the literature.<sup>257</sup>

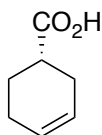
**(R)-Cyclohex-3-ene-1-carboxylic acid (168)**



The following procedure was modified from Miyashita *et al.*<sup>257</sup> To a stirred solution of (S)-4-benzyl-3-((R)-cyclohex-3-ene-1-carbonyl)oxazolidin-2-one **274** (5.0 g, 16.9 mmol, 1.0 equiv.) in THF-water (4:1, 50 mL) were added 30% H<sub>2</sub>O<sub>2</sub> solution (8.27 mL, 84.5 mmol, 5.0 equiv.) and LiOH (1.69 g, 84.5 mmol, 5.0 equiv.) at 0 °C, and the reaction was stirred at RT for 5 h. At 0 °C, Na<sub>2</sub>SO<sub>3</sub> (10.0 g) was added to the reaction mixture, which was then stirred at RT for 15 min. After evaporation of THF under reduced pressure, the resulting aqueous solution was washed with CH<sub>2</sub>Cl<sub>2</sub>, acidified to pH 1 with conc. HCl, and extracted with ether. The ethereal layer was washed with saturated NaCl solution, dried (MgSO<sub>4</sub>), and concentrated *in vacuo* to afford the product as a colourless oil (1.55 g, 73 %, 12.3 mmol).

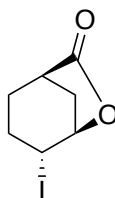
$\delta_{\text{H}}$  (500 MHz; CDCl<sub>3</sub>) 5.72-5.65 (2H, m, CHCH), 2.61 (1H, dddd, *J* 11.5, 9.0, 6.5 and 3.0, CHCO<sub>2</sub>H), 2.32-2.22 (2H, m, CHCH<sub>2</sub>CH), 2.19-2.01 (3H, m, CHCH<sub>2</sub>CH<sub>2</sub>), 1.76-1.68 (1H, m, CHCH<sub>2</sub>CH<sub>2</sub>CH);  $\delta_{\text{C}}$  (125 MHz, CDCl<sub>3</sub>) 182.5 (CO<sub>2</sub>H), 126.9 (CHCH<sub>2</sub>CHCH), 125.1 (CHCH<sub>2</sub>CHCH), 39.2 (CHCO<sub>2</sub>H), 27.3 (CHCH<sub>2</sub>CHCH), 25.0 (CHCH<sub>2</sub>CH<sub>2</sub>CHCH), 24.4 (CHCH<sub>2</sub>CH<sub>2</sub>CHCH); HRMS (ESI) cald. for C<sub>7</sub>H<sub>10</sub>NaO<sub>2</sub> (M + Na<sup>+</sup>) requires 149.0587, found 149.0588. Spectroscopic data consistent with that previously reported in the literature.<sup>258</sup>

**(S)-Cyclohex-3-ene-1-carboxylic acid (161)**



(S)-Cyclohex-3-ene-1-carboxylic acid **161** was synthesized using the same procedure as for the synthesis of (*R*)-cyclohex-3-ene-1-carboxylic acid **168** using (*R*)-4-benzyl-3-((*S*)-cyclohex-3-ene-1-carbonyl)oxazolidin-2-one **162** to afford the product as a colourless oil (1.57 g, 74 %, 12.5 mmol). Spectroscopic data was identical to that of (*R*)-cyclohex-3-ene-1-carboxylic acid **168** and consistent with that previously reported in the literature.<sup>258</sup>

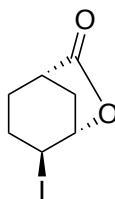
**(1*R*,4*R*,5*R*)-4-Iodo-6-oxabicyclo[3.2.1]octan-7-one (169)**



The following procedure was modified from Schwizer *et al.*<sup>259</sup> To a stirred solution of (*R*)-cyclohex-3-ene-1-carboxylic acid **168** (1.50 g, 11.9 mmol, 1.0 equiv.) in H<sub>2</sub>O (50 mL) was added NaHCO<sub>3</sub> (3.0 g, 35.7 mmol, 3.0 equiv.), followed by a solution of KI (11.8 g, 71.4 mmol, 6.0 equiv.) and iodine (3.31 g, 13.1 mmol, 1.1 equiv.) in H<sub>2</sub>O (30 mL). The reaction was stirred at RT for 24 h and then extracted with CH<sub>2</sub>Cl<sub>2</sub> (3 × 50 mL). The combined organic layers were washed with a saturated solution of Na<sub>2</sub>S<sub>2</sub>O<sub>3</sub> (50 mL). The aqueous layer was extracted with CH<sub>2</sub>Cl<sub>2</sub> (2 × 50 mL). The combined organic layers were dried (MgSO<sub>4</sub>), filtered and concentrated *in vacuo* to afford the product as an off-white solid (2.87 g, 96 %, 11.4 mmol).

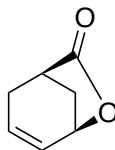
$\delta_{\text{H}}$  (500 MHz; CDCl<sub>3</sub>) 4.82 (1H, t, *J* 5.0, CHICHO), 4.51 (1H, t, *J* 5.0, CHI), 2.80 (1H, d, *J* 12.5, CHICH<sub>2</sub>CHO), 2.67 (1H, br. t, *J* 4.5, CHCOO), 2.49-2.42 (1H, m, CHICH<sub>2</sub>), 2.39 (1H, dd, *J* 13.0 and 6.0, CHICH<sub>2</sub>CHO), 2.12 (1H, dd, *J* 16.5 and 5.0, CHICH<sub>2</sub>), 1.90 (1H, tdd, *J* 13.5, 5.5 and 2.0, CHICH<sub>2</sub>CH<sub>2</sub>), 1.82 (1H, dt, *J* 13.0 and 5.5, CHICH<sub>2</sub>CH<sub>2</sub>);  $\delta_{\text{C}}$  (125 MHz, CDCl<sub>3</sub>) 178.0 (CO<sub>2</sub>), 80.4 (CHO), 38.8 (CHCO<sub>2</sub>), 34.7 (CH<sub>2</sub>CHOCHI), 29.9 (CHICH<sub>2</sub>), 23.9 (CHI), 23.3 (CHICH<sub>2</sub>CH<sub>2</sub>); HRMS (ESI) calcd. for C<sub>7</sub>H<sub>9</sub>INaO<sub>2</sub> (M + Na<sup>+</sup>) requires 274.9539, found 274.9539. Spectroscopic data was identical to that previously reported in the literature.<sup>259</sup>

**(1*S*,4*S*,5*S*)-4-Iodo-6-oxabicyclo[3.2.1]octan-7-one (188)**



(1*S*,4*S*,5*S*)-4-Iodo-6-oxabicyclo[3.2.1]octan-7-one **188** was synthesized using the same procedure as for the synthesis of (1*R*,4*R*,5*R*)-4-iodo-6-oxabicyclo[3.2.1]octan-7-one **169** using (*S*)-cyclohex-3-ene-1-carboxylic acid **161** to afford the product as a colourless oil (2.75 g, 92 %, 1.1 mmol). Spectroscopic data was identical to that of (1*R*,4*R*,5*R*)-4-Iodo-6-oxabicyclo[3.2.1]octan-7-one **169** and consistent with that previously reported in the literature.<sup>260</sup>

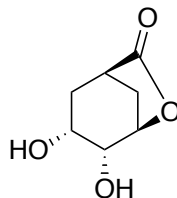
**(1*R*,5*R*)-6-Oxabicyclo[3.2.1]oct-3-en-7-one (170)**



The following procedure was modified from Schwizer *et al.*<sup>259</sup> To a stirred solution of (1*R*,4*R*,5*R*)-4-iodo-6-oxabicyclo[3.2.1]octan-7-one **169** (1.0 g, 4.0 mmol, 1.0 equiv.) in dry THF (50 mL) was added DBU (0.9 mL, 6.0 mmol, 1.5 equiv.) under argon and the mixture was refluxed for 20 h. The reaction mixture was cooled to RT, diluted with Et<sub>2</sub>O (50 mL) and washed with HCl solution (50 mL, 0.5 M) and brine (50 mL). The aqueous layers were further extracted with Et<sub>2</sub>O (3 × 20 mL). The combined organic layers were dried (MgSO<sub>4</sub>), filtered and concentrated *in vacuo*. The crude product was purified by silica chromatography (1:3 EtOAc:Petroleum ether) to afford the product as a yellowish oil (383 mg, 94 %, 3.76 mmol).

$\delta_{\text{H}}$  (500 MHz; CDCl<sub>3</sub>) 6.26-6.21 (1H, m, CHCHCHO), 5.85 (1H, dt, *J* 9.5 and 3.0, CHCHCHO), 4.76 (1H, t, *J* 5.5, CHCHCHO), 2.92 (1H, t, *J* 5.5, CHCO<sub>2</sub>), 2.55-2.22 (3H, m, CHCH<sub>2</sub>CHO, CHCH<sub>2</sub>CO<sub>2</sub>), 2.09 (1H, d, *J* 11.0, CHCH<sub>2</sub>CHO);  $\delta_{\text{C}}$  (125 MHz, CDCl<sub>3</sub>) 179.5 (CO<sub>2</sub>), 130.4 (CHCHCHO), 129.5 (CHCHCHO), 73.4 (CHCHCHO), 38.2 (CHCO<sub>2</sub>), 34.6 (CHOCH<sub>2</sub>CHCO<sub>2</sub>), 29.3 (CH<sub>2</sub>); HRMS (ESI) cald. for C<sub>7</sub>H<sub>9</sub>O<sub>2</sub> (M + H<sup>+</sup>) requires 125.0603, found 125.0597. Spectroscopic data was identical to that previously reported in the literature.<sup>259</sup>

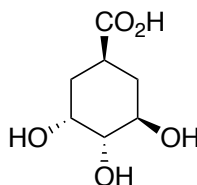
**(1*R*,3*R*,4*R*,5*R*)-3,4-Dihydroxy-6-oxabicyclo[3.2.1]octan-7-one (171)**



The following procedure was modified from Ueda *et al.*<sup>205</sup> To a stirred solution of NMO (361 mg, 3.09 mmol, 1.05 equiv.) in H<sub>2</sub>O (5 mL) and acetone (2 mL) were added K<sub>2</sub>[OsO<sub>2</sub>(OH)<sub>4</sub>] (33.0 mg, 88.0 μmol, 0.03 equiv.) and a solution of (1*R*,5*R*)-6-oxabicyclo[3.2.1]oct-3-en-7-one **170** (300 mg, 2.94 mmol, 1.00 equiv.) in acetone (5 mL). The resulting mixture was stirred at RT for 6 h, and then quenched with saturated aqueous NaHSO<sub>3</sub> (10 mL). The resulting mixture was extracted with EtOAc (3 × 20 mL). The combined organic extracts were washed with brine (20 mL), dried (MgSO<sub>4</sub>), filtered, and concentrated *in vacuo*. The residue was purified by silica chromatography on silica gel (EtOAc) to afford the product as a brown solid (367 mg 79 %, 2.32 mmol, m.p. 160-162 °C).

δ<sub>H</sub> (500 MHz; CDCl<sub>3</sub>) 4.86 (1H, t, J 5.0, CH<sub>2</sub>CHOHCHOH), 4.19 (1H, t, J 4.5, CH<sub>2</sub>CHOHCHOH), 3.96 (1H, dq, J 10.5 and 5.5, CHOCHOCHO), 2.72 (1H, br. s, CH<sub>2</sub>CHOHCHOH), 2.62 (1H, t, J 5.0, CHCO<sub>2</sub>), 2.37 (1H, d, J 12.0, CH<sub>2</sub>CHCO<sub>2</sub>), 2.23-2.15 (3H, m, CH<sub>2</sub>CHOH, CH<sub>2</sub>CHOH), 1.67 (1H, ddd, J 12.5, 11.5 and 2.0); δ<sub>C</sub> (125 MHz, CDCl<sub>3</sub>) 177.9 (CO<sub>2</sub>), 79.2 (CH<sub>2</sub>CHOHCHOH), 67.1 (CH<sub>2</sub>CHOHCHOH), 66.2 (CHOCHOCHO), 36.1 (CHCO<sub>2</sub>), 31.3 (CH<sub>2</sub>CHCO<sub>2</sub>), 30.6 (CHOHCH<sub>2</sub>); HRMS (ESI) cald. for C<sub>7</sub>H<sub>10</sub>NaO<sub>4</sub> (M + Na<sup>+</sup>) requires 181.0477, found 181.0476. Spectroscopic data was identical to that previously reported in the literature.<sup>205</sup>

**(1*R*,3*R*,4*R*,5*R*)-3,4,5-Trihydroxycyclohexane-1-carboxylic acid (167)**



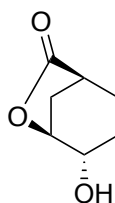
To a solution of (1*R*,3*R*,4*R*,5*R*)-3,4-dihydroxy-6-oxabicyclo[3.2.1]octan-7-one **171** (350 mg, 2.21 mmol, 1.0 equiv.) in a 5:3 mixture of THF (5 mL) and water (3 mL), was added LiOH



(88 mg, 4.42 mmol, 2.0 equiv.) and the reaction stirred for 16 h. The reaction was then acidified to pH 2.0 using 1 M HCl before being concentrated *in vacuo* to afford the product as a white solid (381 mg, 98 %, 2.17 mmol, m.p. 133-135 °C).

$\nu_{\max}/\text{cm}^{-1}$  (neat) 3261 (OH), 1701 (CO);  $\delta_{\text{H}}$  (500 MHz; CD<sub>3</sub>OD) 4.06 (1H, q, *J* 3.5, CHOHCHOHCHOH), 3.75 (1H, ddd, *J* 11.0, 9.5 and 4.5, CHOHCHOHCHOH), 3.27 (1H, dd, *J* 9.0 and 3.0, CHOHCHOHCHOH), 2.82 (1H, tt, *J* 12.5 and 3.5, CHCO<sub>2</sub>H), 2.16-2.19 (1H, m, CH<sub>2</sub>CHCO<sub>2</sub>HCH<sub>2</sub>), 2.03 (1H, dq, *J* 14.0 and 3.5, CH<sub>2</sub>CHCO<sub>2</sub>HCH<sub>2</sub>), 1.61 (1H, ddd, *J* 14.5, 12.5 and 2.0, CH<sub>2</sub>CHCO<sub>2</sub>HCH<sub>2</sub>), 1.41 (1H, q, *J* 12.5, CH<sub>2</sub>CHCO<sub>2</sub>HCH<sub>2</sub>);  $\delta_{\text{C}}$  (125 MHz, CD<sub>3</sub>OD) 177.2 (CO<sub>2</sub>H), 77.3 (CHOHCHOHCHOH), 70.4 (CHOHCHOHCHOH), 70.1 (CHOHCHOHCHOH), 37.2 (CHCO<sub>2</sub>), 36.3 (CH<sub>2</sub>CHCO<sub>2</sub>CH<sub>2</sub>), 34.9 (CH<sub>2</sub>CHCO<sub>2</sub>CH<sub>2</sub>); HRMS (ESI) cald. for C<sub>7</sub>H<sub>12</sub>NaO<sub>5</sub> (M + Na<sup>+</sup>) requires 199.0582, found 199.0581;  $[\alpha]_{\text{D}}^{26}$  (c 1.0, H<sub>2</sub>O): -61.2.

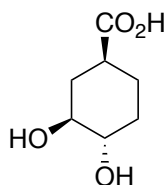
#### (1*S*,4*S*,5*S*)-4-Hydroxy-6-oxabicyclo[3.2.1]octan-7-one (163)



The following procedure was modified from Corey *et al.*<sup>261</sup> To a stirred solution of (*S*)-cyclohex-3-ene-1-carboxylic acid **161** (500 mg, 3.97 mmol, 1.0 equiv.) in CHCl<sub>3</sub> (20 mL) was added *m*-CPBA (751 mg, 4.37 mmol, 1.1 equiv.) and the reaction mixture was stirred at 0 °C for 4 h. Triethyl amine (2.78 mL, 19.9 mmol, 5.00 equiv.) was added and the resulting reaction mixture was heated to 65 °C for a further 4 h. The mixture was diluted with CHCl<sub>3</sub> (50 mL), washed with 1 M HCl (50 mL), brine (50 mL), dried (MgSO<sub>4</sub>) and concentrated *in vacuo*. The resulting residue was purified by silica chromatography (1 : 1 EtOAc : Petroleum ether) to afford the product as a white solid (242 g, 43 %, 1.71 mmol, m.p. 165-166 °C).

$\nu_{\max}/\text{cm}^{-1}$  (neat) 3424 (OH), 1741 (CO), 1160 (C-O);  $\delta_{\text{H}}$  (500 MHz; CDCl<sub>3</sub>) 4.66 (1H, t, *J* 5.5, CHCH<sub>2</sub>CHCO<sub>2</sub>), 4.19 (1H, t, *J* 4.5, CHOH), 2.61 (1H, t, *J* 5.0, CHCO<sub>2</sub>), 2.39 (1H, d, *J* 12.0, CHCH<sub>2</sub>CHCO<sub>2</sub>), 2.21 (1H, dt, *J* 11.5 and 5.5, CHCH<sub>2</sub>CHCO<sub>2</sub>), 2.00-1.76 (4H, m, CHCH<sub>2</sub>CH<sub>2</sub>);  $\delta_{\text{C}}$  (125 MHz, CDCl<sub>3</sub>) 178.8 (CO<sub>2</sub>), 79.1 (CHCH<sub>2</sub>CHCO<sub>2</sub>) 65.3 (CHOH), 38.5 (CHCO<sub>2</sub>), 36.1 (CHCO<sub>2</sub>), 31.3 (CHCH<sub>2</sub>CHCO<sub>2</sub>), 27.5 (CH<sub>2</sub>CH<sub>2</sub>CHOH), 22.8 (CH<sub>2</sub>CH<sub>2</sub>CHOH); HRMS (ESI) cald. for C<sub>7</sub>H<sub>11</sub>O<sub>3</sub> (M + H<sup>+</sup>) requires 143.0708, found 143.0704;  $[\alpha]_{\text{D}}^{26}$  (c 0.5, CHCl<sub>3</sub>): -21.1.

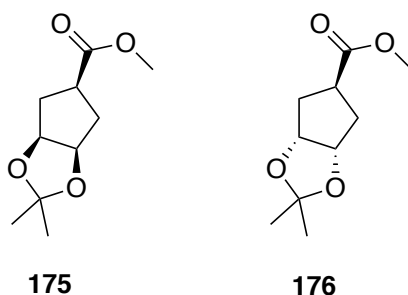
**(1*S*,3*S*,4*S*)-3,4-Dihydroxycyclohexane-1-carboxylic acid (157)**



(1*S*,3*S*,4*S*)-3,4-Dihydroxycyclohexane-1-carboxylic acid **157** was synthesized using the same procedure as for the synthesis of (1*R*,3*R*,4*R*,5*R*)-3,4,5-trihydroxycyclohexane-1-carboxylic acid **167** using (1*R*,4*R*,5*R*)-4-hydroxy-6-oxabicyclo[3.2.1]octan-7-one **163** (200 mg, 1.41 mmol) to afford the product as a viscous oil (236 mg, 92 %, 1.3 mmol).

$\nu_{\max}/\text{cm}^{-1}$  (neat) 3192 (OH), 2936 (CO<sub>2</sub>H), 1700 (CO), 1061 (C-O);  $\delta_{\text{H}}$  (500 MHz; D<sub>2</sub>O) 3.45-3.25 (2H, m, CHOH, CHOH), 2.25 (1H, tt, *J* 12.5 and 3.5, CHCO<sub>2</sub>H), 2.09 (1H, dq, *J* 12.0 and 2.0, CHCOHCH<sub>2</sub>CHCO<sub>2</sub>H), 2.00-1.95 (1H, m, CHOHCH<sub>2</sub>CH<sub>2</sub>), 1.88-1.82 (1H, m, CHOHCH<sub>2</sub>CH<sub>2</sub>), 1.41-1.27 (3H, m, CHCOHCH<sub>2</sub>CHCO<sub>2</sub>H, CHOHCH<sub>2</sub>CH<sub>2</sub>, CHOHCH<sub>2</sub>CH<sub>2</sub>);  $\delta_{\text{C}}$  (125 MHz, D<sub>2</sub>O) 184.8 (CO<sub>2</sub>H), 75.0 (CHOHCH<sub>2</sub>CH<sub>2</sub>), 74.6 (CHOH), 45.5 (CHCO<sub>2</sub>H), 36.7 (CHOHCH<sub>2</sub>CHCO<sub>2</sub>), 32.2 (CH<sub>2</sub>CH<sub>2</sub>CHCO<sub>2</sub>H), 28.3 (CH<sub>2</sub>CH<sub>2</sub>CHCO<sub>2</sub>H); HRMS (ESI) cald. for C<sub>7</sub>H<sub>12</sub>NaO<sub>4</sub> (M + H<sup>+</sup>) requires 183.0633, found 183.0630;  $[\alpha]_{\text{D}}^{25}$  (c 0.15, MeOH): 22.5.

**Methyl (3*aR*,5*r*,6*aS*)-2,2-dimethyltetrahydro-4*H*-cyclopenta[*d*][1,3]dioxole-5-carboxylate (175) and methyl (3*aR*,5*s*,6*aS*)-2,2-dimethyltetrahydro-4*H*-cyclopenta[*d*][1,3]dioxole-5-carboxylate (176)**



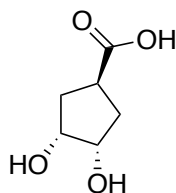
The following procedure was modified from Semak *et al.*<sup>218</sup> To a stirred solution of NMO (487 mg, 4.17 mmol, 1.05 equiv.) in H<sub>2</sub>O (5 mL) and acetone (2 mL) were added K<sub>2</sub>[OsO<sub>2</sub>(OH)<sub>4</sub>] (45 mg, 119  $\mu$ mol, 0.03 equiv.) and a solution of methyl cyclopent-3-ene-1-carboxylate **174** (500 mg, 3.97 mmol, 1.00 equiv.) in acetone (5 mL). The resulting mixture

was stirred at RT temperature for 6 h, and then quenched with saturated aqueous NaHSO<sub>3</sub> (10 mL). The resulting mixture was extracted with EtOAc (3 × 20 mL). The combined organic extracts were washed with brine (20 mL), dried (MgSO<sub>4</sub>), filtered, and concentrated *in vacuo*. The crude mixture was then re-suspended in CH<sub>2</sub>Cl<sub>2</sub> (20 mL) before the addition of 2,2-dimethoxypropane (2 mL) and a catalytic amount of TsOH. The resulting mixture was stirred for a further 2 h before being concentrated *in vacuo*. The crude mixture was then purified by silica chromatography (1:5 EtOAc:Petroleum ether) to afford methyl (3*aR*,5*r*,6*aS*)-2,2-dimethyltetrahydro-4*H*-cyclopenta[*d*][1,3]dioxole-5-carboxylate **175** (270 mg, 34 %, 1.35 mmol) and methyl (3*aR*,5*s*,6*aS*)-2,2-dimethyltetrahydro-4*H*-cyclopenta[*d*][1,3]dioxole-5-carboxylate **176** (421 mg, 53 %, 2.1 mmol) as colourless oils.

Methyl (3*aR*,5*r*,6*aS*)-2,2-dimethyltetrahydro-4*H*-cyclopenta[*d*][1,3]dioxole-5-carboxylate **175**: δ<sub>H</sub> (500 MHz; CDCl<sub>3</sub>) 4.69-4.67 (2H, m, CHO), 3.68 (3H, s, CO<sub>2</sub>CH<sub>3</sub>) 3.03 (1H, tt, *J* 12.0 and 6.0, CHCO<sub>2</sub>CH<sub>3</sub>), 2.13 (1H, dd, *J* 14.0 and 6.0, CHCH<sub>2</sub>), 1.72 (1H, td, *J* 14.0 and 3.5, CHCH<sub>2</sub>), 1.44 (3H, s, C(CH<sub>3</sub>)<sub>2</sub>), 1.28 (3H, s, C(CH<sub>3</sub>)<sub>2</sub>); δ<sub>C</sub> (125 MHz, CDCl<sub>3</sub>) 175.5 (CO<sub>2</sub>CH<sub>3</sub>), 109.1 (C(CH<sub>3</sub>)<sub>2</sub>), 80.1 (CH<sub>2</sub>CHO), 51.9 (OCH<sub>3</sub>), 40.7 (CHCO<sub>2</sub>), 37.1 (CH<sub>2</sub>CHO), 26.2 (C(CH<sub>3</sub>)<sub>2</sub>), 23.9 (C(CH<sub>3</sub>)<sub>2</sub>); HRMS (ESI) cald. for C<sub>10</sub>H<sub>16</sub>NaO<sub>4</sub> (M + Na<sup>+</sup>) requires 223.0946, found 223.0947. Spectroscopic data was identical to that previously reported in the literature.<sup>206</sup>

Methyl (3*aR*,5*s*,6*aS*)-2,2-dimethyltetrahydro-4*H*-cyclopenta[*d*][1,3]dioxole-5-carboxylate **176**: δ<sub>H</sub> (500 MHz; CDCl<sub>3</sub>) 4.64-4.61 (2H, m, CHO), 3.66 (3H, s, CO<sub>2</sub>CH<sub>3</sub>) 2.80 (1H, tt, *J* 8.0 and 3.0, CHCO<sub>2</sub>CH<sub>3</sub>), 2.47 (1H, dd, *J* 14.5 and 3.0, CHCH<sub>2</sub>), 1.86 (1H, ddd, *J* 13.5, 6.5 and 4.0, CHCH<sub>2</sub>), 1.37 (3H, s, C(CH<sub>3</sub>)<sub>2</sub>), 1.26 (3H, s, C(CH<sub>3</sub>)<sub>2</sub>); δ<sub>C</sub> (125 MHz, CDCl<sub>3</sub>) 174.5 (CO<sub>2</sub>CH<sub>3</sub>), 110.5 (C(CH<sub>3</sub>)<sub>2</sub>), 80.6 (CH<sub>2</sub>CHO), 51.9 (OCH<sub>3</sub>), 42.5 (CHCO<sub>2</sub>), 35.1 (CH<sub>2</sub>CHO), 26.1 (C(CH<sub>3</sub>)<sub>2</sub>), 24.2 (C(CH<sub>3</sub>)<sub>2</sub>); HRMS (ESI) cald. for C<sub>10</sub>H<sub>16</sub>NaO<sub>4</sub> (M + Na<sup>+</sup>) requires 223.0946, found 223.0946. Spectroscopic data was identical to that previously reported in the literature.<sup>206</sup>

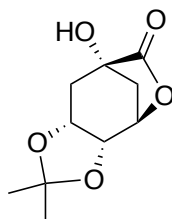
### (1*s*,3*R*,4*S*)-3,4-Dihydroxycyclopentane-1-carboxylic acid (**173**)



To a solution of acetonide **176** (328 mg, 1.64 mmol, 1.0 equiv.) in MeOH (10 mL) was added TsOH (35 mg, 0.20 mmol, 0.12 equiv.) and the reaction was stirred at RT for 1 h. The mixture was then concentrated *in vacuo* and partitioned between EtOAc (20 mL) and saturated NaHCO<sub>3</sub> (20 mL). The layers were separated and the aqueous phase further extracted with EtOAc (2 × 20 mL), the combined organics were then washed with brine, dried (MgSO<sub>4</sub>), filtered and concentrated *in vacuo* to afford the crude diol as a viscous oil. The diol was then dissolved in THF (10 mL) and H<sub>2</sub>O (5 mL), and LiOH was added (40 mg, 2.0 mmol, 1.20 equiv.). The reaction was then stirred at RT for 16 h, acidified (1 M HCl, 5 mL) and concentrated *in vacuo* to afford the product as a viscous oil (162 mg, 78 %, 1.29 mmol).

$\nu_{\max}/\text{cm}^{-1}$  (neat) 3347 (OH), 1652 (C=O), 1025 (C-O);  $\delta_{\text{H}}$  (500 MHz, MeOD) 4.09-4.02 (2H, br. m, CHOH), 3.06 (1H, tt, *J* 9.5 and 3, CHCOOH), 2.09-1.88 (4H, m, CH<sub>2</sub>);  $\delta_{\text{C}}$  (125 MHz, MeOD) 183.2 (CO<sub>2</sub>H), 73.2 (CHOH), 40.1 (CHCOOH), 35.1 (CH<sub>2</sub>); HRMS (ESI) calcd. for C<sub>6</sub>H<sub>10</sub>NaO<sub>4</sub> (M + Na<sup>+</sup>) requires 169.0477, found 169.0475.

**(3a*R*,4*R*,7*S*,8a*R*)-7-Hydroxy-2,2-dimethyltetrahydro-4,7-methano [1,3]dioxolo[4,5-*c*]oxepin-6(4*H*)-one (181)**

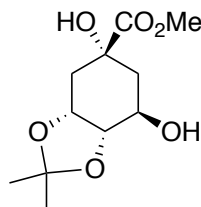


The following procedure was modified from Wang *et al.*<sup>262</sup> To a stirred solution of *D*-(-)-quinic acid (10.0 g, 52.0 mmol, 1.0 equiv.) in acetone (150 mL), was added 2,2-dimethoxypropane (19.2 mL, 156 mmol, 3.0 equiv.) and TsOH (95 mg, 0.50 mmol, 0.01 equiv.), the reaction was heated to reflux for 4 h. The reaction mixture was then concentrated *in vacuo* and re-suspended in EtOAc (150 mL), before being washed with sat. NaHCO<sub>3</sub> solution (50 mL), brine (50 mL), dried (MgSO<sub>4</sub>) and concentrated *in vacuo* to afford the product as a white solid (10.5 g, 94 %, 48.9 mmol).

$\delta_{\text{H}}$  (500 MHz; CDCl<sub>3</sub>) 4.72 (1H, dd, *J* 6.0 and 2.5, CHOCO), 4.50 (1H, td, *J* 7.5 and 3.0, CH<sub>2</sub>CHCH), 4.30 (1H, d, *J* 6.5, CH<sub>2</sub>CHCH), 2.74 (1H, br. s, OH), 2.65 (1H, d, *J* 12.0, CCH<sub>2</sub>COCO), 2.36 (1H, ddd, *J* 14.5, 7.5 and 2.0, CH<sub>2</sub>), 2.30 (1H, dd, *J* 12.0 and 6.5, CCH<sub>2</sub>COCO), 2.18 (1H, dd, *J* 14.5 and 3.0, CH<sub>2</sub>), 1.52 (3H, s, CH<sub>3</sub>), 1.33 (3H, s, CH<sub>3</sub>);  $\delta_{\text{C}}$  (125 MHz, CDCl<sub>3</sub>) 178.9 (CO<sub>2</sub>), 109.9 (C(CH<sub>3</sub>)<sub>2</sub>), 76.0 (CHOCO), 72.3 (CH<sub>2</sub>CHCH), 71.7 (CH<sub>2</sub>CHCH), 71.6 (CCO<sub>2</sub>), 38.4 (CH<sub>2</sub>), 34.4 (CH<sub>2</sub>COCO), 27.1 (CH<sub>3</sub>), 24.2 (CH<sub>3</sub>); HRMS

(ESI) calcd. for  $C_{10}H_{14}NaO_5$  ( $M + Na^+$ ) requires 237.0739, found 237.0731. Spectroscopic data was identical to that previously reported in the literature.<sup>262</sup>

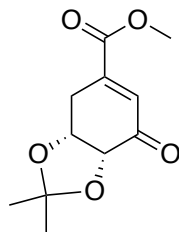
**Methyl (3a*R*,5*R*,7*R*,7a*S*)-5,7-dihydroxy-2,2-dimethylhexahydrobenzo[*d*][1,3] dioxole-5-carboxylate (182)**



The following procedure was modified from Wang *et al.*<sup>262</sup> To a stirred solution of (3a*R*,4*R*,7*S*,8a*R*)-7-hydroxy-2,2-dimethyltetrahydro-4,7-methano [1,3]dioxolo[4,5-*c*]oxepin-6(4*H*)-one **181** (10.2 g, 47.7 mmol, 1.0 equiv.) in MeOH (250 mL), was added NaOMe (2.57 g, 47.7 mmol, 1.0 equiv.) and the reaction was stirred at RT for 4 h. The reaction was quenched via the addition of AcOH (2.0 mL) before being concentrated *in vacuo*. The resulting residue was re-suspended in EtOAc (100 mL), before being washed with water (50 mL), brine (50 mL), dried (MgSO<sub>4</sub>) and concentrated *in vacuo*. The resulting residue was purified by silica chromatography (EtOAc) to afford the product as a colourless oil (9.86 g, 84 %, 40 mmol)

$\delta_H$  (500 MHz; CDCl<sub>3</sub>) 4.49-4.46 (1H, m, CHOH), 4.16-4.06 (1H, m, CHOHCHCH), 3.98 (1H, t, *J* 6.0, CHOHCHCH), 3.81 (3H, s, OCH<sub>3</sub>), 3.35 (1H, br. s, OH), 2.44 (1H, br. s, OH), 2.30-2.22 (2H, m, CH<sub>2</sub>CHOH), 2.10-2.05 (1H, m, CH<sub>2</sub>), 1.88 (1H, ddd, *J* 13.5, 10.5 and 3.0, CH<sub>2</sub>), 1.54 (3H, s, CH<sub>3</sub>), 1.37 (3H, s, CH<sub>3</sub>);  $\delta_C$  (125 MHz, CDCl<sub>3</sub>) 175.8 (CO<sub>2</sub>), 109.4 (C(CH<sub>3</sub>)<sub>2</sub>), 79.9 (CHOHCHCH), 74.0 (CCO<sub>2</sub>), 73.5 (CHOH), 68.3 (CHOHCHCH), 53.3 (OCH<sub>3</sub>), 39.1 (CH<sub>2</sub>), 34.9 (CH<sub>2</sub>CHOH), 28.3 (CH<sub>3</sub>), 25.8 (CH<sub>3</sub>); HRMS (ESI) calcd. for  $C_{11}H_{18}NaO_6$  ( $M + Na^+$ ) requires 269.1001, found 269.0999. Spectroscopic data was identical to that previously reported in the literature.<sup>262</sup>

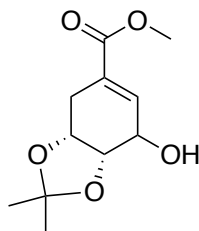
**Methyl (3aR,7aR)-2,2-dimethyl-7-oxo-3a,4,7,7a-tetrahydrobenzo[d][1,3]dioxole-5-carboxylate (183)**



The following procedure was modified from Wang *et al.*<sup>262</sup> To a stirred solution of methyl (3aR,5R,7R,7aS)-5,7-dihydroxy-2,2-dimethylhexahydrobenzo[d][1,3]dioxole-5-carboxylate **182** (9.50 g, 38.6 mmol, 1.0 equiv.), 3.0 Å molecular sieves (20.0 g) and anhydrous pyridine (9.38 mL, 116 mmol, 3.0 equiv.) in anhydrous CH<sub>2</sub>Cl<sub>2</sub> (100 mL) was added PCC (33.2 g, 154 mmol, 4.0 equiv.) and the reaction stirred at RT for 16 h. The reaction mixture was then filtered through Celite<sup>®</sup>, the filtrate washed with brine (50 mL), dried (MgSO<sub>4</sub>) and concentrated *in vacuo*. The crude residue was then purified by silica chromatography (1:1 EtOAc:Petroleum ether) to afford the product as a yellow solid (4.45 g, 51 %, 19.7 mmol).

$\delta_{\text{H}}$  (500 MHz; CDCl<sub>3</sub>) 6.85 (1H, d, *J* 2.5, CCHCO), 4.70 (1H, td, *J* 5.0 and 1.5, CHCHCO), 4.31 (1H, d, *J* 5.0, CHCHCO), 3.87 (3H, s, OCH<sub>3</sub>), 3.22 (1H, d, *J* 20.5, CH<sub>2</sub>), 2.88 (1H, ddd, *J* 20.0, 5.0 and 3.0, CH<sub>2</sub>), 1.41 (3H, s, CH<sub>3</sub>), 1.33 (3H, s, CH<sub>3</sub>);  $\delta_{\text{C}}$  (125 MHz, CDCl<sub>3</sub>) 197.6 (CO), 166.3 (CO<sub>2</sub>Me), 144.4 (CCO<sub>2</sub>Me), 131.4 (CHCCO<sub>2</sub>Me), 109.7 (C(CH<sub>3</sub>)<sub>2</sub>), 75.3 (CHCHCO), 72.7 (CHCHCO), 53.1 (OCH<sub>3</sub>), 27.5 (CH<sub>3</sub>), 26.8 (CH<sub>2</sub>), 26.0 (CH<sub>3</sub>); HRMS (ESI) cald. for C<sub>11</sub>H<sub>14</sub>NaO<sub>5</sub> (M + Na<sup>+</sup>) requires 249.0739, found 249.0735 Spectroscopic data was identical to that previously reported in the literature.<sup>262</sup>

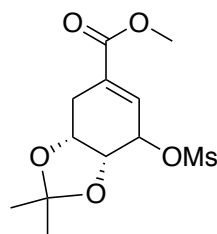
**Methyl (3aR,7aS)-7-hydroxy-2,2-dimethyl-3a,4,7,7a-tetrahydrobenzo[d][1,3]dioxole-5-carboxylate (184)**



The following procedure was modified from Wang *et al.*<sup>262</sup> To a stirred solution of methyl (3a*R*,7a*R*)-2,2-dimethyl-7-oxo-3a,4,7,7a-tetrahydrobenzo[*d*][1,3]dioxole-5-carboxylate **183** (4.00 g, 17.7 mmol, 1.0 equiv.) in MeOH (50 mL) at 0 °C was added NaBH<sub>4</sub> (737 mg, 19.4 mmol, 1.1 equiv.) and the reaction mixture was stirred at this temperature for 30 min. The reaction was quenched with saturated NH<sub>4</sub>Cl solution (5 mL) and the MeOH was removed *in vacuo*. The resulting mixture was re-dissolved in CH<sub>2</sub>Cl<sub>2</sub> (50 mL), washed with brine (50 mL), dried (MgSO<sub>4</sub>) and concentrated *in vacuo* to afford the product as a colourless oil (3.87 g, 96 %, 17 mmol).

$\delta_{\text{H}}$  (500 MHz; CDCl<sub>3</sub>) 6.94 (1H, s, CHCCO<sub>2</sub>Me), 4.64 (1H, ddd, *J* 7.5, 3.5 and 2.5, CHCHCHOH), 4.57 (1H, dd, *J* 6.0 and 4.5, CHCHCHOH), 4.07 (1H, br. s, CHOH), 3.77 (3H, s, OCH<sub>3</sub>), 3.04 (1H, dd, *J* 16.5 and 2.0, CH<sub>2</sub>), 2.65 (1H, br. s, OH), 1.95 (1H, dq, *J* 16.5 and 3.0, CH<sub>2</sub>), 1.33 (3H, s, CH<sub>3</sub>), 1.32 (3H, s, CH<sub>3</sub>);  $\delta_{\text{C}}$  (125 MHz, CDCl<sub>3</sub>) 166.3 (CO<sub>2</sub>Me), 142.6 (CCO<sub>2</sub>Me), 128.5 (CHCCO<sub>2</sub>Me), 109.2 (C(CH<sub>3</sub>)<sub>2</sub>), 76.2 (CHCHCHOH), 72.6 (CHCHCHOH), 68.1 (CHOH), 52.1 (OCH<sub>3</sub>), 26.6 (CH<sub>2</sub>), 26.0 (CH<sub>3</sub>), 24.5 (CH<sub>3</sub>); HRMS (ESI) calcd. for C<sub>11</sub>H<sub>16</sub>NaO<sub>5</sub> (M + Na<sup>+</sup>) requires 251.0895, found 251.0890. Spectroscopic data was identical to that previously reported in the literature.<sup>262</sup>

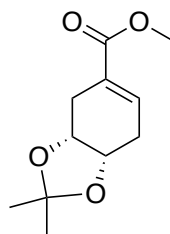
**Methyl (3a*R*,7a*R*)-2,2-dimethyl-7-((methylsulfonyl)oxy)-3a,4,7,7a-tetrahydrobenzo[*d*][1,3]dioxole-5-carboxylate (186)**



To a stirred solution of methyl (3a*R*,7a*S*)-7-hydroxy-2,2-dimethyl-3a,4,7,7a-tetrahydrobenzo[*d*][1,3]dioxole-5-carboxylate **184** (3.70 g, 16.2 mmol, 1.0 equiv.) in CH<sub>2</sub>Cl<sub>2</sub> (100 mL) was added Et<sub>3</sub>N (22.55 mL, 162 mmol, 10.0 equiv.) and methanesulfonyl chloride (6.3 mL, 81.1 mmol, 5.0 equiv.) at 0 °C and the mixture was stirred overnight at RT. The reaction was quenched with 1 M HCl (20 mL) and the mixture extracted with CH<sub>2</sub>Cl<sub>2</sub> (3 × 50 mL), the combined organics were then washed with brine, dried (MgSO<sub>4</sub>), filtered and concentrated *in vacuo* to afford the crude product as an orange solid. The crude product was purified by silica chromatography (2 : 1 EtOAc : Petroleum ether) to afford the product as a white solid (4.11 g, 83 %, 13.4 mmol, m.p. 88-90 °C).

$\nu_{\max}/\text{cm}^{-1}$  (neat) 1701 (C=O), 1351 (S=O), 1063 (C-O);  $\delta_{\text{H}}$  (500 MHz,  $\text{CDCl}_3$ ) 6.95 (1H, br. s, CHCHOS), 5.06 (1H, br. s, CHOS), 4.75-4.71 (1H, m,  $\text{CH}_2\text{CHOCHO}$ ), 4.67-4.63 (1H, m,  $\text{CH}_2\text{CHO}$ ), 3.78 (3H, s,  $\text{OCH}_3$ ), 3.17 (3H, s,  $\text{SCH}_3$ ), 3.07 (1H, d,  $J$  16.5,  $\text{CH}_2$ ), 2.00 (1H, d,  $J$  16.5,  $\text{CH}_2$ ), 1.34 (3H, s,  $\text{CCH}_3$ ), 1.32 (3H, s,  $\text{CCH}_3$ );  $\delta_{\text{C}}$  (125 MHz,  $\text{CDCl}_3$ ) 165.5 ( $\text{CO}_2\text{Me}$ ), 136.2 (CHCOS), 130.8 ( $\text{CCOOMe}$ ), 109.9 ( $\text{C}(\text{CH}_3)_2$ ), 75.7 (CHOS), 75.4 ( $\text{CH}_2\text{CHOCHO}$ ), 72.5 ( $\text{CH}_2\text{CHO}$ ), 52.4 ( $\text{COOCH}_3$ ), 39.2 ( $\text{SCH}_3$ ), 27.2 ( $\text{CH}_2$ ), 25.8 ( $\text{CH}_3$ ), 24.4 ( $\text{CH}_3$ ); HRMS (ESI) calcd. for  $\text{C}_{12}\text{H}_{18}\text{NaO}_7\text{S}$  ( $\text{M} + \text{Na}^+$ ) requires 329.0671, found 329.0672.

**Methyl (3aR,7aS)-2,2-dimethyl-3a,4,7,7a-tetrahydrobenzo[d][1,3]dioxole-5-carboxylate (185)**

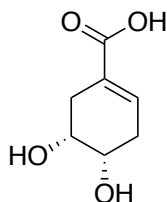


To a stirred solution of  $\text{Pd}_2(\text{dba})_3 \cdot \text{CHCl}_3$  (600 mg, 0.60 mmol, 0.18 equiv.), tributylphosphine (150  $\mu\text{l}$ , 0.60 mmol, 0.18 equiv.) and methyl (3aR,7aR)-2,2-dimethyl-7-((methylsulfonyl)oxy)-3a,4,7,7a-tetrahydrobenzo[d][1,3]dioxole-5-carboxylate **186** (3.30 g, 11.0 mmol, 1.0 equiv.) in dioxane (100 mL) under and argon atmosphere was added a suspension of  $\text{NaBH}_4$  (400 mg, 11.0 mmol, 1.00 equiv.) in  $\text{H}_2\text{O}$  (10 mL) and the reaction was stirred for 2 h at RT. The reaction mixture was then diluted with saturated brine (10 mL) and extracted with  $\text{Et}_2\text{O}$  ( $3 \times 50$  mL), the combined organics were then washed with brine, dried ( $\text{MgSO}_4$ ), filtered and concentrated *in vacuo* to afford the crude product as a black oil. The crude product was purified by silica chromatography (1 : 9 EtOAc : Petroleum ether) to afford the product as a colourless oil (1.59 g, 68 %, 7.48 mmol).

$\nu_{\max}/\text{cm}^{-1}$  (neat) 2985 (C=C-H), 1711 (C=O), 1092 (C-O);  $\delta_{\text{H}}$  (500 MHz,  $\text{CDCl}_3$ ) 7.02 (1H, dt,  $J$  6.0 and 3.0,  $\text{CHCH}_2\text{CHO}$ ), 4.52 (1H, ddd,  $J$  7.0, 4.0 and 3.0,  $\text{CH}_2\text{CHO}$ ), 4.48 (1H, ddd,  $J$  7.0, 5.0 and 2.5,  $\text{CHCH}_2\text{CHO}$ ), 3.74 (3H, s,  $\text{OCH}_3$ ), 2.74 (1H, dd,  $J$  16.5 and 3.0,  $\text{CH}_2\text{C}$ ), 2.50 (1H, dd,  $J$  17.0, 6.0 and 2.0,  $\text{CHCH}_2$ ), 2.29-2.20 (2H, m,  $\text{CH}_2\text{C}$ ,  $\text{CHCH}_2$ ), 1.29 (3H, s,  $\text{CCH}_3$ ), 1.28 (3H, s,  $\text{CCH}_3$ );  $\delta_{\text{C}}$  (125 MHz,  $\text{CDCl}_3$ ) 168.4 ( $\text{CO}_2\text{Me}$ ), 139.5 ( $\text{CHCH}_2$ ), 130.7 ( $\text{CCOOMe}$ ), 108.9 ( $\text{C}(\text{CH}_3)_2$ ), 74.7 ( $\text{CH}_2\text{CHO}$ ), 74.0 ( $\text{CHCH}_2\text{CHO}$ ), 52.2 ( $\text{COOCH}_3$ ), 30.0 ( $\text{CH}_2\text{C}$ ), 28.0 ( $\text{CHCH}_2$ ) 26.7 ( $\text{CH}_3$ ), 24.6 ( $\text{CH}_3$ ); HRMS (ESI) calcd. for  $\text{C}_{11}\text{H}_{16}\text{NaO}_4$  ( $\text{M} + \text{Na}^+$ ) requires 235.0946, found 235.0949;  $[\alpha]_{\text{D}}^{25}$  (c 0.1, MeOH): +33.8.



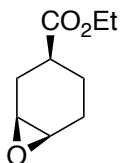
**(4*S*,5*R*)-4,5-Dihydroxycyclohex-1-ene-1-carboxylic acid (51)**



To a solution of methyl (3*aR*,7*aS*)-2,2-dimethyl-3*a*,4,7,7*a*-tetrahydrobenzo[*d*][1,3]dioxole-5-carboxylate **185** (1.50 g, 7.0 mmol, 1.0 equiv.) in MeOH (50 mL) was added TsOH (170 mg, 1.0 mmol, 0.14 equiv.) and the reaction was stirred at RT for 1 h. The mixture was then concentrated *in vacuo* and partitioned between EtOAc (50 mL) and saturated NaHCO<sub>3</sub> (50 mL). The layers were separated and the aqueous phase further extracted with EtOAc (2 × 50 mL), the combined organics were then washed with brine, dried (MgSO<sub>4</sub>), filtered and concentrated *in vacuo* to afford the crude diol as a viscous oil. The diol was then dissolved in THF (50 mL) and H<sub>2</sub>O (25 mL), and LiOH was added (140 mg, 7.00 mmol, 1.00 equiv.). The reaction was then stirred at RT for 16 h, acidified (1 M HCl, 10 mL) and concentrated *in vacuo* to afford the product as a viscous oil (810 mg, 73 %, 5.11 mmol).

$\nu_{\max}/\text{cm}^{-1}$  (neat) 3287 (OH), 2927 (C=C-H), 1709 (C=O), 1089 (C-O);  $\delta_{\text{H}}$  (500 MHz, MeOD) 6.87-6.84 (1H, m, CHCH<sub>2</sub>CHO), 3.92-3.84 (2H, m, CHO), 2.55-2.35 (4H, m, CH<sub>2</sub>),  $\delta_{\text{C}}$  (125 MHz, MeOD) 170.25 (CO<sub>2</sub>H), 137.8 (CHCH<sub>2</sub>), 128.9 (CCOOH), 69.6 (CH<sub>2</sub>CHO), 68.5 (CHCH<sub>2</sub>CHO), 32.3 (CH<sub>2</sub>C), 31.0 (CHCH<sub>2</sub>) 26.7 (CH<sub>3</sub>); HRMS (ESI) cald. for C<sub>7</sub>H<sub>10</sub>NaO<sub>4</sub> (M + Na<sup>+</sup>) requires 181.0477, found 181.0476. [ $\alpha$ ]<sub>D</sub><sup>25</sup> (c 0.5, MeOH): +18.

**Ethyl (1*S*,3*S*,6*R*)-7-oxabicyclo[4.1.0]heptane-3-carboxylate (189)**

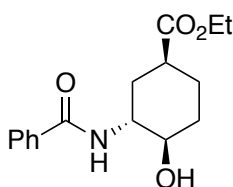


The following procedure was modified from Wang *et al.*<sup>258</sup> To a solution of (1*S*,4*S*,5*S*)-4-iodo-6-oxabicyclo[3.2.1]octan-7-one **188** (2.50 g, 1.0 mmol, 1.0 equiv.) in EtOH (50 mL) was added 2 M NaOH solution (20 mL) and the reaction was stirred at RT for 4 h. The EtOH was

removed *in vacuo* and the resulting residue was re-dissolved in CH<sub>2</sub>Cl<sub>2</sub> (50 mL), the mixture was then washed with brine (50 mL), dried (MgSO<sub>4</sub>) and concentrated *in vacuo*. The crude residue was then purified by silica chromatography (1 : 3 EtOAc : Petroleum ether) to afford the product as a colourless oil (1.41 g 83 %, 0.83 mmol).

$\delta_{\text{H}}$  (500 MHz; CDCl<sub>3</sub>) 4.11 (2H, q, *J* 5.0, CH<sub>2</sub>CH<sub>3</sub>), 3.17-3.14 (2H, m, CHCHO), 2.26-2.08 (4H, m, CHOCH<sub>2</sub>CH<sub>2</sub>, CHOCH<sub>2</sub>CH, CHCO<sub>2</sub>), 1.77 (1H, dddd, *J* 15.0, 11.0, 5.5 and 1.5, CHOCH<sub>2</sub>CH<sub>2</sub>), 1.66-1.53 (2H, m, CH<sub>2</sub>CHCO<sub>2</sub>), 1.24 (3H, t, *J* 7.5, CH<sub>3</sub>);  $\delta_{\text{C}}$  (125 MHz, CDCl<sub>3</sub>) 175.0 (CO<sub>2</sub>), 60.6 (CH<sub>2</sub>CH<sub>3</sub>), 51.9 (CHCH<sub>2</sub>CHO), 50.9 (CHO), 38.2 (CHCO<sub>2</sub>), 26.4 (CHCH<sub>2</sub>CH), 24.3 (CHOCH<sub>2</sub>), 21.2 (CHCH<sub>2</sub>), 14.4 (CH<sub>3</sub>); HRMS (ESI) cald. for C<sub>9</sub>H<sub>14</sub>NaO<sub>3</sub> (M + Na<sup>+</sup>) requires 193.0841, found 193.0836. Spectroscopic data consistent with that previously reported in the literature.<sup>258</sup>

### Ethyl (1*S*,3*R*,4*R*)-3-benzamido-4-hydroxycyclohexane-1-carboxylate (**190**)

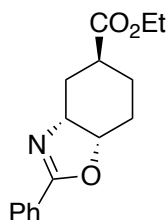


To a solution of ethyl (1*S*,3*S*,6*R*)-7-oxabicyclo[4.1.0]heptane-3-carboxylate **189** in (1.15 g, 6.76 mmol, 1.0 equiv.) in EtOH (10 mL) was added 28 % aqueous ammonia (20 mL). The reaction was stirred at 45 °C overnight and concentrated *in vacuo* to afford the amino alcohol as a yellow oil. The oil was dissolved EtOH (20 mL) and benzoic anhydride (1.68 g, 7.44 mmol, 1.1 equiv.) was then added in an ice-water bath. After 15 min the reaction was allowed to warm to RT and stirred for a further 2 h. The reaction was then concentrated *in vacuo*, and the crude oil purified by silica chromatography (1 : 2 EtOAc : Petroleum ether) to afford the product as a white solid (1.75 g, 89 %, 6.0 mmol, m.p. 138-140 °C).

$\nu_{\text{max}}/\text{cm}^{-1}$  (neat) 3423 (NH), 3310 (OH), 2944 (ArH), 1720 (C=O), 1627 (C=O), 1025 (C-O);  $\delta_{\text{H}}$  (500 MHz; CDCl<sub>3</sub>) 7.76 (2H, d, *J* 7.5, ArH), 7.51 (1H, t, *J* 7.0, ArH), 7.43 (2H, t, *J* 7.5, ArH), 7.18 (1H, br. d, *J* 6.5, NH), 4.19 (2H, q, *J* 7.5, OCH<sub>2</sub>CH<sub>3</sub>), 4.12-4.05 (1H, m, CHN), 3.71 (1H, br. s, OH), 3.56 (1H, td, *J* 9.0 and 4.5, CHOH), 2.72 (1H, quin., *J* 4.0, CHCO<sub>2</sub>), 2.50-2.44 (1H, m, CH<sub>2</sub>CHN), 2.22-2.14 (1H, m, CH<sub>2</sub>CHCO<sub>2</sub>), 1.99-1.91 (1H, m, CH<sub>2</sub>CHOH), 1.73 (1H, br. s, OH), 1.63-1.54 (3H, m, CH<sub>2</sub>CHN, CH<sub>2</sub>CHCO<sub>2</sub> and CH<sub>2</sub>CHOH), 1.29 (3H, t, *J* 7.0, CH<sub>3</sub>);  $\delta_{\text{C}}$  (125 MHz, CDCl<sub>3</sub>) 174.0 (CO<sub>2</sub>CH<sub>2</sub>), 169.3 (CON), 134.2 (ArC<sub>quart.</sub>), 132.0 (ArC), 128.8 (ArC), 127.2 (ArC), 74.2 (CHO), 60.9 (CH<sub>2</sub>CH<sub>3</sub>), 53.1 (CHN), 38.9 (CHCO<sub>2</sub>), 31.5 (CH<sub>2</sub>CHN), 30.7

(CH<sub>2</sub>CHOH), 25.0 (CH<sub>2</sub>CHCO<sub>2</sub>), 14.4 (CH<sub>3</sub>); HRMS (ESI) cald. for C<sub>16</sub>H<sub>21</sub>NNaO<sub>4</sub> (M + Na<sup>+</sup>) requires 314.1363, found 314.1363; [ $\alpha$ ]<sub>D</sub><sup>26</sup> (c 0.15, MeOH): +13.3.

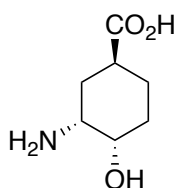
**Ethyl (3aR,5S,7aS)-2-phenyl-3a,4,5,6,7,7a-hexahydrobenzo[d]oxazole-5-carboxylate (191)**



To a solution of ethyl (1S,3R,4R)-3-benzamido-4-hydroxycyclohexane-1-carboxylate **190** (1.5 g, 5.15 mmol, 1.0 equiv.) in CHCl<sub>3</sub> (30 mL) was added SOCl<sub>2</sub> (1.5 mL, 9.82 mmol, 1.9 equiv.) dropwise under an inert atmosphere. The reaction was allowed to stir for 1 h at 40 °C, before the addition of saturated NaHCO<sub>3</sub> (15 mL), the reaction was then stirred for a further 10 min. The organic layer was then separated and the aqueous layer further extracted with CHCl<sub>3</sub> (2 x 20 mL), the combined organics were dried (MgSO<sub>4</sub>), filtered and concentrated *in vacuo* to afford the product as a yellow oil (1.21 g, 86 %, 4.4 mmol).

$\nu_{\max}/\text{cm}^{-1}$  (neat) 2941 (ArH), 1720 (C=O), 1631 (C=N), 1025 (C-O);  $\delta_{\text{H}}$  (500 MHz; CDCl<sub>3</sub>) 7.94 (2H, d, *J* 7.5, ArH), 7.48 (1H, t, *J* 7.5, ArH), 7.41 (2H, t, *J* 7.5, ArH), 4.81 (1H, dt., *J* 9.0 and 5.5, CHOCN), 4.39 (1H, quin., *J* 4.5, CHN), 4.13 (2H, qd, *J* 7.0 and 2.0, OCH<sub>2</sub>CH<sub>3</sub>), 2.59 (1H, dtd, *J* 11.5, 7.0 and 5.0, CHCO<sub>2</sub>), 2.24 (1H, dt, *J* 14.5 and 4.0, CH<sub>2</sub>CHN), 2.01-1.92 (2H, m, CH<sub>2</sub>CHN and CH<sub>2</sub>CHO), 1.88-1.73 (2H, m, CH<sub>2</sub>CHO and CH<sub>2</sub>CHCO<sub>2</sub>), 1.68-1.60 (1H, m, CH<sub>2</sub>CHCO<sub>2</sub>), 1.24 (3H, t, *J* 7.0, CH<sub>3</sub>);  $\delta_{\text{C}}$  (125 MHz, CDCl<sub>3</sub>) 176.0 (CO<sub>2</sub>CH<sub>2</sub>), 164.5 (CON), 131.6 (ArC), 128.5 (ArC), 128.3 (ArC), 128.0 (ArC<sub>quart.</sub>), 77.7 (CHO), 63.2 (CHN), 60.6 (CH<sub>2</sub>CH<sub>3</sub>), 35.7 (CHCO<sub>2</sub>), 28.6 (CH<sub>2</sub>CHN), 25.0 (CH<sub>2</sub>CHO), 20.9 (CH<sub>2</sub>CHCO<sub>2</sub>), 14.3 (CH<sub>3</sub>); HRMS (ESI) cald. for C<sub>16</sub>H<sub>20</sub>NO<sub>3</sub> (M + H<sup>+</sup>) requires 274.1438, found 274.1439; [ $\alpha$ ]<sub>D</sub><sup>26</sup> (c 0.35, MeOH): +28.6.

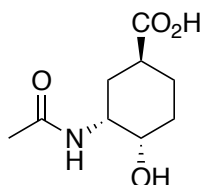
**(1S,3R,4S)-3-amino-4-hydroxycyclohexane-1-carboxylic acid (192)**



Ethyl (3*aR*,5*S*,7*aS*)-2-phenyl-3*a*,4,5,6,7,7*a*-hexahydrobenzo[*d*]oxazole-5-carboxylate **191** (1.20 g, 4.41 mmol, 1.0 equiv.) was dissolved in aqueous HCl (6 M, 50 mL) and heated to reflux overnight. The reaction was then concentrated *in vacuo*, diluted with water and then washed with Et<sub>2</sub>O (5 × 50 mL). The aqueous phase was then concentrated *in vacuo* to afford the product as a white solid (0.65 g, 92 %, 4.05 mmol, m.p. 233-235 °C).

$\nu_{\max}/\text{cm}^{-1}$  (neat) 3283 (NH<sub>2</sub>), 3134 (OH), 2904 (CO<sub>2</sub>H), 1697 (C=O), 1040 (C-O);  $\delta_{\text{H}}$  (500 MHz; D<sub>2</sub>O) 4.06 (1H, dt, *J* 6.5 and 3.0, CHOH), 3.62 (1H, dt, *J* 8.0 and 4.0, CHNH<sub>2</sub>), 2.79 (1H, quin., *J* 6.0 CHCO<sub>2</sub>H), 2.10-1.91 (3H, m, CHCH<sub>2</sub>CHNH<sub>2</sub>, CH<sub>2</sub>CHCO<sub>2</sub>H), 1.85-1.67 (3H, m, CH<sub>2</sub>CHCO<sub>2</sub>H, CH<sub>2</sub>CHOH);  $\delta_{\text{C}}$  (125 MHz, D<sub>2</sub>O) 178.9 (CO<sub>2</sub>H), 65.5 (CHOH), 50.2 (CHNH), 37.1 (CHCO<sub>2</sub>H), 27.1 (CH<sub>2</sub>CHOH), 26.3 (CH<sub>2</sub>CHNH<sub>2</sub>), 22.0 (CH<sub>2</sub>CHCO<sub>2</sub>H); HRMS (ESI) cald. for C<sub>7</sub>H<sub>14</sub>NO<sub>3</sub> (M + H<sup>+</sup>) requires 160.0967, found 160.0968; [ $\alpha$ ]<sub>D</sub><sup>26</sup> (c 0.18, MeOH): +25.7.

### (1*S*,3*R*,4*S*)-3-acetamido-4-hydroxycyclohexane-1-carboxylic acid (**193**)

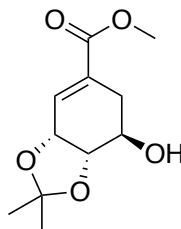


To a solution of (1*S*,3*R*,4*S*)-3-amino-4-hydroxycyclohexane-1-carboxylic acid **192** (100 mg, 0.63 mmol, 1.0 equiv.) in H<sub>2</sub>O (2 mL) was added acetic anhydride (75  $\mu$ L, 0.85 mmol, 1.4 equiv.) followed by sodium acetate (200 mg, 2.52 mmol, 4.0 equiv.) and the reaction stirred at RT for 4 h. The reaction mixture was then acidified using aqueous HCl (2 M, 2 mL), and concentrated *in vacuo* to afford a white tacky solid. The crude was then re-suspended in MeOH (10 mL), filtered and concentrated *in vacuo* to afford the product as a viscous oil (92 mg, 73 %, 0.46 mmol).

$\nu_{\max}/\text{cm}^{-1}$  (neat) 3136 (OH), 2935 (NH), 1699, 1618 (C=O), 1023 (C-O);  $\delta_{\text{H}}$  (500 MHz; D<sub>2</sub>O) 5.12 (1H, dt, *J* 6.0 and 3.0, CHOH), 3.77 (1H, dt, *J* 9.5 and 3.5, CHNH), 2.82 (1H, quin., *J* 5.0, CHCO<sub>2</sub>H), 2.19-2.14 (1H, m, CH<sub>2</sub>CHNH), 2.16 (3H, s, CH<sub>3</sub>CON), 2.07 (1H, ddd, *J* 14.0, 10.0 and 5.0, CH<sub>2</sub>CHNH), 1.96-1.75 (4H, m, CH<sub>2</sub>CHCO<sub>2</sub>H, CH<sub>2</sub>CHOH);  $\delta_{\text{C}}$  (125 MHz, D<sub>2</sub>O) 177.4 (CO<sub>2</sub>H), 171.2 (CONH), 67.7 (CHOH), 46.5 (CHNH), 35.9 (CHCO<sub>2</sub>H), 24.8 (CH<sub>2</sub>CHNH), 22.5 (CH<sub>2</sub>CHOH), 19.8 (CH<sub>2</sub>CHCO<sub>2</sub>H), 18.4 CH<sub>3</sub>; HRMS (ESI) cald. for C<sub>9</sub>H<sub>16</sub>NO<sub>4</sub> (M + H<sup>+</sup>) requires 202.1074, found 202.1075; ; [ $\alpha$ ]<sub>D</sub><sup>26</sup> (c 0.3, MeOH): +7.7.

### 6.9.3 Synthesis of Substrates used to Probe DHCCA Biosynthesis

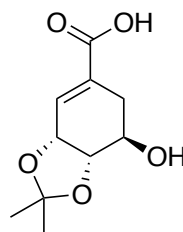
#### Methyl (3a*R*,7*R*,7a*S*)-7-hydroxy-2,2-dimethyl-3a,6,7,7a-tetrahydro benzo[*d*] [1,3]dioxole-5-carboxylate (229)



The following procedure was modified from Chahoua *et al.*<sup>263</sup> To a solution of shikimic acid (1.0 g, 5.7 mmol, 1.0 equiv.) in MeOH (50 mL) was added 2 M HCl solution (2 mL) and the reaction was heated to reflux for 16 h. The reaction was then concentrated *in vacuo* to afford the crude methyl ester. The ester was then re-dissolved in CH<sub>2</sub>Cl<sub>2</sub> (10 mL) and 2,2-dimethoxypropane (10 mL) before a catalytic amount of TsOH was added and the reaction stirred at RT for 4 h. The reaction was then concentrated *in vacuo* and the crude residue purified by silica chromatography (1 : 2 EtOAc : Petroleum ether) to afford the product as a white solid (1.08 g, 83 %, 4.7 mmol).

$\delta_{\text{H}}$  (500 MHz; CDCl<sub>3</sub>) 6.92 (1H, br. t, *J* 2.5, CHCCO<sub>2</sub>Me), 4.74 (1H, dd, *J* 6.0 and 4.0, CHCHCHOH), 4.08 (1H, t, *J* 7.0, CHCHCHOH), 3.89 (1H, td, *J* 8.0 and 5.0, CHOH), 3.77 (3H, s, OCH<sub>3</sub>), 2.79 (1H, dd, *J* 17.5 and 4.5, CH<sub>2</sub>), 2.24 (1H, ddt, *J* 17.5, 8.5 and 2.0, CH<sub>2</sub>), 2.10 (1H, br. s, OH), 1.44 (3H, s, CH<sub>3</sub>), 1.40 (3H, s, CH<sub>3</sub>);  $\delta_{\text{C}}$  (125 MHz, CDCl<sub>3</sub>) 166.7 (CO<sub>2</sub>Me), 134.1 (CHCCO<sub>2</sub>Me), 130.8 (CCO<sub>2</sub>Me), 109.9 (C(CH<sub>3</sub>)<sub>2</sub>), 78.1 (CHCHCHOH), 72.4 (CHCHCHOH), 69.0 (CHOH), 52.3 (OCH<sub>3</sub>), 29.6 (CH<sub>2</sub>), 28.1 (CH<sub>3</sub>), 25.9 (CH<sub>3</sub>); HRMS (ESI) cald. for C<sub>11</sub>H<sub>16</sub>NaO<sub>5</sub> (M + Na<sup>+</sup>) requires 251.0895, found 251.0897. Spectroscopic data was identical to that previously reported in the literature.<sup>263</sup>

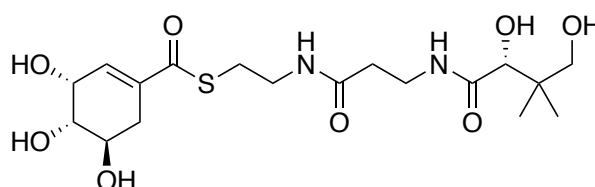
**(3a*R*,7*R*,7a*S*)-7-Hydroxy-2,2-dimethyl-3a,6,7,7a-tetrahydrobenzo [*d*][1,3]dioxole-5-carboxylic acid (227)**



To a stirred solution of methyl (3a*R*,7*R*,7a*S*)-7-hydroxy-2,2-dimethyl-3a,6,7,7a-tetrahydrobenzo[*d*][1,3]dioxole-5-carboxylate **229** (900 mg, 3.95 mmol, 1.0 equiv.) in THF (20 mL) and H<sub>2</sub>O (10 mL) was added LiOH (158 mg, 7.90 mmol, 2.0 equiv.) and the reaction stirred at RT for 16 h. The THF was then removed *in vacuo* and the mixture acidified using 1 M HCl (5 mL). The resulting mixture was extracted with Et<sub>2</sub>O (3 × 20 mL), the combined organics were washed with brine (20 mL), dried (MgSO<sub>4</sub>), filtered and concentrated *in vacuo* to afford the product as a crystalline white solid (668 mg, 79 %, 3.12 mmol).

$\delta_{\text{H}}$  (500 MHz; CD<sub>3</sub>OD) 6.82 (1H, br. s, CHCCO<sub>2</sub>H), 4.76 (1H, dd, *J* 5.5 and 4.0, CHCHCHOH), 4.10 (1H, t, *J* 6.5, CHCHCHOH), 3.88 (1H, q, *J* 6.5, CHOH), 2.60 (1H, dd, *J* 17.5 and 4.5, CH<sub>2</sub>), 2.25 (1H, ddt, *J* 17.5, 7.0 and 1.0, CH<sub>2</sub>), 1.39 (3H, s, CH<sub>3</sub>), 1.38 (3H, s, CH<sub>3</sub>);  $\delta_{\text{C}}$  (125 MHz, CD<sub>3</sub>OD) 169.7 (CO<sub>2</sub>H), 135.3 (CHCCO<sub>2</sub>H), 131.6 (CCO<sub>2</sub>H), 110.5 (C(CH<sub>3</sub>)<sub>2</sub>), 78.5 (CHCHCHOH), 73.7 (CHCHCHOH), 69.0 (CHOH), 30.3 (CH<sub>2</sub>), 28.3 (CH<sub>3</sub>), 26.1 (CH<sub>3</sub>); HRMS (ESI) calcd. for C<sub>10</sub>H<sub>14</sub>NaO<sub>5</sub> (M + Na<sup>+</sup>) requires 237.0739, found 237.0737. Spectroscopic data was identical to that previously reported in the literature.<sup>264</sup>

***S*-(2-(3-((*R*)-2,4-Dihydroxy-3,3-dimethylbutanamido)propanamido)ethyl) (3*R*,4*S*,5*R*)-3,4,5-trihydroxycyclohex-1-ene-1-carbothioate (228)**

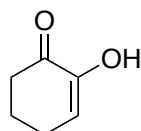


To a stirred solution of (3a*R*,7*R*,7a*S*)-7-Hydroxy-2,2-dimethyl-3a,6,7,7a-tetrahydrobenzo[*d*][1,3]dioxole-5-carboxylic acid **227** (100 mg, 0.47 mmol, 1.3 equiv.), (*R*)-*N*-(3-((2-mercaptoethyl)amino)-3-oxopropyl)-2,2,5,5-tetramethyl-1,3-dioxane-4-carboxamide **61** (161 mg, 0.51 mmol, 1.4 equiv.) and DMAP (13 mg, 0.11 mmol, 0.3 equiv.) in CH<sub>2</sub>Cl<sub>2</sub> (10

mL) was added EDC.HCl (79 mg, 0.51 mmol, 1.4 equiv.) at 0 °C, and the mixture allowed to stir at RT for 16 h. The mixture was then diluted with CH<sub>2</sub>Cl<sub>2</sub> (10 mL), washed with 1 M HCl (10 mL), saturated NaHCO<sub>3</sub> solution (10 mL), dried (MgSO<sub>4</sub>) and concentrated *in vacuo* to afford the crude acetonide as a yellow oil. The crude product was re-dissolved in AcOH : H<sub>2</sub>O (2 : 1, 3 mL) and stirred for 16 h at RT. The reaction was then concentrated *in vacuo* and purified using silica chromatography (9 : 1 EtOAc : MeOH) to give the product as a colourless oil (107 mg, 68 %, 0.25 mmol).

$\nu_{\max}/\text{cm}^{-1}$  (neat) 3306 (OH), 2930 (NH), 1720 (COS), 1638 (CON);  $\delta_{\text{H}}$  (500 MHz; CD<sub>3</sub>OD) 6.80 (1H, br. s, CHCCOS), 4.41 (1H, br. s, CHCHCCOS), 4.01 (1H, dt, *J* 6.5 and 4.5, CH<sub>2</sub>CHOHCHOH), 3.89 (1H, s, CHCONH), 3.71 (1H, dd, *J* 7.0 and 4.5, CH<sub>2</sub>CHOHCHOH), 3.53-3.33 (6H, m, NHCH<sub>2</sub>, CH<sub>2</sub>CH<sub>2</sub>S, CH<sub>2</sub>OH), 3.07 (2H, t, *J* 6.5, CH<sub>2</sub>S), 2.72 (1H, ddt, *J* 18.0, 4.0 and 2.0, CH<sub>2</sub>CCOS), 2.41 (2H, t, *J* 7.0, CH<sub>2</sub>CONH), 2.24 (1H, dd, *J* 18.0 and 5.0, CH<sub>2</sub>CCOS), 0.91 (6H, s, C(CH<sub>3</sub>)<sub>2</sub>);  $\delta_{\text{C}}$  (125 MHz, CD<sub>3</sub>OD) 193.5 (CO<sub>2</sub>S), 176.1 (CH<sub>2</sub>CONH), 174.0 (CHCONH), 137.7 (CCOS), 137.7 (CHCCOS), 77.3 (CHOHC(CH<sub>3</sub>)<sub>2</sub>), 72.5 (CH<sub>2</sub>CHOHCHOH), 70.3 (CH<sub>2</sub>OH), 68.4 (CH<sub>2</sub>CHOHCHOH), 67.3 (CHCHCCOS), 40.4 (CH<sub>2</sub>C(CH<sub>3</sub>)<sub>2</sub>), 40.0 (CH<sub>2</sub>CH<sub>2</sub>S), 36.4 (CH<sub>2</sub>CONH), 36.3 (CH<sub>2</sub>NH), 31.0 (CH<sub>2</sub>CCOS), 29.0 (CH<sub>2</sub>S), 21.3 (CH<sub>2</sub>C(CH<sub>3</sub>)<sub>2</sub>), 20.9 (CH<sub>2</sub>C(CH<sub>3</sub>)<sub>2</sub>); HRMS (ESI) cald. for C<sub>18</sub>H<sub>30</sub>N<sub>2</sub>NaO<sub>8</sub>S (M + Na<sup>+</sup>) requires 457.1621, found 457.1620;  $[\alpha]_{\text{D}}^{25}$  (c 0.1, MeOH): +18.8.

### 2-hydroxycyclohex-2-en-1-one (250)

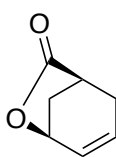


The following procedure was modified from Amon *et al.*<sup>265</sup> A magnetically stirred solution of dimethyl sulfoxide (300  $\mu\text{L}$ , 4.23 mmol, 3.2 equiv.) in CH<sub>2</sub>Cl<sub>2</sub> (18 mL) maintained under an argon atmosphere at -60 °C was treated in a dropwise fashion with TFAA (540  $\mu\text{L}$ , 3.82 mmol, 2.9 equiv.). The resulting clear colourless solution was stirred at -60 °C for 10 min, and then *cis*-1,2-cyclohexanediol (154 mg, 1.33 mmol, 1.0 equiv.) dissolved in a minimum volume of CH<sub>2</sub>Cl<sub>2</sub>/dimethyl sulfoxide was added in a dropwise fashion. The clear colourless solution was stirred at -60 °C for 1.5 h. After the dropwise addition of Et<sub>3</sub>N (1.23 mL, 8.82 mmol, 6.60 equiv.), the light yellow reaction mixture was stirred for a further 1.5 h at -60 °C, warmed to 5 °C, poured into aqueous 2 M HCl (50 mL), and extracted with CH<sub>2</sub>Cl<sub>2</sub> (2  $\times$  30 mL). The combined organic extracts were washed with water (50 mL), dried (MgSO<sub>4</sub>),

filtered and concentrated *in vacuo* to afford a crude residue, which was purified by silica chromatography to afford the product as a white solid (72 mg, 48 %, 0.64 mmol).

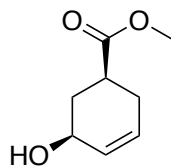
$\delta_{\text{H}}$  (500 MHz,  $\text{CDCl}_3$ ) 6.15 (1H, t,  $J$  4.5, CH), 2.54 (2H, t,  $J$  6.0,  $\text{CH}_2\text{CO}$ ), 2.40 (2H, q,  $J$  5.5, CHCH<sub>2</sub>), 2.01 (2H, quin.,  $J$  6.5,  $\text{CH}_2\text{CH}_2\text{CO}$ );  $\delta_{\text{C}}$  (125 MHz,  $\text{CDCl}_3$ ) 195.8 (CO), 147.2 (COH), 118.7 (CH), 36.6 ( $\text{CH}_2\text{CO}$ ), 24.0 ( $\text{CH}_2\text{CH}$ ), 23.4 ( $\text{CH}_2\text{CH}_2\text{CO}$ ); HRMS (ESI) cald. for  $\text{C}_6\text{H}_8\text{NaO}_2$  ( $\text{M} + \text{Na}^+$ ) requires 135.0422, found 135.0420. Spectroscopic data consistent with that previously reported in the literature.

#### (1*S*,5*S*)-6-Oxabicyclo[3.2.1]oct-3-en-7-one (246)



(1*S*,5*S*)-6-Oxabicyclo[3.2.1]oct-3-en-7-one **246** was synthesized using the same procedure as for the synthesis of (1*R*,5*R*)-6-Oxabicyclo[3.2.1]oct-3-en-7-one **170** using (1*S*,4*S*,5*S*)-4-iodo-6-oxabicyclo[3.2.1]octan-7-one **188** to afford the product as a colourless oil (371 mg, 91 %, 3.0 mmol). Spectroscopic data was identical to that of (1*R*,5*R*)-6-Oxabicyclo[3.2.1]oct-3-en-7-one **170** and consistent with that previously reported in the literature.<sup>266</sup>

#### Methyl (1*S*,5*S*)-5-hydroxycyclohex-3-ene-1-carboxylate (247)

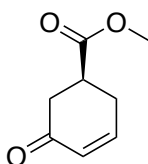


The following procedure was modified from Trost *et al.*<sup>266</sup> To a stirred solution of (1*S*,5*S*)-6-oxabicyclo[3.2.1]oct-3-en-7-one **246** (300 mg, 2.42 mmol, 1.0 equiv.) in MeOH (10 mL) was added  $\text{NaHCO}_3$  (203 mg, 2.42 mmol, 1.0 equiv.). The reaction was stirred for 16 h at RT before being concentrated *in vacuo*. The resulting residue was partitioned between  $\text{Et}_2\text{O}$  (20 mL) and  $\text{H}_2\text{O}$  (20 mL), the organic layer was collected and washed with brine (20 mL), dried ( $\text{MgSO}_4$ ), filtered and concentrated *in vacuo* to afford a crude residue which was columned using silica chromatography ( $\text{Et}_2\text{O}$ ) to afford the product as a colourless oil (298 mg, 79 %).



$\delta_{\text{H}}$  (500 MHz;  $\text{CDCl}_3$ ) 6.79-6.73 (2H, m,  $\text{CHCHCHOH}$ ), 4.76 (1H, q,  $J$  6.5,  $\text{CHCHCHOH}$ ), 3.70 (3H, s,  $\text{OCH}_3$ ), 2.72 (1H, dtd,  $J$  10.5, 7.5 and 3.0,  $\text{CHCO}_2\text{Me}$ ), 2.33-2.23 (3H, m,  $\text{CH}_2$ ,  $\text{CHOHCH}_2\text{CO}_2\text{Me}$ ), 2.07 (1H, d,  $J$  7.5,  $\text{OH}$ ), 1.74 (1H, ddd,  $J$  13.0, 10.5 and 8.0,  $\text{CHOHCH}_2\text{CO}_2\text{Me}$ );  $\delta_{\text{C}}$  (125 MHz,  $\text{CDCl}_3$ ) 175.8 ( $\text{CO}_2\text{Me}$ ), 130.9 ( $\text{CHCHCHOH}$ ), 127.1 ( $\text{CHCHCHOH}$ ), 66.1 ( $\text{CHCHCHOH}$ ), 52.1 ( $\text{OCH}_3$ ), 37.8 ( $\text{CHCO}_2\text{Me}$ ), 34.3 ( $\text{CHOHCH}_2$ ), 27.5 ( $\text{CH}_2$ ); HRMS (ESI) cald. for  $\text{C}_8\text{H}_{13}\text{O}_3$  ( $\text{M} + \text{H}^+$ ) requires 157.0685, found 157.0682. Spectroscopic data consistent with that previously reported in the literature.<sup>266</sup>

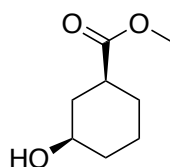
### Methyl (*S*)-5-oxocyclohex-3-ene-1-carboxylate (**245**)



To a stirred solution of methyl (*1S,5S*)-5-hydroxycyclohex-3-ene-1-carboxylate **247** (25 mg, 0.16 mmol, 1.0 equiv.) in  $\text{CH}_2\text{Cl}_2$  (10 mL), was added  $\text{MnO}_2$  (140 mg, 1.6 mmol, 10.0 equiv.) and the reaction allowed to stir in the absence of light for 16 h at RT. The reaction was then filtered through Celite<sup>®</sup> and concentrated *in vacuo* to afford the product as a colourless oil (21 mg, 84 %, 0.13 mmol).

$\nu_{\text{max}}/\text{cm}^{-1}$  (neat) 1738 (C=O), 1671 (C=O), 1156 (C-O);  $\delta_{\text{H}}$  (500 MHz;  $\text{CDCl}_3$ ) 6.96 (1H, dt,  $J$  10.0 and 4.0,  $\text{CHCHCO}$ ), 6.06 (1H, dt,  $J$  10.0 and 2.0,  $\text{CHCHCO}$ ), 3.72 (3H, s,  $\text{OCH}_3$ ), 3.09 (1H, ddt,  $J$  11.0, 9.0 and 5.5,  $\text{CHCO}_2\text{Me}$ ), 2.74-2.58 (4H, m,  $\text{COCH}_2$ ,  $\text{CHCH}_2\text{CH}$ );  $\delta_{\text{C}}$  (125 MHz,  $\text{CDCl}_3$ ) 197.1 (CO), 173.6 ( $\text{CO}_2\text{Me}$ ), 147.9 ( $\text{CHCHCO}$ ), 130.0 ( $\text{CHCHCO}$ ), 52.4 ( $\text{OCH}_3$ ), 39.9 ( $\text{CHCO}_2\text{Me}$ ), 39.8 ( $\text{COCH}_2$ ), 28.1 ( $\text{CHCH}_2\text{CH}$ ); HRMS (ESI) cald. for  $\text{C}_8\text{H}_{11}\text{O}_3$  ( $\text{M} + \text{H}^+$ ) requires 155.0708, found 155.0708;  $[\alpha]_{\text{D}}^{25}$  (c 1.0,  $\text{CHCl}_3$ ): 76.3.

### Methyl (*1S,3R*)-3-hydroxycyclohexane-1-carboxylate (**249**)

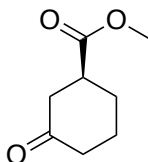


To a stirred solution of methyl (*1S,5S*)-5-hydroxycyclohex-3-ene-1-carboxylate **247** (200 mg, 1.28 mmol, 1.0 equiv.) in MeOH (10 mL) was added palladium on carbon (10 mg) and the reaction placed under a  $\text{H}_2$  atmosphere and stirred at RT for 16 h. The reaction was then

filtered through Celite<sup>®</sup> and concentrated *in vacuo* to afford the product as a colourless oil (184 mg, 91 %, 1.16 mmol).

$\delta_{\text{H}}$  (500 MHz;  $\text{CDCl}_3$ ) 3.68 (3H, s,  $\text{OCH}_3$ ), 3.62 (1H, tt,  $J$  10.0 and 4.0,  $\text{CHOH}$ ), 2.37 (1H, tt,  $J$  12.0 and 4.0,  $\text{CHCO}_2\text{Me}$ ), 2.19 (1H, br. d,  $J$  12.5,  $\text{CHOHCH}_2\text{CH}$ ), 1.95 (1H, br. d,  $J$  12.0,  $\text{CH}_2\text{CHOH}$ ), 1.92-1.81 (2H, m,  $\text{CH}_2$ ,  $\text{CH}_2\text{CHCO}_2\text{Me}$ ), 1.63 (1H, br. s,  $\text{OH}$ ), 1.42 (1H, q,  $J$  12.0,  $\text{CHOHCH}_2\text{CH}$ ), 1.37-1.19 (3H, m,  $\text{CH}_2\text{CHOH}$ ,  $\text{CH}_2$ ,  $\text{CH}_2\text{CHCO}_2\text{Me}$ );  $\delta_{\text{C}}$  (125 MHz,  $\text{CDCl}_3$ ) 175.7 ( $\text{CO}_2\text{Me}$ ), 69.9 ( $\text{CHOH}$ ), 51.9 ( $\text{OCH}_3$ ), 41.8 ( $\text{CHCO}_2\text{Me}$ ), 37.7 ( $\text{CHOHCH}_2\text{CH}$ ), 35.0 ( $\text{CH}_2\text{CHOH}$ ), 28.1 ( $\text{CH}_2\text{CHCO}_2\text{Me}$ ), 23.3 ( $\text{CH}_2$ ); HRMS (ESI) cald. for  $\text{C}_8\text{H}_{15}\text{O}_3$  ( $\text{M} + \text{H}^+$ ) requires 159.1021, found 159.1019. Spectroscopic data consistent with that previously reported in the literature.<sup>267</sup>

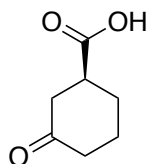
### Methyl (*S*)-3-oxocyclohexane-1-carboxylate (**248**)



To a stirred solution of methyl (1*S*,3*R*)-3-hydroxycyclohexane-1-carboxylate **249** (150 mg, 0.96 mmol, 1.0 equiv.), in acetone (10 mL) at 0 °C was added 1 mL of a prepared solution of Jones' reagent ( $\text{CrO}_3$  (800 mg),  $\text{H}_2\text{SO}_4$  (3 mL),  $\text{H}_2\text{O}$  (3 mL)) and the reaction left to stir at RT for 1 h. The reaction was quenched via the addition of isopropanol (3 mL) and the reaction was concentrated *in vacuo*. The resulting residue was partitioned between  $\text{CH}_2\text{Cl}_2$  (10 mL) and  $\text{H}_2\text{O}$  (10 mL), the organic layer was collected, washed with brine (10 mL), dried ( $\text{MgSO}_4$ ), filtered and concentrated *in vacuo* to afford the product as a colourless oil (84 mg, 56 %)

$\delta_{\text{H}}$  (500 MHz;  $\text{CDCl}_3$ ) 3.69 (3H, s,  $\text{OCH}_3$ ), 2.80 (1H, dtd,  $J$  11.0, 8.0 and 4.0,  $\text{CHCO}_2\text{Me}$ ), 2.53 (2H, d,  $J$  8.0,  $\text{COCH}_2\text{CHCO}_2\text{Me}$ ), 2.37 (1H, dt,  $J$  15.0 and 5.0,  $\text{CH}_2\text{CO}$ ), 2.30 (1H, ddd,  $J$  15.0, 11.0 and 6.0,  $\text{CH}_2\text{CO}$ ), 2.13-2.01 (2H, m,  $\text{CH}_2$ ,  $\text{CH}_2\text{CHCO}_2\text{Me}$ ), 1.87-1.67 (2H, m,  $\text{CH}_2$ ,  $\text{CH}_2\text{CHCO}_2\text{Me}$ );  $\delta_{\text{C}}$  (125 MHz,  $\text{CDCl}_3$ ) 209.3 ( $\text{CO}$ ), 174.3 ( $\text{CO}_2\text{Me}$ ), 52.2 ( $\text{OCH}_3$ ), 43.2 ( $\text{COCH}_2\text{CH}$ ), 43.2 ( $\text{CHCO}_2\text{Me}$ ), 41.0 ( $\text{CH}_2\text{CO}$ ), 27.8 ( $\text{CH}_2\text{CHCO}_2\text{Me}$ ), 24.5 ( $\text{CH}_2$ ); HRMS (ESI) cald. for  $\text{C}_8\text{H}_{13}\text{O}_3$  ( $\text{M} + \text{H}^+$ ) requires 157.0685, found 157.0683. Spectroscopic data consistent with that previously reported in the literature.<sup>268</sup>

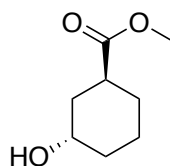
### (S)-3-Oxocyclohexane-1-carboxylic acid (258)



To a stirred solution of methyl (S)-3-oxocyclohexane-1-carboxylate **248** (10 mg, 0.06 mmol, 1.0 equiv.) in THF (2 mL) and H<sub>2</sub>O (1 mL) was added LiOH (2.0 mg, 0.12 mmol, 2.0 equiv.) and the reaction stirred at RT for 16 h. The THF was then removed *in vacuo* and the mixture acidified using 1 M HCl (1 mL). The resulting mixture was extracted with Et<sub>2</sub>O (3 x 5 mL), the combined organics were washed with brine (5 mL), dried (MgSO<sub>4</sub>), filtered and concentrated *in vacuo* to afford the product as a crystalline white solid (9 mg, 96 %, 0.06 mmol).

$\delta_{\text{H}}$  (500 MHz; CD<sub>3</sub>OD) 2.84 (1H, tt, *J* 9.5 and 4.5, CHCO<sub>2</sub>H), 2.58-2.31 (2H, m, COCH<sub>2</sub>CHCO<sub>2</sub>H), 2.25-2.09 (2H, m, CH<sub>2</sub>CO), 2.06-1.67 (4H, m, CH<sub>2</sub>CHCO<sub>2</sub>H, CH<sub>2</sub>);  $\delta_{\text{C}}$  (125 MHz, CD<sub>3</sub>OD) 208.6 (CO), 179.1 (CO<sub>2</sub>Me), 43.9 (COCH<sub>2</sub>CH), 41.3 (CHCO<sub>2</sub>Me), 36.2 (CH<sub>2</sub>CO), 29.5 (CH<sub>2</sub>CHCO<sub>2</sub>H), 22.8 (CH<sub>2</sub>); HRMS (ESI) calcd. for C<sub>7</sub>H<sub>10</sub>NaO<sub>3</sub> (M + Na<sup>+</sup>) requires 165.0528, found 165.0525. Spectroscopic data consistent with that previously reported in the literature.<sup>268</sup>

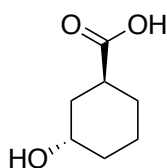
### Methyl (1S,3S)-3-hydroxycyclohexane-1-carboxylate (259)



To a stirred solution of methyl (S)-3-oxocyclohexane-1-carboxylate **248** (50 mg, 0.32 mmol, 1.0 equiv.) in THF (5 ml) cooled to -20 °C was added 1 M K-selectride in THF (0.64 ml, 0.64 mmol, 2.0 equiv.). The reaction was stirred at RT for 1 h before being quenched with saturated NH<sub>4</sub>Cl solution (5 mL) and extracted with diethyl ether (3 x 10 ml). The organic extracts were combined, dried (MgSO<sub>4</sub>) and concentrated *in vacuo*. The crude material was then stirred in 1M HCl (10 ml) for 15 min, neutralised with NaHCO<sub>3</sub>, extracted with diethyl ether (3 x 20 ml), dried with MgSO<sub>4</sub> and concentrated *in vacuo*. The crude material was purified using silica chromatography (1 : 1 Et<sub>2</sub>O:petroleum ether) to afford the product as a colourless oil (14 mg, 28 %, 0.09 mmol).

$\delta_{\text{H}}$  (500 MHz;  $\text{CDCl}_3$ ) 4.08 (1H, quin.,  $J$  4.5,  $\text{CHOH}$ ), 3.66 (3H, s,  $\text{OCH}_3$ ), 2.78 (1H, tt,  $J$  9.5 and 4.5,  $\text{CHCO}_2\text{Me}$ ), 1.92-1.77 (2H, m,  $\text{CHOHCH}_2\text{CH}$ ,  $\text{CH}_2\text{CHOH}$ ), 1.74-1.63 (2H, m,  $\text{CHOHCH}_2\text{CH}$ ,  $\text{CH}_2\text{CHOH}$ ), 1.62-1.26 (4H, m,  $\text{CH}_2$ ,  $\text{CH}_2\text{CHCO}_2\text{Me}$ );  $\delta_{\text{C}}$  (125 MHz,  $\text{CDCl}_3$ ) 176.4 ( $\text{CO}_2\text{Me}$ ), 66.3 ( $\text{CHOH}$ ), 51.7 ( $\text{OCH}_3$ ), 38.0 ( $\text{CHCO}_2\text{Me}$ ), 36.7 ( $\text{CHOHCH}_2\text{CH}$ ), 33.0 ( $\text{CH}_2\text{CHOH}$ ), 28.3 ( $\text{CH}_2\text{CHCO}_2\text{Me}$ ), 20.0 ( $\text{CH}_2$ ); HRMS (ESI) cald. for  $\text{C}_8\text{H}_{15}\text{O}_3$  ( $\text{M} + \text{H}^+$ ) requires 159.1021, found 159.1018. Spectroscopic data consistent with that previously reported in the literature.<sup>267</sup>

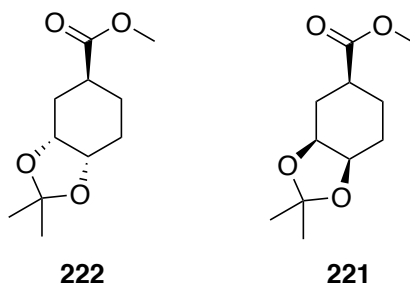
**(1*S*,3*S*)-3-Hydroxycyclohexane-1-carboxylic acid (257)**



To a stirred solution of methyl (1*S*,3*S*)-3-hydroxycyclohexane-1-carboxylate **259** (10 mg, 0.06 mmol, 1.0 equiv.) in THF (2 mL) and  $\text{H}_2\text{O}$  (1 mL) was added LiOH (2.0 mg, 0.12 mmol, 2.0 equiv.) and the reaction stirred at RT for 16 h. The THF was then removed *in vacuo* and the mixture acidified using 1 M HCl (1 mL). The resulting mixture was extracted with  $\text{Et}_2\text{O}$  (3  $\times$  5 mL), the combined organics were washed with brine (5 mL), dried ( $\text{MgSO}_4$ ), filtered and concentrated *in vacuo* to afford the product as a crystalline white solid (9 mg, 96 %, 0.06 mmol).

$\delta_{\text{H}}$  (500 MHz;  $\text{CD}_3\text{OD}$ ) 4.00 (1H, quin.,  $J$  3.5,  $\text{CHOH}$ ), 2.78 (1H, tdd,  $J$  9.5, 5.0 and 4.5,  $\text{CHCO}_2\text{H}$ ), 1.81-1.72 (3H, m,  $\text{CHOHCH}_2\text{CH}$ ,  $\text{CH}_2\text{CHOH}$ ,  $\text{CH}_2\text{CHCO}_2\text{H}$ ), 1.71-1.63 (1H, m,  $\text{CH}_2$ ), 1.62-1.47 (4H, m,  $\text{CH}_2$ ,  $\text{CH}_2\text{CHCO}_2\text{H}$ ,  $\text{CHOHCH}_2\text{CH}$ ,  $\text{CH}_2\text{CHOH}$ );  $\delta_{\text{C}}$  (125 MHz,  $\text{CD}_3\text{OD}$ ) 185.2 ( $\text{CO}_2\text{H}$ ), 67.5 ( $\text{CHOH}$ ), 42.3 ( $\text{CHCO}_2\text{H}$ ), 37.6 ( $\text{CHOHCH}_2\text{CH}$ ), 33.9 ( $\text{CH}_2\text{CHOH}$ ), 30.6 ( $\text{CH}_2\text{CHCO}_2\text{H}$ ), 21.4 ( $\text{CH}_2$ ); HRMS (ESI) cald. for  $\text{C}_7\text{H}_{12}\text{NaO}_3$  ( $\text{M} + \text{Na}^+$ ) requires 167.0684, found 167.0681. Spectroscopic data consistent with that previously reported in the literature.<sup>267</sup>

**Methyl (3aR,5S,7aS)-2,2-dimethylhexahydrobenzo[d][1,3]dioxole-5-carboxylate (222) and Methyl (3aS,5S,7aR)-2,2-dimethylhexahydrobenzo[d][1,3]dioxole-5-carboxylate (221)**



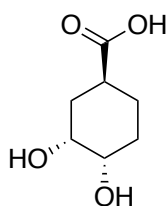
The following procedure was modified from Semak *et al.* To a stirred solution of NMO (878 mg, 7.50 mmol, 1.05 equiv.) in H<sub>2</sub>O (10 mL) and acetone (4 mL) were added K<sub>2</sub>[OsO<sub>2</sub>(OH)<sub>4</sub>] (78 mg, 0.21 mmol, 0.03 equiv.) and a solution of methyl cyclohex-3-ene-1-carboxylate (1.00 g, 7.14 mmol, 1.00 equiv.) in acetone (10 mL). The resulting mixture was stirred at RT for 6 h, and then quenched with saturated aqueous NaHSO<sub>3</sub> (20 mL). The resulting mixture was extracted with EtOAc (3 x 20 mL). The combined organic extracts were washed with brine (20 mL), dried (MgSO<sub>4</sub>), filtered, and concentrated *in vacuo*. The resulting mixture was then re-suspended in CH<sub>2</sub>Cl<sub>2</sub> (20 mL) before the addition of 2,2-dimethoxypropane (4.0 mL) and a catalytic amount of TsOH. The resulting mixture was stirred for a further 2 h before being concentrated *in vacuo*. The crude mixture was then purified by silica chromatography (1:5 EtOAc:Petroleum ether) to afford methyl (3aR,5r,6aS)-2,2-dimethyltetrahydro-4H-cyclopenta[d][1,3]dioxole-5-carboxylate **222** (596 mg, 39 %, 2.78 mmol) and methyl (3aR,5s,6aS)-2,2-dimethyltetrahydro-4H-cyclopenta[d][1,3]dioxole-5-carboxylate **221** (413 mg, 27 %, 1.92 mmol) as colourless oils.

Methyl (3aR,5S,7aS)-2,2-dimethylhexahydrobenzo[d][1,3]dioxole-5-carboxylate **222**:  $\delta_{\text{H}}$  (500 MHz; CDCl<sub>3</sub>) 4.29 (1H, q, *J* 4.0, CHOCH<sub>2</sub>CHCO<sub>2</sub>), 4.10 (1H, dt, *J* 7.0 and 5.5, CHOCHO), 3.67 (3H, s, OCH<sub>3</sub>), 2.67 (1H, tt, *J* 9.5 and 4.5, CHCO<sub>2</sub>), 2.19 (1H, dt, *J* 15.0 and 4, CHOCH<sub>2</sub>CHCO<sub>2</sub>), 1.95-1.75 (3H, m, CHOCH<sub>2</sub>CHCO<sub>2</sub>, CH<sub>2</sub>CHO, CH<sub>2</sub>CHCO<sub>2</sub>), 1.62 (1H, dddd, *J* 14.0, 10.5, 7.5 and 4.0, CH<sub>2</sub>CHO), 1.49 (3H, s, C(CH<sub>3</sub>)<sub>2</sub>), 1.46 (1H, dtd, *J* 17.0, 10.0, 3.5, CH<sub>2</sub>CHCO<sub>2</sub>), 1.33 (3H, s, C(CH<sub>3</sub>)<sub>2</sub>);  $\delta_{\text{C}}$  (125 MHz, CDCl<sub>3</sub>) 176.3 (CO<sub>2</sub>CH<sub>3</sub>), 108.2 (C(CH<sub>3</sub>)<sub>2</sub>), 73.2 (CH<sub>2</sub>CHO), 72.6 (CHCH<sub>2</sub>CHO), 51.9 (OCH<sub>3</sub>), 36.6 (CHCO<sub>2</sub>), 29.4 (CHCH<sub>2</sub>CHO), 28.3 (C(CH<sub>3</sub>)<sub>2</sub>), 27.2 (CH<sub>2</sub>CHO), 26.1 (C(CH<sub>3</sub>)<sub>2</sub>), 23.7 (CH<sub>2</sub>CHCO<sub>2</sub>); HRMS (ESI) cald. for C<sub>11</sub>H<sub>18</sub>NaO<sub>4</sub> (M + Na<sup>+</sup>) requires 237.1103, found 237.1101. Spectroscopic data consistent with that previously reported in the literature.<sup>218</sup>

Methyl (3aS,5S,7aR)-2,2-dimethylhexahydrobenzo[d][1,3]dioxole-5-carboxylate **221**:  $\delta_{\text{H}}$  (500 MHz; CDCl<sub>3</sub>) 4.17-4.14 (1H, m, CHOCHO), 4.07 (1H, dt, *J* 9.5 and 6.0,

CHOCH<sub>2</sub>CHCO<sub>2</sub>), 3.67 (3H, s, OCH<sub>3</sub>), 2.26-2.20 (1H, m, CHCO<sub>2</sub>), 2.16 (1H, dt, *J* 11.0 and 3.0, CHOCH<sub>2</sub>), 2.10-2.06 (1H, m, CHOCH<sub>2</sub>CHCO<sub>2</sub>), 1.75-1.63 (4H, m, CH<sub>2</sub>CHO, CHOCH<sub>2</sub>CHCO<sub>2</sub>, CH<sub>2</sub>CHCO<sub>2</sub>), 1.49 (3H, s, C(CH<sub>3</sub>)<sub>2</sub>), 1.33 (3H, s, C(CH<sub>3</sub>)<sub>2</sub>); δ<sub>c</sub> (125 MHz, CDCl<sub>3</sub>) 175.4 (CO<sub>2</sub>CH<sub>3</sub>), 108.4 (C(CH<sub>3</sub>)<sub>2</sub>), 73.9 (CH<sub>2</sub>CHO), 72.5 (CHCH<sub>2</sub>CHO), 51.9 (OCH<sub>3</sub>), 39.6 (CHCO<sub>2</sub>), 31.7 (CHCH<sub>2</sub>CHO), 28.5 (C(CH<sub>3</sub>)<sub>2</sub>), 26.4 (C(CH<sub>3</sub>)<sub>2</sub>), 26.3 (CH<sub>2</sub>CHO), 22.8 (CH<sub>2</sub>CHCO<sub>2</sub>); HRMS (ESI) cald. for C<sub>11</sub>H<sub>18</sub>NaO<sub>4</sub> (M + Na<sup>+</sup>) requires 237.1103, found 237.1103. Spectroscopic data consistent with that previously reported in the literature.<sup>218</sup>

**(1*S*,3*R*,4*S*)-3,4-Dihydroxycyclohexane-1-carboxylic acid (48)**



To a solution of methyl (3*aR*,5*S*,7*aS*)-2,2-dimethylhexahydrobenzo[*d*][1,3]dioxole-5-carboxylate **222** (350 mg, 1.64 mmol, 1.0 equiv.) in MeOH (30 mL) was added TsOH (35 mg, 0.20 mmol, 0.12 equiv.) and the reaction was stirred at RT for 1 h. The mixture was then concentrated *in vacuo* and partitioned between EtOAc (20 mL) and saturated NaHCO<sub>3</sub> solution (20 mL). The layers were separated and the aqueous phase further extracted with EtOAc (2 × 20 mL), the combined organics were then washed with brine, dried (MgSO<sub>4</sub>), filtered and concentrated *in vacuo* to afford the crude diol as a viscous oil. The diol was then dissolved in THF (10 mL) and H<sub>2</sub>O (5 mL), and LiOH was added (40 mg, 1.4 mmol, 2.0 equiv.). The reaction was then stirred at RT overnight and the THF removed *in vacuo*. The resulting suspension was then acidified (1 M HCl, 10 mL) and extracted with EtOAc (5 × 10 mL). The combined organics were then washed with brine, dried (MgSO<sub>4</sub>), filtered and concentrated *in vacuo* to afford the product as a viscous oil (192 mg, 73 %).

$\nu_{\text{max}}/\text{cm}^{-1}$  (neat) 3147 (OH), 2935 (CO<sub>2</sub>H), 1718 (C=O), 1066 (C-O); δ<sub>H</sub> (500 MHz; D<sub>2</sub>O) 4.05-4.01 (1H, br. m, CHCH<sub>2</sub>CHOH), 3.69 (1H, ddd, *J* 11.0, 4.0 and 3.0, CHOH), 2.55 (1H, tt, *J* 12.0 and 3.5, CHCO<sub>2</sub>H), 2.06-1.99 (1H, m, CHCOHCH<sub>2</sub>CHCO<sub>2</sub>H), 1.96-1.90 (1H, m, CH<sub>2</sub>CHCO<sub>2</sub>H), 1.76-1.60 (3H, m, CHCOHCH<sub>2</sub>CHCO<sub>2</sub>H, CH<sub>2</sub>CHOH), 1.47 (1H, qd, *J* 12.5 and 4.0, CH<sub>2</sub>CHCO<sub>2</sub>H); δ<sub>c</sub> (125 MHz, D<sub>2</sub>O) 183.1 (CO<sub>2</sub>H), 71.2 (CHOH), 69.2 (CHCH<sub>2</sub>CHOH), 38.4 (CHCO<sub>2</sub>H), 33.9 (CHCH<sub>2</sub>CHOH), 26.3 (CH<sub>2</sub>CH<sub>2</sub>CHCO<sub>2</sub>H), 27.0 (CH<sub>2</sub>CHCO<sub>2</sub>H); HRMS (ESI) cald. for C<sub>7</sub>H<sub>13</sub>O<sub>4</sub> (M + H<sup>+</sup>) requires 161.0814, found 161.0813; [α]<sub>D</sub><sup>26</sup> (c 0.2, MeOH): +12.5.

## **7. References**

- 1 A. L. Demain and A. Fang, *Adv. Biochem. Eng. Biotechnol.*, 2000, **69**, 1–39.
- 2 E. D. Brown and G. D. Wright, *Nature*, 2016, **529**, 336–343.
- 3 A. Fleming, *Br. J. Exp. Pathol.*, 1929, **10**, 226–236.
- 4 R. Gaynes, *Emerg. Infect. Dis.*, 2017, **23**, 849–853.
- 5 M. Lobanovska and G. Pilla, *Yale J. Biol. Med.*, 2017, **90**, 135.
- 6 D. A. Dias, S. Urban and U. Roessner, *Metabolites*, 2012, **2**, 303–336.
- 7 S. A. Waksman and H. B. Woodruff, *Exp. Biol. Med.*, 1940, **45**, 609–614.
- 8 K. Lewis, *Nat. Rev. Drug Discov.*, 2013, **12**, 371–387.
- 9 D. Lyddiard, G. L. Jones and B. W. Greatrex, *FEMS Microbiol. Lett.*, 2016, **363**, 84.
- 10 G. D. Wright, *Nat. Prod. Rep.*, 2017, **34**, 694–701.
- 11 A. Schatz and S. A. Waksman, *Exp. Biol. Med.*, 1944, **57**, 244–248.
- 12 I. Chopra and M. Roberts, *Microbiol. Mol. Biol. Rev.*, 2001, **65**, 232–260.
- 13 G. P. Dinos, *Br. J. Pharmacol.*, 2017, **174**, 2967–2983.
- 14 G. L. Marcone, E. Binda, F. Berini and F. Marinelli, *Biotechnol. Adv.*, 2018, **36**, 534–554.
- 15 J. M. Munita and C. A. Arias, *Microbiol. Spectr.*, 2016, **4**.
- 16 C. A. Townsend, *Curr. Opin. Chem. Biol.*, 2016, **35**, 97–108.
- 17 R. J. Worthington and C. Melander, *J. Org. Chem.*, 2013, **78**, 4207–13.
- 18 P. D. Stapleton and P. W. Taylor, *Sci. Prog.*, 2002, **85**, 57–72.
- 19 M. C. Enright, D. A. Robinson, G. Randle, E. J. Feil, H. Grundmann and B. G. Spratt, *Proc. Natl. Acad. Sci.*, 2002, **99**, 7687–7692.
- 20 T. J. Foster, *Trends Microbiol.*, 2019, **27**, 26–38.
- 21 C. Reading and M. Cole, *Clavulanic Acid: a Beta-Lactamase-Inhibiting Beta-Lactam from Streptomyces clavuligerus*, 1977, vol. 11.
- 22 A. M. Geddes, K. P. Klugman and G. N. Rolinson, *Int. J. Antimicrob. Agents*, 2007, **30**, 109–112.
- 23 S. M. Drawz and R. A. Bonomo, *Clin. Microbiol. Rev.*, 2010, **23**, 160–201.
- 24 K. M. Shaeer, M. T. Zmarlicka, E. B. Chahine, N. Piccicacco and J. C. Cho, *Pharmacother. J. Hum. Pharmacol. Drug Ther.*, 2019, **39**, 77–93.
- 25 J. N. Lashinsky Oryan Henig Jason M Pogue Keith S Kaye, *Infect. Dis. Ther.*, 2017, **6**.
- 26 S. Omura, S. Morimoto, T. Nagate, T. Adachi and Y. Kohno, *Yakugaku Zasshi*, 1992, **112**, 593–614.
- 27 P. Fernandes, E. Martens and D. Pereira, *J. Antibiot. (Tokyo)*, 2017, **70**, 527–533.
- 28 F. Liu and A. G. Myers, *Curr. Opin. Chem. Biol.*, 2016, **32**, 48–57.
- 29 J. A. Sutcliffe, W. O'Brien, C. Fyfe and T. H. Grossman, *Antimicrob. Agents Chemother.*, 2013, **57**, 5548–5558.
- 30 A. Imada, M. Kondo, K. Okonogi, K. Yukishige and M. Kuno, *Antimicrob. Agents*



- Chemother.*, 1985, **27**, 821–7.
- 31 I. B. Seiple, Z. Zhang, P. Jakubec, A. Langlois-Mercier, P. M. Wright, D. T. Hog, K. Yabu, S. R. Allu, T. Fukuzaki, P. N. Carlsen, Y. Kitamura, X. Zhou, M. L. Condakes, F. T. Szczypiński, W. D. Green and A. G. Myers, *Nature*, 2016, **533**, 338–345.
- 32 T. Weber, P. Charusanti, E. M. Musiol-Kroll, X. Jiang, Y. Tong, H. U. Kim and S. Y. Lee, *Trends Biotechnol.*, 2015, **33**, 15–26.
- 33 J. Won Park, S. Ryeol Park, K. Kumar Nepal, A. Reum Han, Y. Hee Ban, Y. Ji Yoo, E. Ji Kim, E. Min Kim, D. Kim, J. Kyung Sohng and Y. Joon Yoon, *Nat. Chem. Biol.*, 2011, **7**, 843–852.
- 34 U. Lešnik, T. Lukežič, A. Podgoršek, J. Horvat, T. Polak, M. Šala, B. Jenko, K. Harmrolfs, A. Ocampo-Sosa, L. Martínez-Martínez, P. R. Herron, Š. Fujs, G. Kosec, I. S. Hunter, R. Müller and H. Petković, *Angew. Chemie Int. Ed.*, 2015, **54**, 3937–3940.
- 35 S. Santajit and N. Indrawattana, *Biomed Res. Int.*, 2016, **2016**, 2475067.
- 36 G. Yim, W. Wang, M. N. Thaker, S. Tan and G. D. Wright, *ACS Infect. Dis.*, 2016, **2**, 642–650.
- 37 M. N. Thaker, W. Wang, P. Spanogiannopoulos, N. Waglechner, A. M. King, R. Medina and G. D. Wright, *Nat. Biotechnol.*, 2013, **10**, 922–927.
- 38 G. L. Challis, *J. Med. Chem.*, 2008, **51**, 2618–2628.
- 39 L. Foulston, *Curr. Opin. Microbiol.*, 2019, **51**, 1–8.
- 40 L. Laureti, L. Song, S. Huang, C. Corre, P. Leblond, G. L. Challis, B. Aigle and C. Khosla, *Proc. Natl. Acad. Sci.*, 2011, **15**, 6258–6253.
- 41 V. H. T. Pham and J. Kim, *Trends Biotechnol.*, 2012, **30**, 475–484.
- 42 D. Nichols, N. Cahoon, E. M. Trakhtenberg, L. Pham, A. Mehta, A. Belanger, T. Kanigan, K. Lewis and S. S. Epstein, *Appl. Environ. Microbiol.*, 2010, **76**, 2445–50.
- 43 L. L. Ling, T. Schneider, A. J. Peoples, A. L. Spoering, I. Engels, B. P. Conlon, A. Mueller, T. F. Schäberle, D. E. Hughes, S. Epstein, M. Jones, L. Lazarides, V. A. Steadman, D. R. Cohen, C. R. Felix, K. A. Fetterman, W. P. Millett, A. G. Nitti, A. M. Zullo, C. Chen and K. Lewis, *Nature*, 2015, **517**, 455–459.
- 44 J. Masschelein, M. Jenner and G. L. Challis, *Nat. Prod. Rep.*, 2017, **34**, 712–783.
- 45 L. Eberl and P. Vandamme, *F1000Research*, 2016, **5**, 1007.
- 46 E. Mahenthiralingam, T. A. Urban and J. B. Goldberg, *Nat. Rev. Microbiol.*, 2005, **3**, 144–156.
- 47 K. Scherlach, L. P. Partida-Martinez, H.-M. Dahse and C. Hertweck, *J. Am. Chem. Soc.*, 2006, **128**, 11529–11536.
- 48 M. Yamaguchi, H.-J. Park, S. Ishizuka, K. Omata and M. Hirama, *J. Med. Chem.*, 1995, **38**, 5015–5022.
- 49 Z. Lin, J. O. Falkinham, K. A. Tawfik, P. Jeffs, B. Bray, G. Dubay, J. E. Cox and E. W.

- Schmidt, *J. Nat. Prod.*, 2012, **75**, 1518–1523.
- 50 M. Anwar, A. Kasper, A. R. Steck and J. G. Schier, *J. Med. Toxicol.*, 2017, **13**, 173–179.
- 51 H. Jenke-Kodama, A. Sandmann, R. Müller and E. Dittmann, *Mol. Biol. Evol.*, 2005, **22**, 2027–2039.
- 52 B. Shen, *Curr. Opin. Chem. Biol.*, 2003, **7**, 285–295.
- 53 R. J. Cox and T. J. Simpson, in *Methods in enzymology*, 2009, vol. 459, pp. 49–78.
- 54 C. Olano, B. Wilkinson, C. Sánchez, S. J. Moss, R. Sheridan, V. Math, A. J. Weston, A. F. Braña, C. J. Martin, M. Oliynyk, C. Méndez, P. F. Leadlay and J. A. Salas, *Chem. Biol.*, 2004, **11**, 87–97.
- 55 H. Chen and L. Du, *Appl. Microbiol. Biotechnol.*, 2016, **100**, 541–57.
- 56 J. Staunton and K. J. Weissman, *Nat. Prod. Rep.*, 2001, **18**, 380–416.
- 57 J. Staunton and B. Wilkinson, *Chem. Rev.*, 1997, **97**, 2611–2630.
- 58 A. T. Keatinge-Clay, *Angew. Chemie Int. Ed.*, 2017, **56**, 4658–4660.
- 59 L. Zhang, T. Hashimoto, B. Qin, J. Hashimoto, I. Kozono, T. Kawahara, M. Okada, T. Awakawa, T. Ito, Y. Asakawa, M. Ueki, S. Takahashi, H. Osada, T. Wakimoto, H. Ikeda, K. Shin-ya and I. Abe, *Angew. Chemie Int. Ed.*, 2017, **56**, 1740–1745.
- 60 R. H. Lambalot, A. M. Gehring, R. S. Flugel, P. Zuber, M. LaCelle, M. A. Marahiel, R. Reid, C. Khosla and C. T. Walsh, *Chem. Biol.*, 1996, **3**, 923–36.
- 61 L. Ray and B. S. Moore, *Nat. Prod. Rep.*, 2016, **33**, 150–61.
- 62 C. Bisang, P. F. Long, J. Corte's, J. Westcott, J. Crosby, A.-L. Matharu, R. J. Cox, T. J. Simpson, J. Staunton and P. F. Leadlay, *Nature*, 1999, **401**, 502–505.
- 63 B. J. Dunn, D. E. Cane and C. Khosla, *Biochemistry*, 2013, **52**, 1839–41.
- 64 T. Robbins, J. Kapilivsky, D. E. Cane and C. Khosla, *Biochemistry*, 2016, **55**, 4476–4484.
- 65 D. H. Kwan and F. Schulz, *Molecules*, 2011, **16**, 6092–6115.
- 66 P. Caffrey, *ChemBioChem*, 2003, **4**, 654–657.
- 67 A. T. Keatinge-Clay and R. M. Stroud, *Structure*, 2006, **4**, 737-748.
- 68 X. Xie, A. Garg, A. T. Keatinge-Clay, C. Khosla and D. E. Cane, *Biochemistry*, 2016, **55**, 1179–86.
- 69 J. Zheng and A. T. Keatinge-Clay\*, *J. Mol. Biol.*, 2011, **410**, 105–117.
- 70 C. R. Valenzano, Y.-O. You, A. Garg, A. Keatinge-Clay, C. Khosla and D. E. Cane, *J. Am. Chem. Soc.*, 2010, **132**, 14697–14699.
- 71 X. Xie and D. E. Cane, *Org. Biomol. Chem.*, 2018, **16**, 9165–9170.
- 72 D. H. Kwan, Y. Sun, F. Schulz, H. Hong, B. Popovic, J. C. C. Sim-Stark, S. F. Haydock and P. F. Leadlay, *Chem. Biol.*, 2008, **15**, 1231–1240.
- 73 D. M. Roberts, C. Bartel, A. Scott, D. Ivison, T. J. Simpson and R. J. Cox, *Chem. Sci.*,

- 2017, **8**, 1116–1126.
- 74 M. A. Skiba, A. P. Sikkema, W. D. Fiers, W. H. Gerwick, D. H. Sherman, C. C. Aldrich and J. L. Smith, *ACS Chem. Biol.*, 2016, **11**, 3319–3327.
- 75 M. A. Skiba, M. M. Bivins, J. R. Schultz, S. M. Bernard, W. D. Fiers, Q. Dan, S. Kulkarni, P. Wipf, W. H. Gerwick, D. H. Sherman, C. C. Aldrich and J. L. Smith, *ACS Chem. Biol.*, 2018, **13**, 3221–3228.
- 76 L. Du and L. Lou, *Nat. Prod. Rep.*, 2010, **27**, 255–278.
- 77 U. R. Awodi, J. L. Ronan, J. Masschelein, E. L. C. de Los Santos and G. L. Challis, *Chem. Sci.*, 2017, **8**, 411–415.
- 78 H.-Y. He, H.-X. Pan, L.-F. Wu, B.-B. Zhang, H.-B. Chai, W. Liu and G.-L. Tang, *Chem. Biol.*, 2012, **19**, 1313–1323.
- 79 C. Olano, C. Méndez and J. A. Salas, *Nat. Prod. Rep.*, 2010, **27**, 571.
- 80 A. Kumar and S. Singh, *Crit. Rev. Biotechnol.*, 2013, **33**, 365–378.
- 81 B. Meunier, S. P. De Visser and S. Shaik, *Chem rev*, 2004, **9**, 3947–3980.
- 82 J. R. Cupp-Vickery and T. L. Poulos, *Nat. Struct. Biol.*, 1995, **2**, 144–153.
- 83 F. Zhang, H.-Y. He, M.-C. Tang, Y.-M. Tang, Q. Zhou and G.-L. Tang, *J. Am. Chem. Soc.*, 2011, **133**, 2452–2462.
- 84 M. K. Kharel, P. Pahari, H. Lian and J. Rohr, *Chembiochem*, 2009, **10**, 1305–8.
- 85 J. Staunton and B. Wilkinson, *Chem Rev*, 1997, **7**, 2611–2630.
- 86 J. Xu, E. Wan, C.-J. Kim, H. G. Floss and T. Mahmud, *Microbiology*, 2005, **151**, 2515–2518.
- 87 A. Rascher, Z. Hu, N. Viswanathan, A. Schirmer, R. Reid, W. C. Nierman, M. Lewis and C. R. Hutchinson, *FEMS Microbiol. Lett.*, 2003, **218**, 223–230.
- 88 C. S. Neumann, D. G. Fujimori and C. T. Walsh, *Chem. Biol.*, 2008, **15**, 99–109.
- 89 V. Weichold, D. Milbredt and K.-H. van Pée, *Angew. Chemie Int. Ed.*, 2016, **55**, 6374–6389.
- 90 L.-F. Wu, S. Meng and G.-L. Tang, *Biochim. Biophys. Acta - Proteins Proteomics*, 2016, **1864**, 453–470.
- 91 L. Gu, B. Wang, A. Kulkarni, T. W. Geders, R. V Grindberg, L. Gerwick, K. Håkansson, P. Wipf, J. L. Smith, W. H. Gerwick and D. H. Sherman, *Nature*, 2009, **459**, 731–5.
- 92 E. M. Musiol and T. Weber, *Medchemcomm*, 2012, **3**, 871.
- 93 J. Masschelein, P. Sydor, C. Hobson, R. Howe, C. Jones, D. Roberts, Z. Yap, J. Parkhill, E. Mahenthiralingam and G. L. Challis, *Nat. Chem.*, 2019, **Accepted**.
- 94 E. J. N. Helfrich and J. Piel, *Nat. Prod. Rep.*, 2016, **33**, 231–316.
- 95 E. Shelest, N. Heimerl, M. Fichtner and S. Sasso, *BMC Genomics*, 2015, **16**, 1015.
- 96 D. T. Wagner, Z. Zhang, R. A. Meoded, A. J. Cepeda, J. Piel and A. T. Keatinge-Clay, *ACS Chem. Biol.*, 2018, **13**, 975–983.

- 97 T. J. Buchholz, C. M. Rath, N. B. Lopanik, N. P. Gardner, K. Håkansson and D. H. Sherman, *Chem. Biol.*, 2010, **17**, 1092–1100.
- 98 L. Gu, B. Wang, A. Kulkarni, T. W. Geders, R. V Grindberg, L. Gerwick, K. Håkansson, P. Wipf, J. L. Smith, W. H. Gerwick and D. H. Sherman, *Nature*, 2009, **459**, 731–735.
- 99 D. T. Wagner, J. Zeng, C. B. Bailey, D. C. Gay, F. Yuan, H. R. Manion and A. T. Keatinge-Clay, *Structure*, 2017, **25**, 1045–1055.
- 100 M. Jenner, S. Kosol, D. Griffiths, P. Prasongpholchai, L. Manzi, A. S. Barrow, J. E. Moses, N. J. Oldham, J. R. Lewandowski and G. L. Challis, *Nat. Chem. Biol.*, 2018, **14**, 270–275.
- 101 L. Song, M. Jenner, J. Masschelein, C. Jones, M. J. Bull, S. R. Harris, R. C. Hartkoorn, A. Vocat, I. Romero-Canelon, P. Coupland, G. Webster, M. Dunn, R. Weiser, C. Paisey, S. T. Cole, J. Parkhill, E. Mahenthiralingam and G. L. Challis, *J. Am. Chem. Soc.*, 2017, **139**, 7974–7981.
- 102 E. A. Campbell, N. Korzheva, A. Mustaev, K. Murakami, S. Nair, A. Goldfarb and S. A. Darst, *Cell*, 2001, **104**, 901–912.
- 103 M. Jenner, J. P. Afonso, C. Kohlhaas, P. Karbaum, S. Frank, J. Piel and N. J. Oldham, *Chem. Commun.*, 2016, **52**, 5262–5265.
- 104 E. Mahenthiralingam, L. Song, A. Sass, J. White, C. Wilmot, A. Marchbank, O. Boaisa, J. Paine, D. Knight and G. L. Challis, *Chem. Biol.*, 2011, **18**, 665–677.
- 105 A. M. Jones, M. E. Dodd, J. R. W. Govan, V. Barcus, C. J. Doherty, J. Morris and A. K. Webb, *Thorax*, 2004, **59**, 948–51.
- 106 T. Watanabe, T. Sugiyama, M. Takahashi, J. Shima, K. Yamashita, K. Izaki, K. Furihata and H. Seto, *Agric. Biol. Chem.*, 1990, **54**, 259–261.
- 107 H. Furukawa, H. Kiyota, T. Yamada, M. Yaosaka, R. Takeuchi, T. Watanabe and S. Kuwahara, *Chem. Biodivers.*, 2007, **4**, 1601–1604.
- 108 R. Takeuchi, H. Kiyota, M. Yaosaka, T. Watanabe, K. Enari, T. Sugiyama and T. Oritani, *J. Chem. Soc. Perkin Trans. 1*, 2001, **10**, 2676–2681.
- 109 A. Howard, M. O’Donoghue, A. Feeney and R. D. Sleator, *Virulence*, 2012, **3**, 243–50.
- 110 A. Parmeggiani, I. M. Krab, T. Watanabe, R. C. Nielsen, C. Dahlberg, J. Nyborg and P. Nissen, *J. Biol. Chem.*, 2006, **281**, 2893–2900.
- 111 R. D. Süßmuth and A. Mainz, *Angew. Chemie Int. Ed.*, 2017, **56**, 3770–3821.
- 112 R. Oyama, T. Watanabe, H. Hanzawa, T. Sano, T. Sugiyama and K. Izaki, *Biosci. Biotechnol. Biochem.* 2014, **78**, 766–769.
- 113 M. Leesong, B. S. Henderson, J. R. Gillig, J. M. Schwab and J. L. Smith, *Structure*, 1996, **4**, 253–264.
- 114 L. Moynié, S. M. Leckie, S. A. McMahon, F. G. Duthie, A. Koehnke, J. W. Taylor, M. S. Alphey, R. Brenk, A. D. Smith and J. H. Naismith, *J. Mol. Biol.*, 2013, **425**, 365–377.

- 115 M. S. Kimber, F. Martin, Y. Lu, S. Houston, M. Vedadi, A. Dharamsi, K. M. Fiebig, M. Schmid and C. O. Rock, *J. Biol. Chem.*, 2004, **279**, 52593–52602.
- 116 D. Kostrewa, F. K. Winkler, G. Folkers, L. Scapozza and R. Perozzo, *Protein Sci.*, 2009, **14**, 1570–1580.
- 117 D. L. Akey, J. R. Razelun, J. Tehranisa, D. H. Sherman, W. H. Gerwick and J. L. Smith, *Structure*, 2010, **18**, 94–105.
- 118 A. Keatinge-Clay, *J. Mol. Biol.*, 2008, **384**, 941–953.
- 119 S. Pasta, A. Witkowski, A. K. Joshi and S. Smith, *Chem. Biol.*, 2007, **14**, 1377–1385.
- 120 T. Maier, S. Jenni and N. Ban, *Science*, 2006, **311**, 1258–62.
- 121 J. M. Schwab, A. Habib and J. B. Klassen, *J. Am. Chem. Soc.*, 1986, **108**, 5304–5308.
- 122 J. M. Schwab, J. B. Klassen and A. Habib, *J. Chem. Soc., Chem. Commun.*, 1986, **10**, 357–358.
- 123 P. Caffrey, *Chembiochem*, 2003, **4**, 654–657.
- 124 X. Guo, T. Liu, C. R. Valenzano, Z. Deng and D. E. Cane, *J. Am. Chem. Soc.*, 2010, **132**, 14694–6.
- 125 D. D. Shah, Y.-O. You and D. E. Cane, *J. Am. Chem. Soc.*, 2017, **139**, 14322–14330.
- 126 W. D. Fiers, G. J. Dodge, Y. Li, J. L. Smith, R. A. Fecik and C. C. Aldrich, *Chem. Sci.*, 2015, **6**, 5027–5033.
- 127 D. Gay, Y.-O. You, A. Keatinge-Clay and D. E. Cane, *Biochemistry*, 2013, **52**, 8916–8928.
- 128 M. M. Alhamadsheh, N. Palaniappan, S. Daschouduri and K. A. Reynolds, *J. Am. Chem. Soc.*, 2007, **129**, 1910–1.
- 129 N. Kandziora, J. N. Andexer, S. J. Moss, B. Wilkinson, P. F. Leadlay and F. Hahn, *Chem. Sci.*, 2014, **5**, 3563.
- 130 O. Vergnolle, F. Hahn, A. Baerga-Ortiz, P. F. Leadlay and J. N. Andexer, *ChemBioChem*, 2011, **12**, 1011–1014.
- 131 N. A. Wilson, E. Barbar, J. A. Fuchs and C. Woodward, *Biochemistry*, 1995, **34**, 8931–9.
- 132 W. D. Fiers, G. J. Dodge, D. H. Sherman, J. L. Smith and C. C. Aldrich, *J. Am. Chem. Soc.*, 2016, **138**, 16024–16036.
- 133 D. C. Gay, P. J. Spear and A. T. Keatinge-Clay, *ACS Chem. Biol.*, 2014, **9**, 2374–81.
- 134 H. Luhavaya, M. V. B. Dias, S. R. Williams, H. Hong, L. G. de Oliveira and P. F. Leadlay, *Angew. Chem. Int. Ed. Engl.*, 2015, **54**, 13622–5.
- 135 S. Kosol, M. Jenner, J. R. Lewandowski and G. L. Challis, *Nat. Prod. Rep.*, 2018, **35**, 1097–1109.
- 136 J. Piel, *Nat. Prod. Rep.*, 2010, **27**, 996.
- 137 J. Moldenhauer, X.-H. Chen, R. Borriss and J. Piel, *Angew. Chemie*, 2007, **119**, 8343–8345.

- 138 I. E. Holzbaur, R. C. Harris, M. Bycroft, J. Cortes, C. Bisang, J. Staunton, B. A. M. Rudd and P. F. Leadlay, *Chem. Biol.*, 1999, **6**, 189–195.
- 139 N. Wu, F. Kudo, D. E. Cane and C. Khosla, *J. Am. Chem. Soc.*, 2000, **122**, 4847–4852.
- 140 D. E. Cane, F. Kudo, K. Kinoshita and C. Khosla, *Chem. Biol.*, 2002, **9**, 131–42.
- 141 H. Lu, S.-C. Tsai, C. Khosla and D. E. Cane, *Biochemistry*, 2002, **41**, 12590–7.
- 142 Y. Yin, H. Lu, C. Khosla and D. E. Cane, *J. Am. Chem. Soc.*, 2003, **125**, 5671–5676.
- 143 J. Wu, T. J. Zaleski, C. Valenzano, C. Khosla and D. E. Cane, *J. Am. Chem. Soc.*, 2005, **127**, 17393–404.
- 144 Y. Li, G. J. Dodge, W. D. Fiers, R. A. Fecik, J. L. Smith and C. C. Aldrich, *J. Am. Chem. Soc.*, 2015, **137**, 47.
- 145 X. Xie and D. E. Cane, *Biochemistry*, 2018, **57**, 3126–3129.
- 146 A. S. Worthington, H. Rivera, J. W. Torpey, M. D. Alexander and M. D. Burkart, *ACS Chem. Biol.*, 2006, **1**, 687–691.
- 147 S. Kapur, A. Worthington, Y. Tang, D. E. Cane, M. D. Burkart and C. Khosla, *Bioorg. Med. Chem. Lett.*, 2008, **18**, 3034–3038.
- 148 Luis E. N. Quadri, Paul H. Weinreb, Ming Lei, Michiko M. Nakano, Peter Zuber and Christopher T. Walsh, *Biochemistry*, 1998, **37**, 1585–1595.
- 149 R. Noyori, T. Ohkuma, M. Kitamura, H. Takaya, N. Sayo, H. Kumobayashi and S. Akutagawa, *J. Am. Chem. Soc.*, 1987, **109**, 5856–5858.
- 150 V. Ratovelomanana-Vidal, C. Girard, R. Touati, J. P. Tranchier, B. B. Hassine and J. P. Genêt, *Adv. Synth. Catal.*, 2003, **345**, 261–274.
- 151 J. A. Dale, D. L. Dull and H. S. Mosher, *J. Org. Chem.*, 1969, **34**, 2543–2549.
- 152 N. M. Gaudelli and C. A. Townsend, *J. Org. Chem.*, 2013, **78**, 6412–6426.
- 153 Z. Gao, J. Wang, A. K. Norquay, K. Qiao, Y. Tang and J. C. Vederas, *J. Am. Chem. Soc.*, 2013, **135**, 1735–1738.
- 154 M. B. Hodge and H. F. Olivo, *Tetrahedron*, 2004, **60**, 9397–9403.
- 155 S. G. Davies, J. R. Haggitt, O. Ichihara, R. J. Kelly, M. A. Leech, A. J. Price Mortimer, P. M. Roberts and A. D. Smith, *Org. Biomol. Chem.*, 2004, **2**, 2630.
- 156 W. Igarashi, H. Hoshikawa, H. Furukawa, T. Yamada, S. Kuwahara and H. Kiyota, *Heterocycl. Commun.*, 2011, **17**, 7–9.
- 157 H. Furukawa, H. Hoshikawa, W. Igarashi, M. Yaosaka, T. Yamada, S. Kuwahara and H. Kiyota, *Heterocycl. Commun.*, 2011, **17**, 3–5.
- 158 H. Furukawa, H. Kiyota, T. Yamada, M. Yaosaka, R. Takeuchi, T. Watanabe and S. Kuwahara, *Chem. Biodivers.*, 2007, **4**, 1601–1604.
- 159 U. Galm, L. Wang, E. Wendt-Pienkowski, R. Yang, W. Liu, M. Tao, J. M. Coughlin and B. Shen, *J. Biol. Chem.*, 2008, **283**, 28236–45.
- 160 Z. Yunt, K. Reinhardt, A. Li, M. Engeser, H.-M. Dahse, M. Gütschow, T. Bruhn, G.

- Bringmann and J. Piel, *J. Am. Chem. Soc.*, 2009, **131**, 2297–2305.
- 161 M. V Mendes, N. Antón, J. F. Martín and J. F. Aparicio, *Biochem. J.*, 2005, **386**, 57–62.
- 162 K. Arakawa, K. Kodama, S. Tatsuno, S. Ide and H. Kinashi, *Antimicrob. Agents Chemother.*, 2006, **50**, 1946–52.
- 163 P. Spiteller, L. Bai, G. Shang, B. J. Carroll, T. W. Yu and H. G. Floss, *J. Am. Chem. Soc.*, 2003, **125**, 14236–14237.
- 164 M.-Q. Zhang, S. Gaisser, M. Nur-E-Alam, L. S. Sheehan, W. A. Vousden, N. Gaitatzis, G. Peck, N. J. Coates, S. J. Moss, M. Radzom, T. A. Foster, R. M. Sheridan, M. A. Gregory, S. M. Roe, C. Prodromou, L. Pearl, S. M. Boyd, B. Wilkinson and C. J. Martin, *J. Med. Chem.*, 2008, **51**, 5494–5497.
- 165 S. Kushnir, U. Sundermann, S. Yahiaoui, A. Brockmeyer, P. Janning and F. Schulz, *Angew. Chemie Int. Ed.*, 2012, **51**, 10664–10669.
- 166 T. Brautaset, H. Sletta, A. Nedal, S. E. F. Borgos, K. F. Degnes, I. Bakke, O. Volokhan, O. N. Sekurova, I. D. Treshalin, E. P. Mirchink, A. Dikiy, T. E. Ellingsen and S. B. Zotchev, *Chem. Biol.*, 2008, **15**, 1198–1206.
- 167 Y. Zhou, J. Li, J. Zhu, S. Chen, L. Bai, X. Zhou, H. Wu and Z. Deng, *Chem. Biol.*, 2008, **15**, 629–638.
- 168 R. Reid, M. Piagentini, E. Rodriguez, G. Ashley, N. Viswanathan, J. Carney, D. V Santi, C. R. Hutchinson and R. McDaniel, *Biochemistry*, 2003, **42**, 72–9.
- 169 J. F. Barajas, J. M. Blake-Hedges, C. B. Bailey, S. Curran and J. D. Keasling, *Synth. Syst. Biotechnol.*, 2017, **2**, 147–166.
- 170 P. Power, T. Dunne, B. Murphy, L. N. Lochlainn, D. Rai, C. Borissow, B. Rawlings and P. Caffrey, *Chem. Biol.*, 2008, **15**, 78–86.
- 171 L. Tang, L. Chung, J. R. Carney, C. M. Starks, P. Licari and L. Katz, *J. Antibiot. (Tokyo)*, 2005, **58**, 178–184.
- 172 K. J. Weissman, *Trends Biotechnol.*, 2007, **25**, 139–142.
- 173 M. A. Gregory, H. Petkovic, R. E. Lill, S. J. Moss, B. Wilkinson, S. Gaisser, P. F. Leadlay and R. M. Sheridan, *Angew. Chemie Int. Ed.*, 2005, **44**, 4757–4760.
- 174 S. Mo, D. H. Kim, J. H. Lee, J. W. Park, D. B. Basnet, Y. H. Ban, Y. J. Yoo, S. Chen, S. R. Park, E. A. Choi, E. Kim, Y.-Y. Jin, S.-K. Lee, J. Y. Park, Y. Liu, M. O. Lee, K. S. Lee, S. J. Kim, D. Kim, B. C. Park, S. Lee, H. J. Kwon, J.-W. Suh, B. S. Moore, S.-K. Lim and Y. J. Yoon, *J. Am. Chem. Soc.*, 2011, **133**, 976–985.
- 175 S. J. Moss, I. Carletti, C. Olano, R. M. Sheridan, M. Ward, V. Math, M. Nur-E-Alam, A. F. Braña, M. Q. Zhang, P. F. Leadlay, C. Méndez, J. A. Salas and B. Wilkinson, *Chem. Commun.*, 2006, **10**, 2341–2343.
- 176 S. Weist, B. Bister, O. Puk, D. Bischoff, S. Pelzer, G. J. Nicholson, W. Wohlleben, G. Jung and R. D. Süssmuth, *Angew. Chemie Int. Ed.*, 2002, **41**, 3383–3385.

- 177 J. Kennedy, *Nat. Prod. Rep.*, 2008, **25**, 25–34.
- 178 J. R. Jacobsen, C. R. Hutchinson, D. E. Cane and C. Khosla, *Science*, 1997, **277**, 367–9.
- 179 J. R. Jacobsen, A. T. Keatinge-Clay, D. E. Cane and C. Khosla, *Bioorg. Med. Chem.*, 1998, **6**, 1171–7.
- 180 G. W. Ashley, M. Burlingame, R. Desai, H. Fu, T. Leaf, P. J. Licari, C. Tran, D. Abbanat, K. Bush and M. Macielag, *J. Antibiot. (Tokyo)*, 2006, **59**, 392–401.
- 181 R. J. M. Goss and H. Hong, *Chem. Commun.*, 2005, 3983–3985.
- 182 S. Murli, K. S. MacMillan, Z. Hu, G. W. Ashley, S. D. Dong, J. T. Kealey, C. D. Reeves and J. Kennedy, *Appl. Environ. Microbiol.*, 2005, **71**, 4503–4509.
- 183 C. J. B. Harvey, J. D. Puglisi, V. S. Pande, D. E. Cane and C. Khosla, *J. Am. Chem. Soc.*, 2012, **134**, 12259–12265.
- 184 R. Thiericke and J. Rohr, *Nat. Prod. Rep.*, 1993, **10**, 265.
- 185 M. Winn, J. K. Fyans, Y. Zhuo and J. Micklefield, *Nat. Prod. Rep.*, 2016, **33**, 317–347.
- 186 R. Traber, H. Hofmann and H. Kobel, *J. Antibiot. (Tokyo)*, 1989, **42**, 591–7.
- 187 Y. Yan, J. Chen, L. Zhang, Q. Zheng, Y. Han, H. Zhang, D. Zhang, T. Awakawa, I. Abe and W. Liu, *Angew. Chemie Int. Ed.*, 2013, **47**, 12308–12312.
- 188 E. Kalkreuter and G. J. Williams, *Curr. Opin. Microbiol.*, 2018, **45**, 140–148.
- 189 B. S. Evans, Y. Chen, W. W. Metcalf, H. Zhao and N. L. Kelleher, *Chem. Biol.*, 2011, **18**, 601–607.
- 190 X. Bian, A. Plaza, F. Yan, Y. Zhang and R. Müller, *Biotechnol. Bioeng.*, 2015, **112**, 1343–1353.
- 191 H. Kries, R. Wachtel, A. Pabst, B. Wanner, D. Niquille and D. Hilvert, *Angew. Chemie Int. Ed.*, 2014, **53**, 10105–10108.
- 192 J. Thirlway, R. Lewis, L. Nunns, M. Al Nakeeb, M. Styles, A.-W. Struck, C. P. Smith and J. Micklefield, *Angew. Chemie Int. Ed.*, 2012, **51**, 7181–7184.
- 193 E. M. Musiol-Kroll, F. Zubeil, T. Schafhauser, T. Härtner, A. Kulik, J. McArthur, I. Koryakina, W. Wohlleben, S. Grond, G. J. Williams, S. Y. Lee and T. Weber, *ACS Synth. Biol.*, 2017, **6**, 421–427.
- 194 A. J. Hughes and A. Keatinge-Clay, *Chem. Biol.*, 2011, **18**, 165–176.
- 195 I. Koryakina and G. J. Williams, *ChemBioChem*, 2011, **12**, 2289–2293.
- 196 I. Koryakina, J. McArthur, S. Randall, M. M. Draelos, E. M. Musiol, D. C. Muddiman, T. Weber and G. J. Williams, *ACS Chem. Biol.*, 2013, **8**, 200–208.
- 197 E. Kim, B. S. Moore and Y. J. Yoon, *Nat. Chem. Biol.*, 2015, **11**, 649–659.
- 198 M. Klaus and M. Grininger, *Nat. Prod. Rep.*, 2018, **35**, 1070–1081.
- 199 C. L. Bayly and V. G. Yadav, *Molecules*, 2017, **22**, 235.
- 200 K. A. J. Bozhüyük, F. Fleischhacker, A. Linck, F. Wesche, A. Tietze, C.-P. Niesert and H. B. Bode, *Nat. Chem.*, 2017, **10**, 275–281.



- 201 M. Cummings, R. Breitling and E. Takano, *FEMS Microbiol. Lett.*, 2014, **351**, 116–125.
- 202 R. S. Flannagan, T. Linn and M. A. Valvano, *Environ. Microbiol.*, 2008, **10**, 1652–1660.
- 203 S. Higashibayashi, W. Czechtizky, Y. Kobayashi and Y. Kishi, *J. Am. Chem. Soc.*, 2003, **125**, 14379–14393.
- 204 Y. Kobayashi, W. Czechtizky and Y. Kishi, *Org. Lett.*, 2003, **5**, 93–96.
- 205 K. Ueda, H. Umihara, S. Yokoshima and T. Fukuyama, *Org. Lett.*, 2015, **17**, 3191–3193.
- 206 W. H. Rastetter and D. P. Phillion, *J. Org. Chem.*, 1981, **46**, 3204–3208.
- 207 C. S. Neumann, D. G. Fujimori and C. T. Walsh, *Chem. Biol.*, 2008, **15**, 99–109.
- 208 J. Latham, E. Brandenburger, S. A. Shepherd, B. R. K. Menon and J. Micklefield, *Chem. Rev.*, 2018, **118**, 232–269.
- 209 T. Watanabe, T. Sugiyama, K. Chino, T. Suzuki, S. Wakabayashi, H. Hayashi, R. Itami, J. Shima and K. Izaki, *J. Antibiot. (Tokyo)*, 1992, **45**, 476–84.
- 210 K. C. Nicolaou, P. G. Bulger and D. Sarlah, *Angew. Chem. Int. Ed.*, 2005, **44**, 4442–4489.
- 211 C. C. C. Johansson Seechurn, M. O. Kitching, T. J. Colacot and V. Snieckus, *Angew. Chemie - Int. Ed.*, 2012, **51**, 5062–5085.
- 212 K. M. Herrmann and L. M. Weaver, *Annu. Rev. Plant Physiol. Plant Mol. Biol.*, 1999, **50**, 473–503.
- 213 H. Maeda and N. Dudareva, *Annu. Rev. Plant Biol.*, 2012, **63**, 73–105.
- 214 H. G. Floss, *Nat. Prod. Rep.*, 1997, **14**, 433.
- 215 T. Vogt, *Mol. Plant*, 2010, **3**, 2–20.
- 216 B. S. Moore, H. Cho, R. Casati, E. Kennedy, K. A. Reynolds, U. Mocek, J. M. Beale and H. G. Floss, *J. Am. Chem. Soc.*, 1993, **115**, 5254–5266.
- 217 T.-W. Yu, L. Bai, D. Clade, D. Hoffmann, S. Toelzer, K. Q. Trinh, J. Xu, S. J. Moss, E. Leistner and H. G. Floss, *Proc. Natl. Acad. Sci. U. S. A.*, 2002, **99**, 7968–73.
- 218 V. Semak, T. A. Metcalf, M. A. A. Endoma-Arias, P. Mach and T. Hudlicky, *Org. Biomol. Chem.*, 2012, **10**, 4407.
- 219 M. Johnson, I. Zaretskaya, Y. Raytselis, Y. Merezhuk, S. McGinnis and T. L. Madden, *Nucleic Acids Res.*, 2008, **36**, W5–W9.
- 220 J. Heider, *FEBS Lett.*, 2001, **509**, 345–349.
- 221 P. Stenmark, D. Gurmu and P. Nordlund, *Biochemistry*, 2004, **43**, 13996–14003.
- 222 S. Ricagno, S. Jonsson, N. Richards and Y. Lindqvist, *EMBO J.*, 2003, **22**, 3210–9.
- 223 L.-B. Dong, J. D. Rudolf, D. Kang, N. Wang, C. Q. He, Y. Deng, Y. Huang, K. N. Houk, Y. Duan and B. Shen, *Nat. Commun.*, 2018, **9**, 2362.
- 224 C. L. Berthold, C. G. Toyota, N. G. J. Richards and Y. Lindqvist, *J. Biol. Chem.*, 2008, **283**, 6519–29.
- 225 G. C. Whiting and R. A. Coggins, *J. Sci. Food Agric.*, 1973, **24**, 897–904.

- 226 G. C. Whiting and R. A. Coggins, *J. Biochem.*, 1974, **141**, 35-42.
- 227 N. C. Bruce and R. B. Cain, *Arch. Microbiol.*, 1990, **154**, 179-186.
- 228 T. B. Fitzpatrick, N. Amrhein and P. Macheroux, *J. Biol. Chem.*, 2003, **278**, 19891-19897.
- 229 A. Höppner, D. Schomburg and K. Niefind, *Biol. Chem.*, 2013, **394**, 1505-16.
- 230 Herbert Irschik, Dietmar Schummer, Gerhard Höfle, Hans Reichenbach, and Heinrich Steinmetz and R. Jansen, *J. Nat. Prod.*, 2007, **70**, 1060-1063.
- 231 D. Gallenkamp and A. Fürstner, *J. Am. Chem. Soc.*, 2011, **133**, 9232-9235.
- 232 F. H. Arnold, *Angew. Chemie Int. Ed.*, 2018, **57**, 4143-4148.
- 233 A. Fukii, S. Hashiguchi, N. Uematsu, T. Ikariya and Ryoji Noyori, *J. Am. Chem. Soc.* 1996, **118**, 2521-2522.
- 234 T. Matsuda, R. Yamanaka and K. Nakamura, *Tetrahedron: Asymmetry*, 2009, **20**, 513-557.
- 235 M. Pesic, E. Fernández-Fueyo and F. Hollmann, *ChemistrySelect*, 2017, **2**, 3866-3871.
- 236 L. A. O'Sullivan, A. J. Weightman, T. H. Jones, A. M. Marchbank, J. M. Tiedje and E. Mahenthiralingam, *Environ. Microbiol.*, 2007, **9**, 1017-1034.
- 237 Y. Zhang, *BMC Bioinformatics*, 2008, **9**, 40.
- 238 V. B. Chen, W. B. Arendall, J. J. Headd, D. A. Keedy, R. M. Immormino, G. J. Kapral, L. W. Murray, J. S. Richardson, D. C. Richardson and D. C. Richardson, *Acta Crystallogr. D. Biol. Crystallogr.*, 2010, **66**, 12-21.
- 239 A. T. Drew Wagner, J. Zeng, C. B. Bailey, D. C. Gay, F. Yuan, H. R. Manion and A. T. Keatinge-Clay Correspondence, *Structure*, 2017, **25**, 1045-1055.
- 240 M. H. Medema, R. Kottmann, P. Yilmaz, M. Cummings, J. B. Biggins, K. Blin, I. de Bruijn, Y. H. Chooi, J. Claesen, R. C. Coates, P. Cruz-Morales, S. Duddela, S. Düsterhus, D. J. Edwards, D. P. Fewer, N. Garg, C. Geiger, J. P. Gomez-Escribano, A. Greule, M. Hadjithomas, A. S. Haines, E. J. N. Helfrich, M. L. Hillwig, K. Ishida, A. C. Jones, C. S. Jones, K. Jungmann, C. Kegler, H. U. Kim, P. Kötter, D. Krug, J. Masschelein, A. V Melnik, S. M. Mantovani, E. A. Monroe, M. Moore, N. Moss, H.-W. Nützmann, G. Pan, A. Pati, D. Petras, F. J. Reen, F. Rosconi, Z. Rui, Z. Tian, N. J. Tobias, Y. Tsunematsu, P. Wiemann, E. Wyckoff, X. Yan, G. Yim, F. Yu, Y. Xie, B. Aigle, A. K. Apel, C. J. Balibar, E. P. Balskus, F. Barona-Gómez, A. Bechthold, H. B. Bode, R. Borriss, S. F. Brady, A. A. Brakhage, P. Caffrey, Y.-Q. Cheng, J. Clardy, R. J. Cox, R. De Mot, S. Donadio, M. S. Donia, W. A. van der Donk, P. C. Dorrestein, S. Doyle, A. J. M. Driessen, M. Ehling-Schulz, K.-D. Entian, M. A. Fischbach, L. Gerwick, W. H. Gerwick, H. Gross, B. Gust, C. Hertweck, M. Höfte, S. E. Jensen, J. Ju, L. Katz, L. Kaysser, J. L. Klassen, N. P. Keller, J. Kormanec, O. P. Kuipers, T. Kuzuyama, N. C. Kyrpides, H.-J. Kwon, S. Lautru, R. Lavigne, C. Y. Lee, B. Linquan, X. Liu, W. Liu, A.

- Luzhetskyy, T. Mahmud, Y. Mast, C. Méndez, M. Metsä-Ketelä, J. Micklefield, D. A. Mitchell, B. S. Moore, L. M. Moreira, R. Müller, B. A. Neilan, M. Nett, J. Nielsen, F. O'Gara, H. Oikawa, A. Osbourn, M. S. Osburne, B. Ostash, S. M. Payne, J.-L. Pernodet, M. Petricek, J. Piel, O. Ploux, J. M. Raaijmakers, J. A. Salas, E. K. Schmitt, B. Scott, R. F. Seipke, B. Shen, D. H. Sherman, K. Sivonen, M. J. Smanski, M. Sosio, E. Stegmann, R. D. Süßmuth, K. Tahlan, C. M. Thomas, Y. Tang, A. W. Truman, M. Viaud, J. D. Walton, C. T. Walsh, T. Weber, G. P. van Wezel, B. Wilkinson, J. M. Willey, W. Wohlleben, G. D. Wright, N. Ziemert, C. Zhang, S. B. Zotchev, R. Breitling, E. Takano and F. O. Glöckner, *Nat. Chem. Biol.*, 2015, **11**, 625–31.
- 241 J. D. Thompson, T. J. Gibson and D. G. Higgins, *Curr. Protoc. Bioinforma.*, 2003, **10**, 231-232.
- 242 E. Riva, I. Wilkening, S. Gazzola, W. M. A. Li, L. Smith, P. F. Leadlay and M. Tosin, *Angew. Chemie Int. Ed.*, 2014, **53**, 11944–11949.
- 243 C. Mordant, P. Dünkemann, V. Ratovelomanana-Vidal and J.-P. Genet, *Chem. Commun.*, 2004, 1296–1297.
- 244 R. Touati, V. Ratovelomanana-Vidal, B. Ben Hassine and J.-P. Genêt, *Tetrahedron: Asymmetry*, 2006, **17**, 3400–3405.
- 245 H. Chen, A. S. Olson, W. Su, P. H. Dussault and L. Du, *RSC Adv.*, 2015, **5**, 105753–105759.
- 246 V. Ratovelomanana-Vidal and J.-P. Genêt, *J. Organomet. Chem.*, 1998, **567**, 163–171.
- 247 S. M. Smith, M. Uteuliyev and J. M. Takacs, *Chem. Commun.*, 2011, **47**, 7812.
- 248 Mamoun M. Alhamadsheh, Nadaraj Palaniappan, Suparna DasChouduri and K. A. Reynolds, *J. Am. Chem. Soc.*, 2007, **129**, 1910-1911.
- 249 K. Sugimoto, Y. Kobayashi, A. Hori, T. Kondo, N. Toyooka, H. Nemoto and Y. Matsuya, *Tetrahedron*, 2011, **67**, 7681–7685.
- 250 R. A. Fernandes and S. V. Mulay, *J. Org. Chem.*, 2010, **75**, 7029–7032.
- 251 Z. Gao, J. Wang, A. K. Norquay, K. Qiao, Y. Tang and J. C. Vederas, *J. Am. Chem. Soc.*, 2013, **135**, 1735–1738.
- 252 D. Scott Coffey, Andrew I. McDonald, Larry E. Overman, Michael H. Rabinowitz and P. A. Renhowe, *Synlett*, 2000, **122**, 1043-1053.
- 253 C. A. Brown and V. K. Aggarwal, *Chem. A Eur. J.*, 2015, **21**, 13900–13903.
- 254 K. Ohta, O. Miyagawa, H. Tsutsui and O. Mitsunobu, *Bull. Chem. Soc. Jpn.*, 1993, **66**, 523–535.
- 255 A. D. Steele, K. W. Knouse, C. E. Keohane and W. M. Wuest, *J. Am. Chem. Soc.*, 2015, **137**, 7314–7317.
- 256 G. C. Fu, S. T. Nguyen and R. H. Grubbs, *J. Am. Chem. Soc.*, 1993, **115**, 9856–9857.
- 257 K. Miyashita, T. Tsunemi, T. Hosokawa, M. Ikejiri and T. Imanishi, *Tetrahedron Lett.*,

- 2007, **48**, 3829–3833.
- 258 X. Wang, M. Ma, A. G. K. Reddy and W. Hu, *Tetrahedron*, 2017, **73**, 1381–1388.
- 259 D. Schwizer, J. T. Patton, B. Cutting, M. Smieško, B. Wagner, A. Kato, C. Weckerle, F. P. C. Binder, S. Rabbani, O. Schwarzt, J. L. Magnani and B. Ernst, *Chem. - A Eur. J.*, 2012, **18**, 1342–1351.
- 260 T. Nagata, T. Yoshino, N. Haginoya, K. Yoshikawa, M. Nagamochi, S. Kobayashi, S. Komoriya, A. Yokomizo, R. Muto, M. Yamaguchi, K. Osanai, M. Suzuki and H. Kanno, *Bioorg. Med. Chem.*, 2009, **17**, 1193–1206.
- 261 E. . Corey and H.-C. Huang, *Tetrahedron Lett.*, 1989, **30**, 5235–5238.
- 262 Zhi-Xian Wang, Susie M. Miller, Oren P. Anderson and Yian Shi, *J Org. Chem.*, 1999, **64**, 7675-7677.
- 263 L. Chahoua, M. Baltas, L. Gorrichon, P. Tisnes and C. Zedde, *J. Org. Chem.*, 1992, **57**, 5798–5801.
- 264 S. Jiang, B. Mekki, G. Singh and R. H. Wightman, *Tetrahedron Lett.*, 1994, **35**, 5505–5508.
- 265 C. M. Amon, M. G. Banwell and G. L. Gravatt, *J. Org. Chem.*, 1987, **52**, 4851–4855.
- 266 B. M. Trost and Y. Kondo, *Tetrahedron Lett.*, 1991, **32**, 1613–1616.
- 267 T. D. H. Bugg, C. Abell and J. R. Coggins, *Tetrahedron Lett.*, 1988, **29**, 6779–6782.
- 268 E. Brenna, M. Crotti, F. G. Gatti, D. Monti, F. Parmeggiani, A. Pugliese and F. Tentori, *Green Chem.*, 2017, **19**, 5122–5130.

## **8. Appendices**

## 8.1 Phylogenetic Analysis of Diene-Forming DH Domains (Matt Jenner)

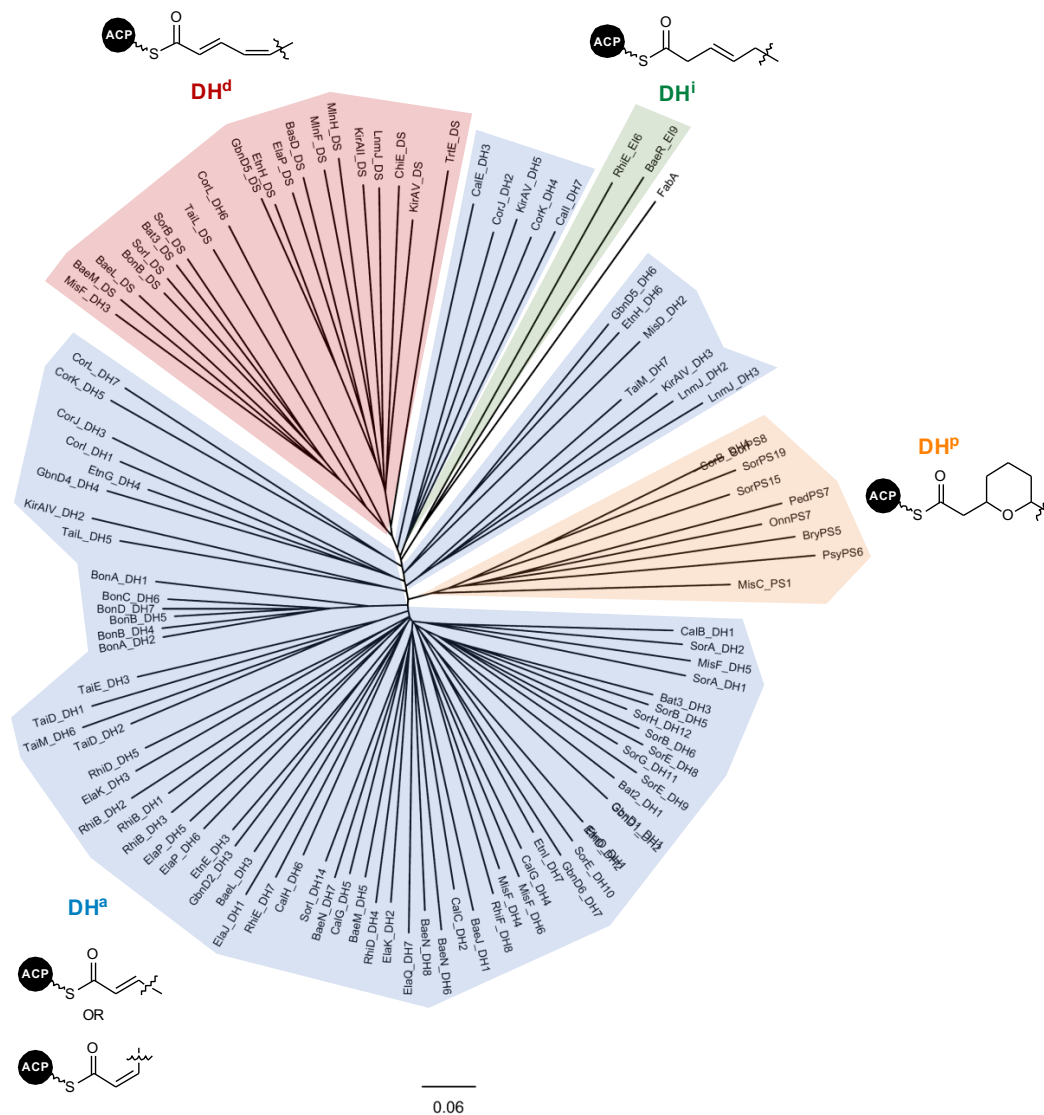


**Figure 8.1** The phylogenetic analysis of DH domains from *trans*-AT PKSs. The colored clades correspond to the function of the DH domain as follows: alkene-forming DH (DH<sup>a</sup>), blue; diene-forming DH (DH<sup>d</sup>), red; Enoyl Isomerase (DH<sup>i</sup>), green; Pyran Synthase (DH<sup>p</sup>), orange.

## 8.2 HRMS of Brominated Encyloxin IIa Derivatives

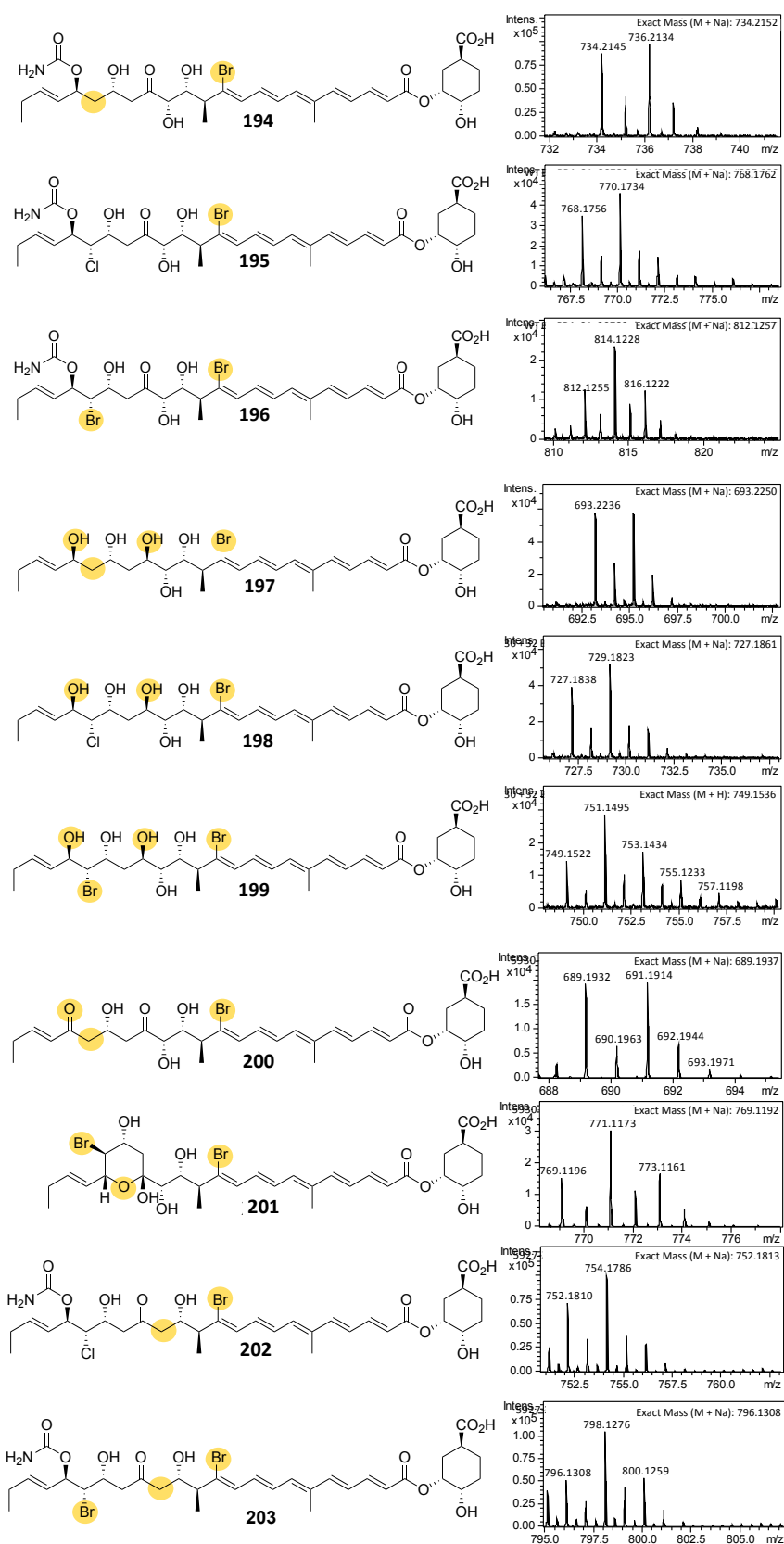
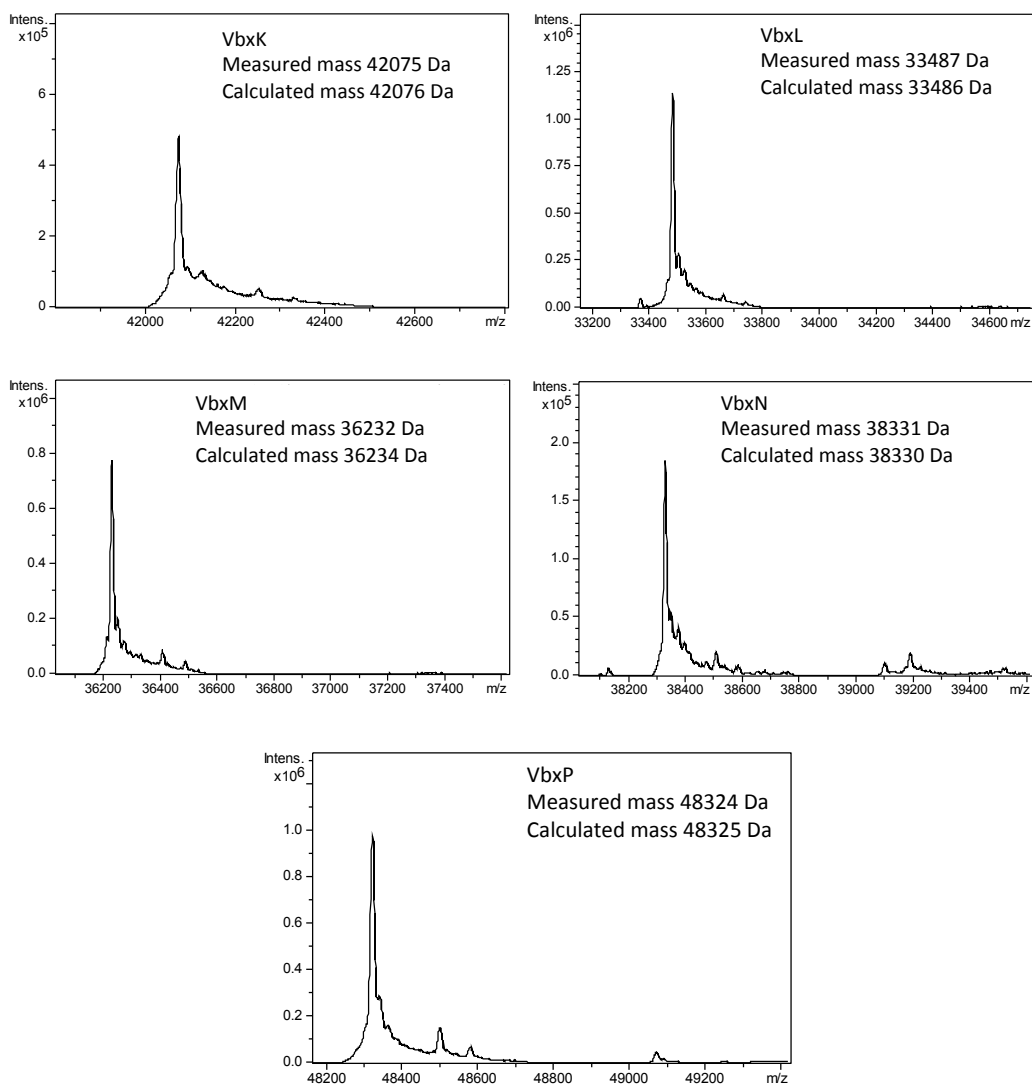


Figure 8.2 The HRMS corresponding to brominated encyloxin IIa derivatives 194-203.

### 8.3 Intact Protein MS of DHCCA Biosynthesis Enzymes



**Figure 8.3** The deconvoluted spectra corresponding to the intact MS of the proteins involved in DHCCA biosynthesis.



## 8.4 Intact Protein MS DH-ACP Control

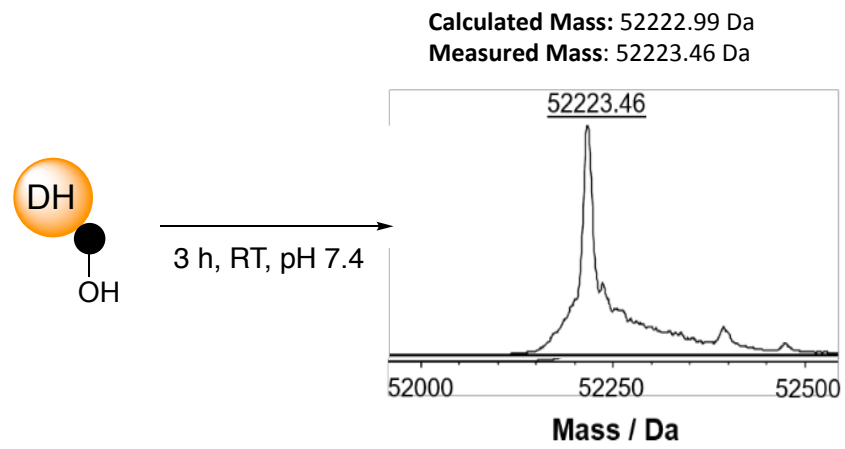


**Figure 8.4** The deconvoluted spectra corresponding to the intact MS of DH-ACP control (no loaded substrate).

## 8.5 Masses of Species from DH-ACP Assays

Substrate	Substrate-Loaded Mass (Theoretical Mass) / Da	Dehydrated Mass(s) (Theoretical Mass(s)) / Da	Rehydrated Mass(s) (Theoretical Mass(s)) / Da	Related Figure
<b>WT GbnD5 DH-ACP</b>				
53	52706.6 (52706.5)	52687.4 (52688.5)	-	Fig. 2.4
54	52705.3 (52706.5)	<i>N.D.</i> (52688.5)	-	Fig. 2.4
64	52658.6 (52660.4)	-	52676.4 (52678.4)	Fig. 2.5
65	52658.8 (52660.4)	-	<i>N.D.</i> (52678.4)	Fig. 2.5
71	52693.6 (52694.5)	-1 x H <sub>2</sub> O 52676.3 (52676.4) -2 x H <sub>2</sub> O 52657.8 (52658.4)	-	Fig. 2.7
72	52657.2 (52658.4)	-	+1 x H <sub>2</sub> O 52674.6 (52676.4) +2 x H <sub>2</sub> O 52695.6 (52694.5)	Fig. 2.7
86	52675.1 (52676.4)	52657.5 (52658.4)	52693.6 (52694.5)	Fig. 2.10
92	52693.6 (52694.5)	-1 x H <sub>2</sub> O 52673.0 (52676.4) -2 x H <sub>2</sub> O 52656.5 (52658.4)	-	Fig. 2.11
99	52657.2 (52658.4)	-	+1 x H <sub>2</sub> O 52675.8 (52676.4) +2 x H <sub>2</sub> O 52695.7 (52694.5)	Fig. 2.12
78	52692.9 (52694.5)	-1 x H <sub>2</sub> O 52675.1 (52676.4) -2 x H <sub>2</sub> O 52657.9 (52658.4)	-	Fig. 2.11
91	52692.9 (52694.5)	-1 x H <sub>2</sub> O 52675.1 (52676.4) -2 x H <sub>2</sub> O 52657.2 (52658.4)	-	Fig. 2.11
98	52675.1 (52676.4)	52657.2 (52658.4)	52694.3 (52694.5)	Fig. 2.12
<b>GbnD5 DH-ACP(H158Y)</b>				
86	52701.2 (52702.4)	<i>N.D.</i>	52719.1 (52720.4)	Fig. 2.10

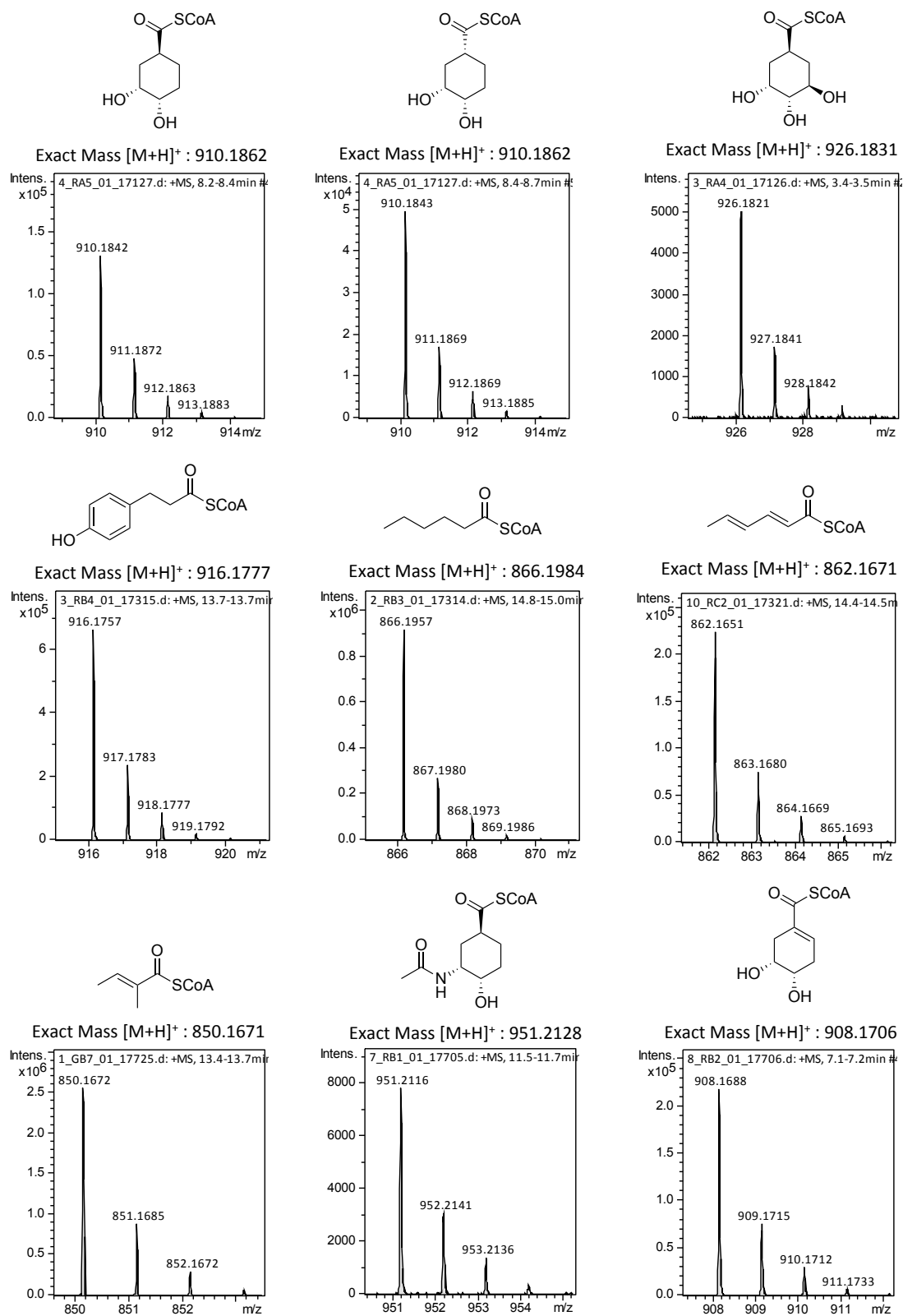
**Table 8.1** The masses of the dehydrated species from the DH-ACP assays.

## 8.6 Putative Functions of the Genes from the Enacyloxin Cluster

Gene	Putative Function
<i>Bamb_5912</i>	Dehydratase involved in DHCCA biosynthesis
<i>Bamb_5913</i>	Shikimate dehydrogenase
<i>Bamb_5914</i>	Enoyl reductase involved in DHCCA biosynthesis
<i>Bamb_5915</i>	NRPS Condensation domain
<i>Bamb_5916</i>	CoA Transferase involved in DHCCA biosynthesis
<i>Bamb_5917</i>	ACP
<i>Bamb_5918</i>	Enone reductase involved in DHCCA biosynthesis
<i>Bamb_5919</i>	<i>trans</i> -AT PKS
<i>Bamb_5920</i>	<i>cis</i> -AT PKS
<i>Bamb_5921</i>	<i>cis</i> -AT PKS
<i>Bamb_5922</i>	<i>cis</i> -AT PKS
<i>Bamb_5923</i>	<i>cis</i> -AT PKS
<i>Bamb_5924</i>	<i>cis</i> -AT PKS
<i>Bamb_5925</i>	<i>cis</i> -AT PKS
<i>Bamb_5926</i>	Type II thioesterase
<i>Bamb_5927</i>	$\alpha$ -Ketoglutarate and non-heme iron-dependent hydroxylase
<i>Bamb_5928</i>	Flavin-dependent chlorinase
<i>Bamb_5929</i>	Hypothetical protein
<i>Bamb_5930</i>	Carbamoyl transferase
<i>Bamb_5931</i>	$\alpha$ -Ketoglutarate and non-heme iron-dependent chlorinase
<i>Bamb_5932</i>	PQQ-Dependent dehydrogenase

**Table 8.2** The putative functions of the genes from the enacyloxin gene cluster.

## 8.7 MS Data for CoAs Generated by VbxP



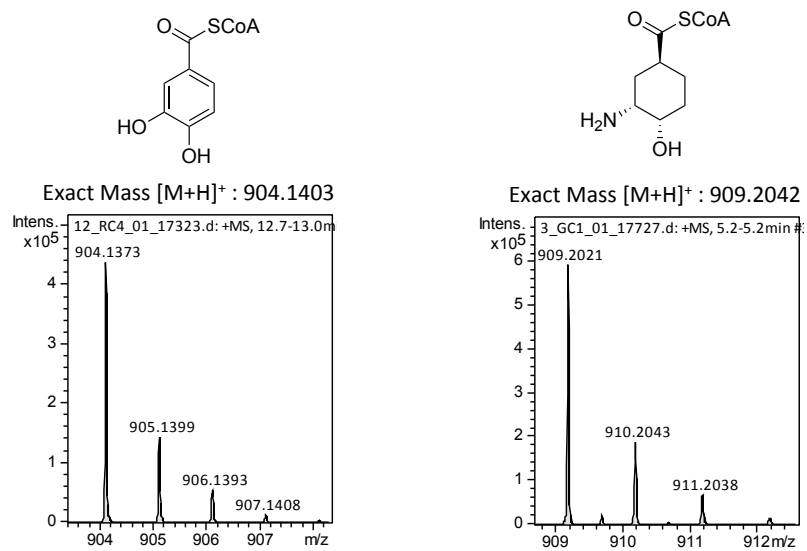


**Figure 8.5** MS data for the CoAs generated using VbxP.